universidad de león

Departamento de Ciencias Biomédicas

Área de Fisiología

UNDERSTANDING THE FUNCTION OF THE MEMBRANE TRANSPORTER ABCG2 BY COMPARISON WITH P-GLYCOPROTEIN: INTERACTION WITH ANTITUMORALS, ANTIBIOTICS, HORMONES AND OTHER COMPOUNDS

"ESTUDIO DE LA FUNCIÓN DEL TRANSPORTADOR DE MEMBRANA ABCG2 MEDIANTE COMPARACIÓN CON LA GLICOPROTEÍNA-P: INTERACCIÓN CON ANTITUMORALES, ANTIBIÓTICOS, HORMONAS Y OTROS COMPUESTOS"

Memoria para la obtención del grado de Doctor

Estefanía Egido de Frutos

León, 2014

universidad de león

INFORME DE LAS DIRECTORAS DE LA TESIS

(Art. 11.3 del R.D. 56/2005)

La Dra. Dña. **Gracia Merino Peláez** y la Dra. Dña. **Anna Seelig,** como Directoras de la Tesis Doctoral titulada "*Understanding the function of the membrane transporter ABCG2 by comparison with P-glycoprotein: interaction with antitumorals, antibiotics, hormones and other compounds*" realizada por Dña. **Estefanía Egido de Frutos** en el programa de doctorado Biomedicina en el departamento de Ciencias Biomédicas, informan favorablemente el depósito de la misma, dado que reúne las condiciones necesarias para su presentación y defensa.

Lo que firman para dar cumplimiento del artículo 11.3 del R.D. 56/2005, en León a___ de _____de 2014.

Fdo: Dra. Merino Peláez

Fdo: Dra. Anna Seelig

universidad de león

ADMISIÓN A TRÁMITE DEL DEPARTAMENTO

(Art. 11.3 del R.D. 56/2005 y 7ª norma complementaria de la ULE)

El órgano responsable del programa de doctorado en Biomedicina, en su reunión celebrada el día___de _____ de 2014, ha acordado dar su conformidad a la admisión a trámite de lectura de la Tesis Doctoral titulada "Estudio de la función del transportador de membrana ABCG2 mediante comparación con la Glicoproteína-P: interacción con antitumorales, antibióticos, hormonas y otros compuestos", dirigida por la Dra. Dña. Gracia Merino Peláez Fernández y la Dra. Dña. Anna Seelig, elaborada por Dña. Estefanía Egido de Frutos y cuyo título en inglés es "*Understanding the function of the membrane transporter ABCG2 by comparison with P-glycoprotein: interaction with antitumorals, antibiotics, hormones and other compounds*".

Lo que firman para dar cumplimiento del artículo 11.3 del R.D. 56/2005, en León a___ de _____de 2014.

El Director del Departamento, La Secretaria,

Fdo: Juan José García Vieítez Fdo: Pilar Sánchez Collado

Parte de la presente memoria será objeto de las siguientes**:**

Publicaciones en preparación

- **Estefanía Egido**, Anna Seelig and Gracia Merino. *BCRP/ABCG2 interaction of the antibiotics pefloxacin, norfloxacin and moxifloxacin: ATPase activity correlation with other in vitro and in vivo experiments using fluoroquinolones*. *Manuscript in preparation.*
- **Estefanía Egido,** Rita Müller, Xiaochun Li-Blatter*, Gracia Merino and Anna Seelig. The Breast Cancer Resistance Protein (ABCG2) and P-Glycoprotein (ABCB1) - Two Uneven Cousins yet with Related Skills***.*** *Manuscript in preparation.*
- **Estefanía Egido,** Rita Müller, Xiaochun Li-Blatter, Gracia Merino and Anna Seelig. *ABCG2/BCRP and P-glycoprotein – hormone analysis of ATPase activity and transport. Manuscript in preparation.*

Parte de la presente memoria ha sido objeto de las siguientes**:**

C**omunicaciones a Congresos**

- **Egido E**, González-Lobato L, Barrera B , Real R , Prieto JG , Álvarez AI, Merino G "*In vitro interaction of the fluoroquinolone Pefloxacin with Breast Cancer Resistance Protein (BCRP/ABCG2)".* 3rd FEBS Meeting: ATP-binding cassette (ABC) proteins: from multidrug resistance to genetic disease**.** Innsbruck, Austria 2010.
- **Egido E**, Li-Blatter X, Müller R, Merino G, Seelig A. "*P-Glycoprotein (MDR1, ABCB1) and Brest Cancer Resistance Protein (BCRP, ABCG2) – Two ABC Transporters with Different Substrate Specificities"*. Biozentrum Symposium. Basilea, Suiza 2011.
- **Egido E**, Müller R, Li-Blatter X, Merino G, Seelig A. "*The function of the ATP binding cassette transporters P-glycoprotein and BCRP in hormone and peptide transport across the membrane".* 13th edition of the Naples Workshop on Bioactive Peptides "Conformation and Activity in Peptides: Relationships and Interactions". Nápoles, Italia 2012.
- **Egido E**, Müller R, Li-Blatter X, Merino G, Seelig A. "*BCRP and P-glycoprotein – Predicting the transport rate on the basis of ATPase activity measurements".* 4th FEBS Meeting: ATP-binding cassette (ABC) proteins: from multidrug resistance to genetic disease**.** Innsbruck, Austria 2012.

Esta Tesis Doctoral se ha desarrollado gracias a la concesión de una **Ayuda para la "Contratación de Personal Investigador de Reciente Titulación Universitaria (PIRTU)" de la Consejería de Educación (Junta de Castilla y León) y del Fondo Social Europeo** (2008-2012).

Gran parte del desarrollo de la presente Tesis Doctoral se ha realizado en el centro de investigación internacional en el laboratorio de la Prof. Dr. Anna Seelig (Biophysical Chemistry Deparment del Biozentrum, University of Basel, Suiza), siendo beneficiaria de la ayudas para movilidad de estudiantes en 2011 de la convocatoria Orden EDU/2719/2011, Ministerio de Educación y de las ayudas para estancias breves en centros de investigación nacionales o extranjeros a realizar en 2010 de la convocatoria Orden EDU/2307/2009, Junta de Castilla y León.

Para el desarrollo de algunas partes también se ha contado con la **financiación de diversas entidades:**

- **JUNTA DE CASTILLA Y LEÓN.**

Título del proyecto: "**Evaluación de nuevos candidatos antitumorales: Estudios in vitro de transporte mediado por la BCRP y estudios in vivo de toxicidad y farmacocinética**". REF. SAN673/LE04/08. Duración: 01/01/2008-31/12/2008. Investigadora Principal: Dra. Gracia Merino Peláez.

- **INSTITUTO BIOMAR SA.**

Título del proyecto: "**Estudio de la biodisposición y toxicidad de nuevos tratamientos antitumorales".** Duración: 2008-2012. Investigadora Principal: Dra. Gracia Merino Peláez.

- **SWISS NATIONAL SCIENCE FOUNDATION.** REF. 3100AO-107793.

La experiencia no es lo que sucede,

si no lo que se hace con lo que sucede.

(A. Huxley)

GENERAL INDEX

Page

LIST OF FIGURES AND TABLES

FIGURES

TABLES

LIST OF ABBREVIATIONS

A-B	apical-to-basolateral
ABC	ATP-binding cassette efflux transporter
ABCG2	breast cancer resistance protein (BCRP)
ABCG2-M-ATPase	inside-out plasma membrane vesicles from mammalian cells with human ABCG2
ABZSO	albendazole sulfoxide
A_D	cross-sectional area of the molecule at the air-water interface
ADME	absorption, distribution, metabolism and excretion
ADP	adenosine diphosphate
ATP	adenosine triphosphate
AUC	area under the plasma drug concentration-time curve
B-A	basolateral-to-apical
BBB	blood brain barrier
BCA	bicinchoninic acid
BCIP	5-bromo-4-chloro-3'-indolyphosphate p-toluidine salt
BSA	bis(trimethylsilyl)acetamide o bovine serum albumin
$C_{12}EO_8$	dodecyloctaglyol
C_6-malt	*6*-tetradecyl- *β* -D-maltopyranoside
Caco-2	heterogeneous human epithelial colorectal adenocarcinoma cells
CFTR	cystic fibrosis transmembrane conductance regulator (ABCC7)
CHAPS	3-[(3-cholamidopropyl) dimethylammonio]-1-propanesulfonate
CIP	ciprofloxacin
CMC	critical micelle concentration
CPT-cAMP	8-(4-Chlorophenylthio) adenosine 3′,5′-cyclic monophosphate sodium salt
C_S	specific drug concentration
CsA	cyclosporine A
Cymal-1	cyclohexyl-Methyl-*β*-D- maltopyranoside
CYP450	cytochrome P450

DGX	digoxin
DHPC	1,2-dicaproyl-*sn*-glycero-3-phosphocholine
DMEM	Dulbecco's modified eagle medium
DMEM	Dulbecco's modified eagle medium
DMSO	dimethyl sulfoxide
DNA	deoxyribonucleic acid
DNR	daunorubicin
DOX	doxorubicin
DPBS	Dulbecco's phosphate buffered saline
DTT	1,4-dithiol-DL-threitol
ECAR	extracellular acidification rate
EDTA	ethylenediaminetetraacetic acid
EGTA	ethylene glycol tetraacetic acid
ERα	estrogen receptor
FBS	fetal bovine serum
Fos-choline-8	n-Octylphosphocholine
Fos-choline-iso-9	2,6-Dimethyl-4-Heptylphosphocholine
FQ	fluoroquinolone
FRET	fluorescence resonance energy transfer
FTC	fumitremorgin C
GF120918	elacridar
GFP	green fluorescent protein
HAP	hydrogen bond acceptor group
HEK	human embrionic kidney cells
HIV	human immunodeficiency virus
HPLC	high-performance liquid chromatography
IAAP	^{125}I-iodoarylazidoprazosin
IC_{50}	concentration of half-maximum inhibition/activation

IgG-AP	goat anti-mouse alkaline phosphatase
IRES	internal ribosome entry site
ITC	isothermal titration calorimetry
K_1	half maximum activation
K_2	half maximum inhibition
K_{aw}	air-water partition coefficient
K_{lw}	lipid-water partition coefficient
K_m	Michaelis-Menten constant
KO	knock-out
Ko143	(3*S*,6*S*,12a*S*)-1,2,3,4,6,7,12,12a-Octahydro-9-methoxy-6-(2-methylpropyl)-1,4-dioxopyrazino[1',2':1,6]pyrido[3,4-*b*]indole-3-propanoic acid 1,1-dimethylethyl ester
K_{tl}	binding constant of the drug from the lipid to the transporter
K_{tw}	binding constant of the drug from the water to the transporter
LLC-PK1	pig kidney epithelial cells
Log D	octanol-water distribution coefficient
Log P	octanol-water partition coefficient
MDCK-II	madin-darby canine kidney cells
MDR	multidrug resistance phenomenon
MEF3.8	murine embryo fibroblast cells
MF	median of fluorescence
mRNA	messenger RNA
MRP	multidrug resistance protein (ABCC)
M_W	molecular weight
MXF	moxifloxacin
MXR	mitoxantrone
NBD	nucleotide binding domain
NBT	nitro-blue tetrazolium chloride
NIH-3T3	mouse embryo fibroblasts

NIH-MDR1-G185	mouse embryo fibroblasts stably transfected with the human MDR1 gene
NMDG	*N*-methyl-D-glucamine
OAT	organic anion transporter
OATP	organic anion transport proteins
OCT	organic cation transporter
OD	optical density
Opti-MEM	serum-free medium
PBS	phosphate buffered saline
P-gp	P-glycoprotein from surface glycoprotein, P for permeability (MDR1, ABCB1)
PGR	progesterone receptor
PhIP	2-amino-1-methyl-6-phenylimidazo[4,5-b] pyridine
Pi	inorganic phosphate
PK	pharmaco*k*inetics
pK_a	acid dissociation constant at logarithmic scale
POPC	1-palmitoyl-2-oleoyl-sn-glycero-3-phosphocholine
QSAR	quantitative structure-activity relationship model
Rh123	rhodamine123
RNA	ribonucleic acid
SAM	surface activity measurement
SAR	structure–activity relationship model
SD	standard deviation
SDS	sodium dodecyl sulfate
Sf9	insect cells from *Spodoptera frugiperda*
siRNA	small interfering RNA
SLC	solute carrier transporter
SNP	single nucleotide polymorphisms
TBS	tris buffered saline
TKI	tyrosine kinase inhibitors

TM	transmembrane
TMD	transmembrane domain
TPT	topotecan
V_0	basal activity in the absence of drugs
V_1	maximum transporter activity
V_2	minimum transporter activity
VB	vinblastine
VRP	verapamil
V_s	rate at a specific drug concentration (C_S) in aqueous solution
WT	wild-type
$\Delta G°$	free energy
π	surface pressure
π_M	lateral packing density of the membrane

Introduction

Breast Cancer Resistance Protein (BCRP, ABCG2) and P-glycoprotein (P-gp, ABCB1, MDR1) are members of the G and B subfamily of the ATP-binding cassette (ABC) efflux transporters, respectively. Both transporters use the energy of ATP hydrolysis for substrate efflux. ABCG2 was identified in 1998 (Doyle et al., 1998) while P-gp was discovered 20 years earlier (Juliano and Ling, 1976). ABCG2 and P-gp are localized in normal tissues and barriers as well as in tumor cells where they transport a wide variety of compounds, including antitumorals, antibiotics and hormones. Moreover, they show overlapping substrate specificity. These transporters are considered as clinically relevant in drug absorption in the intestine, distribution (e.g., at blood-brain barrier) and elimination in the liver and the kidney; ABCG2, also in drug secretion in the mammary gland (Giacomini et al., 2010). Both are the clinically most important efflux transporters at the blood-brain barrier and the intestinal barrier. Furthermore, they are involved in the multidrug resistance phenomenon (MDR). Despite similar functions, the two proteins show practically no protein sequence identity in the transmembrane domains (TMDs) and only little sequence identity in the nucleotide binding domains (NBDs) (~ 20%) (Li et al., 2007). The present knowledge on P-gp and ABCG2 have been extensively reviewed (e.g. Krishnamurthy and Schuetz, 2006; Sharom, 2008; Robey et al., 2009; Poguntke et al., 2010; Mo and Zhang, 2012).

It is thus of great importance in pharmaceutical chemistry and medicine to understand the function of these transporters and to be able to predict their function.

In the case of P-gp, broad knowledge has been gained on its biochemistry, structure and function. It has long been known that P-gp binds its substrates in the lipid membrane; as a consequence, substrate binding to P-gp is a two-step process, a lipid-water partitioning step and a transporter binding step in the lipid membrane. In contrast, comparatively, little is known on ABCG2 structural function (e.g. Matsson et al., 2009; Ni et al., 2010). Numerous computational approaches or models based on Quantitative Structure-Activity Relationships (QSAR) models, Structure–Activity Relationships (SARs) analysis, pharmacophore modeling and molecular docking were developed to predict P-gp inhibitors or substrates (Chen et al., 2012); but only limited models can give satisfactory predictions. In the case of ABCG2, the number of approaches is lower. However, despite different approaches, the nature of drug-transporter interactions in the case of ABCG2 is not yet very clear. A model that can predict ABCG2 substrates and inhibitors accurately is still lacking. In addition, no direct molecular model explaining how ABCG2 works has been reported so far. The **main aim** of the present memory was to understand the ABCG2 function by comparison witn P-gp. For this goal, several specific aims were proposed.

The **first specific aim** of the present investigation was to gain further insight into the similarities and differences between ATPase kinetics and the substrate binding of ABCG2 and P-gp; and in addition, to attempt a prediction explaining the substrate interactions of compounds at the molecular level with both transporters. For this purpose we chose 28 compounds, including electrically neutral, cationic, anionic and zwitterionic species, 20 of which interacted with both transporters.

As it has been already mentioned, one of the major constituents of ABCG2 and P-gp substrates are hydrophobic chemotherapeutics, including topoisomerase inhibitors, anthracyclines, camptothecin analogs, tyrosine kinase inhibitors, antimetabolites, anthracyclines, vinca alkaloids and taxanes (Duan et al., 2009; Mo and Zhang, 2012). Despite the fact that the interaction of these antitumorals with ABCG2 and P-gp have been investigated by means of *in vitro* cell-based and ATPase activity assays as well as by means of *in vivo* experiments, a general understanding regarding their interaction with these two ABC transporters at the molecular level remains to be clarified. Therefore, several antitumorals were also included in the list of compounds to study and explain the substrate interaction with P-gp and ABCG2.

In the field of ABC transporter analysis, a certain disparity has been developed in data interpretation between groups focus in protein science and groups focus in membrane science. However, both items (protein and membrane) function synergistically. Most drugs reach their target by passive diffusion across several membrane lipid bilayer barriers. Transporters such as ABCG2 and P-gp compete with passive drug influx into the cell by binding drugs in the lipid bilayer membrane and moving them back to the extracellular environment at expenses of ATP hydrolysis.

To assess whether a compound is a substrate or an inhibitor of a particular transporter the International Transporter Consortium (Giacomini et al., 2010) recommends bi-directional transport assays with polarized confluent cell monolayers expressing the transporter of interest. Measurement of the substrate-induced ATP hydrolysis was in contrast not recommended because of inconsistency between the ATPase activity and the transport rate of some substrates and inhibitors and a high incidence of false positive and false negatives. However, the rate of ATP hydrolysis and the rate of substrate transport unambiguously correlate, provided, the passive flux across the bilayer membrane is taken into account in a quantitative manner (Seelig, 2007).

The **second specific aim** of the present study was to test the correlation between ATPase activity of both transporters and the rate of substrate transport in transport and accumulation assays by taking into account that most drugs can cross the bilayer membrane by passive diffusion. For this analysis we chose steroid hormones. The interaction between steroid hormones and the two ABC transporters, P-gp and ABCG2, has been extensively studied and published and we used the large amount of transport and accumulation assays provided in literature to compare them with our ATPase activity and SAM results. Steroid hormones moreover have the advantage to be electrically neutral which allows ignoring charge effects and make easier the explanations of the interactions between transporters and steroids.

Another group of compounds with great scientific interest that interact with ABC transporters is the antibiotics. Antibiotics for the treatment of infections include fluoroquinolones, a class of synthetic antimicrobial with remarkably broad spectrum and high antibacterial potency. In a similar way as the second purpose, the **third specific aim** of this investigation was to correlate ABCG2 and P-gp- ATPase activity obtained for five common fluoroquinolones (ciprofloxacin, enrofloxacin, moxifloxacin,

norfloxacin, pefloxacin) with obtained and published data from accumulation and transport cell-based assays, which allows explaining the interactions between these fluoroquinolones and ABCG2 and P-gp at the molecular level. Additionally, to complete the characterization of the interaction of these fluoroquinolones with ABCG2, we evaluate the *in vivo* interaction of moxifloxacin, norfloxacin and pefloxacin with ABCG2.

Bibliographic Revision

1. Membrane transporters

Membrane transporters are membrane-associated specialized proteins that cross cell membrane bilayers and mediate translocation of solutes into and out of cells using active and passive mechanisms (Klaassen and Aleksunes, 2010).

The two major superfamilies of membrane transporters are the ATP-binding cassette (ABC) and solute carrier (SLC) superfamilies. More than 400 membrane transporters in these two major superfamilies have been listed in the human genome (Giacomini et al., 2010).

The members of the superfamily of ATP-binding cassette (ABC) transporters use primary active transport; i.e. substrates pass through transport pumps using energy generated from the hydrolysis of ATP. Solutes are transported across biological membranes against a concentration gradient and/or an electrochemical potential (Klaassen and Aleksunes 2010). The ABC superfamily will be afterwards discussed in more detail among the next paragraphs.

Many of these transporters have been cloned, characterized and localized in tissues and cellular membrane domains in different species of animals and others beings; specially mammals and humans. An extensive selection of human transporters localized in different important barrier tissues (intestine, liver, kidney and brain) is displayed in Figure 1.

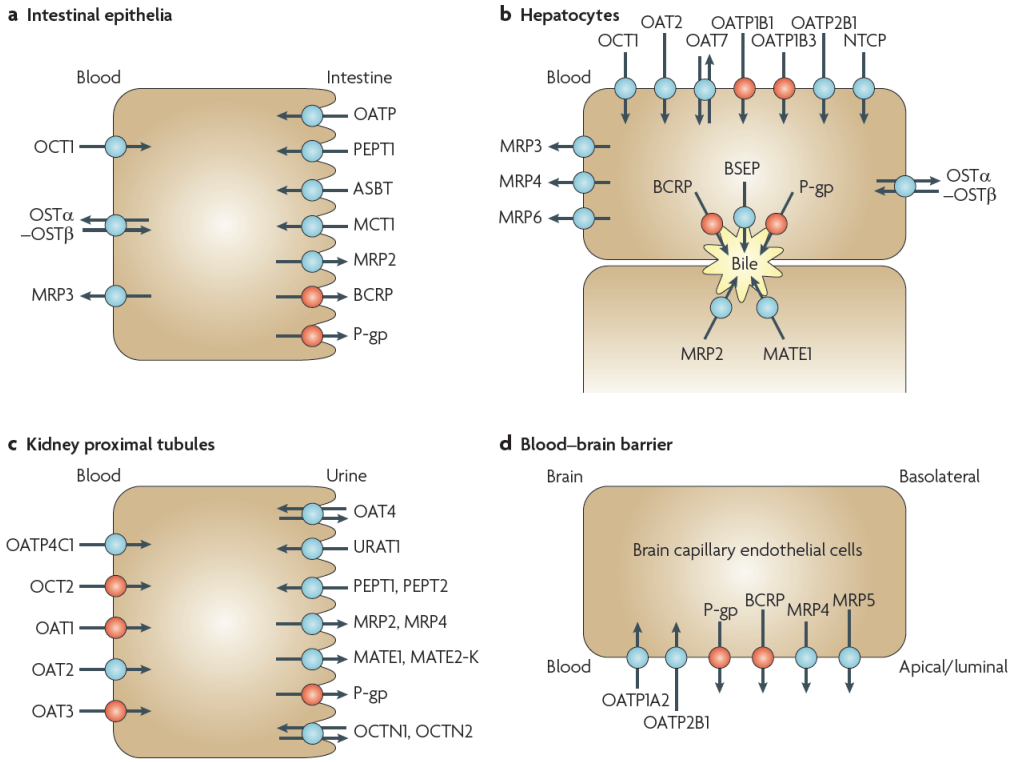

Figure 1. Human transporters in plasma membrane domains of intestinal epithelia (**A**), hepatocytes (**B**), kidney proximal tubules (**C**) and brain capillary endothelial cells (**D**) (Giacomini et al., 2010).

In daily life, organisms are exposed to hydrophobic compounds in food and the environment that pass through the lipid bilayer freely and penetrate the body. Unfortunately, many of them have toxic effects. Thus, living beings have developed mainly two strategies to cope with these hydrophobic toxic substances. One strategy is to conjugate them enzymatically with glutathione, glucuronate, or sulfate, whereby they become more hydrophilic and then detoxified. At the same time, this makes these compounds easier to be recognized by transporters. For instance, several members of the ABC superfamily, the ABCC (MRPs) and ABCG2 proteins, are involved in transporting these marked compounds out of cells (Borst et al., 2000; Schinkel and Jonker, 2003). This pathway is very efficient but has an intrinsic defect, i.e. toxic substances must be marked to be bound and effluxed. The other strategy is to recognize compounds as they pass through the plasma membrane and to excrete them out of the cells. The latter process applies to some ABC proteins such us P-gp and ABCG2 (Sarkadi et al., 2006).

The removal of compounds has significant consequences in drug disease treatments. Drugs are recognize as toxic compounds by transporters and are excreted out of the cell and body. Membrane transporters have a clinical importance as they play a major role in drug absorption and disposition, and therefore modulate the concentration of drugs in the systemic circulation and they also affect intracellular concentrations of drugs. Consequently, transporter-based drug interactions may alter the efficacy or toxicity of the affected drug (Endres et al., 2006).

Membrane transporters play also an essential role by maintaining the integrity of the plasma membrane. The plasma membrane is critical for the life of the cell, not only as maintaining the cytosolic environment differently from the extracellular environment, but also as a platform for the protein assembly, which converts extracellular stimuli into intracellular signals. Transporters assure the proper circulation and distribution of the hundred species of lipids embed in the plasma membrane and take them up from tissues in case of excess (Ueda, 2011).

2. ABC transporters

ATP binding cassette (ABC) transporters are ubiquitous integral membrane proteins that actively transport a wide variety of structurally unrelated compounds across biological membranes. They contain ATP-binding domains that possess ATPase activity (hydrolysis of ATP to ADP) to provide energy for translocating substrates, most often against concentration gradients, across cell membranes. This process is critical for most aspects of cell physiology, including the uptake of nutrients and elimination of waste products, energy generation, and cell signalling. Their dysfunction underlies a number of human genetic diseases. ABC transporters play essential roles in a majority of physiological, pathological, and pharmacological processes; also in drug disposition, therapeutic efficacy and adverse drug reactions (Linton, 2007). Therefore, ABC proteins are clinically and economically important.

They were first described in the 1970s and 1980s with the identification of human P-glycoprotein (P-gp) as the cause of cytotoxic drug resistance (Juliano and Ling, 1976) and characterization of the maltose and histidine bacterial permease systems (Ferenci et al., 1977; Gilson et al., 1982).

2.1. Classification

The ATP-binding cassette (ABC) superfamily of proteins is one of the largest protein families in biology. They are collectively named ABC transporters or proteins because of the highly conserved ATP binding domains (Dassa and Bouige, 2001). ABC transporters are encoded within the genome of every living organism; they have been conserved across the three kingdoms of archaea, eubacteria and eukarya (Dean et al., 2001).

They have been classified into seven subfamilies designated A to G on the basis of phylogenetic relationship, i.e. sequence similarity of the ATP binding domain and domain organization (Dean et al., 2001). The human genome encodes 49 ABC transporters (Sheps et al., 2004), only a fraction of which have been characterized. They are listed in Figure 2.

A	B	C	D	E	F	G
ABCA1	ABCB1(MDR1)	ABCC1(MRP1)	ABCD1(ALDP)	ABCE1	ABCF1	ABCG1
ABCA2	ABCB2(TAP1)	ABCC2(MRP2)	ABCD2		ABCF2	ABCG2(BCRP)
ABCA3	ABCB3(TAP2)	ABCC3	ABCD3(PMP70)		ABCF3	ABCG4
ABCA4	ABCB4(MDR2)	ABCC4	ABCD4			ABCG5
ABCA5	ABCB5	ABCC5				ABCG8
ABCA6	ABCB6	ABCC6				
ABCA7	ABCB7	ABCC7(CFTR)				
ABCA8	ABCB8	ABCC8(SUR1)				
ABCA9	ABCB9	ABCC9(SUR2)				
ABCA10	ABCB10	ABCC10				
ABCA12	ABCB11(BSEP)	ABCC11				
ABCA13		ABCC12				
		ABCC13				

Figure 2. Members of subfamilies (A to G) of human ABC proteins.

From the point of view of function, the ABC superfamily can be divided in two groups (Holland and Blight, 1999). The larger of these contains primary active transporters that utilize the energy of ATP hydrolysis to translocate substrates across cellular membranes. The second group comprises non-transporter ABC proteins that are localized to the cytosol or nucleus and are employed for maintenance and repair of DNA and for gene regulation (George and Jones, 2012).

2.2. Structure

ABC transporters can exist as full or half transporters. The prototypical ABC transporter is a "full transporter"; it is composed by two hydrophobic transmembrane domains (TMDs) with 12 transmembrane (TM) α-helices that form the permeation pathway and the binding sites for transport substrates that also provide specificity. Additionally, it has two hydrophilic cytosolic nucleotide binding domains (NBDs), also known as ATP-binding cassettes, which hydrolyze ATP to power this process. To achieve export, ABC transporters require a minimum of these four core domains (Figure 3). In bacteria, these four domains exist as different separate polypeptides, whereas in eukaryotes, the four domains are often fused into a single large protein. Some of the human transporters have additional domains (many of the "C" subgroup have a third TMD, and CFTR has a cytoplasmic regulatory domain). "Half transporters" are also present and are characterized by a single TMD fused to a single NBD (Figure 3B). Half transporters are able to form homodimers or heterodimers to generate a functional transporter (see Linton, 2007; and Falasca and Linton, 2012 as examples of reviews).

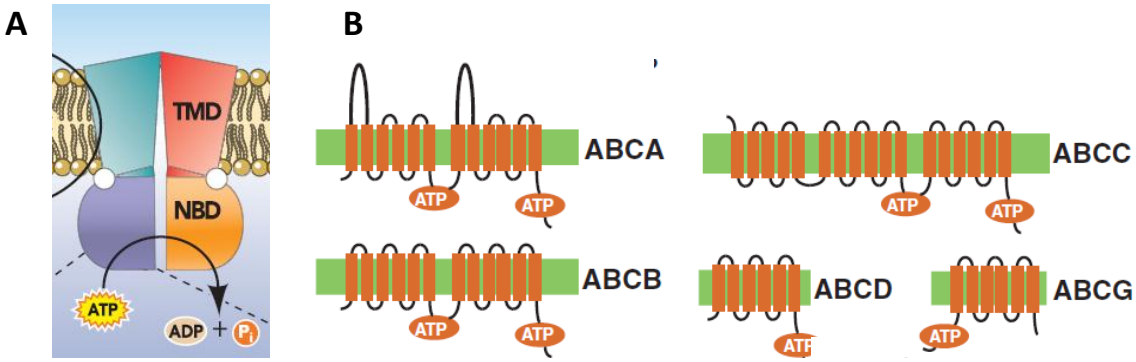

Figure 3. ABC transporters structure. **A**. The four domains of a "full" ABC transporter structure: two transmembrane domains (TMDs) bind ligand, and two nucleotide binding domains (NBDs) which drive transport by ATP binding and hydrolysis (Linton, 2007). **B**. The typical secondary structures (topology) of some families. Full length transporters (ABCA and ABCB) have 12 transmembrane (TM) segments and two cytoplasmic NBDs (represented as ATP). "Half-transporters" (ABCD and ABCG) comprising six TM segments and a cytoplasmic NBD (Ueda, 2011).

The amino acid sequence of TMDs varies considerably through ABC-transporters; it provides the specificity for the transported solute. In contrast, the structure of the NBDs is well conserved among ABC transporters (25-30% identity) (Li et al., 2007). The NBDs of all ABC proteins contain three highly conserved sequence motifs that play an important role in ATP-binding and hydrolysis; the Walker A and Walker B motifs (found in many proteins that bind ATP or GTP) and a signature C motif, which is specific for the ABC superfamily. Each ATP-binding site is formed from the Walker A and B motif of one NBD subunit and the C motif of the partner NBD subunit. The NBDs are closed around two molecules of ATP at the interface.

There are also a few but clinically important examples of atypical ABC proteins because although they have the requisite domains to function as transporters, they act as channels. For instance, the cystic fibrosis transmembrane regulator (CFTR or ABCC7) is a chloride ion channel that when dysfunctional is responsible for the inherited genetic disorder cystic fibrosis in Caucasians (Riordan et al., 1989; Gadsby et al., 2006). The sulphonylurea receptor (SUR or ABCC8) regulates a potassium channel to which it is bound in a quaternary complex (Inagaki et al., 1995).

During 2002-2012, nine prokaryotic ABC transporter structures and two eukaryotic structures have been solved to medium resolution using biochemical, cryoelectron microscopy and fluorescence spectroscopic studies. Crystallization of integral membrane proteins has been an increasing success in several bacterial ABC proteins (see George and Jones, 2012 for review). However, eukaryotic ABC proteins seemed to show more difficulties for crystallization.

2.3. Mechanism of action

It is interesting to note that most ABC transporters are unidirectional. Although the general mechanism for the transport cycle of ABC transporters has not been fully elucidated, it is well known that drug extrusion involves ATP binding and hydrolysis coupled to conformational changes in the transporter (Falasca and Linton, 2012). Drug transport involves two interconnected cycles, first a catalytic cycle of ATP hydrolysis; second, the compound transport cycle.

The model that describes the mechanism of action of ABC transporters is defined more commonly by the **ATP Switch model** (Higgins and Linton, 2004, and updated in Linton and Higgins, 2007). It proposes that the transport-substrate binding domain (TMDs) alternates between two conformations: one open towards the intrafacial side of the membrane with high affinity for drugs, and the other open to the exofacial side of the membrane with low affinity for drugs. This is also coupled to the ATP catalytic cycle of the NBDs. The ATP-switch model is based on biochemical and structural studies of several ABC transporters. It is also known as the “Tweezers-Like” (Chen et al., 2003) and “Processive Clamp” (van der Does and Tampe, 2004) models.

The "ATP Switch" model is divided into four steps or four conformational changes; they are schematized in Figure 4. It is important to appreciate that each step is closely coupled to the next. In the first step drug binds to the TMDs in the high-affinity open NBD dimer conformation, it causes a conformational change in the NBDs and induces an increase of affinity for ATP. In the second step, ATP binding induces formation of the closed NBD dimer, which in turn induces a large conformational change in the TMDs sufficient to translocate drug. The third step starts when the ATP hydrolysis initiates destabilization of the closed NBD dimer. This conformational change at the NBDs induces a corresponding change in conformation of the TMDs which opens the drug binding site to the outside of the cell and simultaneously lower the affinity of the drug binding pockets so that drug is released extracellularly. At the fourth and final step of the cycle, following hydrolysis, the liberated phosphate is released from the protein, and then ADP is released to complete the transport cycle and restore the transporter to its basal configuration (Linton and Higgins, 2007).

For some ABC transporters like P-gp, hydrolysis of both ATPs is necessary for completion of the transport cycle, and the ATPs are hydrolysed nonsimultaneously. In other ABC transporters, such as in MRP1 and CFTR, hydrolysis of only one ATP may be sufficient to drive the protein through the conformational cycle (Linton, 2007). Note that affinity of ABC transporters for ADP is low, and ADP is unable to stabilize the dimeric interaction of NBDs.

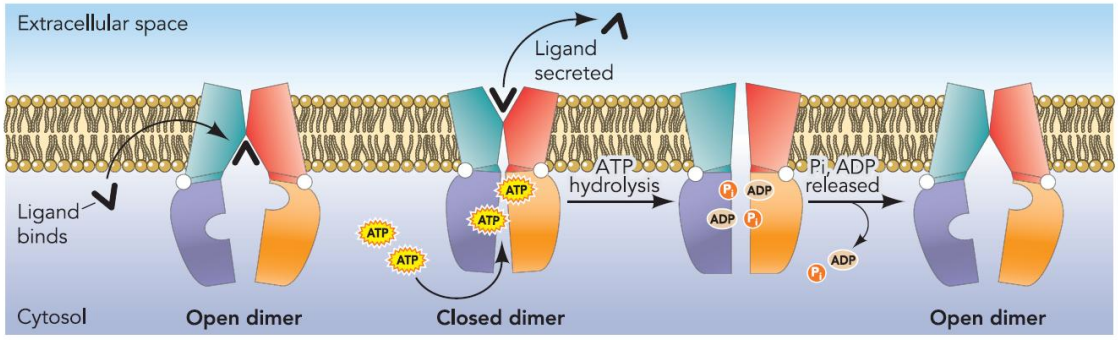

Figure 4. The ATP-switch mechanism for ABC transporters. Ligand binding to a high-affinity pocket formed by the TMDs induces a conformational change in the NBDs resulting in a higher affinity for ATP. Two molecules of ATP bind to the NBDs. The energy released by the formation of the closed NBD dimer causes conformational change in the TMDs. ATP hydrolysis detonates dissolution of the closed NBD dimer resulting in further conformational changes in the TMDs. Finally, phosphate and then ADP release restores the transporter to the open NBD dimer conformation (Linton and Higgins, 2007).

An alternative model is the **Constant Contact model** (Jones and George, 2009). The "Constant Contact" model is based on the early "alternating sites" model that established alternating ATP hydrolysis in each NBD, with one site opening at the point of ATP hydrolysis, and the second site remaining closed with ATP bound and occluded (Senior et al., 1995; Senior and Bhagat, 1998). In the

"Constant Contact" model, one site opens sufficiently for nucleotide release without the need for the NBD monomers to separate fully. Then, as this site closes with a new ATP molecule now bound and occluded, the opposite site becomes primed for hydrolysis and the process repeats in alternating cycles.

Differences between both models can be observed in Figure 5.

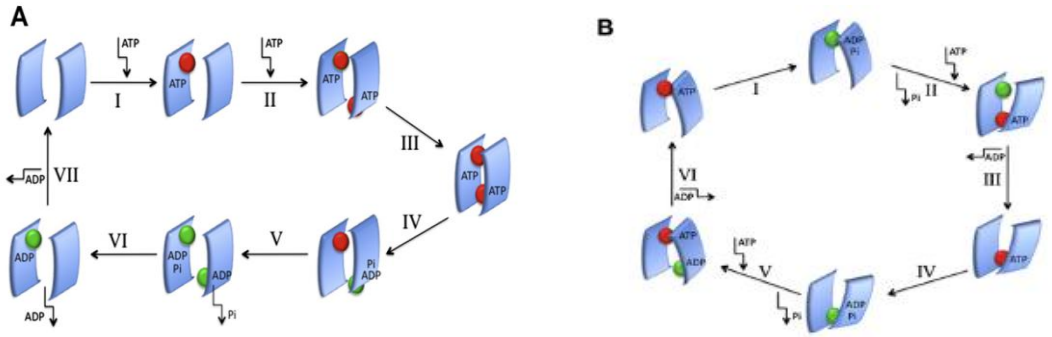

Figure 5. Models for the catalytic cycle of ATP binding and hydrolysis in the ABC transporter NBD dimer. **A**. The Switch Model: Step I is the resting state in which the ABC monomers are separated and nucleotide-free. In Step II the monomers become loaded with ATP, triggering the closure of the interface to form the sandwich dimer (Step III). Steps IV, V, and VI depict hydrolysis of ATP in each site, returning the dimer to the nucleotide-free open state during Step VII, completing the cycle. **B**. Constant Contact Model: In Step I, the ATP-bound active site is closed and the opposite site is empty and ATP hydrolysis occurs. In Step II, the empty site switches to high affinity, enabling ATP binding. In Step III, ATP binding to the empty site and P_i release promotes opening of the ADP-bound site, release of ADP and occlusion of the ATP-bound site. Steps I, II, and III are repeated in the opposite active site during Steps IV, V, and VI, with ADP release in Step VI completing the cycle (George and Jones, 2012).

2.4. Distribution, functions and implications

ATP binding cassette (ABC) transporters are found in all archaea, eubacteria and eukarya living organisms and many species have lots. There are, for example, 28 in *Saccharomyces*, 58 in *Caenorhabditis*, 51 in *Drosophila*, 129 in *Arabadopsis*, and 69 ABC transporters in *E. coli* (Linton, 2007).

ABC transporters are present in the cytoplasmic membrane (extracellular) of bacteria, and in both the plasma membrane and organelle (intracellular) membranes - like endoplasmic reticulum, mitochondria or peroxisome - in eukaryotes. They are also expressed in biological barriers such as the blood-brain, intestine, kidney or liver barriers (Figure 6). Important as well, several members of the human ABC transporter family have been found overexpressed in several different tumour and leukaemia cell types (Gottesman et al., 2002).

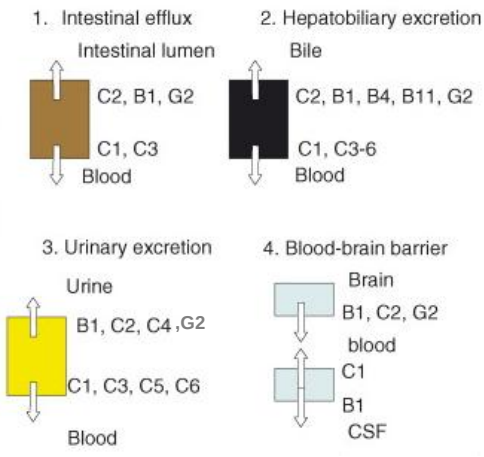

Figure 6. Several ABC transporters expressed in the basolateral or apical side of epithelial cells in barriers: intestine (1), liver (2), kidney (3) and brain (4) (Szakács et al., 2008).

ABC transporters are responsible for the ATP-dependent movement of a wide variety of xenobiotics (exogenous toxins), lipids and metabolic products across the plasma membrane and intracellular membranes (Sharom, 2008). While prokaryotic ABC proteins can be either importers or exporters, eukaryotic family members are exclusively exporters.

Their primordial origin and ubiquitous distribution reflect fundamental import and export requirements, for example, to accumulate essential nutrients such as amino acids, sugars, ions, nucleotides, endogenous metabolites and vitamins in prokaryotes; or to eliminate drugs, toxins, xenobiotics, polysaccharides, lipids, hormones, sterols, bile salts, peptides, and proteases (George and Jones, 2012).

ABC transporters can transport unmodified drugs and drug conjugates. Some transporters as P-gp transport a large number of structurally unrelated compounds; others transport specific compounds or a subset of closely related compounds that can be either physiological or xenobiotic. For instance, ABCA1 eliminates excess cholesterol in peripheral cells by generating HDL (Ueda, 2011).

2.4.1. Implications in organism protection and drug disposition (ADME)

Usually there is overlapping drug specificity; this redundancy indicates that a complex network of efflux pumps is involved in protecting the body from xenobiotics. ABC transporters play a central role in normal physiology by protecting tissues from the toxicity of exogenous xenobiotics and endogenous molecules (Leslie et al., 2005). The tissues or organs that are protected depend on the specific pattern of expression and the activity of each protein in normal tissues.

Therefore, the normal function of some human ABC transporters is to secrete cytotoxic compounds (dietary cytotoxics and therapeutic drugs) from cells. Some of these transporters (P-gp,

ABCG2, and MRP1) are highly expressed in biological barriers such as the barriers in gut, liver and kidneys (in particular in the epithelia), where they restrict the bioavailability of administered drugs (Sarkadi et al., 2006). Thus, ABC transporters are major contributors to the disposition or bioavailability of chemicals within the body by participating in the pharmacokinetics (PK) areas; i.e., absorption, distribution, and elimination (metabolism and excretion). This is commonly referred to as the ADME scheme. These processes dictate the circulating and cellular levels of endogenous and exogenous compounds and, in turn, their physiological and pharmacological activity (Klaassen and Aleksunes, 2010). Studies on knockout mice lacking each of these proteins have confirmed these ideas (Borst and Schinkel, 1996; Zhou et al., 2002).

2.4.2. The MultiDrug Resistance (MDR) phenomenon: use of ABC transporter inhibitors

As already mentioned, several ABC transporters are multidrug efflux pumps; that play an important role in the absorption and disposition of therapeutic drugs (Schinkel and Jonker, 2003). Therefore they affect clinical therapy; resistance to treatment of multiple drugs as antibiotics and antitumorals has been associated with ABC transporters expression in the target tissue. The multidrug resistance (**MDR**) is a complex multifactorial phenomenon where organisms and cells display cross-resistance to a wide range of drugs that are structurally and functionally unrelated, leading to an attenuated therapeutic response in the clinical setting. The phenomenon of MDR was first described in the scientific literature in 1970 (Biedler and Riehm, 1970). Although the active efflux of drugs by ABC transporters is not the only mechanism responsible for MDR, it is considered one of the most frequent.

Chemotherapy has been a major form of treatment for various cancers since 1940s. However, ineffectiveness and failure of chemotherapy with single agent was soon observed (Dean et al., 2005). This is probably due to the ability of cancer cells to mutate spontaneously at a rate of approximately 10^{-7} cells per generation and acquire resistance to the single agent in response to the pressures imposed by the drug treatment via a selection process (Boesen et al., 1994). In order to resolve this issue, the break-through concept of combinational therapy was introduced in the 1960s, which was based on the premise that the emergence of resistant cancers could be prevented with an alternating combination of drugs that have different targets. Nevertheless, MDR has become a persistent clinical problem to successful treatment of a majority of human cancers (Mo and Zhang, 2012). Indeed, the inevitable development of multidrug resistant cancer cells during the course of treatment is a major fundamental obstacle associated with cancer care and MDR is considered the main cause of failure in cancer therapy.

The role of ABC proteins in resistance to anticancer drugs has been known for over 30 years. It was first demonstrated in the 1970s that cancer cells become resistant to chemotherapeutic drugs by acquiring the ability to export multiple drugs by active efflux (Juliano and Ling, 1976). The single gene believed responsible for this multidrug-resistance phenotype was subsequently identified and cloned from multiple mammals as MDR1 (P-gp or ABCB1) (Chen et al., 1996). The concept of a single drug efflux

transporter (P-gp) was revised after multidrug resistance protein 1 (Mrp1) was cloned in the laboratory of Cole & Deeley in 1992 (Cole et al., 1992). A total of 15 family members can function as drug efflux pumps, and have been implicated in potentially conferring resistance to chemotherapeutic agents (Schinkel and Jonker, 2003; Huang and Sadee, 2006). Three ABC efflux pumps were primarily associated with MDR in humans and rodents; P-glycoprotein (P-gp/MDR1/ABCB1), MDR-associated protein (MRP1/ABCC1) and Breast Cancer Resistance Protein (BCRP/ABCG2) (Litman et al., 2001). These efflux pumps are expressed in many tumors, they have broad and, to a certain extent, overlapping substrate specificities, transporting the major drugs currently used in cancer chemotherapy. In recent years it has become increasingly apparent that other ABC transporters may play roles in MDR (Gillet and Gottesman, 2011). Furthermore, a novel and more active involvement of these proteins in cancer progression is emerging (Fletcher et al., 2010). There is the surprising recent discovery that MDR cancer cells can display hypersensitivity to other drugs, a phenomenon described as "collateral sensitivity" (Hall et al., 2009).

The MDR phenomenon is not only restricted to cancer but it can also hamper the chemotherapy of HIV (Lee et al., 1998; Huisman et al., 2000), epilepsy (Loscher and Potschka, 2002), bacterial (Van Bambeke et al., 2000), fungal (Wolfger et al., 2001), and parasitic diseases (Borst and Ouellette, 1995).

One option to overcome MDR is to identify or develop an **ABC inhibitor**, modulator, chemosensitizer or MDR-reversal agent (Robert and Jarry, 2003). They show the same diversity of chemical structure as substrates and appear to act in several different ways, like competitive or non-competitive inhibition. Inhibition of a multidrug ABC transporter is likely to increase the retention time and bioavailability of a therapeutic drug that is a substrate of the transporter. Ideally this would be a non-toxic compound that would inhibit the relevant ABC transporter with high potency and specificity, and which did not adversely affect the pharmacokinetics of the therapeutic drug that would be co-administered to kill the cancer cell (Falasca and Linton 2012). The development of modulators that are effective against MDR tumors, yet nontoxic, has been a major challenge during the past two decades.

P-gp was the first ABC transporter discovered 35 years ago to be involved in cancer drug resistance and consequently the search for inhibitors or reversal agents has concentrated mostly on P-gp mediated MDR. Several compounds have been generated and tested *in vitro* and clinically, and are categorized as three different generations of P-gp inhibitors (Sharom, 2008). The first generation used clinically was generally drugs already used for treatment of other medical conditions and they suffered from the dual problems of high toxicity and low efficacy. Second-generation inhibitors showed improved efficacy at low doses but serious adverse pharmacokinetic interactions were often noted in cases where both, the drug and the inhibitor were substrates for cytochrome P450. Indeed, this implied reduced clearance of the anticancer drug and led to increased toxicity. Third-generation modulators have low

toxicity and show both increased selectivity and high potency against P-gp. There is a hope that these new agents will prove more success in clinical trials for P-gp.

Only a very few of the modulators identified for ABCG2 that could be used in patients have been used in clinical trial. Given the fact that many of the compounds identified as ABCG2 inhibitors also act on P-gp, the possibility of using dual P-gp-ABCG2 modulators clinically appears to be a realistic goal. The involvement of other ABC transporters in clinical MDR has been demonstrated only more recently, and therefore the search for specific inhibitors of these transporters are still in its infancy.

Tyrosine kinase inhibitors such as sunitinib, lapatinib and tyrphostin, which are used to treat malignant cell growth and metastasis, have also been shown to interact and inhibit ABC transporters (Ozvegy-Laczka et al., 2005; Dai et al., 2008). Natural compounds such as curcumin have been also shown to modulate ABC transporter activity and improve the efficacy of antitumorals (Chearwae et al., 2004; Nabekura, 2010). A cell-based screening assay has been developed in a paclitaxel-resistant ovarian cancer cell line to identify small molecule compounds that can reverse chemoresistance (Duan et al., 2009). An uncharacterized molecule, NSC23925, was identified; it inhibits and reverses P-gp resistance but does not inhibit ABCC or ABCG2- mediated MDR (Duan et al., 2009).

Recent work has also focused on ABCC1 that has been closely linked to poor treatment response in several cancers, primarily neuroblastoma (Haber et al., 2006). Reversan, a new potent ABCC1 inhibitor, increased the efficacy of both vincristine and etoposide in murine models of neuroblastoma (Burkhart et al., 2009). In contrast to the majority of inhibitors of multidrug transporters, reversan was not toxic by itself nor did it increase the toxicity of chemotherapeutic drug exposure in mice.

The use of ABC efflux-pump modulators has led to some success in MDR reversal in preclinical studies. However there has been little impact on clinical cancer applications. Very few of the hundreds of modulators-inhibitors identified *in vitro* are suitable for clinical application in cancer treatment. Whether modulation can result in increased patient survival, remains controversial. Therefore, the discovery of novel, potent and nontoxic inhibitors as well as new treatment strategies is needed (Sharom, 2008; Falasca and Linton, 2012).

To understand the **problems to obtain successful inhibitors** it is necessary to consider that oral administered drugs must cross both the apical and basolateral membranes of the enterocyte to enter the bloodstream before meeting the membrane of a cancer cell. If the target cancer cell resides within a tissue barrier, then two further membranes of the endothelial cell must be crossed before the tumour can be targeted. The drug must hence cross three or five membranes before it can act efficaciously (Falasca and Linton, 2012).

An antitumoral drug will find a large number of ABC transporters in its way in the body; P-gp is expressed in the apical membrane of the enterocyte, in the luminal membrane of the blood--brain

barrier, and may also be present in the membrane of the cancer cell. Assuming successful trans-enterocyte transport, the drug will enter the portal vein which drains into the capillaries of the liver. The basolateral membrane of hepatocytes is rich in organic anion transport proteins (OATPs of the SLC0 family of transporters) that import drugs from the portal blood into the hepatocyte. The drug may then be delivered unadulterated to the canalicular membrane for efflux into the bile duct (usually via ABCB1 or ABCG2), or may be oxidized, primarily by cytochrome P450 enzymes (CYP450s), before efflux via ABCC1. There is compelling evidence that these uptake and efflux transporters have co-evolved overlapping substrate and inhibition specificities with the CYP450s (van Waterschoot et al., 2010).

So, while it may have seemed simple at first (if the cancer cell expresses an ABC transporter then inhibit it to gain entry of the therapeutic drug), the problem of drug delivery is far more complex. Even before the transporter content of the cancer cell is taken into account, the therapeutic drug must escape the first pass of the liver and metabolism. ABC transporter inhibitors can have a profound effect on the hepatocyte leading to unexpectedly high systemic concentrations of a therapeutic drug that, because of their cytotoxic nature, impacts on side effects.

Other problems include off-site effects, the inhibition of the normal function of ABC transporters in healthy tissue, and the need of evaluation in combinatorial therapies.

The advent of high-throughput screening technology in the pharmaceutical industry has revolutionized the approach to rational design of novel drugs. Inevitably, this approach has also had an impact in the search for novel inhibitors of ABC transporters. In future clinical trials of combinatorial therapies, it will be important to re-evaluate the safety and efficacy of the co-administered drug therapy in light of likely changes to its pharmacokinetic behavior following inhibition of drug efflux pumps.

Other strategies to treat MDR that are also being developed include nanomedicinal strategies, particularly in nanodelivery technology to overcome drug resistance. Nanoparticle-based therapeutic systems are being exploited to selectively deliver drugs to tumour cells (Dong et al., 2010). Some of these nanoparticles are currently undergoing preclinical studies *in vivo*, as well as advanced stages of clinical evaluation with promising results. Nanoparticles carrying combinations to selectively target and eliminate tumour cells and simultaneously inhibit transporters are subject to intense research effort, and likely to enter clinical trials in the near future.

At the level of gene expression of ABC transporters antisense oligonucleotides or double-stranded small interference RNAs (siRNA), to regulate mRNA levels (Yague et al., 2004), or targeting the signaling pathways that induce ABC transporter expression (Huang et al., 2007) have been used. A combined nanomedicine and siRNA approach was used recently (Susa et al., 2010) to deliver P-pg-targeted siRNA via biocompatible, lipid-modified polymeric nanoparticles. The use of specific antibodies against a variety of ABC transporters is also under preclinical evaluation.

2.4.3. Other implications in cancer

ABC transporters are known to be expressed or overexpressed in several tumour and leukaemia. Therefore, they are involved in the MDR phenomenon. Furthermore, in normal physiology, they play a crucial role in determining anticancer drug bioavailability since they influence drug absorption, distribution and elimination.

Evidence is also emerging of the role played by ABC transporters transporting bioactive signaling molecules in cancer cells such as prostaglandins, leukotrienes, sphingosine- 1-phosphate and lysophosphatidylinositol, that are implicated in cancer cell proliferation, migration, survival and tumourogenesis. This is likely to be important in disease progression (see Falasca and Linton 2012 for review).

ABC transporters also appear to be important in cancer stem cells (Gatti et al., 2011). Recent work on cancer stem cells has revealed that they are protected against widely used chemotherapeutic agents by a variety of mechanisms, such as an increased efficacy in DNA damage repair, hyperactivation of signalling pathways, low division rate, and last but not least, the expression of ABC transporter drug-efflux pumps (Dean et al., 2005). In particular, ABCG2 is frequently expressed in a number of cancer cells and appears to be a marker of cancer stem cells (Ahmed et al., 2008).

2.4.4. Mutations and diseases

ABC proteins protect the body and maintain optimal health. The importance of the physiological roles played by ABC transporters is underlined by the existence of human diseases linked to mutation or malfunction of the ABC transporter. 14 human ABC transporters have been associated with a specific disease state (Borst and Elferink, 2002). For example, members of the ABCA family extrude cholesterol (ABCA1) and phospholipids (ABCA3 and ABCA7). At least 70 mutations in ABCA1 have been linked to Tangier disease (Rust et al., 1999) and overexpression of the gene has been shown to be protective in a mouse model of Alzheimer's disease (Wahrle et al., 2008) while mutations in ABCA3 and ABCA7 are linked to Neonatal surfactant deficiency (Shulenin et al., 2004) and Sjogren syndrome (Harangi et al., 2005), respectively. Members of the ABCB subgroup secrete the short chain phospholipid, platelet-activating factor (ABCB1) and bile constituents (bile acids (ABCB11) and phosphatidylcholine (ABCB4), and their deficiency are associated with ulcerative colitis (Schwab et al., 2003) and intrahepatic cholestasis (Strautnieks et al., 1998), respectively. On the other hand, members of the ABCC subgroup flux, or efflux, chloride ions (CFTR) and bilirubin (ABCC2), and their dysfunction are linked to cystic fibrosis (Riordan et al., 1989) and Dubin Johnson syndrome (Paulusma et al., 1996), respectively. Inactivating mutations in ABCC6 produce progressive ectopic mineralization of the skin, eyes, and arteries causing pseudoxanthoma elasticum (Jansen et al., 2013).

In conclusion, mutations in many ABC transporters are at the root of genetic disorders including bleeding (ABCB7), gout (ABCG2) or cystic fibrosis (ABCC7) diseases, and eye (ABCA4) or liver (ABCB4,

ABCB11) disorders; all of which are caused by the failure to export a specific ligand across a lipid bilayer. In Table 1 some diseases associated to a particular ABC protein are listed.

Single nucleotide polymorphisms (SNP) in ABC transporters may play a role in differences in both protein expression level and transport function, which are in turn expected to affect drug absorption, distribution and elimination; therefore, varying responses to drug therapy and disease susceptibility in a population.

Table 1. Human ABC proteins and associated diseases related with the dysfunction of the correspondent transporter (Ueda, 2011).

Gene (symbol)	Phenotype, disease/function
ABCA subfamily	
ABCA1	HDL deficiency/Cholesterol and phospholipid efflux
ABCA3	Pulmonary surfactant deficiency in newborn
ABCA4 (ABCR)	Stargardt disease 1
ABCA12	Harlequin ichthyosis
ABCA13	Schizophrenia, Bipolar Disorder, Depression
ABCB subfamily	
ABCB1 (MDR1)	Multidrug resistance in cancer/Export of xenobiotics
ABCB2 (TAP1)	Behçet's disease/Antigen peptide transport into ER lumen
ABCB3 (TAP2)	Behçet's disease/Antigen peptide transport into ER lumen
ABCB4 (MDR3)	Intrahepatic cholestasis/Secretion of phosphatidylcholine into bile
ABCB7	Sideroblastic anemia/Transport of iron-sulfate complexes in mitochondria
ABCB11 (BSEP, SPGP)	Intrahepatic cholestasis/Export of bile acid
ABCC subfamily	
ABCC1 (MRP1)	Multidrug resistance in cancer/Export of xenobiotics
ABCC2 (MRP2/cMOAT)	Dubin-Johnson syndrome/Export of bilirubin
ABCC6 (MRP6)	Pseudoxanthoma elasticum
ABCC7 (CFTR)	Cystic fibrosis/Cl^- channel
ABCC8 (SUR1)	PHHI/ATP sensitive K^+ channel regulator in pancreatic β-cells
ABCD subfamily	
ABCD1 (ALDP)	Adrenoleukodystrophy/Peroxysomal transport of very long fatty acid
ABCD2 (ALDR)	Adrenoleukodystrophy/Peroxysomal transport of very long fatty acid
ABCG subfamily	
ABCG2 (BCRP)	Gout/Export of Uric acid
ABCG5	Sitosterolemia/Export of phytosterols
ABCG8	Sitosterolemia/Export of phytosterols

2.4.5. Other physiological functions

The physiological role as self-defense mechanism against xenobiotics is only one aspect of the importance of ABC transporters. They are also involved in diverse cellular processes including maintenance of osmotic homeostasis, nutrient uptake, antigen processing, cell division, bacterial immunity, pathogenesis and sporulation, cholesterol and lipid trafficking, and developmental stem cell biology (van Veen and Konings, 1998; Davidson et al., 2008; George and Jones, 2012).

Many ABC transporters have been found to be involved in lipid homeostasis. ABCB4 and ABCB11 are involved in bile formation as transporters of phospholine and bile salts. ABCA1 is a key molecule in cholesterol pathway, as is required for HDL generation, which is the only pathway

eliminating excess cholesterol from peripheral cells. ABCA2 might be involved in lipid movement, generating the myelin sheath. ABCA3 and ABCA7 are implicated in the biogenesis of pulmonary surfactant; furthermore, they are thought to transport pulmonary surfactant lipids into vesicles. ABCG5 and ABCG8 excrete plan sterols into the canalicular lumen. Finally, ABCA12 perhaps also transport lipids to form the intercellular lipid layers in skin (see Ueda, 2011 for review).

2.5. Influence in drug development: approaches to identify new drugs

The identification of membrane transporters that influence the disposition and safety of drugs is a new challenge for drug development programs, as well as for regulatory agencies worldwide. The presence of these efflux pumps is a serious problem in drug discovery, since many new drug candidates may not be able to cross the intestinal barrier, making them clinically useless for oral administration. Additionally, the presence of transporters in the blood brain barrier may reduce the accumulation of drug in the brain tissue in pharmacotherapy of brain diseases (Sharom, 2008).

Drug transporter information is becoming common in drug labels, and provides important mechanistic ADME information that is useful for patients, physicians, regulatory agencies and research scientists (Giacomini, et al., 2010). For instance, the label for mycophenolate mofetil highlights the role of ABCC2 in the hepatic disposition of mycophenolic acid; the atorvastatin label indicates the role of OATP1B1; and the varenicline label discusses the involvement of OCT2 in its interaction with other drugs. Other examples include the sitagliptin label, which has information about the role of P-gp and oAT3 in the drug's clearance; the cidofovir label, which includes information on the potential modulation of renal toxicity by coadministration of an oAT inhibitor, probenecid; and the lapatinib label, which includes information on P-gp, ABCG2 and OATPs1&2.

The ability to move a test compound rapidly into the clinic and to plan effectively for its clinical development will, in part, depends on preclinical assessments of the interaction of drug candidates with transporters. Of the numerous drug transporters identified so far, P-gp, ABCG2, OATPs, OCTs and OATs are now included to test in drug discovery screening at many pharmaceutical companies (Giacomini, et al., 2010).

2.6. Perspectives

Because defects in the function and expression of ABC proteins are related to various diseases, their functions have been extensively studied; however, the physiological functions and endogenous substrates of many ABC transporters remain elusive. One reason is that it is still difficult to purify eukaryote ABC proteins and to analyze their functions after reconstitution. Even, despite the steady

progress in research and the development of new techniques, many mechanisms of substrate recognition, functions and transport are still unclear. An enormous effort has been done to elucidate these enigmas; however, a long way is still needed to walk.

Future studies will continue to uncover additional novel substrates and inhibitors, physiological functions for ABC transporters, as well as function mechanisms, further, definition of additional roles in human disease.

3. BCRP/ABCG2

3.1. Discovery

Breast Cancer Resistance Protein (BCRP), is a protein variously named BCRP/ABCG2/MXR/ABCP ABC transporter. ABCG2 was discovered independently by three groups from both drug-selected model cell lines and human cDNA library in the late 1990s (1998). The gene responsible for the novel cross-resistance phenotype was first cloned by Doyle and colleagues (Ross's group) from a drug selected human breast cancer cell line MCF-7/ AdVp selected for its unique drug resistance in the presence of a P-gp inhibitor (verapamil); and, although no highly expressed in breast cancer, it was called BCRP for its identification from Breast Cancer Resistant Protein (Doyle et al., 1998). Simultaneously, Allikmets and colleagues (Dean's group) reported a nearly identical gene as an expressed sequence tag and named it ABCP for ATP-Binding Cassette Transporter abundantly expressed in Placenta (Allikmets et al., 1998). Shortly after, the cDNA of ABCG2 was cloned by a third independently group from a mitoxantrone selected human colon carcinoma cell line, S1-M1-80, and was designated MXR for its ability to confer cell-growth resistance to mitoxantrone (Miyake et al., 1999). Then, the Human Gene Nomenclature Committee assigned the gene the name of ABCG2, making it the second gene in the G subfamily of ABC transporters that is made up of only half transporters. Few years later the murine, porcine, rhesus and bovine orthologs of ABCG2 were identified (Allen et al., 1999; Eisenblatter et al., 2003; Ueda et al., 2005; Merino et al., 2009).

Analysis of the phylogenetic relationship of ABCG2 to other members of the ABC transporter superfamily revealed that ABCG2 is only distantly related to P-gp (ABCB1) and MRP1 (ABCC1) but is closely related to ABCG1, a human ortholog of the *Drosophila* white gene (Croop et al., 1997) (Figure 7 A).

3.1.1. ABCG family classification context

The ABCG2 transporter belongs to the ATP-binding cassette subfamily G (ABCG family), five members of this subfamily are known to exist in humans: ABCG1, ABCG2, ABCG4, ABCG5, and ABCG8 (Figure 7 A). They are mammalian homologs of the *Drosophila* white gene. The members consist of one ATP-binding cassette in the amino terminal followed by six putative transmembrane domains, and thus, they are referred to as half-sized ABC transporters. To become functionally active, they form a homodimer (ABCG1, ABCG2, and ABCG4) or a heterodimer (ABCG5 and ABCG8). ABCG members are found in multiple tissues (Figure 7 C). Except for ABCG2, the members of the ABCG family play an important role in efflux transport of cholesterol (Figure 7 B). They facilitate the efflux of excess cholesterol to high-density lipoprotein (HDL) from macrophage to the liver (ABCG1 and ABCG4), and mediate the biliary excretion of cholesterol (ABCG5 and ABCG8). In addition, ABCG5 and ABCG8 also mediate the biliary excretion of sterols, and their intestinal efflux to prevent their accumulation.

Mutations causing a loss of function of ABCG5 or ABCG8 are associated with a rare autosomal-recessive lipid metabolism disorder, sitosterolemia, characterized by accumulation of sterols (see Kusuhara and Sugiyama, 2007; and Woodward et al., 2011 for reviews). To date no functional mutations in ABCG1 and ABCG4 have been linked to any monogenic human disease, although ABCG1 has been implicated in cardiovascular disease, obesity and diabetes (see Tarr et al., 2009 for review).

A

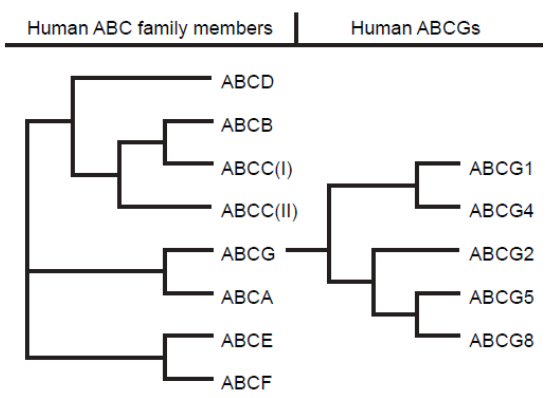

B

Gene name	Aliases	Substrates
ABCG1	ABC8	Cholesterol
ABCG2	BCRP, MXR, ABCP	Very broad
ABCG4		Cholesterol
ABCG5 ABCG8	Sterolin-1 Sterolin-2	Cholesterol Phytosterols, shellfish sterols

C

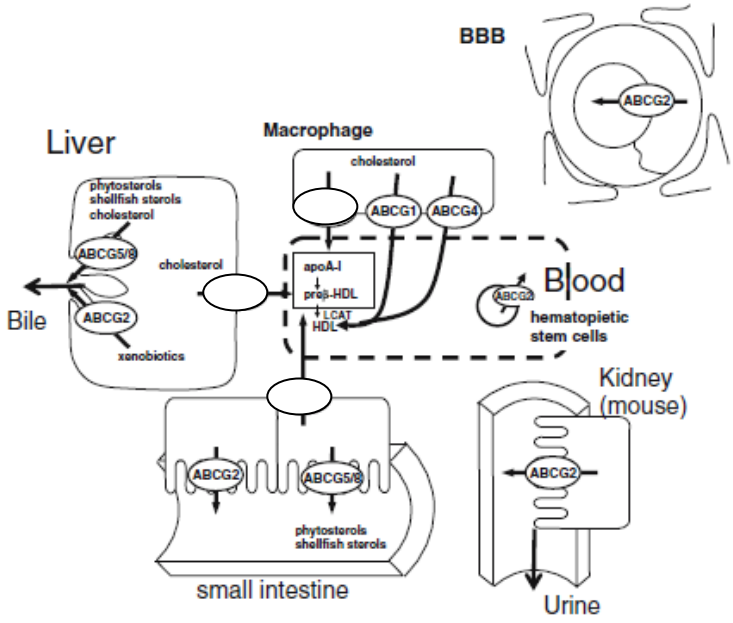

Figure 7. **A**. Phylogenetic tree of all human ABC genes and specifically the ABCG subgroup of genes (Woodward et al., 2011). **B**. Names and substrates of the ABCG family (Kusuhara and Sugiyama, 2007). **C**. Schematic diagram of expression localization of the members of ABCG family (Kusuhara and Sugiyama, 2007).

3.2. Structure, membrane topology and mechanism of transport

The human ABCG2 gene lengths over 66 kb and is constituted by 16 exons and 15 introns. The resulting protein is 655 amino acid residues long, a 72 kDa protein on an SDS gel under reducing conditions (Bailey-Dell et al., 2001). ABCG2 gene is localized in chromosome 4 between 4q21-4q22 (Knutsen et al., 2000).

The human ABCG2 protein is considered a **"half-transporter"** consisting of two domains: amino-terminal ATP-binding domain (NBD) and carboxyl-terminal transmembrane domain (TMD). Little is known about the structure of ABCG2, although the membrane topology of ABCG2 has recently been determined experimentally. Knowledge about membrane topology of ABCG2 is important for understanding the structural basis of ABCG2 action and for homology modeling of the transporter. The topology analysis suggested that the TMD of ABCG2 consists of 6 putative transmembrane (TM) α-helices segments (Wang et al., 2008).

As all other ABC transporters, ABCG2 contains the characteristic motifs involved in the binding of ATP at the interface of two cytosolic nucleotide-binding domains (NBDs): the Walker-A and -B motifs, and the Q- and H-loops, as well as A-loop, belong to the cis-NBD; whereas the ABC signature is located on the trans-NBD (Rosenberg et al., 2010). In addition, the D-loop is involved in protein–protein interactions between the two monomers of the dimer. Each NBD is fused to a transmembrane domain (TMD) containing six alpha-helical loops connected by two intracellular and three extracellular loops (Figure 8); they are involved in drug binding and translocation.

It has been widely accepted that a functional ABC transporter requires two TMDs and two NBDs which form a central substrate translocation pathway. Thus, because of its half size nature, ABCG2 has been thought to function as an active transporter as a homo-**dimer**, with evidence provided in several earlier studies (Kage et al., 2002; Litman et al., 2002; Bhatia et al., 2005). The prior study by Kage et al. (2002) revealed that ABCG2 migrated as a 70 kDa band on SDS-PAGE under reducing condition, but as a 140 kDa complex in the absence of reducing agents, suggesting that ABCG2 could form a homodimer bridged by disulfide bonds. Litman et al. (2002) also observed a molecular mass shift of ABCG2 from 72 kDa to 180 kDa after treatment with chemical crosslinking agents. Bhatia et al. (2005) showed that chimeric fusion proteins containing two ABCG2 monomers fused with or without a linker peptide were properly targeted to the plasma membrane and retained drug transport activity.

However, emerging evidences have suggested that ABCG2 may exist as a higher order of homo-oligomer on plasma membranes. Using sucrose density gradient sedimentation and non-denaturing gel electrophoresis, Xu et al. (2004) provided evidence of ABCG2 oligomer formation. Likewise, the electron microscopy (EM) analysis of ABCG2 protein particles in detergent solutions identified an octameric state that was organized as a tetramer of dimmers (McDevitt et al., 2006). The recent cryo-EM analysis of 2D crystals revealed that ABCG2 could form a tetrameric complex (two ABCG2 dimers) (Rosenberg et al.,

2010). Recently, dimer/oligomer formation of ABCG2 was determined using fluorescence resonance energy transfer (FRET) microscopy (Ni et al., 2010b). At present, the role of oligomerization in ABCG2 function is not yet clear and the physiological significance of such high molecular-weight oligomers is still questionable (see Ni et al., 2010a and Mo et al., 2012 for reviews).

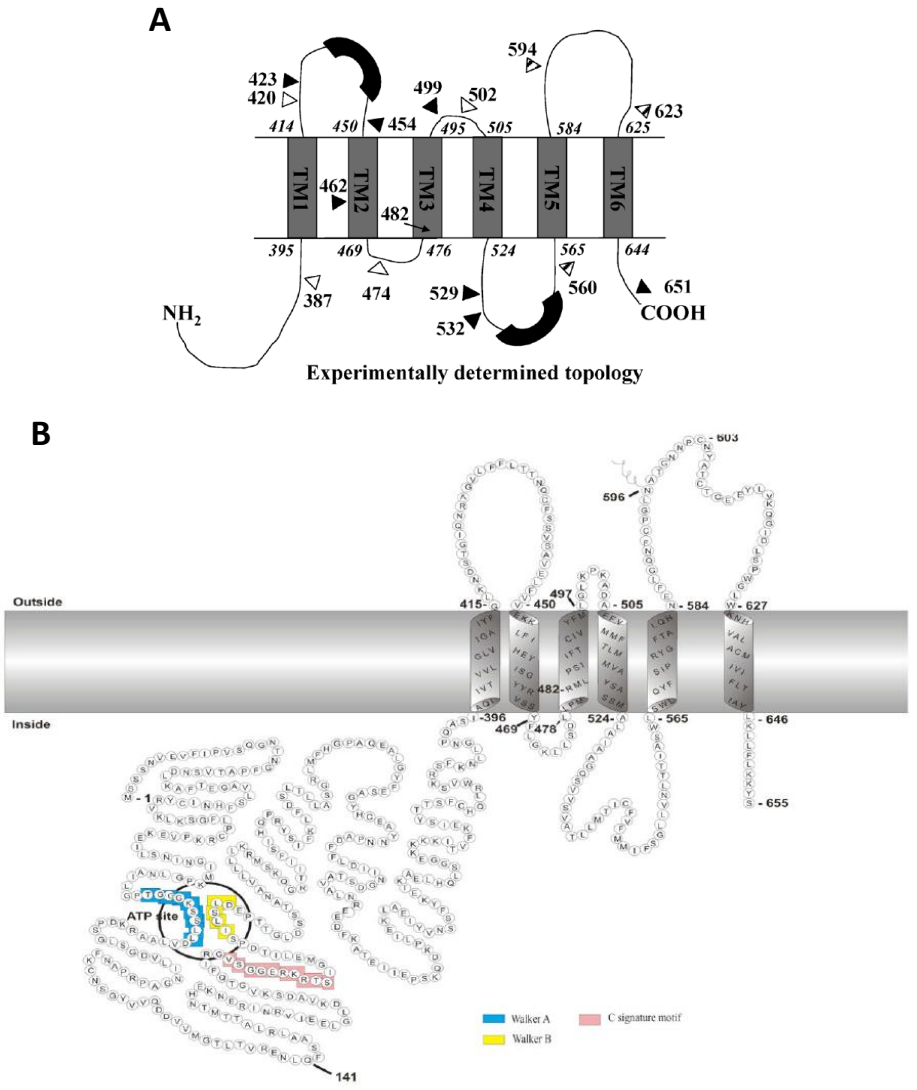

Figure 8. Topology model representations of ABCG2 deduced from experimental results. **A.** First homology model published for ABCG2. The transmembrane domains (TM) and different extra-membrane loops are illustrated. Triangles indicate approximate positions of the hemagglutinin tag insertions performed in the study (Wang et al., 2008). **B**. Schematic illustration of the membrane topology of ABCG2 based on the experimentally determined membrane topology of ABCG2. The ATP site (the Walker A (blue) and Walker B (yellow) motifs), and the C signature (pink) motif are indicated (Ni et al., 2010a). Numbers indicate the aminoacid number.

Taken together, despite extensive studies, it is still not clear whether the minimal functional unit of ABCG2 in the plasma membrane is a homodimer or a homooligomer, neither the effect of the dimeric or oligomeric state of ABCG2 on drug binding and transport. This requires further investigation into the mechanisms by which ABCG2 forms homodimers or homooligomers.

Although there were major differences between the experimental and the computer predicted topology models (Figure 8 A), Rosenberg et al. (2010) demonstrated that, except for two regions, the overall topology structure of ABCG2 deduced from the experimental data is surprisingly similar to that of P-gp observed in its X-ray structure by Aller et al. (2009). The amino acid identity between the TMDs of ABCG2 and the first half of P-gp is approximately 18% (Rosenberg et al., 2010).

At present, there are only two structural studies for ABCG2. McDevitt et al. (2006) reported the first electron microscopy (EM) analysis of single protein particles of ABCG2 purified from insect cells. A 3D structure was reconstructed at a low resolution; only the overall shape and oligomeric state of the ABCG2 complex could be visualized. Most recently, Rosenberg et al. (2010) determined the first projection structures of ABCG2 purified from Pichia pastoris by cryo-EM of well-diffracting 2D crystals at medium resolution. The dimension of the asymmetric unit cell of the crystals indicated that there were 4 ABCG2 monomers (two ABCG2 dimers) in one unit cell, indicating the existence of an oligomeric complex of ABCG2. Importantly, ABCG2 showed significant conformational changes in 2-D crystals grown in the absence and presence of mitoxantrone; ABCG2 appears to have a more compact configuration in the presence of mitoxantrone. This was the first experimental evidence showing substrate binding induced conformational changes in ABCG2, which has implications for transport mechanism of the transporter. The number of TM α-helices, and their orientations in the membrane was not resolved; it will require the calculation of a 3D map at a high resolution.

To further illustrate drug binding and transport mechanism of ABCG2, **homology models** have been developed in different laboratories. The first model of ABCG2 was constructed using the crystal structure of MsbA from Vibrio cholera (VcMsbA) as the template for TM segments (Li et al., 2007) (Figure 9 C). Two additional models of ABCG2 were predicted based on the crystal structure of the bacterial exporter Sav1866 (Dawson et al., 2006) as the template (Hazai and Bikadi, 2008; Polgar et al., 2010). These studies were based on the computer-predicted ABCG2 topology and, differed significantly from the experimental structure. Rosenberg et al. (2010) developed homology models based on the experimental topology structure of ABCG2 using as well the crystal structures of atomic published templates of MsbA (Ward et al., 2007), P-gp (Aller et al., 2009), Sav1866 (Dawson et al., 2006) and MalK (Chen et al., 2003) transporters (Figure 9 A and B). Several features concerning ABCG2 structure were elucidated by these models (see Ni et al., 2010a for review).

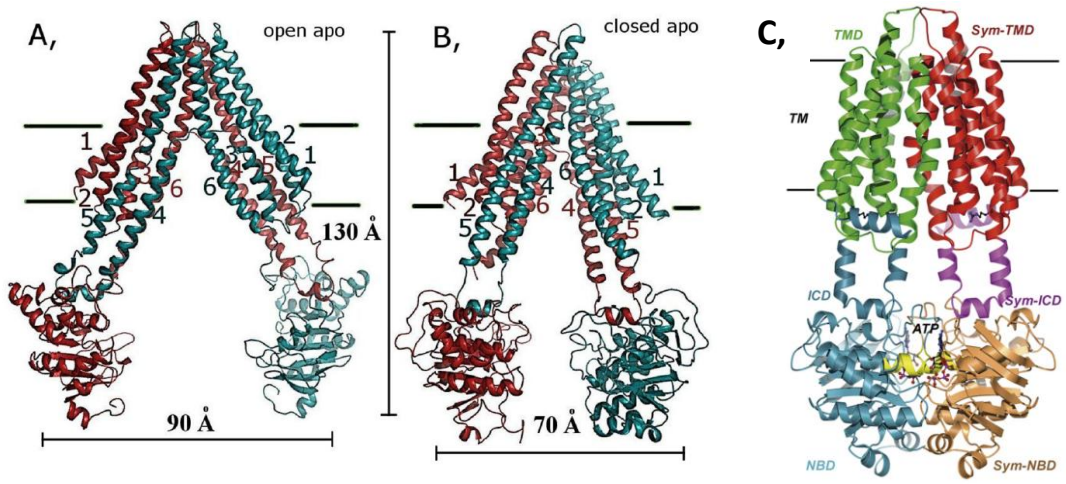

Figure 9. **A.** Homology models of ABCG2. Open (**A**) and closed (**B**) conformations, representing a substrate-free state and a substrate-bound state, respectively (Rosenberg et al., 2010). The TM α-helices of each ABCG2 monomer are labeled with numbers 1 – 6 in different colors. The dimensions of one ABCG2 monomer are presented. **C**. Structure diagram of the dimeric model of ABCG2 (Li et al., 2007). The putative boundaries of the lipid bilayer are indicated with straight lines.

To prove drug **binding** in ABCG2, direct drug binding interactions with ABCG2 have been investigated using photo-affinity labeling and mass spectrometryanalysis (Alqawi et al., 2004; Ejendal et al., 2006; McDevitt et al., 2006). The prazosin analogue [125I]-IAAP is the photo-active compound that is most frequently used, also [125I]-IAA-rhodamine 123 and [3H]-azidopine. At present, the residues potentially involved in interactions of the photo-active substrates with ABCG2 have not been identified. In addition, there is only a few equilibrium or kinetic binding studies for substrates or inhibitors of ABCG2 (Pozza et al., 2006; McDevitt et al., 2008).

Earlier studies suggested multiple **binding sites** in ABCG2 that may not or only partially overlap (Nakanishi et al., 2003; Xia at al., 2005). Existence of two or three distinct but symmetrical binding sites has been suggested for the wild-type Arg482 ABCG2 and the R482G mutant isoform, respectively (Ejendal and Hrycyna, 2005; Clark et al., 2006). However, more recent studies propose two single binging sites for ABCG2 (Glavinas et al., 2007). Even, it was hypothesized two binging sites for each substrate or inhibitor of ABCG2, one high affinity site (*K*m in a low μM range) and one low affinity site (Pozza et al., 2006).

Although the locations of these binding sites are not yet clear (Xia at al., 2005), substrate-binding sites are likely located in the central cavity surrounded by TM α-helices (Rosenberg et al., 2010). Furthermore, these binding sites are possibly hydrophobic (Coburger et al., 2010). It has been seen from homology models that the entry of the open nucleotide-free structure (Figure 9 B) is large enough (70 Å) compared to that for P-gp (30 Å) (Aller et al., 2009) to allow access of a bulky of ABCG2 big or charged

substrates from either the inner leaflet of the plasma membrane or cytoplasm (Rosenberg et al., 2010). It is widely extended the idea that ABCG2 take compounds directly from the aqueous phase in the cytoplasm (e.g. Sarkadi et al., 2006). Nonetheless, some current authors have proposed that as in the case of P-gp, the lipid membrane is an important part in the efflux function of ABCG2 (Sharom, 2008). Hence, passive membrane partitioning of the compound significantly influences its access and binding to the transporter; in a word: drug-transporter interaction (Matsson et al., 2007). Accordingly, compounds would accumulate in the plasma membrane before being taken by ABCG2, meaning that plasma membrane plays a major role in the presentation of drugs to the transporter. All these features are in agreement with a two-step interaction model (proposed initially for P-gp by Sauna and Ambudkar, 2001), i.e. partitioning of drug from water into the membrane, and subsequent transfer of drug from the lipid to the binding pocket of the ABCG2 transporter (Figure 10) (Matsson et al., 2007; Sharom, 2008). In this two-step mechanism the drug's capacity to insert into the cell membrane and to interact with the binding site of the transporter are important. Therefore, ABCG2 has been proposed to work as a "flipase", where compounds are "flipped" from the inner to the outer leaflet of the bilayer, from which they can rapidly partition into the aqueous phase (Sharom, 2008), or a floppase (Homolya et al., 2011). It was also said that hydrogen bonds, nitrogen atoms and interactions involving π-electron systems, such as π - π and π -cation interactions, play a role in binding to ABCG2 (Matsson et al., 2007).

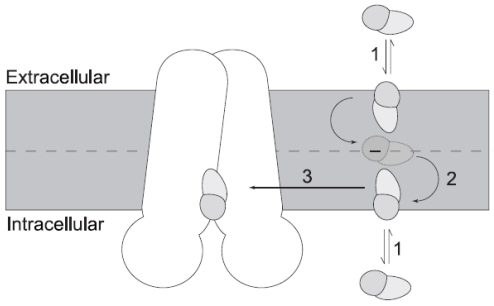

Figure 10. A proposed two-step model for drug binding to ABCG2. The schematic illustration shows the efflux transporter ABCG2 inserted in the plasma membrane. An extracellularly applied compound needs to partition to the plasma membrane (1). After flip-flop from the outer to the inner membrane leaflet (2) and lateral diffusion in the membrane, the compound can bind to the transporter (3) (Matsson et al., 2007).

Recently, it was demonstrated that mitoxantrone has a high rate of passive membrane partitioning and is expelled by the ABCG2 multidrug transporter directly from the plasma membrane instead than from the cytoplasma (Homolya et al., 2011), confirming the importance of membrane partitioning and the two-step model for ABCG2.

Despite this last finding, up to date, all these statements are more closely to speculations; direct demonstrable experimental results have not yet been presented. Additionally, how ATP binding and/or hydrolysis is coupled with drug transport in ABCG2 is not known. Only one study showed that ATP binding alone could convert the drug binding site from a high to a low affinity state (McDevitt et al., 2008), suggesting that it is ATP binding, not ATP hydrolysis, that appears to initiate drug transport by ABCG2.

All ABC transporters display constitutive **ATPase activity**. The basal ATPase activity is modulated by compounds acting by a biphasic pattern, stimulating activity at low concentrations and inhibiting at higher concentrations, whereas others show only activation or inhibition (Doige et al., 1992; Garrigo et al., 1997; Litman et al., 1997). Like other multidrug transporters, ABCG2 shows basal and drug-induced ATPase activity (Krishnamurthy and Schuetz, 2006). In fact, ATP hydrolysis (ATPase activity) of ABCG2 has been reported in numerous studies (McDevitt et al., 2009). ATP hydrolysis by ABCG2 was confirmed by photo-labeling of ABCG2 under hydrolytic conditions with 8-azido ATP in the presence of vanadate and Mg2+ or Co2+ (Ozvegy et al., 2002; Mao et al., 2004). Further investigations are needed for a quantitative analysis of the ABCG2 ATPase activity. To the present, most of the experimental ATPase activity searches for ABCG2 have been concentrated exclusively to elucidate whether a tested compound is a substrate and/or an inhibitor of the transporter.

Membrane composition and packing density of plasma vesicle membranes have been demonstrated to be important in drug ATPase activity stimulation for P-gp (Aänismaa et al., 2008). In the case of ABCG2, it was suggested that the different behavior of the vesicle membranes from insect cells Sf9 and from mammalian cells was due to the membrane composition (Glavinas et al, 2007). In fact, it was found that lipid membrane environment affects transport kinetics of ABCG2 because differences in cholesterol composition affect ATPase transport in these membranes (Pal et al., 2007). The addition of cholesterol could significantly potentiate ATPase activity of ABCG2 and its substrate stimulation characteristics (Pal et al., 2007). Depletion of cholesterol levels lowers ABCG2 ATPase activity but did not alter cell viability or transporter subcellular localization or expression (Storch et al., 2007). Therefore, although ABCG2 is expressed at appreciable level in Sf9 with high ATPase activity, a main problem is due to its dependence on cholesterol (Pal et al., 2007; Telbisz et al., 2007) which is nearly absent in insect cells (Nicolle et al., 2009).

3.3. Regulation of ABCG2 expression

The expression of ABCG2 in normal and cancer cells appears to be regulated at different levels including gene amplification, epigenetic modifications (by de/methylation or acetylation) and transcriptional and post-transcriptional regulation by microRNAs.

ABCG2 gene consists of 16 exons, and a putative TATA less promoter has been suggested upstream of exon 1, where the binding motifs of estrogen receptor (ERα) and hypoxia-inducible factor 1 (HIF1) are located (Kusuhara et al., 2007). Few data are available regarding molecular mechanisms controlling ABCG2 expression. Krishnamurthy and colleagues were the first to demonstrate that hypoxia regulates ABCG2 expression (Krishnamurthy et al., 2004). ABCG2 may be controlled at the promoter level by sex hormones as estrogen, progesterone, and testosterone (Imai et al., 2005; Wang et al., 2006). ABCG2 expression is strongly induced in the mammary gland during lactation (Jonker et al., 2005). ABCG2 expression in the ducts of breast lobules appears to be hormonally regulated by down regulation by either 17beta-estradiol or dexamethasone. Additionally, there is up regulation by progesterone in placenta. ABCG2 expression is minimally affected by liver X receptor (LXR), pregnance X receptor (PXR) or constitutively active receptor (CAR) activators (Krishnamurthy et al., 2006). Thus, ABCG2 is not regulated by nuclear receptors that upregulate genes involved in cellular detoxification. Transcription factors shown to be involved in regulating ABCG2 expression include estrogen receptor alpha (ERα), hypoxia-inducible factor 1 (HIF-1), peroxisome proliferator-activated receptor gamma (PPARγ), progesterone receptor (PGR) and aryl hydrocarbon receptor (AHR) (see Nakanishi and Ross 2012 and Mo et al., 2012 for review).

3.4. Distribution

At the initial report of Doyle and colleagues, authors noted the highest level of human ABCG2 expression in the placenta, with lower levels in the brain, prostate, small intestine, testis, ovary, colon and liver (Doyle et al., 1998). Soon after, Maliepaard et al. (2001) localized expression of human ABCG2 mRNA prominently in placental syncytiotrophoblasts, epithelium of small intestine and colon, liver canalicular membranes, and ducts and lobules of mammary tissue; it is also expressed in cardiac muscle, ovary, venous endothelium, and in capillaries but only sporadic in arterioles. ABCG2 expression was not significant in blood cells as leukocytes, erythrocytes and platelets (Maliepaard et al., 2001). ABCG2 is expressed in alveolar pneumocytes, sebaceous glands, islet and acinar cells of the pancreas, interstitial cells of testes, zona reticularis of the adrenal gland, cortical tubules of the kidney, spinal cord, endocervical cells of uterus, squamous epithelium of cervix, and prostate epithelium (Aust et al., 2004; Fetsch et al., 2006). ABCG2 is localized in other tissues as thyroid, parathyroid, heart, spleen and thymus. ABCG2 is prominently expressed in stem cells from various sources, including bone marrow and skeletal muscle (Zhou et al., 2001). The ABCG2 tissue location and a schematic overview of ABCG2 through the body are represented in Table 2 and Figure 11.

Within the human gastrointestinal tract, ABCG2 mRNA expression was maximal in the human duodenum and decreased continuously down to the rectum (terminal ileum 93.7%, ascending colon 75.8%, transverse colon 66.6%, descending colon 62.8% and sigmoid colon 50.1%, as compared with the

level in duodenum) (Gutmann et al., 2005). In brain capillaries and choroids plexus there is higher expression of ABCG2 compared to P-gp or MRP1 (Tanaka et al., 2005).

Table 2. The cellular localization (apical or basolateral) of ABCG2 in a particular tissue (reviewed by Klaassen and Aleksunes, 2010).

Cellular Localization	Tissue	Cell Types	References
Bcrp			
Apical	Liver	Hepatocytes	Maliepaard et al., 2001; Jonker et al., 2002
Apical	Gallbladder	Epithelium	Aust et al., 2004
Apical	Kidney	Proximal tubule cells	Jonker et al., 2002
Apical	Small Intestine	Enterocytes	Maliepaard et al., 2001; Jonker et al., 2002
Apical	Brain	Brain capillaries, choroid plexus	Cooray et al., 2002; Hori et al., 2004; Lee et al., 2005b
Apical	Fetal membranes	Visceral yolk sac, amnion	Aleksunes et al., 2008b; Yeboah et al., 2008
Apical/Basolateral	Placenta	Syncytiotrophoblasts	Maliepaard et al., 2001; Jonker et al., 2002
Apical	Testes	Endothelial cells	Bart et al., 2004; Enokizono et al., 2007
Apical	Epididymis	Body, head	Enokizono et al., 2007
Apical	Mammary gland	Epithelia from lactating gland	Maliepaard et al., 2001; Pulido et al., 2006; Wang et al., 2008b
Apical	Eye	Retinal capillary endothelial cells	Asashima et al., 2006
Apical	Lung	Epithelium, glands, endothelial cells	Scheffer et al., 2002c
N.D.	Heart	Capillary endothelial cells and arterioles	Meissner et al., 2006

N.D, not determined.

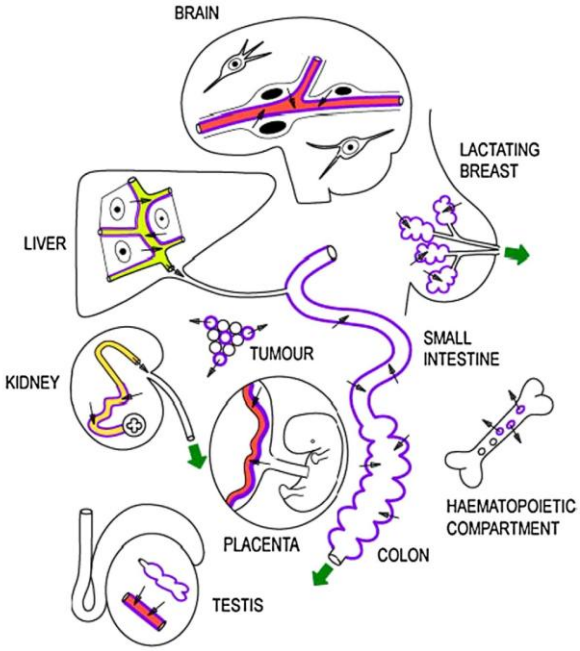

Figure 11. Schematic overview of ABCG2 expression throughout the body. Small arrows indicate the direction of ABCG2-mediated transport. Wide arrows indicate net body excretion of ABCG2 substrates. Expression of ABCG2 in endothelial cells of blood capillaries and veins, or in "side population" cells throughout many tissues in the body is not indicated (Vlaming et al., 2009).

ABCG2 is predominantly localized to the plasma membrane and almost exclusively expressed on the apical surface of polarized cells as enterocytes or hepatocytes or breast (Maliepaard et al., 2001). ABCG2 is unique among the ABC half-transporters in its localization to the plasma membrane rather than to an intracellular membrane of a subcellular organelle.

Concerning differences in ABCG2 distribution among species, a similar distribution of mouse and rat ABCG2 expression has been reported with high ABCG2 mRNA in rodent kidneys, liver, small intestine, placenta and testes; the highest expression was found in kidney for both species (Tanaka et al., 2005). In mice, the expression of ABCG2 in the brain capillary endothelial cells is low. In the kidney, ABCG2 expression is high in mice, but smaller in humans (Maliepaard et al., 2001; Xia et al., 2005).

There is also a sex difference among species. Hepatic ABCG2 mRNA is higher in male mice and humans, respectively, compared with female counterparts; as a result, ABCG2 substrates as nitrofurantoin or topotecan exhibit greater biliary excretion in male wild-type mice relative to female mice (Merino et al., 2005). Male-predominant expression of ABCG2 was observed in rat kidney and mouse liver; male-predominant expression of ABCG2 in rat kidney appears to be due to the suppressive effect of estradiol, and male-predominant expression of ABCG2 in mouse liver appears to be due to the inductive effect of testosterone (Tanaka et al., 2005).

Many of above mentioned tissues harbor secretory or barrier function including hepatocytes, proximal tubules, enterocytes, trophoblasts, placenta, and mammary glands as well as brain and retinal capillary endothelial cells (Maliepaard et al., 2001; Cooray et al., 2002; Jonker et al., 2002; Asashima et al., 2006; Pulido et al., 2006; Aleksunes et al., 2008). This specific tissue distribution profile of ABCG2 is closely related to the physiological role of human ABCG2 suggesting a protective role (see below).

3.5. Function

3.5.1. Protection limiting substrate penetration and tissue distribution

The primary biological and physiological role of ABCG2 is the protection against xenobiotic absorption and towards toxic metabolites excretion preventing the accumulation of both extracellular and intracellular toxins in cells, organs, and in the body as a whole. ABCG2 is also responsible for the efflux of sulfate and glucuronide conjugates of xenobiotics and hormones, which are mostly products of phase II metabolism (Dietrich et al., 2003; Álvarez et al., 2011), suggesting that ABCG2 has a major role in extruding toxic metabolites via the biliary pathway.

The expression of ABCG2 in the gastrointestinal tract, and also in the liver supports the protective role of ABCG2 against xenobiotic absorption and towards toxic metabolite excretion. Indeed, the primary mechanism by which ABCG2 reduces oral drug levels could be by either reducing **intestinal** uptake or mediating **hepatobiliary** drug excretion (Schnepf and Zolk, 2013). Altered oral

pharmacokinetics with increased plasma concentrations in Abcg2 knockout animals compared with their wild-type controls were reported for several compounds, such as trans-resveratrol conjugates, axitinib, methotrexate, topotecan, the investigational cyclin-dependent/Aurora kinase inhibitor JNJ-7706621, sulfasalazine, ciprofloxacin, nitrofurantoin, 2-amino-1-methyl-6-phenylimidazo[4,5-b] pyridine (PhIP), aflatoxin B1, 2-amino-3- ethylimidazo[4,5-f]quinoline and 3-amino-1,4-dimethyl-5H-pyrido[3,4-b]indole (see Schnepf and Zolk, 2013 for review).

The observation that both oral and intravenous AUCs similarly increased in knockout and wild-type mice suggests that Abcg2 may have a limited effect on intestinal methotrexate uptake but may primarily influence biliary methotrexate excretion (Vlaming et al., 2011). However, to estimate the relative contribution of intestinal versus hepatic Abcg2 to the bioavailability of ABCG2 substrates is very hard. This is also the case of the antitumoral topotecan, where increased oral bioavailability of topotecan in knockout mice (Jonker et al., 2002; Kruijtzer et al, 2002) could be due to decreased hepatobiliary excretion or limitation of uptake at the intestinal barrier.

Since a high level of Abcg2 is found in the **renal** proximal tubules in rodents, it is possible that ABCG2 is also involved in the tubular secretion of organic compounds. However, compared with the role in the intestine and the liver, much less is known about the role of renal ABCG2. It was first demonstrated that ABCG2 can play a role in the renal excretion of organic sulfates (Mizuno et al., 2004). However, renal elimination of another ABCG2 substrate, 4 MUS, which is predominantly excreted in the urine, was not affected in knockout mice. A more recent study assessed the effect of ABCG2 on the excretion of the ABCG2 substrate drugs nitrofurantoin and sulfasalazine (Huang et al., 2012). A possible role of ABCG2 in sulfasalazine urinary excretion was reported in rats. In contrast, urinary excretion of nitrofurantoin, which is eliminated primarily through the kidneys, was unaffected in knockout rats. These findings make clear that for several ABCG2 substrates, such as 4 MUS or nitrofurantoins, overlapping renal secretion pathways exist compensating for the ABCG2 deletion.

Dated today, two dozens of clinical studies have been done to test the *in vivo* role of ABCG2 in human pharmacokinetics regarding the influence of the gastrointestinal, hepatobiliary and renal systems (see Schnepf and Zolk, 2013 for review).

The **Blood Brain Barrier** (BBB) is formed by brain microvascular endothelial cells. In addition to the highly developed tight junctions between adjacent cells, the BBB expresses multiple xenobiotic transporters characterized by broad substrate specificities, such as ABCG2. BBB serves as a crucial barrier restricting drug access into the brain. It was not straightforward to unequivocally establish a functional role of ABCG2 at the BBB (Jonker et al., 2002; Zhou et al., 2002, Vlaming et al., 2009). This is illustrated by a number of studies, with sometimes contradicting outcomes. Cisternino et al. (2004) stated that Abcg2, and not P-gp, restricts the uptake of prazosin and mitoxantrone into the brain. Nonetheless, no difference in the brain distribution of mitoxantrone (Lee et al., 2005) and other ABCG2 substrates, such as pitavastatin and fluoroquinolones, was found between wild-type and knockout mice

(Hirano et al., 2005; Ando et al., 2007). The functional role of ABCG2 in the BBB was also demonstrated by the study of Breedveld et al. (2005), where imatinib entry into the brain was restricted by ABCG2, although subsequent analysis showed that P-gp plays a significant role in limiting brain penetration of imatinib rather than ABCG2 (Bihorel et al., 2007). However, they showed that when P-gp is saturated the contribution of Abcg2 in reducing imatinib passage across the BBB becomes detectable. Enokizono et al. (2008) demonstrated the same phenomenon for PhiP and prazosin.

In subsequent studies, the relevance of P-gp and/or ABCG2 to the brain efflux of a variety of drugs, including several tyrosine kinase inhibitors, anti-HIV agents and antiepileptic drugs was demonstrated. Both transporters appeared to contribute similarly to the efflux of some drugs; however, in other cases, the brain penetration of the drug appeared to be mainly limited by one or the other transporter (see Schnepf and Zolk, 2013 for review). Collectively, the data suggest the cooperation of ABCG2 and P-gp at the BBB, the remaining transporter can largely compensate for the loss of function of the deleted one, in the case of single knockout mice.

ABCG2 protein is abundantly expressed in the **placenta** and fetal membranes in humans and rodents (Maliepaard et al., 2001; Aleksunes et al., 2008). The expression of Abcg2 changes with gestational age; however, the physiological function of this variable expression during gestation is not known (Mao, 2008). ABCG2 in the placenta serves to protect the human fetus by causing the efflux of toxins from the placenta back into the maternal circulation. This was first documented after topotecan accumulated in murine Abcg2-knockout fetuses to a greater extent than in wild-type fetuses (Jonker et al., 2000). Glyburide and nitrofurantoin are routinely prescribed for pregnant patients for the treatment of gestational diabetes and urinary tract infections, respectively. Thus, investigators have questioned if the fetus maintains very low concentrations of these drugs. Inhibition of ABCG2 disrupts glyburide efflux (Gedeon et al., 2008); in support of this, glyburide concentrations are higher in Abcg2-knockout fetuses compared with wild type (Zhou et al., 2008). Likewise, the concentration of the antibiotic nitrofurantoin is 5-fold higher in fetuses from Abcg2-knockout mice (Zhang et al., 2007). These findings indicate the protection of the fetus via ABCG2. It is noteworthy that a human ABCG2 variant (Q141K) is associated with reduced ABCG2 protein accumulation in placenta (Kobayashi et al., 2005).

The ability of the **mammary gland** to concentrate pharmaceuticals such as nitrofurantoin and cimetidine in human breast milk was recognized (Oo et al., 1995; Gerk et al., 2001). More recently, it was hypothesized that drug transporters may be important in the active transport of chemicals into breast milk. Studies have shown that ABCG2 is localized to the apical epithelial surface of the mammary glands of humans, sheep, cows, goats and rats (Maliepaard et al., 2001; Pulido et al., 2006; Wang et al., 2008; Lindner et al., 2013). ABCG2 expression is strongly induced during late pregnancy and lactation in mammary gland, but not in virgin or non lactating mammary gland epithelia of mice, cows and humans (Jonker et al., 2005). Pharmacological inhibition of ABCG2 using GF120918 (note that P-gp is not expressed in lactating mammary glands, therefore, not inhibited by GF120918) blocked excretion of

nitrofurantoin into milk of lactating rats (Wang et al., 2008). Moreover, the milk-to plasma ratio of nitrofurantoin was 80-fold higher in wildtype mice than in Abcg2-deficient mice (Merino et al., 2005b). Likewise, ABCG2 transports fluoroquinolone antibiotics such as ciprofloxacin and danofloxacin at the breast (Merino et al., 2006; Real et al., 2011). Endogenous molecules and vitamins such riboflavin (vit B2), biotin (vit H), but not folic acid (B9), vit K1 or Vit B12 (van Herwaarden et al., 2007) are examples of vitamins excreted to milk by ABCG2. In addition to excrete pharmaceuticals and nutrients, ABCG2 also transfers dietary carcinogens (aflatoxin B1 and other heterocyclic amines) into breast milk (Jonker et al., 2005; van Herwaarden et al., 2006). ABCG2 function in the mammary glands is somewhat of a double-edged sword; it prevents xenobiotic accumulation in the mother and simultaneously delivers potentially toxic chemicals to newborns. The paradox function of ABCG2 in mammary gland, because not only vitamins but also noxious xenobiotics are pumped into milk, has been extensively discussed (see van Herwaarden et al., 2006 and Vlaming et al., 2009, as examples); nonetheless a clear conclusion of why ABCG2 is induced in the lactating mammary gland has yet to be elucidated.

ABCG2 efficiently restricts the accumulation of various pharmaceuticals (including dantrolene, triamterene, and prazosin) and other compounds such PhiP, and the phytoestrogens daidzein, genistein, cumestrol within the **testes** (Enokizono et al., 2007 and 2008). These data indicate a prominent role of ABCG2 in reducing xenobiotic entry across the blood-testes barrier. The physiological function of Abcg2 at the blood-testis barriers might be particularly important with respect to (phyto)estrogens, many of which have been identified as Abcg2 substrates (Enokizono et al., 2007), because these compounds are known to influence reproductive functions, e.g. reducing testicular weight and sperm count (Adeoya-Osiguwa et al., 2003). A physiological function cannot be excluded, but male fertility (and hence sperm function) in knockout mice does not seem to be compromised (Jonker et al., 2002; Zhou et al., 2002).

Using single- and double-knockout mice, it was demonstrated that Abcg2 and P-gp account for the side population phenotype of **stem cells** of mammary glands (Jonker et al., 2005b). On the other hand, only Abcg2 conferred the side population phenotype in bone marrow and skeletal muscle (Zhou et al., 2002; Jonker et al., 2005b). In addition, Abcg2-knockout hematopoietic cells are more sensitive to mitoxantrone in drug-treated transplanted mice (Zhou et al., 2002). Taken together, these findings suggest that ABCG2 serves to protect stem cells against xenobiotic toxicity. There is a possible dual role of ABCG2 in maintaining human pluripotent stem cells in an undifferentiated state fluxing a compound important for differentiation and in protecting these stem cells from xenobiotics or other toxins (Zhou et al., 2001; Bunting, 2002). Based on similar concept, ABCG2 has also been proposed to play a role in protecting putative cancer stem cells (see Mo et al., 2012 for review). However, in some studies it was reported that cancer cells with or without ABCG2 expression are equally tumorigenic (Raaijmakers et al., 2005) and, thus, raising a question whether ABCG2 plays any role in the stemness of cancer cells. Further studies are clearly needed to elucidate the expression and role of ABCG2 in putative cancer stem cells.

ABCG2 seems to be implicated in **skin photosensitivity protection**. Porphyrins have very important roles in biological processes, nevertheless, they are highly efficient photosensitizers and an excess can cause severe cellular damage (Krishnamurthy et al., 2007), therefore their synthesis and distribution must be carefully regulated. Abcg2 knockout mice are generally healthy but can develop phototoxic lesions on light-exposed skin after feeding with diets containing a high percentage of alfalfa due to accumulation of pheophorbide a (a phototoxic porphyrin catabolite of chlorophyll) (Jonker et al., 2002). A similar phototoxicity can be observed in Abcg2-knockout mice administering pheophorbide a (Jonker et al., 2002). Furthermore, a heme precursor, protoporphyrin IX (PPIX), accumulates in the plasma and erythrocytes of Abcg2 knockout mice (Jonker et al., 2002). Because of the ability of ABCG2 to transport porphyrins and heme, the role of ABCG2 in protecting against hypoxic injury has been investigated in Abcg2- knockout mice (Krishnamurthy et al., 2004). ABCG2 is up-regulated in progenitor cells under low-oxygen conditions in an attempt to lower heme and/or porphyrin levels and ensure cell survival (Krishnamurthy et al., 2004). Moreover, *in vitro* mutant ABCG2 expressing cells are more susceptible to phototoxicity (Tamura et al., 2006; 2007). However, the physiological function of ABCG2-mediated transport of PPIX remains unclear, as no functional abnormalities have been described in Abcg2 knockout mice that could be directly attributed to the altered PPIX levels (Vlaming et al., 2009). One possibility is that ABCG2 helps to reduce porphyrin toxicity in liver and other cells in situations of porphyrin excess. More research is needed to elucidate ABCG2's role in heme homeostasis and skin photosensitivity reactions.

3.5.2. Clinical implications

3.5.2.1. In ADME

The positive impact of the protective role of ABCG2 is that it protects the body from the toxicity of xenobiotics while the negative impact is that ABCG2 impedes therapeutic agents to reach their targets for treating tumors or other illness. ABCG2 limits oral availability at the level of intestinal absorption and mediates hepatobiliary and renal excretion of its substrates and thus influences the pharmacology via pharmacokinetics and side effects of many drugs. Indeed, there is an impact of ABCG2 in absorption, distribution, metabolism and excretion (ADME), see Figure 12. In "absorption", ABCG2 can restrict drug absorption by pumping drugs out of intestinal epithelial cells, a barrier to xenobiotics, remember the already commented experiments with elacridar and topotecan (Kruijtzer et al., 2002). It has been shown that ABCG2 acts synergistically with other transporters in drug absorptions (Xia et al., 2005).

ABCG2 regulates the pharmacological and/or toxicological effect of drugs also because it limits their distribution in the different barriers through the body. Renal and hepatobiliary elimination comprise the phase of excretion. Hepatic uptake and biliary excretion determine the drug concentration in the liver, and they may affect the pharmacological effects and/or toxic side effects. The function of

ABCG2 at the level of biliary and renal excretion has effects in bioavailability of many drugs (see Schnepf and Zolk, 2013 for review).

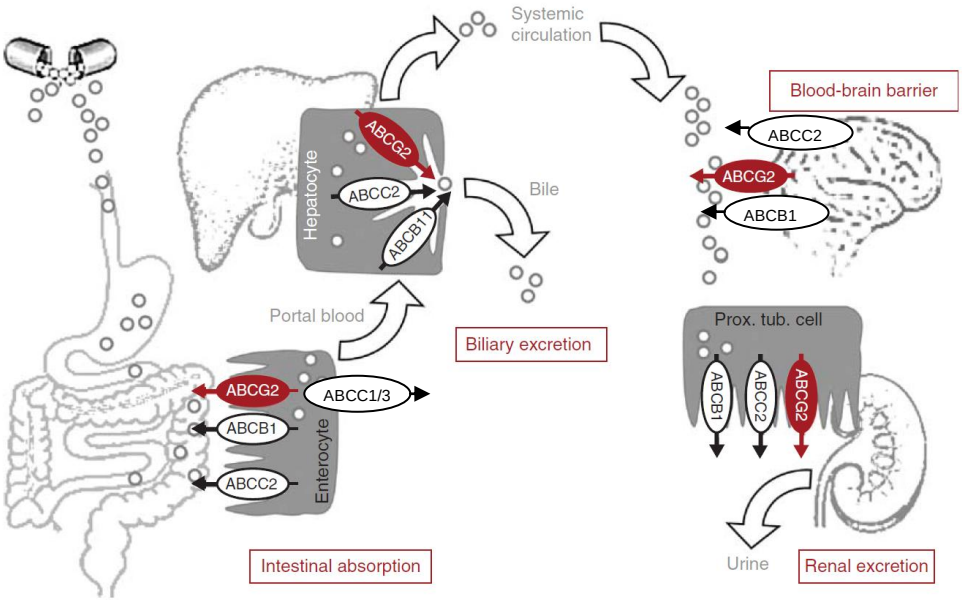

Figure 12. ABCG2 tissue expression and tissue-specific functions have implications in absorption (intestine), distribution (barriers as BBB) and excretion (biliary and renal) of an oral administrated compound (Poguntke et al., 2010).

3.5.2.2. In Cancer and MDR

As it was already said, ABCG2 was originally identified in anticancer drug-resistant human cancer cell lines obtained by *in vitro* selection confering resistance to anticancer drugs, such as mitoxantrone, doxorubicin, and daunorubicin, decreasing their cellular accumulation (Doyle et al., 1998). Subsequent analyses have shown that overexpression of ABCG2 results in the acquisition of resistance to anticancer drugs, such as topoisomerase inhibitors (topotecan, its metabolite SN- 38, irinotecan, belotecan, 9-aminocamptothecin), the antifolate agent methotrexate, flavopiridol, or bisantrene (Kusuhara and Sugiyama, 2007). ABCG2 seems to have a strong tendency to interact with clinically important kinase inhibitors including imatinib, nilotinib, gefitinib, canertinib, erlotinib, and lapatinib. Functional and pharmaceutical interactions between ABCG2 and imatinib or gefitinib have been extensively examined, and these data indicate that, although these kinase inhibitors are substrates for ABCG2, they exhibit potent inhibitory activity against this ABC transporter when used at relatively high concentrations (see Noguchi et al., 2009 for review). On the other side, ABCG2 transfected cells have been shown to display only minimal resistance to etoposide and depsipeptide (Robey et al., 2003) but no resistance to cisplatin, paclitaxel, or vincristine (Doyle et al., 1998). Furthermore, ABCG2 restricts the bioavailability of orally administered anticancer agents that are ABCG2-substrates like these drugs.

Since undesired toxic effects of chemotherapeutic drugs on the digestive organs are a significant problem during clinical cancer chemotherapy, the functional activity of ABCG2 is an important consideration for ABCG2-transportable drug pharmacokinetics in patients (Noguchi et al., 2009).

The expression of ABCG2 is associated with a poor response to cancer chemotherapy and is responsible for the development of clinical drug resistance, thus in the MDR phenomenon (Roos et al., 2000; Steinbach et al., 2002). The influence of ABCG2 on resistance of human cancers to antineoplastic pharmaceuticals should be viewed as the combined effects of the role that the transporter plays in normal tissues affecting drug absorption, distribution, metabolism and excretion (ADME), and the effects of the expression of the transporter in neoplastic tissues to produce active efflux of chemotherapeutic molecules (Natarajan et al., 2012). Inhibition of ABCG2 function may be a viable pharmacologic anticancer strategy from two perspectives. First, in cancers that naturally have high levels of ABCG2, ABCG2 inhibition can increase the intracellular level of the chemotherapeutic agent, thereby increasing cytotoxicity. Second, inhibition of ABCG2 would increase systemic drug levels (Krishnamurthy and Schuetz, 2006).

ABCG2 overexpression is commonly observed in cells derived from various types of human solid tumors selected with drugs, such as mitoxantrone, topoisomerase inhibitor topotecan, flavopiridol, and imatinib, and seems to be independent of P-gp or MRP expression (Nakanishi and Ross, 2012). Despite the original identification of ABCG2 in a breast cancer cell line, the expression of this transporter is quite variable among primary breast carcinomas. Expression of ABCG2 in other tumor types is also changeable; detection is more frequent in adenocarcinomas of the digestive tract, endometrium, and lungs (Diestra et al., 2002). ABCG2 has been reported to be overexpressed in solid tumors in subpopulations of cells with ‘‘stem-like’’ properties: quiescence, drug resistance, enhanced self-renewal capacity and tumorigenicity, and expression of other markers characteristic of stem cells. The extent to which ABCG2 contributes to drug resistance in these subpopulations is currently under active investigation. Subpopulations of stem-like cells expressing ABCG2 were found in cell lines or primary tumor samples from a wide assortment of solid tumors, including head and neck cancer, breast carcinoma, small cell and non-small cell lung cancer, gastrointestinal cancers including pancreatic, colon and hepatocellular, uterus and ovarian cancer, gliomas, malignant peripheral nerve sheath tumors, osteosarcoma, prostate cancer, Ewing’s sarcoma, odontogenic tumors, transitional cell carcinoma of the bladder, melanoma and neuroblastoma (Natarajan et al., 2012). Taken together, these results are consistent with the putative role of ABCG2 in clinical drug resistance in solid tumors and suggest that ABCG2 expression has prognostic value.

ABCG2 has the potential to play an important role in drug resistance in hematologic malignancies, as it is frequently expressed on malignant hematopoietic and lymphoid cells, and some of the drugs used to treat these cancers are ABCG2 substrates. Additionally, ABCG2 is expressed on stem cells in leukemias, potentially contributing to their resistance to eradication by chemotherapy or

targeted therapies. ABCG2 expression might be a significant prognostic factor in leukemia. Several studies have found a positive relationship between ABCG2 expression and drug resistance in acutemyelogenous leukemia (AML) and acute lymphocytic leukemia (ALL). Nonetheless, conclusions about the impact of ABCG2 overexpression on clinical outcome or on prognosis in AML or ALL require caution; a few studies have failed to find significant correlation of ABCG2 with these leukemias. To clearly delineate the role of ABCG2 in drug resistance in leukemia, larger studies of ABCG2 expression in clinical samples are necessary (see Natarajan et al., 2012 for review).

3.5.2.3. In polymorphisms and mutants

The expression and function of endogenous ABCG2 can be affected by **natural**ly occurring **variants** caused by single nucleotide **polymorphisms** (SNPs) of the coding region of ABCG2 gene. SNPs variants are known to impair ABCG2 expression and function, thus they may have significant physiological and pharmacological relevance; in addition, cells expressing these variants may confound results based on mRNA expression (Ross and Nakanishi, 2010). ABCG2 is a highly polymorphic transporter with over 80 SNPs in the ABCG2 gene (Tamura et al., 2007). A list of some genetic SNPs in ABCG2 characterized *in vitro* is shown in Table 3. Non-synonymous SNPs have been reported; among them, the most frequently observed in the ABCG2 coding region occur in exon 2 (G34A, resulting in a V to M mutation in amino acid 12), and in exon 5 (C421A, resulting in a Q141K mutation). The altered ABCG2 primary structure resulting from these polymorphisms generally causes loss or reduction in transporter expression and/or function, including variations to drug efflux, response or toxicity; reduced ATPase activity and influence the pharmacokinetics of drugs, such as topotecan, diflomotecan and 9-aminocamptothecin (Ieiri, 2012). It was recently recognized that healthy individuals of the Jr(a)-blood type carry two null alleles of ABCG2 despite the important physiologic role understood for ABCG2 (Saison et al., 2012; Zelinski et al., 2012).

There are mainly four categories of **non-natural ABCG2 mutants**. First, mutations that do not affect plasma membrane expression but alter substrate specificity and/or overall transport activity, as Arg482 or His457. In the second category, mutations affect biogenesis with decreased stability, lower expression and/or altered subcellular distribution of ABCG2. As examples, Arg383 in the linker region has been shown to be crucial for biogenesis of ABCG2; Gly406 and Gly410 in the GXXXG dimerization motif in TM1 of ABCG2 have been investigated for their impact on potential dimerization; Gly553 has been shown to be critical for plasma membrane targeting and proper folding of the transporter. In the third category, mutations cause alterations in chemical modifications such as N-linked glycosylation or disulfide bond formation in ABCG2. The only N-linked glycosylation site in ABCG2 is Asn596. In the fourth category, mutations do not have major effects on both plasma membrane expression and function of ABCG2. Such mutants include K473A and H630X, suggesting that these residues are likely not critical for expression and function of ABCG2 (see Ni et al., 2010b for review).

Table 3. Genetic ABCG2 single nucleotide polymorphisms SNPs characterized *in vitro* and consequences in transporter expression and/or function (Klaassen and Aleksunes, 2010).

Nucleotide Change	Amino Acid Change	In Vitro Function	Protein Expression/Localization
ABCG2	BCRP		
G34A	V12M	↔	Normal/intracellular
C376T	Gln126STOP	N.D.	Absent
C421A	Q141K	↓	Normal/reduced
G445C	A149P	↔	Normal
G448A	R163K	↔	Normal
C496G	Q166E	↔	Normal/reduced
A616C	I206L	↓ ↔	Normal
T623C	F208S	N.D.	Reduced
T742C	S248P	N.D.	Normal
C805T	P269S	↓ ↔	Normal
T1291C	F431L	↓	Normal/reduced
G1322A	S441N	↓	Reduced
T1465C	F489L	↓ ↔	Normal/reduced
A1768T	N590Y	↓ ↔	Increased
G1858A	D620N	↓ ↔	Normal

↓, reduced function; ↔, no change in function; N.D. not determined.

One of the most known mutations is Arg 482, found in some anthracycline resistant cancer cell lines. It has either threonine (T) or glycine (G) instead of arginine (R) at the amino acid position 482, suggesting it to be a "hot spot" for mutation. R482T and R482G mutations confer strong resistance to anthracycline including doxorubicin, daunorubicin, epirubicin (Honjo et al., 2001), as well as bisantrene and fluorescence dyes rhodamine 123 and lysotracker green. On the other hand, they are unable to transport methotrexate and its derivates (Volk et al., 2002), and folic acid. ABCG2, amino acid 482 mutations have yet to be found in clinical samples, suggesting that this observation has limited clinical relevance (Xia et al., 2005; Mo and Zhang, 2012).

3.5.2.4. In others

A genome-wide association study identified a common single-nucleotide polymorphism in ABCG2 as a determinant of serum urate levels and risk of **gout**. Gout patients had genotype combinations of the Q141K and Q126X variants that resulted in more than a 75% reduction of ABCG2 function (Dehghan et al., 2008; Matsuo et al., 2009; Woodward et al., 2009). Since these first studies, the relation of ABCG2 with the risk of gout has been studied in many diverse populations and is constantly observed with comparable effects (see Woodward et al., 2011 for review). Subsequent functional analysis *in vitro* demonstrated that urate is indeed a substrate of ABCG2 and that this apical efflux transporter is important in the renal secretion of urate. Based on the function of ABCG2 in urate excretion, one possible side effect of ABCG2 inhibitors could be the increase of serum urate concentrations and gout attacks. ABCG2 dysfunction has been characterized as a major cause of gout.

There are recent evidences suggesting a novel role ABCG2 in the removal of the peptide amyloid-β, a hallmark of **Alzheimer** disease, from the brains of mice (see Abuznait and Kaddoumi, 2012

for review). In addition, Alzheimer's patients with cerebral amyloid angiopathy overexpress ABCG2; moreover it has been shown that ABCG2 protein coprecipitates with amyloid-β in diseased tissue samples compared with age-matched controls (Xiong et al., 2009). These observations may reveal novel risk factors for accumulation of amyloid beta and the development of Alzheimer's disease.

3.6. Interaction with compounds

3.6.1. Substrates and inhibitors

The list of **substrates** of ABCG2 has been steadily expanding since its discovery. Because ABCG2 was first identified from chemotherapy- resistant cancer cells, early functional analysis focused upon anticancer drugs. Consequently, one of the major constituents of ABCG2 substrates are anticancer drugs, including topoisomerase inhibitors, anthracyclines, camptothecin (CPT) analogs, tyrosine kinase inhibitors (TKI), and antimetabolites (Mo and Zhang, 2012). However, ABCG2 has broad substrate specificity; it has been shown to transport a wide spectrum of structurally and functionally diverse substrates such as anticancer drugs, antibiotics, antivirals, sulfate and glucuronide conjugates of sterols and xenobiotics, natural compounds and toxins, carcinogens, fluorescent dyes, photosensitizers, endogenous compounds and HMG-CoA reductase inhibitors (see Xia et al., 2005; Krishnamurthy and Schuetz, 2006; Robey et al., 2009 as examples of reviews). The substrates of ABCG2 are identified *in vitro* directly by cellular or vesicular transport assays, or indirectly by substrate-stimulated ATPase activity or cytotoxicity assays. A list of selected substrates is displayed in Table 4.

Fumitremorgin C (FTC) was the first ABCG2 **inhibitor** described; however, its clinical development was not possible due to its neurotoxicity, which led to the development of a new nontoxic analogue of FTC, Ko143. Ko143 appeared to be a specific and potent inhibitor of both human and murine ABCG2 (Allen et al., 2002). Subsequently, other FTC-type inhibitors, including the indolyl diketopiperazines (van Loevezijn et al., 2001) and tryprostatin A (Woehlecke et al., 2003) were described.

The first inhibitors reported were also inhibitors of P-gp or MRP1 such as cyclosporine a, reserpine, elacridar (GF120918), tariquidar (XR-9576) and biricodar (VX-710). Additional classes of inhibitors include pyridines and dihydropyridines such as nimodipene and nicardipene; tyrosine kinase inhibitors (TKIs) such as imatinib and nilotinib (most likely as competitive inhibitors); flavonoids such as quercetin and tectochrysin; taxane derivatives, steroids and derivates; HIV protease inhibitors including ritonavir, saquinavir and nelfinavir, and bisindolylmaleimides and indolcarbazole kinase inhibitors. An extensive summary list is displayed at Table 5. The list of reported ABCG2 inhibitors has been growing rapidly. There are different ways to classify ABCG2 inhibitors (called also modulators): according to either (a) the specificity of inhibitors, (b) their chemical class or (c) their origin (naturally compounds,

clinically-used drugs, designed inhibitors …) (see Nicolle et al., 2009; Robey et al., 2009; Ni et al. 2010; Mo and Zhang, 2012, as examples of reviews).

Table 4. Summary of ABCG2 substrates classified in groups. For references of each compound see Mo et al. (2012).

Topoisomerase inhibitors
- Mitoxantrone (topoisomerase II inhibitor)
- Bisantrene (topoisomerase II inhibitor)
- Etoposide (topoisomeriase II inihibitor)
- Becatecarin (topoisomerase II inhibitor)
- NB-506, J-107088 (topoisomerase I inhibitors)

Anthracyclines (Topoisomerase II inhibitors)
- Daunorubicin
- Doxobucincin
- Epirubicin
- Pirarubicin

Camptothecin analogs (Topoisomerase I inhibitors)
- Topotecan
- SN-38
- CPT-11
- 9-aminocamptothecin
- NX211
- DX-8951f
- Homocamptothecins
- BN80915 (diflomotecan)
- Gimatecan
- Belotecan

Tyrosine kinase inhibitors
- Gefitinib
- Dasatinib
- Erlotinib
- Vandetanib
- Nilotinib
- Sorafenib
- Tandutinib
- CI1033 (Pan-HER TKI)
- CP-724,714 (HER2 TKI)
- Symadex (fms-like tyrosine kinase 3 inhibitor)

Antimetabolites
- MTX, MTX diglutamate, MTX triglutamate (antifolate)
- GW1843, Tomudex (antifolates)
- Trimetrexatte, piritrexim, metoprine, pyrimethamine (lipophilic antifolates)
- 5-fluorouracil (pyrimidine analog)
- CdAMP (nucleotide), cladribine (nucleoside)

Other anticancer drugs
- Flavopiridol (cyclin-dependent kinase inhibitor)
- JNJ-7706621 (CDK and aurora kinases inhibitor)
- Bicalutamide (non-steroidal anti-androgen)
- NSC73306
- Phenethyl isothiocyanate (PEITC)
- TH-337 (indazole-based tubulin inhibitors)

Sufate and glucuronide conjugates of xenobiotics
- Estrone 3-sulfate (E1S)
- 17beta-estradiol sulfate
- DHEAS
- 4[35S]-methylumbelliferone sulfate
- E3040 sulfate
- Troglitazone sulfate
- 3-O-sulfate conjugate of 17alpha-ethinylestradiol
- SN-38-glucuronide
- [3H]17beta-estradiol-17beta-D-glucuronide
- [14C]4-methylumbelliferone glucuronide
- BP-3-sulfate and BP-3-glucuronide
- Phenolic MPA glucuronide

Photosensitizers
- Pheophorbide a
- Pyropheophorbide a methyl ester
- Chlorine E6
- 5-aminolevulinic acid
- Phytoporphyrin
- HPPH

Natural compounds and toxins
- Folic acid
- Urate
- Genistein
- Riboflavin (vitamin B2)
- Vitamin K3, plumbagin
- Glutathione (GSH)
- Sphingosine 1-phosphate
- PhIP (carcinogen)
- PPIX (heme precursor)

Fluorescent dyes
- Rhodamine 123
- Hoechst 33342
- Lysotracker green
- BODIPY-prazosin
- D-luciferin (firefly luciferase substrate)
- Cholyl-L-lysyl-fluorescein (fluorescent bile salt derivative)
- BODIPY-FL-dihydropyridine

Others
- [(125)I]Iodoarylazidoprazosin (IAAP), [(3)H]azidopine
- Sulfasalazine (anti-inflammatory)
- Erythromycin (macrolide antibiotic)
- Ciprofloxacin, ofloxacin, norfloxacin,enrofloxacin, grepafloxacin, ulifloxacin antibiotics)
- Nitrofurantoin (urinary tract antibiotic)
- Moxidectin (parasiticide)
- Albendazole suloxide and oxfendazole (anthelmintics)
- Ganciclovir (antiviral drug)
- Zidovudine (NRTI)
- Lamivudine (NRTI)
- Leflunomide and A771726 (antirheumatic drugs)
- Diclofenac (analgesic and anti-inflammatory drug)
- Cimetidine (histamine H2-receptor antagonist)
- ME3277 (hydrophilic glycoprotein IIb/IIIa antagonist)
- Pitavastatin (HMG-CoA reductase inhibitor)
- Rosuvastatin (HMG-CoA reductase inhibitor)
- Dipyridamole (thromboxane synthase inhibitor)
- Glyburide (hypoglycemic agent)
- Nicardipine, nifedipine, nitrendipine (Ca^{2+} channel blocker)
- Olmesartan medoxomil (angiotensin II AT1-R antagonist)
- Befloxatone (selective monoamine oxidase inhibitor)
- Prazosin (alpha-1-adrenergic receptor antagonist)
- Riluzole (Na^{+} channels blocker)
- Amyloid-beta
- Zoledronic acid (osteotropic compound)
- Hesperetin conjugates (flavonoid)
- Kaempferol (flavonoid)

Table 5. Summary of ABCG2 inhibitors classified in groups. For references of each compound see Xia et al. (2005) and Mo et al. (2012).

Xenobiotics	ABCB1 inhibitors
Fumitremorgin C and Ko-143	Elacridar (GF120918)
GF-120918	Cyclosporin A
BIB-E	PSC0833
Flavopiridol	Pyridines derivatives
CI-1033	Tariquidar (XR9576)
Novobiocin	Chromanone derivatives
Reserpine	Tyrosine kinase inhibitors (TKI)
Prazosin	CI1033
VX-710 and VX-853, diethylstillbesterol	Gefitnib (Iressa, ZD1839)
Tamoxifen and derivatives (TAG-111 and TAG-139), toremifene	Imatinib mesylate (Gleevec, STI571)
Imatinib	Nilotinib
Gefitinib	Erlotinib
HIV protease inhibitors (e.g., ritonavir, saquinavir)	Lapatinib
Tryprostatin	Sunitinib
UCN-01	Other inhibitors
Cyclosporin A	Flavonoids
Digoxin	Curcumin
Pantoprazole and omeprazole	PZ compounds
Statins (e.g., lovastatin, simvastatin, cerivastatin, pitavastatin)	Xanthine
Steroids	FTC
Beclomethasone, 6α-methylprednisolone, corticosterone, triamcinolone, dexamethasone, betamethasone	Pipecolinate derivative (VX-710)
Endogenous steroid and conjugates	Taxane derivatives
Oestrone-3-sulfate	Tetrahydroisoquinolin-ethyl-phenylamines
17β-Oestradiol sulfate	Novobiocin
17β-Oestradiol dehydroepiandrosterone sulfate	UCN-01
Taurolithocholate	
Taurolithocholate sulfate	
Dietary compounds	
Flavonoids (e.g. apigenin, biochanin A, chrysin, genistein, kaempferol, hesperetin, naringenin and silymarin)	
Isothiocyanates	
Dihydropyridines (e.g. niguldipine, nicardipine and nitrendipine)	

Dynamic inhibitors including PZ- 39 have been recently found to inhibit ABCG2 activity and induce ABCG2 degradation by accelerating its endocytosis and trafficking to lysosomes. Xanthenes have also been shown to be dynamic inhibitors. “Static” inhibitors include FTC or flavonoids (Peng et al., 2009; 2010). In addition to modulating ABCG2 function, directly inhibition of the ABCG2 expression gene has been considered. For instance, hammerhead ribozyme, RNA interference or antisense oligonucleotide have been designed and proved to reduce ABCG2 expression (Kowalski et al., 2001; 2002; 2004; Ee et al., 2004).

It has been speculated that there are multiple ABCG2 modulation sites, although the locations of these binding sites are not yet clear. Additionally, it has been suggested the existence of different inhibition mechanisms (Ahmed-Belkacem et al., 2005; Xia et al., 2005).

Because of the role of ABCG2 in MDR, considerable efforts have been paid to identify chemosensitizing agents targeting ABCG2 to reverse ABCG2-mediated MDR. ABCG2 inhibitors have potential uses in increasing oral bioavailability or penetration of substrate drugs, potentially leading to more effective cancer treatments. However, despite the explosion of publications identifying ABCG2 inhibitors, none has been used in the clinical setting. Targeting ABCG2 degradation and inhibiting ABCG2 expression may provide a novel mechanism of ABCG2 inhibition that may become an effective way of reversing ABCG2-mediated MDR (Mo and Zhang, 2012).

There is a considerable **overlap** in substrate and inhibition specificity between ABCG2 and other ABC transporters. An example of proportions of overlapping between ABCG2, P-gp and MRP2 inhibition is show in Figure 13 A.

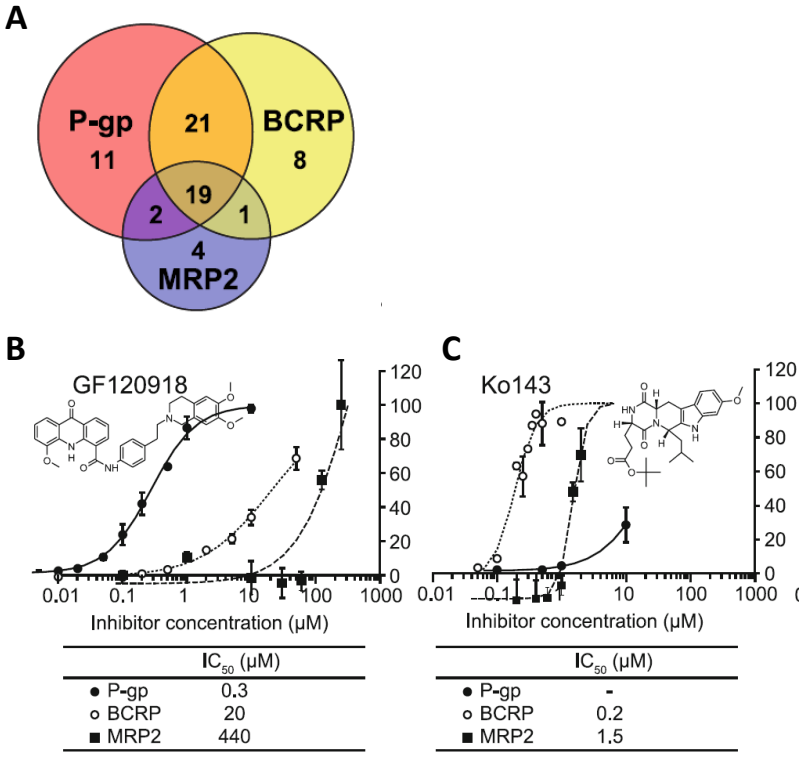

Figure 13. A. Overlapping inhibition of the major efflux transporters P-gp, ABCG2 (BCRP) and MRP2 (Matsson et al., 2009). 66 compounds were studied; the number of specific inhibitors was 11, 8 and 4 for P-gp, ABCG2 and MRP2, respectively. A large overlap was observed between P-gp and ABCG2, with 40 inhibitors in common. **B** and **C**. Concentration dependent inhibitory effect of GF120918 (B) and Ko143 (C), on P-gp, ABCG2 and MRP2 transport (Matsson et al., 2009). IC_{50} values, defined as the concentration resulting in half-maximum inhibition, were determined using non-linear regression. GF120918 and Ko143 showed preferential affinity towards P-gp and ABCG2, although MRP2 is affecting at higher concentrations.

ABCG2 transport substrate profile largely overlaps with P-gp and includes topotecan, SN-38, bisantrene, kinase inhibitors as imatinib, prazosin, antibiotics as cimetidine, antiviral drugs, amyloid beta, rhodamine 123 and Hoechst 33342. ABCG2 transport is partly overlapping with MRP1 and MRP2 substrates such as methotrexate, pravastatin, oestradiol- 17β-glucuronide and SN-38-glucuronide; as well as P-gp, MRP1 and MRP2 substrates, such as etoposide and anthracyclines (daunorubicin, doxorubicin) (Doyle et al., 1998; Miyake et al., 1999; Litman et al., 2000; Kawabata et al., 2002). In contrast, ABCG2 does not recognize the well-known P-gp substrates paclitaxel, colchicine, verapamil, vinblastine, or calcein AM. ABCG2 also does not recognise the MRP substrates calcein, cisplatin, glutathione or glutathione conjugates (Bates et al., 2001). The ABCG2 substrates also overlap with solute carrier transporter substrates (Lee and Kim, 2004), such as the organic cation transporter substrate, cimetidine; organic anion transporter substrates, methotrexate, oestrone sulfate and oestradiol sulfate; and organic anion transporting protein (OATP) substrates, statins, oestradiol glucuronide and oestrone sulfate.

It is then likely that part of the attempts which failed to abolish cancer cell multidrug resistance, by specifically inhibiting P-gp, was attributable to co-expression of ABCG2 in addition to P-gp. Therefore, ABCG2-specific inhibitors are urgently required in order to fully abolish multidrug resistance. Pharmacological inhibition studies and transporter deficient mice demonstrated that P-gp and ABCG2 play distinct and overlapping functions in pumping chemicals from the brain (see Klassen and Alekssunes, 2010 for review). Thus, it has been suggested that the overlap between ABCG2 and P-gp can lead to a synergistic effect of the transporters in limiting drug penetration across tissue barriers such as the blood-brain barrier (Kodaira et al., 2010; Polli et al., 2009). It has extensively accepted that GF120918 is a potent inhibitor of P-gp and ABCG2, whereas Ko143 shows almost 300-fold more inhibition potency to ABCG2 than P-gp (Allen et al., 2002). Nevertheless, caution should be paid in how to interpret the inhibition potency of an inhibitor-compound. Given a specific transporter, the inhibition of a compound is concentration dependent. For example at the concentration of 1μM, GF120918 highly inhibits P-gp but not ABCG2; however, at 10 μM both transporters are inhibited (Figure 13 B). In contrast, Ko143 inhibits ABCG2 since very low concentrations (0.2 μM) and P-gp starts to be inhibited at concentrations higher than 10 μM (Figure 13C) (Matsson et al., 2009).

ABCG2 could be solubilized from membranes using **detergents** such as 3-[(3-cholamidopropyl) dimethylammonio]-1-propanesulfonate (CHAPS) (Pozza et al., 2006), foscholine derivatives (McDevitt et al., 2006), or ndodecyl- β-D-maltoside (DDM) (Rosenberg et al., 2010). Purified ABCG2 in detergent solution was active in drug binding (McDevitt et al., 2006) or ATP hydrolysis (Pozza et al., 2006; Rosenberg et al., 2010). However, these kinds of detergents have been show to interact with P-gp (Li-Blatter et al., 2009); as a result, detergents may influence and interfere P-gp transport results if the transporter has been solubilized with detergents. So far, no research have been done for ABCG2 in this direction, there is no knowledge of the interaction of ABCG2 with detergents but taking in account the large number of compounds that overlap for both transporters, it could be hypotized that detergents

also interact with ABCG2. It should be notice that it has been shown that purified ABCG2 in detergents solution is active in hydrolyzing ATP but with a relatively low basal activity (Pozza et al., 2006; Rosenberg et al., 2010). This is probably due to detergent-ABCG2 interactions presumably as inhibitors. Further investigations are needed in this field.

3.6.2. Chemical properties of the compounds

Regarding **hydrophobicity**, in addition to hydrophobic substrates such as mitoxantrone, ABCG2 can also transport hydrophilic conjugated organic anions, particularly the sulfated conjugates with high affinity. ABCG2 transports either hydrophobic or hydrophilic, neutral, negatively or positively **charge**d molecules (Xia et al., 2005; Krishnamurthy and Schuetz, 2006; Ni et al., 2010). Enokizono et al. (2008) found that the ABCG2-specific substrates were weak acids, whereas basic or neutral ABCG2 substrates were also P-gp substrates. Hydrophilic compounds as methotrexate, sulfasalazine, cimetidine, and nitrofurantoin are described as very good substrates but not inhibitors of ABCG2; a low intrinsic affinity for the transporter in combination with poor membrane permeability probably explains the absence of an inhibitory effect for these compounds (Matsson et al., 2007). Indeed, a developed three-dimensional pharmacophore model based on a set of ABCG2 inhibitors, consisted of two hydrophobic centers (Figure 14) (Matsson et al., 2007), resembling that hydrophobic compounds act more as ABCG2 inhibitors.

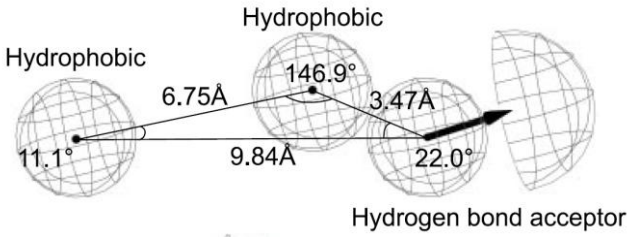

Figure 14. Three-dimensional orientation of the ABCG2 inhibitors. A threepoint pharmacophore model was developed based on a set of ABCG2 inhibitors. The model consisted of two hydrophobic centers and one hydrogen bond acceptor feature. The arrow indicates the optimal direction of electron sharing in the hydrogen bond, and the hemisphere indicates the optimal placement of a hydrogen bond donor group in the ABCG2 binding site (Matsson et al., 2007).

The inhibitor specificities of P-gp, ABCG2 and MRP2 were shown to be highly overlapping (Matsson et al., 2009). Compounds were transported more specifically usually at low concentrations. General ABC (P-gp, MRP2, ABCG2) inhibitors were more lipophilic and aromatic than specific inhibitors and non-inhibitors for these transporters. It seemed that lipophilic multi-specific inhibitors interact with a site distinct from the ATP-binding domain, possibly located in the membrane–protein interface. However, lipophilicity (as log P or log D) has been shown to be a predictor of inhibition of ABCG2 by a few groups but not for others (Gandhi and Morris, 2009; Ni et al., 2010).

Hydroxyl (–OH) and amino (nitro: N) groups in compounds form **hydrogen-bonds** and have been reported to be an important component for ABCG2 drug- transporter recognition and interaction, particularly hydrogen (H)-donor affects positively to ABCG2 inhibition (Yoshikawa et a., 2004; Saito et al., 2006; Boumendjel et al., 2007; Pick et al., 2008). Certainly, the abundance of nitrogen atoms was important for discriminating ABCG2 inhibitors from non-inhibitors in a QSAR (Quantitative Structure-Activity Relationships) study (Matsson et al., 2007; 2009) because the ABCG2 inhibitors contained a larger number of nitrogen atoms, in particular aromatic nitrogens. It should be noted that when ABCG2 was discovered it was mentioned that amino acids in the intracellular loops and the transmembrane domains of the ABCG2 protein contain a large number of aromatic and hydrogen bond donor side chains (Doyle et al., 1998). A correlation between drug affinity and the frequency of hydrogen bond acceptor patterns was presented for P-gp (Seelig, 1998; Gatlik-Landwojtowicz et al., 2006), a similar correlation for ABCG2 has been suggested (Cramer et al., 2007; Matsson et al., 2007). The large number of aromatic and hydrogen bond donor side chains in the intracellular loops and TMDs for both P-gp and ABCG2 could well contribute to the overlapping substrate specificity of the two transporters (Doyle et al., 1998; Matsson et al., 2007).

A common aspect that increases ABCG2 inhibition is **planar structure**; methyl groups and hydroxyl groups can both increase or decrease inhibitory potency depending on the group of compounds analyzed and the localization in the structure (Gandhi and Morris, 2009).

Nothing so far has been published related to the correlation of **amphiphilicity** with ABCG2.

It has been commented that ABCG2 transports more efficiently in acidic environments, this **pH dependency** is specific for ABCG2, as it is not happening in P-gp, MRP2 or MRP5 (Breedveld et al., 2007; Li et al., 2011). However, there is discrepancy between both authors concerning the dependency of ionization state of the substrate in acidic environments. Other authors found only in some cases higher ATPase activity and transport kinetics at acidic pH compared to neutral (Glavinas et al., 2007).

3.6.3. Structure-activity relationships (SARs)

The transporting mechanism, substrate properties and computational models (*in silico*) for ABC transporters have been discussed in several reviews (Ha et al., 2007; Demel et al., 2008; Ecker et al., 2008; Demel et al., 2009; Seeger and van Veen, 2009). *In silico* models can be used to predict pharmacokinetic and pharmacodynamic properties during drug discovery and development phases before performing *in vitro* and *in vivo* experiments, and can be used to synthesize drugs with favorable physicochemical properties. The two most common approaches applied in *in silico* models are development of Quantitative Structure-Activity Relationships (QSAR) models and Structure–Activity Relationships (SARs) models. QSAR models correlate *in vivo* biological activity to physicochemical properties of compounds while SARs attempt to explain chemical moieties or structural features that contribute to or are detrimental to the biological activity (Gandhi and Morris, 2009).

SAR analysis for ABCG2 has been reported for taxane-based reversal agents (paclitaxel ananogues), flavonoids, tamoxifen analogues, cyclin-dependent kinase inhibitors, tariquidar analogues, GF120918 analogues, camptothecin analogues, acridone derivatives, ginsenosides, chalcones, dihydropyridines, tryprostatin A analogues and FTC analogues (see Gandhi and Morris, 2009 and Ni et al., 2010 for reviews).

Common features among SARs and QSARs models for ABCG2 inhibition are a planar structure (required for binding to the protein and inhibiting), hydrogen bonding (related with ABCG2 inhibition), polarizability and lipophilicity. However, for compounds with similar chemical structures such as flavonoids, contradicting results were obtained in different laboratories with respect to which substitutions would have favorable or detrimental effects on ABCG2 inhibition (Gandhi and Morris 2009). In addition, most ABCG2 datasets available for *in silico* modeling are comprised from congeneric series of compounds; however, as a problem, the results from one series usually cannot be applied to another series of compounds (Gandhi and Morris, 2009). In conclusion, despite different published approaches, the nature of drug-ABCG2 transporter interactions is not yet very clear. To date, none of the existing SAR or QSAR models are sufficiently precise to discriminate efficiently between the different characteristics involved in interactions with ABCG2 to be able to accurately predict ABCG2 substrates and/or inhibitors. Thus, a model that can predict ABCG2 substrates and inhibitors accurately is still lacking. In addition, no direct molecular model has been reported so far. Note that all current Q(SAR) models were developed through indirect modeling based on chemical structures of inhibitors.

4. P-glycoprotein

4.1. Discovery

ABCB1, also called as MDR1 (because the ABCB1 encoding gene was related with the MDR phenomenon), P-glycoprotein (because is a surface glycoprotein, P for permeability) or as the abbreviation P-gp, was the first human ABC transporter described. Victor Ling's group discovered it from drug- resistant Chinese hamster ovary cells mutants in 1976 and named it as P-gp (Juliano and Ling, 1976); then, it was purified in 1979 by the same group (Riordan and Ling, 1979). Subsequently, it was shown that P-gp transports structurally unrelated compounds out of the cell at the expense of ATP (Gottesman and Pastan, 1993). Ten years after P-gp discovery, it was isolated from a multidrug-resistant carcinoma cell line and its encoding gene was identified as MDR1 or ABCB1 (Chen et al., 1986; Ueda et al., 1986). Its role in multidrug resistance in cancer cells was also reported. Thus, P-gp was the first ABC transporter discovered to be involved in cancer drug resistance 30 years ago and consequently it became the primary focus of biomedical research in this field and is the best characterized in MDR (Falasca and Linton, 2012).

4.2. Structure, membrane topology and mechanism of transport

P-glycoprotein (P-gp, ABCB1, MDR1) is a transmembrane protein composed of 1280 amino acids (170 kDa). In humans P-gp is encoded by multiple MDR genes, including *ABCB1* (old nomenclature *MDR1*-gene) and *ABCB4* (old nomenclature *MDR3*-gene), although P-gp most often indicates the ABCB1 gene product; whereas in mice two multidrug resistance proteins are encoded by the genes *Abcb1a*- and *Abcb1b*-genes (old nomenclature *Mdr1a* and *Mdr1b*-genes) (Schinkel et al., 1997; Gottesman and Pastan, 1993).

Throughout the past decade, the structure of P-gp has usually been characterized by **homology model**ing techniques (Seigneuret and Garnier-Suillerot, 2003; Stenham et al., 2003; Pajeva et al., 2004). However, earlier attempts to model the 3D structure of P-gp suffered from low sequence identity to the template protein (Chen et al., 2012). Encouragingly, in 2009, the X-ray structure of apo murine P-gp and two additional P-gp X-ray structures in complex with two cyclopeptidic inhibitors were reported by Aller et al. (2009). They found that P-gp is a pseudo-symmetrical heterodimer with each monomer consisting of two bundles of six transmembrane (TM) helices and two nucleotide-binding domains (NBDs) separated by 30 A° (Figure 15 A). The murine P-gp shares 87% sequence identity with the human homolog.

The **structural topology of P-gp** therefore **consists of** two halves regions. Both halves contain six hydrophobic transmembrane domains (TMD), followed by a large internal cytoplasmic domain with an ATP-binding site (NBD) (van der Bliek et al., 1988; Devault and Gros, 1990; Aller et al., 2009). An

intracellular flexible polypeptide loop connects both halves. The amino and carboxyl termini of P-gp are located intracellularly (Figure 15 B). Three glycosylation sites are located on the first extracytoplasmic domain. P-gp has also four phosphorylation sites located in the linker region. However, the functional significance of phosphorylation is not well understood, mutational studies where P-gp lacked all phosphorylation sites revealed that phosphorylation is not essential for P-gp to interact with drugs (Germann et al., 1996). There is 43% sequence homology between the two halves, the necessity of both homologues halves and the intracellular linker region for drug transport and ATPase activity has been demonstrated (Chen et al., 1986; Loo and Clarke., 1994; Hrycyna et al., 1998; Takada et al., 1998). Like other ABC-transporters, P-gp has typical conserved sequence motifs in the NBDs consisting on Walker A, Walker B, signature C motifs, and the Q-, D-, and H-loops (Ambudkar et al., 2006). The function of NBDs is to bind ATP, thus providing energy for substrate binding.

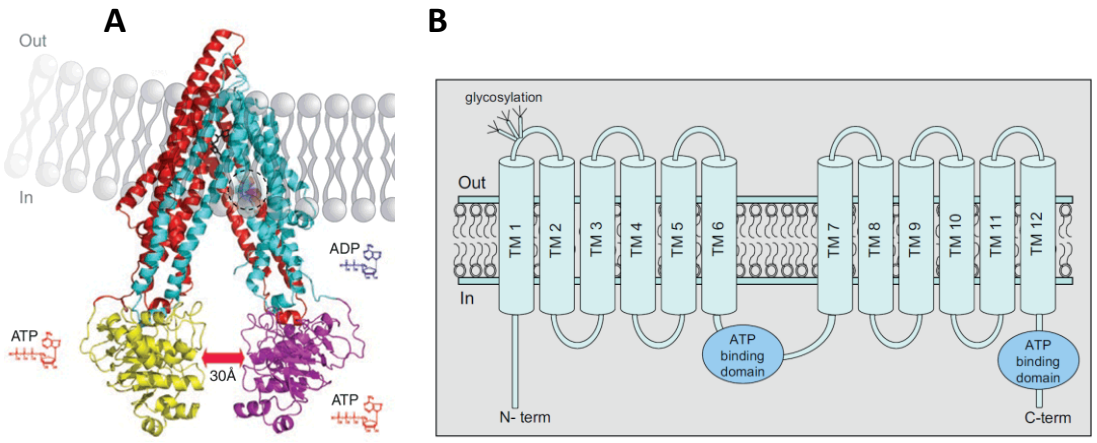

Figure 15. **A**. The X-ray structure of murine P-gp at 3.8 Å resolution (Aller et al., 2009). **B.** Membrane topology model of P-gp structure (TM: transmembrane domain) (Fu and Arias, 2012).

To date, the detailed mechanism for P-gp transporting substrates out of cells is still subjected to considerable controversy (Oldham et al., 2008; Locher, 2009; Chen et al., 2012). In order to mediate drug transport, P-gp has to couple the energy from drug **binding**, ATP binding and ATP hydrolysis, to the conformational changes that most probably alter the drug binding affinity and/or the accessibility of drug-binding sites (van Veen et al., 2001). Several models have been proposed, for example a model was proposed where two ATP are hydrolyzed per one drug molecule transported, one ATP was used to change the drug binding site from high to low affinity and the second ATP was used to reset P-gp back to its high binding affinity conformation (Ramachandra et al., 1998; Sauna and Ambudkar, 2000). One classic hypothesis is the ‘’ATP Switch” model where the release of drug occurs via ATP binding and dimerization of NBDs and the energy from ATP hydrolysis is used for resetting P-gp back to its high affinity conformation (Higgins and Linton, 2004; Linton and Higgins, 2007). In the ”two step drug

binding" model, the first step is the drug partitioning into the lipid bilayer described by the lipid-water partition coefficient (K_{lw}) and the second step is the drug binding to P-gp from the lipid phase depicted by the binding constant of drug to P-gp from the lipid phase (K_{tl}). The binding constant of the drug from the aqueous phase to P-gp (K_{tw}) is thus a product of these two binding constants, $K_{tw} = K_{lw} \times K_{tl}$ (Figure 16) (Seelig and Landwojtowicz, 2000; Gatlik-Landwojtowicz et al., 2006).

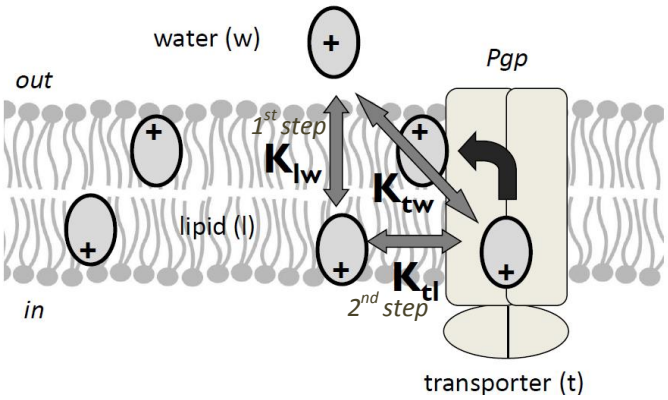

Figure 16. The two-step drug binding model. Relationship between the lipid to the water partition coefficient (K_{lw}), the binding constant of the drug from lipid to the transporter (K_{tl}) and the binding constant of the drug from the water to the transporter (K_{tw}). The grey ovals indicate an applied cationic compound. (Based on Seelig and Gatlik-Landwojtowicz, 2005).

The amphipathic nature of P-gp substrates allows them to partition into the lipid bilayer; this is consistent with the fact that the drug-binding sites of P-gp are accessible from the lipid bilayer (Shapiro and Ling, 1997; Shapiro et al., 1999; Chen et al., 2001). This led to the proposal of two models of drug transport. In the hydrophobic "vacuum cleaner" model P-gp binds its substrates from the inner leaflet of the lipid bilayer and transports them out to the extracellular bulk water phase. In the "flippase" model drugs are flipped from the inner to the outer leaflet of lipid bilayer where they can diffuse to the extracellular medium. Investigations supporting one or the other model have been published; however, for both models, the binding process comprises two steps; partitioning of drug from water into the membrane, and subsequent transfer of drug from the lipid to the binding pocket of the protein (remember Figure 16). Thus, drugs approaching the extracellular side of the plasma membrane will partition into the outer leaflet, and then diffuse into the inner leaflet, from where they will bind to P-gp (Eytan et al., 1996). Compound must achieve passive diffusion, thus if it is highly charged or too large it will not be able to diffuse or diffuse very slowly.

The location and the number of drug-**binding site(s)** of P-gp have been the interest of many research groups. The already commented intriguing question of how P-gp interact with a wide variety of of structurally diverse compounds has led to propose that P-gp possesses multiple drug-binding sites (Shapiro et al., 1999). The site-directed mutagenesis and the photoaffinity labeling experiments

suggested that the different substrates have different, but maybe overlapping drug-binding binding sites and that the major sites of drug interactions are located within P-gp TMDs in the middle of the lipid bilayer (Bruggemann et al., 1992; Greenberger, 1993; Demmer et al., 1999). However, the type and number of drug binding site(s) is still not clear (Sharom et al., 2005; Sauna and Ambudkar, 2007; Chen et al., 2012). The results of some studies have suggested the existence of a single large flexible binding pocket (Aller et al., 2009) or two "functional" drug-binding sites (the H-site, which binds Hoechst 33342, and the R-site, which binds rhodamine 123) (Sharom et al., 2005), some three and some even four binding sites (Dey et al., 1997; Shapiro and Ling, 1997; Martin et al. 2000a; Loo and Clarke, 2002; Lugo and Sharom, 2005).

A kinetic model was proposed assuming that P-gp has two binding regions, one activating binding region occupied at low substrate concentrations, and one inhibitory binding region, occupied at high substrate concentrations (Litman et al., 1997a and b; Ambudkar et al., 1999). Binding of drug to the activating region will enhance P-gp activity and thus ATP hydrolysis, whereas binding to the inhibitory region will reduce P-gp activity, leading to a decrease in the ATP hydrolysis, see Figure 17 A (Sauna and Ambudkar, 2001; Gatlik-Landwojtowicz et al., 2004). Substrates with a high affinity from drug to the transporter have a higher propensity to occupy both binding regions, and therefore to inhibit P-gp already at low aqueous concentrations (Li-Blatter et al., 2009). Moreover, if two different intrinsic substrates are applied simultaneously, the substrate with the higher binding affinity to the transporter will influence the bioavailability of the second drug (Van Asperen et al., 1998). These compounds having a high affinity to P-gp are called modulators (Seelig and Landwojtowicz, 2000; Seelig and Gatlik-Landwojtowicz, 2005), they generally enhance P-gp activity, and thus ATP hydrolysis. The kinetic model was mathematically evaluated as a modified Michaelis-Menten equation (Figure 17 B), based on uncompetive inhibition (Litman et al., 1997a). However, if only activation occurs, the dissociation constant (K_1) and the maximum activity (V_1) correspond to the simple Michaelis-Menten parameters (Seelig and Landwojtowicz, 2000).

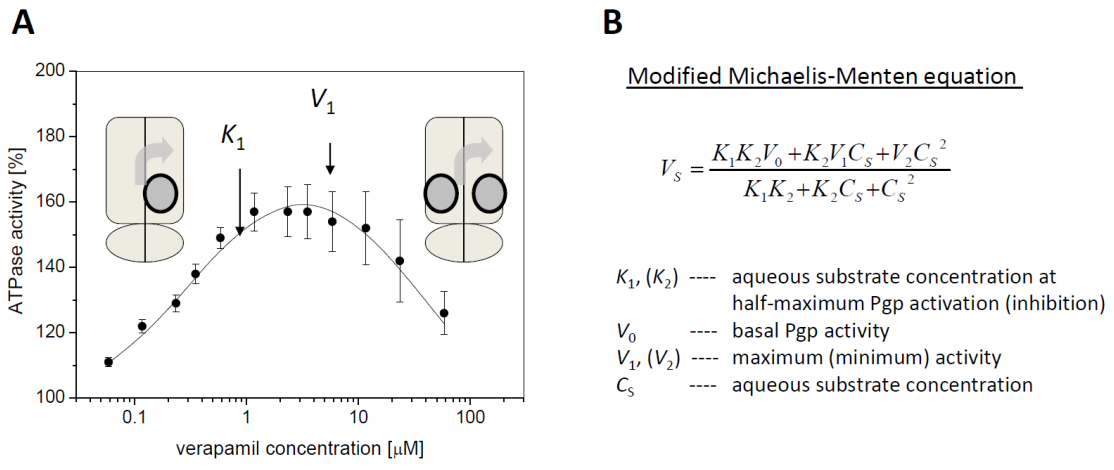

Figure 17. (Legend in next page)

Figure 17. **A.** Two binding regions kinetic model. At low drug concentrations the activating binding region is occupied and enhances P-gp ATPase activity, at high substrate concentrations the inhibitory binding region is also occupied and reduces P-gp ATPase activity. **B**. Modified Michaelis-Menten equation and parameters. (Based on Litman et al., 1997a and Gatlik-Landwojtowicz et al., 2006).

It has been proposed that the feature which distinguishes groups of compounds is their rate of spontaneous movement across the membrane (Eytan et al., 1996). Substrates are suggested to cross membranes at a low rate. After they have been effluxed, they will rapidly repartition into the outer leaflet, cross slowly to the inner leaflet and interact with P-gp once again, but the transporter will be able to maintain a substrate concentration gradient (Seelig and Gatlik-Landwojtowicz, 2005; Sharom, 2008). Hence, the export rate of drug is faster than the rate of passive diffusion into the cell (influx) and the drug will barely reach the cytosol (Figure 18 A). Modulators, on the other hand, appear to cross membranes very rapidly, faster than the rate of P-gp-mediated transport. Passive influx is distinctly faster than active efflux and the drug will reach the cytosol even if it is a substrate for an efflux transporter (Figure 18 B). Thus, the protein engages in a futile cycle of modulator transport, but cannot either generate a modulator gradient or transport other substrates. Therefore, although modulators inhibit transport of other drugs, it is difficult to measure the rate at which they are themselves transported; despite P-gp is working at high rate there is no net transport, see below (Seelig, 2007).

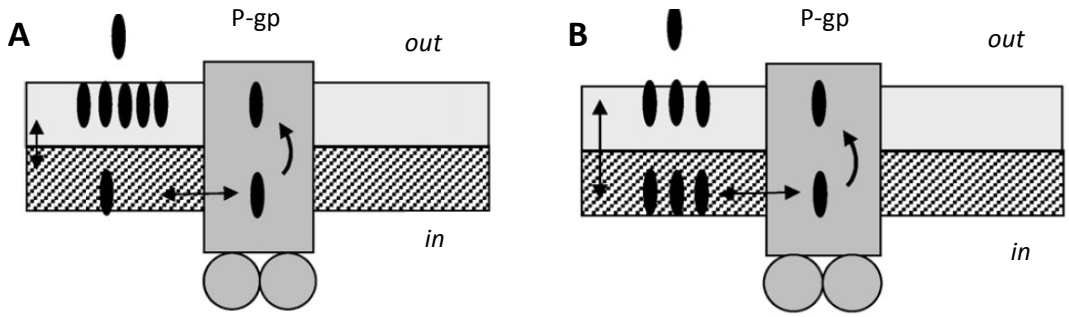

Figure 18. A. A compound which diffuses the membrane at low rate is maintained by P-gp with a concentration gradient (Nervi et al., 2010). **B**. A compound which diffuse the membrane rapidly, faster than the rate of P-gp efflux (Nervi et al., 2010). The extracellular and the cytosolic membrane leaflets are indicated as grey and hatched, horizontal rectangles, respectively. The black ovals indicate the compound applied.

The molecular mechanism of substrate recognition, binding, and transport by P-gp has been a matter of enormous effort in research and debate. The importance of the identification of molecular properties required for the recognition of compounds by P-gp is the use in rationally directing lead optimization towards the desired P-gp interaction (e.g. efflux, inhibition or no interaction) (Raub, 2006).

Efflux (which is the sum of passive influx and active efflux) depends on the expression level of the transporter and the concentration of the drug applied (Seelig, 2007). Note that usually, compounds can act as substrates or inhibitors of P-gp depending on the concentration, at low concentrations they are substrates and at higher inhibitors (Seelig and Landwojtowicz, 2000).

The ATP-binding domains act as ATPase, which converts ATP to ADP to provide the energy required for P-gp to pump substrates across membranes, often against steep concentration gradients (Buxbaum, 1999). Both NBDs are essential for proper functioning of P-gp and ATP must bind to both NBDs to allow activity of the entire P-gp protein (Romsicki and Sharom, 1998). However, whether hydrolysis of both bound ATP molecules is necessary to produce activity is uncertain (Kimura et al., 2007). It seems that ATP binding rather than **ATP hydrolysis** drives the major role in the P-gp transport process (Sauna and Ambudkar, 2000).

4.3. Distribution

P-gp is normally expressed at the apical membrane of endothelial cells in many important physiological barriers, including the intestinal epithelia, on the biliary canalicular membrane of liver hepatocytes, renal proximal tubular cells, the placenta and fetal-maternal barrier, blood-testis barrier, blood-nerve barrier the adrenal gland and endothelial capillaries of the brain comprising the blood–brain barrier (BBB) (Figure 19 A) (Thiebaut et al., 1987; Cordon-Cardo et al., 1990; Klaassen and Aleksunes, 2010). It has been seen also expressed in some pluripotent stem cells and cancer stem cells as well as being commonly over-expressed in tumor cell lines.

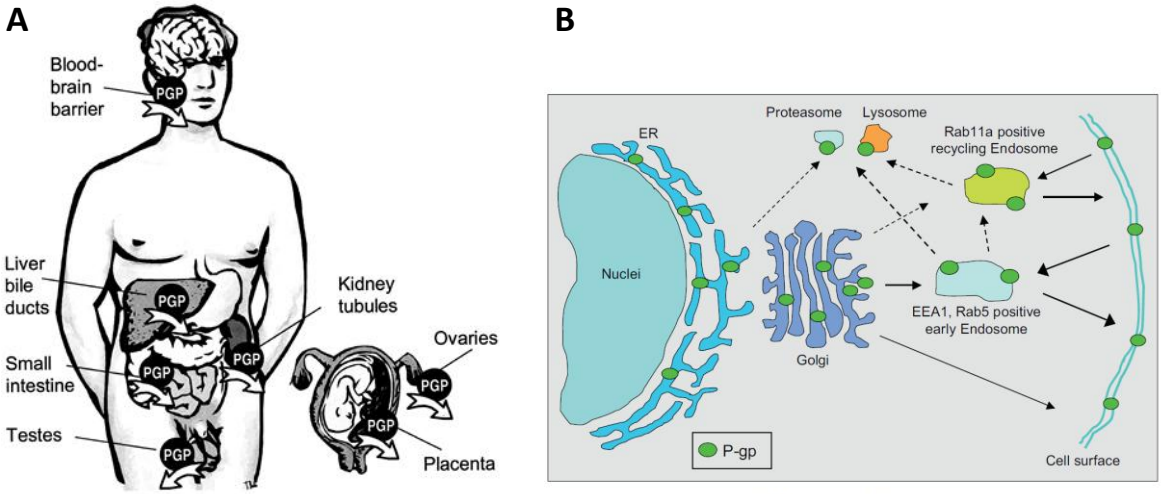

Figure 19. P-gp tissue distribution. **A**. P-gp distribution at barrier sites (Marzolini et al., 2004). **B**. Generic model of cellular localization of P-gp and possible traffic/cycling routes (Fu and Arias, 2012).

P-gp is also localized in intracellular compartments, such as endoplasmic reticulum (ER), Golgi, endosomes and lysosomes, conversely P-gp mitochondria localization remains controversial. Cycles between endosomal compartments and the plasma membrane act in a microtubular-actin dependent manner (Sai et al., 1999; Fu et al., 2004; Fu and Roufogalis 2007). The sites of P-gp synthesis (ER), modification (Golgi), trafficking/recycling (endosomes) and degradation (lysosome, proteasome) are indicated in Figure 19 B.

It has been shown that expression levels of P-gp depend on genetic, age, diet or medication (Seelig and Gatlik-Landwojtowicz, 2005).

4.4. Function and implications

4.4.1. Protection limiting substrate penetration and tissue distribution

P-gp tissue distribution and its drug transport activity reveals its primary role thought to be cellular and tissue protection of the organism against toxic xenobiotics (Borst and Schinkel, 2013). Knockout mouse studies support the idea of this protective function of P-gp; mice lacking the Abcb1a- and Abcb1b-genes were hypersensitive to several xenobiotic toxins, however they did not show dramatic physiological abnormalities (Schinkel, et al., 1995; Schinkel, 1997). Efflux activity associated with P-gp would reduce intestinal drug absorption while enhancing drug elimination though the liver and kidney. At barrier sites such as the blood-brain barrier, testes and placenta, P-gp would limit tissue exposure to potentially toxic P-gp substrate compounds. This function is similar to ABCG2.

Other physiological functions where P-gp could be implicated are transport of lipids (van Helvoort et al., 1996), regulation of apoptosis (Johnstone et al., 2000), indirect modulation of chloride channel activity (Valverde et al., 1992) and cholesterol esterification (Luker et al., 1999). It was also postulated that the subcellular P-gp location contributes to the protection of DNA (Molinari et al., 1998; Calcabrini et al., 2000; Munteanu et al., 2006).

4.4.2. Clinical implications

4.4.2.1. In ADME

In Abcb1a/Abcb1b knock-out mice, tissue concentrations of P-gp substrates are higher than in normal mice, suggesting that P-gp plays a role in determining oral drug bioavailability (Schinkel, 1997). Similarly to ABCG2 and other ABC transporters, P-gp significantly modulates the absorption, distribution, metabolism and excretion (ADME) properties of drugs. After oral administration most drugs enter to the blood circulation mainly within the small intestine via passive diffusion where P-gp is highly expressed thus hampering the *absorption* of drugs. Absorbed drugs have to be transported from the site of administration to the site of action in order to be effective. The brain for example is frequently targeted

by drugs. However, the brain is separated from the blood circulation by the BBB where P-gp is highly expressed in the BBB and thus exports its substrates back to the bloodstream (Tatsuta et al., 1992; Schinkel, et al., 1996).

Drugs are *metabolized* mainly in the liver but also the small intestine and the kidney contribute significantly to the overall drug metabolism. The effect of P-gp on the metabolism of drugs in the liver and kidney is minimal because P-gp is localized at the exit site of hepatocytes and renal epithelial cells. In contrary, in intestine P-gp is localized at the entrance site of epithelial cells and thus drugs are exposed to P-gp prior to intracellular distribution and metabolism. The intestinal P-gp extrudes drugs from the inside of epithelial cells back to the intestinal lumen. However, a portion of the extruded drugs are reabsorbed back into the epithelial cells. In this way, P-gp prolongs the intracellular residence time of drugs and increases the probability of drugs to get caught by the metabolizing enzymes (Hochman et al., 2000; Glavinas et al., 2004). The elimination of the drugs from the body via *excretion* by the liver and kidney is also affected as drugs at first cross the basolateral membrane of renal epithelial cells or hepatocytes and then diffuse to the apical membrane where P-gp contributes to the excretion of drugs into the urine or bile (Glavinas et al., 2004).

4.4.2.2. In cancer and MDR

As it has already said, the best known multidrug resistance (MDR) protein is P-gp (see Ambudkar et al., 1999; Litman et al., 2001; Zhou, 2008 for reviews). Nonetheless, it should be note that the classical MDR phenotype is characterized by cross resistance patterns against a variety of drugs; if a cell become resistant, it will be to all the drugs substrates for the efflux transporters (Seelig and Gatlik-Landwojtowicz, 2005). About half of human cancers express P-gp at levels sufficient to confer multidrug resistance; cancers from liver, intestine, kidney, breast and ovaries exhibit high endogenous P-gp levels even before the chemotherapy. It is well established that P-gp overexpression in tumour cells reduces the accumulation of different chemotherapeutics including taxanes (e.g. paclitaxel), vinca alkaloids (e.g. vincristine) and anthracyclines (e.g. doxorubicin). Indeed, P-gp involves resistance to cytotoxic drugs in about 50% of human cancers (Gottesman and Ling, 2006). In hematological malignancies, such as leukemias, lymphomas and multiple myelomas, the low levels of P-gp expression observed initially are markedly increased after chemotherapy treatment and relapse (Sharom, 2008). Association between P-gp expression and failure of treatment with substrate drugs is well established in several hematopoietic cancers (Sikic, 1999) and myeloid leukaemia (Gottesman et al., 2002; Sikic, 2006).

Most strategies for reversing MDR have focused on modulation or inhibition of P-gp activity (Ambudkar et al., 1999; Seelig and Gatlik-Landwojtowicz, 2005), which can be achieved by inhibition of ATP binding or hydrolysis (e.g. azido-ATP, NBD chloride) (al-Shawi and Senior,1993; al-Shawi et al., 1994), selectively blocking the expression of individual multidrug resistance proteins in cancer cells (Pichler et al., 2005), inhibition of conformational changes via antibody binding (e.g. UIC2) (Mechetner and Roninson, 1992) or by non-competitive or competitive inhibitor which direct interacts with P-gp

binding sites. Especially in this last approach, a lot of effort has been made in order to find suitable P-gp-inhibitors for clinical use, but either due to their poor modulatory activity, toxicity at high concentration, or unpredictable pharmacokinetic interactions in the presence of chemotherapeutic agents (Krishna and Mayer, 2000; Huisman et al., 2003; Thomas and Coley, 2003), only a few significant advances have been made.

Moreover human P-gp accounts for other significant clinical problems; for instance, a compound having a high affinity for the transporter may change the bioavailability of another co-administrated drug that was usually effluxed by P-gp, leading to unexpected side-effects (Van Asperen et al., 1998).

4.4.2.3. In polymorphisms and mutants

P-gp variants carrying spontaneous mutations have been found in cultured cell lines; the first one to be identified was G195V, which caused increased resistance to colchicines, while resistance to several other drugs was unchanged (Kioka et al., 1989). Another cell line with a spontaneous deletion of F335 showed altered resistance to several substrates (Chen et al., 1997).

Over 50 SNPs in the human ABCB1 gene have been reported in patients (Schwab et al., 2003; Marzolini et al., 2004; Kimchi-Sarfaty et al., 2007). Although genetic polymorphism in P-gp have been reported to change the mRNA expression, protein expression and function of P-gp, several SNP in P-gp have failed to show this association (Leschziner et al., 2007), leading to inconclusive results overall. SNP expression in cultured cell lines has shown that many of these variants have from no effect to modest changes on P-gp surface expression, transport function, substrate specificity and/or drug-stimulated ATPase activity (Leschziner et al., 2007). Moreover, the majority of attempts to demonstrate an association between *ABCB1* genotype/haplotype and pharmacokinetics or clinical outcome for P-gp substrates have been inconclusive (Leschziner et al., 2007).

Since P-gp play a central role in tissue defense against toxic substrates, it has been suspected that polymorphisms might alter susceptibility of individuals to disease. In fact, P-gp polymorphisms are associated with increased susceptibility to ulcerative colitis (e.g. Potocnik et al., 2004), colon cancer (e.g. Potocnik et al., 2001), renal epithelial tumors (Siegsmund et al., 2002), Parkinson's disease (Drozdzik et al., 2003), and possibly other human diseases. See Zhou et al., 2008 for a more extended review in MDR1 polymorphisms.

4.5. Interaction with compounds

4.5.1. Substrates and inhibitors

P-gp has been shown to transport a wide range of structurally dissimilar compounds that are hydrophobic and amphipatic, ranging in size from less than 200 to almost 1900 Da. Many of these

molecules are clinically important, including anticancer drugs, HIV-protease inhibitors, analgesics, antihistamines, H2-receptor antagonists, immunosuppressive agents, cardiac glycosides, calcium-channels blockers, antibiotics, steroids, cyclic peptides, antiemitics… (Sharom, 1997) Compounds interacting with P-gp also include physiological substrates as steroid hormones, lipids, peptides, cytokines… (see Sarkadi et al., 2006 for review).

Owing to the importance of P-gp on MDR and ADME, extensive studies have been carried out to identify P-gp substrates or develop more-potent, -selective and -specific P-gp inhibitors (Polli et al., 2001). The polyspecificity (i.e. promiscuity) of P-gp in substrate and inhibitor recognition makes designing effective candidate compounds difficult (Demel et al., 2009).

Several compounds have been generated and tested *in vitro* and clinically as P-gp inhibitors; they are categorized in three different generations of P-gp inhibitors (see Darby et al., 2011, and Falasca and Linton, 2012 for a more detailed reviews). The first-generation inhibitors included the use of drugs developed for other conditions such as verapamil (an antihypertensive), quinine (an antimalarial) and cyclosporine A (an immunosuppressant). Despite their efficacy in inhibiting ABCB1-dependent drug efflux *in vitro* (Tsuruo et al., 1981), these inhibitors failed to provide a positive effect in the clinical setting due to undesired side effects and were prone to pharmacokinetic complications. These compounds are substrates at low concentrations and inhibitors at higher concentrations, therefore, lacked specificity and potency and consequently they were characterized by high toxicity (Ozols et al., 1987).

Second-generation of P-gp inhibitors were designed to specifically target this transporter; consequently they were more selective and less toxic. Valspodar (formerly PSC833) a derivative of cyclosporine A and the piperidine derivative Biricodar (VX-710) for example, where identified as more potent inhibitors with higher specificity for P-gp than the first-generation compounds. However, they also failed to improve outcome in Phase III clinical trials when co-administered with other anticancer drugs due to pharmacokinetic interactions, especially in cases where both, the drug and the inhibitor were substrates for cytochrome P450 (Falasca and Linton, 2012).

The third-generation inhibitors were specifically designed to overcome the limitations of the second generation, and so inhibitor development focused on compounds that lacked inhibition of the CYP450s and did not alter the pharmacokinetics of the anticancer drugs. Currently, tariquidar (an anthranilamide, XR9576), elacridar (an acridone caroxamide), zosuquidar (LY335979) and CBT-1 (both quinolone derivatives) and laniquidar (a piperidine) are at various stages of clinical trial. They are characterized by higher potency and lower toxicity than their predecessors. However, side effects and drug-drug interactions have been also reported for these types of inhibitors. Clearly, therefore, difficulties remain with this strategy that may or may not be overcome. Careful personalized therapy and dosing to minimize side effects could help; indeed, studies are ongoing with these inhibitors (Lancet et al., 2009; Ruff et al., 2009; Kelly et al., 2011).

4.5.2. Chemical properties of the compounds

One of the most puzzling and constant feature related to P-gp is how this protein can recognize and transport hundreds of structurally dissimilar compounds including therapeutic drugs, natural products, detergents and peptides. Progress in this field has been made, but it is still far away from a complete understanding. Classically P-gp interacts with hydrophobic, amphiphilic, lipid-soluble compounds, with molecular weights in the range of 200 to 2000 Da, often with aromatic rings and a neutral or positive charge at physiological pH (Gottesman and Pastan, 1993; Seelig et al., 1994; Schinkel et al., 1996; Sharom, 2008). Compounds with negative charge have been shown initially to not interact with P-gp (Seelig, 1998). It was proposed that hydrophobicity, amphiphilicity and number and strength of electron donor patterns (hydrogen bond acceptor groups) regulate the interaction with P-gp (Seelig, 1998; Seelig and Landwojtowicz, 2000). Later, authors found that the interaction of a compound with P-gp depends on compound partitioning, which is controlled by drug chemistry (specially cross-sectional area (AD) and the charge (pK_a)) and drug concentration, lateral packing density of the membrane (π_M), expression level of the transporter and metabolic state of cells (Gatlik-Landwojtowicz et al., 2006; Aänismaa and Seelig, 2007). It was earlier suggested that the lipid bilayer is important in drug recognition (Romsicki and Sharom, 1999). The importance of amphiphilicity and hydrophobicity are a prerequisite for binding to lipid membranes, thus, to P-gp (Seelig and Landwojtowicz, 2000; Sharom 2008). Additionally, the involvement of the lateral packing density of the membrane as an essential factor for the interaction of the transport process, as it has been previously said, is representative of the importance of the lipid membrane in P-gp function. Therefore, to be able to explain the P-gp efflux process at molecular level it is important to characterize the interacting drug, the lipid membrane and the efflux transporter (Seelig, 2007).

The intrinsic affinity of the transporter for its substrates may be weaker but more specific than to the lipid bilayer; this was confirmed by a thermodynamic analysis of the drug-binding process within a lipid bilayer (Gatlik-Landwojtowicz et al., 2006). The low dielectric constant ($\varepsilon \approx 2$) and enhancing of electrostatic interactions such as the π-electrons of aromatic ring and a cation in the lipid bilayer determines the nature of substrate-P-gp binding interactions. In a lipid environment, electrostatic and dipolar interactions (according to Coulomb's law) are improved due to low dielectric constant. Consequently, hydrogen-bond formation (dipole-dipole) for substrate recognition can take place (Seelig and Gatlik-Landwojtowicz, 2005). The sequences of putative transmembrane helices of P-gp have a high percentage of amino acids residues with hydrogen bond donor side chains arranged in an amphipathic manner. It has been suggested that the binding of the drug to P-gp occurs via specific hydrogen bonds formation patterns (Seelig, 1998; Seelig and Landwojtowicz, 2000). They are arranged in a particular spatial distance, called type I and type II units, between hydrogen bond acceptors (HAP) of the drug and the hydrogen bond donor side chains of the transmembrane α-helices of P-gp. Three dimensional structural analysis of hundred P-gp-substrates revealed that all of them carried at least two hydrogen bond acceptor groups in a specific distance of 2.5 ± 0.5 Å (type I unit) or three with a distance of 4.6 ±

0.6 Å between the two outer hydrogen bond acceptor groups (type II unit) (Seelig, 1998). Furthermore, it was proposed that the strength of substrate binding to P-gp increases with the number and strength of individual hydrogen bond formed. Molecules that contain at least one type I or one type II unit are predicted to be P-gp substrates. For transport, at least two type I patterns or one type I and one type II pattern are required. Moreover, if two substrates are applied simultaneously to P-gp the compound with the higher potential to form hydrogen bonds generally acts as an inhibitor. In addition, type I patterns are the principle recognition elements for P-gp; on the other hand, type II patterns not only interact with P-gp, but are also responsible for induction of P-gp over-expression and thus for the development of drug resistance. Type II patterns are especially abundant in antibiotics and in drugs targeted to DNA (e.g. antitumor and antiviral drugs) (Seelig and Landwojtowicz, 2000).

4.5.3. Structure-activity relationships (SARs)

For P-gp, numerous computational approaches or models based on QSAR analyses, pharmacophore modeling and molecular docking were developed to predict P-gp inhibitors or substrates (e.g. Ha et al., 2007; Demel et al., 2008; Seeger and van Veen, 2009). Rather than developing computational models based on complicated statistical techniques, earlier attempts were made to find a set of simple rules based on structural and functional features that could characterize the interactions between a substrate or inhibitor and P-gp (Zamora et al., 1988; Pearce et al., 1989; Gottesman and Pastan, 1993; Seelig, 1998). For example, Seelig suggested a set of well-defined structural elements required for an interaction with P-gp (Seelig, 1998), this was already explained in the previous section.

A lot of effort has been dedicated to predict P-gp inhibitors or substrates and understand the mechanism of action for the P-gp inhibitors or substrates. Currently, only limited *in silico* models can give satisfactory predictions. How to improve the prediction accuracy of the models still remains a significant challenge (Chen et al., 2012).

5. Important compounds for this study

5.1. Steroid hormones

Hormones are endogenous molecules that work as chemical messengers; they transport a signal from one cell to cells in other parts of the organism. In cells expressing the specific receptor for the hormone, the hormone binds to the receptor, resulting in the activation of a signal transduction mechanism that ultimately leads to cell type-specific responses related with their growth, function, or metabolism. The rate of hormone biosynthesis and secretion is often regulated by a homeostatic negative feedback control mechanism which depends on factors that influence the metabolism and excretion of hormones. Common effects of hormones on the body include regulation of growth, apoptosis, immune system, metabolism, preparation of the body for a new phase of life, and control of the reproductive cycle and sexual characteristics. Notoriously, a variety of exogenous chemical compounds, both natural and synthetic, have hormone-like effects on both humans and wildlife. Their interference with the different processes of natural hormones in the body results in same changes as endogenously produced hormones do (Crisp et al., 1998).

Mammalian hormones are classified in three chemical classes: peptide-hormones, lipid-derived hormones and monoamines (derived from aromatic amino acids). Lipid and phospholipid-derived hormones are synthesized from lipids such as linoleic acid and arachidonic acid and phospholipids. The main classes of lipid-derived hormones are the steroid hormones which are generally synthesized from cholesterol in the gonads and adrenal glands. They are classified in five groups: glucocorticoids, mineralocorticoids, androgens, estrogens, and progestogens. Steroid hormones help control metabolism, inflammation (e.g. glucocorticoids), immune functions, salt and water balance (e.g. mineralocorticoids), development of sexual characteristics (e.g. androgens and estrogens), and the ability to withstand illness and injury. The term steroid includes both hormones produced by the body and artificially produced medications that duplicate the action for the naturally occurring steroids.

5.1.1. Steroid hormones used in this study

Cortisol, known also as hydrocortisone, is a glucocorticoid produced by the adrenal gland. It is released in response to stress and a low level of blood glucocorticoids. Its primary functions are to increase blood sugar through stimulating gluconeogenesis (and it activates anti-stress and anti-inflammatory pathways); suppress the immune system; regulate lipolysis, proteolysis, bone formation and carbohydrate metabolism (Simmons et al., 1984; Coderre et al., 1991; Djurhuus et al., 2002). Hydrocortisone is the pharmaceutical term for cortisol. It is used as an immunosuppressive drug, given by injection in the treatment of severe allergic reactions such as anaphylaxis and angioedema. It can be used topically for allergic rashes, eczema, psoriasis and certain other inflammatory skin conditions. It may also be injected into inflamed joints resulting from diseases such as gout.

Dexamethasone is a potent synthetic glucocorticoid steroid member, acting as an anti-inflammatory and immunosuppressant. Dexamethasone is used to treat many inflammatory and autoimmune conditions, such as rheumatoid arthritis and bacterial meningitis (Brouwer et al., 2010). Cancer patients undergoing chemotherapy are given dexamethasone to counteract certain side effects of their antitumor treatment, like development of edema. Dexamethasone is also used as a direct chemotherapeutic agent in certain hematological malignancies, especially in the treatment of multiple myeloma.

Estradiol, named also as E2 (because it has two hydroxyl groups in its molecular structure, see Figure 20), 17β-estradiol or oestradiol; is the predominant estrogen during reproductive years (except in pregnancy periods). Estradiol is also present in males, however in lower levels. This hormone is produced principally in ovaries; smaller amounts of estradiol are also synthesized by the adrenal cortex, and (in men), by the testes. It can be also produced as an active metabolic product of testosterone. Estradiol has not only a critical impact on reproductive (female and male) and sexual functioning and pregnancy in human female (Carreau et al., 2003), but also affects other organs, including the bones (Carani et al., 1997) and brain (Simerly, 2002). In cases of hypoestrogenism, estradiol preparations are prescribed. If severe side effects of low levels of estradiol in a woman's blood are experienced (commonly at the beginning of menopause), hormone replacement therapy may be prescribed. In contrast, inducing a state of hypoestrogenism may be beneficial in certain situations where estrogens are contributing to unwanted effects, e.g., certain forms of breast cancer and premature closure of epiphyses. In addition, a derivative form of estradiol, ethinylestradiol, is a major component of hormonal contraceptive devices.

Progesterone is the major naturally occurring human progestogen. It is involved in the female menstrual cycle, pregnancy (supporting gestation) and embryogenesis. Progesterone is produced in the ovaries, the adrenal glands, and, during pregnancy, in the placenta. The use of progesterone and its analogues have many medical applications, both to address acute situations and the long-term decline of natural progesterone levels. For instance, it is used to control persistent anovulatory bleeding, to prepare uterine lining in infertility therapy and to support early pregnancy. It has also been demonstrated to be beneficial in preventing preterm birth (Fonseca et al., 2007).

Tamoxifen is a synthetic first generation selective estrogen receptor modulator. It is a mixed agonist/antagonist steroid as tamoxifen is an antagonist of the estrogen receptor in breast tissue but it is an agonist in other tissues such as the endometrium. Tamoxifen is the usual anti-estrogen therapy for hormone receptor-positive breast cancer in women because some breast cancer cells require estrogen to grow (Jordan, 2006). Tamoxifen has been used to treat premature puberty (Eugster et al., 1999), infertility (Steiner et al., 2005), bipolar disorders (Yildiz et al., 2008) and other problems.

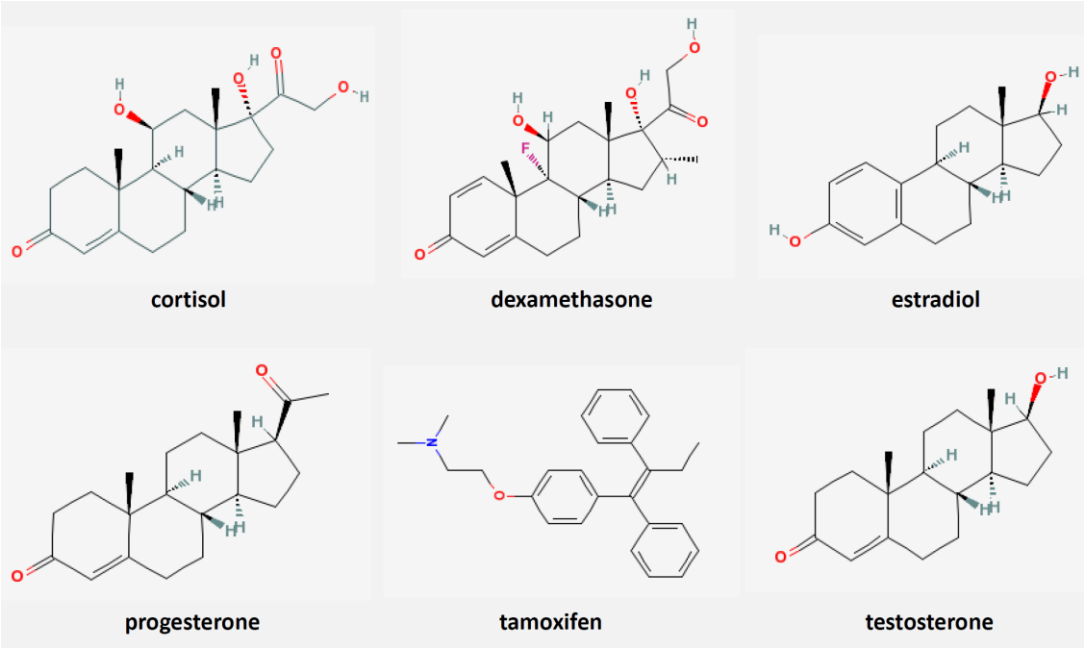

Figure 20. Structure of steroid hormones used in this study, including cortisol, dexamethasone, estradiol, progesterone, tamoxifen and testosterone.

Testosterone is the principal male sex steroid hormone (androgen) as it plays a key role in the development of male reproductive tissues and promotes secondary sexual characteristics. It has also anabolic effects including protein synthesis and bone maduration. Testosterone is primarily secreted in the testicles of males and the ovaries of females, although small amounts are also secreted by the adrenal glands. The original and primary use of testosterone is for the treatment of males who have too little or no natural endogenous testosterone production-males with hypogonadism. However, over the years, testosterone has also been given for many other conditions and purposes besides replacement, with varying success but higher rates of side effects or problems. Examples include reducing infertility, correcting lack of libido or erectile dysfunction, correcting osteoporosis, encouraging penile enlargement, encouraging height growth, encouraging bone marrow stimulation and reversing the effects of anemia, and even appetite stimulation (e.g. Davis et al., 2008).

5.1.2. Interaction of steroid hormones with ABCG2 and P-gp

Hormone regulation of ABC transporters has been a matter of extensive research. The presence of steroid-response elements (ERE, PRE) has already been reported in the ABCG2 promoter (Ee et al., 2004; Wang et al., 2008). Key players in hormone regulation events are nuclear receptors which may affect ABCG2 expression (Ee et al., 2004; Wang et al., 2008). Various glucocorticoids, including dexamethasone, efficiently interact with progesterone receptors (PGR) (Leo et al., 2004). Indeed, dexamethasone has been shown to down-regulate ABCG2 expression levels in breast cancer cells (Honorat et al., 2008). In addition, hormones such as estradiol and progesterone can regulate ABCG2

expression in human placental BeWo cells (Imai et al., 2005; Wang et al., 2008). Note that progesterone and estradiol are the two most important steroid hormones produced by the human placenta during pregnancy. Additionally, several studies have shown that pregnancy can affect expression and function of ABC transporters such as P-gp and MRP2 (Cao et al., 2002; Gil et al., 2005; Mathias et al., 2005). On the other hand, male-predominant expression of ABCG2 in rat kidney appears to be due to the suppressive effect of estradiol and male-predominant expression of ABCG2 in mouse liver appears to be due to the inductive effect of testosterone (Tanaka et al., 2005). In the case of P-gp, for example, it has been reported not to be induced by dexamethasone (Matsunaga et al, 2006).

Due to the critical importance of steroid hormones in multiple body processes and the involvement of ABC transporters in bioavailability of many compounds, interactions of steroid hormones with ABCG2 and P-gp ABC transporters have been also extensively studied (Table 6).

Table 6. Summary of *in vitro* experiments (including transport and accumulation) published for each steroid hormone and transporter (ABCG2 or P-gp). The type of experiment, the cell line used, concentrations and results are listed. The references are organized in alphabetic order per each transporter. When it was indicated or possible to calculate from the publication, the % of inhibition is written. *Radiolabeled compounds. Abbreviations: cyclosporine A (CsA), daunorubicin (DNR), digoxin (DGX), ^{125}I-iodoarylazidoprazosin (IAAP), non-transfected cells (NT), prazosin (PR), mitoxantrone (MXR), 2-Amino-1-methyl-6-phenylimidazo [4, 5-b] pyridine (PhIP), rhodamine123 (Rh123), topotecan (TPT), transfected cells (T), vinblastine (VB).

Cortisol

Transporter	Experiment	Cell type	Concentration [µM]	Result	Reference
ABCG2	Transport with cells (Transwell)	LLC-PK1 T	0.01 *	No substrate	Imai et al., 2003
	Transport with vesicles (with estrone-3-sulfate* at 50 nM)	K562 T	10 and 30 *	~30% inhibition	Imai et al., 2003
	Accumulation of MXR at 1 µM (flow cytometry)	Saos-2 T	50	~0% inhibition	Matsson et al., 2007
	Accumulation of MXR at 10 µM (flow cytometry)	MEF3.8 T	50	0% inhibition	Pavek et al., 2005
P-gp	Accumulation of VB at 23-45 nM *	SW620 Ad300 NT	30	No inhibition	Barnes et al., 1996
	Accumulation	MDR CEM "T"	1 *	Substrate	Farrel et al., 2002
	Transport with cells (Transwell)	LLC-PK1 T	0.009 *	Substrate	Karssen et al., 2001
	Transport with cells (Transwell)	LLC-PK1 T	0.01 *	Substrate	Ueda et al., 1992
	Efflux studies	DC-3F NT	1 *	Substrate	van Kalken et al., 1993
	Accumulation	DC3F/ A2780	1 *	Substrate	van Kalken et al., 1993
	Accumulation of DNR at 0.4 µM	A2780 NT	50 to 150	Inhibition	van Kalken et al., 1993
	Accumulation of VB at 1 µM *	J774.2 T?	50	No inhibition	Yang et al., 1989
	Transport with cells (Transwell)	LLC-PK1 T	50	Substrate	Yates et al., 2003

Dexamethasone

Transporter	Experiment	Cell type	Concentration [μM]	Result	Reference
ABCG2	Accumulation of MXR at 10 μM (flow cytometry)	MCF-7 T?	1-10	Inhibition	Elihan et al., 2010
	Transport with cells (Transwell)	MDCK-II T	2 *	No substrate	Pavek et al., 2005
	Transport with cells (Transwell) (with PhIP* at 2 μM)	MDCK-II T	50	~50% inhibition	Pavek et al., 2005
	Accumulation of MXR at 10 μM (flow cytometry)	MEF3.8 T	50	13% inhibition	Pavek et al., 2005
P-gp	Accumulation of VB at 23-45 nM *	SW620 Ad300 NT	30	No inhibition	Barnes et al., 1996
	Transport with cells (Transwell)	LLC-PK1 T	2 *	Substrate	Schinkel et al., 1995
	Transport with cells (Transwell)	LLC-PK1 T	0.02 *	Substrate	Ueda et al., 1992
	Accumulation of VB at 1 μM *	J774.2 T?	50	No inhibition	Yang et al., 1989
	Transport with cells (Transwell)	LLC-PK1 T	50	Substrate	Yates et al., 2003

Estradiol

Transporter	Experiment	Cell type	Concentration [μM]	Result	Reference
ABCG2	Accumulation of TPT at 20 μM (flow cytometry)	K562 T	100	Inhibition	Imai et al., 2002
	Transport with cells (Transwell)	LLC-PK1 T	0.01 *	No substrate	Imai et al., 2003
	Transport with vesicles	K562 T	0.03 *	No substrate	Imai et al., 2003
	Transport with cells (Transwell) (with MXR* at 50 nM)	LLC-PK1 T	30	Inhibition	Imai et al., 2003
	Transport with vesicles (with estrone-3-sulfate* at 50 nM)	K562 T	10 and 30 *	~50% inhibition	Imai et al., 2003
	Transport assay	*L. lactis* T	0.5 *	Substrate	Janvilisri et al., 2003
	Accumulation of MXR at 1 μM (flow cytometry)	Saos-2 T	50	58% inhibition	Matsson et al., 2007
	Transport with cells (Transwell)	MDCK-II T	2 *	Slight substrate	Pavek et al., 2005
	Transport with cells (Transwell) (with PhIP* and TPT* at 2 μM)	MDCK-II T	100	~100% inhibition	Pavek et al., 2005
	Accumulation of Bodipy-PR at 0.25 μM * (flow cytometry)	HEK T	100	Inhibition	Robey et al., 2003
P-gp	Accumulation of VB at 23-45 nM *	SW620 Ad300 NT	30	No inhibition	Barnes et al., 1996
	Transport with cells (Transwell)	MDCK-II T	No specified	No substrate	Kim & Benet., 2004
	Accumulation of VB at 1 μM *	J774.2 T?	50	No inhibition	Yang et al., 1989

Progesterone

Transporter	Experiment	Cell type	Concentration [μM]	Result	Reference
ABCG2	Transport with cells (Transwell) (with MXR* at 50 nM)	LLC-PK1 T	50	~25% inhibition	Imai et al., 2003
	Transport with vesicles (with estrone-3-sulfate* at 50 nM)	K562 T	10 and 30 *	~20% inhibition	Imai et al., 2003
	Accumulation of MXR at 1 μM (flow cytometry)	Saos-2 T	50	56% inhibition	Matsson et al., 2007
P-gp	Accumulation of VB at 23-45 nM *	SW620 Ad300 NT	30	Inhibition	Barnes et al., 1996

P-gp	Transport with cells (Transwell)	LLC-PK1 T	0.001 to 50 *	No substrate	Ueda et al., 1992
	Transport with cells (Transwell) (with CsA at 20 µM)	BeWo NT	0.05	No substrate	Ushigome et al., 2000
	Accumulation of DNR at 0.4 µM	A2780 NT	25 to 150	Inhibition	van Kalken et al., 1993
	Accumulation of VB at 1 µM *	J774.2 T?	50	Inhibition	Yang et al., 1989
	Efflux assays	J774.2 T?	1 *	No substrate	Yang et al., 1990

Tamoxifen

Transporter	Experiment	Cell type	Concentration [µM]	Result	Reference
ABCG2	Accumulation of MXR at 1 µM (flow cytometry)	Saos-2 T	50	64% inhibition	Matsson et al., 2007
	Accumulation of TPT at 20 µM (flow cytometry)	K562 T	30	Slight inhibition	Sugimoto et al., 2003
P-gp	Transport with cells (Transwell)	Caco-2	100	No substrate	Bekaii-Saab et al., 2004
	Transport with cells (Transwell) (with Rh123 at 5 µM)	Caco-2	10, 30, 60	Inhibition	Bekaii-Saab et al., 2004
	Accumulation	KB3-1 NT	20 *	No substrate	Callaghan & Higgins, 1995
	Accumulation of VB at 21 nM *	KB3-1 NT	0-60 *	Inhibition	Callaghan & Higgins, 1995

Testosterone

Transporter	Experiment	Cell type	Concentration [µM]	Result	Reference
ABCG2	Transport with cells	HEK T	0.03 *	No substrate	Gardner et al., 2008
	Accumulation of IAAP* at 3-5 nM	MCF-7 T	40	~5% inhibitor	Gardner et al., 2008
	Accumulation of MXR at 1 µM (flow cytometry)	Saos-2 T	50	6% inhibition	Matsson et al., 2009
P-gp	Accumulation of VB at 23-45 nM *	SW620 Ad300 NT	30	No inhibition	Barnes et al., 1996
	Transport with cells (Transwell) (with DNR at 35 nM or DGX at 25 nM)	LLC-GAS-COL150 T	50	No inhibition	Katoh et al., 2001
	Accumulation of DNR at 35 nM *	LLC-GAS-COL150 T	50	No inhibition	Katoh et al., 2001
	Accumulation of DNR at 0.4 µM	A2780 NT	50 to 150	Inhibition	van Kalken et al., 1993
	Accumulation of VB at 1 µM *	J774.2 T?	50	Inhibition	Yang et al., 1989

Cortisol has been reported not to be a substrate of ABCG2 in transport assays performed with polarized cells LLC-PK1 (Imai et al., 2003). This hormone has been described as a non-inhibitor of ABCG2 in accumulation assays with mitoxantrone (Pavek et al., 2005; Matsson et al., 2007). In comparison, a slight inhibition was reported by Imai et al. (2003) in transport assays with vesicles. To our knowledge, no ATPase assay with cortisol *versus* ABCG2 is available in scientific literature. When cortisol has been studied regarding the interaction with P-gp, it has been always described as a P-gp substrate in transport assays with LLC-PK1 cells (Ueda et al., 1992; Karssen et al., 2001; Yates et al., 2003); also in efflux studies and accumulation assays (van Kalken et al., 1993; Farrel et al., 2002). Cortisol was earlier described as well as a P-gp inhibitor (van Kalken et al., 1993). However, other authors reported cortisol not to be an

inhibitor of P-gp in accumulation assays (Yang et al., 1989; Barnes et al., 1996), in murine and human cells lines, respectively. P-gp ATPase activity has been measured with cortisol using vesicles from Sf9 insect cell (Rao et al., 1994) with a complete bell-shape curve as result. It was also measured in vesicles from hamster lung fibroblast where only activation of P-gp ATPase was found (Orlowski et al., 1996).

Dexamethasone has been described to not interact with the ABCG2 transporter, non as a substrate, probably neither as an inhibitor (Pavek et al., 2005). In contrast, recently it has been shown to be an ABCG2 inhibitor (Elaihan et al., 2010). Dissimilarly, dexamethasone has been shown to be a P-gp substrate in transcellular transport experiments with LLC-PK1 polarized cells (Ueda et al., 1992; Schinkel et al., 1995; Yates et al., 2003), also *in vivo* with knock-out mice (Schinkel et al., 1995); but not a P-gp inhibitor in accumulation evaluations (Yang et al., 1989; Barnes et al., 1996). No ATPase activity assays with ABCG2 or P-gp are published in literature for this steroid.

Estradiol was found to be a non-substrate of human ABCG2 in transport assays performed with LLC-PK1 cells and K562 (human immortalised myelogenous leukemia) cells at nM range concentrations (Imai et al., 2003); a slight substrate in MDCK-II cells at 2 µM (Pavek et al., 2005) and a substrate in *L. lactis* cells at 0.5 µM (Janvilisri et al., 2003). This fact demonstrates the importance of the kind of cells and the concentration employed in each experiment, already commented previously. As an ABCG2 inhibitor, no discrepancy between groups has been shown, estradiol has been always described as an ABCG2-inhibitor (Imai et al., 2002; 2003; Robey et al., 2003; Pavek et al., 2005; Matsson et al., 2007). A full bell-shape curve has been found in ABCG2-ATPase activity assays with vesicles from *L. lactis* (Janvilisri et al., 2003). Concerning the interaction of estradiol with P-gp, few experiments have been reported with no successful interaction between the steroid and the transporter neither as substrate or inhibitor (Yang et al., 1989; Barnes et al., 1996; Kim and Benet., 2004). However, when estradiol was studied in ATPase activity assays with vesicles from insect cells, a full P-gp bell-shape curve was obtained (Rao et al., 1994).

Regarding the interaction of progesterone with ABCG2, it has been studied only as an ABCG2 inhibitor. Low inhibition has been reported using transport and accumulation assays with different cell types (Imai et al., 2003; Matsson et al., 2007) (Table 6). A full bell-shape curve was found in ABCG2-ATPase activity assays with vesicles from *L. lactis* (Janvilisri et al., 2003). This steroid has been found not to be a P-gp substrate in transport assays at any concentration tried, i.e. between 0.001 to 50 µM (Yang et al., 1990; Ueda et al., 1992; Ushigome et al., 2000); but it has been described as a P-gp inhibitor in accumulation assays (Yang et al., 1989; van Kalken et al., 1993; Barnes et al., 1996) (Table 6). From the study of progesterone it was suggested that both transport and transport antagonism correlated with steroid hydrophobicity (Yang et al., 1989; Barnes et al., 1996). Progesterone has been broadly given as an example of a typical full bell-shape ATPase activity compound for P-gp despite the use of different cell types (Rao et al., 1994; Orlowski et al., 1996; Litman et al., 1997a; Kim and Benet., 2004).

Tamoxifen has been studied as well only as an ABCG2 inhibitor in accumulation experiments (Sugimoto et al., 2003; Matsson et al., 2007). Again, a full bell-shape curve was resulted in ABCG2-ATPase activity assays with vesicles from *L. lactis* also for this steroid (Janvilisri et al., 2003). Tamoxifen has been described not to be a P-gp substrate but an inhibitor in accumulation assays (Lee et al., 1994; Callaghan and Higgins, 1995), Caco-2 cell monolayers in a transwell system (Bekaii-Saab et al., 2004) and also in other studies (Gottesman et al., 1996; Wang et al., 2000). Relating to P-gp ATPase activity *versus* tamoxifen, full bell-shapes curves have been found in two studies using insect cells and mammary cells (Rao et al., 1994; Litman et al., 1997a).

Testosterone was found not to interact as a substrate or as an inhibitor of ABCG2 (Gardner et al., 2008; Matsson et al., 2009). As in the case of previous commented steroids, a full bell-shape curve was obtained in ABCG2-ATPase activity assays with vesicles from *L. lactis* also for this steroid (Janvilisri et al., 2003). In comparison, when working with vesicles from Sf9 cells or mammalian cells, only inhibition ABCG2-ATPase activity curves were acquired (Glavinas et al., 2007). Testosterone was found not to act as a P-gp inhibitor at concentrations lower than 50 µM (Barnes et al., 1996; Katoh et al., 2001); however, at higher concentrations, testosterone inhibits P-gp (van Kalken et al., 1993; Yang et al., 1989). No ATPase activity assay is published so far with P-gp *versus* testosterone.

In summary, interactions of steroid hormones with ABCG2 and P-gp ABC transporters have been extensively tested, especially regarding transepithelial transport experiments with polarized cells and accumulation assays (Table 6). ABCG2-ATPase activity assays are mainly shown in one publication by Janvilisri et al. (2003) and concerning P-gp-ATPase activity assays, they had been performed mostly by three groups (Rao et al., 1994; Orlowski et al., 1996; Litman et al., 1997a). In conclusion, in general, hormones are not substrates of ABCG2 (except, maybe, estradiol), and not all of them interact as inhibitors of ABCG2 (exceptions are dexamethasone, estradiol, and tamoxifen) in transport and accumulation assays. However, ABCG2-ATPase activity is visible for all of them. In the case of P-gp, only cortisol and dexamethasone are substrates in transport assays. Progesterone, tamoxifen and testosterone are the only inhibitors in accumulation experiments. In contrast, again a P-gp-ATPase activity is achieved for all these steroids. An explanation of these, apparently, inconsistencies has not been yet presented. A general understood of steroid hormones regarding their mechanism of interaction with P-gp and ABCG2 has not been yet precisely explained.

5.2. Fluoroquinolones

The quinolone antibiotics are synthetic compounds developed through structural modification of the “4-quinolone” molecule. They have been employed in the treatment of bacterial infections for nearly 50 years. The first quinolone, nalidixic acid, was identified as a remarkably effective agent in the treatment of urinary tract infections, but it suffered from poor oral absorption and a short half-life,

while its efficacy was limited to a narrow range of anaerobic Gram-negative organisms (Ball, 2000; Scholar, 2002). Thus, intensive studies led to the development of successive **generations** of synthetic antimicrobial drugs that mainly improved their *in vitro* antimicrobial activity by increasing the spectrum of activity and enhancing potency.

One of the earliest quinolone modifications was substitution of a hydrogen by a fluorine atom at position 6 of the 4-quinolone ring, resulting in these agents being referred to as fluoroquinolones (FQs); flumequine was the first FQ (Ball, 2000; Scholar, 2002). Second-generation FQs (e.g., ciprofloxacin, enoxacin, norfloxacin, and ofloxacin) demonstrated increased activity against Gram-negative bacteria, as well as *Staphylococcus* species, and improved tissue penetration, thus, they could be used for certain respiratory tract and soft-tissue infections. Third generation FQs (e.g., grepafloxacin, levofloxacin, pefloxacin and sparfloxacin) have prolonged half-life and are also effective against some Gram-positive organisms and atypical pathogens, including species of *Chlamydia*, *Haemophilus*, *Legionella*, and *Mycoplasma* (Lipsky and Baker, 1999; Ball, 2000; Scholar, 2002). Together with excellent oral bioavailability, their therapeutic indications were expanded to illness treatment of community-acquired pneumonia, chronic bronchitis, pyelonephritis, and prostatitis (Hooper, 2000; Oliphant and Green, 2002). Fourth-generation compounds (e.g., gatifloxacin, moxifloxacin, and trovafloxacin) exhibit a further enhancement of activity against a still wider range of bacterial pathogens, increasing their therapeutic indications further, including penicillin- and cephalosporin-resistant pneumonias (Lipsky and Baker, 1999; Ball, 2000; Scholar, 2002).

FQs are widely employed as orally and parenterally administered drugs in the treatment of bacterial diseases, including severe systemic infections because of their broad spectrum and potent antibacterial activity (Peterson, 2001, Blondeau, 2004). In fact, since their introduction in the late 1980s, they have become the most commonly prescribed class of antibiotics to adults in USA (Linder et al., 2005) and were in the fifth position in Europe in 2002 (Goossens et al., 2005), increasing each year.

Nonetheless, FQs have been associated with a number of significant **adverse effects**, which has resulted in a restriction of FQ use as primary therapeutics for many indications (Mandell and Tillotson, 2002; Stahlmann, 2002; Sprandel and Rodvold, 2003). The most common adverse effects associated with these agents range from mild effects on the gastrointestinal tract, such as nausea, vomiting, and diarrhea to moderate or severe phototoxicity to extremely serious CNS effects, including seizures, anxiety, and toxic psychosis (Mandell and Tillotson, 2002; Stahlmann, 2002; Sprandel and Rodvold, 2003). In some cases, toxicity appears to be associated with particular moieties present in the chemical structure of FQs (Mandell and Tillotson, 2002; Stahlmann and Lode, 2002). A number of other rare adverse events have been reported, including severe renal (crystalluria, interstitial nephritis, hemolytic-uremic syndrome, and acute renal failure) and hepatic toxicities, cardiac effects, hypoglycemia, and tendon rupture (Lipsky and Baker, 1999; Scholar, 2002). Currently, further structural modifications aimed improving their pharmacokinetic properties and reducing adverse reactions are being

investigated. Certainly, some later fourth-generation FQs (e.g., gemifloxacin) exhibit significant reduction in adverse effects (Ball, 2000).

Fluoroquinolone **mechanism of action** against bacteria consists on inhibition of two enzymes involved in bacterial DNA synthesis, DNA gyrase and topoisomerase IV, both of which are DNA topoisomerases that human cells lack and that are essential for bacterial DNA replication, thereby enabling these agents to be both specific and bactericidal (Hooper, 1999).

One important problem for FQs is the development of **resistances**; therefore, they are often used when other treatments failed. Fluoroquinolone resistance develops through two main mechanisms: alterations in the drug target enzymes and alterations in access to the drug target enzymes. Alterations in the drug target enzymes may be sub-classified as mutations in DNA gyrase and mutations in topoisomerase IV. Alterations in access to the drug target enzymes include the expression of multidrug resistant (MDR) membrane-associated efflux pumps, which actively pump drug out of the bacterial cell. MDR efflux pumps have been shown to reduce fluoroquinolone activity and contribute to low-level resistance (Hooper, 1999). Additionally, in Gram-negative organisms, decreased levels of outer membrane proteins responsible for drug diffusion, such as general diffusion porins, have also been shown to reduce the accumulation of drug within the cytoplasm (Hirai et al., 1986; 1987). This mechanism of reducing drug diffusion into the cell acts in concert with MDR efflux pumps to contribute to bacterial resistance (Hooper, 1999).

Concerning the **pharmacokinetic properties,** FQs are rapidly absorbed from the intestine and distributed in tissues and fluids, with a bioavailability of nearly 90% for some of them. Not surprisingly, urine and biliary FQ concentrations often greatly exceed those in plasma as a consequence of the excretory functions of the kidney and liver. Indeed, for many FQs, their unchanged urinary levels are considerably high against most urinary pathogens, explaining their therapeutic success in the treatment of urinary tract infections (Sorgel et al., 1989; Scholar, 2002). Similarly, for those FQs which undergo extensive intestinal secretion or hepatic metabolism, the unchanged drug and metabolite concentrations in feces are high, rendering their effectiveness in the treatment of many gastrointestinal infections (Sorgel et al., 1989; Scholar, 2002).

5.2.1. Fluoroquinolones used in this study

Ciprofloxacin (Figure 21) is a second-generation fluoroquinolone antibiotic. Its spectrum of activity includes most strains of bacterial pathogens responsible for respiratory, urinary tract, gastrointestinal, and abdominal infections, including Gram-negative (*E. coli, H. influenzae, K. pneumoniae, L. pneumophila* and *P. aeruginosa*), and Gram-positive (methicillin-sensitive but not methicillin-resistant *S. aureus, S. pneumoniae, S. epidermidis, E. faecalis*, and *S. pyogenes*) bacterial pathogens (Solomkin et al., 2010). Ciprofloxacin is valued for this broad spectrum of activity, excellent tissue penetration, and for their availability in both oral and intravenous formulations. This is why it is

one of the most commonly prescribed antibacterial (Nelson et al., 2007). Its bioavailability is approximately 70-80% and the biotransformation is hepatic, with an elimination half life of 4 h.

Enrofloxacin is a veterinary fluoroquinolone similar to ciprofloxacin (Figure 21); indeed, it is partly de-ethylated *in vivo* to ciprofloxacin. It has shown its efficacy in the treatment of the main bacterial processes affecting farm animals as enrofloxacin has antibacterial activity against a broad spectrum of Gram-negative and Gram-positive bacteria including *S. aeruginosa, Klebsiella, E. coli, Enterobacter, Shigella, Yersinia or Staphylococcus* (Schroder, 1989; Martinez et al., 2006).

Moxifloxacin (Figure 21) is a fourth-generation synthetic fluoroquinolone with activity against Gram-positive and Gram-negative bacteria such as *S. aureous, S. epidermis, S. pneumoniae, H. influenza, B. anthracis, Klebsiella* or *Enterobacter.* As a result it is administrated via oral, intravenous and in the eye to treat respiratory infections as bronchitis and sinusitis, conjunctivitis, skin and intraabdominal infections, and other infections including meningitis, pneumonia, anthrax and tuberculosis (Miravitlles and Anzueto 2008; Fouad and Gallagher 2011). Following oral administration, moxifloxacin is rapidly and almost completely absorbed, with an absolute bioavailability of approximately 91% (Stass et al., 2001). Moxifloxacin, as a new FQ exhibits wider systemic distribution characteristics and longer duration of action as compared to the older compounds (Stein, 1996; Zlotos et al., 1998). This may partially be a consequence of increased plasma protein binding, resulting in decreased elimination. This FQ also exhibits increased tissue penetration, allowing reaching higher intracellular concentrations (Stein, 1996; Zlotos et al., 1998). Systemically, this translates into significantly greater FQ levels in target organs. Moxifloxacin is excreted via renal and biliary/fecal pathways as unchanged drug as well as in the form of metabolites (Stass et al., 2002).

Norfloxacin is the main active pefloxacin metabolite and discloses the same potent antibacterial activity (Thibault et al., 1981). Norfloxacin (Figure 21) as a second-generation FQ was the first FQ used in the management of ocular infectious diseases, introduced for the treatment of bacterial conjunctivitis. It is also employed in urinary, including cystitis infections, moreover in gonorrhea and prostatitis. Administrated via oral, intravenously or in eye, norfloxacin demonstrated anti-pseudomonal activity, activity against Gram-negative bacilli, as well as limited activity against susceptible Gram-positive bacteria, such as *S. aureous, S. epidermis, K. pneumoniae, E. coli* or *Enterobacter* (Ito et al., 1980). Norfloxacin is rapidly absorbed after oral administration with a large distribution volume (Gilfillan et al., 1984; Wise 1984); however, other authors state that bioavailability of this FQ is certainly low, 30-40% (Sörgel et al., 1989). After 1 hour, concentrations of drug in organs were higher than the plasma levels; tissues with higher concentrations were kidney and liver (Gilfillan et al., 1984). It has been suggested that the main site of norfloxacin metabolism is liver; however, it is mainly excreted via active renal tubular secretion to urine. Six metabolites of norfloxacin have been described.

Pefloxacin (Figure 21) is a third generation fluoroquinolone. Its administration via oral or intravenous is used to treat urinary, genitourinary, gastrointestinal, respiratory, skin, bone and joint

infections due to susceptible bacteria such as *E. coli, Enterobacter, Salmonella, Legionella, Shigella, Yersinia, Vibrio*… In the first and more complete study of *in vivo* pharmacokinetics for pefloxacin using several species (Montay and Tassel, 1984), this fluoroquinolone was shown to be well absorbed by oral route. Importantly, except in brain, concentrations in most of the organs and tissues tested in rats and dogs were higher than the plasma levels, indicating an extensive distribution, explaining why pefloxacin is successful in many kinds of infections. The antimicrobial activity was due to unchanged drug in a percentage of 84% in human plasma, with half-life ranges from 1.9 h in mice to 8.6 h in humans. Pefloxacin is excreted and metabolized in kidney and liver, thus, urine and bile contained uncharged drug and several metabolites, where the principal metabolite was norfloxacin. When antibacterial activity of pefloxacin metabolites was analyzed, only norfloxacin was found to be as active as pefloxacin *in vitro* (Montay and Tassel, 1984). Therefore, the antimicrobial activity in urine was essentially due to pefloxacin and norfloxacin.

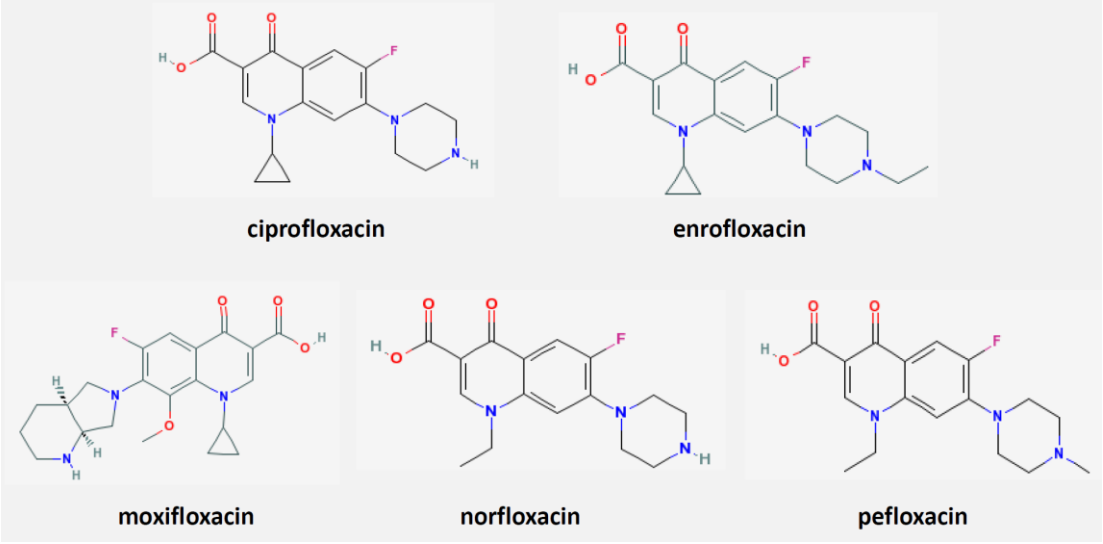

Figure 21. Structure of several fluoroquinolone used in this study, including ciprofloxacin, enrofloxacin, moxifloxacin, norfloxacin and pefloxacin. The common feature for all of them is the fluorine atom at position 6 of the 4-quinolone ring.

5.2.2. Interaction of fluoroquinolones with ABCG2 and P-gp

One of the most important problems in the clinical use of fluoroquinolones, apart from the adverse effects, is the development of resistances. There is increasing evidence to suggest that interference between drugs and ATP binding cassette (ABC) proteins is a key mechanism underpinning clinically important drug interactions (Marchetti et al., 2007). The possible role of ABC transporters in the evolution of resistances to antibiotics was earlier suggested (Putman et al., 1999). In addition, it has been proposed that the interaction of ABC transporters with fluoroquinolones could be associated with

the emergence of resistances (Merino et al., 2006; Michot et al., 2004). Moreover, ABC transporters could affect fluoroquinolone pharmacokinetics and then the efficacy of the antibiotic treatment.

It has been already reported that the bioavailabilities of several fluoroquinolones are affected by the ABCG2 activity (e.g., ciprofloxacin (Merino et al., 2006), enrofloxacin (Pulido et al., 2006), danofloxacin (Real et al., 2011)), indicating that ABCG2 plays a role in the pharmacokinetics and milk secretion of these antibiotics. However, not all fluoroquinolones share this transport mechanism *in vivo*; for example, no *in vivo* interaction between sparfloxacin and ABCG2 could be found in our laboratory (Real, Egido and Merino, unpublished results). It was suggested that minor structural differences in fluoroquinolones may play a key role in transporter recognition (Michot et al., 2004). On the other hand, fluoroquinolones have been shown to be weak inhibitors for efflux transporters (Haritova et al., 2007). Certainly, several fluoroquinolones have been shown not to interact as inhibitors of ABCG2, e.g. ciprofloxacin, norfloxacin (Merino et al., 2006) and enrofloxacin (Pulido et al., 2006).

Concerning the interaction of ciprofloxacin with ABCG2, it has been shown to be an *in vitro* substrate employing MDCK-II cells (Merino et al., 2006; Haslam et al., 2011) and Caco-2 cells (Haslam et al., 2011) in transcellular experiments. Furthermore, this interaction was also visible when ciprofloxacin was applied to animal models (Merino et al., 2006; Ando et al., 2007). On the contrary, no effect on inhibition of ABCG2 was found by addition of ciprofloxacin in mitoxantrone accumulation assays (Merino et al., 2006) (Table 7).

Ciprofloxacin has earlier been suggested not to be a substrate of P-gp in *in vitro* transport assays with Caco-2 cells using verapamil as inhibitor (Cavet et al., 1997). Two years later, Dautrey et al. (1999) showed that P-gp has no *in vivo* effect on ciprofloxacin. Subsequent studies revealed similar results. For instance, *in vitro* transcellular transport assays with LLC-PK1 cells (de Lange et al., 2000; Yamaguchi et al., 2004; Park et al., 2011), MDCK-II (Lowes and Simmon, 2002; Park et al., 2011), Caco-2 (Lowes and Simmon, 2002; Yamaguchi et al., 2004) and mouse macrophages (Michot et al., 2004; 2005), showed no interaction of ciprofloxacin as P-gp substrate. Similarly, *in vitro* experiments of transport (de Lange et al., 2000) and accumulation assays (Haritova et al., 2007) demonstrated no P-gp inhibition using ciprofloxacin. In addition, no significant effect was obtained when the possible role of ciprofloxacin on P-gp *in vivo* was evaluated using mice (de Lange et al., 2000) and rats (Rodriguez-Ibañez et al., 2006; Haslam et al., 2011). By contrast, a possible interaction between ciprofloxacin and P-gp *in vivo* (with rats) and *in vitro* (with Caco-2 cells) was proposed by Rodríguez-Ibañez et al. (2003). Indeed, Ruiz-García et al. (2002), in transport assays with Caco-2 cells, found a positive interaction of ciprofloxacin as a substrate of P-gp. This result was also found for MDCK-I cells by Park et al. (2011). In conclusion, generally, ciprofloxacin was found not to interact with P-gp as a substrate nor as an inhibitor neither when studied with transport assays using several types of cells, nor when studied in *in vivo* experiments. However, in few cases, typically working with Caco-2 cells, it has been possible to show ciprofloxacin as a P-gp substrate.

Table 7. Summary of published results about the interaction of each fluoroquinolone with the transporters ABCG2 and P-gp. The type of experiment, the used cell line or tissue, the concentrations and results are listed. The references are organized in alphabetic order per each transporter. When it was indicated or possible to calculate from the publication, the % of inhibition is written. Acronyms: albendazole sulfoxide (ABZSO), ciprofloxacin (CIP), cyclosporine A (CsA), doxorubicin (DOX), fumitremorgin (FTC), genistein (GEN), intravenous (iv), Knock-out (KO), mitoxantrone (MXR), moxifloxacin (MXF), oral (o), rhodamine 123 (Rho-123), verapamil (VRP), vinblastine (VB), wild-type (WT).[a] For *in vitro* experiments cell type used, for *in vivo* and *ex vivo* experiments tissue or fluid analyzed. For *in vivo* experiments, the animal and the via used for administration are indicated. Concentrations not accurately specified by the authors are indicated with an interrogation symbol.

Ciprofloxacin

Transporter	Experiment	Cell type/ Tissue [a]	Concentration [μM]	Result	Reference
ABCG2	*In vivo*, WT & KO mice, iv	Bile, brain, kidney & liver	3	*In vivo* substrate	Ando et al.,2007
	Transport (with Ko143 at 1 μM)	MDCK-II & Caco-2	10	Substrate	Haslam et al.,2011
	Ex vivo secretory permeability (with Ko143 at 0.1-10 μM)	Human & rat intestine	30 & 100	Substrate	
	Transport	MDCK-II	10	Substrate	Merino et al.,2006
	Accumulation of MXR at 5 μM	MDCK-II	100	No inhibitor	
	In vivo, WT & KO mice, o and iv	Milk & plasma	33	*In vivo* substrate	
P-gp	Transport (with VRP at 100-500 μM)	Caco-2	100	No substrate	Cavet et al., 1997
	Transport of VB at 10 mM	Caco-2	3000	No inhibitor	
	In vivo, rat, iv (with several substrates)	Bile, intestinal fluid & plasma	38	No *in vivo* substrate	Dautrey et al., 1999
	Transport	LLC-PK1	10	No substrate	de Lange et al., 2000
	Transport of Rho-123 at 1 μM	LLC-PK1	100	~10% inhibition	
	In vivo, WT & KO mice, intra-arterial infusion	Brain	0.05/min	No *in vivo* substrate	
	Ex vivo secretory permeability (with VRP at 100 μM)	Rat intestine	100	No substrate	Haslam et al.,2011
	Accumulation of Rho-123 at 0.1 & 0.5 μM	Hen splenocytes	1.6-50	~6% inhibition	Haritova et al., 2007
	Transport	MDCK-II, Caco-2 & T84	10	No substrate	Lowes & Simmons, 2002
	Transport of VB at 10 μM	MDCK-II	10?	No inhibitor	
	Accumulation of CIP (with VRP at 100 μM & GF120918 at 1 (2) μM)	Mouse macrophage	50 (16.5)	No substrate	Michot et al., 2004 (2005)
	Transport	MDCK-I	25 & 100	Substrate	Park et al.,2011
	Transport	LLC-PK1 & MDCK-II	25	No substrate	
	Transport (with several inhibitors)	Caco-2	50	Possible interaction	Rodríguez-Ibañez et al., 2003
	In vivo, rat, i*n situ* perfusion in gut (with several inhibitors)	Luminal fluid	50	Possible interaction	
	In vivo, rat, i*n situ* perfusion in gut (with VRP at 2 mM)	Luminal fluid	1.5	No *in vivo* substrate	Rodríguez-Ibañez et al., 2006
	Transport (with several inhibitors)	Caco-2	50?	Substrate	Ruiz-García et al.,2002

Pgp	Transport (with several inhibitors)	LLC-PK1 & Caco-2	2	No substrate	Yamaguchi et al., 2004

Enrofloxacin

Transporter	Experiment	Cell type/ Tissue [a]	Concentration [µM]	Result	Reference
ABCG2	Transport	MDCK-II	10	Substrate	Pulido et al., 2006 & Real et al., 2011
	Accumulation of MXR at 5 µM	MDCK-II	200	Human inhibition No mice inhibition	Pulido et al., 2006
	In vivo, sheep, iv (with GEN at 3 µM and ABZSO at 7 µM)	Milk & plasma	7	*In vivo* substrate	
P-gp	Accumulation of Rho-123 at 0.1 & 0.5 µM	Hen splenocytes	1.6-50	~9% inhibition	Haritova et al., 2007

Moxifloxacin

Transporter	Experiment	Cell type/ Tissue [a]	Concentration [µM]	Result	Reference
ABCG2					
P-gp	Transport (with several inhibitors)	Calu-3	50	Substrate	Brillault et al., 2009
	Accumulation of MXF (with VRP at 100 µM & GF120918 at 2 µM)	Mouse macrophage	11.4	No substrate	Michot et al., 2005
	Accumulation of MXF (with VRP at 100 µM)	Mouse macrophage	50	MXF [c]	Vallet et al., 2011
	In vivo, human, o	Plasma	11.4/day	No *in vivo* substrate	Weiner et al., 2007

Norfloxacin

Transporter	Experiment	Cell type/ Tissue [a]	Concentration [µM]	Result	Reference
ABCG2	Transport	MDCK-II	10	Substrate	Merino et al.,2006
	Accumulation of MXR at 5 µM	MDCK-II	200	No inhibitor	
P-gp	Transport	LLC-PK1	10	No substrate	de Lange et al., 2000
	Transport of Rho-123 at 1µM	LLC-PK1	100	~10% inhibition	
	In vivo, WT & KO mice, intra-arterial infusion	Brain	0.05/min	No *in vivo* substrate	
	Transport of VB at 10 µM	MDCK-II	10?	No inhibitor	Lowes & Simmons, 2002
	Transport of CsA at 0.0068 µM	MDCK-II	500	No inhibitor	Sikri et al., 2004
	Accumulation of DOX at 5 µM	P388	500	Inhibitor	Zhao et al., 2002

Pefloxacin

Transporter	Experiment	Cell type/ Tissue [a]	Concentration [µM]	Result	Reference
ABCG2	Transport	MDCK-II	3	Substrate	Kodaira et al., 2011
P-gp	Transport	LLC-PK1	10	No substrate	de Lange et al., 2000
	Transport of Rho-123 at 1µM	LLC-PK1	100	~10% inhibition	
	In vivo, WT & KO mice, intra-arterial infusion	Brain	0.05/min	No *in vivo* substrate	
	Transport	LLC-PK1	3	Substrate	Kodaira et al., 2011
	Transport of VB at 10 µM	MDCK-II	10?	No inhibitor	Lowes & Simmons, 2002

Pgp	*In vivo*, rat, iv (with CsA at 8.3 μM)	Bile, brain & plasma	21.5	No *in vivo* substrate	Tsai 2001

Enrofloxacin was found to interact as an ABCG2 substrate *in vitro* (Pulido et al., 2006; Real et al., 2011) and *in vivo* (Pulido et al., 2006). No inhibition in mice but in human was obtained when studying the interaction as inhibitor of ABCG2 by the same authors. This FQ has been shown not to inhibit P-gp in accumulation assays (Haritova et al., 2007). To our knowledge, no more literature is available regarding the interaction of enrofloxacin with P-gp.

Moxifloxacin interaction with P-gp has been widely studied, although obtaining opposite results in transepithelial transport assays studying the drug as a substrate (Michot et al., 2005; Brillault et al., 2009) and no clear effect in *in vivo* experiments with humans (Weiner et al., 2007). However, there is a lack of knowledge concerning a direct interaction of moxifloxacin with ABCG2 (Table 7).

Norfloxacin has been shown to be subject to active intestinal efflux (Griffiths et al., 1994; Rabbaa et al., 1996), thus, it could be an indication that an ABC transporter is involved in its pharmacokinetics. Indeed, norfloxacin is *in vitro* transported by ABCG2 (Merino et al., 2006). Therefore, ABCG2 could be the best candidate to be involved in norfloxacin pharmacokinetics. The interaction of norfloxacin with ABCG2 in mitoxantrone accumulation assays was also published by Merino et al. (2006); no significant inhibition interaction between drug and transporter was found. Norfloxacin was not detected in maternal milk in human after oral administration (Wise, 1984); however, it was detected in milk from other species as sheep (Soback et al., 1994) and cows (Gips and Soback, 1999). Consequently, ABCG2 might be also involved in norfloxacin milk pharmacokinetics. However, P-gp seems not to interact with norfloxacin as a substrate *in vitro* (with LLC-PK1) nor *in vivo* (with mice) (de Lange et al., 2000), neither as an inhibitor in transport assays (de Lange et al., 2000; Lowes and Simmons, 2002; Sikri et al., 2004) with LLC-PK1 and MDCK-II, respectively. Nevertheless, in accumulation assays with doxorubicin, Zhao et al. (2002) found norfloxacin as an inhibitor of P-gp.

Pefloxacin has been suggested to be actively transported in monocytes (Memin et al., 1996) and intestine (Gilfillan et al., 1984). Pefloxacin *in vitro* interaction with murine Abcg2 in MDCK-II cells has been demonstrated (Kodaira et al., 2011). However, since species differences have been reported regarding fluoroquinolone transport (Merino et al., 2006; Real et al., 2011), human ABCG2 transport remains to be demonstrated. In addition, pefloxacin has been detected in female lactating milk in species such as humans (Giamarellou et al., 1989), goats (Abd El-Aty and Goudah, 2002), and camels, (Goudah et al., 2008). This fact may indicate the possible role of ABCG2 in the mammary glad to efflux this fluoroquinolone to milk, still not elucidated. The role of P-gp in pefloxacin transport has been shown to be negligible as a substrate, both *in vitro* (de Lange et al., 2000) and *in vivo* (de Lange et al., 2000;

Tsai, 2001), also as an inhibitor (de Lange et al., 2000; Lowes and Simmons, 2002). Nonetheless, current results have shown pefloxacin as a P-gp substrate (Kodaira et al., 2011).

Besides, despite the interaction of several fluoroquinolones with ABCG2 and P-gp have been published with cell-based and *in vivo* experiments (summarized in Table 7), ATPase activity assays neither a complete general understanding of this family of antibiotics regarding the interaction with these two ABC transporters at the molecular level has not been yet presented. It should be noted that fluoroquinolones are zwitterionic compounds and very hydrophilic (Mulgaonkar et al., 2012); these characteristics may play a big role in the interactions with P-gp and presumably with ABCG2. For instance, it is already known that usually, P-gp does not take negative charged compounds (Seelig, 1998) and hydrophilic compounds are hardly taken by P-gp.

In conclusion, a general understanding of fluoroquinolones regarding the molecular mechanism for interaction with P-gp and ABCG2 has not been yet precisely explained. Furthermore, the possible effect of ABCG2 on the pharmacokinetics of norfloxacin, pefloxacin and moxifloxacin remains to be clarified.

6. Methodological bases for the study of drug interactions with ABC transporters: advantages and disadvantages

Due to the high number of possible transporter-based drug interactions, it is impossible to test each one of these in the clinic. Therefore, laboratory methods to predict the potential of a clinically significant interaction between a substrate and a drug that acts as an inhibitor or an inducer need to be explored. Thus, *in vitro* assays with cells or tissues and *in vivo* methods with laboratory animals have been developed to predict those interactions that are likely to be clinically significant. Different studies may assign the same compound differently, which additionally complicates literature mining. Indeed, ~ 25% of the compounds were assigned inconsistently concerning the interaction with ABCG2 (Poguntke et al., 2010). Therefore, often a combination of assays is required to accurately describe the full interaction spectrum of a given compound with ABC transporters. The pros and cons of the most common assays used to study drug interactions with ABC transporters are summarized in Table 8.

Table 8. Summary of pros and cons of different *in vitro* and *in vivo* models, most of them used in this study.

	Assay	**Advantages**	**Disadvantages**	**References**
In vitro	ATPase activity	Low cost, high-throughput, simplicity and reproducibility. Tool to identify substrates and inhibitors.	Inconsistency between ATPase activity and the transport rate of some drugs, false positives and negatives hits, the disposition of substrates cannot be monitored.	Glavinas et al., 2004; Hegedus et al., 2009; Nicolle et al., 2009; Giacomini et al., 2010
	Vesicular transport	High-throughput. Tool to identify substrates and inhibitors.	Sensitive to the passive permeability: false negative hits.	Xia et al., 2005; Hegedus et al., 2009
	Photoaffinity labeling	Tool for studying details of the molecular mechanism.	Technologically complex and difficult procedures, generally does not distinguish between substrates and inhibitors.	Hegedus et al., 2009
	Cytotoxicity	The accumulation of compounds can be reflected by cytotoxicity.	Assay limited to antiproliferate compounds	Xia et al., 2005; Hegedus et al., 2009
	Transcellular transport	Tool to identify substrates and inhibitors.	Problems with endogenous transporters; passive permeability: false negative hits, high cost and work.	Xia et al., 2005; Glavinas et al., 2007; Poguntke et al., 2010
	Accumulation	Tool for studying transporter function, tool to identify inhibitors.	False negative hits, as it may underestimate compounds with low permeability, little information on molecular mechanisms.	Xia et al., 2005; Glavinas et al., 2007; Sharom, 2008; Poguntke et al., 2010
	Cytosensor microphysiometer	Tool for studying details of the cellular metabolism in real time.	False negative hits. High cost and work.	Landwojtowicz et al., 2002; Gatlik-Landwojtowicz et al., 2004; Aänismaa and Seelig, 2007
In vivo	Knock-out mice	Tool for studying pharmacokinetics, pharmacodynamics and drug-drug interactions.	Expensive, low-throughput. Many variables should be considered carefully in the interpretation of data and extrapolation across species.	Vlaming et al., 2009; Giacomini et al., 2010

6.1. *In vitro* experiments

6.1.1. Membrane-based assay systems

One possible option for low cost and high-throughput analysis of ABC multidrug transporters is the application of isolated membrane preparations from cells overexpressing the protein of interest (Sharom et al., 1999; Glavinas et al., 2004). The use of low ionic strength buffers, containing no bivalent cations, throughout the membrane preparation steps promotes the formation of open membrane sheets and/or inside-out vesicles (Steck et al., 1970). This membrane arrangement is crucial, since the substrate binding sites have to be accessible to both ATP and the investigated molecules. Transporter-expressing membranes produced can be collected by ultracentrifugation; the pellet is then suspended in hypotonic or isotonic buffer and stored at -80 °C or in liquid nitrogen until use (Hegedus et al., 2009). Membrane-based assay systems include ATPase activity assays, vesicular transport assay and photoaffinity labeling.

ATPase activity assays. As stated previously, ABC transporters need ATP to perform the transport of the drug out of the cell. Thus a process coupled to drug efflux is hydrolysis of ATP, leading to formation of ADP and inorganic phosphate (Pi). Any drug that interacts with the transporter influences the ATP consumption and thus the formation of inorganic phosphate. However, the hydrolyzing step occurs inside the cell, which is rather difficult to monitor. The solution is to work with inside-out vesicles: the cells are disrupted, and then the membrane fragments containing the ABC protein are isolated with several centrifugation steps. Afterward, these fragments reassemble predominantly as inside-out (the nucleotide-binding sites toward the exterior) vesicles. In those vesicles, the inorganic phosphate appears in the medium upon ABC transporter activation; a following colorimetric reaction is used to measure the Pi release concentration (e.g. Doige and Sharom, 1992). In the case of transported substrates, an increased turnover and related ATP hydrolysis can be monitored. Furthermore, since some ABC transporters as P-gp and ABCG2 have a basal ATPase activity in the absence of externally applied drug due to transport of endogenous substrate in the membranes or a partially uncoupled form of the protein (Ozvegy et al., 2001; Al-Shawi et al., 2003), even the effect of an inhibitor of the transporter will be measurable, since inhibitors decrease the basal transporter activity.

The first documentation of the applicability of such an assay system was with the P-gp protein (Doige and Sharom, 1992; Sarkadi et al., 1992). Due to their relatively high protein expression yields, baculovirus-infected insect ovary cells (Spodoptera frugiperda, Sf9) are widely used to attain membranes overexpressing various ABC transporters (Sarkadi et al., 1992; Bakos et al., 2000; Bodo et al., 2003). As a caveat, transporters in Sf9 membrane vesicles may be functionally impaired due to the low cholesterol content of the insect cell membranes or because of improper protein glycosylation in these cells. It has been shown that differences in the glycosylation status of several ABC multidrug transporters, including ABCG2, do not affect functionality (see Hegedus et al., 2009 for review).

Membranes prepared from human expression systems have also been widely used in the field of ABC transporters (Loe et al., 1996; Sharom et al., 1999; Hirohashi et al., 2000). Unfortunately, these expression systems usually yield significantly lower expression levels that are insufficient to measure the ATPase activity of the transporter. Regarding ABCG2, most of the studies used ABCG2-enriched insect cell plasma membranes, although plasma membranes from other expression systems such as HEK cells, *P. pastoris*, and *L. lactis* or purified ABCG2 were also utilized (Ni et al., 2010b). The first ABCG2 ATPase activity assays using Sf9 membranes were reported on the R482G version of the transporter (Ozvegy et al., 2001). In the case of P-gp, some of the cell lines such as human KB 3-1, HEK293, and Chinese hamster ovary LR- 73, due to high level of other ATPases and/or alkaline phosphate, are not suitable for the measurement of P-gp-associated ATPase activity in crude membranes. In these cases, P-gp has to be at least partially purified to assay its ATPase activity. Mouse NIH-3T3 fibroblasts are more appropriate, due to the low level of background ATPases and other phosphatases activities (Ambudkar, 1998).

To analyze data obtained from ABCG2 ATPase activity release, results have been generally evaluated with the classical Michaelis– Menten kinetics (Ozvegy et al., 2001), probably in most of the cases the achieved ATPase curves were simple, i.e. only activation or only inhibition. However, the P-gp ATPase activity measured as a function of the substrate concentration generally yields bell-shaped profiles which are best interpreted in terms of two-site binding models (Litman et al., 1997b; Al-Shawi et al., 2003). The model proposed by Al-Shawi et al. (2003) is based on non-competitive inhibition and assumes that the transporter is blocked if the second site is occupied, whereas the model proposed by Litman et al. (1997b) is based on un-competitive or substrate inhibition and allows for transport, although at a reduced rate, even if the second binding site is occupied. Various competition experiments supported the latter model and suggest that the two binding sites are juxtaposed (Gatlik-Landwojtowicz et al., 2006; Li-Blatter et al., 2009). The model proposed by Litman et al. (1997b) is a modified Michaelis–Menten equation (for the equation see Figure 17). It assumes that the same compound can act as substrate and inhibitor depending on the concentration apply, i.e. a transporter activation if one substrate molecule per transporter is bound and inhibition if a second substrate molecule per transporter is bound.

It should be noted that crude membrane preparation of a cell is a mixture of various intracellular organelle membranes and plasma membranes. As a result, different type ATPases contribute to the activity measured in these membranes. To overcome this problem, a battery of inhibitors such as sodium azide, EGTA, and ouabain should be used to inhibit these ATPases (Ambudkar, 1998). In addition, transporter ATPase activity is inhibited by vanadate; this drug permits ATP hydrolysis in one NBD, but after dissociation of inorganic phosphate, the vanadate enters the active site forming a stable complex with ADP (ATP-transporter-ADP-vanadate) and, thus, impeding ATP hydrolysis in the other NBD (Urbatsch et al., 1995). Therefore, vanadate is used often in negative controls in ATPase activity assays. Some problems which may be found in the experiment procedure and should be taken into account are irreversible drug association which reduces membrane partitioning, and, in turn,

binding to the transporter (Aänismaa and Seelig, 2007). Drugs which are especially prone to association include progesterone and daunorubicin. For compounds which are especially prone to aggregation, the quality of data decreases with increasing concentration (Gatlik-Landwojtowicz et al., 2006). Another potential problem could be vesicle aggregation which makes difficult to measure in the inhibitory part of the curve; the addition of high amounts of charged drugs can lead to vesicle aggregation (Aänismaa and Seelig, 2007). In addition, compounds that are transported with a low turnover rate may not yield detectable amount of inorganic phosphate liberation in the ATPase activity assay, and thus false negative results would be obtained (Hegedus et al., 2009).

The simplicity and reproducibility of the ATPase activity assay makes it a practical technique, indeed it is one of the most widely used in high-throughput assays to screen for compounds that interact with various ABC transporters (Ishikawa et al., 2005; Sarkadi et al., 2006). Numerous substrates, for which a transport assay may not be applicable, have been identified based on increased ABC-ATPase activity. These compounds include some of the most hydrophobic substrates of ABCG2, including prazosin and various tyrosine kinase inhibitors (Hegedus et al., 2009). Strengths comprise also that it is a relatively inexpensive screening tool, which, besides detecting the interaction of test drugs and ABC transporters, may also indicate the nature of the interaction (Glavinas et al., 2007). Drawbacks of this technique include inconsistency between ATPase activity and the transport rate of some substrates and inhibitors; a high incidence of false positives and negatives (due to the ATPase assay system is not always suitable for distinguishing among potential substrates, inhibitors, or other types of transporter modulators; even, most inhibitors either stimulate or do not modify activity and are difficult to differentiate from substrates); and the requirement of high substrate concentrations (Glavinas et al., 2004; Nicolle et al., 2009; Giacomini et al., 2010) (Table 8).

Vesicular transport assay is the measurement of the ATP-dependent direct transport of drugs into inside-out membrane vesicles. By using the assay in a direct setup, an increased accumulation of a transported substrate in the ABC transporter-expressing inside-out membrane vesicles can be detected. Similarly to the ATPase assay, the vesicular transport assay can also be used in an indirect (inhibition-type) setup (Saito et al., 2006). The hydrophobic nature of the tested compounds, quite characteristic for the substrates of ABC transporters, can be a major obstacle in a vesicular transport assay, since hydrophobic compounds bearing medium or high passive membrane permeability cannot be trapped inside the membrane vesicles, no net accumulation can be measured, and that may result in false negative hits. Another possible drawback of this system might be that it requires radioactively or fluorescently labeled test-compounds, which are more expensive (Hegedus et al., 2009). However, because the disposition of substrates cannot be monitored in the ATPase assays, the preferred method in industry often remains the indirect vesicular transport assay with an appropriate probe compound.

Photoaffinity labeling assays are applied for studying ABC transporter function regarding a direct substrate/modulator binding to the ABC transporter proteins. In this methodology, ABC

transporter-expressing membranes or isolated proteins are incubated with labeled photoaffinity compounds and then irradiated to promote covalent linkage of the labeled compound to the protein. Radioactively labeled ABC transporters are then solubilized, and separated by gel electrophoresis, and protein labeling (drug-binding) is then visualized and quantitated by autoradiography. A general drawback of these studies is that ABC multidrug transporters form low-affinity interactions with a great variety of hydrophobic compounds, and the interaction sites and intensities may directly depend on the tested drug, as well as on the actual conformation of the transporter (Hegedus et al., 2009). These experiments are technologically complex and imply difficult procedures. Moreover, direct photolabeling is generally not suitable for distinguishing between substrates and inhibitors.

6.1.2. Cell-based assay systems

Cell-based assay systems can be used in drug discovery to identify substrates and inhibitors for individual transporters. In addition, these systems can be used to assess transport mechanisms (Giacomini et al., 2010). Cell-based assays include cytotoxicity experiments, trans-cellular transport, accumulation assays and cytosensor microphysiometer assays. Transfected cell lines can be used to characterize drug transporter interactions. Cultured cell lines used to study drug transporter interactions include cell monolayers such as MDCK, LLC-PK1, HEK293 or CHO cells grown on solid support. Such monolayers can be used to assess uptake and efflux by single recombinant transporters, or by multiple recombinant transporters, and kinetic measurements can be obtained. A limitation of certain single transfected cells is that they often lack the endogenous uptake or efflux transporters to provide a complete mechanism for trans-cellular transport of a molecular entity (Giacomini et al., 2010). Similarly, endogenous transporters and drug-metabolizing enzymes can have a significant influence on the results, obscuring the effects of the transfected transporter (e.g. Goh et al., 2002).

Cytotoxicity experiments are widely applied for investigating ABC multidrug transporter function in which the extrusion of drugs bearing cytotoxic or antiproliferative effects can be tested. Following the incubation of ABC protein expressing cells with the test compound, the number of living cells is determined, and by assessing the drug concentration resulting in 50% cell death, the IC_{50} values are calculated. In a direct assay setup, ABC transporter-expressing cells show elevated IC_{50} values for the actively extruded compounds, compared to the parental cells. In an indirect setup, combined treatment with a well-defined cytotoxic transporter substrate and a potential transporter inhibitor or competing substrate (test compound) is performed. In most cases, ABC transporter interaction with the test compound results in a decreased IC_{50} value for the cytotoxic ABC transporter substrate (Hegedus et al., 2009).

The cytotoxicity assay proved to be an excellent method for the interaction of ABCG2 with small molecules like protein kinase inhibitors (PKI). As a restriction, these measurements are limited to antiproliferate compounds (Xia et al., 2005; Hegedus et al., 2009).

The **transcellular transport assay**, namely also as transepithelial transport or bidirectional transport, is a traditional method for identifying substrates of transporters recommended in the FDA Draft Guidance for Industry and the International Transporter Consortium White Paper (Giacomini et al., 2010). It is an *in vitro* tool for investigating vectorial transport across tight cell layers. Pharmacological barriers contain at least one tight cell layer, which is deterministic of the barrier's substance trafficking properties. Therefore, a representative immortalized cell line in a monolayer transport setup is believed to be an excellent *in vitro* tool for modeling pharmacological barriers (van Breemen and Li, 2005; Schlatter et al., 2006). Developments of porous plastic materials with surfaces suitable for cell culture were integral to the advent of higher throughput monolayer transport experiments. The cells are grown on a polyethylene or polycarbonate membrane filter which allows the cells to be polarized and to express the multidrug transporter on one side only, namely the apical side (corresponding to the lumen of the stomach, or the blood vessel at the blood-brain barrier). The cells will grow until confluence is reached, and the endothelial cells will build tight junctions between them. In each dish, there are two compartments that are commonly designated as apical and basolateral, denoting the membrane orientation of polarized cell layers. The tested compound is then first applied in the basolateral compartment and the presence of drug is monitored (usually by HPLC or mass spectrometry) in the apical compartment; this experiment is called B to A. In a second parallel experiment, the drug is applied in the apical compartment, and the presence of drug is monitored in the basolateral compartment; this experiment is called A to B. The difference between the basolateral-to-apical (B-A) and the apical-to-basolateral (A-B) transport is assessed and the calculated ratio is referred to as “efflux ratio”. If a drug is not a substrate for the ABC protein, the presence of the drug in both compartments will be identical, thus the ratio B-A/A-B will be 1. Since the ABC transporter is expressed only in the apical side, a substrate applied to the basolateral compartment will accumulate more rapidly in the apical compartment (see Figure 22, left side). In contrast, if applied in the apical compartment the drug will be effluxed by the transporter, leading to no or a slow presence of the drug in the basolateral compartment. Therefore, compounds with an efflux ratio (B-A/A-B) greater than 1.5 or 2 are considered to be subjects to active efflux processes. In the case of some efficiently transported compounds, the efflux ratio falls in the range of hundreds (Liang et al., 2000). A third parallel recommended proof to determine if the compound is a specifically substrate of the studied transporter is to perform the experiment adding specific inhibitors of the transporter in addition to the potential substrate. The result will yield an efflux ratio similar to that when the compound is not a substrate of the transporter as the transporter is inhibited (see Figure 22, right side).

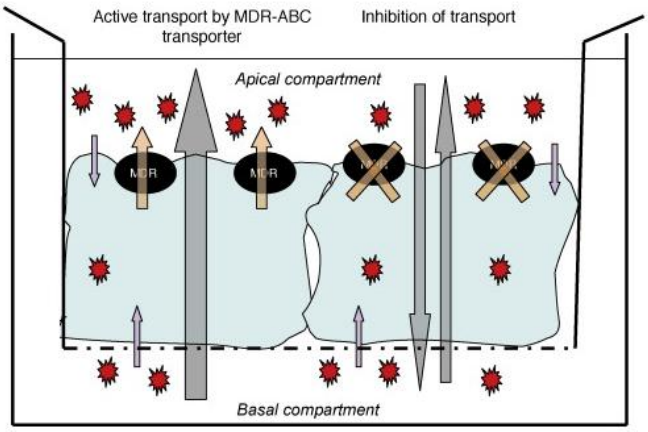

Figure 22. Model of transcellular transport by an apically localized ABC transporter. In a tight monolayer culture of polarized cells, the tested compound has to cross the cellular membranes in order to penetrate through the cells. In case of an apically localized MDR–ABC transporter, the basal to apical (B–A) flux of the transported substrate (represented by stars) will dominate (left panel). When the function of the transporter is inhibited, passive diffusion will determine the distribution of the substrate, and the basal to apical and the apical to basal (B–A = A–B) fluxes will be equal (right panel) (Szakács et al., 2008).

Polarized monolayer cells overexpressing the ABC transporter are used in transport assays. MDCK-II (Madin-Darby canine kidney), a cell line derived from canine kidney proximal tubule epithelial cells, is the most prominent and widely-used for this purpose (Jonker et al., 2000; Pavek et al., 2005; Hegedus et al., 2009). Importantly, polarized MDCK-II cells may express intrinsic transporters, hence, the substrate specificities of which may overlap with those of the transfected transporter (Taub et al., 2005). It is therefore crucial to run parallel experiments using the parental and mock-transfected cell line.

It should be noted that passive permeability of the tested compounds is an important factor influencing the design of monolayer experiments, since it may counteract active transport processes. Moreover, parameters, such as incubation time and concentration range, have to be accurately chosen and tightly controlled when studying extremely hydrophobic compounds (Hegedus et al., 2009). Concentration equilibrium between the two compartments is reached rapidly and sample retrieval in the saturation phase might significantly underestimate the speed of the transport. It is important to note that the compound may also diffuse at a rate comparable to its active ABC-dependent efflux, when active transport is often masked by high passive permeability producing false negative hits (Xia et al., 2005; Poguntke et al., 2010). Of note, high affinity of a drug for the transporter in a cell-free assay does not always translate into a high efflux ratio in cellular models. Decreasing the initial concentration might increase the overall impact of transporters on the net transport, but this might also strain analytical capabilities. In contrast, low passive permeability compounds that are not actively transported require long incubation periods and high initial concentrations to ensure detectable final amounts in the receptor compartment (Sun and Pang, 2008). An additional problem could be that the compound might

be metabolized within the cell where the parent drug, its metabolite, or both (in a competitive manner) are transported (Poguntke et al., 2010). Other disadvantages of this classic tool include high cost and work (Glavinas et al., 2007) (Table 8).

Accumulation assays. ABC drug-efflux pumps are able to transport fluorescent compounds. Therefore, accumulation assays have been proved as a very useful tool for exploring the transport activity of the ABC proteins in intact cells, like quantification of the uptake of these dyes by flow cytometry, and ABC transporter inhibition by other substrates and modulators (Sharom, 2008). Small series of inhibitors were studied checking their ability to induce intracellular accumulation of fluorescent drugs such as mitoxantrone, pheophorbide A, BODIPY-prazosin, LysoTracker, topotecan, Hoechst 33342, rhodamine 123 and doxorubicin. This was done by means of flow cytometry using whole cells, either transfected or drug-selected (Honjo et al., 2001). Parallel tests with several substrates have been recommended (Robey et al., 2001; Giri et al., 2009). The accumulation assay is useful in studying the transporter specificity, for example by combining P-gp and ABCG2 substrates (Nicolle et al., 2009). This technique has been classified as an excellent indicator of transporter function (Sharom, 2008).

The first functional assay using this technique with ABCG2 was developed by Robey et al. (2001). These studies showed that flow cytometric measurement of mitoxantrone or prazosin inhibited by fumitremorgin was a sensitive and specific method for measuring the function of ABCG2 in both selected and unselected cell lines. Mitoxantrone was chosen as a model substrate to follow ABCG2 mediated efflux because mitoxantrone levels are readily measured using fluorescence detection (Doyle et al., 1998; Gupta et al., 2004). To date, the most popular ABCG2 probe substrate for the *in vitro* identification of ABCG2 inhibitors is mitoxantrone, which has been used in > 50% of all published studies (Poguntke et al., 2010). The preferential use of one probe substrate (e.g. mitoxantrone) might be favorable in view of standardization. ABCG2-dependent efflux and drug resistance assays (cytotoxicity assay) are the popular test methods which together make up about 90% to test inhibitors of ABCG2.

GFP-ABCG2 is suitable for studying drug transport by flow cytometry, as demonstrated by measuring the transport of mitoxantrone (Orbán et al., 2008). Using a specific inhibitor, either Ko143 or FTC (Allen et al., 2002), and comparing the results with those of the GFP-tagged species, the transport characteristics of the applied fluorescent drug can be rapidly and reliably assessed. This double control system makes the assay especially reliable and informative, allowing the investigator to identify modulators or inhibitors of the transporter, or confirm potential substrates in a short period of time (Hegedus et al., 2009).

Data are usually evaluated by calculating the inhibitory potencies of compounds from the median of fluorescence (MF). Thereby, shift of the MF caused by the tested compound in ABCG2 cells is related to the shift of MF caused by the potent ABCG2 inhibitor Ko143 (Pavek et al., 2005). The inhibitory potency is then calculated according to the following equation: Inhibitory potency = (MF of

cells with tested compound - MF of cells without inhibitor / MF of cells with Ko143 – MF of cells without inhibitor) x 100 % (Pavek et al., 2005). A schematic explanation of the process is presented in Figure 23.

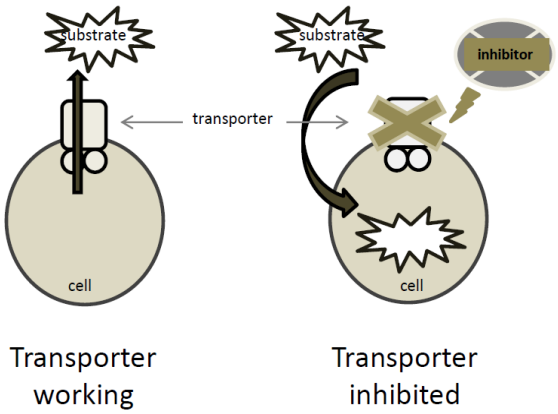

Figure 23. Schematic representation of the basics of accumulation assays. When the transporter is working, the substrate is extruded out of the cell and, therefore, not accumulated in the cell and no fluorescence is detected. Oppositely, when the transporter is "blocked" by an inhibitor, the fluorescence of the substrate accumulated in the cell is visible.

It has to be noted that this method may underestimate compounds with low permeability (Xia et al., 2005). In addition, it provides little information on the nature of the interaction or on molecular mechanisms (Glavinas et al., 2007; Poguntke et al., 2010) (Table 8). It has been suggested that the correct classification of compounds as inhibitors or non-inhibitors of ABCG2 requires several different prototype substrates to be investigated (Giri et al., 2009). According to Poguntke et al. (2010), nearly a third of the compounds classified as non-inhibitors of ABCG2 in one experimental set up actually inhibit ABCG2 in a different experimental set up; for example using another known substrate.

Accumulation assays are also widely used with the P-gp transporter (Sarkadi et al., 2006) with the same basis as explained for ABCG2 (Figure 23).

Cytosensor microphysiometer assays. The rate of ATP synthesis in living cells can be measured by monitoring the extracellular acidification rate, ECAR, using a Cytosensor microphysiometer (Parce et al., 1989; McConnell et al., 1992). Cytosensor microphysiometer in the field of ABC transporters was an approach developed initially to study drug-induced ATPase activity of P-gp in real time (Landwojtowicz et al., 2002). The use of ATP by an ABC transporter is directly correlated to the production of lactate as a result of glycolysis; lactate is extruded as lactic acid out of the cell (Figure 24). Thus, upon P-gp activation, the environmental medium will be acidifed; this acidification can be assessed using a cytosensor microphysiometer, which is a micro pH-meter. The ECAR describes the efflux rate of acidic metabolites and, thus, reflects the overall energy metabolism of cells. Results obtained with this method

are comparable to those obtained with the ATPase activity assay; however it has the advantage to handle living cells instead of reconstituted inside-out membrane vesicles (for details see Landwojtowicz et al., 2002; Gatlik-Landwojtowicz et al., 2004; Gatlik-Landwojtowicz et al., 2006; Aänismaa and Seelig, 2007).

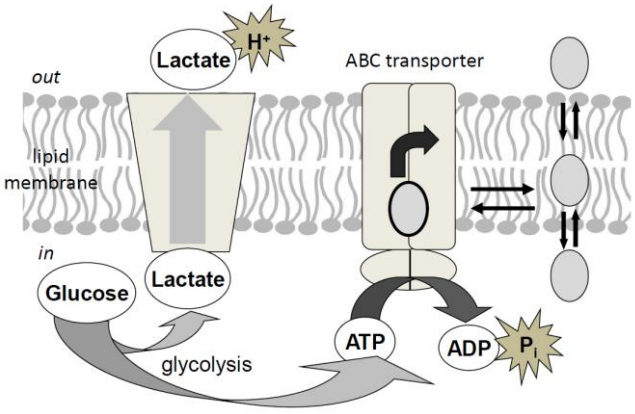

Figure 24. Glucose is used in glycolysis to produce lactate and ATP. The ATP can be used for the ABC transporters energy, where it implicates inorganic phosphate release (P_i) which can be measured by a colorimetric reaction. As a consequence of lactate production, there is extrusion of protons (H^+) out of the cells and the medium is acidified; acidification can be measured for instance with a pH-meter (Seelig, unpublished).

6.2. *In vivo* experiments

The *in vivo* function of transport proteins can be assessed using multiple approaches. Numerous transporter-gene knockout (lacking expression of the transporter) and naturally occurring transporter-deficient animal models have been characterized in recent years. Transporter gene knockout mice have been genetically engineered and are useful for pharmacokinetic and toxicologic studies. Indeed, knockout models have illustrated the role of transporters in physiology, protection of major blood–tissue barriers, and the absorption and excretion of xenobiotics and endogenous compounds (Giacomini et al., 2010; Klaassen and Alleksunes, 2010).

Knockout mice lacking Abcg2 were primarily generated by Jonker et al. (2002). The use of genetically modified Abcg2 knockout mice has been proved as a useful tool in studying the *in vivo* function of this efflux pump (Vlaming et al., 2009). Work relying mainly on the use of Abcg2 knockout mice has revealed important contributions of ABCG2 to the protection in blood-brain, blood-testis and blood-fetal barriers. In addition, several other physiological functions of ABCG2 have been observed, including extrusion of porphyrins and/or porphyrin conjugates from hematopoietic cells, liver and harderian gland, as well as secretion of vitamin B2 (riboflavin) and possibly other vitamins (biotin, vitamin K) into breast milk (see Vlaming et al., 2009 as a review of recent findings in Abcg2 knockout mice regarding physiological and pharmacological roles of ABCG2). Whether ABCG2 functions as

efficiently in humans as in mice will first have to be investigated in more detail before extrapolating directly from the mouse to humans. Nevertheless, it has been considered that knockout mice are valuable tools to determine the *in vivo* effects of ABCG2 for many drugs that are currently used in the clinic, as well as for the characterization of newly discovered drugs (Vlaming et al., 2009). In the case of P-gp, some transgenic animal models have been established (like double knock-out mice, mdr1a and mdr1b) to study the effect of the absence of P-gp on the bioavailability of drugs (Schinkel et al., 1996). Evidence obtained in *Abcg2*$^{-/-}$/*Mdr1a*$^{-/-}$/*Mdr1b*$^{-/-}$ triple knockout mice treated with lapatinib and other compounds suggested that ABCG2 and P-gp may have a combined effect at the blood–brain barrier (Polli et al., 2009; Tang et al., 2012; Tang et al., 2013).

Animal models are an important issue in the development of drugs after the *in vitro* step and before starting studies with humans. Specifically, genetically knockout animal models have become important tools in evaluating the effect of transporters in the pharmacokinetics, pharmacodynamics and drug-drug interactions of drug molecules (Xia et al., 2005; Vlaming et al., 2009). The use of these methodologies is often needed for better understanding of transporter-mediated efflux and uptake of drug molecules. However*, in vivo* studies are relatively expensive and low-throughput; moreover, species, strain, sex, diet and housing condition differences, as well as compensatory mechanisms, are a limitation of knockout and mutant animal models. All these variables should be considered carefully in the interpretation of data and in attemptions to extrapolate findings across species (Giacomini et al., 2010). Gender differences in the expression of certain transporters may exist; higher hepatic ABCG2 expression in males has been established in both mice and humans (Merino et al., 2005a). Direct translation of preclinical transport findings to the clinic is challenging because of species differences in transporter expression, substrate affinity, physiological function and interplay between transporters and enzymes (Table 8). Caution needs to be taken when using these transgenic animal models to interpret the results also because deletion of one transporter might cause upregulation of another (Xia et al., 2005). For instance, although the mRNA levels of P-gp, Mrp1, Mrp4 and Oatp2 in brain were not changed in Abcg2$^{-/-}$ mice (Lee et al., 2005), there was about three times more Abcg2 mRNA in the microvessels of brains from Mdr1a/1b$^{-/-}$ mice than in those from wild-type mice (Cisternino et al., 2004). However, these differences in the level of mRNA of the different transporters did not imply changes of protein expression (Agarwal and Elmquist, 2012).

7. Methodological bases for the study of the passive influx

Estimations of rates of passive influx of drugs allow comparisons with the rates of efflux processes of ABC transporters (Seelig and Gatlik-Landwojtowicz, 2005). For instance, the knowledge of the passive influx of a compound gives an idea of the potential interaction of this drug with a specific ABC transporter.

7.1. Surface activity measurements (SAM)

Hydrophobicity and membrane partitioning are typically estimated from the octanol-water partition coefficient (Log P). The air-water interface is a better alternative because it mimics the lipid bilayer, it orders the compounds in a similar way as the lipid bilayer (amphiphilic drugs are oriented with the non-polar core to the air and the polar to the water) and secondly, the dielectric constant of air ($\varepsilon \approx 1$) is closer to the dielectric constant of the hydrophobic core region of the membrane ($\varepsilon \approx 2$) than to the dielectric constant of octanol ($\varepsilon \approx 10$) (Seelig and Gatlik-Landwojtowicz, 2005). In addition, the octanol system is isotropic; oppositely, the membrane system is anisotropic. It is therefore not surprising that octanol-water partition coefficient measurements do not correlate satisfactorily with the ability of a drug to diffuse through a lipid membrane. As an alternative a method which does not involve lipids or organic solvents has been suggested, that is the Surface Activity Measurement (SAM) (Seelig et al., 1994). It should be noted that P-gp allocrits are typically amphiphilic and thus surface-active (Seelig and Gatlik-Landwojtowicz, 2005). The simple permeability predictions on the basis of SAMs provide an estimation of rates of passive influx of drugs and allow for comparison with the rates of efflux processes (Seelig and Gatlik-Landwojtowicz, 2005). Remember that in the "two step drug binding" model, the first step is the drug partitioning into the lipid bilayer described by the lipid-water partition coefficient (K_{lw}) and the second step is the drug binding to P-gp from the lipid phase depicted by the binding constant of drug to P-gp from the lipid phase (K_{tl}). The binding constant of the drug from the aqueous phase to P-gp (K_{tw}) is thus a product of these two binding constants, $K_{tw} = Kl_w \times K_{tl}$ (Figure 16) (Seelig and Landwojtowicz, 2000; Gatlik-Landwojtowicz et al., 2006). With this method the lipid-water partition coefficient (K_{lw}) is measured and K_{tl}, which cannot be measured directly (Seelig and Gatlik-Landwojtowicz, 2005), can be evaluated with the measurement of the transporter-water partition coefficient (K_{tw}) by ATPase activity measurements or ECAR by a Cytosensor microphysiometer.

The surface pressure is measured with a Wilhelmy plate in Teflon troughs and the measurement yields pressure *versus* concentration (p/Log C) curves. The approach is based on the measurement of the Gibbs adsorption isotherm which is a quantitative measure for the tendency of a drug to move to the air-water interface (the air-water partition coefficient, $K_{aw,}$ is obtained). The analysis of the Gibbs adsorption isotherm yields three physical-chemical parameters of a drug molecule: the minimum concentration to induce surface activity (C_o), the surface cross-sectional area of the molecule

at the air-water interface (A_D) (while adding a compound the pressure is increased), and the critical micelle concentration (CMC), when no more compound concentration fit in the surface (see Figure 25). From the p/Log C curve, the K_{aw} and A_D of the compound can be determined and knowledge of the two parameters allows estimation of the lipid-water partition coefficient (K_{lw}) for any type of membrane (Fisher et al., 1998). Thermodynamics and kinetic evaluations of SAM technique were discussed in detail previously (Seelig et al., 1994; Fisher et al., 1998; Gerebtzoff et al., 2004; Nervi et al., 2010).

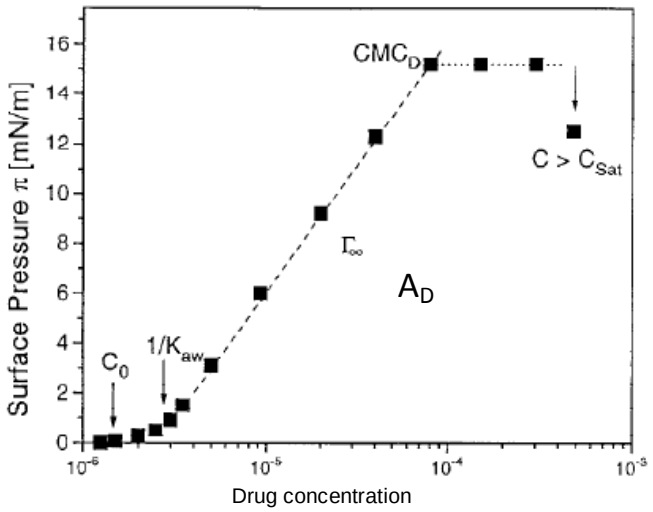

Figure 25. Surface pressure as a function of drug concentration, p/Log C plot. The p/Log C curve yields the cross-sectional area of the molecule (A_D), the critical micelle concentration (CMC), the air-water partition coefficient (K_{aw}) and the minimum concentration to induce surface activity (C_o). (Based on Seelig and Gatlik-Landwojtowicz, 2005).

It should be noted that for compounds with low amphiphilicity or amphiphilicity changing in the process of aggregation, the measured Gibbs adsorption isotherm cannot be satisfactorily simulated. For these compounds neither A_D nor K_{aw} can be properly determined (Fisher et al., 1998). In addition, deviations at very low drug concentrations are due to adsorption to the surface of the Teflon trough. For more hydrophilic compounds adsorption is less pronounced.

This method has allowed to improve the understanding of P-gp fundamentals; however, this field in the case of ABCG2 typical compounds has not been yet investigated.

7.2. Isothermal titration calorimetry (ITC)

Isothermal titration calorimetry (ITC) is a quantitative physical technique used to determine the thermodynamic parameters such us the binding affinity, enthalpy changes, and binding stoichiometry of the interaction between two or more molecules in solution. From these initial measurements, Gibbs energy changes and entropy changes can be determined. The lipid-water partition

coefficient (K_{lw}) of a compound can also be calculated by ITC. Therefore, the binding constants of a drug to the transporter can be deduced also by using ITC.

ITC is one of the latest techniques to be used in characterizing binding affinity of ligands for proteins. It is typically used in screening. ITC is particularly useful as it gives not only the binding affinity but also the thermodynamics of the binding which allows for further optimization of compounds (Weber and Salemme, 2003).

Aims of Research

Taking all together, with this background, the principal aim of the present memory was therefore to understand the ABCG2 function by comparison with P-gp. For this purpose, the specific aims were:

1. To gain further insight into similarities and differences of the two transporters, ABCG2 and P-gp, regarding ATPase activity, substrate specificity and substrate-activity relationship. Additionally, to attempt a prediction explaining the substrate interactions of compounds at the molecular level comparing both transporters.
    a. To characterize different drugs for their interaction with ABCG2 and P-gp by measuring the basal and substrate-induced ATPase activity in inside-out plasma membrane vesicles of cells over-expressing the respective transporters.
    b. To characterize the compounds by means of surface activity measurements to assess their air-water partition coefficients and the cross-sectional areas in their membrane bound conformation which allow an estimation of the lipid-water partition coefficients.
    c. To correlate the parameters obtained from both previous experiments.
2. To test the correlation between ATPase activity of both transporters and the rate of substrate transport in transport and accumulation assays with steroid hormones.
    a. To analyse the measurement of the hormone-induced ABCG2 and P-gp ATPase activity in inside-out plasma membrane vesicles of cells over-expressing the respective transporters.
    b. To analyse the estimation of the hormone passive flux by means of surface activity measurements.
    c. To correlate ATPase activity with transport and accumulation assays by taking into account the passive diffusion.
3. To study the correlation between ATPase activity and the outcome from other *in vitro* and *in vivo* experiments for both transporters using fluoroquinolones.
    a. To evaluate the ABCG2 and P-gp ATPase activity of five fluoroquinolones in inside-out plasma membrane vesicles.
    b. To study the *in vitro* transepithelial transport and the effect on mitoxantrone accumulation assays of the fluoroquinolones using ABCG2-transduced cells.
    c. To perform *in vivo* experiments with wild-type and Abcg2-knockout mice using these antibiotics.

d. To correlate ATPase activity with transport, accumulation experiments and *in vivo* assays using also published data related to the interaction of these fluoroquinolones with ABCG2 and P-gp.

Materials and Methods

1. Materials

1.1. Chemicals and reagents

Cimetidine, ciprofloxacin, hydrocortisone (cortisol), 8-(4-Chlorophenylthio) adenosine 3′,5′-cyclic monophosphate sodium salt (CPT-cAMP), daunorubicin-HCl, dexamethasone, digoxin, enrofloxacin, β-estradiol, etoposide, famotidine, forskolin, glybenclamide, Ko143, methotrexate, mitoxantrone-2HCl, nizatidine, norfloxacin, pefloxacin mesylate dihydrate, prazosin-HCl, progesterone, promazine-HCl, ranitidine-HCl, (-)-riboflavin, sulfasalazine, tamoxifen, testosterone, *(R/S)*-verapamil-HCl, colchicine, *L*-ascorbic acid (ascorbic acid), 3-[(3-Cholamidopropyl) dimethylammonio]-1-propanesulfonate (CHAPS), dodecyloctaglyol ($C_{12}EO_8$), heptanoic acid, maltose, sodium deoxycholate and sodium hexanoate, were purchased from Sigma-Aldrich (Steinheim, Germany; and St. Louis, MO, USA) and Tocris (Bristol, UK).

Cyclohexyl-Methyl-*β*-D- maltopyranoside (Cymal-1), *6*-tetradecyl- *β* -D-maltopyranoside (C_6-malt)**,** n-Octylphosphocholine (Fos-choline-8), 2,6-Dimethyl-4-Heptylphosphocholine (Fos-choline-iso-9), were obtained from Anatrace (Maumee, OH, USA). 1,2-dicaproyl-*sn*-glycero-3-phosphocholine (DHPC) was bought to Avanti Polar Lipids (Alabaster, AL, USA).

Complete EDTA-free protease inhibitor cocktail tablets were obtained from Roche Diagnostics (Mannheim, Germany). 1,4-dithiol-DL-threitol (DTT) and Tris ultrapure from AppliChem (Darmstadt, Germany). Bicinchoninic acid (BCA) protein assay reagents from Pierce (Rockford, IL). All other chemicals were either from Sigma-Aldrich or Merck.

PBS, DPBS, cell culture media: Dulbecco's Modified Eagle Medium (DMEM) with and without pyruvate and/or glutaMax, Opti-MEM medium as well as all other compounds and reagents required for cell culture such as fetal bovine serum (FBS), Trypsin 0.05% with EDTA, L-glutamine, and antibiotics were purchased from Gibco, Invitrogen (Basel, Switzerland), from Life Technologies, Inc., (Carlsbad, CA, USA) and from MP Biomedicals (Solon, OH, USA).

1.2. Cell lines, cell culture and membrane vesicles

Mouse embryo fibroblasts stably transfected with the human MDR1 gene (NIH-MDR1-G185) were a generous gift from Dr. M.M. Gottesman and Dr. S.V. Ambudkar (National Institutes of Health, Bethesda, MD). Cell culture was done as described previously (Nervi et al., 2010; Gatlik-Landwojtowicz et al., 2004). Cells were grown in a monolayer culture in DMEM (4.5 g/L glucose) supplemented with FBS (10% v/v), penicillin (100 U/mL), streptomycin (100 μg/mL) and L-glutamine (146 mg/L) at 37 °C in an atmosphere containing CO_2 (5%). They were kept under growth selection with 0.15 µM colchicine. Confluent cell cultures were passaged twice a week using trypsin–EDTA.

The adherent spontaneously immortalized embryo fibroblast cell line derived from triple knockout Mdr1a/b$^{-/-}$, Mrp1$^{-/-}$mice (MEF3.8) and the subclon cells stably transduced with the human ABCG2 and mouse Abcg2 were explained in detail by Allen et al. (1999). MDCK-II (Madin Darby canine kidney) cell lines, parental and subclones transduced with murine Abcg2 and human ABCG2 were described elsewhere (Jonker et al., 2000; Jonker et al., 2002; Pavek et al., 2005). All these cell types were kindly provided by Dr. A.H. Schinkel (Netherlands Cancer Institute, Amsterdam, The Netherlands). Cells were grown under identical conditions as were previously described by Allen et al. (1999; 2000). They were cultured in DMEM with glutamax supplemented with FBS (10% v/v), penicillin (50 U/ml) and streptomycin (50 µg/ml) at 37 °C in an atmosphere with 5% CO_2 and were passaged every 3-4 days by trypsinization with trypsin-EDTA.

Inside-out plasma membrane vesicles from isolated mammalian cells containing human ABCG2 (ABCG2-M-ATPase) were obtained from SOLVO Biotechnology (Budapest, Hungary) (Glavinas et al., 2007).

1.3. Animals

Animals used were male and female Abcg2$^{-/-}$ and wild-type mice of a 99% FVB genetic background, 9-14 weeks old. They were kindly supplied by Dr. A.H. Schinkel, (Netherlands Cancer Institute, Amsterdam, The Netherlands). Animals were maintained at a controlled temperature with a 12-h light/dark cycle; they received a standard rodent diet (Panlab, Barcelona, Spain) and water *ad libitum*. Mice were housed and handled according to the guidelines of the Research Committee of Animal Use of the University of Leon (Spain), the "Principles of Laboratory Animal Care" and the European law (EC Directive 86/609).

2. Methods for ABCG2 expression quantification

2.1. Western Blotting

Samples of plasma membrane vesicles from ABCG2-transduced MEF3.8 cells or ABCG2-M-ATPase from SOLVO containing the human ABCG2 were fractionated on a 10% sodium dodecyl sulfate Polyacrylamide gel electrophoresis (SDS-PAGE). Then, it was transferred to a nitrocellulose membrane (Protran® cellulosenitrate BA85. Sigma- Aldrich. Steinheim, Germany) at 120-150 mAmp during 60 min at 4 ºC. After washing the membrane twice in TBS for 10 min at room temperature, it was incubated in 3% BSA in TBS/tween (blocking solution) for 60 min at room temperature to block the unspecific joins. The membrane was washed twice for 10 min in TBS/tween at room temperature.

The membrane was then incubated with the ABCG2-specific primary antibody BXP-21 (sc-58222, Santa Cruz Biotechnology, Inc. Heidelberg, Germany) in TBST buffer, 60 min at room temperature, dilution 1:200. Soon after, it was washed four times for 5 minutes with TBS/tween at room temperature. Goat anti-mouse IgG-AP (alkaline phosphatase) (sc-2008, Santa Cruz Biotechnology, Inc. Heidelberg, Germany) was used as the secondary antibody, in TBST buffer, 45 min at room temperature, dilution 1:2000. The membrane was next washed four times in blocking solution buffer, once in TBS and once with alkaline phosphatase buffer pH 9.5.

For final enzyme detection, the NBT/BCIP reaction was applied; i.e. the colorimetric detection was performed with the combination of NBT (nitro-blue tetrazolium chloride) and BCIP (5-bromo-4-chloro-3'-indolyphosphate p-toluidine salt) which yields an intense, insoluble black-purple precipitate when reacted with alkaline phosphatase.

Quantity analysis was done using the Quantity One® Software Version 4.2 from Bio-Rad.

2.2. Quantification of the enhanced GFP in MEF3.8 cells

When ABCG2-overexpressing MEF3.8 cells were generated (Pavek et al., 2005), they were transduced with a monocistronic vector containing ABCG2 followed by an internal ribosome entry site (IRES) and the enhanced green fluorescent protein (GFP) (Figure 26). Assuming that the two proteins, ABCG2 and GFP were translated the same number of times, at least to a first approximation (despite the fact that the IRES site in the cloning vector is between GFP and ABCG2), allowed a rough estimation of the cellular GFP and thus ABCG2 concentration. To estimate the ABCG2 expression level in the MEF3.8 cells, the GFP fluorescence intensity was measured in a Spectramax M2 spectrometer in 96-well microtiter opaque plates adding titrations of concentration of cells (100 µl/well) in suspension. Confluent cells were previously trypsinized, counted with a hemocytometer, centrifuged and

resuspended in PBS containing 20% glycerol. After a previous scanning, the wavelengths chosen were 488 nm for excitation and 510 nm for emission. Lysis of cells did not improve the fluorescence intensity; therefore, whole cells were used. For each measurement, samples were freshly prepared and at least 4 independent measurements with 4 replicas each were performed. Cells maintained in culture between 1-6 weeks where used to assure a constant ABCG2 expression level. The final fluorescence results were obtained by subtracting the fluorescence background of the PBS-glycerol alone. Fluorescence of parental MEF3.8 cells was also checked. The results were compared with titrations of pure GFP protein (full-length GFP with a N-terminal His-tag, expressed in *E. coli*. from Merck Millipore Bioscience, Massachusetts, USA) to determine the number of GFP molecules per cell; this number corresponds approximately to the number of ABCG2 molecules.

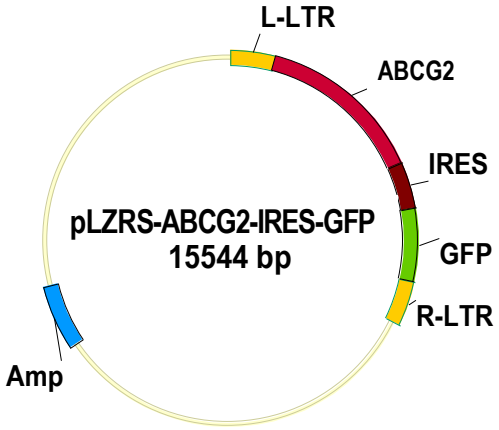

Figure 26. Monocistronic vector containing ABCG2 followed by an internal ribosome entry site (IRES) and the enhanced green fluorescent protein (GFP) used to transfect ABCG2 over-expressed cells (Michiels et al., 2000).

3. Membrane-based assay systems

3.1. Plasma membrane vesicle preparation

The NIH-MDR1-G185 cell membranes were prepared as described previously in detail (Aänismaa and Seelig, 2007) with minor changes. Briefly, cells were grown in 15 cm dishes until confluence. Then, cells washed with PBS were scraped into ice-cold PBS and resuspended in ice-cold buffer A (10 mM Tris-HCl pH 7.5, 10 mM NaCl, 1 mM $MgCl_2$ and protease inhibitors). After a centrifugation at 1000g_{max} for 10 min at 4 °C, the pellet was resuspended in buffer A (5 mL/ 4×15 cm dishes) and disrupted with a "One Shot" cell disrupter (Constant Systems Ltd, Warwickshire, U.K.) at 400 bar. The "One Shot" cell disrupter uses pressure to force a sample through a small fixed orifice at high speed. By transferring the cell sample from a region of high pressure to one of low pressure cells disrupt

(Aänismaa and Seelig, 2007). The cell lysate was diluted 1:1 in ice-cold buffer B (10 mM Tris-HCl pH 7.4, 50 mM *N*-methyl-D-glucamine, NMDG, 120 mM sucrose, protease inhibitors). Subsequent centrifugations were executed; unbroken cells, cell debris and nuclei were pelleted at 800g_{max} for 10 min at 4 °C; then, mitochondria were removed at 6000g_{max} for 10 min at 4 °C.

Ultracentrifugation in a TFT45.94 rotor (100000g_{max}, 1 h, 4 °C) was used to pellet the crude membranes. The membranes were resuspended in buffer B, homogenized by several passages through a 23-gauge needle, and quickly frozen in aliquots at -80 °C until use. The protein concentration of the membrane vesicles (usually between 6-11.5 mg/mL) was determined by BCA protein assay using bovine serum albumin as a standard. The amount of P-gp was estimated as 1.1 % of the total protein content and vesicles exhibited a predominantly inside–out orientation (Aänismaa and Seelig, 2007). The lateral membrane packing density in vesicles was assumed to correspond approximately to that of living cells (Nervi et al., 2010). A schematic illustration of the steps to prepare plasma membrane vesicles is shown at Figure 27.

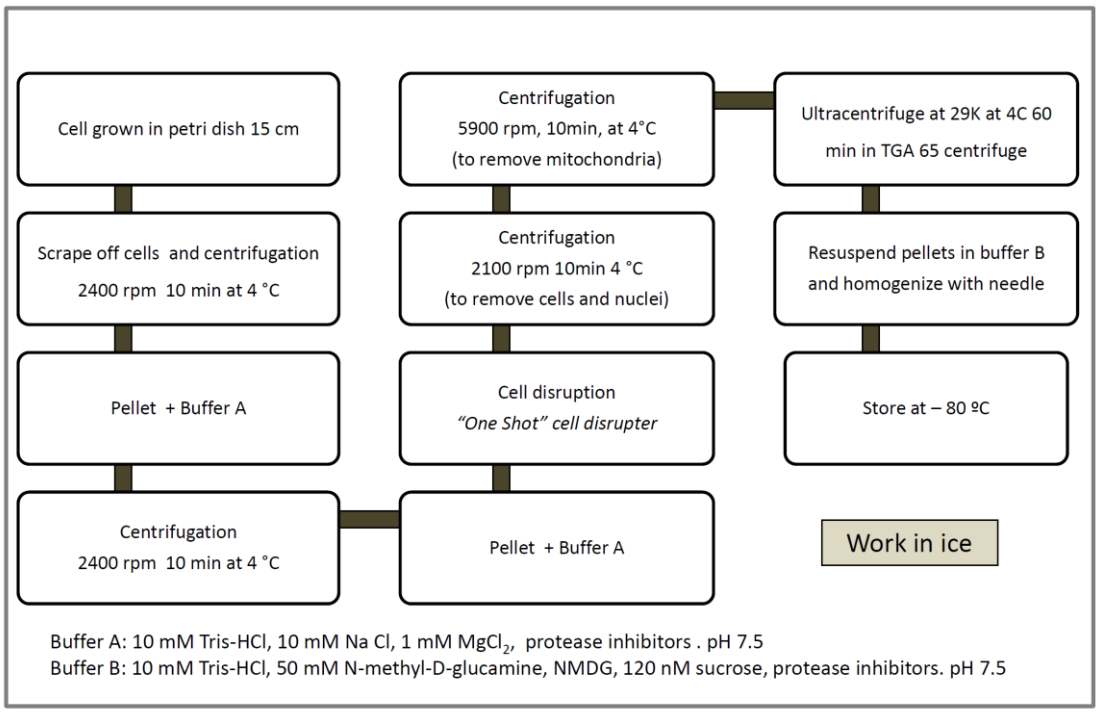

Figure 27. Schematic representation of steps for the procedure of plasma membrane vesicle preparation from cells.

Inside-out plasma membrane vesicle preparations from MEF3.8 cells transduced with human ABCG2 were prepared similarly. A reduction in the first centrifugation step with ice-cold buffer A at

500g_{max} instead of 1000g_{max} was applied to prepare these membranes. The final protein content of the membrane vesicles determined by BCA protein assay was 0.7-5 mg/ml.

3.2. ABCG2 plasma membrane vesicles ATPase activity assay optimization

To optimize the conditions to perform the ATPase activation assays with ABCG2-M-ATPase membrane vesicles from SOLVO, some preliminary tests were realized. We basically used the same conditions previously described by Litman et al. (1997a) with small modifications from Aänismaa and Seelig (2007) (for more details, see below). Several parameters were checked: incubation time at 37 °C (30-90 min), final working concentration of membrane (0.025-1.25 mg/ml), pH dependency (pH= 5-8.5), vanadate concentrations (10^{-7}- 0.5 mM) and ATP dependency (0.07-6.35 mM). For time of incubation and concentration of membrane dependent experiments, sulfasalazine was used as the titrated drug. Sulfasalazine is the best known compound to test ABCG2-M-ATPase membranes (Glavinas et al., 2007). For pH dependent assays MES buffer (25 mM adjusted to pH 6.4 at 25 °C) and Tris/HCl (25 mM adjusted to pH 7.4 or 8.4 at 25 °C) were used. ATP dependent assays were done using a titration of ATP in the presence of $MgSO_4$ at 10 mM instead of 2.5 mM to avoid aggregation.

Optimization of NIH-MDR1-G185 cell membranes vesicles preparations was previously published (Ambudkar, 1998; Aänismaa and Seelig, 2007).

3.3. ATPase activity measurements

The P-gp and ABCG2 associated ATP hydrolysis were determined by quantifying the release of inorganic phosphate (Pi) with a colorimetric assay according to Litman et al. (1997a) with small modifications (Aänismaa and Seelig, 2007). The plasma membrane vesicles were diluted to a protein concentration of 0.1 mg/mL for P-gp and 0.075 mg/mL for ABCG2, in ice-cold phosphate release assay buffer (25 mM Tris–HCl pH 7.4, 50 mM KCl, 3 mM ATP, 2.5 mM $MgSO_4$, 3 mM DTT, 0.5 mM EGTA, 2 mM ouabain, and 3 mM sodium azide). The pH was adjusted to pH 7.4 at room temperature, this yielding a pH 7.0 at the temperature of the ATPase assay (37 °C). Buffer (50 μl) was added to each well of a 96-well microtiter plate. Dilutions of the compounds were prepared either in aqueous solution or DMSO and drug solutions (1 µl if diluted in DMSO or 5 µl if diluted in aqueous solution) were added to each well (total volume of 60 µl). Drugs and membranes were incubated for 1 hour in a water bath at 37°C. Then, the reaction was stopped by cooling the plate on ice for several minutes. 200 µl of freshly prepared ice cold stop solution (ascorbic acid 1% (w/v), SDS 0.9% (w/v), sulfuric acid 1.43% (v/v) and ammonium molybdate 0.2% (w/v)) were added to each well. After mixing, the plates were then incubated for 30 minutes at room temperature and the inorganic phosphate release quantified colorimetrically at 820 nm

using a Spectramax M2 (Molecular Device, Sunnyvale, CA). A diagram of the consecutive steps for the ATPase activity measurements is displayed in Figure 28.

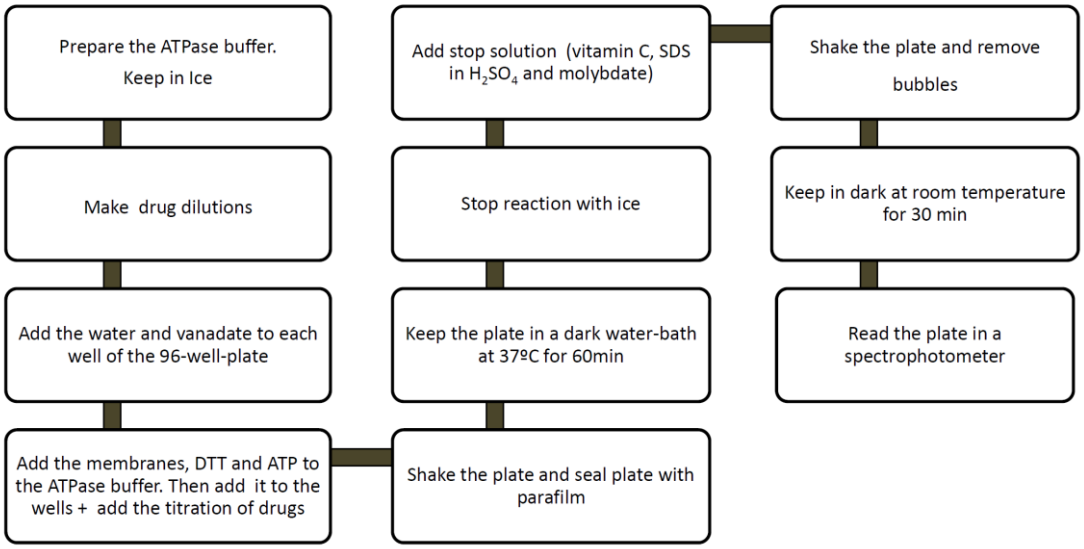

Figure 28. Schematic representation of steps for the procedure of ATPase activity measurements.

Vanadate control (used to inhibit the ATPase activity of endogenous ABC transporters) was subtracted from measurements to obtain the either P-gp or ABCG2 related ATPase activity. Measurements were performed in duplicates or quadruplicates and at least two independent experiments were made for each drug. The assays were performed either by hand with a multichannel pipette or with the Zephyr Compact Liquid Handling Workstation (Caliper Life Sciences, Hopkinton, USA). The vanadate-sensitive activity in latter cases was obtained executing the experiment with four measurements.

As a consequence of the physical-chemistry characteristics of the compounds, most of them had to be diluted in DMSO for this assay; only cimetidine, CTP-cAMP, mitoxantrone, nizatidine, pefloxacin and ranitidine could be dissolved in water. For the fluoroquinolones ciprofloxacin, enrofloxacin and norfloxacin, an initial amount of approximately 10 µl of NaOH 1M was necessary to be dissolved, completing later with nanopure water. The final DMSO concentration was 1.7% (v/v); this concentration did not affect the assay.

Data were finally analyzed by the Hill coefficient or a modified Michaelis–Menten equation:

Hill coefficient. The vanadate and the ATP dependence of the ATPase activity were fitted to the Hill equation (Equation 1), where y is the ATPase activity, x the concentration of the used drug, IC_{50} the concentration of half-maximum inhibition/activation and n the Hill coefficient describing cooperativity of the binding process.

(1)

$$y = \frac{1}{1+(x/IC_{50})^{n}}$$

Modified Michaelis–Menten equation. The kinetic evaluation of the drug-induced ATP hydrolysis was analyzed using a modified Michaelis–Menten equation according to the model proposed by Litman et al. (1997a).

$$V_s = \frac{K_1 K_2 V_0 + K_2 V_1 C_s + V_2 C_s^2}{K_1 K_2 + K_2 C_s + C_s^2} \quad (2)$$

Where V_s is the rate at a specific drug concentration (C_S) in aqueous solution, V_0 is the basal activity in the absence of drugs, V_1 and V_2 are the maximum and minimum transporter activity, respectively; K_1 and K_2 are the half maximum activation and inhibition, respectively. The model is based on the principle of uncompetitive inhibition (the same compound can act as substrate and inhibitor depending on the concentration applied) and assumes two binding sites; occupation of the first binding site leads to activation of the transporter and occupation of the second binding site leads to inhibition of the transporter. For details see Gatlik-Landwojtowic et al., 2006. As it will be widely discussed afterwards, this model is also applicable to fit data from the ABCG2 transporter.

K_{tw} (the binding constant of the substrate from water to the transporter). The binding constant of the substrate from water to the transporter (K_{tw}) is the half-maximum ($1/K_1$) activation from the modified Michaelis–Menten equation in ATPase activity measurements (Seelig and Gatlik-Landwojtowicz, 2005).

$$K_{tw} = \frac{1}{K_1} \quad (3)$$

4. Cell-based assay systems

4.1. Transport assays

Directional transepithelial transport studies were performed using MDCK-II cell subclones in 6-well Transwell plates (Transwell 3414, Corning Life Science, Corning, NY, USA) as previously described (Real et al., 2011) (Figure 29 A). Cells seeded at a density of 1 x 10^6 cell/well were grown for 3 days. As a control, transepithelial resistance was measured in each well using a Millicell-ERS ohmmeter (Millipore, Bedford, MA, USA) before and after the experiment; only wells with a resistance of ≥ 150 ohms were used. When the selective and potent ABCG2 inhibitor Ko143 was applied, it was present in both

compartments during pre-incubation and during the assay at 1 μM. 2 hours before the experiment was started, the culture medium on each side of the filters was replaced with Opti-MEM (serum-free medium), either with or without Ko143. The experiment was started by replacing the medium in the donor compartment (apical or basolateral) with fresh Opti-MEM containing the substrate to be tested (10 μM) in the presence or absence of Ko143. Samples were taken at 2 and 4 h and stored at -20 °C until HPLC analysis. At least three independent assays were performed with each drug. Results were represented as the percentage of drug concentration found in the acceptor compartment related to the total drug added to the donor compartment at the beginning of the assay. Relative transport ratios were calculated by dividing percentages of apically directed (B-A) by basolaterally directed (A-B) transports of drug after 4 h (Figure 29 B).

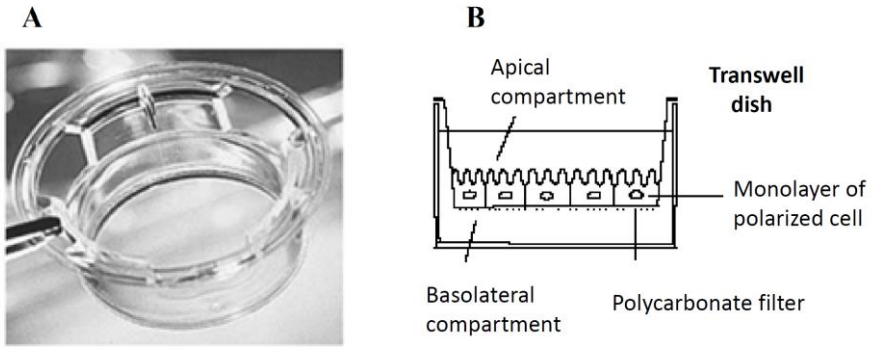

Figure 29. A. Transwell dish employed to perform transport assays with polarized cells. **B**. Different sections of a transwell dish.

4.2. Accumulation experiments

Mitoxantrone (MXR) accumulation measurements were performed based on previous published methods (Pavek et al., 2005) to test fluoroquinolones as ABCG2 inhibitors. Briefly, cells were grown in 24-well plates for 36 hours until sub-confluence, washed with PBS and then pre-incubated for 1 hour with Opti-MEM with or without Ko143 (1 μM), moxifloxacin or pefloxacin at different concentrations. Incubation was performed with the fluorescence substrate MXR (10 μM) in Opti-MEM with or without the tested inhibitors for 1 hour. Subsequently, in order to stop the reaction and retain the accumulation of the fluorescent substrate, cells were washed with ice-cold PBS, trypsinized, collected and resuspended in PBS with 2.5% FBS. Relative cellular accumulation of MXR (excitation and emission wavelengths 635 and 650 nm, respectively) of at least 5,000 cells was quantified by flow cytometry using a CYAN cytometer (Beckman Coulter®, Fullerton, CA, USA) testing the median of fluorescence (MF). Data from the histogram plots of the tested populations were processed using SUMMIT version 4.3 software (Innovation Drive, Fort Collins, CO, USA). Possible background fluorescence of the fluoroquinolones was evaluated; it was found to be negligible in all cases. Samples

were gated on forward scatter versus side scatter to exclude cell debris and clumps. At least three independent experiments were performed.

ABCG2 expression prevents accumulation of MXR in ABCG2-transduced cells; therefore, MXR is accumulated in cells lacking ABCG2 (parental) but not in cells expressing this transporter (human ABCG2 and murine Abcg2-transduced cells). ABCG2 inhibition increases accumulation of MXR in the ABCG2-transduced cells. The accumulation of MXR is reflected in the MF.

4.3. Cytosensor measurements

The rate of ATP synthesis in ABCG2 transduced living cells was measured by monitoring the extracellular acidification rates, ECARs, in real time using an eight-channel Cytosensor® Microphysiometer (Molecular Devices, Menlo Park, CA, USA) (McConnel et al., 1992). The Cytosensor (Figure 30) detects micro-pH changes in the extracellular fluid of cells in the flow chamber. The ECAR was shown to correspond to the rate of lactate efflux due to proton excretion as a result of glycolysis (for details see references Landwojtowicz et al., 2002; Gatlik-Landwojtowicz et al., 2004; Gatlik-Landwojtowicz et al., 2006). The procedure was performed similarly to the extensively previously described experiments with P-gp (Landwojtowicz et al., 2002; Gatlik-Landwojtowicz et al., 2004; Gatlik-Landwojtowicz et al., 2006; Aänismaa and Seelig, 2007; Nervi et al., 2010).

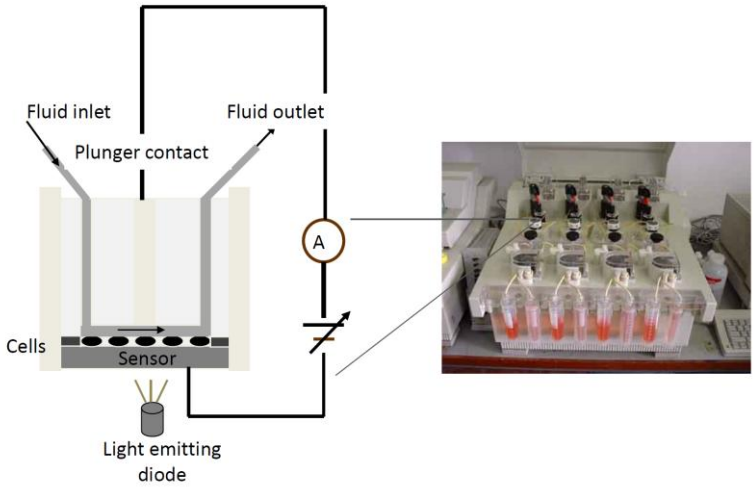

Figure 30. An eight-channel Cytosensor® Microphysiometer. One chamber is illustrated in detail indicating where the cells are attached to the polycarbonate membrane, the flow circuit of medium and the pH sensor system (Seelig, unpublished).

Briefly, cells were seeded at a density of 1-4 x10^5 cells per cup in the culture medium and were kept at 37°C overnight to allow for attachment to the polycarbonate membrane. The calibration of the instrument was discussed in detail elsewhere (Gatlik-Landwojtowicz et al., 2004). For quantification of

ECARs the cells were prepared 4 h prior to the Cytosensor experiment, since the number of cells seeded remained approximately constant within this period of time. Measurements were performed at pH 7.4 and temperature of 37 °C. Due to the flow chambers it is possible to maintain approximately constant drug concentrations, which allows the establishment of steady state conditions.

The pump cycles for stimulation of ABCG2 with drugs were based in previous published experiments for P-gp (Landwojtowicz et al., 2002; Gatlik-Landwojtowicz et al., 2004; Gatlik-Landwojtowicz et al., 2006). The acidification rates were measured during periodic interruptions of the flow of the medium through the flow chambers. During the pump-off period in each pump cycle the rate of extracellular pH changes were calculated by the Cytosoft program (Molecular Devices, Menlo Park, CA, USA.). The actual cellular response can be given either in percentage over the basal activity or in absolute values of protons per cell, per second (H+/cell/s) (Gatlik-Landwojtowicz et al., 2004; Gatlik-Landwojtowicz et al., 2006).

5. Methods for studying the passive influx

5.1. Surface activity measurements (SAMs)

Experiments were basically performed as described previously (Seelig et al., 1994; Fischer et al., 1998; Gerebtzoff et al., 2004). Buffer (Tris/HCl 50 mM with 114 mM NaCl) was freshly prepared before use with ultrapure water and adjusted to pH 7.4 at ambient temperature. Measurements were performed also at room temperature. A Teflon trough designed by Fromherz (Mayer Feintechnik, Göttingen Germany) (Fromherz and Marcheva 1975) was used, with 20 mL filling volume each compartment. To maintain a constant humidity, the trough was covered by a Plexiglas hood. The surface pressure was monitored with filter paper (Whatman N° 1, 15×16 mm) connected to a Wilhelmy balance (Figure 31).

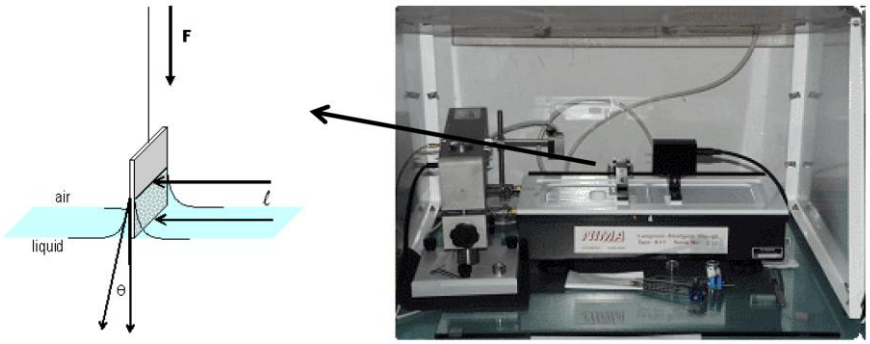

Figure 31. A Wilhelmy balance built as a Teflon trough used to perform Surface Activity Measurements. The interface between air and liquid achieved in the filter paper is drawn more in detailed.

Before each measurement, the trough and the filter paper were cautiously cleaned with methanol and distilled water. The filter paper was left in buffer up to equilibrium and then, the surface tension of the buffer was set to zero. Stock solutions (0.1-1000 mM) of each compound were prepared in pure water, water with NaOH (fluoroquinolones), DMSO or methanol, and serial aliquots were injected using a Hamilton syringe. The surface pressure *vs* the concentration of the compound was recorded until equilibrium, the critical micelle concentration (CMC). Since methanol itself shows some surface activity, compounds dissolved in it were corrected for the intrinsic surface pressure of methanol; the corrected SAM curves were in good agreement with SAM curves measured in purely aqueous solutions (Seelig et al., 1994). No further corrections were needed since the added volume compensated for the loss of solvent due to evaporation (Fischer et al., 1998). 1-4 independent measurements were performed.

From SAM experiments we could determine the next equations and coefficients:

Gibbs adsorption isotherm equation. This equation describes the thermodynamics of drug absorption at the air–water interface. SAM data are fitted to this equation.

$$d\pi = RT\Gamma d\ln C \qquad (4)$$

π is the surface pressure, RT is the product of the gas constant and the absolute temperature, C is the concentration of the compound in solution in the monolayer trough and Γ is the surface excess concentration of the compound at the air–water interface.

K_{aw} (air-water partition coefficient). Combining the Gibbs adsorption isotherm equation and the Szyszkowski equation (π = RTΓ_∞ln(K_{aw}C + 1)), it is possible to calculate the air-water partition coefficient (K_{aw}) as described below.

$$K_{aw}C = e^{\pi \cdot A_S N_A / RT} - 1 \qquad (5)$$

Where *C* is the concentration in the Teflon trough, *k* is the Boltzmann constant and T the absolute temperature, π is the pressure, N_A is the Avogadro number, and A_S is the surface active molecule at the interface. The last two parameters are obtained by surface activity measurements. The cross sectional area A_D can be assumed to be similar to the A_S (Fischer et al., 1998).

K_{lw} (lipid-water partition coefficient). Knowledge of the air-water partition coefficient (K_{aw}) and the cross sectional area (A_D) of a drug allows estimation of the lipid-water partition coefficient (K_{lw}) according to Equation 6 (Fischer et al., 1998).

$$K_{lw} = K_{aw} \cdot e^{-\pi_M A_D / kT} \qquad (6)$$

Here *k* is the Boltzmann constant and π_M is the lipid packing density of the membrane.

Calculation of passive influx. Passive influx can be calculated on the basis of stokesian diffusion taking into account the lateral membrane packing density (Seelig, 2007). The flux (Φ) is defined as the product of the permeability coefficient (P) and the concentration gradient between the intracellular and extracellular environment (ΔC). If only the initial external aqueous concentration (C) is considered, the flux can be expressed as:

$$\Phi = C \,.\, P \tag{7}$$

After a series of calculations and deductions (see Seelig, 2007), it can be assumed that the passive influx (Φ) into the cell can be calculated as:

$$\Phi \cong \left(\kappa \cdot \; e^{-\pi_{\mathrm{m}} A_{\mathrm{D}}/\mathrm{kT}}\right) \Big/ r_{\mathrm{D}} \tag{8}$$

Where π_M is the lipid packing density of the membrane, A_D is the cross sectional area of the drug, k is the Boltzmann constant, r_D is the radius of the diffusing molecule and κ comprises the membrane thickness (Δx) and the viscosity of the membrane (η).

$$\kappa = \mathrm{b} \cdot \frac{kT}{6\pi\eta\Delta x} \tag{9}$$

Therefore, the passive influx for uncharged drugs depends essentially on the radius (r_D) of the diffusing molecule and the packing density of the membrane (π_M), and for charged drugs, it depends in addition on the pK_a of the drug and the pH of the environment (Seelig, 2007).

5.2. Isothermal titration calorimetry (ITC)

ITC was performed with a VP ITC instrument (Microcal, Northampton, MA). Measurements were performed at 37 °C. Buffer solutions (50 mM Tris, 114 mM NaCl or 50 mM MOPS, 154 mm ionic strength) were freshly prepared and the pH was adjusted to 7 or 7.4 at 37 °C. A suspension of lipid vesicles formed from 1-palmitoyl-2-oleoyl-sn-glycero-3-phosphocholine (POPC) was injected into the compound solution in the calorimeter cell by using a Hamilton syringe; both, lipid and compound, are suspended in the same buffer. As a control, lipid vesicles were injected into the calorimeter cell containing buffer without compound. Solutions were degassed before use. The injection volumes were 3.5-12 μL. The calorimeter was calibrated electrically. The data were acquired by computer software developed by MicroCal.

For all compounds, injections gave rise to exothermic heats of reaction, produced by the partitioning of the compound into the membrane. The partition coefficient, K_{lw}, describes a linear

relation between the equilibrium concentration of the compound (free) in solution, C_{eq}, and the molar ratio of the compound bound per lipid, X_b. $X_b = K_{lw} C_{eq}$

6. Other determined parameters

K_{tl} (the binding constant from lipid to the transporter). The binding constant of the substrate from water to the transporter (K_{tw}) can be considered as the product of the lipid-water partition coefficient (K_{lw}) of the substrate and its binding constant from the lipid to the transporter (K_{tl}), Equation 10 (Seelig and Gatlik-Landwojtowicz, 2005).

$$K_{tw} = K_{lw} \cdot K_{tl} \quad (10)$$

Therefore, the binding constant from lipid to the transporter (K_{tl}) can be calculated as

$$K_{tl} = K_{tw} / K_{lw} \quad (11)$$

Free energies. The free energy of partitioning into the air-water interface ($\Delta G°_{aw}$) the free energy of partitioning into the lipid-water interface ($\Delta G°_{lw}$) the free energy of the binding constant of the substrate from water to the transporter ($\Delta G°K_{tw}$) and the free energy of the binding constant from lipid to the transporter ($\Delta G°K_{tl}$) are obtained as follows.

$$\Delta G°_X = -RTln(C_w K_X) \quad (12)$$

$$\Delta G°_{tw} = \Delta G°_{lw} + \Delta G°_{tl} \quad (13)$$

Where C_w is the molar concentration of water (C_w=55.5 $molL^{-1}$ at 24 ± 1°C and C_w=55.3 $molL^{-1}$ at 37°C) *X* is *aw, lw, tw* or *tl*, and *R* is the gas constant.

7. Pharmacokinetic studies

Abcg2$^{-/-}$ and wild-type mice were orally administered with norfloxacin or pefloxacin (10 mg/kg) by gavage into the stomach, 300 μl of drug solution per 30 g body weight. Norfloxacin solution was prepared at 1 mg/ml in saline (0.9% NaCl) and 1% NaOH, and pefloxacin at 1 mg/ml in saline (0.9% NaCl). Animals were fasted 3 h before administration. After anesthesia with isoflurane, blood was collected either by orbital bleeding, using heparinized capillary tubes, or cardiac puncture. Immediately thereafter, mice were sacrificed by cervical dislocation.

In experiments with male mice, organs were removed, intestinal content was separated from intestinal tissue and bile was obtained from the gall-bladder at 30 min for pefloxacin and 30 and 60 min for norfloxacin. Blood was collected at 5, 15, 30, 60 or 120 min after administration.

Norfloxacin was also administered orally to male wild-type and knockout mice for 7 days, one daily dose at 10 mg/kg. Plasma concentrations of norfloxacin at 15 min post-dosing every two days were analysed. Animals were kept in metabolic cages, and feces and urine were also collected at 24 h after the first administration; additionally, urine was collected at 60 min after this first administration.

In milk secretion experiments, females with ~10-day-old pups were used. To stimulate milk secretion, oxytocin (200 µl of 1 IU/ml solution) was administered subcutaneously 20 min before milk collection. 15 min after drug administration, blood and milk were collected. Milk samples were obtained from mammary glands by vacuum suction.

Subsequently, heparinized blood samples were centrifuged at 1000 g for 10 min and plasma was collected. Plasma, bile, milk and tissues were stored at -20 °C until HPLC analysis. Three to seven animals were used for each time point.

The area under the plasma concentration-time curve (AUC) from t = 0 to the last sampling point was calculated by the linear trapezoidal rule. Tissue-to-plasma ratios were obtained by dividing the drug concentration in milk, bile or liver by the plasma concentration at the same sampling point.

8. HPLC analysis

The conditions for HPLC analysis of the fluoroquinolones were established as described previously, with slight modifications (Garcia et al., 2000; Tsai, 2001; Merino et al., 2006). The chromatographic system consisted of a Waters 2695 separation module and a Waters 2998 UV photodiode array detector. Samples maintained at 4°C were separated on a reversed-phase column (Phenomenex Synergi 4 μm Hydro-RP 80 Å) at room temperature. UV absorbance was measured at 278 nm. Integration was performed using Empower software (Waters, Milford, MA, USA).

For the analysis of transport samples, 50 μl of the culture media from transport assays were directly injected into the HPLC system. The mobile phase consisted of orthophosphoric acid (25 mM, pH 3.0) and acetonitrile (70:30, v/v; for moxifloxacin and 80:20, v/v; for pefloxacin). The flow rate of the mobile phase was set at 1.5 ml/min for both fluoroquinolones. Calibration curves from standard samples in Opti-MEM were performed at a concentration range of 0.16 - 5 μg/ml for moxifloxacin and 0.07 - 5 μg/ml for pefloxacin.

For the analysis of samples from pharmacokinetic experiments, organs were defrosted and the entire organ or the intestinal content was homogenized in 2 ml of sodium phosphate buffer 0.5 M pH 7.0 with a Polytron homogenizer (Kinematica AG, Lucerne, Switzerland), based on a modified method

from Montay and Tassel (1985). Aliquots of 100 μl of plasma, or tissue homogenate, or 50 μl of bile were analysed to determine norfloxacin and/or pefloxacin concentrations. To process the samples, 10 μl of enrofloxacin (12.5 μg/ml) as an internal standard and 300 μl of dichloromethane were added to each aliquot. Samples were shaken and the water and organic phases were separated by centrifugation at 5000 g for 5 min. Then, the organic phase was evaporated to dryness under a nitrogen stream, resuspended with 100 μl of methanol and injected into the HPLC system. The mobile phase consisted of citrate buffer (25 mM, pH 5.0), acetonitrile and triethylamine (83:17:0.1, v/v/v). The flow rate of the mobile phase was set at 1 ml/min. Standard samples were prepared using the appropriate matrix and the range of concentrations used was 0.08 - 80 μg/ml. Sample peak area ratios (fluoroquinolone/enrofloxacin) were used for comparison with the standard curve.

9. Statistical Analysis

Results are presented as means ± standard deviation (SD). The two-sided unpaired Student *t* test was used to assess the statistical significance of differences between two sets of data. Differences were considered to be statistically significant when $P < 0.05$.

Results

1. Comparison of ATPase activity, substrate specificities and substrate-activity relationships between ABCG2 and P-glycoprotein

The ABCG2 and P-gp, both members of the ATP-transporter family, exhibit a very low sequence homology; however they show overlapping substrate specificity. The first aim of the present investigation was to gain further insight into similarities and differences of the two transporters concerning ATPase activity, substrate specificity and substrate-activity relationship. To this purpose we characterized 28 drugs for their interaction with ABCG2 and P-gp by measuring the basal and substrate-induced ATPase activity of ABCG2 and P-gp in inside-out plasma membrane vesicles of cells over-expressing the respective transporters (ABCG2-M-ATPase and NIH-MDR1-G185 plasma membrane vesicles, respectively) using a colorimetric assay. Previously, we analyzed the ABCG2 membrane vesicles and optimized the conditions for the ATPase activity measurement. Moreover, we characterized the compounds by means of surface activity measurements; we assessed their air-water partition coefficients and their cross-sectional areas in their membrane bound conformation which allowed an estimation of their lipid-water partition coefficients. This procedure let to explain some of the mechanistics and activity of the two transporters. The principles derived with drugs were verified with 10 detergents by measuring their interaction with the transporters *via* ATPase activity. Cytosensor measurements were also performed with cells over-expressing the ABCG2 transporter. In addition, the present results were combined with a structural analysis.

1.1. Quantification of ABCG2 expression

NIH-MDR1-G185 cells were previously characterized by FACS flow cytometery using the human P-gp-specific mouse monoclonal antibody MRK16 and fluorescent FITC-labeled species anti-mouse polyclonal secondary antibodies (Landwojtowicz et al., 2002). The number of P-gp molecules per cell has been calculated (Ambudkar et al., 1997).

However, the level of ABCG2 expression in the ABCG2-M-ATPase membranes is not known. Thus, to properly characterize the used ABCG2-M-ATPase plasma membrane vesicles for ABCG2 ATPase activity analysis, the level of ABCG2 expression was measured. The corresponding intact cells of ABCG2-M-ATPase membranes which would allow an estimation of the expression level using ABCG2 antibodies are not available. The level of ABCG2 expression in the ABCG2-M-ATPase membranes was therefore studied by combining three different approaches. We used the well characterized MEF3.8 cells for calibration (Pavek et al., 2005). First of all, we performed a Western blot analysis; secondly, we quantified levels of enhanced GFP expression in ABCG2-transduced MEF3.8 cells; thirdly, we compared the ATPase activity between ABCG2-transduced MEF3.8 and ABCG2-M-ATPase plasma membrane vesicles to get an estimation of the number of ABCG2 molecules per cell of the ABCG2-M-ATPase membranes.

1.1.1 Western Blot analysis

First, we compare the expression level of human ABCG2 in the plasma membrane vesicles from ABCG2-transduced MEF3.8 cells and from ABCG2-M-ATPase mammalian cells by means of a Western blot using BXP-21 monoclonal antibody (Figure 32). A densitometric analysis taking into account 11 gels, yielded an at least 7-fold higher ABCG2 concentration in ABCG2-M-ATPase membranes than in ABCG2-transduced MEF3.8 cell membranes.

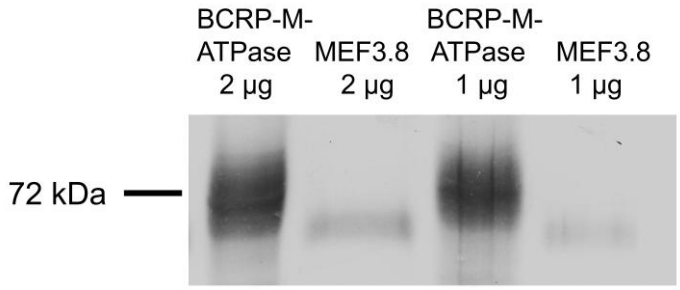

Figure 32. Representative Western Blot analysis of ABCG2 (BCRP) in plasma membrane vesicles from MEF3.8 cells transduced with human ABCG2 and ABCG2-M-ATPase vesicles from mammalian cells from SOLVO. 1-2 µg of protein were separated by 10% SDS-PAGE and blotted on a nitrocellulose membrane. The monoclonal antibody BXP-21 was used to detect ABCG2, followed by an AP conjugated second antibody.

1.1.2 ABCG2 quantification with the enhanced GFP in MEF3.8 cells

MEF3.8 cells were transduced with a monocistronic vector containing ABCG2 followed by an internal ribosome entry site (IRES) and the enhanced green fluorescent protein (GFP) (Pavek et al., 2005). Hence, secondly, we quantified the cellular GFP using a calibration curve made with commercially available GFP in aqueous solution (Figure 33 A) which allowed a rough estimation of ABCG2 expression.

The fluorescence background of the parental MEF3.8 cells lacking GFP was similar to that of the solvent (PBS containing 20% glycerol) (Figure 33 B); different solvents were tested and the same fluorescence background was found for all of them (not shown). Errors due to GFP adsorption to the well-plate could be excluded by comparing fluorescence measurements obtained with and without pre-coating the measured cells with BSA (Wilma Van Esse et al., 2011). A lysation of cells did not yield to a higher fluorescence compared to intact cells. The samples had to be very concentrated, because at cell concentrations lower than $0.3x10^6$ cells, the GFP fluorescence corresponds to the fluorescence background and errors were observed (see Figure 33 B).

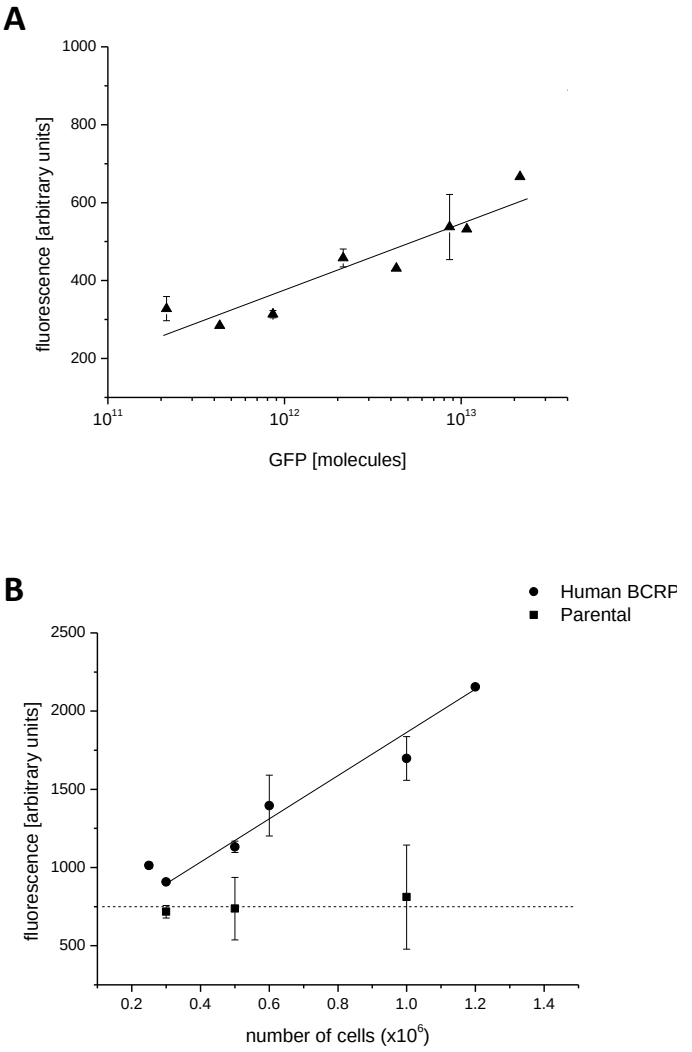

Figure 33. ABCG2 quantification with the enhanced GFP in MEF3.8 cells. **A**. Titration curve with pure GFP. **B**. Titration of GFP fluorescence in MEF3.8 cells transduced with human ABCG2 (circles) and parental cells (squares). The fluorescence background is indicated with a dashed line.

Comparing the fluorescence obtained for the MEF3.8 cells transduced with human ABCG2 with the titration curve of commercial GFP, the calibration yielded approximately 10^6 to 10^7 GFP/ABCG2 molecules per MEF3.8 cell. Although it is not yet answered if the minimal functional unit of ABCG2 is a homodimer or homooligomer (Ni et al., 2010 a and b), for the following calculations we assumed further that ABCG2 functions as a homodimer (Kage et al., 2002; Litman et al., 2002; Bhatia et al., 2005), rather than a homotetramer (two ABCG2 dimers) (Xu et al., 2004; McDevitt et al 2006; Rosenberg et al., 2010) which yielded $5x10^5$ to $5x10^6$ molecules of functional ABCG2 per cell. With these numbers, the level of ABCG2 in ABCG2-M-ATPase membranes was estimated as $7\times(5x10^5 – 5x10^6)$ molecules per cell, i.e., $3.5x10^6$ - $3.5x10^7$ molecules per cell (taken into account the 7-fold higher ABCG2 concentration obtained in ABCG2-M-ATPase membranes than in MEF3.8 cell membranes by Western blot, Figure 32).

As MEF3.8 cells and NIH-MDR1-G185 cells are fibroblats we can assume that the total protein content is identical. NIH-MDR1-G185 cells have in the order of 10^6 molecules of P-gp (Ambudkar et al., 1997). We have determined 10^5 to 10^6 ABCG2 dimer-molecules per MEF3.8 cells, which is in the same order of magnitude as P-gp. We can therefore assume that the amount of transporter is 1% from the total protein concentration in the MEF3.8 membranes, as it is for NIH-MDR1-G185 cells (Aanismaa and Seelig, 2007).

1.1.3 Comparison of the quantitative expression of ABCG2 in membranes from transduced MEF3.8 cells and ABCG2-M-ATPase membranes by ATPase activity measurements

For further comparison expression of ABCG2 in the two cell lines, we titrated ABCG2 in ABCG2-transduced MEF3.8 plasma membranes and ABCG2-M-ATPase membranes with sulfasalazine, the compound with the best bellshaped curve interacting with ABCG2 in ATPase activity assays (Glavinas et al., 2007), under identical conditions. We had previously checked that the optimal conditions to perform ATPase activity assays with ABCG2-M-ATPase membranes were also valid for the MEF3.8 membranes (for conditions see below). We performed the same measurements at different protein membrane concentration.

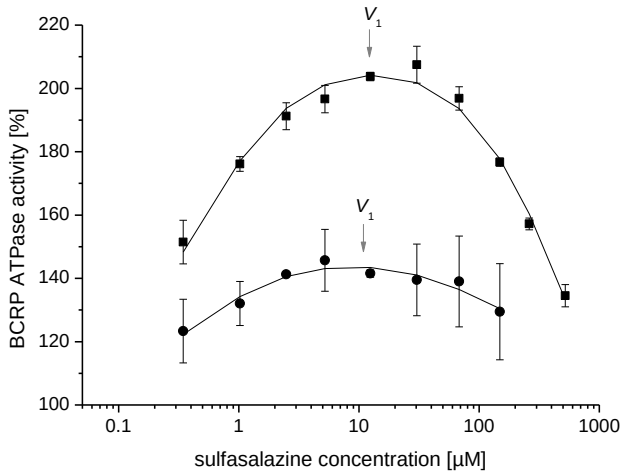

Figure 34. Sulfasalazine human-ABCG2-ATPase activity titration in vesicles from MEF3.8 (circles) and ABCG2-M-ATPase membranes (squares) at 0.075 mg/ml protein. The titration curves are the average of two measurements presented as means and error bars correspond to standard deviations (SD).

As seen in Figure 34 the ATPase activity increased with the concentration of sulfasalazine up to a maximum and decreased again at high concentrations yielding bell-shaped curves in both cell lines. The basal activity was defined as 100 % and the increase over basal values is displayed as a function of

sulfasalazine concentration (Log scale). The solid lines represent fits of a two-site binding model (Equation 2) to the data. The analysis yielded the concentration of half-maximum activation, K_1 (i.e. 0.68 µM for ABCG2-M-ATPase membranes and 0.39 µM for membranes from MEF3.8 cells), and inhibition, K_2 (600.41 µM for ABCG2-M-ATPase membranes and 137.89 µM for membranes from MEF3.8 cells), respectively; as well as the maximum, V_1 (2.11-fold for ABCG2-M-ATPase membranes and 1.47-fold for membranes from MEF3.8 cells), and minimum, V_2 (0.43-fold for ABCG2-M-ATPase membranes and 1.15-fold for membranes from MEF3.8 cells), activity.

To compare ATPase activity differences, the maximum activity (V_1) was plotted as a function of plasma membrane protein concentration (Figure 35). The figure clearly shows the higher ATPase activity with ABCG2-M-ATPase membranes.

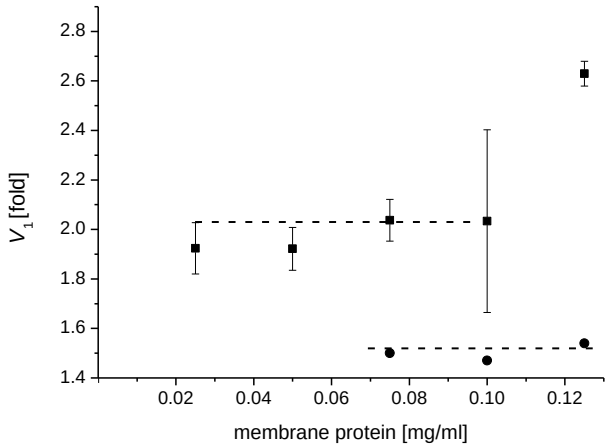

Figure 35. The maximum activity (V_1), obtained from phosphate measurements using plasma membrane vesicles containing human-ABCG2 from MEF3.8 cells (circles) or ABCG2-M-ATPase from mammalian cells (squares), plotted as a function of plasma membrane concentration of protein. Sulfasalazine was used as titrant.

As seen in Figure 36, the sulfasalazine-induced ATPase activity was around 5-fold higher in ABCG2-M-ATPase membranes than in MEF3.8 plasma membranes (observe for instance the difference between both V_1; i.e. the average of V_1 is ~ 80 nmol min^{-1} mg^{-1} for ABCG2-M-ATPase membranes and ~ 15 nmol min^{-1} mg^{-1} for membranes from MEF3.8 cells, therefore $V_{1\ ABCG2\text{-}M\text{-}ATPase}$ / $V_{1\ MEF3.8} \approx 5$. In addition, the difference between both V_0; i.e. the average of V_0 is ~ 40 nmol min^{-1} mg^{-1} for ABCG2-M-ATPase membranes and ~ 8 nmol min^{-1} mg^{-1} for membranes from MEF3.8 cells, therefore $V_{0\ ABCG2\text{-}M\text{-}ATPase}$ / $V_{1\ MEF3.8} \approx 5$), which is in good agreement with the estimation of the expression level of ABCG2 by Western blot (Figure 32); i.e. the 7-fold higher ABCG2 concentration obtained in ABCG2-M-ATPase membranes than in MEF3.8 cell membranes by Western blot.

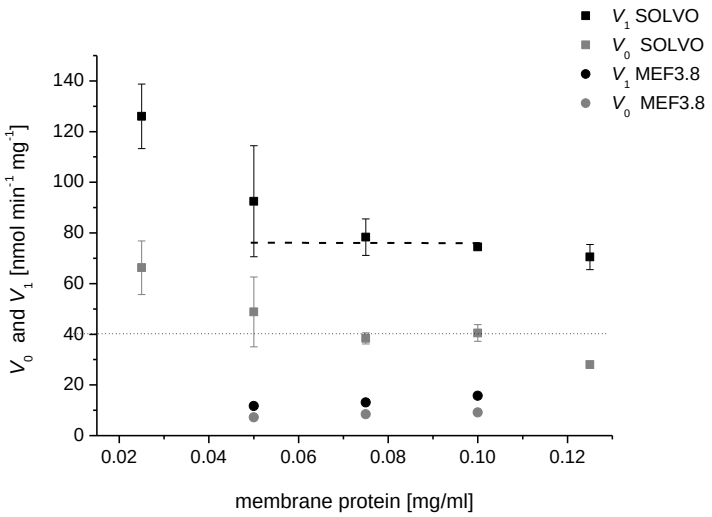

Figure 36. Basal activity (V_0) and the maximum sulfasalazine induced activity (V_1) in nmol min^{-1} mg^{-1} represented as a funtion of membrane protein concentration. The basal activity from Glavinas et al., 2007 at 20 µg/well of membrane vesicles is indicated with a stippling line. Results from MEF3.8 plasma membrane are also included for comparison.

1.2. Optimization of conditions for ABCG2-ATPase activity measurements

To optimize the experimental conditions of ATPase activity measurements with the ABCG2-M-ATPase plasma vesicle membranes we performed dependent experiments on each variable. The appropriate concentration of protein, the optimal incubation time, pH, vanadate and ATP concentrations, respectively, were assessed.

Concentration of plasma membrane protein. To determine the appropriate concentration of plasma membrane protein needed in the experiments, titrations of sulfasalazine were performed using various dilutions of membrane protein (0.025-0.125 mg/ml). The ATPase activity as a function of protein concentration (Log scale) yielded a bell-shaped dependence for each protein concentration used (Figure 37). The average basal activity (V_0) as well as the maximum sulfasalazine induced activity (V_1) (Figure 36) were constant in the protein concentration range of (0.05 - 0.1) mg/ml and were determined as a V_0 = 39.21 ± 2.27 nmol min^{-1} mg^{-1} and V_1 = 76.83 ± 4.96 nmol min^{-1} mg^{-1}, respectively. For comparison, data from MEF3.8 plasma membranes were, V_0 = 8.14 nmol min^{-1} mg^{-1} and V_1 = 13.08 nmol min^{-1} mg^{-1}. A closer inspection of Figures 36 and 37 shows that increasing membrane concentration yielded slightly increasing half maximum activation/inhibition (K_1, K_2) values and also slightly increasing maximum activities (V_1). 0.075 mg/ml was chosen as an appropriate concentration of protein for the ATPase activity experiments as an intermediate concentration.

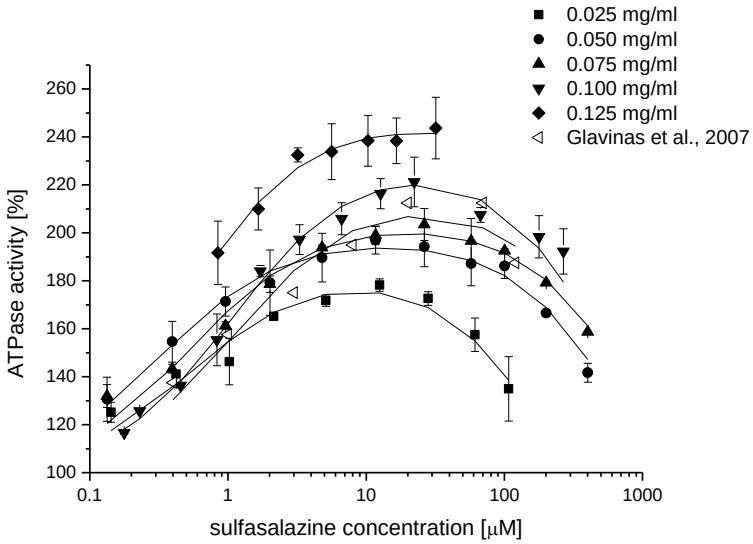

Figure 37. ABCG2-ATPase activity represented as a function of sulfasalazine concentration in ABCG2-M-ATPase membranes at 0.025 to 0.125 mg/ml of membrane protein. Results from Glavinas et al. (2007) at 20 μg/well of membrane vesicles are also represented for comparison.

Time of incubation. Secondly, we tested the incubation time dependence by stimulating the ABCG2-ATPase activity with sulfasalazine at 30 min, 45 min, 60 min and 90 min incubation time. Sulfasalazine was applied at a concentration range of 0.41 – 27.37 μM. We could see an approximately linear correlation between time and the optical density signal up to 60 min of incubation in water bath kept at 37 °C for the protein concentration of 0.075 mg/ml (Figure 38). 60 min was chosen for subsequent experiments.

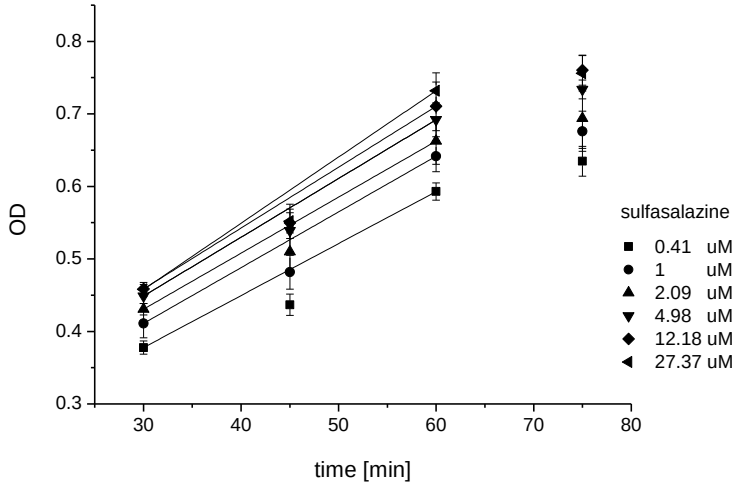

Figure 38. Optical density (OD) represented as a function of time of incubation for sulfasalazine in the concentration range of 0.41 – 27.37 μM in ABCG2-ATPase activity with ABCG2-M-ATPase membranes.

Buffer pH. When the experiment was performed at different buffer pH values (between 5 and 8.5), no effect was observed in the basal activity between pH 6 and 8 (Figure 39). ABCG2 appeared not to be affected by the pH in this range. The basal ATPase activity is used in this experiment to make sure that there is not any probable interference from a drug on the pH.

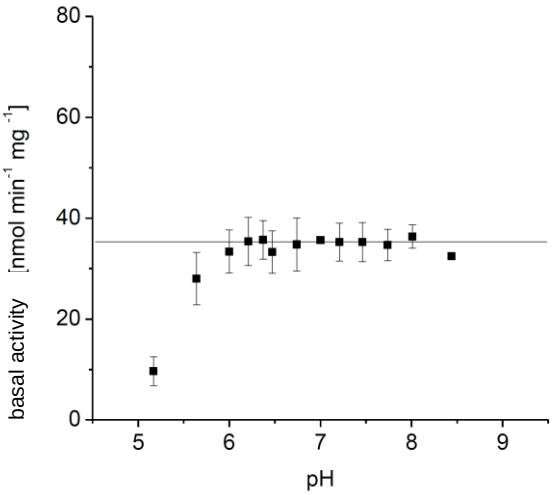

Figure 39. The effect of pH in the buffer of ATPase activity assays shown with ABCG2-M-ATPase plasma vesicle membranes. The basal ATPase activity is represented as a function of the pH.

Vanadate concentration. Vanadate is a pentavalent phosphate analog whose structure is similar to ATP and is often used to block ABC-transporters in the post-hydrolysis state (Urbatsch et al., 1995). The optimal vanadate concentration to inhibit ABCG2 ATPase activity was assessed by measuring the ATPase activity as a function of vanadate concentration (Figure 40). The curve was fitted to the Hill equation (Equation 1) yielding the concentration of half-maximum activation determined as $K_{0.5}$ = 4.06 µM. A complete inhibition of the ATPase was achieved at a vanadate concentration of 0.1 mM. A concentration of 0.5 mM of vanadate was chosen to perform the ATPase activity assays in the following experiments to guarantee a complete protein inhibition, as used previously for P-gp (Litman et al., 1997 a and b).

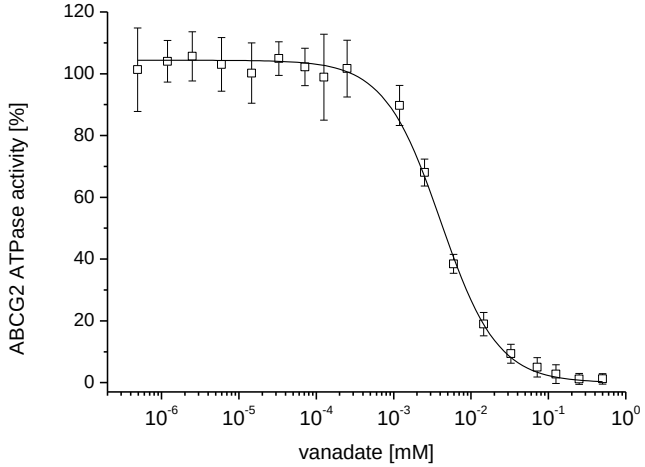

Figure 40. ATPase activity in ABCG2-M-ATPase plasma membrane vesicles represented as a function of the vanadate concentration. The line represents curve fit according to Hill equation.

ATP concentration. The ABCG2 ATPase activity was also measured as a function of the ATP concentration. The ATPase activity rose with increasing ATP concentration up to a maximum around 3 mM ATP and then decreased at higher concentrations, showing a bell-shaped activity curve. Considering the activating ATP concentration range only (C_{ATP} = 0 - 3 mM), data in Figure 41 could be well fitted with the Hill equation (Equation 1) yielding the concentration of half-maximum activation and the maximum activity determined as $K_{0.5}$ = 0.92 mM and V_{max} = 40.7 nmol min^{-1} mg^{-1}. The full curve could also be fitted to the un-competitive Michaelis-Menten equation (Equation 2).

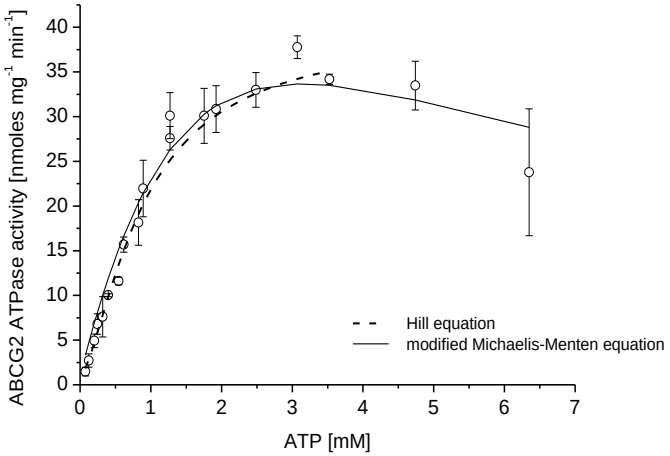

Figure 41. ATPase activity in ABCG2-M-ATPase plasma membrane vesicles measured as a function of the ATP concentration. The lines represent curve fitted according to Hill equation (dashed line) or the modified Michaelis-Menten equation (solid line).

For the following, in ABCG2-ATPase activity assays the plasma membrane protein concentration was C_{prot} = 0.075 mg/ml, the incubation time was t = 60 min, the vanadate concentration was C_V = 0.5 mM and the ATP concentration was C_{ATP} = 3 mM. All experiments were performed at pH 7.0 and 37 °C.

1.3. ATPase activity measurements in plasma membrane vesicles for P-gp and ABCG2

1.3.1. ATPase activity assays with 28 compounds

To compare ATPase activity, substrate specificities and substrate-activity relationships between P-gp and ABCG2, 28 compounds were tested. The compounds investigated are displayed in Table 9. The list of compounds include those with potential P-gp recognition patterns (Seelig, 1998) (daunorubicin, dexamethasone, digoxin, etoposide, glybenclamide, promazine, tamoxifen, verapamil), steroid hormones (cortisol, estradiol, progesterone, testosterone), typical compounds for ABCG2 interaction (Ko143, methotrexate, mitoxantrone, prazosin, sulfasalazine, riboflavin), the H_2 receptor antagonists (cimetidine, famotidine, nizatidine, ranitidine), fluoroquinolones (ciprofloxacin, enrofloxacin, norfloxacin, pefloxacin), CPT-cAMP and forskolin. Note that dexamethasone apart from a typical P-gp substrate, is also a synthetic steroid hormone. The compounds listed in Table 9 were classified according to the electric charge at physiological pH, as electrically neutral, basic, anionic, and zwitterionic. Moreover we defined three groups describing the molecular distribution of polar and non-polar centers in the molecule. Compounds in group I display an amphiphilic charge distribution with a polar and a hydrophobic end, molecules in group II have a hydrophilic core flanked on each side by hydrophobic centers, and molecules in group III have a hydrophobic core flanked on each side by a polar center (Figure 42).

Table 9. Compounds tested with ATPase activity and kinetic parameters of P-gp and ABCG2 activation. The concentration of half-maximum activation (inhibition), K_1 (K_2), and the maximum (minimum) transporter activity, V_1 (V_2), were obtained from phosphate release measurements in plasma membrane vesicles. The kinetic parameters for each compound were calculated using all results obtained.

				P-gp				ABCG2			
Charge [a]	Charge distrib.[b]	N°	Compound	K_1 (μM)	K_2 (μM)	V_1 (fold)	V_2 (fold	K_1 (μM)	K_2 (μM)	V_1 (fold)	V_2 (fold)
O	I	1	cortisol	129.81	nd	1.95	nd	nd	485.48	nd	0.23
	I	2	dexamethasone	286.29	nd	2.50 [c]	nd	nd	267.58	nd	0.00
	I	3	progesterone	36.60	141.51	4.89	0.71	nd	31.23	nd	0.49
	I	4	testosterone	191.00	305.00	4.50 [c]	2.56	nd	160.67	nd	0.19
	II	5	Ko143	3.06	10.52	3.21	0.00	nd	0.01	nd	0.10
	III/I	6	digoxin	12.07	nd	1.96	nd	nd	82.13	nd	0.00
	III	7	estradiol	nd	nd	nd	nd	nd	4.65	nd	0.62
	III	8	etoposide	102.23	424.17	1.55	1.24	nd	102.31	nd	0.45
	III	9	forskolin	143.15	nd	1.49	nd	nd	25.56	nd	0.64
(+)	II	10	prazosin	13.10	3117.51	3.36	2.63	1.19	210.06	1.49	1.28
	III	11	cimetidine	1975.10	nd	1.84 [c]	nd	320.12	nd	1.36 [c]	nd
	III	12	famotidine	1716.92	nd	2.22 [c]	nd	394.68	50485.9	1.37	0.00
	III	13	nizatidine	5255.03	nd	3.22 [c]	nd	1085.36	nd	1.30	nd
	III	14	ranitidine	nd	nd	1.65 [c]	nd	nd	298.50	nd	0.82
+	I	15	promazine	82.00	2150.00	2.50	0.10	nd	20.92	nd	0.48
	I	16	tamoxifen	1.47	nd	1.60	nd	nd	8.88	nd	0.32
	II/I	17	verapamil	1.00	843.60	2.50	1.00	nd	159.88	nd	0.01
	III	18	daunorubicin	5.50	43.50	1.40	0.80	10.83	77.08	1.95	0.94
	III	19	mitoxantrone	nd	nd	nd	nd	75.67	nd	1.28 [c]	nd
-	II/I	20	glybenclamide	80.85	460.23	5.33	0.00	nd	35.54	nd	0.13
	III	21	CPT-cAMP	-	-	-	-	80.36	nd	1.47	nd
	III	22	methotrexate	-	-	-	-	nd	nd	nd	nd
	III	23	riboflavin	-	-	-	-	121.16	9410.66	1.72	0.02
	III	24	sulfasalazine	-	-	-	-	1.67	1100.53	2.26	0.00
+/-	III	25	ciprofloxacin	-	-	-	-	665.02	nd	1.42 [c]	nd
	III	26	enrofloxacin	-	-	-	-	19.51	361.31	1.56	1.28
	III	27	norfloxacin	-	-	-	-	947.55	nd	1.26 [c]	nd
	III	28	pefloxacin	-	-	-	-	160.23	5155.29	1.60	0.00

[a] Electric charge classification at pH 7.4 for the compounds. O, neutral; (+) partially cationic; +, cationic; -, anionic; +/-, zwitterionic. [b] Charge distribution on the molecular structure: I, polar – non-polar; II, non-polar – polar – non-polar; III, polar – non-polar - polar. [c] Maximum not reached. *nd*: not determined.

Note that verapamil (include in group II in Table 9), glybenclamide (include in group II in Table 9) and digoxin (include in group III in Table 9) can fold and can thus adopt also the structure of group I (Table 9 and Figure 42); thus, they are amphiphilic.

Charge distribution	I	II	III
Representation of the structure			
Compounds	cortisol, promazine, dexamethasone, tamoxifen, progesterone, testosterone, digoxin, verapamil, glybenclamide	Ko143, prazosin	cimetidine, enrofloxacin, methotrexate, ranitidine, ciprofloxacin, estradiol, mitoxantrone, riboflavin, CPT-cAMP, etoposide, nizatidine, sulfasalazine, daunorubicin, famotidine, norfloxacin, forskolin, pefloxacin

Figure 42. Schematic representation of the compounds structured by the hydrophobic (black) and the hydrophilic (white) groups.

P-gp and ABCG2 activity in inside-out plasma membranes vesicles from NIH-MDR1-G185 cells and ABCG2-M-ATPase, respectively, were measured for the 28 compounds listed in Table 9. Figures 43 to 45 show the rate of P-gp and ABCG2 activity as a function of substrate concentration (Log scale). The concentration range chosen for ATPase activity measurements was derived from surface activity measurements (see next Section 1.4 at results). Titrations were generally started at the concentration slightly below where the surface activity pressure starts to increase and ended at the CMC or solubility limit of the compound. For several compounds it could even not be possible to achieve this limit because problems with solubility and/or the basal activity. Drug-stimulated P-gp and ABCG2 activity is expressed as a percentage of the basal activity (taken as 100%). The solid lines in Figures 43 to 45 were fitted to the modified Michaelis-Menten model (Equation 2) proposed by Litman et al. (1997a), assuming P-gp activation upon binding of a first drug molecule at low concentration, and inhibition upon binding of a second drug molecule at high concentration. The titration curves are shown as examples representing the average of two measurements.

Compounds in Figures 43 to 45 are organized according to their functional classification or the nature of their effect upon the P-gp and ABCG2 ATPase activity in the following manner: Figure 43 and Figure 44 include the compounds that interact with both transporters; Figure 45 includes the compounds that interact only with ABCG2. Additionally, compounds from Figure 43 have neutral charge; compounds from Figure 44 are mostly positive electrically charged and compounds from Figure 45 are essentially positive and/or negative charged.

The activation profiles of typical P-gp compounds show a characteristic bellshaped dependence on the logarithm of concentration in Figures 43 and 44 A and B. Promazine, verapamil, glybenclamide, Ko143, progesterone and etoposide enhanced the P-gp ATPase activity at low concentrations up to a

maximum and reduced it again at higher concentrations that are still well below the CMC. The P-gp response with Ko143 is surprising and it has never been published before. The P-gp titration curves of other compounds in Figures 43 and 44 A and B showed only activation (tamoxifen, forskolin, cortisol, testosterone, dexamethasone and digoxin). In contrast, all compounds in Figures 43 and 44 A and B barely enhanced but rather reduced the ABCG2 ATPase activity already at low concentrations, indicating that they interact with ABCG2 directly inhibiting it.

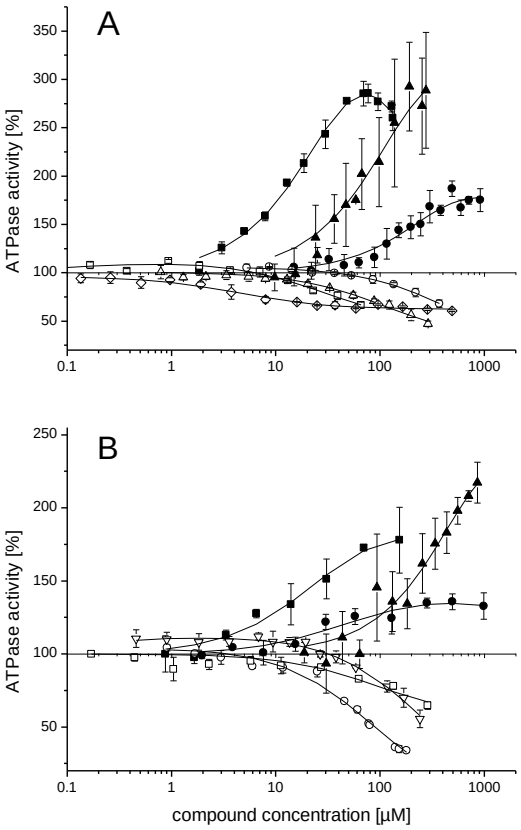

Figure 43. ATPase activity in inside-out plasma membrane vesicles as a function of the substrate concentration for P-gp (closed symbols) and ABCG2 (open symbols). The titration curves shown as examples represent the average of two measurements, standard deviation are given. Solid lines are fits to the modified Michaelis-Menten equation (Equation 2). **A**: cortisol (●), estradiol (♦), progesterone (■), testosterone (▲). **B**: dexamethasone (▲), digoxin (■), etoposide (●).

Figure 44 C shows the compound-induced P-gp and ABCG2 ATPase activity profiles in inside–out membrane vesicles for daunorubicin and prazosin, which are the only two relatively hydrophobic compounds with a full bell-shaped curve for both transporters, with an ascending branch at low concentrations and descending branch at higher concentrations. ATPase activity measurements for H_2 receptor antagonists are represented in Figure 44 D; only an activation part of the ATPase activity curve was acquired for all four drugs when the compounds were evaluated with P-gp. The same phenomenon

was observed with the protein ABCG2, except for ranitidine, which had only inhibition of ATPase activity. A different scale has been used to plot the H_2 receptor antagonists as they are more hydrophilic and it was necessary to apply higher concentrations to achieve the curve of ATPase activity. The electric charge of these compounds at pH 7.4 is cationic.

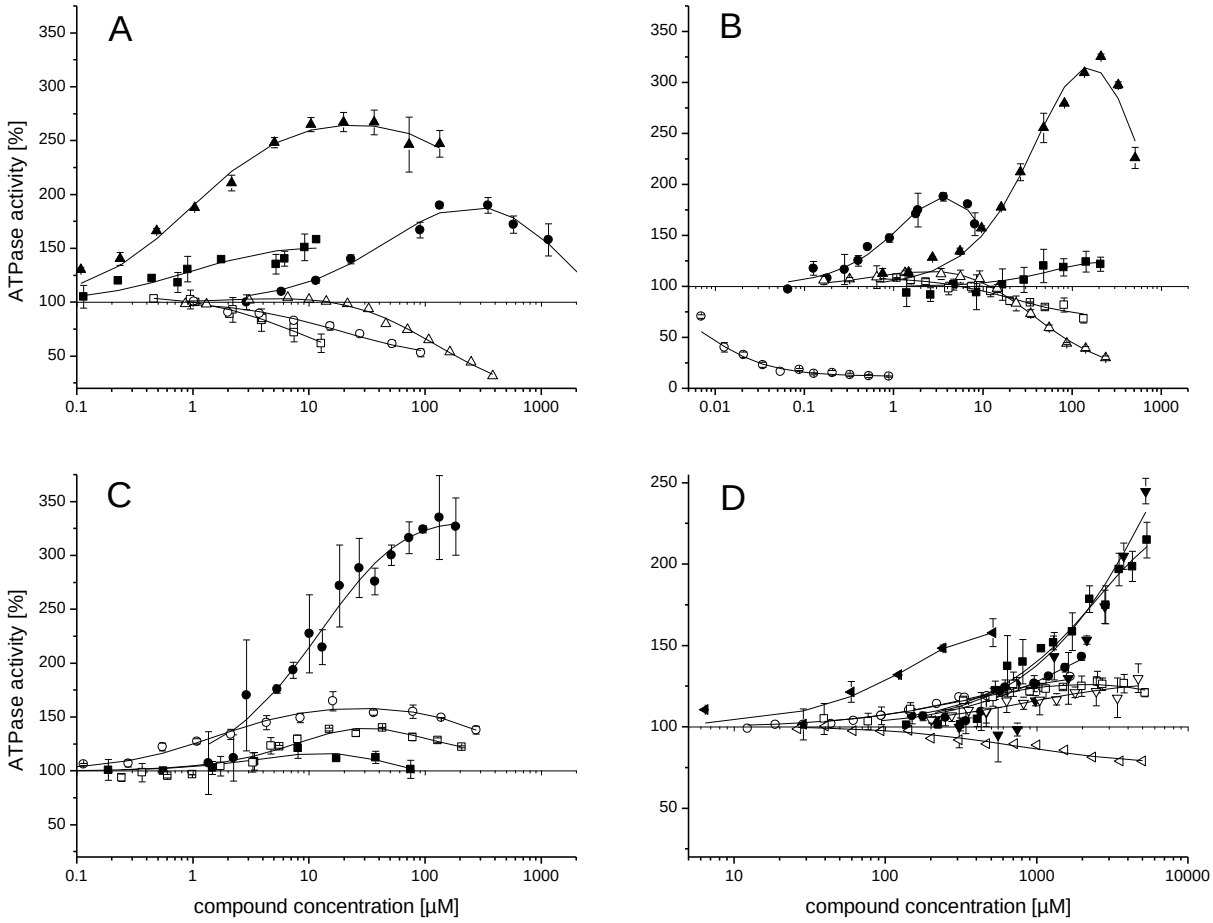

Figure 44. ATPase activity in inside-out plasma membrane vesicles as a function of the substrate concentration for P-gp (closed symbols) and ABCG2 (open symbols). The titration curves shown as examples represent the average of two measurements, standard deviation are given. Solid lines are fits to the modified Michaelis-Menten equation (Equation 2). **A**: promazine (•), tamoxifen (■), verapamil (▲). **B**: forskolin (■), glybenclamide (▲), Ko143 (•). **C**: daunorubicin (■), prazosin (•). **D**: cimetidine (•), famotidine (■), nizatidine (▼), ranitidine (◄).

The titration curves shown in Figure 45 include compounds which did not appear to interact with P-gp (Data not shown). It is important to remark that the ATPase curve for P-gp was negligible with points with a tremendous scatter using the fluoroquinolones (ciprofloxacin, enrofloxacin, pefloxacin,

norfloxacin), CPT-cAMP, estradiol, methotrexate, mitoxantrone, riboflavin and sulfasalazine (Data not shown). Sulfasalazine is the compound with the best ATPase response for ABCG2. Mitoxantrone, riboflavin and CPT-cAMP implied only ATPase activation on their curves; the curve of mitoxantrone is similar to the beginning of the CPT-cAMP one (Figure 45 A). Methotrexate did not stimulate the ATPase activity of ABCG2 (Data not shown). Excluding pefloxacin, the hydrophilic fluoroquinolones, represented in Figure 45 B, showed scanty activation curves for the ABCG2 transporter. These compounds have positive and/or negative charge (Table 9).

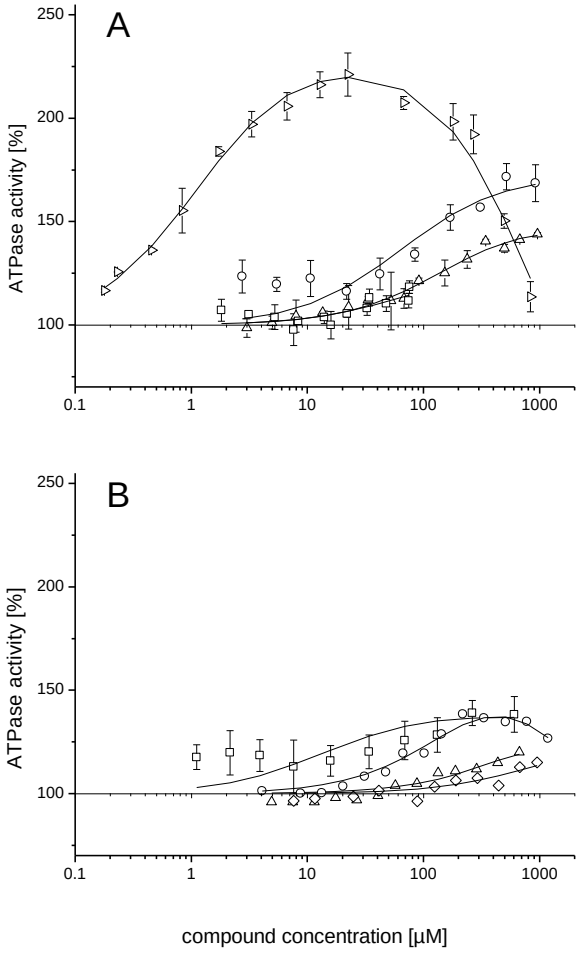

Figure 45. ATPase activity in inside-out plasma membrane vesicles as a function of the substrate concentration for ABCG2 (open symbols). The titration curves shown as examples represent the average of two measurements, standard deviation are given. Solid lines are fits to the modified Michaelis-Menten equation (Equation 2). **A**: CPT-cAMP (▲), mitoxantrone (■), riboflavin (●), sulfasalazine (►). **B**: ciprofloxacin (▲), enrofloxacin (■), norfloxacin (♦), pefloxacin (●).

Data from the automated fit program to Equation 2 yielded the concentration of half-maximum activation (K_1) and inhibition (K_2) as well as the maximum (V_1) and minimum rate (V_2) from P-gp and

ABCG2 ATPase activity, respectively. The kinetic parameters derived from phosphate release measurements in plasma membrane vesicles are summarized in Table 9 and correspond to average values of one to six independent experiments (n=2 or 4 each experiment).

Kinetic parameters for the inhibitory part of the curve, K_2 and V_2, could not be calculated for several compounds because the inhibitory part of the ATPase activity curve was affected by vesicle aggregation and/or compound association (written as *nd* in Table 9). The ATPase activity curve obtained for these compounds was only a fraction of the activation branch (Figures 43 to 45). Therefore, probably the maximum activity (V_1) is subestimated for these compounds and the inverse of the half maximum activation ($1/K_1$) overestimated (cimetidine, cortisol, dexamethasone, etoposide, famotidine, forskolin, nizatidine, ranitidine, tamoxifen for P-gp and cimetidine, ciprofloxacin, CPT-cAMP, famotidine, mitoxantrone, nizatidine, norfloxacin for ABCG2) (Figures 43 to 45 and Table 9).

Conversely, half of the analyzed compounds showed only an inhibition curve with the ABCG2 transporter (Figures 43 and 44). Consequently, the half-maximum activation (K_1) and the minimum activity (V_1) were not possible to calculate (Table 9).

A closer look at the ATPase activity profiles in inside-out plasma membrane vesicles shows that for very hydrophilic compounds inhibition could not be reached (e.g. H_2 receptor antagonists for both transporters, Figure 44 D), whereas for the very hydrophobic compounds activation is barely visible or not present at all (e.g. Figure 43 for ABCG2).

Taken together, 20 of the analyzed compounds interact with both transporters. Half of them showed only inhibition curves for ABCG2 and activation or the bell-shaped (firstly activation and secondly inhibition) curve for P-gp (Figure 43 and ranitidine in the Figure 44 D). Only 4 of the compounds had a complete ATPase activity curve (bell-shaped): daunorubicin and prazosin (Figure 44 C) for both transporters, and sulfasalazin and pefloxacin for ABCG2 (Figure 45). 9 compounds produced only stimulation of ATPase activity (the H_2 receptor antagonist cimetidine, famotidine and nizatidine from Figure 44 D for both transporters, and CPT-cAMP, mitoxantrone, riboflavin, and the fluoroquinolones ciprofloxacin, enrofloxacin and norfloxacin for ABCG2, Figure 45). In general, P-gp shows greater fold-stimulation of ATPase activity than ABCG2 with the compounds used in this study.

To go further, based on the tested set of compounds, it is possible to classify the compounds according to electric charge *vs* the trend results in ATPase activity measurements for the compounds with P-gp and ABCG2 (Table 10). It is evident that the ability of the compounds to act as modulators on ATPase activity measurements can be reasonably well predicted on the basis of the electric charge and hydrophobicity. The more hydrophobic electrically neutral and cationic compounds induced full bell-shaped ATPase activity curves for P-gp, whereas they barely activated but strongly inhibited ABCG2 (Figure 43 and Figure 44 A, C).Additionaly, cationic compounds can also produce activation of the ABCG2 transporter, especially if they are slightly cationic. The more hydrophilic compounds (e.g. Figure 44 D) induced only the activating branch of the curve in the case of P-gp, whereas they induced almost full

bell-shaped ABCG2-ATPase activity curves. Secondly, zwitterionic and anionic compounds interact only with ABCG2. There are two exceptions for anionic compounds. For instance, glybenclamide interacts activating the P-gp-ATPase activity and inhibiting the ABCG2-ATP-ase activity. The other exception is metotrexate which does not yield any ATPase activity with none of the two transporters. In the case of ABCG2, the compounds of intermediate hydrophobicity induced almost full bell-shaped ATPase activity curves (Figure 45).

Table 10. Classification of compounds according to electric charge *vs* the trend results in ATPase activity measurements for the compounds interacting with P-gp and ABCG2 transporters.

	ATPase activity	
Electric charge	**ABCG2**	**P-gp**
neutral	strong inhibition	activation
cationic	activation/inhibition	activation
anionic	activation	no interaction
zwitterionic	activation	no interaction

1.3.2. ATPase activity assays with other molecules

Additionally, to deeper investigate the behavior of the ABCG2-ATPase activity, we tested several detergents which were previously proven to be ideal model compounds for the study of P-gp activity because the hydrophobic as well as the hydrophilic part of the molecule can be systematically varied (Li-Blatter et al., 2009; Li-Blatter and Seelig, 2010; Li-Blatter et al., 2012).

Titrations in ABCG2-M-ATPase membrane vesicles with CHAPS, C_6-maltoside, Cymal-1, $C_{12}EO_8$, fos-choline-8, fos-choline-iso-9 detergents are displayed in Figure 45. We also performed ATPase activity measurements using sugars (maltose), acids (ascorbic acid, heptanoic acid, sodium deoxycholate, sodium hexanoate) and lipids (DHPC); see Figure 46 and Table 11. No interaction was reported for maltose, ascorbic acid, heptanoic acid and fos-choline-iso-9 as their ATPase activity was negligible (Data not shown).

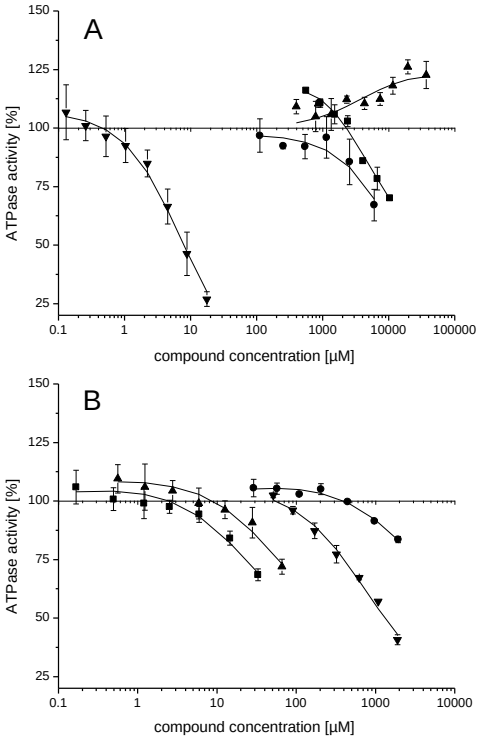

Figure 46. ATPase activity in inside-out plasma membrane vesicles as a function of the substrate concentration for ABCG2. The titration curves shown as examples represent the average of two measurements, standard deviation are given. Solid lines are fits to the modified Michaelis-Menten equation (Equation 2). Lipids, acids, detergents and sugars are included. **A**: C_6-maltoside (■), Cymal-1 (•), $C_{12}EO_8$ (▼), sodium hexanoate (▲). **B**: CHAPS (■), DHPC (▼), fos-choline-8 (•), sodium deoxycholate (▲).

Table 11. Kinetic parameters of ABCG2 activation for lipids, acids, detergents and sugars. The concentration of half-maximum activation (inhibition), K_1 (K_2), and the maximum (minimum) transporter activity, V_1 (V_2), obtained from phosphate release measurements in plasma membrane vesicles.

Charge [a]	Compound	K_1 [μM]	K_2 [μM]	V_1 [fold]	V_2 [fold]	Nº of experiments	Interaction with ABCG2
neutral	C_6-maltoside	46.10 [b]	4610.42	1.28	0.43	2	inhibition
	Cymal-1	150.94 [b]	15094.37	0.97	0.00	2	inhibition
	$C_{12}EO_8$	0.07 [b]	6.93	1.07	0.00	2	inhibition
	maltose	nd	nd	1.28	0.93	2	no interaction
anionic	ascorbic acid	nd	nd	1.11	0.88	2	no interaction
	heptanoic acid	nd	nd	1.11	1.02	2	no interaction
	sodium hexanoate	4145.18	2719830	1.26	0.00	4	activation
zwitterionic	CHAPS	0.24 [b]	24.06	1.06	0.42	2	inhibition
	DHPC	7.28 [b]	727.87	1.06	0.19	2	inhibition
	fos-choline-8	26.75 [b]	2675.24	1.07	0.49	2	inhibition
	fos-choline-iso-9	nd	nd	1.09	0.92	4	no interaction
	sodium deoxycholate	0.52 [b]	52.33	1.09	0.44	2	inhibition

[a] Electric charge classification at pH 7.4 for the compounds. [b] estimated K_1 ($K_1 = K_2 / 100$). *nd*: not determined.

We observed that, accordingly with previous results (Table 9 and Figures 43-45), neutral compounds (C_6-maltoside, Cymal-1 and $C_{12}EO_8$) inhibited the ATPase activity of ABCG2 (Figure 46 and Table 11). Even, zwitterionic compounds which are very hydrophobic (CHAPS, DHPC, fos-choline-8, sodium deoxycholate) also inhibited the ATPase activity of ABCG2 (Figure 46 and Table 11). More hydrophilic anionic compounds showed only the activating branch of the ATPase activity curve (sodium hexanoate) (Figure 46 and Table 11). However, for compounds (maltose, ascorbic acid, heptanoic acid or fos-choline-iso-9) without patterns in their molecular structure to partition into the lipid bilayer of the membrane (no type I and/or type II units of HAP (Seelig, 1998)) the ATPase signal was negligible, independently from the charge and concentration tested; no interaction was found between the compound and ABCG2 (Table 11). Membrane partitioning is thus required for an interaction with ABCG2 as demonstrated previously for P-gp. A two-step binding model is therefore adequate for both exporters.

1.4. Estimation of membrane partitioning of drugs (passive influx)

1.4.1. Surface activity measurements (SAM)

Injection of an amphiphilic drug into a monolayer trough filled with buffer is followed by partitioning of the drug between the aqueous phase and the air-water interface. Molecules in the air-water interface orient the hydrophilic residue to the aqueous phase and the hydrophobic residue into the air. At low concentrations the surface pressure, π, increased slowly, then reached a constant slope up to the critical micelle concentration (CMC) from which there was no further increase in surface pressure (for further information see Gerebtzoff et al., 2004 and Fischer et al., 1998).

The surface activity as a function of concentration (π/logC plot), concentration in Log scale, was measured at pH 7.4 for the compounds listed in Table 9 and 12 and plotted in Figure 47. The fitting of the slope on the quasilinear part corresponds with the Gibbs adsorption Isotherm (solid line) (Equation 4). In several cases, due to the lack of amphiphilicity of the compounds, there is not a quasilinear part (e.g. compounds from Figure 47 G).

Data obtained from SAM experiments are summarized in Table 12. The point of constant surface pressure at high concentrations is defined as the critical micelle concentration of the drug, CMC. However, this point could not be reached for many of the compounds because precipitation was achieved before arriving to the CMC (e.g. digoxin and etoposide from Figure 47 B), or because they were too hydrophilic (e.g. H_2 receptor antagonists in Figure 47 E, except famotidine). For this reason, in Table 12 the ultimate column was named as *Solubility limit or CMC*. From the linear slope of the π/log*C* plot, the cross-sectional area (A_D) was derived and the air-water partition coefficient (K_{aw}) was then evaluated by fitting the data to Equation 5.

In Table 12 compounds are classified according to their charge, as already said: neutral (no charge), slightly cationic, cationic, anionic, zwitterionic. Where stated, pK_a values in Table 12 were taken from previously published literature; pK_a value is not a characteristic parameter for neutral compounds, therefore, this value is not provided for these compounds. No pK_a value was found for CPT-cAMP.

Table 12. Parameters from surface-activity measurements (the air-water partition coefficient (K_{aw}), the Critical Micelle Concentration of drugs (CMC) or solubility limit), net charge of the compounds, pK_a values, LogP and LogD values. Data obtained for the 28 compounds listed in Table 9.

Charge [a]	Charge distrib. [b]	N°	Compound	MW base [g/mol]	pK_a [c]	LogP [d]	LogD [d]	K_{aw} [mM^{-1}]	Solubility limit/CMC [mM]
O	I	1	cortisol	362.5		1.28	1.28	2.08	> 2.56
	I	2	dexamethasone	392.5		1.68	1.68	5.56	> 1.50
	I	3	progesterone	314.4		4.15	4.15	146.00	0.09
	I	4	testosterone	288.4		3.37	3.37	103.42	0.36
	II	5	Ko143	469.6		4.75	4.75	15647.9	0.01
	III/I	6	digoxin	780.9		2.37	2.37	262.21	0.23
	III	7	estradiol	272.4		3.75	3.75	nd	nd
	III	8	etoposide	588.6		1.16	1.16	6.95	2.01
	III	9	forskolin	410.5		1.36	1.36	52.10	> 0.17
(+)	II	10	prazosin	419.8	6.5 [10]	1.69	2.08	nd	nd
	III	11	cimetidine	252.3	6.9 [7]	-0.11	-0.25	5.96	> 8.51
	III	12	famotidine	337.5	6.7 [8]	-1.95	-1.27	282.03	0.32
	III	13	nizatidine	331.4	1.9, 6.7 [3]	0.76	-0.69	0.37	> 10.00
	III	14	ranitidine	350.9	1.9, 8.1 [3]	0.98	0.19	4.58	> 11.10
+	I	15	promazine	321.0	9.4 [2]	3.93	2.67	*4.80	*2.86
	I	16	tamoxifen	371.5	8.5 [5]	6.35	5.10	1310.00	0.02
	II/I	17	verapamil	491.1	8.9 [6]	5.04	3.28	*166.00	*5.00
	III	18	daunorubicin	563.9	8.4 [1]	1.73	1.00	*589.00	*0.30
	III	19	mitoxantrone	517.4	5.9, 8.1 [14]	1.19	-1.58	5.32	1.00
-	II/I	20	glybenclamide	494.0	6.3 [9]	3.79	3.15	758.90	0.45
	III	21	CPT-cAMP	493.8	nd	0.50	1.34	300.00	0.70
	III	22	methotrexate	454.4	3.2, 4.5, 5.6 [13]	-0.5	-5.10	142.22	0.08
	III	23	riboflavin	376.4	9.7 [4]	-0.92	0.09	9.30	> 4.36
	III	24	sulfasalazine	398.4	2.3, 7.9 [17]	3.94	-0.10	368.55	> 3.52
+ / -	III	25	ciprofloxacin	331.3	6.4, 8.3 [11]	-0.81	-1.35	0.97	5.91
	III	26	enrofloxacin	359.4	6.3, 7.8 [12]	1.15	1.08	16.25	> 4.00
	III	27	norfloxacin	319.3	6.2, 8.4 [15]	-0.92	-0.92	nd	nd
	III	28	pefloxacin	465.5	6.3, 7.6 [16]	0.88	-0.82	2.46	3.51

[a] Electric charge classification at pH 7.4 for the compounds. O, neutral; (+) partially cationic; +, cationic; -, anionic; +/-, zwitterionic. [b] Charge distribution on the molecular structure: I, polar – non-polar; II, non-polar – polar – non-polar; III, polar – non-polar - polar. [c] pK_a values are from literature (see below) or from Sigma or Merck labels, no pK_a value was found for CPT-cAMP; the pK_a value is not a characteristic parameter for neutral compounds. [d] LogP and LogD values from www.chemicalize.org. *nd*: not determined. * Data from literature: Seelig et al., 1994; Seelig and Landwojtowicz, 2000; Gerebtzoff et al., 2004; Aänismaa et al., 2007. References: Frézard and Garnier-Suillerot, 1998 (1); Seiler, 1974 (2); Dumanovic et al., 1997 (3); Sigma (4); Kannan et al., 2010 (5); Hasegawa et al., 1984 (6); Avdeef and Berger, 2001 (7); Islam and Narurkar, 1993 (8); Sheppard and Robinson, 1997 (9); Sigma (10); Völgyi et al., 2007 (11); Escribano et al., 1997 (12); Szakács and Noszál, 2006 (13); Gennaro, 1995 (14); Barbosa et al., 2001 (15); Bassi et al., 1994 (16); Box et al., 2007 (17).

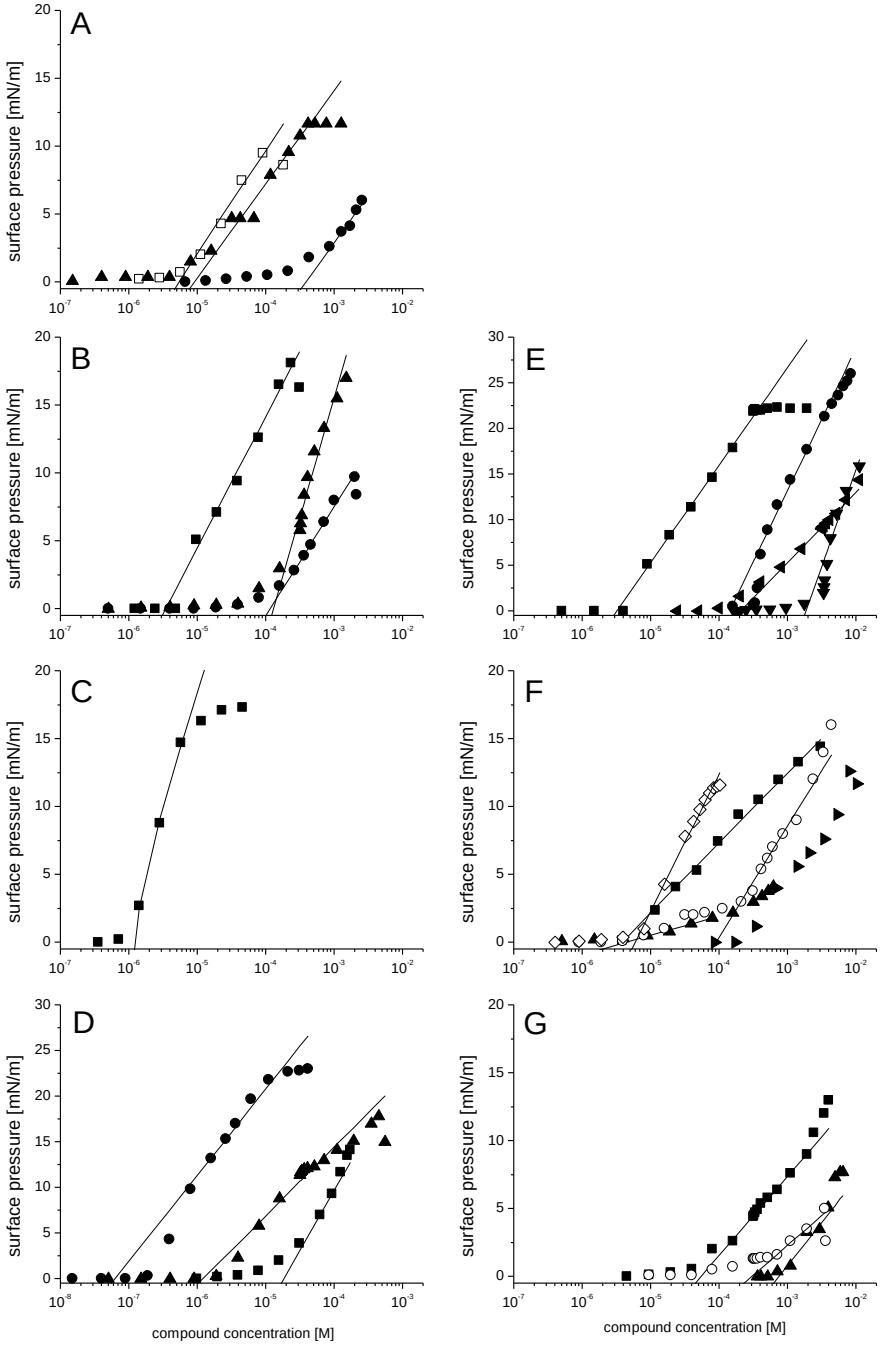

Figure 47. Surface-activity measurements as a function of concentration (surface pressure (π)/ logC plots). **A**: cortisol (•), progesterone (□), and testosterone (▲). **B**: dexamethasone (▲), digoxin (■), etoposide (•). **C**: tamoxifen. **D**: forskolin (■), glybenclamide (▲), Ko143 (•). **E**: cimetidine (•), famotidine (■), nizatidine (▼), ranitidine (◄). **F**: CPT-cAMP (▲), methotrexate (◊), mitoxantrone (■), riboflavin (○), sulfasalazine (►). **G**: ciprofloxacin (▲), enrofloxacin (■), pefloxacin (○). The solid line is the fit to the Gibbs adsorption isotherm equation (Equation 4).

Daunorubicin, verapamil and promazine are exceptions, since these compounds have been extensively previously studied (Seelig et al., 1994; Seelig and Landwojtowicz, 2000, Gerebtzoff et al., 2004; Aänismaa et al., 2007); therefore, they have been not studied more, neither plotted. It is important to note that for estradiol, norfloxacin and prazosine, no surface activity could be detected; thus, no representation of these compounds was possible in Figure 47.

The air-water partition coefficient (K_{aw}) reflects the amphiphilicity of a compound; it covers a broad range from $K_{aw} \sim 10^2$ M^{-1} (very hydrophilic compounds) to $K_{aw} \sim 10^8$ M^{-1} (very hydrophobic compounds). The compound with the highest K_{aw} was Ko143. Surface activity results reflected that the compounds analyzed can be divided in two groups. The first group of compounds, with important surface activity, show the typical constant linear slope up to the critical micelle concentration (CMC) from which there was no further increase in surface pressure; therefore, they are amphiphilic (e.g. testosterone, progesterone, Figure 47 A). These compounds are the typical P-gp substrates (Seelig and Gatlik-Landwojtowicz, 2005). The second group of compounds are compounds very low surface active, with strange slopes of surface activity as sigmoid slopes (e.g. tamoxifen and Ko143, Figure 47 C and D), steps (e.g. riboflavin and glybenclamide Figure 47 D and F) and/or for which the CMC is not possible to achieve (e.g. dexamethasone and nizatidine, Figure 47 B and E) or the surface activity decrease when arriving at the CMC (e.g. etoposide and pefloxacin, Figure 47 A and G). The latter two cases can be explained by means of aggregation problems. Certainly, at the end of some of those experiments the aggregates of the drugs where visible. This second group comprises the non-amphiphilic compounds; as it was already said, for compounds with low amphiphilicity or amphiphilicity changing in the process of aggregation the measured Gibbs adsorption isotherm cannot be satisfactorily simulated. As a result, for these compounds neither the cross-sectional area (A_D) nor the air-water partition coefficient (K_{aw}) could be properly determined, therefore neither the lipid-water partition coefficients (K_{lw}) (Fischer et al., 1998). In these cases, the K_{aw} stated in Table 12 is just an estimated value.

Importantly, in this latter set are included the typical ABCG2 substrates (Figure 47 F and G). Cross-sectional area is important for passive diffusion (Fischer et al., 1998). It is not possible to obtain the cross-sectional area for typical ABCG2 compounds because they are not amphiphilic and most likeky cross the membrane slowly. Surface activity curves for all the typical compounds which interact with ABCG2 have in some way a sigmoid cross section, which maybe indicative of absorption to the Teflon trough (Ko143) or maybe indicative of an orientation charge (methotrexate, mitoxantrone, riboflavin, sulfasalazine and fluoroquinolones, Figure 47 D, E, F) (Fischer et al., 1998). An explanation for the kind of steps found in these π /Log C curves is that non-amphiphilic compounds can form not only a monolayer but several in surface activity measurements given each one its own surface activity.

1.4.2. Isothermal titration calorimetry (ITC)

A second technique was used for further analyze the lipid-water partition coefficients. ITC measurements were performed with some of the compounds (digoxin, Ko143, methotrexate, nizatidine, ranitidine, riboflavin and sulfasalazine). The lipid-water partition coefficients (K_{lw}) obtained were higher in comparison with those calculated from the surface activity measurements (except for Ko143 which was smaller) (Table 13). Interestingly, all the lipid-water partition coefficients obtained for these compounds where in the range of 10^3 M^{-1} (except for sulfasalazine which was 322 M^{-1}) (Table 13).

Table 13. Lipid-water partition coefficients (K_{lw}) obtained from surface-activity measurements (SAM) and isothermal titration calorimetry (ITC) measurements. The cross-sectional areas of the molecules (A_D) obtained from surface-activity measurements are also indicated.

	K_{lw} [M^{-1}]		A_D [$Å^2$]
Compound	**SAM**	**ITC**	**SAM**
digoxin	279.00	1300	97.64
Ko143	13871.00	5073	100.27
methotrexate	201.00	1950	93.60
nizatidine	16.00	2500	44.60
ranitidine	0.82	1763	123.00
riboflavin	2.74	1500	115.97
sulfasalazine	0.22	322	276.97

Taken all together, these results give an idea of the difficulty of non-typical amphiphilic compounds to partition into the membrane. The lipid-water partition coefficients (K_{lw}) of amphiphilic molecules can be determined in good agreement by ITC and by surface activity measurements, taking into account the air-water partition coefficient (K_{aw}) the cross-sectional area (A_D) of the molecule, and the packing density of the lipid membrane. In the case of non-amphiphilic molecules the situation is more complex as seen in Table 13, because the molecules adopt a large area at the air-water interface which leads to an underestimation of the lipid-water partition coefficient. However, the lipid-water partition coefficient determined by ITC may also be biased due to mere adsorption of the molecules to the head group region of the lipid bilayer, instead of penetration into the hydrophobic core region.

1.5. Correlation parameters

1.5.1. Correlation between the maximum rate of ATP hydrolysis and the binding affinity of the drug from water to the transporter

The maximum rate of the ATPase activity (V_1) (Log scale) (Table 9), measured in inside-out membrane vesicles was plotted as a function of the free energy of binding of the compound from the aqueous phase to the activating binding region of the transporter ($\Delta G°_{tw\,(1)}$) (Figure 48) to investigate the relationship between ATP hydrolysis at the NBDs and substrate binding and release at the TMDs. The values of $\Delta G°_{tw\,(1)}$ were derived from the concentration of half-maximum activation (K_1), Equations 3 and 12. Compounds whose ATPase activity parameters or surface activity could not be determined (Tables 9 and 12) are not represented in this plot.

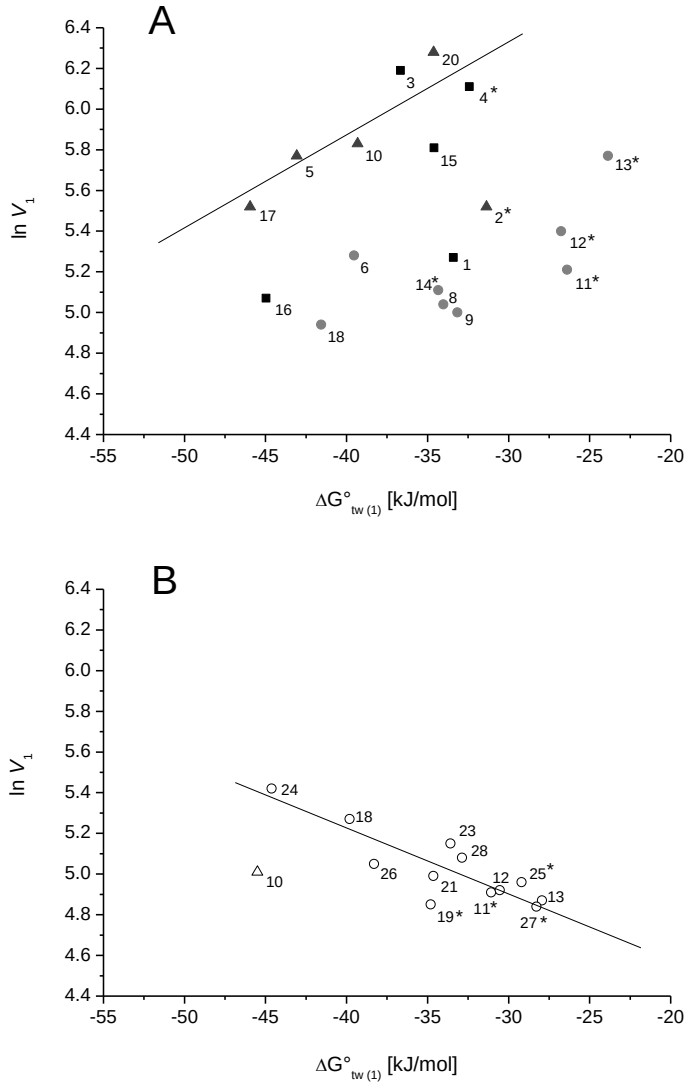

Figure 48. (Legend in next page)

Figure 48. The logarithm of the maximum activity (ln V_1), obtained from phosphate measurements at pH 7.4 plotted as a function of the free energy of binding of the substrate from water to the transporter ($\Delta G^\circ_{tw\ (1)}$) for P-gp (**A**), ABCG2 (**B**). The maximum activity (V_1) is expressed as a percentage of the basal rates taken as 100%. Compounds are classified according to the charge distribution pattern from Table 9: I (■), II (▲), III (●). Data represented are the averages of all results obtained from each compound. For the compounds correlation number-name, see Tables 9 or 12. * Compounds with only ascendant branch of ATPase activity.

The more negative the free energy of binding, the higher is the affinity of the compound to the transporter P-gp; the higher affinity of the compounds to the transporter, the lower is the ATPase activity and thus the rate of transport (Li-Blatter et al., 2009). The rate of ATP hydrolysis decreases with decreasing free energy of binding of the compound from water to the transporter ($\Delta G^\circ_{tw\ (1)}$) (or increasing binding affinity of the drug from water to the transporter). A linear correlation was observed for typical P-gp compounds in Aänismaa and Seelig (2007). A similar trend was observed when we plotted our results (Figure 48 A). Outliers from this linear correlation in the present set of compounds are essentially due to a low amphiphilicity of the molecules; observe that many of these outliers correspond to type III compounds (marked in grey) and several of them are typical ABCG2 compounds. Therefore, as expected, these typical P-gp compounds are type I and II. It is already known that the higher the affinity of the drugs to the P-gp transporter, the lower is the ATPase activity and thus the rate of transport. Compounds with a high affinity from water to the transporter have a higher tendency to occupy both binding regions, to bind strongly and therefore to lead to a lower ATPase activation or to inhibit P-gp already at low aqueous concentrations (Li-Blatter et al., 2009).

On the other hand, as seen in Figure 48 B, the rate of ABCG2 ATPase activity increases linearly with increasing affinity of the compound from water to the transporter (i.e., decreasing free energy of binding of the drug from water to the transporter). The behavior of ABCG2 is thus just opposite to the behavior of P-gp. Thereby the compounds following this linear correlation are very hydrophilic, non amphiphilic, carry many hydrogen bond acceptor groups, and are essentially type III compounds, whereas the more hydrophobic compounds are outliers to the left side in Figure 48 B (not included).

In summary, we can conclude that the rate of P-gp- ATPase activity and transport decrease with the affinity of the substrates to the transporter and is the opposite for ABCG2.

1.5.2. Correlation between the concentration of half-maximum activation and the air-water partition coefficient

If the log ($1/K_1$) (proportional to the free energy of binding from water to the activating binding region of the transporter, $\Delta G^\circ_{tw\ (1),}$ see Equations 3 and 12) is plotted against the logarithm of the air-water partition coefficient (log K_{aw}), the binding constant from the lipid to the transporter (K_{tl}) is

obtained (see Equation 11)(Figure 49). An approximately linear correlation is attained for this parameter for both transporters, P-gp and ABCG2, as shown in Figure 49.

Compounds whose ATPase activity parameters or surface activity could not be determined (Tables 9 and 12) were not represented in this plot. The surface activity results of estradiol, norfloxacin and prazosin showed marginal effects (Table 12); consequently, these compounds are not plotted in the Figure 49.

Figure 49 shows further that cimetidine, famotidine, nizatidine and prazosin have a somewhat higher affinity to ABCG2 than to P-gp, whereas the inverse is true for daunorubicin. In terms of free energies of binding from water to the exporter these differences are however small. It should be also noted that outliers from the correlation line (placed under the line) are due to the pH used in surface measurements (pH=7.4) is not favorable for those charged compounds. This pH is critical for some compounds where dissociation may occur and can influence and vary the obtained results.

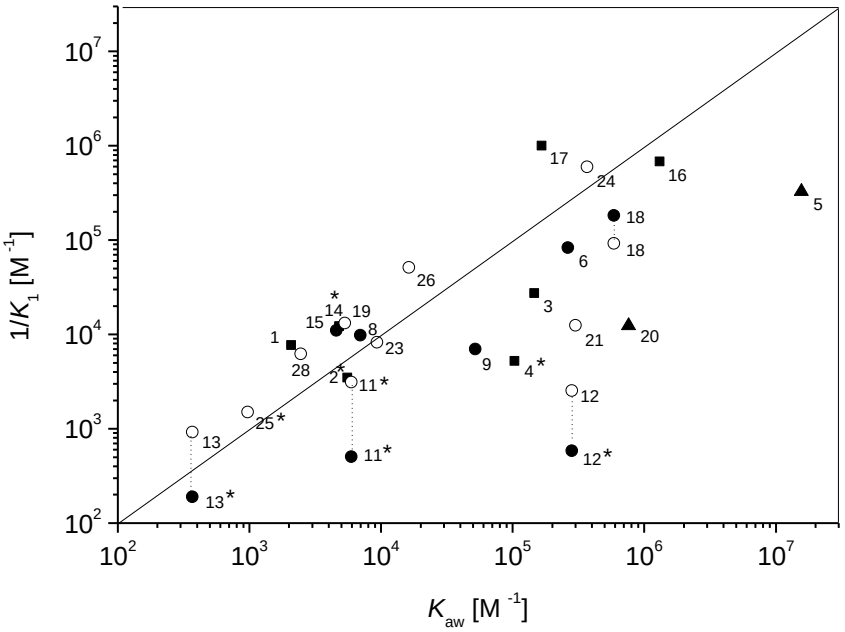

Figure 49. The inverse of the half maximum activation ($1/K_1$), obtained from ATPase activity measurements at pH 7.4 plotted as a function of the air-water partition coefficient (K_{aw}) for P-gp (closed symbols), ABCG2 (open symbols). Compounds are classified according to the charge distribution pattern from Table 9: I (■), II (▲), III (•). Half maximum activation (K_1) data are the averages of all results obtained from each compound. The K_{aw} data were obtained from surface-activity measurements. For the compounds correlation number-name, see Tables 9 or 12. * Compounds with only ascendant branch of ATPase activity.

1.6. Cytosensor measurements

When cytosensor experiments were performed (for details see Landwojtowicz et al., 2002 and Gatlik-Landwojtowicz et al., 2004) with parental and human ABCG2 transfected MEF3.8 cells; attempts

at different conditions such as different drugs and concentrations, pump cycle, pump-off period, number of cells seeded were not successful to observe a signal from acidification attributable to the transporter. In Table 14 all the experiments tried with the different conditions are summarized.

We might say that these results are possibly related not with a lack of activity of the ABCG2 transporter in the presence of compounds, but most probably with the fact that at the worked concentrations we are only at the beginning of the curve of ECAR activation which most likely corresponds to a basal ATPase activity. For instance, we have demonstrated that there is ATPase activity of ABCG2 with sulfasalazine at the tested concentrations (Figure 45 A); and, as we have commented, it is already know that results obtained with this method are comparable to those obtained with the ATPase activity assays (Landwojtowicz et al., 2002; Gatlik-Landwojtowicz et al., 2004; Gatlik-Landwojtowicz et al., 2006; Aänismaa and Seelig, 2007). We know from previous investigations that more concentrations of the compound are needed in living cells than in vesicles to obtain ATPase activity (Nervi et al., 2010) and the curve of ATPase activity is shifted to the right side in the concentration scale for living cells; therefore, due to problems of precipitation of typical ABCG2 compounds at elevated concentrations (as a result of the high hydrophobicity), it is not possible to work at the concentrations were we could see the ECAR of ABCG2 in cytosensor experiments with sulfasalazine.

Table 14. Cytosensor measurements performed with parental and human ABCG2 transfected MEF3.8 cells. Conditions of the experiments as density of seeded cells, drugs and concentrations, stimulation, pump cycle and pump-off period are displayed.

Nº experiment	Density of seeded cells	Drug and concentration	Stimulation	Pump cycle	Pump-off
1	2.7 - 10.7 × 10^5	sulfasalazine 5 concentrations (1-10 µM)	2 points	2-min (1 min 40 s - 20 s)	13 s (from 1 min 45 s to 1 min 58 s)
2	5 - 8 × 10^5	sulfasalazine 3 concentrations (0.5,1,2 µM)	2 points	2-min (1 min 40 s - 20 s)	5 s (from 1 min 30 s to 1 min 35 s)
3	5 - 8 × 10^5	sulfasalazine 3 concentrations (1, 50, 100 µM)	4 points	2-min (1 min 40 s - 20 s)	13 s (from 1 min 45 s to 1 min 58 s)
4	5 - 8 × 10^5	sulfasalazine 3 concentrations (1, 10, 100 µM)	4 points	2-min (1 min 40 s - 20 s)	13 s (from 1 min 45 s to 1 min 58 s)
5	5 - 8 × 10^5	sulfasalazine 1 concentration (1 µM)	6 points	1:30-min (1 min 10 s - 20 s)	13 s (from 1 min 15 s to 1 min 28 s)
6	5 - 8 × 10^5	curcumin 1 concentration (1 µM)	5 points	2-min (1 min 40 s - 20 s)	13 s (from 1 min 45 s to 1 min 58 s)
7	5 - 8 × 10^5	etoposide 3 concentrations (1, 10, 100 µM)	2 points	2-min (1 min 40 s - 20 s)	13 s (from 1 min 45 s to 1 min 58 s)
8	5 - 8 × 10^5	verapamil 3 concentrations (1, 10, 500 µM)	2 points	2-min (1 min 40 s - 20 s)	13 s (from 1 min 45 s to 1 min 58 s)

2. ABCG2 and P-glycoprotein interaction with steroid hormones – Correlation of ATPase activity and transport

The second aim of the present analysis was to test the correlation between ATPase and the rate of substrate transport in transepithelial transport assays by taking into account that most drugs can cross the bilayer membrane by passive diffusion (Seelig, 2007). For the present analysis we chose steroid hormones which have been extensively tested in transport and accumulation assays (Table 6). Most of the steroid hormones moreover have the advantage to be electrically neutral which allows ignoring charge effects. Cortisol, dexamethasone, estradiol, progesterone, tamoxifen and testosterone were used. First, we analyzed the hormone-induced ABCG2 and P-gp ATPase activity, respectively, as a function of concentration based on data substracted from Figures 44 and 45 and Table 9 from the previous section. On the basis of surface activity measurements (SAM) previously obtained, we characterized the compounds by the Gibbs adsorption isotherm which yields the cross-sectional area (A_D), the air-water partition coefficient (K_{aw}) and the solubility limit of a compound based on data substracted from Figures 47 and Table 12 from the previous section. The parameters obtained from this analysis allowed predicting the passive flux of the different steroids across the lipid membrane (Seelig et al., 1994). Third, we discussed and correlated our results with collected published data from bi-directional transport assays and accumulation experiments of steroid hormones with ABCG2 and P-gp (see Discussion section).

2.1. ATPase activity measurements in plasma membrane vesicles for P-gp and ABCG2

ABCG2 and P-gp ATPase activity in inside-out plasma membranes ABCG2-M-ATPase vesicles and vesicles from NIH-MDR1-G185 cells, respectively, were measured for the six steroid hormones by monitoring the rate of inorganic phosphate release. Data are subtracted from Figures 44 and 45 and Table 9. Figure 50 shows the ABCG2 and P-gp ATPase activity as a function of compound concentration (Log scale) where drug-stimulated ATPase activity is expressed as percentage of the basal activity (taken as 100%). The concentration ranges chosen were somewhat below the point where the pressure started to increase in SAM and ended at the CMC or solubility limit. The titrated curves are shown as examples representing the average of one measurement done in duplicate. Values are presented as means ± standard deviations (SD); SD values are not visible when they are smaller than the symbol used. The solid lines are fitted to the modified Michaelis-Menten model (Equation 2).

The P-gp-ATPase activation profile of progesterone (Figure 50 B) showed a characteristic bellshaped dependence on the logarithm of concentration; enhanced the P-gp ATPase activity at low concentrations up to a maximum and reduced it again at higher concentrations that are still well below the CMC. The P-gp-ATPase activity curves obtained for cortisol, dexamethasone, tamoxifen and

testosterone were only the rising branch because the solubility limit was reached close to the maximum P-gp-ATPase activity (Figure 50). The P-gp ATPase curve was negligible in the case of estradiol (Data not shown). On the other hand, all compounds barely enhanced but rather reduced the ABCG2 ATPase activity already at low concentrations, indicating that they strongly interact with ABCG2 causing a direct inhibition (Figure 50).

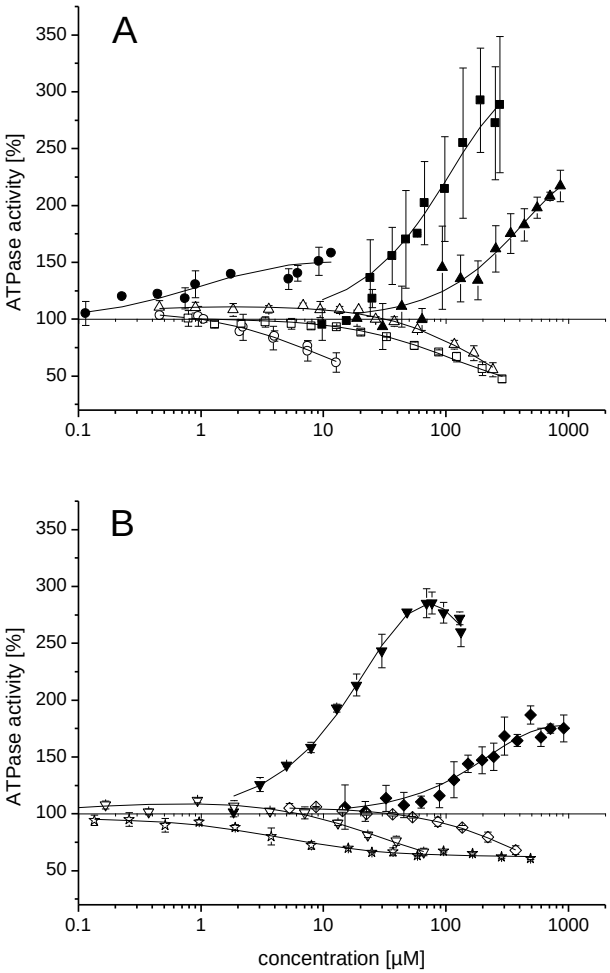

Figure 50. Representative plots of ATPase activity in inside-out plasma membrane vesicles as a function of the substrate concentration for ABCG2 (open symbols) and P-gp (closed symbols). Each point represents the mean ± SD values from a single experiment performed in duplicate. Solid lines are fitted to the modified Michaelis-Menten equation (Equation 2). **A**: dexamethasone (▲), tamoxifen (●), testosterone (■). **B**: cortisol (♦), estradiol (*), progesterone (▼).

Data corresponding to average values of two to six independent phosphate release experiments (all measurements were done in duplicates) were evaluated using an automated fit program made by A. Seelig's group to Equation 2, yielding the kinetic parameters summarized in Table 15. Data are subtracted from Table 9.

Table 15. Kinetic parameters for ABCG2 (A) and P-gp (B) activation with steroid hormones. The concentration of half-maximum activation (inhibition), K_1 (K_2), and the maximum (minimum) transporter activity, V_1 (V_2), obtained from phosphate release measurements in plasma membrane vesicles. Number of independent experiments (all measurements were done in duplicates).

		ABCG2				P-gp			
N°	**Compound**	K_1 [µM]	K_2 [µM]	V_1 [fold]	V_2 [fold]	K_1 [µM]	K_2 [µM]	V_1 [fold]	V_2 [fold]
1	cortisol	4.85 [b]	485.48	1.09	0.23	129.81	*nd*	1.95	*nd*
2	dexamethasone	2.68 [b]	267.58	1.13	0.00	286.29	*nd*	2.50	*nd*
3	estradiol	0.05 [b]	4.65	0.96	0.62	*nd*	*nd*	*nd*	*nd*
4	progesterone	0.31 [b]	31.23	1.08	0.49	36.60	141.51	4.89	0.71
5	tamoxifen	0.09 [b]	8.88	1.08	0.32	1.47	*nd*	1.60	*nd*
6	testosterone	1.61 [b]	160.67	1.01	0.19	191.00	*nd*	4.50	*nd*

[b] estimated K_1 ($K_1 = K_2 / 100$). *nd*: not determined

For P-gp, kinetic parameters for the inhibitory part of the curve, K_2 and/or V_2, could not be calculated (cortisol, dexamethasone, tamoxifen and testosterone; written as *nd* in Table 15) because the inhibitory part of the activity profile was difficult to reach since the drug concentration used in the phosphate release assay can lead to drug association and/or precipitation, and vesicle aggregation may occur (Aanismaa and Seelig, 2007). Furthermore, the maximum activity (V_1) is probably underestimated for these compounds. The analyzed compounds with the ABCG2 transporter showed only inhibition vanadate-sensitive activity, thus, K_1 was not possible to calculate but it was estimated as $K_1 = K_2 / 100$ in Table 15.

2.2. Surface activity measurements (SAM)

To estimate the capacity of the compounds to cross the membrane by passive diffusion we characterized the compounds by surface activity measurements. The surface activity as a function of concentration was subtracted from Figure 47 and plotted in Figure 51. As seen in this figure, the surface pressure (π) increased at low concentrations, then reached a constant slope up to the critical micelle concentration (CMC) from which there was no further increase in surface pressure (for further information see Fischer et al., 1998; Gerebtzoff et al., 2004). The fitting of the slope on the quasilinear part (solid line) corresponds to the Gibbs adsorption Isotherm (Equation 4). From this equation, the cross-sectional area (A_D) was derived and the air-water partition coefficient (K_{aw}) was then evaluated by

fitting the data to Equation 5. Data obtained from SAM are summarized in Table 16 (some of them are from Table 12).

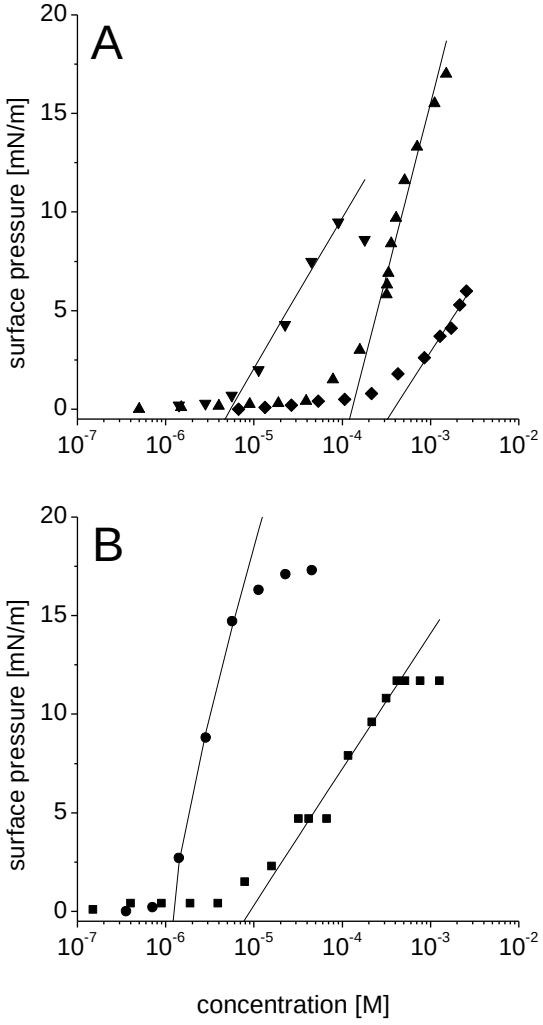

Figure 51. Surface-activity measurements as a function of concentration (Gibbs adsorption isotherms). **A**: cortisol (♦), dexamethasone (▲), progesterone (▼). **B**: tamoxifen (●), testosterone (■). The solid lines are fits data according to Gibbs adsorption isotherm equation (Equation 4).

Dexamethasone, progesterone, tamoxifen and testosterone displayed full SAM curves, from surface of zero until the CMC (Figure 51). Testosterone and progesterone SAM curves end at pressure limits considerably lower than expected for these typical amphiphilic compounds (π limit ≈ 10) (see Gerebtzoff et al., 2004). Dexamethasone and tamoxifen slopes were rather steep.

The point of constant surface pressure at high concentrations, the CMC, could not be reached for cortisol because of precipitation of the compound at $3x10^{-3}$ M; thus, the quasilinear part is almost

negligible (Figure 51 A), indicating the lack of amphiphilicity of the compound. No surface activity could be detected for estradiol; the slight response of surface activity seemed to be due to the surface activity of the solvent, DMSO (Data not shown).

Table 16. Parameters from surface-activity measurements of steroid hormones, partially substracted from Table 12: air-water partition coefficient (K_{aw}), cross sectional area (A_D), solubility limit or critical micelle concentration (CMC) and the maximum surface pressure (π). XLogP values from Pubmed (www.ncbi.nlm.nih.gov/pccompound) are also indicated. Not determined (*nd*).

N°	Compound	MW_{base} [g/mol]	K_{aw} [M^{-1}]	A_D [Å]	Solubility limit or CMC [mM]	π limit [mN/m]	XLogP
1	cortisol	362.5	2.08×10^3	135.50	> 2.56	> 6.00	1.6
2	dexamethasone	392.5	5.56×10^3	54.00	> 1.50	> 17.00	1.9
3	estradiol	272.4	*nd*	*nd*	*nd*	*nd*	4.0
4	progesterone	314.4	1.46×10^5	125.35	0.09	9.50	3.9
5	tamoxifen	371.5	1.31×10^6	62.63	0.02	17.00	7.1
6	testosterone	288.4	1.03×10^5	138.00	0.36	9.00	3.3

Predictions of passive influx for cortisol, dexamethasone, progesterone and testosterone were then calculated using data obtained from surface activity measurements (Equation 8). Passive influx as a function of concentration is represented in Figure 52. It should be remembered that net transport (from transepithelial assays) is the sum of active efflux (ATPase activity) plus the passive flux (calculated from SAM experiments) (Seelig, 2007). Note that the active flux represented in Figure 52 is an estimation range of the average of common ATPase activity results for both transporters, ABCG2 and P-gp. For progesterone and testosterone the passive flux (solid lines) is higher than the active flux (dashed lines) at almost any concentration. Therefore, although active efflux is obviously present (see Figure 50), the net transport could be negligible at concentrations higher than ~ 0,1 µM. In contrast, cortisol and dexamethasone, if are applied at concentrations lower than the range of mM in transepithelial transport assays, the net transport can be visible in these experiments due to active efflux is higher than passive flux (Figure 52). On the other hand, if applied at higher concentrations, where passive flux starts to be higher than active efflux, the net transport might be not visible. These deductions can be applied to both ABC transporters ABCG2 and P-gp.

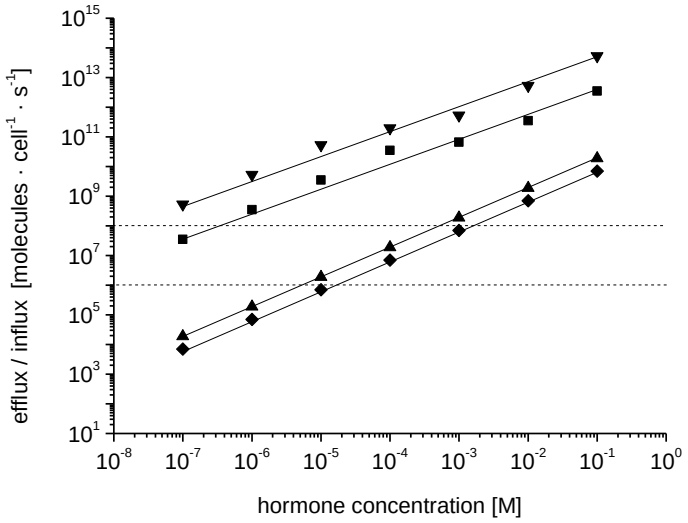

Figure 52. Passive influx and active efflux as a function of concentration. Lines representation: dotted - active efflux; solid – passive influx. Solid, grey arrows indicate approximations of K_1 values concentrations from P-gp-ATPase activity assays and dashed, grey arrows from ABCG2-ATPase activity. Cortisol (♦), dexamethasone (▲), progesterone (▼), testosterone (■).

3. ABCG2 and P-glycoprotein interaction with fluoroquinolones: ATPase activity correlation with other *in vitro* and *in vivo* experiments using these antibiotics

Although the bioavailability of several fluoroquinolones is known to be reduced by ABCG2 (Merino et al., 2006; Pulido et al., 2006; Real et al., 2011), this statement is not fulfilled for every members of this family of antibiotics. On the other hand, the interaction of these antibiotics with P-gp has thoroughly been studied (e.g. de Lange et al., 2000; Lowes and Simmons, 2002). However, a complete understanding of this family of antibiotics regarding the interaction with these two transporters has not been yet precisely explained. The third aim of this investigation was to provide a comparison between ABCG2 and P-gp ATPase activity with other *in vitro* and *in vivo* experiments using fluoroquinolones (ciprofloxacin, enrofloxacin, moxifloxacin, norfloxacin and pefloxacin). For this purpose, we evaluated the ABCG2 and P-gp ATPase activity of these five fluoroquinolones based on data partially subtracted from Figure 45 from previous sections. In addition, we completed their *in vitro* and *in vivo* interaction with these two ABC transporters. All of them have being extensively studied with P-gp. Therefore, moxifloxacin and pefloxacin, widely used fluoroquinolones in human medicine, were studied with ABCG2; *in vitro* transepithelial transport and mitoxantrone accumulation assays with ABCG2-transduced cells, and *in vivo* experiments with wild-type and Abcg2-knockout mice were performed. Ciprofloxacin, enrofloxacin and norfloxacin are three well-known ABCG2 substrates, as their interaction with ABCG2 was already characterized *in vitro* (Merino et al., 2006; Pulido et al., 2006). In addition, ciprofloxacin and enrofloxacin have been described as Abcg2 *in vivo* substrates (Merino et al., 2006; Pulido et al., 2006). A correlation of transport, accumulation and *in vivo* experiments with ATPase activity assays was discussed using also published data related to the interaction of these five fluoroquinolones with ABCG2 and P-gp.

3.1. ATPase activity measurements in plasma membrane vesicles for P-gp and ABCG2

In order to explain the interaction of the studied fluoroquinolones with ABCG2 and P-gp at the molecular level, the ABCG2- and P-gp-ATPase activity of the five fluoroquinolones (ciprofloxacin, enrofloxacin, moxifloxacin, norfloxacin and pefloxacin) was monitored by measuring the rate of phosphate release from inside-out plasma membrane vesicles purchased from mammalian cells (ABCG2-M-ATPase and NIH-MDR1-G185, respectively) (Glavinas et al., 2007). Figure 53 shows the rate of ATPase activity as a function of fluoroquinolone concentration (Log scale), where drug-stimulated ATPase activity is expressed as percentage of the basal activity (taken as 100%). Data were partially subtracted from Figure 45. The titrated curves are shown as examples representing one measurement in duplicate or quadruplicate. Values are presented as means ± SD; for compounds measured in

quadruplicate no SD values are available. The solid lines are fits to the data using the modified Michaelis-Menten model (Litman et al., 1997a).

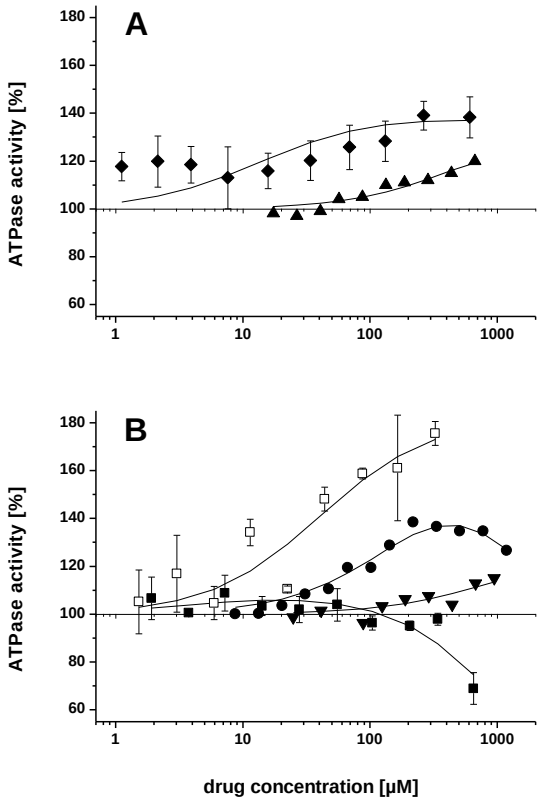

Figure 53. ABCG2 (filled symbols) and P-gp (open symbols) ATPase activity measured as a function of compound concentration in inside-out plasma membrane vesicles. The ATP hydrolysis was determined by quantification of the released inorganic phosphate with a colorimetric assay. The titration profiles shown as examples represent results of one measurement in duplicate or quadruplicate; error bars (sometimes smaller than the symbols) indicate SD. Solid lines are fits to the modified Michaelis-Menten equation (Equation 2). **A**. ciprofloxacin (▲), enrofloxacin (♦). **B**. moxifloxacin (■), norfloxacin (▼), pefloxacin (●).

Regarding ciprofloxacin, enrofloxacin and norfloxacin (Figure 53), due to their hydrophilic nature (mostly negative LogP, see Table 12), only the rising branch of the drug-induced ABCG2-ATPase activity curves could be measured due to solubility problems at high concentrations. This phenomenon is more remarkable for ciprofloxacin and norfloxacin as enrofloxacin seems to have reached the maximum (V_1). As seen in Figure 53 B, moxifloxacin barely enhanced but rather reduced the ABCG2-ATPase activity. In the case of pefloxacin, it showed an almost complete bell-shaped ATPase activity profile for ABCG2.

Data from Figure 53 indicate that ciproflocaxin and norfloxacin will interact as substrates of ABCG2 in the range of µM and mM; nevertheless achieve inhibition with these drugs will be difficult due to problems of solubility and aggregation (related with its high hydrophilicity) at the very high concentrations (might be at the range of M) needed for inhibition. Enrofloxacin will be an ABCG2 substrate up to ~1 mM, at higher concentrations it will work as an inhibitor. Pefloxacin will be seen as an ABCG2 substrate up to ~500 µM, after that it will act as an inhibitor. Moxifloxacin might interact with ABCG2 as a substrate up to a concentration ~600 µM, after that it will be an inhibitor.

Concerning the interaction of these drugs with P-gp, only moxifloxacin interacts well with this transporter (Figure 53 B). For the other fluoroquinolones studied, the ATPase curves for P-gp were negligible low (Data not shown).

Data from the phosphate release experiments were evaluated according to the modified Michaelis-Menten equation (Equation 2), yielding the concentrations of half-maximum activation (K_1) and inhibition (K_2), and the maximum (V_1) and minimum (V_2) rates. The derived kinetic parameters for each fluoroquinolone are summarized in the Table 17 and were partially substracted from Table 9. The ABCG2 ranking of K_1 values (moxifloxacin < enrofloxacin < pefloxacin < ciprofloxacin < norfloxacin) reflects the hydrophobicity of the drugs: moxifloxacin > enrofloxacin > pefloxacin > ciprofloxacin > norfloxacin. This hydrophobicity ranking is also shown by the LogP values (the atomic based prediction of the octanol/water partition coefficient, LogP) indicated in the Table 12; moxifloxacin has not been included in Table 12 but it will be longer argued in the discussion section. V_1 values reveal the obtained curve for each compound: no ABCG2 activation for moxifloxacin (lowest V_1), slight ABCG2 activation for norfloxacin (also small V_1), medium ABCG2 activation for ciprofloxacin and enrofloxacin (also medium V_1) and notable ABCG2 activation for pefloxacin (highest V_1). Note that for norfloxacin the ABCG2 K_2 value is so high that it was not possible to determine.

Table 17. Kinetic characteristic parameters of ABCG2 and P-gp ATP hydrolysis obtained from ATPase activity measurements in plasma membrane vesicles with fluoroquinolones. [a]

Transporter	Drug	K_1 [µM]	K_2 [µM]	V_1 [fold]	V_2 [fold]
ABCG2	ciprofloxacin	665.02	683.04	1.42	1.15
	enrofloxacin	19.51	361.31	1.56	1.28
	moxifloxacin	2.35	861.37	1.17	0.46
	norfloxacin	947.55	*nd*	1.26	1.13
	pefloxacin	160.23	5155.29	1.60	0.00
P-gp	moxifloxacin	38.23	4199.85	2.21	0.00

[a] Derived from the modified Michaelis-Menten equation (Equation 2): concentration of half-maximum activation (inhibition), K_1 (K_2), the maximum (minimum) transporter activity, V_1 (V_2). *nd*: not determined.

3.2. ABCG2 transepithelial transport assays

For comparison purposes, data from transepithelial transport and mitoxantrone assays with ABCG2 for moxifloxacin and pefloxacin were not available. Thus, transepithelial transport experiments with confluent cell monolayers were performed with these fluoroquinolones using the MDCK-II cell lines, parental as well as their subclones transduced with murine Abcg2 and human ABCG2. Fluoroquinolones vectorial transport was tested at 10 μM either in the absence or presence of the specific ABCG2 inhibitor Ko143 at 1 μM.

3.2.1. Moxifloxacin

Moxifloxacin vectorial transport using the three MDCK-II cell lines is represented in Figure 54. Moxifloxacin showed no significant net transport in the parental cell line (Figure 53 A). In both transduced cell lines (murine Abcg2 and human ABCG2), there was a slight increase in the basal to apical (B-A) moxifloxacin translocation (Figure 53 B, C) compared with the parental.

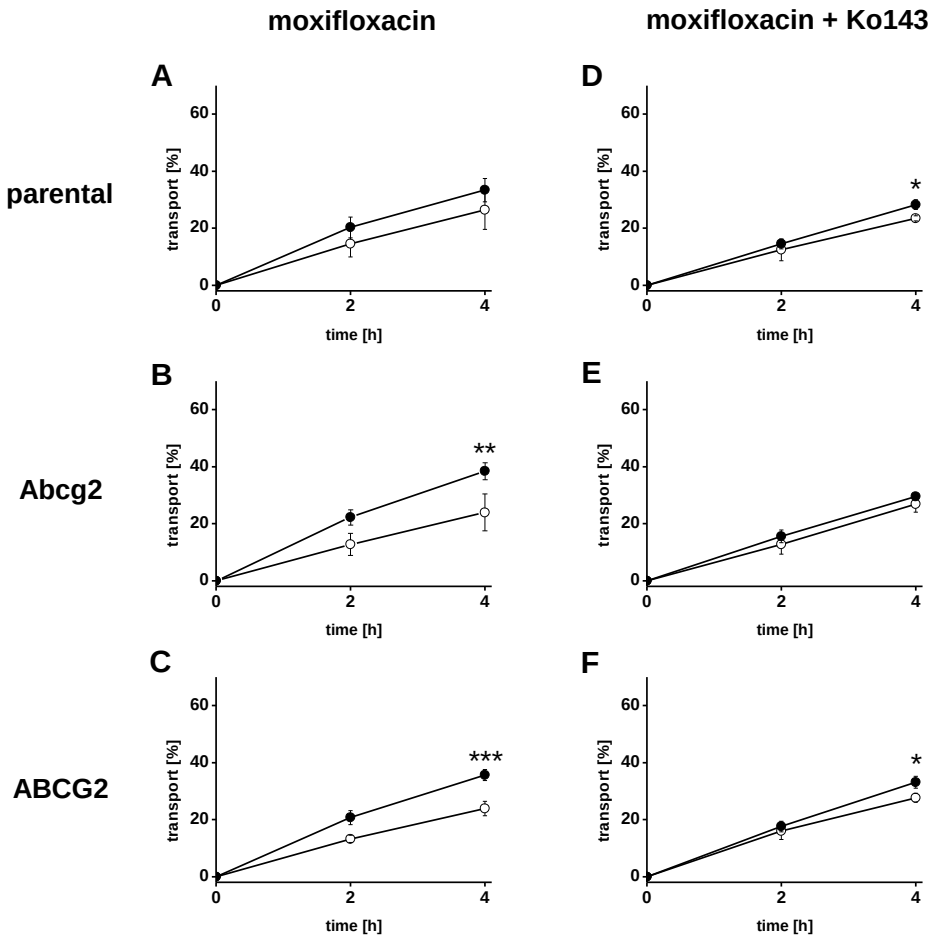

Figure 54. (Legend in next page)

Figure 54. Transepithelial transport of moxifloxacin (10 µM) across monolayers of MDCK-II-parental (**A, D**), MDCK-II-Abcg2 (murine Abcg2) (**B, E**) and MDCK-II-ABCG2 (human ABCG2) (**C, F**) transduced cells. The experiment was started by adding moxifloxacin to one compartment (basolateral or apical); after 2 and 4 hours, the percentage of drug in the opposite compartment was measured by HPLC. Transport was conducted in the absence (A, B, C) or in the presence (D, E, F) of the ABCG2 inhibitor Ko143 at 1 µM, added to both compartments. Translocation from the apical to the basolateral compartment, A-B (open circles); translocation from the basolateral to the apical compartment, B-A (filled circles). Results are the means, error bars (frequently within the symbols) indicate SD (n = 3-5). Significant differences between AB and BA translocation at 4 hours tested by Student's t test (*, $p < 0.05$; **, $p < 0.01$; ***, $p < 0.001$).

The resulting transport ratios (B-A/A-B) calculated at 4 hours of starting the experiment for Abcg2- and ABCG2- transduced cells (r = 1.68 ± 0.42 and 1.51 ± 0.19, respectively) showed not significant differences compared with the parental cell line (r = 1.32 ± 0.27). According to the International Transporter Consortium (Giacomini et al., 2010) moxifloxacin is a poor or non-substrate for ABCG2 since the transport ratios for Abcg2- and ABCG2-transduced cells were < 2. The low ABCG2-mediated transport was reduced when Ko143 was added; however, although very small, a remaining significant transport was observed in the case of parental and ABCG2-transduced cells at 4 hours (Figure 54 D, F), indicating the possible involvement of another ABC transporter such as P-gp in the process. From these results it could be concluded that moxifloxacin is not an *in vitro* substrate of ABCG2 at the concentration tested.

3.2.2. Pefloxacin

Pefloxacin vectorial transport using the three MDCK-II cell lines is represented in Figure 55. Studying pefloxacin, apically and basolaterally directed transports in the parental cell line were similar (Figure 55 A). However, for murine Abcg2-transduced cells the apically directed translocation was considerably increased and basolaterally directed transport was drastically decreased compared with the parental cell line (Figure 55 B). In the human ABCG2-transduced cells, the effects were analogous, but to some extent less pronounced (Figure 55 C). Transport ratios (B-A/A-B) at 4 hours were significantly higher for both transduced cell lines compared to parental cells, with values for murine Abcg2-transduced cells significantly higher than for human ABCG2-transduced cells (r = 34.17 ± 3.44 and 3.83 ± 0.35, respectively). Using Ko143, the Abcg2/ABCG2 mediated transport in the transduced cells was reduced to values similar to the parental cell line (Figure 55 D, E, F). As a result, it can be stated that pefloxacin is efficiently transported by murine Abcg2 and human ABCG2.

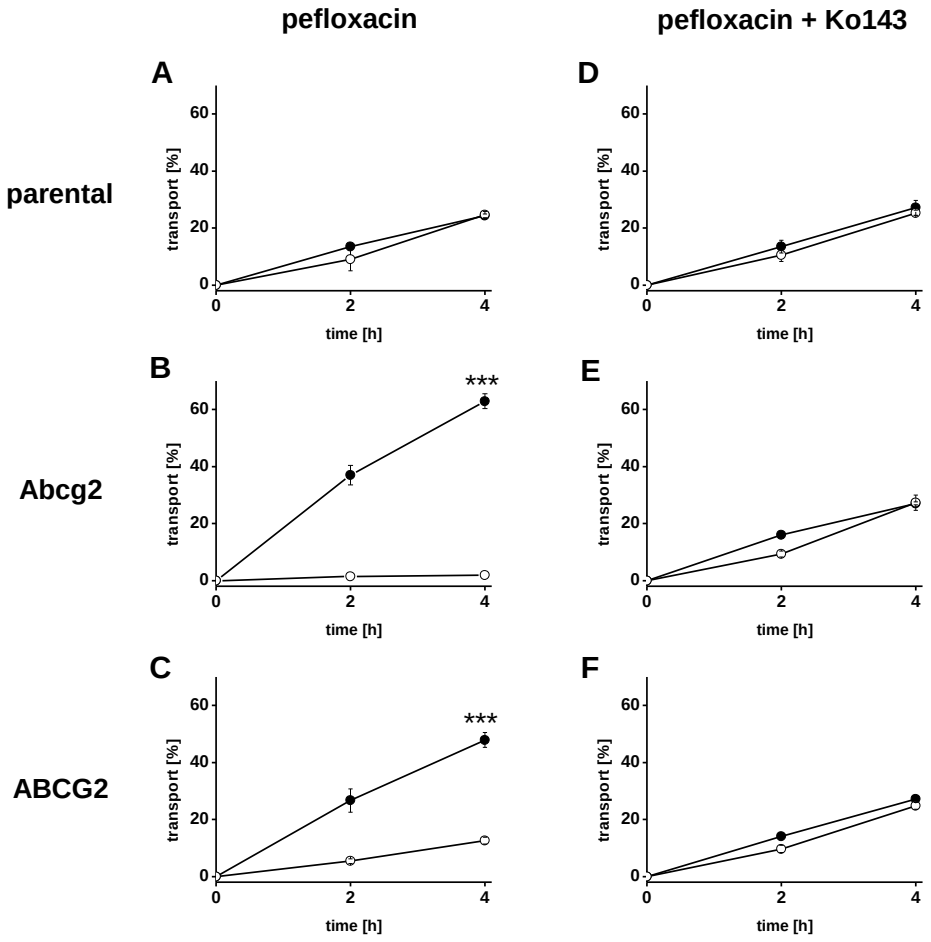

Figure 55. Transepithelial transport of pefloxacin (10 µM) across monolayers of MDCK-II-parental (**A, D**), MDCK-II-Abcg2 (murine Abcg2) (**B, E**) and MDCK-II-ABCG2 (human ABCG2) (**C, F**) transduced cells. The experiment was started by adding pefloxacin to one compartment (basolateral or apical); after 2 and 4 hours, the percentage of drug in the opposite compartment was measured by HPLC. Transport was conducted in the absence (A, B, C) or in the presence (D, E, F) of the ABCG2 inhibitor Ko143 at 1 µM, added to both compartments. Translocation from the apical to the basolateral compartment, A-B (open circles); translocation from the basolateral to the apical compartment, B-A (filled circles). Results are the means, error bars (frequently within the symbols) indicate SD (n = 3). Significant differences between AB and BA translocation at 4 hours tested by Student's t test (***, $p < 0.001$).

3.3. Mitoxantrone accumulation

A common assay used to elucidate whether a compound is an inhibitor of ABCG2 is to analyze the accumulation of a known substrate applied together with the compound to be tested (Hegedus et al., 2009). The antibiotic-mediated inhibition of murine Abcg2 and human ABCG2 was examined using the MDCK-II cell lines (parental and transduced subclones) employing MXR as a fluorescent substrate.

MXR accumulation was measured using flow cytometry. As expected, the accumulation of MXR (10 μM) was increased in Abcg2- and ABCG2-transduced cells by ABCG2 inhibition with Ko143 (1 μM), used as a positive control, to levels similar to those in the parental cells. However, no inhibitory effect was found when moxifloxacin (50 to 500 μM) or pefloxacin (50 and 250 μM) were applied (Figure 56). These data are in agreement with the lack of ABCG2 inhibition reported before for ciprofloxacin and norfloxacin (Merino et al., 2006). These findings suggest that the investigated fluoroquinolones do not act as ABCG2 inhibitors at the tested concentrations.

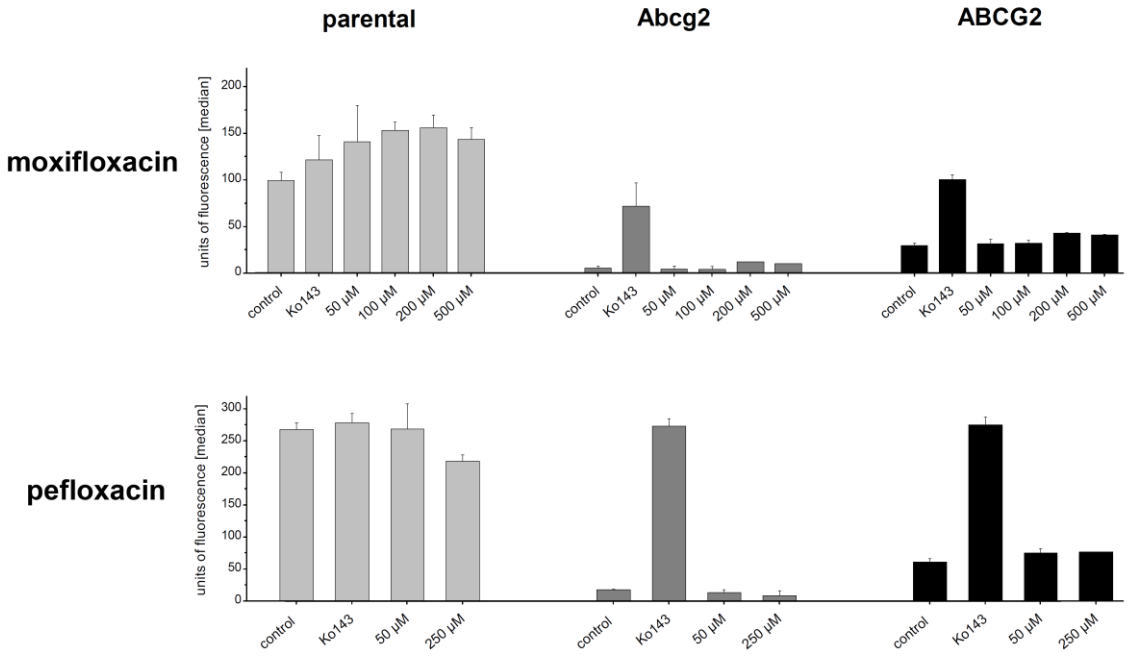

Figure 56. Inhibition of ABCG2 efflux activity. Effect of moxifloxacin and pefloxacin at different concentrations on accumulation of mitoxantrone (10 µM) in parent MEF3.8 cells and in their human ABCG2- and murine Abcg2- transduced cell lines. Cells were pre-incubated with or without Ko143 (1 µM). The tested compounds were analyzed by flow cytometry. Columns are the means of units of fluorescence (median), error bars indicate SD (n = 2-3).

3.4. *In vivo* pharmacokinetics with mice

To complete the characterization of the interaction of the fluoroquinolones used in this study with ABCG2, based on our *in vitro* experiments with pefloxacin (Figure 55) and on previous results from our group indicating that norfloxacin is an *in vitro* Abcg2 substrate (Merino et al., 2006), norfloxacin and pefloxacin were tested as *in vivo* substrates. Male Abcg2$^{-/-}$ and wild-type mice were orally administered with norfloxacin or pefloxacin (10 mg/kg) and fluoroquinolone contents in different fluids and tissues

were analyzed. Ciprofloxacin and enrofloxacin have been reported previously as *in vivo* ABCG2 substrates (Merino et al., 2006; Pulido et al., 2006).

Moxifloxacin was not analyzed extensively *in vivo* as no *in vitro* interaction was found (Figure 54). As expected, a trial performed administering moxifloxacin via oral (200 mg/kg) taking plasma at 120 min postdosing, gave no differences between Abcg2$^{-/-}$ and wild-type male mice (12.07 ± 5.15 *vs* 11.95 ± 4.98 µg/ml, respectively), n=3-5.

3.4.1. Norfloxacin

Plasma concentrations after norfloxacin administration were significantly higher in Abcg2$^{-/-}$ mice compared with wild-type animals over the whole range of time period analyzed (5-120 min) (Figure 57 A).

The calculated $AUC_{0\text{-}120}$ was 1.5-fold higher for Abcg2$^{-/-}$ compared to wild-type mice (0.56 ± 0.03 *µ*g·h/ml *versus* 0.36 ± 0.02 *µ*g·h/ml, respectively, $p < 0.05$), indicating an important role of Abcg2 in the oral pharmacokinetics of this antibiotic. The plasma concentration time curves showed that norfloxacin absorption and distribution occur during the first 30 min (maximum), followed by a first phase of rapid clearance (up to 60 min) and a second phase with slower elimination; indeed, between 60 and 120 min the concentrations remained almost at the same level (Figure 57 A).

Hepatic concentrations were ~2-fold higher in Abcg2$^{-/-}$ compared with wild-type mice at 30 and 60 min postdosing, with statistically significant differences (Figure 57 B and D). On the other hand, norfloxacin bile levels were 6-fold and 3-fold lower in Abcg2$^{-/-}$ mice compared with wild-type mice at 30 and 60 min, respectively. Similar results were obtained when liver or bile concentrations were normalized to plasma concentrations (Figures 57 C and E). These results show the relevant role of Abcg2 in the bile elimination of norfloxacin.

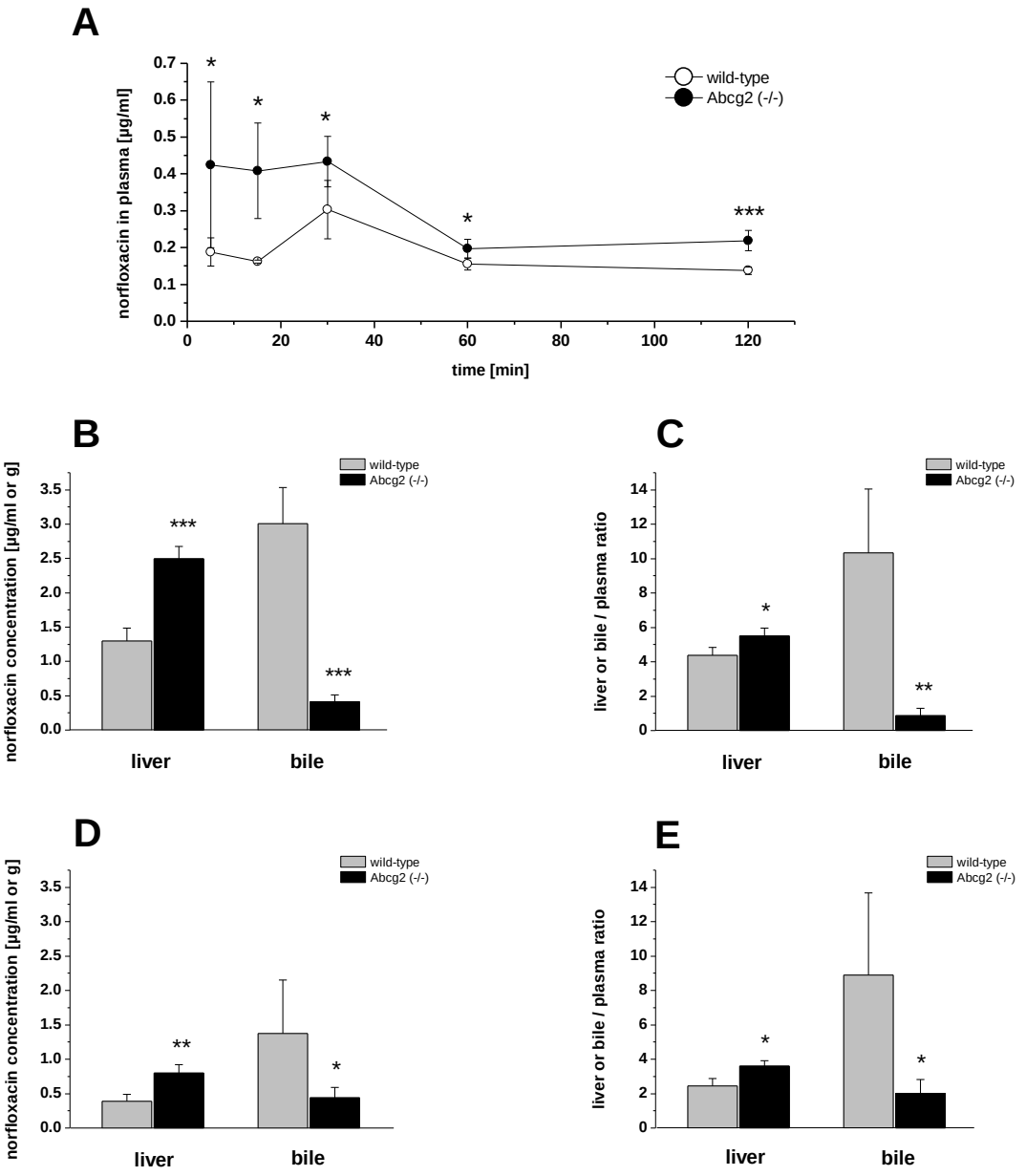

Figure 57. Effect of Abcg2 on plasma, liver and bile concentrations of norfloxacin after its oral administration at 10 mg/kg to male wild-type and Abcg2$^{-/-}$ mice. Time profiles of plasma concentrations(**A**). Norfloxacin concentrations in the liver and bile at 30 min (**B**) and 60 min (**D**) postdosing. Norfloxacin tissue-to-plasma ratios at 30 min (**C**) and 60 min (**E**) postdosing. Drug levels were determined by HPLC. Values are means; error bars represent SD. n = 3-7. Statistically significant differences between wild-type and Abcg2$^{-/-}$ mice (*, $p < 0.05$; **, $p < 0.01$).

Levels of norfloxacin significantly differed between Abcg2$^{-/-}$ and wild-type male mice also in other tissues analyzed after 60 min of administration (Table 18 and Figure 58). Plasma, liver and bile concentrations at 60 min postdosing are also included in Table 18 for comparison.

Table 18. Concentrations of norfloxacin detected in mice tissues at 60 min after oral administration of norfloxacin (10 mg/kg).

Tissue or content	norfloxacin concentration		ratio Abcg2$^{-/-}$ / WT
	wild-type (WT)	Abcg2$^{-/-}$	
	[μg/ml or μg/g]	[μg/ml or μg/g][a]	[fold]
bile	1.38 ± 0.77	0.44 ± 0.15 *	0.32
brain	*nd*	*nd*	*nd*
kidney	0.18 ± 0.02	0.30 ± 0.07 *	1.67
liver	0.38 ± 0.10	0.79 ± 0.12 **	2.08
spleen	0.13 ± 0.00	0.14 ± 0.01 *	1.07
small intestine	4.14 ± 1.41	2.12 ± 0.63 *	0.51
intestinal content	59.87 ± 6.37	22.31 ± 2.93 ***	0.37
plasma	0.15 ± 0.02	0.20 ± 0.03 *	1.33

[a] *, $p < 0.05$; ***, $p < 0.001$ (comparing wild-type and Abcg2$^{-/-}$ mice). Results are mean ± SD. n = 3-6. *nd*: not detected.

The range of relative accumulation of norfloxacin for both groups of mice in the tested tissues was IC > small intestine > bile – liver > kidney > spleen. The significantly higher levels of this antibiotic in the kidney of Abcg2$^{-/-}$ mice reflect the higher plasma levels in these animals since differences disappear when normalized by plasma concentration (Figure 58 B). The 2-fold higher levels of this drug in the small intestine of wild-type compared to Abcg2$^{-/-}$ mice is probably related to the greater accumulation of this fluoroquinolone in the intestinal content of wild-type mice, potentially implying an Abcg2-mediated transport of norfloxacin directly into the lumen of this organ. However, considering the differences in bile levels (Figure 57 B and C), Abcg2-mediated hepatobiliary transport into the intestinal lumen is also probably involved in the elevated amounts of norfloxacin found in the intestinal content in wild-type animals. It is remarkable that norfloxacin was not detected in brain after 60 min of its administration (Table 18).

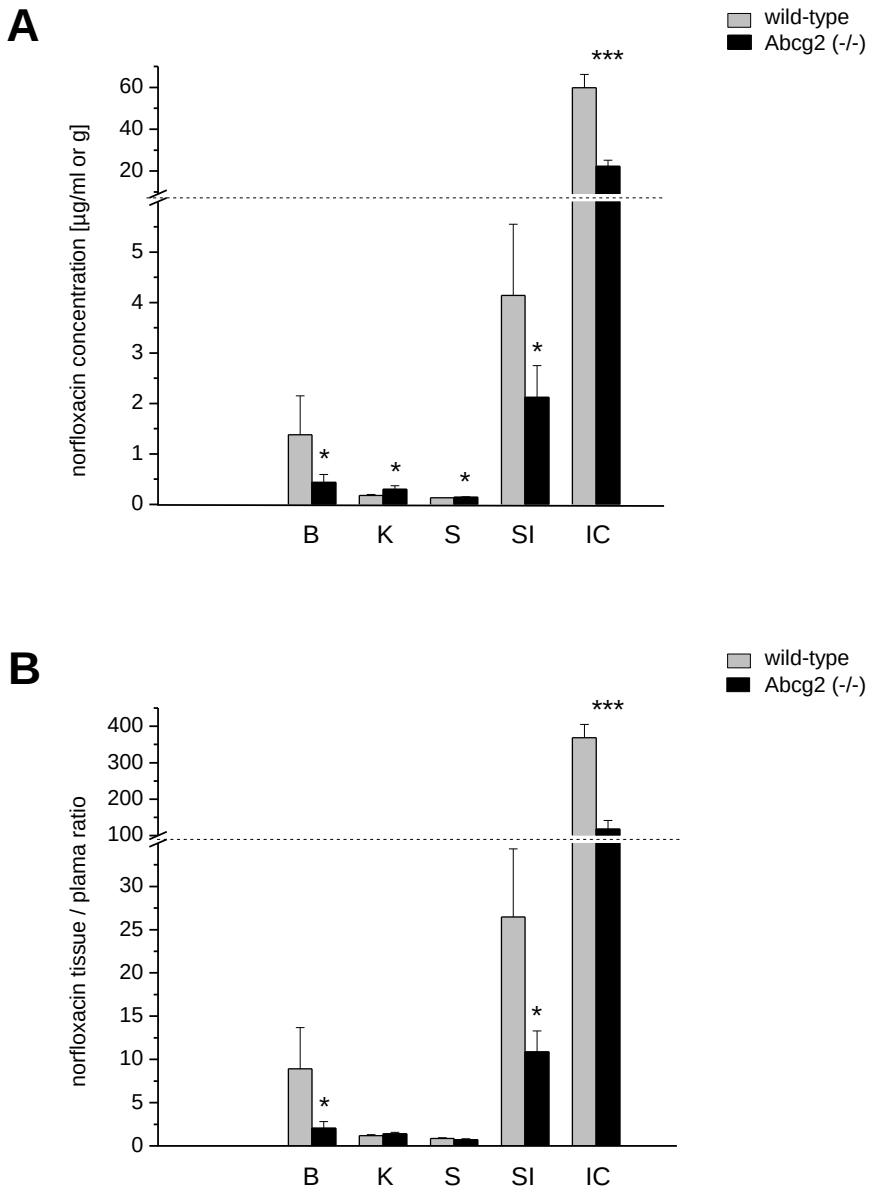

Figure 58. The effect of Abcg2 on tissues and contents concentrations (**A**) and tissue-to-plasma ratios (**B**) of norfloxacin after 60 min of oral administration at 10 mg/kg to male wild-type and Abcg2$^{-/-}$ mice. Levels of drug were determined by HPLC. Values are means; error bars represent SD. n=3-7. B: bile, K: kidney, S: spleen, SI: small intestine, IC: intestinal content. Statistically significant differences between wild-type and Abcg2$^{-/-}$ mice: *, $p < 0.05$; **, $p < 0.01$; ***, $p < 0.001$.

No norfloxacin was detected in milk from female mice for both genotypes after 15 min of oral administration at 10 mg/kg to wild-type and Abcg2$^{-/-}$ mice (Figure 59).

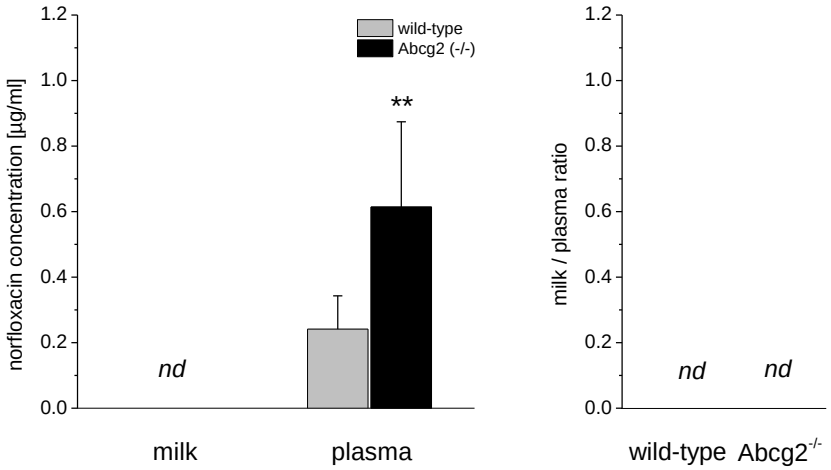

Figure 59. The effect of Abcg2 on milk and maternal plasma concentrations and milk-to-plasma ratios of norfloxacin after 15 min after oral administration at 10 mg/kg to female wild-type and Abcg2$^{-/-}$ mice. Levels of drug were determined by HPLC. Values are means; error bars represent SD. n=6-8. Statistically significant differences between wild-type and Abcg2$^{-/-}$ mice: **, $p < 0.01$. *nd*: no detected (milk) or determined (ratios).

As other antibiotics, fluoroquinolones are usually administered for several days (around one week) in treatments against bacteria. Therefore, in a further investigation, we wanted to analyze the evolution of the pharmacokinetics of norfloxacin for one week. Norfloxacin was administered orally to male wild-type and knockout mice for 7 days, once daily dose at 10 mg/kg. Plasma concentrations of norfloxacin at 15 min post-dosing every two days is represented in Figure 60.

Results reflect again higher levels of fluoroquinolone in knockout mice compared to wild-type. The calculated AUC_{0-t} was 2-fold higher for Abcg2$^{-/-}$ compared to wild-type mice (2.77 ± 0.28 μg·h/ml *versus* 1.35 ± 0.07 μg·h/ml, respectively, $p < 0.05$); indicating once more the relevance of Abcg2 in the pharmacokinetic of this antibiotic even at chronic treatment.

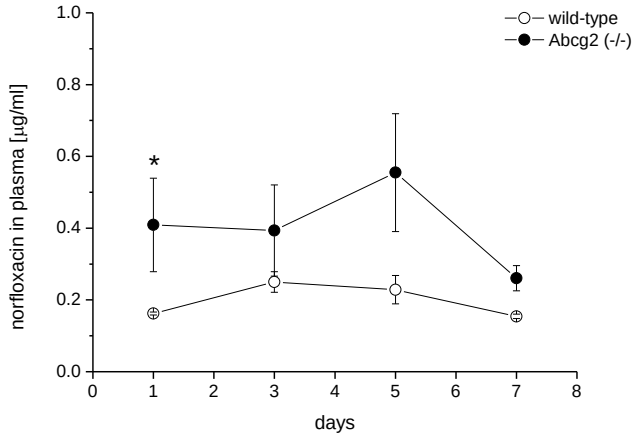

Figure 60. Plasma concentration of norfloxacin after 15 min of oral administration to male wild-type and ABCG21$^{-/-}$ mice at 10 mg/kg daily for 7 days. Plasma levels of compound were determined by HPLC. Results are means; error bars indicate S.D. n=2-3. Statistically significant differences between wild-type and Abcg2$^{-/-}$ mice: *, $p < 0.05$.

In the latter experiment, animals were kept in metabolic cages, and feces and urine were also collected at 24 h after the first administration; additionally, urine was collected at 60 min after this first administration. Samples were analyzed by HPLC. Extremely higher levels of norfloxacin in urine were detected in Abcg2$^{-/-}$ mice compared to wild-type at 60 min (417.76 ± 121.90 *vs* 5.69 ± 5.19 μg/ml, respectively; $p < 0.05$) and at 24 h after the first administration (145.70 ± 203.83 *vs* 2.25 ± 1.39 μg/ml, respectively), probably reflecting plasma levels. Due to the high inter-individual variation, no significant differences were reported at 24 h. No differences in the levels of norfloxacin in feces were found between both genotypes after 1 day of the starting of the experiment (1.49 ± 0.30 μg/ml for wild-type mice *vs* 1.27 ± 0.48 μg/ml for knockout mice).

3.4.2. Pefloxacin

The plasma concentration of pefloxacin after its administration as a function of time represented in Figure 61 A showed similar profiles in Abcg2$^{-/-}$ and wild-type male mice (sample points 5-60 min). Although significant changes were observed in plasma concentrations at 30 min, no significant differences between both groups were observed for the $AUC_{0\text{-}60}$ (1.62 ± 0.08 μg·h/ml for wild-type *versus* 1.44 ± 0.08 μg·h/ml for Abcg2$^{-/-}$, respectively). The time profiles of the plasma concentrations suggest a rapid drug adsorption and distribution, due to the fact that 5 min (or earlier) after administration the plasma pefloxacin level had already reached its maximum.

Tissue distribution was determined at 30 min after pefloxacin oral dosage in male mice. Liver and bile drug concentrations in Abcg2$^{-/-}$ were comparable with those in wild-type mice, with or without normalizing for plasma levels (Figure 61 B, C).

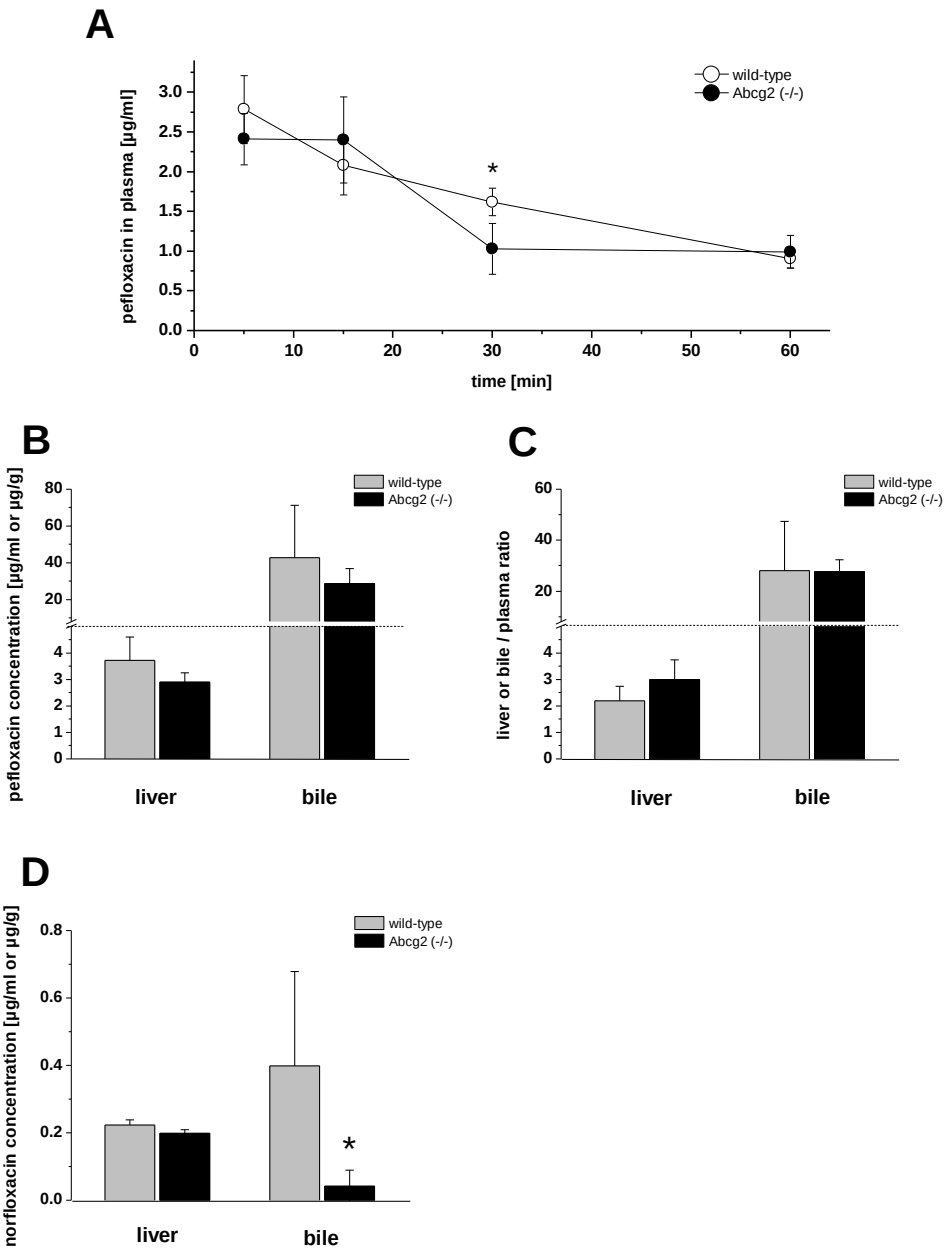

Figure 61. Effect of Abcg2 on plasma, liver and bile concentrations of pefloxacin and norfloxacin after its oral administration of pefloxacin at 10 mg/kg to male wild-type and Abcg2$^{-/-}$ mice. Time profiles of plasma concentrations of pefloxacin (**A**). Pefloxacin concentrations in liver and bile (**B**) and tissue-to-plasma ratio (**C**) at 30 min postdosing. (**D**) Norfloxacin concentrations in liver and bile at 30 min postdosing of pefloxacin. Tissue-to-plasma ratio of norfloxacin concentrations in liver and bile could not be determined since norfloxacin was not detected in plasma. Levels of drugs were determined by HPLC. Values are means; error bars represent SD. n = 3-6. Statistically significant differences between wild-type and Abcg2$^{-/-}$ mice (*, $p \leq 0.05$).

Norfloxacin, as pefloxacin metabolite, could also be detected in samples from tissues of mice administrated with pefloxacin (30 min post-dosing), but not in plasma. In contrast to the pefloxacin results, significant differences were observed in norfloxacin accumulation in the bile between wild-type

and Abcg2$^{-/-}$ mice (0.40 ± 0.28 *vs* 0.04 ± 0.04 μg/ml, respectively; 10-fold, wild-type / Abcg2$^{-/-}$, $p < 0.05$) (Figure 61 D), as well as in the intestinal content (1.16 ± 0.19 *vs* 0.71 ± 0.19 μg/ml, respectively; 1.6-fold, wild-type / Abcg2$^{-/-}$, $p < 0.01$). In the case of the small intestine, concentrations showed a slight reduction in Abcg2$^{-/-}$ mice (0.26 ± 0.05 μg/ml for wild-type mice and 0.22 ± 0.04 µg/ml for knockout mice); however, the differences were not statistically significant. This metabolite was not detected in brain, kidney or spleen. These findings further confirm that Abcg2 significantly affects the hepatobiliary elimination of norfloxacin.

Additionally, levels of pefloxacin in milk from female mice showed significant differences between both groups, Abcg2$^{-/-}$ and wild-type, after 15 min of pefloxacin oral administration at 10 mg/kg (Figure 62). However, these differences disappeared when levels of pefloxacin in milk were normalized with levels in plasma, the milk-to-plasma ratios (Figure 62). Levels of norfloxacin in milk from female mice administered with pefloxacin were negligible low, at the limit of HPLC detection (Data not shown).

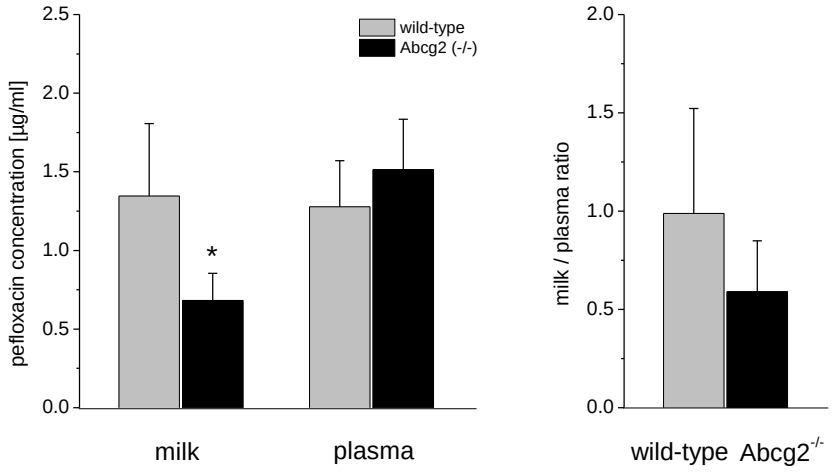

Figure 62. The effect of Abcg2 on milk and maternal plasma concentrations and milk-to-plasma ratios of pefloxacin after 15 min of oral administration at 10 mg/kg to female wild-type and Abcg2$^{-/-}$ mice. Levels of drug were determined by HPLC. Values are means; error bars represent SD. n=4-8. Statistically significant differences between wild-type and Abcg2$^{-/-}$ mice: *, $p < 0.05$.

In summary, it has been demonstrated that Abcg2 activity significantly decreases the systemic exposure and increases hepatobiliary excretion of norfloxacin but not of pefloxacin under the experimental conditions used.

Discussion

1. Comparison of ATPase activity, substrate specificities and substrate-activity relationships between ABCG2 and P-glycoprotein

To understand the function of ABCG2 *via* the comparison with the P-gp transporter to gain further insight into similarities and differences of the two transporters ATPase activity, substrate specificity and substrate-activity relationship were studied with a combination of results from ATPase activity of ABCG2 and P-gp in inside-out plasma membrane vesicles (ABCG2-M-ATPase and NIH-MDR1-G185 plasma membrane vesicles, respectively) and surface activity measurements.

As mentioned earlier, it is a problem to obtain plasma membrane vesicles with high enough expression levels of ABCG2 to be able to stimulate and measure ATPase activity (Glavinas et al., 2007; Ni et al., 2010). This is why most of the studies published used ABCG2-enriched insect cell membranes (Sf9) where ABCG2 is expressed at appreciable level giving high ATPase activity. The effects of substrates and inhibitors on ABCG2- dependent membrane ATPase activity in Sf9 cells have been shown to correlate with the effects of these compounds in ABCG2-overexpressing mammalian cells (Ozvegy et al., 2001). However, a main problem is due to its dependence on cholesterol (Pal et al., 2007; Telbisz et al., 2007) which is nearly absent in insect cells; membrane composition of Sf9 cells is largely different from that of mammals and this fact might likely affect also the ATPase activity results. In fact, it was suggested that the different behavior of the vesicle membranes from insect cells Sf9 and from mammalian cells was due to the membrane composition (Glavinas et al, 2007). It should be noted that membrane composition and packing density of plasma vesicle membranes have been demonstrated to be important in drug ATPase activity stimulation, at least for P-gp (Aänismaa et al., 2008). Thus, we decided to use the alternative assay with mammalian membranes proposed by Glavinas et al. (2007).

To be able to perform ATPase activity assays, quantification of the protein expression in this model is first needed. Regarding P-gp, an attempt of quantification was published with a FACS analysis in two different types of P-gp transfected cell lines, including the NIH-MDR1 cells (Gatlik-Landwojtowicz et al., 2004). For NIH-MDR1 cells, the number of P-gp molecules per cell has been assessed (Ambudkar et al., 1997).

Despite the fact that methods for ABCG2 expression have been broadly employed in a qualitative manner, quantification of the ABCG2 protein has not been yet properly achieved. The expression level of ABCG2 in ABCG2-M-ATPase plasma membrane vesicle from SOLVO was unknown.

Since the corresponding intact cells of ABCG2-M-ATPase membranes which would allow an estimation of the expression level using ABCG2 antibodies are not available, three different approaches were used to estimate the ABCG2 expression in the ABCG2-M-ATPase membranes by comparing with the quantification of ABCG2 in ABCG2-transduced MEF3.8 cells. We performed Western blot analysis with both type of vesicles, we quantified the level of enhanced GFP expression in MEF3.8 cells and, then

we compare the ATPase activity between MEF3.8 and ABCG2-M-ATPase plasma membrane vesicles. These experiments yielded a 5 to 7 fold higher expression level in ABCG2-M-ATPase plasma membrane vesicles compare to vesicles from MEF3.8 cells (Figures 32 and 36).

We are aware that the use of GFP quantification as a method to quantify ABCG2 has several limitations. For instance, due to the IRES site in the cloning vector is between the GFP and ABCG2, it would be possible that both proteins were not translated the same number of times. In addition, GFP may adhere to the plate. Nevertheless, we pre-coated with BSA to prevent adherence to the plate of the fluorophore as it was described elsewhere (Wilma van Esse et al., 2011) and similar results were observed when we performed the experiment without this pre-incubation, indicating that the possible adherence is barely insignificant. Furthermore, reflections and other interferences might occur during the reading of the plate in the spectrometer. Despite these inconvenients, to our knowledge, this was the first attempted to quantify ABCG2 and to give the number of molecules/cell. In addition, the three approximations performed yielded similar conclusions with respect to the number of ABCG2 molecules per cell.

We could estimate the level of ABCG2 expression in the ABCG2-M-ATPase membranes as ≈ 10^6 to 10^7 ABCG2 molecules/cell. Our knowledge from previous experiences in our lab indicates that it is possible to observe the ATPase activity in membranes made from cells expressing over 10^5 molecules of ABC transporter. It should be noted that this is in agreement with the results obtained from the membranes generated from MEF3.8 cells, where we could barely detect ATPase activity (Figure 34) and the calculated ABCG2 dimer-molecules/cell were ≈ 10^5 to 10^6. For NIH-MDR1 cells, the number calculated previously was $1.95x10^6$ P-gp molecules/cell (Ambudkar et al., 1997).

The basal ATPase activity of P-gp in plasma membranes formed from MDR1 transfected mouse embryo fibroblasts (NIH-MDR1-G185), expressing $1.9x10^6$ P-gp per cell (Ambudkar et al., 1997), was previously determined as V_0 = 12.3 ± 1.3 nmol min^{-1} mg^{-1} protein (Aänismaa and Seelig, 2007). The basal ATPase activity from ABCG2 transfected mouse embryo fibroblasts (MEF3.8), estimated to express $5x10^5$ to $5x10^6$ ABCG2 dimers per cell, was determined as V_0 = 8.2 ± 1.0 nmol min^{-1} mg^{-1} protein (Figure 36). The basal activity of ABCG2 in ABCG2-M-ATPase membranes was determined as V_0 = 39.21 ± 2.3 nmol min^{-1} mg^{-1} protein (Figure 36), whereby mammalian cells were estimated to express around $3.5x10^6$ to $3.5x10^7$ ABCG2 dimers per cell. Assuming that the three different cell lines exhibited a comparable total protein concentration and taking into account the number of molecules per cell, **the basal ATPase activity is** somewhat **lower for ABCG2 than for P-gp**.

Comparing with published information, it has been reported that, in general, ABCG2 exhibits a basal ATPase activity that is considerably lower than that of P-gp (Ni et al., 2010), in agreement with our conclusion. One exception was found with insect Sf9 vesicles membrane where the basal ABCG2-ATPase activity was 3-5 higher than for the P-gp-containing membranes (Ozvegy et al., 2001). As it has been already discussed, Sf9 insect cells largely differ from mammalian cells.

Additionally, results showed comparable K_1 parameter in both membranes (i.e. 0.68 µM for ABCG2-M-ATPase membranes and 0.39 µM for membranes from MEF3.8 cells, Figure 35), indicating that the packing density of both membranes is similar (ABCG2-M-ATPase membranes and membranes from MEF3.8 cells). Taking into account that MEF3.8 cells and NIH-MDR1-G185 cells are both mouse embryo fibroblasts, probably all three cells have analogous membrane packing density.

It should noted that as the latter membranes are commercially purchased from a company, no information about them is given to the suppliers; we could not get the type of cells from which they were made, neither any physical or molecular characteristic of the cells. However, we could obtain this important insight, a similar packing density, necessary in further calculations.

After the analysis of the ABCG2 expression in ABCG2-M-ATPase plasma membrane vesicles, optimization of conditions for ABCG2-ATPase activity assays were performed.

Optimization of conditions for P-gp-ATPase activity assays with NIH-MDR1 cells has been broadly completed (e.g. Aänismaa and Seelig, 2007). The appropriate concentration of protein, the optimal incubation time, pH, vanadate and ATP concentrations, respectively, were assessed in this study then for the ABCG2-M-ATPase plasma membrane vesicles. To the best of our knowledge, this was the first time that this complete optimization was performed for any kind of vesicle membranes over-expressing ABCG2. Notably, the optimal conditions assessed for measuring the ATPase activity of ABCG2 were identical to those assessed previously for measuring the ATPase activity of P-gp, except that the plasma membrane protein concentration used for P-gp was somewhat higher (0.1 mg/ml) (Litman et al., 1997 a and b; Aänismaa and Seelig, 2007) compared to the 0.075 mg/ml we chose for ABCG2.

From the concentration dependency experiments we could get the average of ABCG2 basal activity V_0 = 39.21 ± 2.27 nmol min^{-1} mg^{-1} (Figure 36), which is in good agreement with previous measurements as Glavinas et al. (2007) obtained a basal activity of around 40 nmol min^{-1} mg^{-1} for the same vesicle membranes.

ABCG2-ATPase activity assays were also performed at different buffer pH values (between 5 and 8.5) and no effect was observed in the basal activity between pH 6 and 8 (Figure 39). These results of pH dependence are similar to those obtained for P-gp (Aänismaa and Seelig, 2007) but are different to other ABC transporter, Sav1866, where more pronounce dependency of the pH was found (Beck et al., 2013). On present results, at lower pH, the basal ABCG2-ATPase activity decreased with a sigmoid curve (Figure 39). It has been commented that ABCG2 transports more efficiently in acidic environments and this pH dependency is specific for ABCG2, as this is not the case for P-gp, MRP2 or MRP5 (Breedveld et al., 2007; Li et al., 2011). Other authors found only in some cases higher ATPase activity with ABCG2-M-ATPase plasma membrane vesicles in acidic environments (pH=5.5) (Glavinas et al., 2007). This could be due to this decreasing in the basal ATPase activity at this low pH.

A complete inhibition of the ABCG2-ATPase was achieved at a vanadate concentration of 0.1 mM (Figure 40) for the ABCG2-M-ATPase vesicle membranes, with a K_i value of 4.06 µM. Ozvegy et al. (2001) found that vanadate-inhibition of the ABCG2-ATPase activity occurred with a K_i value of about 20 µM Na-orthovanadate for Sf9 cells. Both values from the two different cell lines are by some means comparable. The ABCG2-ATPase activity measured as a function of the ATP concentration presented a semi-full bell-shape curve for the ABCG2-M-ATPase vesicle membranes (Figure 41). The decrease in ATPase activity can be probably attributable to the accumulation and binding of ADP (Beck et al., 2013). Analogous measurements were performed previously with the same membrane vesicles, however at higher concentrations, which yielded only the ascendant branch of the activity curve (Glavinas et al., 2007).

Following the optimization of the conditions for ABCG2 ATPase activity assays, ABCG2- and P-gp-ATPase activity experiments were performed with 28 compounds.

ATPase activity results performed with both transporters, ABCG2 and P-gp, displayed in Figures 43 to 45 are in agreement with other results published with the compounds analyzed, although not performed with the same cell membranes. For instance, daunorubicin, methotrexate, prazosin, progesterone and tamoxifen for P-gp (Litman et al., 1997; Ramachandra et al., 1998) and daunorubicin, digoxin, Ko143, mitoxantrone, ranitidine, sulfasalazine, testosterone, verapamil for ABCG2 (Ozvegy et al., 2001; Glavinas et al., 2007). Nonetheless, there are two remarkable cases regarding the interaction of compounds with ABCG2. First, methotrexate was shown to be transported in Sf9 membranes and ABCG2-M-ATPase vesicle membranes (Ozvegy-Laczka et al., 2005; Glavinas et al., 2007); however only at very low concentrations (pmol range). This is in agreement with our results, where we could not see anymore ABCG2- nor P-gp-ATPase activity for this compound at µM range. The other case is that all compounds analyzed in vesicle membranes obtained from *L. lactis* cells displayed activation and inhibition curves for ABCG2 (Janvilisri et al., 2003), i.e. hormones for which we have found only ATPase inhibition curves. The differences may be due to the different lipid composition between both types of cells (In 't Veld et al., 1991), also together with the higher amount of protein membrane that Janvilisri et al. (2003) used in their ATPase-activity experiments (~ 1 mg/ml) compared to us (0.075 mg/ml). We have shown that the higher concentrations of protein membrane in ATPase activity assay, the easier is to obtain ATPase activation (Beck et al., 2013).

From Figures 43 and 45 and Table 9, it can be deduced that, in general, K_1 values of P-gp are similar to K_2 values of ABCG2 for neutral compounds. An analysis of data obtained from Janvilisri et al. (2003) showed that these authors obtained full activation and inhibition ABCG2-ATPase activity curves for compounds where we could see only inhibition. Results from Janvilisri et al. (2003) reveal that K_2 values are aproximalety ten times higher than K_1 values. This is in agreement with our results for the compounds where we could see a complete curve of ABCG2-ATPase (Table 9). Nonetheless, factors of

K_2/K_1 ~100 (prazosin) and ~1000 (riboflavin and sulfasalazine) could also be observed for some of our compounds (Table 9).

As it was published by Aänismaa and Seelig (2007), regarding P-gp interactions with compounds, maximum ATPase activity requires high millimolar concentrations for very hydrophilic drugs (e.g. H_2 receptor antagonist), micromolar concentrations for hydrophobic drugs (e.g. steroid-hormones), and nanomolar concentrations for even more hydrophobic drugs (e.g. Ko143). This statement seems to be also valid for the ABCG2 transporter (Figures 43 to 45).

Usually, compounds can act as P-gp substrates or inhibitors depending on the concentration, at low concentrations act as substrates and at higher as inhibitors, this yield to bell-shape curves in the ATPase activity (Seelig and Landwojtowicz, 2000). As seen for P-gp (see e.g. promazine and verapamil) and ABCG2 (e.g. sulfasalazine) (Figures 43 to 45) both exporters were in principle able to produce full bell-shaped ATPase activity curves which are best interpreted with a two-site binding model, assuming activation if one molecule is bound to the exporter and inhibition if two molecules are bound to the exporter.

Similarly, the ABCG2 drug-modulation of ATPase activity in a biphasic pattern, stimulating activity at low concentrations and inhibiting at higher concentrations, could have seen in few reported cases. For instance working with vesicle membranes from *L. lactis* (Janvilisri et al., 2003; Cooray et al., 2004) (Figure 63 D), high-five intect cells (Dai et al., 2008) or with the drug sulfasalazine (Glavinas et al, 2007) (Figures 63 A and 45 A).

In most of the published concentration dependent ATPase activity graphics, only activation or inhibition curves were shown (e.g. Ozvegy et al., 2001; Ozvegy-Laczka et al., 2004; Glavinas et al., 2007) (Figure 63 A, B and C).

Probably due to the “simple” curves obtained (only inhibition or only activation), data evaluation of ABCG2 ATPase activity is usually calculated using the simple Michaelis- Menten kinetic (e.g. Ozvegy et al., 2001; Wu et al., 2007; Robey et al., 2009). Data evaluation of compounds for which it is only possible to measure the activation branch of the ATPase curve is more a simple Michaelis-Menten kinetics (as other authors evaluate usually the ATPase activity titration curves; e.g. Ozvegy et al., 2001; Wu et al., 2007; Robey et al., 2009) than the used modified Michaelis–Menten equation proposed by Litman et al. (1997a) for bell-shaped P-gp-ATPase activity profiles (Equation 2 and Figure 18). Certainly, in the modified Michaelis–Menten equation, if only activation occurs, the dissociation constant (K_1) and the maximum activity (V_1) correspond to the simple Michaelis-Menten parameters (Seelig and Landwojtowicz, 2000).

Full curves could only be measured for a few compounds; i.e. daunorubicin and prazosine for both transporters (Figure 44) or sulfasalazine for ABCG2 (Figure 45). Hydrophilic, non-amphiphilic compounds generally revealed only the rising part of the activity curve, because the solubility limit of

the compound was reached before the inhibitory part (i.e. occupation of the second binding site) started. Amphiphilic, hydrophobic molecules showed in contrast only the inhibitory part of the curve.

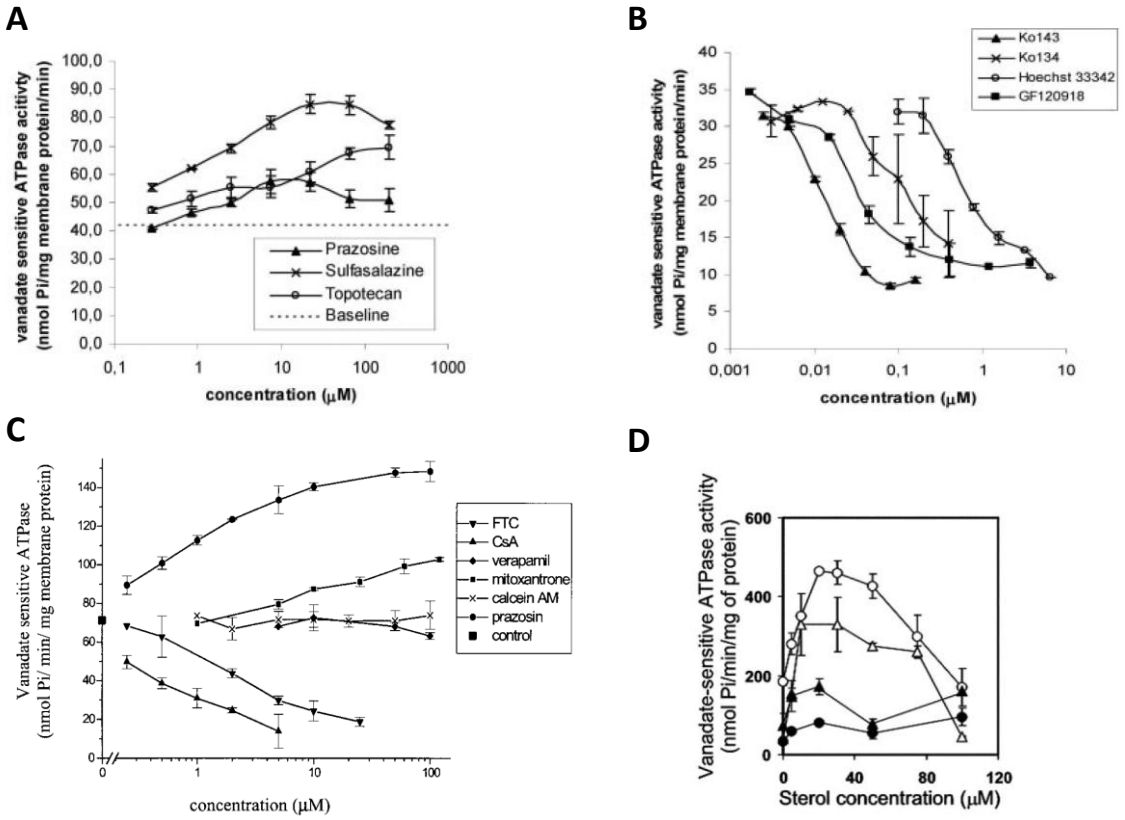

Figure 63. Previously published effects of various compounds on the vanadate sensitive ABCG2-ATPase activity in inside-out membrane vesicles. **A** and **B**. MXR-M vesicles (Glavinas et al., 2007). **C**. Isolated Sf9 membranes of ABCG2 (Ozvegy et al., 2001). **D.** Vesicles of *L. lactis;* in the presence of increasing concentrations of estradiol (*circles*) or cholesterol (*triangles*) (Janvilisri et al., 2003).

A comparison between ABCG2 and P-gp by means of substrate-activity relationship: structural analysis was performed taking into account the charge and hydrophobicity in relation with ATPase activity results from the 28 compounds analyzed.

A classification of the 28 compounds utilized according to their electric charge *versus* the trend results in ATPase activity measurements for the compounds with P-gp and ABCG2 is displayed in Table 10. It was known that P-gp interacts with neutral and cationic charged compounds at physiological pH but not with anionic (Schinkel et al., 1996; Seelig, 1998; Sharom, 2008). Our results are in the same trend (Table 10); note that zwitterionic compounds include also anionic charge. Concerning ABCG2, it was reported that it interacts with neutral, negatively or positively charged molecules (Xia et al., 2005;

Krishnamurthy and Schuetz, 2006; Ni et al., 2010). Our results are in agreement with those in the sense of interaction with the transporter, although ATPase activity assays gave different ABCG2-ATPase activity for each one (Table 10). Neutral and cationic compounds are highly attracted by ABCG2 (have high affinity to the transporter), whereas negatively charged and zwitterionic compounds are bound less strongly and are transported more rapidly (Figure 48).

As a remark, the typical ABCG2 substrates yielded no proper curves of P-gp-ATPase activity (Figure 45 for ABCG2 and Data not shown for P-gp) or lower P-gp-ATPase activity as for daunorubicin (Figure 44 C), an indicative of the scant interaction with the P-gp transporter. This fact might be explained by means of charge as these compounds are overcoat anionic and zwitterionic (with a negative charge) and anionic compounds do not interact with P-gp (Seelig, 1998). Additionally, it is necessary to remember that partitioning into the lipid membrane is the rate-limiting step for the interaction of a substrate with P-gp (Seelig and Landwojtowicz, 2000; Aänismaa and Seelig, 2007). P-gp is efficient in transporting amphiphilic compounds which diffuse well the membrane, at a high rate (Seelig et al., 1994). As a consequence, the rate of P-gp-ATPase activity is usually high. The compound must achieve passive diffusion; thus, if it is highly charged and/or non-amphiphilic, as the typical ABCG2 substrates, the drug will diffuse very slowly (see the "Surface activity" and "Charge" sections at this discussion). Therefore, because of the physico-chemical characteristics of **typical ABCG2 substrates, if transported by P-gp, they will be transported slowly**.

Hydrophobicity has been a common feature among published SARs and QSARs models for both ABCG2 and P-gp (Seelig, 1998; Seelig and Landwojtowicz, 2000; Gandhi and Morris, 2009). Regarding our results, we show that the more hydrophobic compounds induced full bell-shaped ATPase activity curves for P-gp and essentially inhibitory ATPase activity curves with a dominant descending branch for ABCG2 (Figures 43 and 44). The more hydrophilic compounds, which had to be applied at higher concentration (e.g. Figure 44 D), induced only the ascending branch of the P-gp-ATPase activity curves (due to solubility limits of the drug, the inhibitory concentration range could not be reached), whereas they induced almost full bell-shaped ABCG2-ATPase activity curves, suggesting that **the substrate-affinity is significantly higher for ABCG2 than for P-gp**. Titration curves showing only the inhibitory branch accurred in the case of drugs with high affinity to the membrane and to the transporter. In agreement to our conclusions, hydrophilic compounds were described in literature as very good substrates but not inhibitors of ABCG2 while hydrophobic compounds act more as ABCG2 inhibitors (Matsson et al., 2007). Furthermore, classically P-gp has been considered to interact with hydrophobic, amphiphilic, lipid-soluble compounds (Gottesman and Pastan, 1993; Schinkel et al., 1996; Sharom, 2008).

A classification of the compounds according to the distribution of hydrophobic and hydrophilic centers in the molecule is displayed in Figure 42. Typical amphiphilic compounds usually display a hydrophilic and a hydrophobic center, and insert into the membrane *via* the lipophilic (hydrophobic)

part (type I). Compounds with two hydrophobic ends and a hydrophilic center can either have planar and rigid structure, not be able to bend well and hardly insert into the membrane; or bend and insert into the membrane more easily from the hydrophobic core, as amphiphilic compounds (type II). Type II compounds with a rigid structure hardly cross the membrane and would be supposed not to interact with P-gp but only with ABCG2. Nonetheless they have a slightly cationic charge that implies finding ATPase activation for both transporters (prazosin); or neutral (Ko143) charge, therefore ABCG2 inhibition is obtained. Similarly, compounds with two hydrophilic ends and a hydrophobic center can either bend easily (e.g. H_2 receptor antagonist family) or not (e.g. the rest of the compounds from type III). Type III compounds are planar and rigid molecules that have difficulties to cross the membrane; however, they can be sub-classified by their charge in anionic and zwitterionic (typical ABCG2 substrates, they do not interact with P-gp) and neutral (they activate P-gp-ATPase activity and inhibit ABCG2-ATPase activity). The H_2 receptor antagonists, except ranitidine, interact activating both transporters due to the slightly cationic charge; as ranitidine is more hydrophobic (highest XLogP, see Table 12), it interacts directly inhibiting the ABCG2.

Typical ABCG2 substrates are generally type III compounds. As a result, we could conclude that they often exhibit two hydrophilic polar ends (one can be cationic, the other anionic) and a smaller hydrophobic center (which can be a phenol group). Therefore, these compounds have low amphiphilicity.

SAR analysis obtained from Gandhi and Morris (2009) shows that a common aspect required for ABCG2 binding and inhibiting is planar structure. We have also seen that planar structure is necessary for ABCG2 binding; in contrast, we have observed that this planar structure is related with the activation but no with the inhibition of ABCG2-ATPase activity.

From the point of view of the molecular structure, sulfasalazine and glybenclamide are similar at first sight, but differ considerably in their interaction with ABCG2, the former activating and the latter inhibiting ABCG2. Both molecules are negatively charged, while glybenclamide is flexible, can fold, and thereby adopt an amphiphilic structure (type I in Figure 42), sulfasalazine is rigid, planar and non-amphiphilic (type III in Figure 42). Amphiphilic compounds generally inhibit, whereas non-amphiphilic compounds activate ABCG2.

A general conclusion that can be observed from the structural analysis of ATPase results (Figures 43 to 45 and Tables 9 and 12) is that **a compound which activates the P-gp-ATPase activity will act as inhibitor for ABCG2-ATPase (usually these compounds will present neutral or positive charge and will have a hydrophobic nature), except if it is slightly cationic**, e.g. daunorubicin, H_2 receptor antagonists and prazosin. Oppositely, **a compound which activates the ABCG2-ATPase activity will not affect the P-gp-ATPase activity (these compounds will present negative charge and will be hydrophilic)**. Although there must be exceptions (further insights are needed to elucidate them), this

statement might be useful to predict interactions with these two ABC transporters. It seems that both transporters have complementary transport functions concerning the type of compounds transported.

An ABCG2 and P-gp comparison by means of kinetics: ATPase activity-transport is presented below.

In known typical compounds which interact with ABCG2 (Figure 45), results show mostly curves with low ATPase activity (with the exception of sulfasalazine). In addition, with the exception of daunorubicin, most compounds induced a distinctly higher ATPase activity in P-gp than in ABCG2 (Figures 43 to 45). It seems, therefore, that substrates for ABCG2 are transported more slowly than for P-gp; in summary, **ABCG2 exhibits generally a lower substrate-induced activity than P-gp.** This fact can be observed in other published ABCG2-ATPase activity results, where basal ABCG2-ATPase activity could only be stimulated up to 2-fold by its substrates such as prazosin (Ozvegy et al., 2001; 2002; Glavinas et al., 2007; Pal et al., 2007), mitoxantrone (Ozvegy et al., 2001; 2002) or topotecan (Glavinas et al, 2007) (Figure 63 A and C). Ozvegy et al. (2001) associated the relatively smaller magnitude of additional drug-stimulation of ABCG2-ATPase to the relatively high-level of basal ABCG2-ATPase activity found in Sf9 cells. On the other hand, Glavinas et al. (2007) related the low ABCG2-ATPase activity to a low turnover rate that does not yield detectable amount of inorganic phosphate in the ATPase assay. It has been also suggested that this insensitivity of ABCG2 ATPase activity to drug-stimulation is maybe due to the presence of endogenous substrates or a partially uncoupled form of ABCG2 (Hegedus et al., 2009). Note that basal ATPase activity of MRP1 could not be strongly stimulated by its substrates either (Mao et al., 1999).

Despite the low rate of ABCG2-ATPase activity and transport, it can be concluded that **ABCG2 works very efficiently** with its typical compounds. This fact explains our results from experiments with cytosensor. When cytosensor experiments were performed with parental and human-ABCG2 transfected MEF3.8 cells, no signal from acidification was achieved attributable to the transporter from all attempts tried at different conditions (Table 14). However, probably, it does not mean a lack of activity of the ABCG2 transporter. At the low concentrations possible to use in the experiments, in the activation branch of the ATPase activity curve, to make sure not to kill the cells and to have ABCG2 activation, we are only at the beginning of the curve of extracellular acidification rate (ECAR) (remember that ATPase activity curves are shifted to the right in the concentration scale in living cells compare to experiements with vesicles (Nervi et al., 2010)) where the ABCG2 transporter is effectively taking and exporting each molecule of compound that slowly diffuses across the membrane. To use higher concentrations with typical ABCG2 compounds make no sense as we will probably achieve also problems of precipitation as a result of their high hydrophobicity.

To our knowledge, no cytosensor microphysiometer experiments studying the transport of ABCG2 have been published up to today, probably due to problems to obtain any ABCG2-related signal.

We also compared ABCG2 and P-gp by means of thermodynamics: affinity- substrate specificity.

Figure 48 shows the rate of transport (logarithmic scale) plotted as a function of the free energy of substrate binding from water to the transporter ($\Delta G°_{tw}$). Figure 48 reveals several general trends. First, as we have said, the higher the rate of ATPase activity induced by a substrate, the less negative is the free energy of substrate binding to the transporter (i.e., the lower is the affinity to the transporter) for P-gp and the trend is the inverse for ABCG2. It has been previously shown that ideal P-gp substrates, i.e. substrates with a certain amphiphilicity, exhibit a linear correlation between the logarithm of the rate of ATPase activity and substrate affinity (Äänismaa and Seelig, 2007). Indeed, the outliers from the linear correlation of P-gp-ATPase activity versus affinity in the present set of compounds are essentially due to the low amphiphilicity of these specific compounds painted in grey in Figure 48 (type III). A second trend is that each compound has more negative free energy for ABCG2 than for P-gp. Therefore, although the rate of transport for most compounds is lower in the case of ABCG2 than in the case of P-gp (lower V_1 values for ABCG2 compared to P-gp), the substrate affinity is higher for ABCG2 than for P-gp.

Again, complementary patterns are shown in the case of the compound affinity to the ABCG2 and P-gp transporters. Compounds with a high affinity from drug to P-gp occupy both binding sites and have a high propensity to enhance P-gp activity and thus P-gp-ATP hydrolysis (Li-Blatter et al., 2009). These compounds are called modulators (Seelig and Landwojtowicz, 2000; Seelig and Gatlik-Landwojtowicz, 2005).

We were also interested in testing whether ABCG2 binds its substrates in the lipid membrane as P-gp does (Seelig and Landwojtowicz, 2000; Sharom 2008). It was detected from Rosenberg et al. (2010) studies that the entry of the open nucleotide-free ABCG2 structure (Figure 9 B) is large enough (70 Å) to allow access of ABCG2 substrates from either the inner leaflet of the plasma membrane or cytoplasm, compare to that for P-gp (30 Å) (Aller et al., 2009). As already commented, we have seen that the surface activity for typical ABCG2 compounds is hardly measurable, yielding low air-water coefficients (K_{aw}) (Table 12) and high cross sectional areas (AD) (Data not shown). Consequently, lipid-water partition coefficients (K_{lw}) are small (Data not shown). On the other hand, compounds which are able to properly cross the lipid membrane with high air-water coefficients (K_{aw}) and lipid-water partition coefficients (K_{lw}), directly inhibit the ABCG2 transporter. As the lipid-water partition coefficient (K_{lw}) appears to take an unimportant role in ABCG2, it could apparently seem that ABCG2 might take compounds from the aqueous phase. Additionally, the low importance of amphiphilicity and hydrophobicity (prerequisite for binding to lipid membrane (Seelig and Landwojtowicz, 2000; Sharom, 2008)) for ABCG2 transport, may give an erroneous idea of a possible insignificant role of the lipid membrane in the process.

In an additional step, we tested with ATPase activity measurements in inside-out plasma membrane vesicles containing ABCG2 several detergents, sugars, acids and lipids (Figure 46 and Table

11). These compounds exhibit relevant hydrogen bond acceptor patterns and can or cannot partition into the lipid membrane. We found that only those compounds which can partition into the membrane also interacted with ABCG2. These outcomes prove that membrane partitioning is a prerequisite for a compound to interact with ABCG2; thus, this transporter cannot take compounds directly from the aqueous phase as it has been extensively thought (e.g. Sarkadi et al., 2006). As a result, the recent findings showing that mitoxantrone is expelled by ABCG2 directly from the plasma membrane (Homolya et al., 2011) were not fortuity. Partitioning into the lipid membrane seems to be the rate-limiting step for the interaction of a substrate with ABCG2 as it was demonstrated for P-gp (Seelig and Landwojtowicz, 2000; Aänismaa and Seelig, 2007). Matsson et al. (2007) already suggested that membrane partitioning was an important factor for drug interaction with ABCG2 as the two descriptors of their QSAR analysis are correlated to the passive membrane permeability: lipophilicity (octanol-water partition coefficient) and molecular polarizability. In conclusion, **ABCG2 and P-gp bind the substrates in the lipid membrane.**

Hence, **a "two-step binding" model is valid for both transporters**. The first step is the drug partitioning from water into the lipid bilayer, described by the lipid-water partition coefficient (K_{lw}); subsequent second step is the drug binding from the lipid phase to the transporter, described by the binding constant of drug to the transporter from the lipid phase (K_{tl}). This model was proposed initially for P-gp by Sauna and Ambudkar (2001) and suggested latter for ABCG2 by Matsson et al. (2007) (Figure 10).

From these data we also concluded that an analogous equation can be written for both transporters, the binding constant of the drug from the aqueous phase to the transporters (K_{tw}) is thus a product of the two binding constants, K_{lw} and K_{tl}. (Equation 13, Figure 16). Indeed, the free energy ($\Delta G°$) from the water to the transporter binding constants (K_{tw}) were calculated and plotted for both transporters in Figure 47.

Importantly, whereas **hydrophobic interactions seem to explain the higher affinity of substrates to ABCG2, this aspect is absent in P-gp.** Despite partitioning into the lipid membrane is essential for compounds to interact with ABCG2, lipid-water partition coefficient (K_{lw}), amphiphilicity and hydrophobicity (necessary for membrane partition) appeared to take not a very important role in ABCG2 (commented above). Whereby, the interaction between substrates and the ABCG2 transporter seems to exhibit a hydrophobic component in addition to the hydrogen bonding component which is different from P-gp. This hydrophobic contribution explains the higher affinity of substrates to ABCG2 in the lipid membrane. Indeed, it was suggested that ABCG2 binding sites are possibly hydrophobic (Coburger et al., 2010).

Another important feature to take in account from the ABCG2-ATPase activity measurements performed with the latter set of compounds is that detergents interact with ABCG2. Detergents are commonly used to solubilize ABCG2 from membranes, for instance 3-[(3-cholamidopropyl)

dimethylammonio]-1-propanesulfonate (CHAPS) (Pozza et al., 2006), foscholine derivatives (McDevitt et al., 2006), or maltoside derivates (Rosenberg et al., 2010). We have seen that all these three kinds of detergents interact inhibiting the ABCG2-ATPase activity (Figure 46 and Table 11). Therefore, when purified ABCG2 in detergent solution was found to be active in drug binding (McDevitt et al., 2006) or ATP hydrolysis (Pozza et al., 2006; Rosenberg et al., 2010), but with a relatively low basal activity, we could assert that the reason may be the inhibition of ABCG2 by the used detergents. This kind of detergents has been also shown to interact with P-gp (Li-Blatter et al., 2009); as a result, if the transporter has been solubilized with detergents, they may influence and interfere with transport results.

Although there is a considerable overlap between ABCG2 and P-gp substrates (Figures 43 to 45 revealed that out of the 27 compounds interacting with ABCG2, 20 interacted also with P-gp), the analysis revealed significant and characteristic differences. For instance, remember the complementary patterns of typical compounds for each transporter regarding charge, hydrophobicity, amphiphilicity and affinity. These facts suggest that **ABCG2 and P-gp have different substrate binding locations**.

Different studies suggested multiple binding sites in ABCG2 that may not or only partially overlap (Nakanishi et al., 2003; Xia at al., 2005), two or three distinct but symmetrical binding sites (Ejendal and Hrycyna, 2005; Clark et al., 2006), two single binging sites (Glavinas et al., 2007) or two binging sites for each substrate or inhibitor of ABCG2, one high and one low affinity sites (Pozza et al., 2006). Although the locations of these binding sites are not yet clear (Xia at al., 2005), it has been hypothesized that substrate-binding sites are likely located in the central cavity surrounded by TM α-helices (Rosenberg et al., 2010). In the case of P-gp, it has been suggested different but maybe overlapping drug-binding binding sites, possibly the major sites of drug interactions are located within P-gp TMDs in the middle of the lipid bilayer (Bruggemann et al., 1992; Greenberger, 1993; Demmer et al., 1999). However, the type and number of drug binding site(s) is still not clear (Sharom et al., 2005; Sauna and Ambudkar, 2007; Chen et al., 2012). Further investigations are needed to precisely localize the binding sites for each transporter.

Additionally, a second structural analysis was performed regarding the hydrogen acceptor groups (HAP) from the molecular structure. In a lipid environment, electrostatic and dipolar interactions (according to Coulomb's law) are enhanced due to the low dielectric constant; consequently, hydrogen-bond formation (dipole-dipole) for substrate recognition can take place (Seelig and Gatlik-Landwojtowicz, 2005).. The analysis of the hydrogen acceptor groups is displayed in Table 19. The following hydrogen acceptors have been taken into account: =O, -O-, and ternary nitrogen groups.

From this table it can be observed that, in general, typical ABCG2 compounds have between 4 and 6 hydrogen acceptors. The range of hydrogen acceptors is broad for typical P-gp compounds. As a conclusion, **hydrogen acceptors are important for both transporters and the substrate affinity to**

ABCG2 and P-gp seem to be due to hydrogen bonding interactions. As for both transporters substrate membrane partitioning is a prerequisite for interaction, substrate affinity to ABCG2 and P-gp seems to be essentially due to hydrogen bonding interactions. In fact, a correlation between drug affinity and the frequency of hydrogen bond acceptor patterns was presented for P-gp (Seelig, 1998; Gatlik-Landwojtowicz et al., 2006); a similar correlation has been suggested for ABCG2 (Matsson et al., 2007). The large number of hydrogen bond donor side chains in the intracellular loops and TMDs for P-gp and ABCG2 has been assumed to contribute to the overlapping substrate specificity of the two transporters (Doyle et al., 1998; Matsson et al., 2007). Remarkably, it was seen that H-donor affects positively to ABCG2 inhibition; in contrast, H-acceptor is beneficial for P-gp binding and inhibition (Bates et al., 2001; Pick et al., 2008; Liu et al., 2008). Note that hydrogen bonding is a common feature among ABCG2 SARs and QSARs models in literature (Gandhi and Morris, 2009).

Table 19. Number of hydrogen acceptors groups (HAP) and hydroxyl groups from the molecular structure of each drug from the set of 28 compounds.

Charge	Charge distrib.	N°	Compound	HA groups	Hydroxyl groups
O	I	1	cortisol	2	3
	I	2	dexamethasone	2	3
	I	3	progesterone	1	0
	I	4	testosterone	1	1
	II	5	Ko143	6	0
	III	6	digoxin	8	6
	III	7	estradiol	0	2
	III	8	etoposide	9	3
	III	9	forskolin	4	3
(+)	II	10	prazosin	8	0
	III	11	cimetidine	3	0
	III	12	famotidine	5	0
	III	13	nizatidine	2	0
	III	14	ranitidine	1	0
+	I	15	promazine	2	0
	I	16	tamoxifen	2	0
	II	17	verapamil	6	0
	III	18	daunorubicin	6	4
	III	19	mitoxantrone	2	4
-	II	20	glybenclamide	5	0
	III	21	CPT-cAMP	5	2
	III	22	methotrexate	7	2
	III	23	riboflavin	5	4
	III	24	sulfasalazine	6	1
+ / -	III	25	ciprofloxacin	4	1
	III	26	enrofloxacin	5	1
	III	27	norfloxacin	4	1
	III	28	pefloxacin	5	1

It is, therefore, essential to note that $\Delta G°_{tw}$ can be calculated for both transporters as the sum of $\Delta G°_{lw}$ and $\Delta G°_{tl}$ (Equation 13). Hence, both factors are important for ABCG2 but influence interactions disimilarly. For instance, compounds with high LogD values cause inhibition of ABCG2; however, if they present a high number of hydrogen bonds is positive for the interaction with the transporter. Note that $\Delta G°_{lw}$ is related to LogD and $\Delta G°_{tl}$ to hydrogen bonds.

Hydroxyl and nitrogen groups have been reported to be also important for ABCG2 drug-transporter recognition and interaction (Yoshikawa et al., 2004; Saito et al., 2006; Boumendjel et al., 2007; Matsson et al., 2007; Pick et al., 2008, Gandhi and Morris, 2009; Matsson et al., 2009). It could be possible that hydroxyl groups and primary and secondary nitrogens groups are also influencing the interaction of the compounds with ABCG2. However, in our set of data, althought compounds activating ABCG2 ATPase activity present always hydroxyl groups, also compounds interacting with P-gp can have these hydroxyl groups (for instance, digoxin and daunorubicin present a high number of them) (Table 19).

In summary, both ABC transporters, ABCG2 and P-gp, display complementary functions and patterns (Table 20). ABCG2 exhibited a lower basal and generally also a lower substrate-induced activity however a higher substrate-affinity than P-gp. Typical ABCG2 substrates, if transported by P-gp, they are also transported slowly. Despite the relatively slow rate of ATPase activity and transport, ABCG2 transport its substrates very efficiently. The rate of P-gp-ATPase activity and transport decreased with the affinity of the substrates to the transporter and is the opposite for ABCG2. The substrate affinity to ABCG2 as well as to P-gp seems to be essentially due to hydrogen bonding interactions. The higher affinity of substrates to ABCG2 in the lipid membrane seems to be due a hydrophobic contribution which is absent in P-gp. The two transporters seem to bind their substrates in the lipid membrane, thus, a two-step mechanism is valid for both. ABCG2 substrates are non-amphiphilic, hydrophilic and electrically zwitterionic or anionic, whereas typical compounds which interact with P-gp are amphiphilic, hydrophobic and electrically neutral or cationic. Although there is considerable overlap between ABCG2 and P-gp substrates, respectively, the analysis revealed significant and characteristic differences. Both transporters seem to have the same recognition elements except for charge and hydrophobic interactions.

Table 20. Summary of conclusions of typical characteristics for the ABCG2 and P-gp transporters.

Characteristics	ABCG2	P-gp
Basal and induced activity	lower	higher
Affinity	higher	lower
H - bond interactions	yes	yes
Hydrophobic interactions	yes	no
Membrane mediated binding (2steps)	yes	yes
Typical interacting compounds	non-amphiphilic, zwitterionic or anionic	amphiphilic, neutral or cationic

To our knowledge, no direct molecular model has been reported so far for ABCG2. Remember that all current QSAR models were developed through indirect modeling based on chemical structures of inhibitors. In this studio a direct molecular structural analysis has been performed based on experimental data which has allowed explaining and predicting the interaction of compounds as substrates and/or inhibitors with the ABCG2 and P-gp transporters.

2. ABCG2 and P-glycoprotein interaction with steroid hormones – Correlation of ATPase activity and transport

As it was described elsewhere, the rate of ATP hydrolysis by P-gp correlates linearly with the rate of effective transport (Ambudkar et al., 1997; Omote and Al-Shawi, 2002). Thereby, it is important to note that transport measured in transport assays with confluent cell monolayers does not reveal effective transport, but apparent or net transport that is the sum of effective transport and passive influx of substrates (Seelig and Gatlik-Landwojtowicz, 2000; Seelig, 2007).

The second aim of the present analysis was to test the correlation between ATPase and the rate of substrate transport in transepithelial transport and accumulation assays by taking into account also that most drugs can cross the bilayer membrane by passive diffusion (Seelig, 2007). For this purpose we used six steroid hormones which have two principal advantages, first they have been extensively tested in *in vitro* assays (Table 6), second most of them have neutral charge which allows ignoring charge effects. We analyzed the hormone ABCG2- and P-gp- ATPase activity and passive fluxes across the lipid membrane were determined by SAM. The results were then compared with published data from bi-directional transport and accumulation experiments of steroid hormones with the two ABC transporters.

Figure 49 shows the ATPase activity of ABCG2 and P-gp as a function of the steroid hormone concentration. The P-gp-ATPase activity curves obtained for cortisol, dexamethasone, tamoxifen and testosterone showed only the rising branch due to the fact that solubility limit was reached close to the maximum of ATPase activity. Only the P-gp-ATPase activity of progesterone displayed almost a full bell-shaped curve. Although neutral, estradiol is not interacting with P-gp due to the lack of hydrogen bond acceptors patterns (Seelig, 1998). It should be noted that, despite the mentioned compounds enclose charges (neutral for all except tamoxifen that is cationic) which are appropriate to interact with P-gp (Schinkel et al., 1996; Sharom, 2008), they are not typically amphiphilic, a second requisite needed to be taken by the P-gp transporter. For instance, the surface activity slope of cortisol was not possible to measured up to the CMC, finishing at a low surface pressure (Figure 51). Dexamethasone and tamoxifen displayed a sigmoid surface active curve. The progesterone and testosterone surface pressure curves were completed but ending in a relatively low maximum of pressure (Figure 51). In addition, the measurement of Gibbs adsorption isotherm in surface activity could not be determined for this compound.

Concerning ABCG2, as expected from the lack of charge of these steroids (see above), the rates of ATPase activity barely increase above basal values but rather decrease to lower values with concentration for the six hormones under the present conditions.

The ATPase activity assays already published for the six steroid hormones studied were also reviewed. It is summarized in Table 21, where the cell type, the concentration applied and obtained results are displayed. Basically, in almost every results of ABCG2- and P-gp-ATPase activity published, full curves of activation and inhibition were achieved (Table 21).

Table 21. Summary of ATPase activity assays published for steroid hormones with the ABCG2 and P-gp transporters. The cell line used, concentrations and results (A: activation, I: inhibition) with each transporter are listed.

Transporter	Compound	Cell type	Conc. [μM]	Result	Reference
ABCG2	**Estradiol**	*L. lactis*	0-100	A, I	Janvilisri et al., 2003
	Progesterone	*L. lactis*	0-100	A, I	Janvilisri et al., 2003
	Tamoxifen	*L. lactis*	0-1000	A, I	Janvilisri et al., 2003
	Testosterone	*L. lactis*	0-100	A, I	Janvilisri et al., 2003
		Sf9 and ABCG2-M-ATPase	100	I	Glavinas et al., 2007
P-gp	**Cortisol**	Sf9	1-1000	A, I	Rao et al., 1994
		DC-3F	0.1-1000	A	Orlowski et al., 1996
	Estradiol	Sf9	1-1000	A, I	Rao et al., 1994
	Progesterone	Sf9	1-1000	A, I	Rao et al., 1994
		Sf9	0.1-100	A	Kim and Benet., 2004
		DC-3F	0.4-350	A, I	Orlowski et al., 1996
		CHO (CR1R12)	0.1-400	A, I	Litman et al., 1997
	Tamoxifen	Sf9	1-40	A, I	Rao et al., 1994
		CHO (CR1R12)	0.1-400	A, I	Litman et al., 1997

Considering P-gp, published P-gp-ATPase activity results are consistent with our results with cortisol (Orlowski et al., 1996) and progesterone (Rao et al., 1994; Orlowski et al., 1996; Litman et al., 1997; Kim and Benet., 2004) (Table 21). Two of the results which are not in agreement with ours are either because published data are activation and inhibition profiles for cortisol and we only achieved activation, or because they can find P-gp-ATPase activity with estradiol and we did not (Figure 50 and Table 21) (Rao et al., 1994). These experiments were performed with Sf9 insect cells. As it has been reported, the cited differences may be due to the high different lipid composition between cell types (In 't Veld et al., 1991). Sf9 are insect cells, animal that phylogenetically is far from mammalian animals. It should be also noted that these authors used vesicle membranes at high protein concentration (2-4 mg/ml), and remember that the amount of protein that we use in the P-gp-ATPase activity

measurements is 0.1 mg/ml. It has been shown that the higher concentration of protein membrane in ATPase activity assays, the easier is to obtain ATPase activation (Beck et al., 2013).

In the case of tamoxifen, published results from literature (Rao et al.,1994; Litman et al., 1997) show activation and inhibition P-gp-ATPase activity; however, the used concentrations were higher than the ones we used. The reason why we did not use higher concentrations than 10 µM in tamoxifen P-gp-ATPase activity assays was due to the problems we found in the vanadate curves from that concentration, probably resembling aggregation problems.

Concerning ABCG2, the experiment performed with the same membranes that we used in the present memory with progesterone got similar results (Glavinas et al., 2007). The other publication available in literature with ABCG2-ATPase activity assays displayed activation and inhibition curves for estradiol, progesterone, tamoxifen and testosterone and we obtained only inhibition curves (Janvilisri et al., 2003) (Table 21 and Figure 50). However, these authors used vesicle membranes obtained from *L. lactis* cells at high protein concentration (~1 mg/ml), which is favorable to get ATPase activation (Beck et al., 2013). Remember that the amount of protein that we use in the ABCG2-ATPase activity measurements is 0.075 mg/ml.

It is clear from the plots in Figures 50 and 51 that there is a correlation between the SAM and the ATPase activity results, in both cases the curves ended where problems of precipitation of the compound or the CMC were achieved. Moreover, as it was reported by Aanismaa and Seelig, 2007, ATPase activity requires micromolar concentrations for these hydrophobic drugs.

Despite the similar structure of these steroid hormones, small differences make them behave differently. Cortisol and dexamethasone are the compounds with the lower K_{aw} (2.08×10^3 and 5.56×10^3, respectively) and XLogP values (1.6 and 1.9, respectively) (Table 16). They are also the two compounds with the highest number of hetero-atoms (5 oxygen and nitrogen atoms; dexamethasone has also a fluorine atom) (Figure 20). All these features considered together imply that these compounds are the ones crossing the membrane with more difficulty. On the other hand, tamoxifen is the compound with the highest K_{aw} (1.31×10^6) and XLogP (7.1) values (Table 16), with two hetero-atoms (Figure 20); thus the one which crosses the membrane more rapidly. Progesterone and testosterone are in the middle, with K_{aw} (1.46×10^5 and 1.03×10^5, respectively) and XLogP values (3.9 and 3.3, respectively) (Table 16), and enclosing two oxygen atoms. From estradiol, although not possible to measure in SAM experiments, we can say that its XLogP value is similar to progesterone; therefore, its hydrophobicity is located also in the middle of the ranking for these six steroids.

Predictions of passive influx for cortisol, dexamethasone, progesterone and testosterone were calculated from surface activity measurements and represented in Figure 52. As expected, for the less hydrophobic hormones, cortisol and dexamethasone, if applied at concentrations lower than the range of mM, the passive flux is lower than the active flux (ATPase activity) (Figure 52), as they cross the membrane slowly and the ABC transporter can cope with the molecules located at the membrane. On

the other hand, if applied at higher concentrations, the passive flux starts to be higher than active efflux. In contrast, for the more hydrophobic steroids, progesterone and testosterone, the passive flux is higher than the active flux at almost any concentration (Figure 52).

In a further step we compared the results obtained from ATPase activity measurements with several *in vitro* transport and accumulation experiments previously published (Table 6 and Figure 50). A schematic representation comparing our ATPase activity data with published transport and accumulation assays is displayed in Figure 64. When the percentage of inhibition was published (Pavek et al., 2005; Matsson et al., 2007; Matsson et al., 2009) or possible to be calculated (Imai et al., 2003; Pavek et al., 2005), a compound with less than 10% of inhibition was considered a non-inhibitor and with more than 10% an inhibitor. For inhibition data from van Kalken et al. (1993), Elahian et al. (2010) and Sugimoto et al. (2003) no percentage of inhibition was possible to calculate. A detailed look to the published results compared with the ATPase activity results displayed consistent correlations taking into account the meaning of net transport *vs* active transport.

It should be noted that available data on transporter interaction with drugs have to be considered carefully. The information collected with different assays may suggest opposite or diverse results; nonetheless, this is mainly due to the differences between intrinsic and apparent substrate (see below), the presence of two binding regions leading to inhibition at high substrate concentration, but also due to differences in the lipid composition and the lateral packing density of membranes from the different cell lines used in these assays (Seelig and Gerebtzoff, 2006).

Substrates usually cross membranes at a low rate; after they have been effluxed by the transporter they will rapidly diffuse into membrane again and interact with the transporter once more; however the transporter will be able to maintain a substrate concentration gradient (Seelig and Gatlik-Landwojtowicz, 2005; Sharom, 2008). Hence, the export rate of drug is faster than the rate of passive diffusion into the cell (influx) and the drug will barely reach the cytosol (Figure 18 A).

The difference between intrinsic substrates and apparent substrates should also be emphasized. Intrinsic substrates are compounds recognized by ABC transporters, thus leading to an increase in the basal ATP hydrolysis activity of the transporter. Intrinsic substrates have a small cross-sectional area and/or charge and thus diffuse too fast to be effectively accumulated in the apical side (donor compartment), leading thus to a ratio B-A /A-B around 1 in transcellular transport experiments (Seelig and Gerebtzoff, 2006). Therefore, despite being substrates they are not visible in cell transport assays. Apparent substrates are intrinsic substrates large or charged enough to diffuse slowly through the cell membrane so that the transporter will be able to efficiently efflux them out of the cell (Fischer et al., 1998; Seelig and Gatlik-Landwojtowicz, 2005). They give a value higher than 2 in the B-A /A-B ratio in transcellular transport assays (Schwab et al., 2003) and net transport is shown.

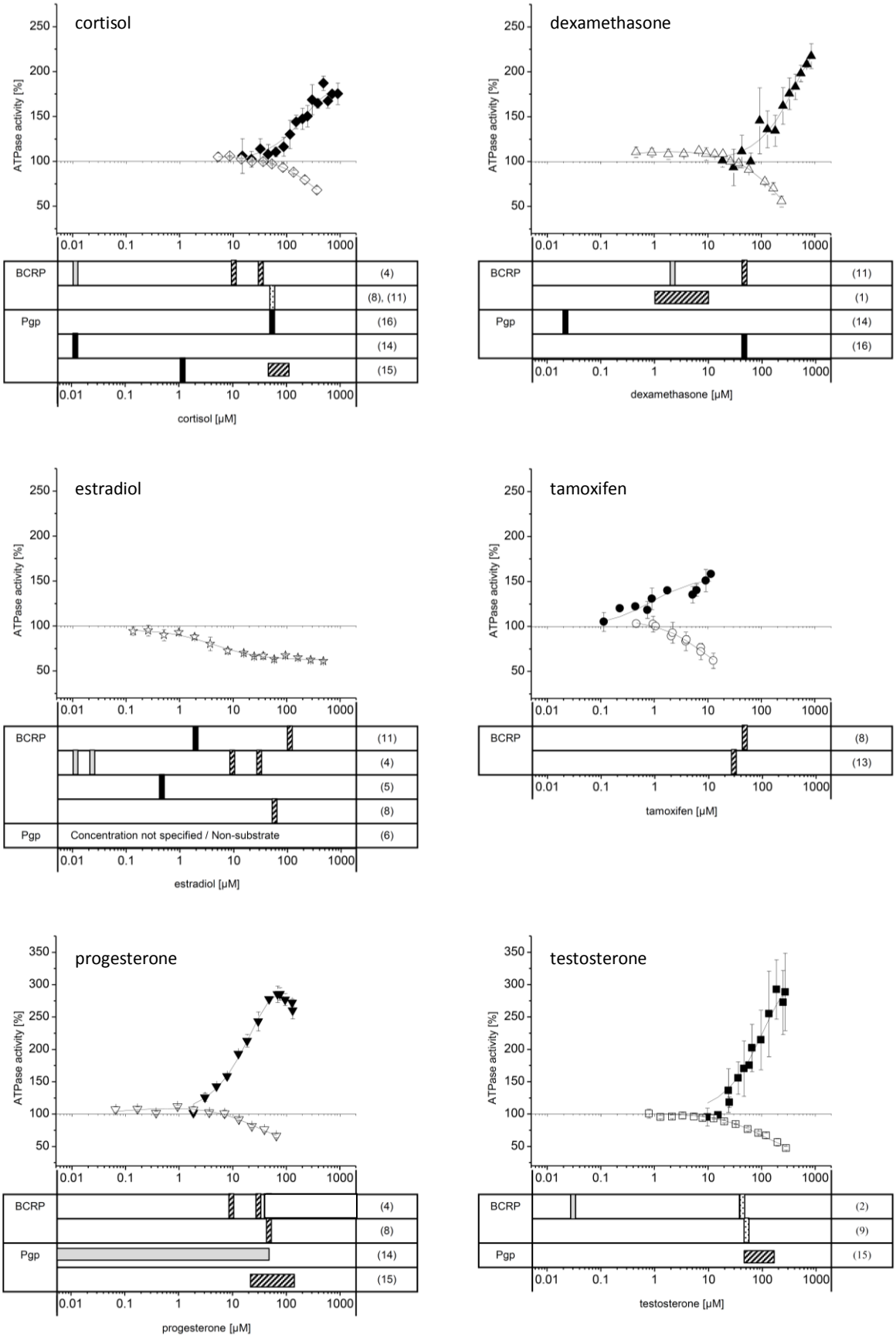

Figure 64. (Legend in next page)

Figure 64. Correlation of the ATPase activity with transport and accumulation published results for ABCG2 and P-gp with steroid hormones. Single concentrations are represented as vertical lines, range of concentrations are represented as horizontal lines. Pattern for the achieved interactions with the transporter: substrate (black filled symbols); non-substrate (grey filled symbols); inhibitor (dashed symbols); non-inhibitor (dotted symbols). When a percentage of inhibition was deduced, less than 10% is represented as non-inhibitor and more than 10% as inhibitor. ATPase activity plots: ABCG2 (open symbols) and P-gp (filled symbols). Numbers in the right column of the tables indicate reference order. References: Elihan et al., 2010 (1); Gardner et al., 2008 (2); Glavinas et al., 2007 (3); Imai et al., 2003 (4); Janvilisri et al., 2003 (5); Kim and Benet, 2004 (6); Litman et al., 1997 (7); Matsson et al., 2007 (8); Matsson et al., 2009 (9); Orlowski et al., 1996 (10); Pavek et al., 2005 (11); Rao et al., 1994 (12); Sugimoto et al., 2003 (13); Ueda et al., 1992 (14); van Kalken et al., 1993 (15); Yates et al., 2003 (16). For further details see Table 6.

From present analysis, we could conclude that cortisol and dexamethasone are apparent substrates and progesterone and testosterone are intrinsic substrates for ABC transporters. It fact, as it is visible in Figure 64 and Table 6, this report is true concerning the interaction of these hormones with the ABCG2 and P-gp transporters, although there is not much research published with the ABCG2 concerning transport assays to elucidate these compounds as substrates. In three publications where transepithelial transport assays were performed with cortisol, at 0.01, 1 and 50 µM, respectively (Ueda et al., 1992; van Kalken et al., 1993; Yates et al., 2003) and in three publications done with dexamethasone, at 0.02, 2 and 50 µM, respectively (Ueda et al., 1992; Schinkel et al., 1995; Yates et al., 2003) net transport was reported. Note that these two steroid hormones are thus apparent substrates at the broad range of concentrations studied, i.e. from nm to µM. Remember that this is consistent with what we have learnt from Figure 52, if cortisol and dexamethasone are applied at concentrations lower than the range of mM in transepithelial transport assays, the net transport can be visible in these experiments due to active efflux is higher than passive flux. On the other hand, if they would be applied at higher concentrations, where passive flux starts to be higher than active efflux, the net transport might be not visible.

Conversely, progesterone is an intrinsic substrate as, despite it displays activation in P-gp-ATPase activity profiles (Figure 50), no interaction has been found at any concentration in cellular transport assays; for instance from nm up to 50 µM of progesterone (Ueda et al., 1992; Ushigome et al., 2000) (Figure 64 and Table 6). This is again consistent with our findings from Figure 51, where we could predict that the net transport (see below) may be negligible at concentrations higher than ~ 0,1 µM. We could not find any reference with testosterone tried as a substrate in transcellular transport assays (Figure 64 and Table 6). As we have said, tamoxifen is the hormone with the highest K_{aw} and XLogP values, even more hydrophobic than progesterone and testosterone, hence also an intrinsic substrate; in fact, it has been described not to be a substrate of P-gp in accumulation assays (Callagan and Higgis, 1995) (Table 6). Estradiol, although at a concentration not specified, it was seen as not a substrate of P-gp (Kim and Benet, 2004); this is consistent with our results where no P-gp-ATPase activity was found.

Cortisol and dexamethasone with P-gp showed apparent transport that is already visible at very low concentrations (nM range) of the compound, where the transporter still works at basal values (Figure 64). This is also why steroids that barely enhance but rather reduced the ABCG2-ATPase activity assays can be observed as substrates in transepithelial transport assays at concentrations where the transporter is working at basal activity. For that reason, estradiol was found to be ABCG2 substrate at 0.5 and 2 μM concentrations (Janvilisri et al., 2003; Pavek et al., 2005); however, not at lower concentrations, 0.01 and 0.03 μM (Imai et al., 2003) (Figure 64). A remarkable aspect is that in the case of Pavek et al. (2005), they state that estradiol is hardly, if at all, transported by ABCG2 at a concentration (2 μM) where there is already inhibition in ATPase activity; note that in the case of inhibitors, despite the ABC transporter is working at high rate there is no net transport (Seelig, 2007). In the cases where the compound was established as no substrate it could be either due to at very low concentrations there may not be enough drug in the membrane to make a visible effect, or might be due to the loss of compound applied; note that some compounds have tendency to stick to membranes and plastic surface (Yahya et al., 1988). The same phenomenon might happen for instance for cortisol applied at 0.01 μM (Imai et al., 2003), dexamethasone used at 2 μM (Pavek et al., 2005) and testosterone at 0.03 μM (Gardner et al., 2008), as these compounds were reported not to be ABCG2 substrates at the mentioned concentrations (Figure 64).

If the steroid hormones are applied at high concentrations they **inhibit** the transporter and at the same time they diffuse rapidly. Passive influx is distinctly faster than active efflux and the drug will reach the cytosol even if it is a substrate for an efflux transporter (Figure 18 B). Thus, the protein is kept in a useless cycle of transport, but cannot either generate an inhibitor gradient or transport other substrates. Therefore, although inhibitors hamper transport of other drugs, it is difficult to measure the rate at which they are themselves transported (Seelig, 2007). Remember that usually, compounds can act as substrates or inhibitors of ABCG2 and P-gp depending on the concentration, at low concentrations they are substrates and at higher inhibitors (Seelig and Landwojtowicz, 2000). For instance, estradiol could be shown as an ABCG2 substrate at concentrations of 0.5 and 2 μM (Janvilisri et al., 2003; Pavek et al., 2005) and as ABCG2 inhibitor at higher concentrations, i.e. from 10 to 100 μM (Figure 64 and Table 6) (Imai et al., 2002; 2003; Pavek et al., 2005; Matsson et al., 2007; Robey et al., 2003).

Note that inhibition can be directly predicted from ATPase activity, for instance the previous example of estradiol for ABCG2. Estradiol is found to be an inhibitor when the ATPase profile is decreasing at lower levels than basal ABCG2-ATPase activity (Figure 64). Another example is tamoxifen applied at 30 and 50 μM, interacting with ABCG2 (Sugimoto et al., 2003; Matsson et al., 2007); and progesterone interacting with ABCG2 at concentrations from 10 to 50 μM (Imai et al., 2003; Matsson et al., 2007).

In some cases, results differ between authors and/or different experiments from the same authors. Pavek et al. (2005) using dexamethasone at 50 μM in flow cytometry with mitoxantrone at 10

μM achieved 13% inhibition of ABCG2, and approximately 50% at the same concentration using the compound to inhibit transepithelial transport of PhiP in cells; this is because 50 μM is in the border-line of inhibition, these authors could see sometimes more inhibition (transport assay) than others (flow cytometry) (Table 6). On the other hand, Elahian et al. (2010), using also mitoxantrone at 10 μM as substrate in flow cytometry, reported to inhibit ABCG2 with dexamethasone already from 1 μM. Inhibition maybe also vary depending on the applied substrate.

It is important to know that there is inhibition, thus the transport rate is reduced, when both binding sites of the transporter are occupied. Most of the experiments performed to elucidate if a compound is an inhibitor of ABCG2 or P-gp, either with transport or accumulation assay employ a typical substrate of the transporter and the compound to be tested as inhibitor, e.g. all these types of experiments from Table 6. As both drugs applied can occupy the binding sites, if applied together, they will contribute in synergy to the inhibition of the transporter. In consequence, the inhibition of the transporter will depend on the concentration of all compounds included in the experiment. Therefore, if one of the two drugs is applied at a concentration close to V_{max} in ATPase activity assays, inhibition can occur even if the concentration of the second drug is not yet inhibitory. This could be the case of Elahian et al. (2010), as using mitoxantrone as substrate in flow cytometry, reported to inhibit ABCG2 with dexamethasone already from 1 μM, where the ABCG2-ATPase activity is at basal levels (Figure 64). Other example is the case of van Kalken et al. (1993) and Yang et al. (1989); these authors could see inhibition of P-gp with progesterone and testosterone at a concentrations of hormones (50 to 150 μM) where the curve of P-gp-ATPase is in the activation phase but close to V_{max} due to the additional concentrations of daunorubicin (Figure 64 and Table 6). They also found inhibition of P-gp with cortisol but at concentrations of steroid that correspond to the beginning of the curve of ATPase activity.

Testosterone was found to inhibit the ABCG2 transporter only at a percentage of around 5% at hormone concentrations of 40 and 50 μM (Gardner et al., 2008; Matsson et al., 2009); concentrations where the curve of ABCG2-ATPase activity is starting to decrease. The results are reasonable as the other compound added in the inhibition assay was applied at very low concentration, i.e. IAAP at 3-5 nM or mitoxantrone at 1 μM, respectively (Figure 64 and Table 6).

The apparently puzzling results of ABCG2 inhibition with cortisol where Pavek et al. (2005) and Matsson et al. (2007), both at 50 μM, could not see inhibition but Imai et al. (2003) at lower concentrations (10 and 30 μM) could, can be well understood by means of the material used in each experiment. In experiments performed with vesicles (Imai et al., 2003), drug can directly access the binding site from the aqueous phase, thus, less concentration is necessary to inhibit the transporter. In contrast, in assays with cells (Matsson et al., 2007; Pavek et al., 2005), higher concentrations are required to inhibit the transporter as the drug has to diffuse across the lipid bilayer to access the binding site (Nervi et al., 2010) (Figures 18 and 64, and Table 6).

In summary, if the transporter (ABCG2 or P-gp) can cope with passive drug influx as in the case of cortisol and dexamethasone, the ATPase activity profile can be directly interpreted in terms of substrate on the rising side of the curve and in terms of inhibitor on the declining side of the curve. If passive influx is higher than active efflux the compounds are no longer substrates but they still act as inhibitors as shown for progesterone and testosterone.

In conclusion, we have demonstrated that the rate of ATP hydrolysis and the rate of transport unambiguously correlate by taking into account the passive flux across the bilayer membrane. We have verified that steroid substrates for ABCG2 and P-gp can be reliably predicted at any concentration by combining results from ATPase activity assays with results from surface activity measurements. Inhibitors of ABCG2 and P-gp can be derived directly from ATPase assays. This approach is less labor-intensive than other *in vitro* experiments as transport assays and also reveal under which conditions a compound acts as a substrate and/or an inhibitor of ABCG2 and P-gp. In addition, it yields detailed insight into the transporter function. A summary of the conclusions is displayed in Figure 65.

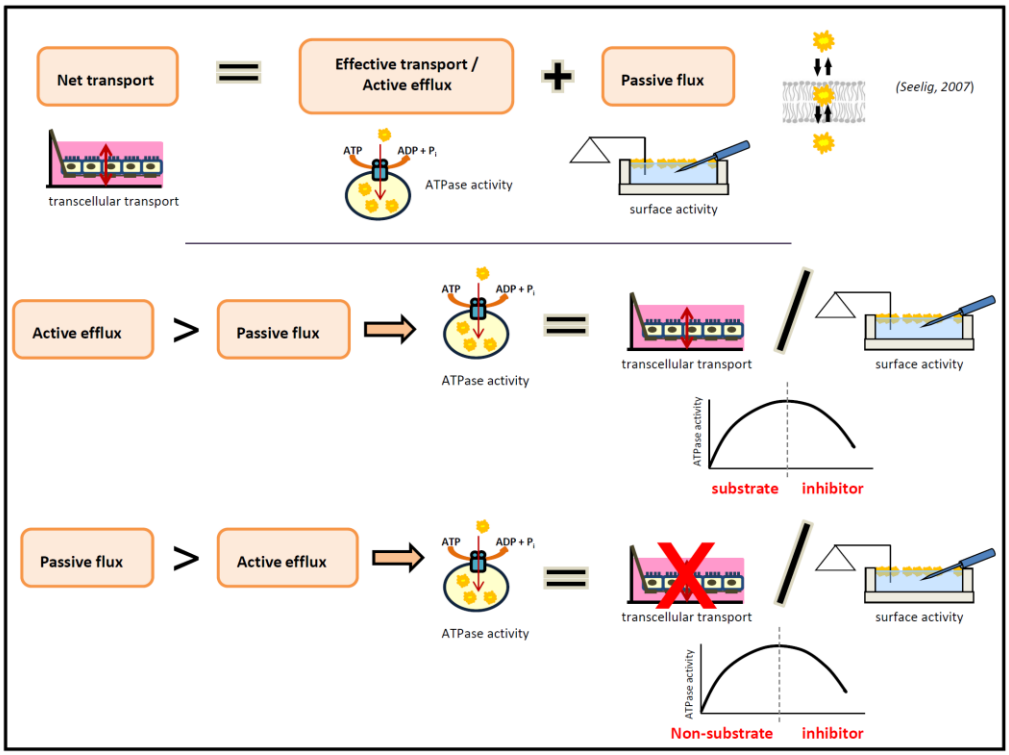

Figure 65. Schematic summary of conclusions obtained from the correlation of ATPase activity with other *in vitro* (transport and accumulation assays) results taking into account passive flux, regarding the interaction with the ABCG2 and P-gp transporters with steroid hormones.

3. ABCG2 and P-glycoprotein interaction with fluoroquinolones: ATPase activity correlation with other *in vitro* and *in vivo* experiments using these antibiotics

In the third aim of the present study we have characterized the interaction of a group of fluoroquinolones with ABCG2 performing different assays (transepithelial transport, MXR accumulation and *in vivo* experiments with wild-type and Abcg2-knockout mice) to correlate these assays with the outcome of ATPase activity; the P-gp transporter was included too.

A summary of the experiments from this study and their respective results with the five fluoroquinolones used in ATPase activity assays interacting with ABCG2 is displayed in Table 22; previously published data were also included.

Table 22. Summary of assays from the present and previously published articles to study the interaction of fluoroquinolones with murine Abcg2 and human ABCG2.

Drug[a]	*in vitro*						*in vivo*		XLogP[d]
	Transepithelial transport (MDCK-II)[b]		MXR accumulation (MDCK-II)[b]		ATPase activity (ABCG2-M-ATPase membrane vesicles)[c]		Pharmacokinetics (Abcg2$^{-/-}$ and wild-type mice)		
	Conc [μM]	outcome[e]	Conc [μM]	outcome[e]	Conc [μM]	outcome[e]	Conc [μM]	outcome[e]	
CIP	10	S (1)	100	no I (1)	~20-700	A	33	S (1)	- 1.10
ENR	10	S (2)	200	no I[f] (2)	~1-600	A	7	S[g] (2)	- 0.20
MXF	10	no S	50 - 500	no I	~2-600	I above 500 μM	-	-	0.60
NOR	10	S (1)	200	no I (1)	~20-1000	A	31	S	- 1.00
PEF	10	S	50 & 250	no I	~8-1000	A & I above 500 μM	21.5	no S	0.30

[a] CIP: ciprofloxacin, ENR: enrofloxacin, MXF: moxifloxacin, NOR: norfloxacin, PEF: pefloxacin. [b] Cells transduced with murine Abcg2 and human ABCG2. [c] Vesicles from cells containing human ABCG2. [d] XLogP values are from Pubmed (www.ncbi.nlm.nih.gov/pccompound). [e] A: activation, I: inhibition, S: substrate. Literature references in brackets. [f] Enrofloxacin was found to inhibit human ABCG2 but not murine Abcg2. [g] *In vivo* experiments with enrofloxacin were done with sheep in presence of ABCG2 inhibitors instead of mice. References: Merino et al., 2006 (1); Pulido et al., 2006 (2).

Figure 66 shows the correlation of the ATPase activity of ABCG2 and P-gp with other assays from our study and other previously published articles for the fluoroquinolones included in our study.

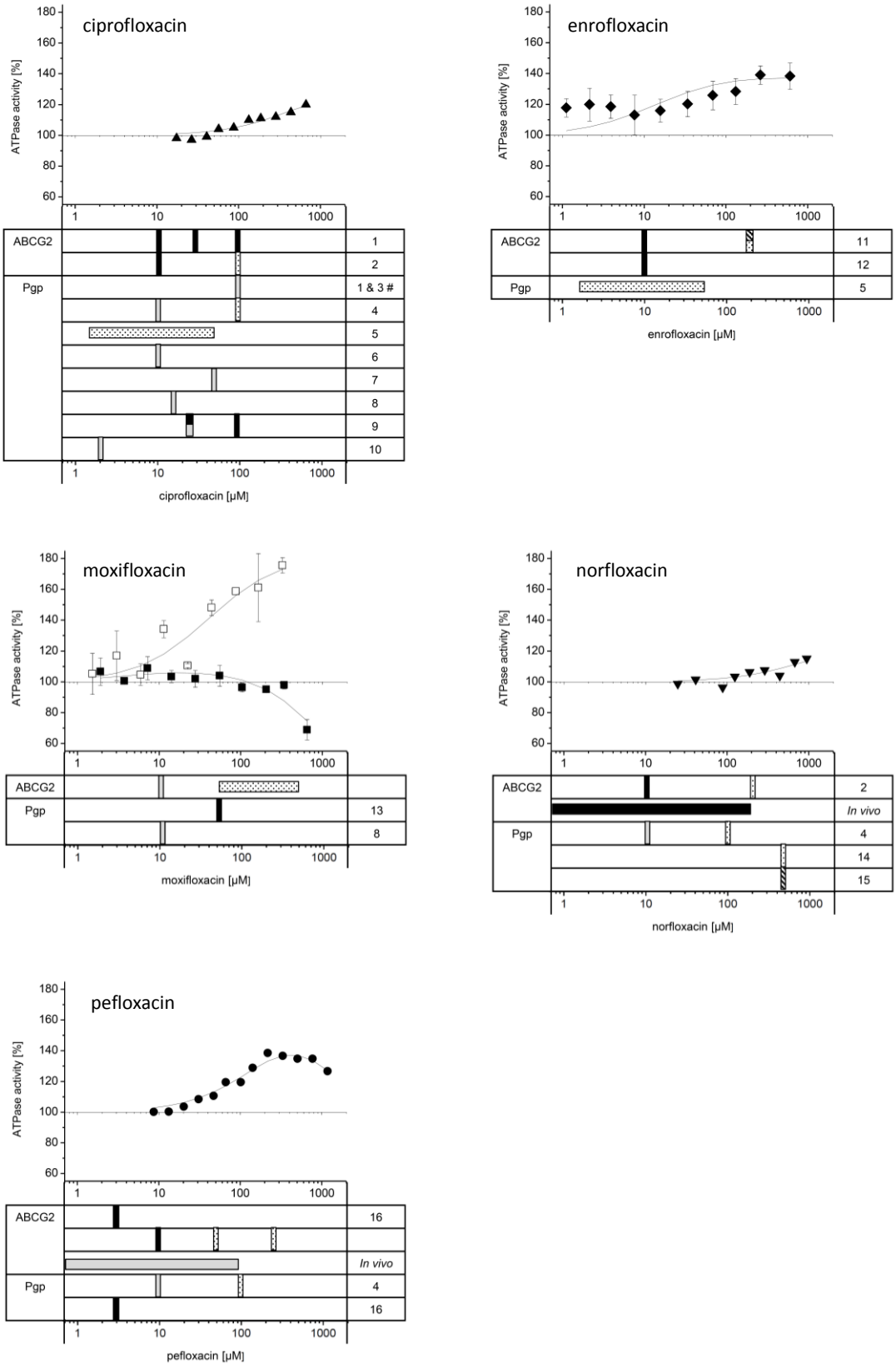

Figure 66. (Legend in next page)

Figure 66. Correlation of the ATPase activity with the *in vitro* and *ex vivo* published results for ABCG2 and P-gp with fluoroquinolones; results from current study are also included. Single concentrations are represented as vertical lines, range of concentrations are represented as horizontal lines. Pattern for the achieved interactions with the transporter: substrate (black filled symbols); non-substrate (grey filled symbols); inhibitor (dashed symbols); non-inhibitor (dotted symbols). When a percentage of inhibition was deduced, less than 10% is represented as non-inhibitor and more than 10% as inhibitor. ATPase activity plots: ABCG2 (filled symbols) and P-gp (open symbols). # Cavet et al., 1997; ciprofloxacin at 3 mM (concentration out of the plot), no inhibitor. Numbers in the right column of the tables indicate reference order; no numbered gaps are results from current study. References: Haslam et al., 2011 (1); Merino et al., 2006 (2); Cavet et al., 1997 (3); de Lange et al., 2000 (4); Haritova et al., 2007 (5); Lowes and Simmons, 2002 (6); Michot et al., 2004 (7); Michot et al., 2005 (8); Park et al., 2011 (9); Yamaguchi et al., 2004 (10); Pulido et al., 2006 (11); Real et al., 2011 (12); Brillault et al., 2009 (13); Sikri et al., 2004 (14); Zhao et al., 2002 (15); Kodaira et al., 2011 (16). For further details see Table 7.

Figure 66 includes, apart from the results obtained in our study, the *in vitro* transport and accumulation assays and *ex vivo* published results displayed in Table 7 where the drug concentration and the transporter-drug interaction were clearly specified. *In vivo* results were not included because the real effective concentration of drug in each tissue or fluid was not always possible to determine from the experiments published in literature.

A detailed look to the published results together with our results and compared with the ATPase activity results (Figure 66 and Table 7), displayed consistent correlations. Except for moxifloxacin, all fluoroquinolones were shown to be substrates but not inhibitors of ABCG2 in each experiment which corresponds with the activation curves of ATPase activity. Moreover, with few exceptions, they do not interact with P-gp. In comparison, these drugs exhibited ABCG2 activation ATPase profiles but no ATPase activity curve for P-gp was obtained (Figure 53). These correlations are discussed in detail below.

Regarding *in vitro* assays with ABCG2, as seen in Table 22, the calculated octanol-water partition coefficients of these fluoroquinolones (XLogP < 1) are small or even negative, which means that the compounds are very hydrophilic; as a consequence, the permeability coefficients are also small (Seelig, 2007). Passive influx is negligibly small for ciprofloxacin, enrofloxacin, norfloxacin and pefloxacin (Figure 47 and Table 12); thus, the ATPase activity profiles correlate directly with the active efflux and bi-directional transport assays (see Table 22). In fact, ABCG2 net transport is already visible at 10 µM, drug concentration where the ATPase activity is at basal rate for all these fluoroquinolones (Figure 53). For the most hydrophobic compound, moxifloxacin (highest XLogP, see Table 22), passive influx can however no longer be ignored. Therefore, the negligibly net transport of moxifloxacin at 10 μM (Figure 54, 66), where the ATPase activity is at basal rate (Figure 53), is explained by passive influx is distinctly faster than the active efflux by the transporter (Seelig and Gatlik-Landwojtowicz, 2005; Seelig, 2007). As expected, the trial performed administering moxifloxacin via oral yielded no differences between Abcg2$^{-/-}$ and wild-type male mice. Since this drug interacts with P-gp (Brillault et al., 2009) and MDCK-II cells

contain endogenous canine P-gp (Goh et al., 2002), this fact could explain the remaining scant but still significant transport differences in parental and transduced cells with the ABCG2 inhibitor Ko143 (Figure 54). Precisely because of these endogenous transporters, additional corroboration with specific inhibitors in transport assays is recommended (Giacomini et al., 2010).

Results from MXR accumulation assays are also in perfect agreement with the results from ATPase activity assays at the concentrations tested as shown in the following. From the analysis of these compounds as ABCG2 inhibitors, considering moxifloxacin, the inhibition in ATPase activity starts around 500 μM in membrane vesicles (Figure 53), but when the inhibitory effect was tested using MXR accumulation assays up to 500 μM of antibiotic, no inhibition was found (Figure 56). We have demonstrated that in living cells, ATPase activity curves of slowly diffusing compounds are shifted to lower concentrations compared to ATPase activity curves in inside-out membrane vesicles (Nervi et al., 2010). Thus, a higher concentration of moxifloxacin would be needed to achieve inhibition of ABCG2 in cell-based assays; however, since moxifloxacin at 500 μM is already half of the lethal single oral dose for mice and only ~6 times lower than the lethal one for monkeys (von Keutz and Schluter, 1999), higher concentrations were neither used in accumulation assays nor tried in *in vivo* experiments. On the other hand, in the case of ciprofloxacin (Merino et al., 2006; Haslam et al., 2011), enrofloxacin (Pulido et al., 2006; Real et al., 2011), norfloxacin (Merino et al., 2006) and pefloxacin (Figure 56), they were not found to inhibit ABCG2 in accumulation assays at concentrations around 100-250 μM (Table 22). In fact, it is difficult to inhibit ABCG2 ATPase activity with these antibiotics because the inhibitory part of the ATPase curve (Figure 53) cannot be achieved due to problems of solubility caused by their zwitterionic character.

Our data show that pefloxacin is an *in vitro* substrate of Abcg2/ABCG2 (Figure 55); furthermore, previously published results reported that its metabolite norfloxacin is also an *in vitro* Abcg2/ABCG2 substrate (Merino et al., 2006). In addition, both fluoroquinolones show an activation of the ABCG2-ATPase activity (Figure 53). Based on these facts and in order to determine a correlation between *in vitro* and *in vivo* results, experiments with Abcg2$^{-/-}$ and wild-type mice using pefloxacin and norfloxacin were performed at 10 mg/kg, usual diary dose for humans. Pefloxacin metabolism is produced mainly in the liver, given several metabolites, including norfloxacin. It has been reported that norfloxacin could be detected in bile and urine in several species administered with pefloxacin, but not in mice urine (Montay et al., 1985). We therefore, measured also norfloxacin in mice administered with pefloxacin.

In the case of norfloxacin administration, differences in drug levels between Abcg2$^{-/-}$ and wild-type were observed for all the tissues analyzed including plasma and bile (Figures 57 and 58, Table 18) indicating that Abcg2 is involved in the systemic exposure of this drug and plays a major role in the hepatobiliary and probably direct transport into the intestinal lumen. Intestinal active secretion of this antibiotic was already suggested (Griffiths et al., 1994), although the transporter involved was not identified. Furthermore, in our *in vivo* pefloxacin experiments, norfloxacin was detected in tissues with a

high accumulation of pefloxacin (i.e. intestine and bile) showing significant differences in norfloxacin levels for both types of animals in the case of bile and intestinal content. It is remarkable that the tissues with higher differences between both groups of mice (i.e. liver, intestine) are the tissues with the highest levels of Abcg2 (Tanaka et al., 2005). It is noteworthy that the tissues with higher differences between both groups of animals have tight junctions (i.e. liver, intestine, kidney), the slower diffusion of compounds in these compact membranes facilitate the active transport of ABCG2. Our *in vivo* data related to the effect of Abcg2 on plasma and tissue distribution of norfloxacin may imply important biological and therapeutic significance. The expression and function of this transporter vary with gender (Merino, van Herwaarden et al., 2005), polymorphism (e.g. (Ni et al., 2010)) or Abcg2-inhibitor coadministration (e.g., (Krishnamurthy and Schuetz, 2006; Mo and Zhang, 2012); thus these factors could affect the bioavailability, efficacy and resistance development of this fluoroquinolone. Further research on this direction will be needed to fully understand these factors.

On the other hand, norfloxacin could not be detected in milk in none of the two groups of animals (Figure 59). Although norfloxacin was detected in milk from sheeps-ewe (Soback et al., 1994) and cows (Gips and Soback, 1999), norfloxacin was not detected in maternal milk in humans after oral administration (Wise, 1984).

Regarding pefloxacin, in general no differences between Abcg2$^{-/-}$ and wild-type mice were observed in the tissues analyzed suggesting that, apparently, Abcg2 does not seem to be involved in the systemic exposure of pefloxacin at the dose used. Additional factors such as the potential *in vivo* involvement of other transporters that may interact with pefloxacin (i.e. P-gp, (Kodaira et al., 2011)) could conceal an *in vivo* effect of ABCG2. Furthermore, a methyl group in pefloxacin is the only structural difference with norfloxacin. This minor structural variance appears to increase drug bioavailability to ~100% for pefloxacin (Hooper and Wolfson, 1985) compared to only ~40% for norfloxacin (Neu, 1992), supporting the potential relevance of an ABC transporter interaction in the process for the latter. In addition, other chemical features of the molecules could also play a role in the ABCG2 interaction.

The role of ABCG2 in milk disposition of several fluoroquinolones (i.e. ciprofloxacin, danofloxacin and enrofloxacin) has been reported (Merino et al., 2006; Pulido et al., 2006; Real et al., 2011). We could not observe such an effect for pefloxacin (Figure 62). However, this result is in agreement with the other findings regarding the lack of interaction of ABCG2 with this antibiotic *in vivo*.

The *in vivo* results regarding the interaction of fluoroquinolone drugs with Abcg2 can be also explained taking in account their hydrophobicity (Table 22). Ciprofloxacin, norfloxacin and enrofloxacin are the most hydrophilic fluoroquinolones (see XLogP in Table 22), crossing the membranes with more difficulty which means that Abcg2 can compete with passive influx; consequently, they are the fluoroquinolones showing the best *in vivo* ABCG2 interactions. As pefloxacin is in the middle in the sequence of hydrophobicity, this could explain why sometimes we observed transport (*in vitro*) but not

others (*in vivo*) (Table 22). Finally, in the case of moxifloxacin, a highly hydrophobic drug, *in vitro* ABCG2 net transport is not reported and, probably, neither *in vivo*.

When correlating *in vitro* and *in vivo* assays, differences in pH at the uptake site is an important issue to be considered as it has a strong influence on the protonation state of these zwitterionic drugs. *In vitro* experiments were performed at physiological pH=~7.4; in this environment, the compounds are zwitterionic. This fact implies a low passive diffusion; the antibiotic is easily taken by the ABCG2 transporter and appears as a substrate. Contrary, in *in vivo* assays with oral administrations, the uptake takes place in the stomach, where the pH=~2; or the small intestine, with a pH=~6. Thus, the fluoroquinolones are weakly cationic and can cross membranes more easily. This explains why, given orally, fluoroquinolones are rapidly absorbed from the intestine and distributed in tissues and fluids.

Our findings *a priori* could suggest the need to study the interaction of each single molecule with ABC transporters. As we have reported, not every compound of a family necessarily interacts in a similar manner. *In vitro* and *in vivo* differences in the ABCG2 interaction with norfloxacin and pefloxacin underline the importance of performing *in vivo* experiments. Many factors such as physiological functions or interplays with enzymes can affect in an *in vivo* system. Hence, the International Transporter Consortium (Giacomini et al., 2010) asserts that *in vivo* models should be established, in particular with compounds with poor solubility and limited permeability, such as norfloxacin. However, as we have demonstrated, taking in account the physicochemical properties of the compounds, it is possible to estimate the interaction of each compound with the ABCG2 transporter.

Considering the interaction of fluoroquinolones with the P-gp transporter, the extensive available results from *in vitro* experiments performed with the five fluoroquinolones compared with our ATPase activity assays (Figure 53) were compiled and displayed in Figure 66. A comparison contrasting the ATPase activity with other *in vitro* results is also indicated in the same figure at the specific indicated concentration. It should be initially taking in account that negative compounds have been described to hardly interact with P-gp (Seelig, 1998), therefore, as fluoroquinolones are zwitterionic charged, it is expected that these antibiotics do not interact with this transporter. However, due to fluoroquinolones have patterns to interact with P-gp if somehow they are able to cross the membrane in enough concentrations (Seelig, 1998), hydrophobic fluoroquinolones may interact with the transporter. Figure 66, thus, shows constant consistencies. Indeed, ciprofloxacin has been constantly found not to interact with P-gp as a substrate when studied with transport assays in several types of cells (with Caco-2 cells (Cavet et al., 1997; Lowes and Simmon, 2002; Yamaguchi et al., 2004), LLC-PK1 cells (de Lange et al., 2000; Yamaguchi et al., 2004; Park et al., 2011), MDCK-II (Lowes and Simmon, 2002; Park et al., 2011) and mouse macrophages (Michot et al., 2004; 2005); nor as inhibitor (de Lange et al., 2000; Haritova et al., 2007); neither in *in vivo* experiments (Dautrey et al., 1999; de Lange et al., 2000; Rodriguez-Ibañez et al., 2006; Haslam et al., 2011). All these results are in agreement with the absent of P-gp-ATPase activity for ciprofloxacin. By contrast, a possible interaction between ciprofloxacin and P-gp *in vivo* (with rats)

and *in vitro* (with Caco-2 cells) was proposed by Rodríguez-Ibañez et al. (2003). Indeed, Ruiz-García et al. (2002), in transport assays with Caco-2 cells found a positive interaction of ciprofloxacin as a substrate of P-gp. This result was also found for MDCK-I cells by Park et al. (2011). It should be noted that in Caco-2 cells many other transporters are expressed, for instance ABCG2, and may have interfered the results (Xia et al., 2005; Seithel et al., 2006).

Enrofloxacin has been seen not to inhibit P-gp in accumulation assays (Haritova et al., 2007), as expected from the absent of ATPase activity. Again, as reflected from ATPase activity results, P-gp seems not to interact with norfloxacin as a substrate *in vitro* nor *in vivo* (de Lange et al., 2000), neither as inhibitor in transport assays (de Lange et al., 2000; Lowes and Simmons, 2002; Sikri et al., 2004) with LLC-PK1 and MDCK-II, respectively.

The role of P-gp in pefloxacin transport has been shown to be negligible as a substrate, both *in vitro* (de Lange et al., 2000) and *in vivo* (de Lange et al., 2000; Tsai, 2001), also as an inhibitor (de Lange et al., 2000; Lowes and Simmons, 2002). Nonetheless, current results have shown pefloxacin as P-gp substrate in transport assays (Kodaira et al., 2011). This could be explaned by means of hydrophobicity, as pefloxacin is in the middle in the sequence of hydrophobicity (Table 22), it could be that the passive flux was quick enough to be able to be taking by P-gp despite the negative charge. This is also why, as in the case of ABCG2, sometimes transport was observed (Kodaira et al., 2011) but not others (de Lange et al., 2000).

As we have explained, moxifloxacin is the fluoroquinolone with the higher XLogP, the most hydrophobic, crossing the membranes easily. This fact allows interacting with P-gp and obtaining an activation curve of ATPase activity (Figure 53). When moxifloxacin interaction with P-gp has been studied, opposite results were obtained in transepithelial transport assays studying the drug as a substrate (Michot et al., 2005; Brillault et al., 2009) and no clear effect in *in vivo* experiments with humans (Weiner et al., 2007). Brillault et al. (2009) applied the antibiotic at a concentration around K_1 in the P-gp-ATPase activity (50 µM) (Table 17), therefore, it was possible to see the drug as a substrate in transport assays (Figure 66). In contrast, Michot et al. (2005) could not see moxifloxacin as a substrate as they applied the antibiotic at a concentration (10 µM) were the P-gp-ATPase activity was still not present (Figure 66) and active efflux could not cope with passive flux.

In conclusion, due to their zwitterionic character fluoroquinolones, in general, interact as *in vitro* substrates but not inhibitors for ABCG2 but they do not interact with P-gp (unless they are hydrophobic enough). In addition, we showed no *in vivo* interaction of pefloxacin with murine Abcg2; however norfloxacin bioavailability is widely affected by the transporter. We could explain our findings about the interactions of fluoroquinolones with ABCG2 and P-gp considering the physicochemical properties of the compounds (as charge and hydrophobicity) and their influence on active efflux and

passive flux. A schematic summary of the conclusions for the ABCG2 transporter is displayed in Figure 67.

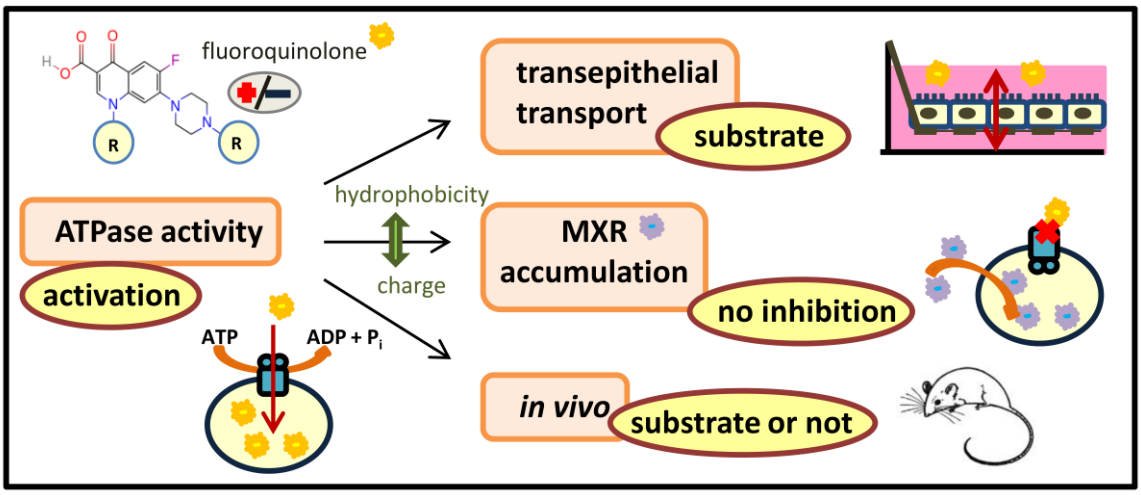

Figure 67. Schematic summary of conclusions obtained from the correlation of ATPase activity with other *in vitro* (transport and accumulation assays) and *in vivo* (with wild-type and knock-out mice) results for fluoroquinolones regarding the interaction with the ABCG2 transporter.

Conclusions

First.- Although there is a considerable overlap between ABCG2 and P-gp substrates, our analysis revealed significant and characteristic differences. Both transporters seem to have preference for a specific type of charge and the extent of hydrophobicity and amphiphilicity. Indeed, ABCG2 substrates are non-amphiphilic, rather hydrophilic and more zwitterionic or anionic (although ABCG2 interacts with compounds with any charge), whereas typical compounds which interact with P-gp are amphiphilic, hydrophobic and electrically neutral or cationic. ABCG2 and P-gp have hydrogen acceptor groups as recognition elements.

Second.- ABCG2 exhibits a lower basal and generally also a lower substrate-induced activity. Typical ABCG2 substrates, if transported by P-gp, they are also transported slowly. Despite the relatively slow rate of ATPase activity and transport, ABCG2 transports non-amphiphilic compounds very efficiently because those compounds generally have a very low rate of diffusion across the lipid bilayer.

Third.- For both exporters bell-shaped activity curves were obtained and the two transporters bind their substrates in the lipid membrane, thus, a two-step binding model is valid for both.

Forth.- ABCG2 exhibits a higher substrate-affinity than P-gp. The substrate affinity to ABCG2 as well as to P-gp seems to be essentially due to hydrogen bonding interactions. The higher affinity of substrates to ABCG2 in the lipid membrane seems to be due to a hydrophobic contribution which is absent in P-gp. Whereas the rate of transport in P-gp decreases with increasing the affinity of the drug to the transporter, it increases with increasing the affinity in ABCG2. ABCG2 and P-gp substrates seem to have different substrate binding locations.

Fifth.- The rate of ATP hydrolysis and the rate of transport unambiguously correlate. This can be shown by taking into account the passive flux across the bilayer membrane. If the transporter can cope with passive drug influx, the ATPase activity profile can be directly interpreted in terms of transport. The compound acts as a substrate in the concentration range of the rising side of the ATPase activity curve and as an inhibitor in the concentration range of the declining side of the curve. If passive influx is higher than active efflux the compounds are no longer substrates but they still act as inhibitors.

Sixth.- Substrates for ABCG2 and P-gp can be reliably predicted at any concentration by combining results from ATPase activity assays with results from surface activity measurements. Inhibitors of ABCG2 and P-gp can be derived directly from ATPase activity

assays. This approach reveal under which conditions a compound acts as a substrate and/or an inhibitor of ABCG2 and P-gp. In addition, it yields detailed insight into the transporter function.

Seventh.- Taking in account the physicochemical properties of fluoroquinolones (as charge and hydrophobicity), it is possible to estimate the interaction of each compound with the ABCG2 and P-gp transporters. Due to their zwitterionic character, in general, fluoroquinolones interact as *in vitro* substrates but not inhibitors for human ABCG2 and barely interact with P-gp.

Eighth.- There is no *in vivo* interaction of moxifloxacin and pefloxacin with murine Abcg2; however, norfloxacin bioavailability is widely affected by the transporter.

Ninth.- The pair P-gp and ABCG2 exhibits the perfect mach. Both transporters work optimally for the type of compounds for which they are adapted to. The two exporters handle compounds that are at the same time water soluble and membrane soluble. Due to the overlap in substrate specificity, an escape is difficult.

Resumen

1. Introducción

Las proteínas *Breast Cancer Resistance Protein* (BCRP, ABCG2) y glicoproteína-P (P-gp, ABCB1, MDR1) son miembros de las subfamilias G y B de la superfamilia de los transportadores ABC de membrana (*ATP-binding cassette*). Ambos transportadores usan la energía de hidrólisis de ATP para transportar sus sustratos. ABCG2 fue identificada en 1998 (Doyle y cols., 1998) mientras que P-gp fue descubierta 30 años antes (Juliano y Ling, 1976). ABCG2 y P-gp están localizadas en tejidos y barreras del organismo, así como en células tumorales donde transportan una amplia variedad de compuestos, incluidos antitumorales, antibióticos y hormonas. Además, existe solapamiento entre ambos transportadores en cuanto a los compuestos que interaccionan con ellos. Estos transportadores están considerados como clínicamente relevantes en absorción de fármacos en el intestino, en la distribución (por ejemplo en barreras como la hematoencefálica) y en la eliminación en el hígado y el riñón; ABCG2, además está implicada en la secreción de compuestos en la glándula mamaria (Giacomini y cols., 2010). Así mismo, ABCG2 y P-gp están implicados en el fenómeno de multi-resistencia a fármacos (MRD). A pesar de tener funciones similares, estas dos proteínas no presentan prácticamente secuencias homólogas en los dominios transmembrana (TMDs) y tan sólo algunas en los dominios de unión a nucleótidos (NBDs) (~ 20%) (Li y cols., 2007). El conocimiento existente hasta la fecha de ABCG2 y P-gp ha sido extensamente revisado (como ejemplos ver Krishnamurthy y Schuetz, 2006; Sharom, 2008; Robey y cols., 2009; Poguntke y cols., 2010; Mo y Zhang, 2012).

Por tanto, es de gran importancia en la industria química y médica entender las funciones de estos dos transportadores ABC y ser capaces de predecir su funcionamiento.

En el caso de P-gp, existe un amplio conocimiento sobre su bioquímica, estructura y función. P-gp se une a los compuestos en la membrana lipídica; como consecuencia, la unión sustrato-transportador ocurre en dos pasos, primero hay un paso del sustrato desde el componente acuoso a la bicapa lipídica y en un segundo paso ocurre la unión al transportador en la membrana. Sin embargo, en lo que respecta a ABCG2, se sabe poco de su función estructural (ej: Matsson y cols., 2009; Ni y cols., 2010). Se han desarrollado numerosos modelos basados en relaciones cuantitativas de estructura-actividad (QSAR), análisis de relaciones de estructura-actividad (SAR), modelos de farmacóforos y acoplamiento celular para predecir sustratos e inhibidores de P-gp (Chen y cols., 2012), aunque pocos modelos permiten dar predicciones satisfactorias. En el caso de ABCG2, el número de modelos al respecto es menor y a pesar de ellos, la naturaleza de las interacciones entre los compuestos y el transportador ABCG2 aún no está clara. Aún no existe un patrón para poder predecir sustratos e inhibidores de ABCG2 correctamente. Además, no existe un modelo molecular directo que explique cómo funciona este transportador. Teniendo en cuenta todo esto, el **objetivo principal** de la presente memoria fue entender el funcionamiento del transportador de membrana ABCG2 comparándolo con P-gp. Para este propósito, fueron propuestos tres objetivos específicos, expuestos a continuación.

El **primer objetivo específico** de esta investigación fue tratar de conseguir un mayor conocimiento de las diferencias y semejanzas entre ABCG2 y P-gp en cuanto a la cinética de ATPasa y la unión a sustrato. Además, intentamos realizar una predicción que explique las interacciones de los compuestos a nivel molecular con ambos transportadores. Para este propósito, escogimos 28 compuestos, incluyendo compuestos eléctricamente neutros, positivos, negativos y zwiteriónicos (con carga positiva y negativa), 20 de los cuales interaccionan con ambos transportadores. Entre los compuestos se encuentran antitumorales, antibióticos y hormonas.

En el campo de estudio de los transportadores ABC, existe una cierta disparidad en la interpretación de los datos entre grupos de investigación orientados hacia la ciencia de la *proteína* y los orientados hacia la *membrana.* Sin embargo, tanto proteína como membrana funcionan sinérgicamente. La mayoría de los compuestos alcanzan su objetivo atravesando mediante difusión pasiva varias bicapas lipídicas. Proteínas como ABCG2 y P-gp compiten con la entrada en la célula por difusión pasiva de los compuestos transportándolos de nuevo hacia el medio extracelular desde la membrana lipídica a expensas de la hidrólisis de ATP.

Para evaluar si un compuesto es sustrato o inhibidor de un transportador, el Consorcio Internacional de Transportadores (Giacomini y cols., 2010) recomienda realizar experimentos de transporte transepitelial con monocapas de células polarizadas que expresan el transportador a estudiar. Por el contrario, no se recomiendan ensayos de hidrólisis de ATP mediante inducción por sustrato debido a inconsistencias entre la actividad ATPasa y el ratio de transporte de algunos sustratos e inhibidores y también por la alta incidencia de falsos positivos y negativos. Sin embargo, el ratio de hidrólisis de ATP y el ratio de transporte se correlacionan si se tiene también en cuenta cuantitativamente la difusión pasiva a través de la membrana lipídica (Seelig, 2007).

El **segundo objetivo específico** de este trabajo de investigación fue evaluar la correlación entre la actividad ATPasa de ambos transportadores y el ratio de transporte en ensayos *in vitro* de transporte y acumulación teniendo en cuenta que la mayoría de los compuestos pueden cruzar las membranas lipídicas mediante difusión pasiva. Para este análisis escogimos seis hormonas esteroideas. La interacción entre hormonas esteroideas y los dos transportadores ABC, ABCG2 y P-gp, ha sido extensamente estudiada y nosotros utilizamos la gran cantidad de ensayos de transporte y acumulación existentes en literatura para compararlos con nuestros resultados. Las hormonas esteroideas además tienen la ventaja de ser eléctricamente neutras, lo que permite ignorar posibles efectos de la carga y hacer más fácil la interpretación de las interacciones entre los transportadores y las hormonas.

Otro grupo de compuestos de gran interés científico que interacciona con los transportadores ABC son los antibióticos, entre los que se incluyen las fluoroquinolonas, un tipo de antimicrobianos sintéticos con un amplio espectro de actividad y una gran potencia antibacteriana. De forma similar al segundo objetivo, el **tercer objetivo específico** de la presente memoria fue correlacionar la actividad

ATPasa de ABCG2 y P-gp obtenida con cinco fluoroquinolonas de uso común (ciprofloxacina, enrofloxacina, moxifloxacina, norfloxacina y pefloxacina) con los datos obtenidos en este trabajo y otros publicados de ensayos *in vitro*, que permiten una explicación de las interacciones entre estas fluoroquinolonas y los transportadores ABCG2 y P-gp a nivel molecular. Además, para completar la caracterización de la interacción de estas fluoroquinolonas con ABCG2, evaluamos la interacción *in vivo* de moxifloxacina, norfloxacina y pefloxacina con ABCG2.

2. Revisión bibliográfica

2.1. Transportadores de membrana

Los transportadores de membrana son proteínas especializadas asociadas a la membrana lipídica celular que median la translocación de solutos hacia dentro y fuera de las células utilizando mecanismos pasivos y activos (Klaassen y Aleksunes, 2010).

Las dos principales superfamilias de transportadores de membrana son los transportadores ABC (*ATP-binding cassette,* casete de unión al ATP) y los transportadores de solutos (SLC, *solute carrier*). Se han descrito más de 400 transportadores de membrana pertenecientes a estas dos superfamilias en el genoma humano (Giacomini y cols., 2010). Muchos de ellos han sido clonados y caracterizados. En la Figura 1 (Página 9) se puede ver un ejemplo de algunos de los más importantes localizados en diferentes tejidos.

En la vida diaria, los organismos están expuestos a compuestos hidrofóbicos presentes en la comida y el medio ambiente que atraviesan libremente las bicapas lipídicas y penetran en el organismo. Desgraciadamente, muchos de ellos son tóxicos; sin embargo, por fortuna algunos transportadores de membrana se han especializado en funciones de detoxificación (Sarkadi y cols., 2006). Por el contrario, este hecho tiene importantes consecuencias en el tratamiento contra enfermedades, ya que algunos fármacos son reconocidos como tóxicos por los transportadores y son excretados fuera de la célula y del organismo, impidiendo su acción contra la enfermedad (Endres y cols., 2006). Además, los transportadores de membrana también juegan un papel esencial en el mantenimiento de la integridad de la membrana plasmática (Ueda, 2011).

2.2. Transportadores ABC

Los transportadores ABC son proteínas integrales de membrana ubicuas que transportan activamente, a través de membranas biológicas y a expensas de la utilización de la energía generada por la hidrólisis de ATP, una amplia variedad de compuestos no relacionados estructuralmente. Estas proteínas han sido **clasificadas** en siete subfamilias designadas de la A a la G en base a su relación

filogenética, por la semejanza en las secuencias de los dominios de unión al ATP (Dean y cols., 2001) (Figura 2, Página 11).

Estructuralmente, los transportadores ABC pueden existir como una única cadena polipeptídica (*full-transporter*) o como dos proteínas separadas (*half-transporter*). El prototipo de transportador ABC es el *full-transporter,* que está compuesto por dos dominios hidrofóbicos transmembrana (TMD, *transmembrane domains*) y dos dominios hidrofílicos de unión a ATP (NBD, *nucleotide binding domains*). Para realizar su función, los transportadores ABC requieren como mínimo estos cuatro dominios. Los *half-transporters* se caracterizan por tener un único TMD unido a un NBD; éstos son capaces de formar homodímeros o heterodímeros para obtener un transportador funcional (Figura 3, Página 12) (ver Falasca y Linton, 2012 como ejemplo de revisión). La secuencia de aminoácidos de los TMD varía considerablemente entre transportadores ABC; por el contrario, la estructura de los NBD está bien conservada.

Aunque el **mecanismo** general del ciclo **de transporte** de los transportadores ABC no se conoce con exactitud, es bien sabido que implica unión de ATP y se presupone que la hidrólisis de éste está ligada a cambios conformacionales en el transportador (Falasca y Linton, 2012). El transporte conlleva dos ciclos interconectados, primero el ciclo catalítico de la hidrólisis de ATP y después el ciclo de transporte del compuesto. Existen dos modelos para explicar el mecanismo de acción de los transportadores ABC, el modelo *ATP Switch* (Higgins y Linton, 2004) que propone que los TMDs alternan entre dos conformaciones (Figura 4, Página 14) y el modelo *Constant Contact* (Jones y George, 2009), que está basado en posiciones alternas abiertas y cerradas, sin necesidad de cambios conformacionales (Figura 5, Página 15).

Los transportadores ABC están **presentes en** las membranas citoplásmaticas de bacterias (extracelulares) y en las membranas plasmáticas y de orgánulos (intracelulares) en eucariotas. Están localizados en barreras biológicas tales como la hematoencefálica, en el intestino, riñón, o hígado (Figura 6, Página 16) y en varios tipos de células tumorales (Gottesman y cols., 2002).

Su amplia y conservada distribución refleja su papel primordial de **transporte** acumulando nutrientes como aminoácidos, azúcares, iones, nucleótidos, metabolitos y vitaminas o eliminando fármacos, toxinas, xenobióticos (toxinas exógenas), hormonas, sales biliares, lípidos, péptidos y proteasas (George y Jones, 2012). A su vez, los transportadores ABC pueden transportar compuestos sin modificar o conjugados, estructuralmente diferentes o específicos. Los transportadores ABC también transportan moléculas de señalización en células cancerosas que están implicadas en la proliferación, migración y supervivencia de las mismas (Falasca y Linton, 2012).

La **función** principal de detoxificación y protección de los tejidos de xenobióticos y otras moléculas endógenas tiene serias **implicaciones** en la terapia clínica, ya que son uno de los principales factores que afectan a la disposición o biodisponibilidad de compuestos en el organismo participando en

su farmacocinética; esto es, en la absorción, distribución y eliminación (metabolismo y excreción) de fármacos, fenómeno conocido como ADME. También es importante su implicación en la multiresistencia a tratamientos con antibióticos y antitumorales, siendo los transportadores ABC uno de los principales mecanismos del fenómeno de multirresistencia a fármacos (MDR), fenómeno multifactorial en el que los organismos y las células presentan resistencia cruzada a un amplio rango de fármacos que no están relacionados estructuralmente ni funcionalmente, desencadenando una atenuación progresiva y constante de la respuesta a los tratamientos clínicos. De hecho, el inevitable desarrollo de MDR es un problema persistente en el éxito del tratamiento de los cánceres humanos (Mo y Zhang, 2012). También afecta a la terapia contra bacterias, hongos, parásitos, VIH y epilepsia. Tres transportadores ABC han sido principalmente asociados con MDR: la glicoproteína-P (P-gp), la *Breast Cancer Resistance Protein* (ABCG2) y la proteína asociada a MDR (MRP1) (Litman y cols., 2001). Una opción para luchar contra el fenómeno MDR es el desarrollo de inhibidores de transportadores ABC, que ha supuesto un gran reto en el que se ha invertido mucha investigación en las últimas dos décadas. Sin embargo, aunque el uso de inhibidores de transportadores ABC ha tenido éxito en estudios preclínicos, ha tenido poco impacto en aplicaciones clínicas. Muy pocos de los cientos de inhibidores identificados *in vitro* son válidos para su aplicación en tratamientos clínicos contra el cáncer. Por tanto, es necesario el descubrimiento de inhibidores nuevos, potentes y no tóxicos así como de nuevas estrategias de tratamiento (Falasca y Linton, 2012). Una posible explicación al fracaso de estos inhibidores es el que el inhibidor tiene que atravesar varias membranas en el organismo donde podrá a su vez interaccionar con otros transportadores e incluso con el citocromo P450, creándose procesos complejos que pueden desembocar incluso en efectos adversos. Por estas razones, la presencia de estas bombas exportadoras supone también un serio problema en el desarrollo de nuevos fármacos. Actualmente, muchas compañías farmacéuticas incluyen en sus pruebas de desarrollo de medicamentos, ensayos sobre la posible interacción con transportadores ABC (Giacomini, y cols., 2010).

La función de defensa de los transportadores ABC es sólo un aspecto de la importancia biológica de estas proteínas. Así, también están involucradas en diversos procesos celulares como el mantenimiento de la homeostasis osmótica y lipídica, tráfico de colesterol y lípidos, toma de nutrientes, división celular, desarrollo de células madre, formación de bilis, inmunidad bactericida, patogénesis y esporulación (van Veen y Konings, 1998; Davidson y cols., 2008; George y Jones, 2012).

La importancia del papel fisiológico fundamental que poseen los transportadores ABC se refleja claramente en las enfermedades humanas ligadas a la mutación o malformación de alguna de estas proteínas. Alteraciones en 14 transportadores ABC humanos han sido asociadas con alguna enfermedad específica (Borst y Elferink, 2002); estos desordenes genéticos incluyen: hemorragia (ABCB7), gota (ABCG2), fibrosis quística (ABCC7), problemas en la vista (ABCA4) o en el hígado (ABCB4, ABCB11) (Tabla 1, Página 22).

A pesar del enorme esfuerzo científico volcado en la investigación de los transportadores ABC, muchas funciones fisiológicas y compuestos que interaccionan con estas bombas exportadoras, así como los mecanismos de reconocimiento y transporte aún se desconocen o no están claros.

2.3. BCRP/ABCG2

La *Breast Cancer Resistance Protein* (BCRP/ABCG2/MXR/ABCP) humana fue descubierta en 1998 independientemente por tres grupos a partir de células seleccionadas con fármacos (Allikmets y cols., 1998; Doyle y cols., 1998; Miyake y cols., 1999). Después se fueron identificando ortólogos de otras especies: ratón, macaco, vaca y cerdo (Allen y cols., 1999; Eisenblatter y cols., 2003; Ueda y cols., 2005; Merino y cols., 2009). El análisis filogenético demuestra que esta proteína está cercana a ABCG1, el ortólogo humano del gen blanco de *Drosophila* y lejanamente relacionada con otros transportadores ABC como P-gp (ABCB1) o MRP1 (ABCC1) (Figura 7 A, Página 26). ABCG2 pertenece a la subfamilia G de los transportadores ABC (ABCG). Esta familia de transportadores son *half-transporters* localizados en múltiples tejidos (Figura 7 C, Página 26). Excepto ABCG2, sus miembros juegan un papel importante en el transporte de colesterol (Figura 7 B, Página 26).

Estructuralmente ABCG2 es por tanto un *half-transporter*, aunque poco se sabe de su estructura. Estudios de topología de membrana sugieren que sus TMD consisten en 6 segmentos transmembranales de hélices alfa (Figura 8, Página 28) (Wang y cols., 2008). Hasta la actualidad, existen sólo dos estudios de estructura realizados con microscopía electrónica; en el primero sólo se pudo observar la forma general de un complejo oligomérico de ABCG2 (McDevitt y cols., 2006) y el más reciente supuso la primera evidencia experimental de que la unión de un compuesto induce cambios conformacionales en ABCG2 (Rosenberg y cols., 2010). Por ser un *half-transporter*, se ha propuesto que ABCG2 tiene que funcionar como transportador activo en forma de homo-dímero (Kage y cols., 2002; Litman y cols., 2002; Bhatia y cols., 2005) u oligómero (Xu y cols., 2004; McDevitt y cols., 2006; Rosenberg y cols., 2010). Sin embargo, el papel y el significado biológico de una posible oligomerización es aún cuestionable (Ni y cols., 2010; Mo y cols., 2012).

Mucho se ha discutido en cuanto a los **sitios de unión** de ABCG2, postulándose que podrían ser dos o varios (Nakanishi y cols., 2003; Ejendal y Hrycyna, 2005; Xia at al., 2005; Clark y cols., 2006; Pozza y cols., 2006; Glavinas y cols., 2007); la localización de estos sitios de unión tampoco está aún clara, aunque se cree que probablemente estén localizados en la cavidad central rodeada por las alfa hélices (Rosenberg y cols., 2010) y que éstos sean hidrofóbicos (Coburger y cols., 2010). Se ha comprobado mediante modelos de homología que la entrada de la estructura abierta de ABCG2 es lo suficientemente grande (70 Å), comparada con P-gp (30 Å) (Aller y cols., 2009) como para permitir el acceso a ABCG2 de compuestos grandes o con carga desde la membrana plasmática o el citoplasma (Rosenberg y cols., 2010) (Figura 9, Página 30). La idea de que ABCG2 toma los compuestos directamente desde el citoplasma está ampliamente extendida (ver por ejemplo Sarkadi y cols., 2006). Sin embargo, algunos

autores han propuesto que la membrana lipídica es también una parte importante para la función exportadora de ABCG2, siendo necesario que los compuestos entren y se acumulen en ella antes de poder ser tomados por el transportador (Matsson y cols., 2007; Sharom, 2008) (Figura 10, Página 31). De hecho, recientemente se ha demostrado que la mitoxantrona difunde pasivamente a la membrana y es expulsada por ABCG2 directamente desde la membrana plasmática y no desde el citoplasma (Homolya y cols., 2011). A pesar de este descubrimiento, hasta la fecha, todas estas declaraciones son más bien especulaciones y aún no ha sido presentado un experimento directo que lo demuestre.

Por ser un transportador ABC, ABCG2 presenta **actividad ATPasa** basal e inducida (Krishnamurthy y Schuetz, 2006; McDevitt y cols., 2009). La hidrólisis de ATP en ABCG2 fue confirmada mediante experimentos de *photo-labeling* (Ozvegy y cols., 2002; Mao y cols., 2004). Hasta la fecha, la experimentación realizada con la actividad ATPasa de ABCG2 se ha concentrado prácticamente en averiguar si un compuesto es sustrato o inhibidor del transportador; por tanto, aún es necesaria la investigación del análisis cuantitativo de la actividad ATPasa de ABCG2. Además, es importante saber que la composición de la membrana puede afectar la cinética de ABCG2; se ha visto que las diferencias en la cantidad de colesterol afectan a la actividad ATPasa, siendo directamente proporcional la cantidad de colesterol y la actividad ATPasa (Pal y cols., 2007; Storch y cols., 2007). Igualmente, existe un comportamiento diferente de la actividad ATPasa entre vesículas obtenidas de células de insecto Sf9 y de mamífero, probablemente debido a la ausencia de colesterol en los insectos (Pal y cols., 2007; Telbisz y cols., 2007; Nicolle y cols., 2009).

ABCG2 se encuentra **localizado** en numerosos tejidos y barreras del organismo incluidos la placenta, ovario, útero, próstata, testículos, cerebro, intestino, colon, hígado, riñón, glándula mamaria, endotelio de venas y capilares, pulmones, pancreas, glándula adrenal, tiroides, corazón, bazo, timo; así como en células tumorales (Tabla 2 y Figura 11, Página 34) (Doyle y cols., 1998; Maliepaard y cols., 2001; Zhou y cols., 2001). Este transportador está localizado predominantemente en la membrana plasmática y se expresa casi exclusivamente en la superficie apical de células polarizadas como enterocitos o hepatocitos. Existen diferencias de distribución de esta proteína entre especies, así la distribución en ratas y ratones es similar, con la máxima expresión de ABCG2 en riñón, sin embargo la expresión en este órgano es menor en humanos (Maliepaard y cols., 2001). También hay diferencias entre sexos, pues por ejemplo, ABCG2 hepático es mayor en machos que en hembras en ratones y humanos; de esta manera, la excreción biliar de fármacos como nitrofurantoína o topotecan es mayor en ratones machos que en hembras (Merino y cols., 2005).

La **función** fisiológica primaria de ABCG2 es la protección contra xenobióticos y metabolitos tóxicos, previniendo la acumulación de tóxicos intra y extra celulares en células, órganos y en el organismo en general. Esta función mediante la cual ABCG2 reduce los niveles de tóxicos orales puede deberse a una reducción en la absorción gastrointestinal o a su papel en la excreción hepatobiliar y/o

renal (Schnepf y Zolk, 2013). El papel de esta proteína en la protección del cerebro a través de la barrera hematoencefálica (BBB, *Blood Brain Barrier*) no fue fácil de esclarecer, pues fueron necesarios muchos estudios y a veces con resultados contradictorios (Jonker y cols., 2002; Zhou y cols., 2002, Vlaming y cols., 2009). El papel en la placenta para proteger al feto fue documentado después de observar una mayor acumulación de topotecan en el feto de ratones sin Abcg2 (*knockout*) comparados con la cepa silvestre (*wild-type*) (Jonker y cols., 2000). Su función en la glándula mamaria supone un arma de doble filo pues previene la acumulación de tóxicos en la madre y simultáneamente distribuye tóxicos nocivos al neonato, aunque también vitaminas esenciales; esta paradoja ha sido extensamente discutida (van Herwaarden y cols., 2006 o Vlaming y cols., 2009, como ejemplos), sin embargo aún no se ha encontrado una conclusión clara. Por otra parte, existe una posible función dual de ABCG2 en el mantenimiento de células madre pluripotentes bombeando compuestos necesarios para la diferenciación y a su vez protegiéndolas de toxinas (Zhou y cols., 2001; Bunting, 2002); la misma función se ha propuesto también para células madre tumorales (Mo y cols., 2012). Las **implicaciones** clínicas de esta función de protección incluye la limitación de la biodisponibilidad oral de fármacos al nivel intestinal, hepatobiliar y renal y su efecto sobre las farmacocinéticas, produciendo además efectos secundarios para muchos medicamentos (Schnepf y Zolk, 2013). Este impacto en el esquema ADME puede verse en la Figura 12 (Página 40). Además, se sabe que existe una sobreexpresión de ABCG2 en tumores sólidos o en leucemias como resultado de la adquisición de resistencia a determinados antitumorales como la mitoxantrona, daunorubicina, metotrexato, bisantreno, inhibidores de las quinasas o topoisomerasas (Kusuhara y Sugiyama, 2007; Nakanishi y Ross, 2012). Esta expresión de ABCG2 está asociada con una menor respuesta a la quimioterapia y es responsable del desarrollo de resistencias, como el fenómeno MDR (Roos y cols., 2000; Steinbach y cols., 2002). La identificación de sobreexpresión de ABCG2 podría utilizarse como un factor de pronóstico en tumores y leucemias (Natarajan y cols., 2012). Se sabe que el transportador ABCG2 también está implicado en dos enfermedades, gota (ABCG2 transporta urato) (Dehghan y cols., 2008; Matsuo y cols., 2009; Woodward y cols., 2009) y Alzheimer (ABCG2 transporta el péptido beta amiloide) (Xiong y cols., 2009; Abuznait y Kaddoumi, 2012).

La función y la expresión de ABCG2 puede verse afectada por variantes naturales causadas por polimorfismos de un nucleótido (SNP, *single nucleotide polymorphisms*) en el gen de ABCG2, pudiendo tener importantes implicaciones fisiológicas y farmacológicas (Ross y Nakanishi, 2010). ABCG2 es un transportador altamente polimórfico con más de 80 SNP descritos su gen (Tabla 3, Página 43) (Tamura y cols., 2007).

Se ha visto que ABCG2 **transporta** un amplio espectro de **sustratos** estructural y funcionalmente muy diversos como antitumorales, antibióticos, antivirales, conjugados sulfatos y glucurónidos de esteroles y xenobióticos, compuestos naturales y tóxicos, metabolitos… (Tabla 4, Página 45) (Xia y cols., 2005; Krishnamurthy y Schuetz, 2006; Robey y cols., 2009). La fumitremorgina (FTC) fue

el primer **inhibidor** de ABCG2 descrito y pronto su análogo no tóxico: Ko143 (Allen y cols., 2002). Desde entonces, el número de inhibidores ha crecido extensamente incluyéndose en la lista grupos de compuestos como piridinas, inhibidores de la tirosina quinasa, flavonoides, derivados de taxano, esteroides, inhibidores del VIH… (Tabla 5, Página 46) (Nicolle y cols., 2009; Robey y cols., 2009; Ni y cols. 2010; Mo y Zhang, 2012). Debido al papel de ABCG2 en MDR, se ha realizado un esfuerzo considerable para identificar agentes para revertir MDR; sin embargo, a pesar de la explosión de publicaciones identificando inhibidores de ABCG2, ninguno ha sido usado a nivel clínico (Mo y Zhang, 2012). Existe un solapamiento considerable de sustratos e inhibidores entre ABCG2 y otros transportadores ABC como P-gp, MRP1 o MRP2 (Figura 13 A, Página 47) y con los transportadores de solutos (SLC) (Doyle y cols., 1998; Miyake y cols., 1999; Litman y cols., 2000; Kawabata y cols., 2002; Lee y Kim, 2004). Por tanto, es posible que en parte los fracasos en la supuesta inhibición específica de ABCG2 o P-gp para paliar MDR se deban a la co-expresión de varios transportadores y a un solapamiento en la afinidad del inhibidor.

ABCG2 puede ser solubilizado apartir de membranas utilizando detergentes (McDevitt y cols., 2006; Pozza y cols., 2006; Rosenberg y cols., 2010) que se conoce que interaccionan con P-gp (Li-Blatter y cols., 2009), influenciando e interfiriendo en los resultados de transporte cuando el transportador P-gp ha sido solubilizado con dichos detergentes. Hasta el momento, no se ha realizado ninguna investigación al respecto con ABCG2, pero teniendo en cuenta el solapamiento entre ambos transportadores, es posible que los detergentes también interaccionen con ABCG2. El ABCG2 purificado con detergentes es activo pero tiene una actividad ATPasa basal baja (Pozza y cols., 2006; Rosenberg y cols., 2010), pudiendo ser un indicativo de la interacción de los detergentes como inhibidores de la ABCG2. Nuevas investigaciones son necesarias al respecto.

ABCG2 transporta compuestos hidrofóbicos, hidrofílicos, neutros, o cargados negativa o positivamente (Xia y cols., 2005; Krishnamurthy y Schuetz, 2006; Ni y cols., 2010). Compuestos hidrofílicos como el metotrexato, la sulfasalazina, cimetidina o nitrofurantoína son descritos como buenos sustratos pero no inhibidores de ABCG2; siendo una posible explicación para la ausencia de inhibición la baja afinidad por el transportador en combinación con la poca permeabilidad en la membrana; por el contrario, los compuestos hidrofóbicos actúan más como inhibidores (Matsson y cols., 2007). Los inhibidores que se solapan entre los transportadores P-gp, MRP2 y ABCG2 son más lipofílicos y aromáticos que los específicos o los compuestos que no son inhibidores (Matsson y cols., 2009). Los inhibidores de ABCG2 contienen un gran número de átomos de nitrógeno (Matsson y cols., 2007; 2009) que tienden a formar puentes de hidrógeno, un elemento importante para el reconocimiento e interacción entre el compuesto y el transportador ABCG2 (Yoshikawa et a., 2004; Saito y cols., 2006; Boumendjel y cols., 2007; Pick y cols., 2008). Se ha sugerido una correlación entre la afinidad de ABCG2 por el sustrato y la frecuencia de patrones aceptores de puentes de hidrógeno (Cramer y cols., 2007; Matsson y cols., 2007). Un aspecto importante que incrementa la inhibición de ABCG2 es la estructura plana (Gandhi y Morris, 2009).

Los modelos *in silico* (computacionales), pueden ser usados en el desarrollo de un fármaco para predecir propiedades farmacocinéticas y fármacodinámicas antes de realizar experimentos *in vitro* e *in vivo* y para sintetizar medicamentos con propiedades fisicoquímicas favorables. Los dos modelos más comunes son los análisis de relaciones de estructura-actividad (SAR, *Structure–Activity Relationships*) y las relaciones cuantitativas de estructura-actividad (QSAR, *Quantitative Structure-Activity Relationships*); QSAR se utiliza para correlacionar parámetros de actividad *in vivo* con propiedades fisicoquímicas, mientras que SAR intenta explicar las propiedades estructurales o químicas que influyen en la actividad biológica (Gandhi y Morris, 2009). Se han publicado varios trabajos al respecto con ABCG2, relacionados sobre todo con su inhibición, sin embargo, la naturaleza de las características que determinan las interacciones de los compuestos con el transportador ABCG2 aún no está clara y no es posible predecir sustratos o inhibidores; tampoco existe un modelo molecular directo.

2.4. Glicoproteína-P

La glicoproteína-P (P-gp, ABCB1, MDR1) fue el primer transportador humano ABC descrito (Juliano y Ling, 1976), por tanto es el más estudiado, conocido y caracterizado, inclusive por su implicación en resistencias al cáncer y en MDR (Falasca y Linton, 2012).

En cuanto a su **estructura**, se trata de un típico *full- transporter,* con sus dos mitades homólogas de 6 hélices alfa transmembrana hidrofóbicas (TMD) unidas por un gran dominio interno citoplasmático y con dos sitios de unión al ATP (NBD) (Figura 15 B, Página 53) (Devault y Gros, 1990). Durante la pasada década, la estructura de P-gp se caracterizó mediante varios modelos de homología; en el último, realizado por Aller y cols. (2009) se encontró un pseudo heterodímero simétrico con cada monómero formado por dos grupos de seis TMD y dos NBD separados por 30 Å (Figura 15 A, Página 53). El homólogo de ratón, compartía el 87% de la identidad en la secuencia. En la actualidad, el mecanismo detallado de transporte de P-gp es todavía objeto de considerable controversia (Oldham y cols., 2008; Locher, 2009; Chen y cols., 2012). Se han propuesto varios modelos, uno de ellos es el *ATP Switch,* comentado anteriormente, donde el compuesto se transporta vía unión y dimerización de ATP en los NBD y la energía de la hidrólisis de ATP se usa para devolver a P-gp a su conformación inicial (Higgins y Linton, 2004; Linton y Higgins, 2007). En el modelo de unión en "dos pasos": en el primer paso el compuesto entra en la bicapa lipídica y está descrito por el coeficiente de partición lípido-agua (K_{lw}); y el segundo paso consiste en la unión del compuesto a P-gp desde la membrana, definido por la constante de unión del lípido al transportador (K_{tl}) (Figura 16, Página 54) (Seelig y Lywojtowicz, 2000; Gatlik-Lywojtowicz y cols., 2006). La naturaleza anfipática de los compuestos típicos que interaccionan con P-pg les permite entrar en la membrana lipídica, este hecho es consistente con que los sitios de unión de P-gp sean accesibles desde la bicapa lipídica (Shapiro y Ling, 1997; Shapiro y cols., 1999; Chen y cols., 2001). Por tanto los compuestos tienen que conseguir difusión pasiva, pero si están muy cargados o son muy grandes no serán capaces de difundir o lo harán muy despacio.

Sobre los **sitios de unión** de los compuestos a P-gp, se ha hipotetizado mucho y se han propuesto dos, tres o múltiples, quizás solapados; sin embargo el tipo y número aún no está claro (Sharom y cols., 2005; Sauna y Ambudkar, 2007; Chen y cols., 2012). Se ha propuesto un modelo cinético asumiendo dos sitios de unión, una región de activación de la actividad de P-gp (y por tanto de hidrólisis de ATP) a bajas concentraciones del sustrato y otra de inhibición a altas concentraciones (Figura 17 A, Página 55), pudiendo un mismo compuesto actuar como sustrato o inhibidor dependiendo de la concentración (Litman y cols., 1997a y b; Ambudkar y cols., 1999; Sauna y Ambudkar, 2001; Gatlik-Lywojtowicz y cols., 2004). Los compuestos con mucha afinidad por el transportador tienden a ocupar directamente ambas regiones y a inhibirlo incluso desde concentraciones bajas (Li-Blatter y cols., 2009). Este modelo cinético ha sido matemáticamente evaluado con una ecuación modificada de Michaelis-Menten (Figura 17 B, Página 55), basada en inhibición no competitiva (Litman y cols., 1997a). Sin embargo, si sólo existe activación, la cinética se corresponde con la ecuación simple de Michaelis-Menten (Seelig y Lywojtowicz, 2000).

P-gp está **distribuido** en tejidos y barreras fisiológicas como intestino, hígado, riñón, placenta o cerebro (Figura 19 A, Página 57) (Thiebaut y cols., 1987; Cordon-Cardo y cols., 1990; Klaassen y Aleksunes, 2010), donde se expresa en la membrana apical de las células. También en células madre y tumorales. Así mismo, también se localiza en compartimentos intracelulares como el retículo endoplasmático, Golgi, endosomas y lisosomas (Fu y Roufogalis 2007). Se ha demostrado que los niveles de expresión de P-gp son dependientes de la edad, la genética, la dieta o los fármacos (Seelig y Gatlik-Lywojtowicz, 2005).

Como tal transportador ABC, la principal **función** de P-gp es la protección del organismo frente a tóxicos (endógenos y exógenos) (Borst y Schinkel, 2013). Estudios con ratones *knockout* sostienen esta idea pues estos ratones deficientes en P-gp son hipersensibles a tóxicos (Schinkel, y cols., 1995; Schinkel, 1997). Por consiguiente, de manera similar a ABCG2 y a otros transportadores ABC, está función protectora tiene **implicaciones** en ADME y en MDR para infinidad de fármacos. La mitad de los cánceres humanos, incluyendo cánceres sólidos, leucemias, linfomas y mielomas; expresan P-gp a niveles suficientes como para conferir MDR incluso antes de la quimioterapia (Gottesman y Ling, 2006; Sharom, 2008). La mayoría de las estrategias para revertir MDR se han centrado en modular o inhibir la actividad de P-gp (Ambudkar y cols., 1999; Seelig y Gatlik-Lywojtowicz, 2005). Se han desarrollado tres generaciones de inhibidores buscando ser potentes, selectivos y específicos; a pesar de la multitud de estudios realizados, debido a su toxicidad, a efectos secundarios o a interacciones farmacocinéticas inesperadas con la presencia de agentes quimioterapéuticos, aún existen problemas para encontrar inhibidores adecuados (Falasca y Linton, 2012).

Otras funciones fisiológicas donde P-gp podría estar implicado son el transporte de lípidos, la regulación de la apoptosis, la modulación indirecta de la actividad del canal de cloruro, la esterificación

de colesterol y la protección del ADN (Valverde y cols., 1992; van Helvoort y cols., 1996; Molinari y cols., 1998; Luker y cols., 1999; Calcabrini y cols., 2000; Johnstone y cols., 2000; Munteanu y cols., 2006).

Se han descrito unos 50 SNP del gen ABCB1 en pacientes humanos que están asociados con un incremento en la susceptibilidad a ciertas enfermedades como colitis, cánceres o Parkinson (Zhou y cols., 2008).

P-gp **transporta** un amplísimo rango de **compuestos** dispares en estructura que son hidrofóbicos y solubles en lípidos, anfipáticos, con un tamaño entre 200 y 2000 Da, a menudo con anillos aromáticos y carga neutra o positiva (Gottesman y Pastan, 1993; Seelig y cols., 1994; Schinkel y cols., 1996; Sharom, 2008). Muchas de estas moléculas son fármacos incluyendo antitumorales, inhibidores de VIH, analgésicos, antihistaminas, antagonistas del receptor de H2, agentes inmunosupresores, antibióticos, etc. Y también hay moléculas fisiológicas como hormonas, lípidos o péptidos (Sarkadi y cols., 2006; Sharom, 1997). Se ha propuesto que la hidrofobicidad, la anfifilicidad y la entrada del compuesto en la membrana (*partitioning*) son los factores que regulan la interacción de un compuesto con P-gp (Seelig, 1998; Seelig y Lywojtowicz, 2000; Gatlik-Lywojtowicz y cols., 2006; Aänismaa y Seelig, 2007), por tanto para explicar el proceso de P-gp a nivel molecular es importante caracterizar el compuesto, la membrana lipídica y la actividad del transportador (Seelig, 2007). *Partitioning* está controlado por la carga, el área de la sección (AD) y la concentración del compuesto, la densidad de empaquetamiento de la membrana (π_M), el nivel de expresión del transportador y el estado metabólico de las células.

Uno de los primeros modelos *in silico* propuestos para estudios de estructura-actividad se basaba en una serie de elementos estructurales bien definidos requeridos para la interacción con P-gp (Seelig, 1998). Partía de la premisa de que la unión de un compuesto a P-gp ocurre por la formación de puentes de hidrógeno (HAP); éstos se pueden organizar en distancias espaciales llamadas patrones de tipo l y tipo ll. Las moléculas que contiene al menos una unidad de estos tipos son predecibles de ser sustratos de P-gp; además, cuantas más unidades contengan mayor será la unión al transportador. Por otra parte, los patrones de tipo ll también son responsables de la inducción de sobre expresión de P-gp y del desarrollo de resistencias; de hecho, estos patrones son especialmente abundantes en antibióticos y antitumorales (Seelig y Lywojtowicz, 2000). A pesar del enorme esfuerzo dedicado, con numerosos modelos *in silico* (como SAR o QSAR), a predecir sustratos e inhibidores de P-gp y entender su mecanismo de interacción con el transportador, actualmente tan sólo algunos modelos limitados dan predicciones satisfactorias (Chen y cols., 2012).

2.5. Compuestos importantes para este estudio

Hormonas esteroideas. Las hormonas son moléculas endógenas que funcionan como mensajeros químicos transportando señales entre células repartidas por todo el organismo. Las

hormonas esteroideas se sintetizan generalmente a partir de colesterol y se clasifican en cinco grupos: glucocorticoides (control de la inflamación), mineralocorticoides (control del balance de sales y agua), andrógenos, estrógenos y progestágenos (control caracteres sexuales). El término esteroide incluye hormonas producidas en el organismo y también medicamentos generados artificialmente.

En este estudio se utilizaron seis hormonas esteroideas cuyas estructuras pueden verse en la Figura 20 (Página 66). El cortisol es un glucocorticoide entre cuyas funciones se incluye el actuar en situaciones de estrés incrementando el azúcar en sangre y suprimiendo el sistema inmune; la hidrocortisona es el término farmacéutico para cortisol, utilizándose en reacciones alérgicas severas y otros procesos inflamatorios (Coderre y cols., 1991; Djurhuus y cols., 2002). La dexametasona es un glucocorticoide sintético utilizado para tratar procesos inflamatorios y autoinmunes, así como antitumoral (Brouwer y cols., 2010). El estradiol es el estrógeno predominante durante los años fértiles en la mujer (excepto en períodos de embarazo), aunque está también presente en hombres; controla funciones reproductivas, sexuales y de gestación (Carreau y cols., 2003). La progesterona es el principal progestágeno natural humano, está involucrada en el ciclo menstrual y en el embarazo, y se usa para tratar infertilidad o como apoyo al principio del embarazo (Fonseca y cols., 2007). El tamoxifen es un estrógeno sintético que se usa para el tratamiento de cáncer de mama, de infertilidad o en pubertad prematura (Steiner y cols., 2005; Jordan, 2006). La testosterona es el principal andrógeno, estando relacionado con el desarrollo de los tejidos y los caracteres sexuales masculinos (Davis y cols., 2008).

La regulación de los transportadores ABC por hormonas es un tema de extensa investigación; así mismo, las interacciones de hormonas esteroideas con los transportadores ABCG2 y P-gp han sido estudiadas ampliamente, especialmente mediante experimentos de transporte transepitelial con células polarizadas y ensayos de acumulación (Tabla 6, Página 67). Los ensayos de actividad ATPasa de ABCG2 con hormonas se limitan prácticamente a una publicación (Janvilisri y cols., 2003); referido a P-gp, estos ensayos se han realizado sobre todo por tres grupos de investigación (Rao y cols., 1994; Orlowski y cols., 1996; Litman y cols., 1997a). Se ha visto que en general estas hormonas esteroideas no son sustrato de ABCG2 (excepto, quizás estradiol), y algunas interaccionan como inhibidores (dexametasona, estradiol y tamoxifen) en experimentos de transporte y acumulación. Sin embargo, la actividad ATPasa de ABCG2 es visible para las seis hormonas. En el caso de P-gp, sólo cortisol y dexametasona son sustratos en ensayos de transporte. La progesterona, el tamoxifen y la testosterona son los únicos inhibidores en experimentos de acumulación. Como contraste, de nuevo existe actividad ATPasa de P-gp para todos estos esteroides. Aún no se ha presentado una explicación para estas aparentes inconsistencias; tampoco existe un conocimiento general de las hormonas esteroideas explicando el mecanismo de interacción con ABCG2 y P-gp.

Fluoroquinolonas. Las fluoroquinolonas (FQ) son antibióticos sintéticos con un átomo de flúor en la posición 6 del anillo de la quinolona. Son administradas de forma oral y parenteral para el

tratamiento de enfermedades bacterianas, incluyendo infecciones sistémicas severas, debido a su amplio espectro de actuación y su potente actividad antibacteriana (Peterson, 2001, Blondeau, 2004). De hecho, son unos de los antibióticos prescritos más comunes en el mundo (Goossens y cols., 2005; Linder y cols., 2005). Sin embargo, presentan dos problemas fundamentales, el primero lo constituyen los efectos adversos que ha dado lugar a la restricción de FQ para muchas indicaciones (Myell y Tillotson, 2002; Stahlmann, 2002; Spryel y Rodvold, 2003). El otro problema es el desarrollo de resistencias y su implicación en el fenómeno MDR; por ello, suelen ser utilizados cuando otros tratamientos fallan (Hooper, 1999). Las FQ son rápidamente absorbidas desde el intestino, distribuidas por el organismo y excretadas; aquellas que tienen un metabolismo renal suelen ser utilizadas para el tratamiento de infecciones urinarias y las que tienen un metabolismo intestinal o hepático para el tratamiento de infecciones gastrointestinales (Sorgel y cols., 1989; Scholar, 2002).

Cinco fluoroquinolonas se han utilizado en este estudio (Figura 21, Página 75). La ciprofloxacina es una de las FQ más prescritas y utilizadas debido a su amplio espectro de actividad, su excelente penetración tisular y su disponibilidad (Nelson y cols., 2007). La enrofloxacina es una FQ veterinaria similar a la ciprofloxacina utilizada en el tratamiento de las principales infecciones de animales de granja (Schroder, 1989; Martinez y cols., 2006). La moxifloxacina se utiliza para tratar infecciones entre las que se encuentran conjuntivitis, bronquitis, meningitis, neumonía o tuberculosis (Miravitlles y Anzueto 2008; Fouad y Gallagher 2011). La norfloxacina es el principal metabolito de la pefloxacina y tiene la misma potencia antibacteriana (Thibault y cols., 1981); se utiliza para tratar infecciones urinarias y del ojo. La pefloxacina se utiliza además en el tratamiento de infecciones gastrointestinales, respiratorias, de la piel, los huesos y las articulaciones.

Se ha propuesto que la interacción de transportadores ABC con FQ podría estar asociada con el desarrollo de resistencias (Merino y cols., 2006; Michot y cols., 2004); además éstos podrían afectar las farmacocinéticas de FQ y la eficacia en el tratamiento con antibióticos. De hecho, se ha demostrado que ABCG2 afecta a la biodisponibilidad y farmacocinéticas de varias FQ (ciprofloxacina (Merino y cols., 2006), enrofloxacina (Pulido y cols., 2006), danofloxacina (Real y cols., 2011)). Sin embargo, esto no es extensivo a todas las fluoroquinolonas; por ejemplo, en nuestro laboratorio no se pudo encontrar una interacción *in vivo* entre la esparfloxacina y ABCG2 (Real, Egido y Merino, resultados sin publicar). Se ha sugerido que pequeñas diferencias estructurales en FQ podrían tener un papel fundamental en el reconocimiento por el transportador (Michot y cols., 2004). Por tanto, falta por clarificar el posible efecto de ABCG2 en las farmacocinéticas de norfloxacina, pefloxacina y moxifloxacina. Por otra parte, se ha visto que las FQ en principio no interaccionan como inhibidores de ABCG2 (ej: ciprofloxacin, norfloxacin, enrofloxacin) (Merino y cols., 2006; Pulido y cols., 2006). En cuanto al transportador P-gp, se ha publicado una gran cantidad de trabajos donde se intenta elucidar su posible interacción con las cinco fluoroquinolonas objeto de nuestro estudio *in vitro* e *in vivo*; y prácticamente en la totalidad de los resultados no se encontraron interacciones entre FQ y P-gp ni como sustrato ni como inhibidor (Tabla 7,

Página 77) (ej: de Lange y cols., 2000; Lowes y Simmon, 2002). Hay que tener en cuenta que las FQ son muy hidrofílicas y tienen carga híbrida (Mulgaonkar y cols., 2012), dos características que no compaginan bien con compuestos que suelen ser transportados por P-gp (Seelig, 1998). Por otra parte, no existe publicado ningún estudio de actividad ATPasa con ninguno de los dos transportadores, ABCG2 ni P-gp. Tampoco se ha presentado una explicación clara de las interacciones entre FQ con ABCG2 y P-gp a nivel molecular.

2.6. Bases metodológicas para el estudio de la interacción de compuestos con transportadores ABC: ventajas y desventajas

Ensayos *in vitro* e *in vivo* se han desarrollado para predecir las interacciones entre fármacos y otros compuestos y los transportadores ABC. Diferentes estudios pueden asignar un mismo compuesto de manera diferente (sustrato y/o inhibidor); es por ello que normalmente es necesaria una combinación de diferentes experimentos para describir adecuadamente la interacción (Poguntke y cols., 2010).

En los experimentos ***in vitro*** se incluyen los realizados con membranas y los realizados con células (Tabla 8, Página 81). La aplicación de preparaciones de membranas aisladas de células que sobre-expresan la proteína de interés supone una opción relativamente barata y con alto rendimiento (Sharom y cols., 1999; Glavinas y cols., 2004). Estos sistemas incluyen ensayos de actividad ATPasa, transporte vesicular y marcaje de fotoafinidad (*photoaffinity labeling*). Los ensayos de actividad ATPasa se basan en que la activación de un transportador ABC implica la hidrólisis de ATP con formación de ADP y fosfato inorgánico; este último se puede medir mediante una reacción colorimétrica en vesículas invertidas, en las que los NBD están hacia el exterior. Además, se puede medir el efecto de un inhibidor ya que disminuye la actividad ATPasa basal del transportador ABC (Ozvegy y cols., 2001; Al-Shawi y cols., 2003). Las células que más se han empleado para estos análisis incluyen células de insecto (Sf9) y fibroblastos de ratón (NIH-3T3), ya que normalmente las células humanas expresan niveles insuficientes del transportador como para medir actividad ATPasa (Ambudkar, 1998; Bodo y cols., 2003; Ni y cols., 2010b). Para analizar la cinética de los datos obtenidos, para ABCG2 normalmente se ha venido usando la cinética clásica de Michaelis-Menten (Ozvegy y cols., 2001); para P-gp Litman y cols., (1997 b) propusieron la ecuación modificada de Michaelis-Menten ya comentada. Dos de las dificultades que se pueden presentar en esta técnica son la agregación de los compuestos testados o de las vesículas (Aänismaa y Seelig, 2007). Algunas ventajas son la simplicidad, reproducibilidad y el altísimo rendimiento, además de permitir caracterizar compuestos hidrofóbicos (Ishikawa y cols., 2005; Sarkadi y cols., 2006; Hegedus y cols., 2009). Por el contrario pueden encontrarse inconsistencias entre la actividad ATPasa y el ratio de transporte de algunos sustratos e inhibidores y falsos positivos y negativos (Giacomini y cols., 2010).

El transporte vesicular es la medida directa de compuestos que son transportados como sustratos por proteínas ABC en vesículas invertidas; de manera indirecta también se pueden testar inhibidores. Una limitación de este tipo de ensayo es que no se pueden medir compuestos hidrofóbicos, dando lugar a falsos negativos, otra es que se necesitan compuestos fluorescentes o radioactivos que encarecen el experimento (Hegedus y cols., 2009). El *photoaffinity labeling* se utiliza para estudiar detalles del mecanismo molecular de la función de los transportadores ABC; se trata de procedimientos complejos y difíciles que no suelen distinguir entre sustratos e inhibidores (Hegedus y cols., 2009).

Los métodos en los que se utilizan células sirven para diferenciar entre sustratos en inhibidores y para evaluar mecanismos de transporte (Giacomini y cols., 2010). Se suelen utilizar células transfectadas que crecen en monocapas en soportes sólidos; algunas de las más utilizadas son MDCK, LLC-PK1 y HEK293. Es importante saber que la presencia de transportadores endógenos puede influir sobre los resultados obtenidos (Goh y cols., 2002). Los sistemas basados en células incluyen experimentos de citotoxicidad, transporte transcelular, experimentos de acumulación y con microfisiómetro *Cytosensor*. Los experimentos de citotoxicidad se utilizan para investigar la función del transportador utilizando compuestos tóxicos o antiproliferativos (lo que de partida supone una limitación) e indirectamente para valorar un inhibidor potencial (Hegedus y cols., 2009). El ensayo de transporte transcelular, transepitelial o bidireccional es un método tradicional para identificar sustratos. El compuesto es aplicado en un compartimento y su presencia es monitorizada (normalmente mediante HPLC o espectrometría de masas) en el compartimento opuesto (ambos compartimentos están separados por una monocapa de células polarizadas sobreexpresando el transportador ABC). La diferencia entre la concentración del compuesto en ambas direcciones es el ratio de transporte (diferencia entre el transporte basal-apical y el apical- basal, B-A/A-B) (Figura 22, Página 87), si es mayor de 1,5 o 2 se considera que el compuesto es sustrato; puesto que la dirección predominante será la dirección basal-apical al estar el transportador más expresado en la parte apical. Las principales limitaciones de este experimento son el gran trabajo y coste que supone; además de la medición exclusivamente de transporte neto (ver apartado de *Resultados y Discusión*), dando lugar a falsos negativos (Giacomini y cols., 2010; Glavinas y cols., 2007).

En los ensayos de acumulación se puede cuantificar el transporte de compuestos fluorescentes por el transportador ABC, y evaluar inhibidores y la especificidad de transporte mediante citometría de flujo (Sharom, 2008). En el caso de evaluación de inhibidores, aunque se recomienda testar paralelamente varios sustratos (Nicolle y cols., 2009), el sustrato más utilizado en el caso de ABCG2 es la mitoxantrona (MXR) (Poguntke y cols., 2010). La expresión de ABCG2 previene la acumulación de MXR y su inhibición aumenta su acumulación (Figura 23, Página 89). Los datos son evaluados calculando las potencias inhibidoras de los compuestos a partir de las medianas de fluorescencia. Uno de los problemas fundamentales que tiene esta técnica son los falsos negativos al infra-estimar compuestos con poca permeabilidad (Xia y cols., 2005). En los experimentos con microfisiómetro *Cytosensor*, un

micro pH-metro, se estudia la activación de actividad ATPasa en tiempo real con células vivas, monitorizando la tasa de acidificación extracelular (ECAR) ya que la utilización de ATP está indirectamente relacionada con la producción de lactato como resultado de la glicolisis y éste se elimina en forma de ácido (Figura 24, Página 90). Los resultados obtenidos son comparables con los de ensayos de actividad ATPasa (Lywojtowicz y cols., 2002; Gatlik-Lywojtowicz y cols., 2004; Gatlik-Lywojtowicz y cols., 2006; Aänismaa y Seelig, 2007).

Los experimentos ***in vivo*** suelen realizarse con modelos animales *knockout* modificados genéticamente en su mayoría. Estos modelos han servido para ilustrar el papel de transportadores ABC en fisiología, protección en barreras y absorción y excreción de compuestos; además de para evaluar el efecto de los transportadores en las farmacocinéticas, farmacodinámicas e interacciones entre fármacos en el proceso de desarrollo de medicamentos (Giacomini y cols., 2010; Klaassen y Alleksunes, 2010). Se ha probado que los ratones Abcg2 y Mdr1 *knockout* son una herramienta útil en el estudio *in vivo* de la función de ABCG2 y P-gp, incluido el papel de ABCG2 como exportador de compuestos a la leche (Vlaming y cols., 2009; Tang y cols., 2013). Los problemas que tienen estos modelos son el elevado precio, la difícil reproducibilidad y extrapolación entre especies y la cantidad de variables que deben considerarse a la hora de interpretar los datos (Xia y cols., 2005; Giacomini y cols., 2010).

2.7. Bases metodológicas para el estudio de la difusión pasiva

La estimación de la difusión pasiva da una idea de la potencial interacción de un compuesto con un transportador ABC específico y se puede utilizar para compararlo con los ratios de transporte de la proteína (Seelig y Gatlik-Lywojtowicz, 2005). La partición en la membrana se estima comunmente mediante el coeficiente de partición octanol-agua (Log P), sin embargo, la interfase aire-agua es una alternativa mejor ya que asemeja la bicapa lipídica (ordena los compuestos de la misma manera). Una estimación de la difusión pasiva utilizando la interfase aire-agua es la **medida de actividad de superficie** (SAM); esta presión de superficie se mide con un plato Wilhelmy en cubetas de teflón y de las medidas se obtienen curvas de presión *versus* concentración (p(π)/Log C) (Figura 25, Página 93); la técnica está basada en la medida de la isoterma de Gibbs. Del análisis de los datos se obtiene el coeficiente de partición aire-agua (K_{aw}) y el área transversal de superficie (A_D) de la molécula analizada (Figura 25, Página 93) y con ellos se puede estimar el coeficiente de partición lípido-agua (K_{lw}) (Seelig y cols., 1994; Fisher y cols., 1998; Gerebtzoff y cols., 2004; Nervi y cols., 2010). SAM no se puede determinar apropiadamente para compuestos que no son anfifílicos (con una parte polar y otra apolar en su estructura) (Fisher y cols., 1998), pues una de las características fundamentales de los compuestos que se encuentran y que penetran fácilmente en la membrana es precisamente esa anfifilicidad. Otra alternativa para determinar la difusión pasiva y calcular K_{lw} es la técnica de **calorimetría de titulación isotérmica (ITC).**

3. Objetivos

Con estos antecedentes, el principal objetivo de la presente memoria fue estudiar la función del transportador ABCG2 mediante su comparación con P-gp. Para este propósito, los objetivos específicos fueron:

4. Conseguir un conocimiento más extenso de las similitudes y diferencias entre ambos transportadores, ABCG2 y P-gp, en relación a la actividad ATPasa, la especificidad y las relaciones de estructura-actividad. Así mismo, intentar conseguir una predicción de las interacciones de los compuestos a nivel molecular con ambos transportadores.
    a. Caracterizar la interacción con ABCG2 y P-gp de diferentes compuestos midiendo la actividad ATPasa a nivel basal y la inducida en vesículas de membrana obtenidas a partir de células que sobre-expresan el transportador objeto de interés..
    b. Caracterizar la actividad de superficie de los compuestos para evaluar los coeficientes de partición aire-agua y las aéreas transversales en su conformación de unión a la membrana, lo que permitirá una estimación de los coeficientes de partición lípido-agua.
    c. Correlacionar los parámetros obtenidos en los experimentos anteriores.
5. Estudiar la correlación entre la actividad ATPasa de ambos transportadores y el ratio de transporte en experimentos de transporte y acumulación con hormonas esteroideas.
    a. Analizar la medición de la actividad ATPasa de ABCG2 y P-gp inducida por hormonas en vesículas de membrana obtenidas a partir de células que sobre-expresan el transportador objeto de estudio.
    b. Analizar la estimación de la difusión pasiva de las hormonas mediante medidas de actividad de superficie.
    c. Correlacionar la actividad ATPasa con experimentos de transporte y acumulación teniendo en cuenta la difusión pasiva.
6. Estudiar la correlación entre la actividad ATPasa y los resultados de otros experimentos *in vitro* e *in vivo* para ambos transportadores utilizando fluoroquinolonas.
    a. Evaluar la actividad ATPasa de ABCG2 y P-gp de cinco fluoroquinolonas en vesículas de membrana.

b. Estudiar el transporte transepitelial *in vitro* de las fluoroquinolonas y su efecto sobre los ensayos de acumulación de mitoxantrona usando células transducidas con ABCG2.

c. Realizar experimentos *in vivo* con ratones de tipo *wild-type* y Abcg2-*knockout* utilizando estos antibióticos.

d. Correlacionar la actividad ATPasa con experimentos de transporte, acumulación e *in vivo* empleando también datos de resultados publicados relacionados con la interacción de estas fluoroquinolonas con ABCG2 y P-gp.

4. Materiales y Métodos

Células. Los fibroblastos embrionarios de ratón transfectados de forma estable con el gen MDR1 humano (NIH-MDR1-G185) fueron generosamente donados por los Dr. M.M. Gottesman y Dr. S.V. Ambudkar (National Institutes of Health, Bethesda, MD). Las células fueron cultivadas como se ha descrito previamente (Nervi y cols., 2010; Gatlik-Lywojtowicz y cols., 2004). Los fibroblastos embrionarios derivados del triple *knockout* Mdr1a/b$^{-/-}$, Mrp1$^{-/-}$mice (MEF3.8) y las células renales de perro (MDCK-II) con sus respectivos subclones transducidos de forma estable con los genes ABCG2 humano y Abcg2 de ratón (Allen y cols., 1999; Jonker y cols., 2000; Jonker y cols., 2002; Pavek y cols., 2005) fueron proporcionados amablemente por el Dr. A.H. Schinkel (Netherlys Cancer Institute, Amsterdam, The Netherlys). Las células crecieron en idénticas condiciones a las descritas por Allen y cols. (1999; 2000). Las vesículas de membrana invertidas de células de mamífero con ABCG2 humana (ABCG2-M-ATPasa) fueron compradas a la empresa SOLVO Biotechnology.

Métodos para la cuantificación de la expresión de ABCG2. Se realizó *Western blotting* o *inmunoblotting* con vesículas de membrana de células MEF3.8 y vesículas ABCG2-M-ATPasa, primero fraccionándolas en un SDS-PAGE al 10% y transfiriéndolas después a una membrana de nitrocelulosa que fue incubada con un anticuerpo primario específico de BCRP (BXP-21) y posteriormente con un anticuerpo secundario de cabra (Ig-AP), que se reveló mediante la reacción enzimática colorimétrica NBT/BCIP. El análisis cuantitativo se realizó utilizando el programa *Quantity One® Software Version* 4.2 de Bio-Rad.

Se cuantificó la proteína verde fluorescente (GFP) de las vesículas provenientes de células MEF3.8 en un espectrofotómetro *Spectramax M2*, corrigiendo por la fluorescencia del medio de solución y comparando con valoraciones de la proteína GFP pura. Esta proteína está presente en estas células porque el vector que se utilizó para la transducción de ABCG2 contiene también GFP (Figura 26, Página 104) (Pavek y cols., 2005); por tanto, a modo de aproximación se puede considerar que ambas proteínas (ABCG2 y GFP) se expresan en la misma cantidad.

Experimentos basados en membranas. La preparación de vesículas de membrana NIH-MDR1-G185 se realizó como se ha descrito en detalle anteriormente (Aänismaa y Seelig, 2007). En la Figura 27 (Página 105) se puede ver una ilustración esquemática de los diferentes pasos empleados en el procedimiento. A modo de resumen, una vez que las células crecieron hasta la confluencia, se aislaron y centrifugaron varias veces para eliminar las distintas fracciones celulares (mitocondrias, núcleos…), después se pasaron por un *"One Shot" cell disrupter* que genera las vesículas invertidas y tras una última centrifugación (esta vez ultracentrifugación), las vesículas se homogenizaron y se almacenaron a -80 ºC. La concentración final de proteína se determinó mediante el ensayo BCA con BSA. La preparación de vesículas de membrana a partir de células MEF3.8 transducidas con ABCG2 humana se realizó de manera similar, con una pequeña variación en la primera centrifugación, aplicando menos revoluciones.

Optimización de los ensayos de actividad ATPasa. La optimización de las condiciones para realizar los ensayos de actividad ATPasa con membranas NIH-MDR1-G185 ha sido previamente publicada (Ambudkar, 1998; Aänismaa y Seelig, 2007). Para optimizar dichos parámetros para el caso de las vesículas ABCG2-M-ATPasa se utilizaron las condiciones descritas previamente por Litman y cols. (1997a) y Aänismaa y Seelig (2007) para realizar los ensayos de actividad ATPasa y se analizaron los parámetros: tiempo de incubación a 37 °C (30-90 min), concentración de membrana (0,025-1 mg/ml), dependencia de pH (pH= 5-8,5), concentración de vanadato (10^{-7}- 0,5 mM) y dependencia de ATP (0,07-6,35 mM). Para los experimentos dependientes del tiempo de incubación y la concentración de membrana se utilizó la sulfasalazina como fármaco evaluado, por ser considerado el mejor compuesto para testar membranas ABCG2-M-ATPasa (Glavinas y cols., 2007).

Medidas de actividad ATPasa. La hidrólisis de ATP asociada a la actividad de ABCG2 y P-gp fue determinada cuantificando la liberación de fosfato inorgánico mediante un ensayo colorimétrico de acuerdo con Litman y cols. (1997a) con pequeñas modificaciones (Aänismaa y Seelig, 2007). En la Figura 28 (Página 107) se puede ver un diagrama de los pasos consecutivos de este experimento. Básicamente, tras la preparación del buffer ATPasa a pH 7,4 a temperatura ambiente (que incluye inhibidores de varias ATPasa inespecíficas, Ambudkar, 1998) y de las diluciones del compuesto a testar (en agua o DMSO), se añadieron a los pocillos de una placa de 96 pocillos vanadato (utilizado como control negativo por inhibir la actividad ATPasa (Urbatsch y cols., 1995)), el buffer con las membranas (0,1 mg/mL para P-gp y 0,075 mg/mL para ABCG2) y ATP, y las diluciones del compuesto (volumen total del pocillo: 60 µl). Después de agitar, se incubaron durante 60 minutos en oscuridad a 37 ºC tras lo cual se paró la reacción con hielo y la solución stop; la reacción colorimétrica resultante de la última incubación se midió mediante un espectrofotómetro *Spectramax M2*. El rango de concentraciones escogidas para testar fue entre un punto algo más bajo que cuando la presión comienza a incrementarse en SAM hasta la CMC o el límite de solubilidad. Los datos fueron analizados con el coeficiente de Hill (Ecuación 1) o con la Ecuación modificada de Michaelis-Menten (Ecuación 2). De la Ecuación 2 se derivan los parámetros cinéticos K_1 (concentración con la que se obtiene la mitad de la activación máxima, K_2

(concentración con la que se obtiene la mitad de la inhibición máxima), V_1 (máxima actividad de transporte) y V_2 (mínima actividad de transporte). Los resultados se expresaron considerando la actividad basal como 100% y el incremento o disminución sobre estos valores basales se exponen en función de la concentración de compuesto (escala Log).

Experimentos basados en células. Los estudios de transporte transepitelial se realizaron cultivando en placas *Transwell* hasta la confluencia los tres tipos celulares de MDCK-II para ABCG2. Después de comprobar que la resistencia transepitelial fuese óptima, se pre-incubó las placas durante 2 horas con medio Opti-MEM (libre de suero) con o sin el potente y selectivo inhibidor de ABCG2, Ko143 (1 μM). El experimento comenzó añadiendo en el compartimento donante (apical o basal) el sustrato a testar (10 μM) en presencia o ausencia de Ko143. Se tomaron muestras a las 2 y 4 h que se congelaron hasta su análisis mediante HPLC. Los resultados se representaron como el porcentaje de compuesto recogido en el compartimento aceptor en relación a la concentración añadida al compartimento donante al comienzo del experimento (Figura 29, Página 109). Se calcularon también los respectivos ratios de transporte (B-A/A-B) a las 4 horas de comenzar el experimento.

Los experimentos de acumulación de mitoxantrona (MXR) para testar las fluoroquinolonas como inhibidores se realizaron basándose en los métodos publicados anteriormente por Pavek y cols. (2005). Brevemente, las células cultivadas en placas de 24 pocillos hasta la sub-confluencia se pre-incubaron 1 hora con Opti-MEM con o sin Ko143 (1 μM) y diferentes concentraciones de las fluoroquinolonas a testar. La incubación se realizó con MXR (10 μM) con o sin Ko143 durante una hora. Después de parar la incubación, se cuantificó la acumulación de MXR con un citómetro de flujo *CYAN cytometer* midiendo la mediana de fluorescencia. Los datos de los histogramas se procesaron utilizando el software *SUMMIT version 4.3*.

La actividad ATPasa de ABCG2 en células vivas a tiempo real se midió utilizando un microfisiómetro *Cytosensor* (Figura 30, Página 110) monitorizando el ratio de acidificación extracelular (ECAR). El procedimiento se llevó a cabo de manera similar a los experimentos descritos con P-gp (Lywojtowicz y cols., 2002; Gatlik-Lywojtowicz y cols., 2004; Gatlik- Lywojtowicz y cols., 2006; Aänismaa y Seelig, 2007; Nervi y cols., 2010), incluyendo la calibración del instrumento y los ciclos de estimulación de ABCG2 con los compuestos a testar. De manera concisa, tras calibrar el *Cytosensor,* a las células crecidas durante la noche se les expuso a ciclos de flujo del medio con los compuestos a testar y se realizaron medidas de acidificación con el programa *Cytosoft* durante los periodos de interrupción del flujo. Los resultados se pueden expresar en porcentaje de actividad respecto a la basal o en valores absolutos de protones por célula por segundo (H+/cell/s).

Métodos para estudiar la difusión pasiva. Las medidas de actividad de superficie (SAM) se realizaron como se ha descrito anteriormente (Seelig y cols., 1994; Fischer y cols., 1998; Gerebtzoff y cols., 2004). Las mediciones se realizaron en una cubeta de teflón de 20 ml diseñada por Fromherz

(Fromherz y Marcheva 1975), con buffer (Tris/HCl 50 mM y 114 mM NaCl) ajustado a pH 7,4 a temperatura ambiente. Tras una cuidadosa limpieza del aparato e instrumentos, la presión de superficie se monitorizó con un papel de filtro conectado a una balanza Wilhelmy (Figura 31, Página 111), previamente equilibrada, inyectando soluciones madre seriadas de cada compuesto preparadas en agua, DMSO o metanol. Se monitorizaron las curvas SAM hasta alcanzar el equilibrio, la CMC (concentración crítica micelar) (Figura 25, Página 93). Los datos se representaron en gráficas p/Log C donde la parte lineal ascendente fue ajustada a la Ecuación de la isoterma de Gibbs (Ecuación 4) (línea sólida). A partir de los datos obtenidos se calcularon el coeficiente de partición aire-agua (K_{aw}) (Ecuación 5), y el flujo debido a la difusión pasiva (Ecuación 7, 8, 9).

A modo de comparación y corroboración también se realizaron medidas de calorimetría de titulación isotérmica (ITC). Se inyectó una suspensión de vesículas lipídicas de POPC en la solución del compuesto en el calorímetro previamente calibrado; el lípido y el compuesto están suspendidos en buffer, que fue el mismo que para SAM. Los resultados fueron obtenidos mediante un programa informático diseñado por MicroCal.

Determinación de parámetros. Como ya se ha comentado anteriormente, a partir del coeficiente de partición aire-agua (K_{aw}) y del área transversal de superficie (A_D) de la molécula analizada (obtenidos por SAM) se puede estimar el coeficiente de partición lípido-agua (K_{lw}) (Ecuación 6). La constante de unión del sustrato desde el agua al transportador (K_{tw}) es la inversa de la mitad del máximo de activación (K_1) de la Ecuación modificada de Michaelis-Menten en las medidas de actividad ATPasa (Seelig y Gatlik- Lywojtowicz, 2005) (Ecuación 2). La constante de unión del lípido al transportador (K_{tl}) no se puede medir, pero se puede estimar a partir de las dos constantes anteriores (Ecuación 11), considerando que en el modelo de unión en "dos pasos" K_{tw} es el producto de K_{lw} y K_{tl} (Ecuación 10) (Figura 16, Página 54) (Seelig y Gatlik- Lywojtowicz, 2005). También se calcularon las energías libres de estas tres constantes (Ecuación 12 y 13).

Estudios farmacocinéticos *in vivo*. Los ratones knockout y wild-type (proporcionados amablemente por el Dr. A.H. Schinkel, (Netherlands Cancer Institute, Amsterdam, The Netherlands) fueron administrados en ayunas por vía oral con norfloxacina o pefloxacina (10 mg/kg). Una vez anestesiados se recogieron muestras de sangre a distintos tiempos y los animales fueron sacrificados por dislocación cervical. En los experimentos realizados con machos, se recogieron órganos y fluidos, y de las hembras se tomaron muestras de leche con una bomba de succión. En el experimento de administración crónica, la norfloxacina fue administrada por vía oral diariamente a 10 mg/kg durante 7 días y se recogieron muestras de sangre cada dos días; además, los ratones se mantuvieron en jaulas metabólicas y se tomaron muestras de heces y orina a las 24 h de comenzar el experimento y también de orina a los 60 min después de esta primera administración. Se extrajo el plasma de las muestras de sangre heparinizada y todas las muestras de plasma, órganos y fluidos se congelaron hasta su análisis

mediante HPLC. Se calcularon los ratios de concentración en tejido en relación a la concentración en plasma y las áreas bajo la curva de concentraciones plasmáticas (AUC).

Análisis por HPLC. Las condiciones para el análisis de muestras conteniendo fluoroquinolonas por cromatografía líquida de alta eficacia (HPLC) fueron establecidas como se describió anteriormente, con ligeras modificaciones (Garcia y cols., 2000; Tsai, 2001; Merino y cols., 2006). Las muestras mantenidas a 4 ºC se separaron a 278 nm en una columna de fase reversa tipo *Phenomenex Synergi* a temperatura ambiente en un sistema cromatográfico *Waters*; la integración se realizó con el software *Empower.* Las muestras de transporte fueron inyectadas directamente en el HPLC y analizadas con una fase móvil de ácido ortofosfórico y acetonitrilo (75:25 v/v aprox.). Las muestras del análisis farmacocinético fueron homogenizadas y después procesadas para eliminar los restos orgánicos y utilizando enrofloxacina como estándar interno fueron inyectadas en el HPLC usando una fase móvil de buffer citrato y acetonitrilo (83:17 v/v). En ambos casos se realizaron curvas de calibración con muestras estándar.

Análisis estadístico. Los resultados se representaron como la media ± la desviación estándar (SD) de al menos 3 experimentos independientes realizados en cada caso. Para evaluar las diferencias significativas se aplicó el test de *t* de Student.

5. Resultados y Discusión

5.1. Comparación de la actividad ATPasa, la especificidad y las relaciones de estructura-actividad entre ABCG2 y P-gp

Para conseguir el primer objetivo de este trabajo de investigación caracterizamos la interacción de 28 compuestos con ABCG2 y P-gp midiendo la actividad ATPasa basal e inducida de ABCG2 y P-gp en vesículas de membrana. Para ello, previamente analizamos las vesículas utilizadas para los ensayos con ABCG2 y optimizamos las condiciones de los ensayos de actividad ATPasa. Además, realizamos medidas de actividad de superficie (SAM) con los 28 compuestos. Los resultados de ambos experimentos nos permitieron calcular diferentes coeficientes. Con este procedimiento explicamos la actividad, características y mecanismos de estos dos transportadores; estos principios fueron confirmados realizando el mismo procedimiento con otras 10 moléculas, incluidos detergentes. Además, se realizaron experimentos con *Cytosensor* testando ABCG2.

Cuantificación de la expresión de ABCG2. Para poder realizar estudios de actividad ATPasa primero es necesario cuantificar la expresión de proteína de la célula original o de sus vesículas. Las células NIH-MDR1-G185 han sido caracterizadas y la expresión de P-gp cuantificada previamente (Ambudkar y cols., 1997; Lywojtowicz y cols., 2002; Gatlik-Lywojtowicz y cols., 2004). La expresión de

ABCG2 ha sido ampliamente estudiada de una forma cualitativa, pero no se conocen casos de cuantificación. Como se ha comentado anteriormente, es difícil conseguir vesículas de membrana con niveles suficientes de ABCG2 como para poder estimular la actividad ATPasa (Glavinas y cols., 2007; Ni y cols., 2010); por ello la mayoría de los trabajos publicados utilizan células Sf9 de insecto, que por su parte presentan el problema de carecer de colesterol, siendo la composición de la membrana muy diferente de la de los mamíferos, lo que afecta a los resultados (Glavinas y cols, 2007; Aänismaa y cols., 2008; Pal y cols., 2007; Telbisz y cols., 2007). Por esta razón, preferimos utilizar las vesículas ABCG2-M-ATPasa de mamífero propuestas por Glavinas y cols. (2007). Las correspondientes células de donde provienen las vesículas de membranas ABCG2-M-ATPasa que permitirían la cuantificación de la expresión de ABCG2 no están disponibles. Por tanto, el nivel de expresión de ABCG2 en dichas vesículas fue estudiado combinando tres aproximaciones, comparando las vesículas ABCG2-M-ATPasa con vesículas provenientes de células MEF3.8 transducidas con ABCG2 humana.

Primero se realizó *Western blotting* con ambos tipos de membrana (Figura 32, Página 120) y del consiguiente análisis densitométrico se dedujo que la concentración de ABCG2 en las membranas ABCG2-M-ATPasa era al menos 7 veces mayor que en las de MEF3.8.

Después se cuantificó la proteína GFP de las células MEF3.8 (Figura 33, Página 121). Comparando la fluorescencia obtenida de las células con curvas de calibrado de GFP comercial, se obtuvo que hay aproximadamente 10^6-10^7 moléculas de GFP/ABCG2 por célula de MEF3.8; considerando que la unidad funcional de ABCG2 es un homodímero habrá entre 5×10^5- 5×10^6 moléculas de ABCG2 funcional por célula. Por tanto, teniendo en cuenta los resultados de *Western blotting,* para las membranas ABCG2-M-ATPasa, la expresión de ABCG2 será de entre $7\times(5\times10^5 - 5\times10^6)$, es decir, $3{,}5\times10^6 - 3{,}5\times10^7$ moléculas por célula. A modo de comparación, se calculó que para las células NIH-MDR1-G185 había del orden de 10^6 moléculas de P-gp por célula (Ambudkar y cols., 1997), que está en el mismo orden de magnitud que los $10^5 - 10^6$ dímeros de ABCG2 para las células MEF3.8 (las células MEF3.8 y NIH-MDR1-G185 son fibroblastos).

Somos conscientes de que utilizar GFP como método para cuantificar ABCG2 tiene varias limitaciones. Para empezar, debido a que en el vector de clonación el sitio IRES se encuentra entre GFP y ABCG2, podría ser posible que ambas proteínas no se traduzcan el mismo número de veces. Además, GFP se podría adherir a la placa utilizada para el experimento, aunque esto no parece afectar demasiado al resultado final pues cuando se realizó la pre-incubación con BSA recomendada por Wilma van Esse y cols. (2011) para prevenir la adherencia, se obtuvieron los mismos resultados que sin dicha pre-incubación. Incluso podrían ocurrir otras interferencias como reflejos durante la lectura de la placa. A pesar de las limitaciones que puedan presentar los tres métodos empleados, las tres aproximaciones dieron lugar a conclusiones similares respecto al número de moléculas ABCG2 por célula.

La tercera aproximación consistió en la comparación de ensayos de actividad ATPasa con vesículas de membrana ABCG2-M-ATPasa y obtenidas de células MEF3.8 utilizando sulfasalazina como compuesto analizado bajo las mismas condiciones (ver más abajo la optimización de las condiciones para el ensayo de ATPasa); comprobamos primero que las condiciones utilizadas para las vesículas ABCG2-M-ATPasa eran también válidas para las de MEF3.8. Se realizaron experimentos a diferentes concentraciones de proteína. De la Figura 36 (Página 124) se deduce que la actividad ATPasa inducida con sulfasalazina fue alrededor de 5 veces mayor en las membranas ABCG2-M-ATPasa que MEF3.8 (observando la diferencia entre ambos V_1, máxima actividad), lo que está en concordancia con los resultados obtenidos del *Western blotting* (Figura 32, Página 120).

De manera adicional, los resultados mostraron parámetros K_1 comparables para ambas vesículas (ABCG2-M-ATPasa y vesículas provenientes de células MEF3.8) (Figura 34, Página 122), indicando que la densidad de empaquetamiento de la membrana de ambas células es similar. Teniendo en cuenta que las células MEF3.8 y NIH-MDR1-G185 son fibroblastos, es posible que entonces la densidad de empaquetamiento sea similar para los tres tipos celulares y por tanto que las tres tengan concentraciones de proteína total comparables.

Optimización de la condiciones de actividad ATPasa para ABCG2 con las vesículas de membrana ABCG2-M-ATPasa. La concentración de proteína fue probada en el rango 0,025-0,125 mg/ml usando sulfasalazina y se observó que V_1 es constante en el rango de concentraciones 0,05 – 0,1 mg/ml (Figuras 36 y 37, Páginas 124 y 125); por tanto se escogió 0,075 mg/ml como una concentración apropiada para realizar los experimentos, por ser la intermedia. Añadir que obtuvimos una media de actividad basal de ABCG2 semejante a la obtenida por los autores de estas membranas (Figura 36, Página 124) (Glavinas y cols., 2007). Además, teniendo en cuenta que las tres líneas celulares presentan una cantidad de proteína total similar y el número de moléculas de transportador por célula, se deduce que la actividad ATPasa basal es menor para ABCG2 que para P-gp (Figura 36, Página 124). De acuerdo con nuestra conclusión se ha dicho que, en general, ABCG2 presenta una actividad ATPasa basal que es considerablemente menor que la de P-gp (Ni y cols., 2010); una excepción la presentan los ensayos realizados con Sf9 (Ozvegy y cols., 2001).

Para el tiempo de incubación a 37 °C probado entre 30 y 90 min se observó una correlación lineal hasta 60 min (Figura 38, Página 125) y se escogió 60 min para los sucesivos experimentos. El pH del buffer se examinó entre pH= 5-8,5, no se observó ningún efecto en la actividad ATPasa basal entre los pH 6 y 8 (Figura 39, Página 126); los subsiguientes experimentos se realizaron por tanto a pH fisiológico (pH 7,0 a 37 ºC). Estos resultados son similares a los obtenidos para P-gp (Aänismaa y Seelig, 2007) pero difieren de otro transportador ABC, Sav1866, donde se encontró una dependencia del pH más pronunciada (Beck y cols., 2013). En nuestros resultados, a pH < 6 la actividad ATPasa basal de ABCG2 disminuye de forma sigmoidea (Figura 39, Página 126). Se ha comentado que el transporte de

ABCG2 es más eficiente en ambientes ácidos y que esta dependencia del pH es específica de ABCG2, pues no se da en P-gp, MRP2 o MRP5 (Breedveld y cols., 2007; Li y cols., 2011). Otros autores encontraron sólo en algunos casos esta mayor actividad ATPasa de ABCG2 con vesículas ABCG2-M-ATPasa a pH=5,5 (Glavinas y cols., 2007), que podría ser debido a esta disminución de la actividad basal a pH bajo.

La optimización de la concentración de vanadato se analizó entre 10^{-7}- 0,5 mM, obteniéndose una inhibición completa de la actividad ATPasa a la concentración de 0,1 mM (Figura 40, Página 127); por tanto para realizar los sucesivos experimentos de actividad ATPasa se escogió la concentración de 0,5 mM para garantizar la inhibición. Estos datos son comparables a los obtenidos por Ozvegy y cols. (2001) para las células Sf9. La actividad ATPasa de ABCG2 en función de la concentración de ATP (0,07-6,35 mM) dio lugar a una curva en forma de campana (primero activación a bajas concentraciones y segundo inhibición a altas concentraciones) con el máximo de actividad a la concentración 3 mM de ATP aproximadamente (Figura 41, Página 127), concentración escogida para subsiguientes experimentos. La disminución de la actividad ATPasa podría ser atribuida a la acumulación y unión de ADP (Beck y cols., 2013). Ensayos similares realizados anteriormente con las vesículas ABCG2-M-ATPasa a mayores concentraciones de membrana y de $MgCl_2$ dieron lugar a curvas sólo ascendentes (Glavinas y cols., 2007).

La optimización de las condiciones para realizar los ensayos de actividad ATPasa de P-gp con membranas NIH-MDR1-G185 ha sido realizada anteriormente (Litman y cols., 1997 a y b; Ambudkar, 1998; Aänismaa y Seelig, 2007). Las condiciones obtenidas para medir la actividad ATPasa de ABCG2 fueron idénticas a las asignadas para P-gp, excepto que la concentración de membrana utilizada para P-gp es algo mayor. Esta ha sido la primera vez que se optimizan las condiciones para alguna vesícula de membrana sobre-expresando ABCG2.

Medidas de actividad ATPasa en vesículas de membrana para ABCG2 y P-gp. Actividad ATPasa con 28 compuestos. La lista de compuestos escogidos para este estudio se encuentra en la Tabla 9 (Página 129); incluye compuestos típicos que interaccionan con P-gp o ABCG2, hormonas, fluoroquinolonas y otros. Los compuestos se clasificaron de acuerdo a su carga eléctrica a pH fisiológico y también se definieron tres grupos en base a la distribución molecular de grupos polares (hidrofílico) o no polares (hidrofóbico) en su estructura: los compuestos del grupo I son anfifílicos con una terminación polar y otra apolar, los compuestos del grupo II tienen un centro polar y dos ramas apolares, los compuestos del grupo III tienen un centro apolar y dos ramas polares (Figura 42, Página 130).

Los compuestos de las Figuras 43 a 45 (Páginas 131 a 133) están organizados de acuerdo a cómo interaccionan con los transportadores ABCG2 y P-gp: en las Figuras 43 y 44 interaccionan con ambos transportadores y en la Figura 45 sólo con ABCG2; además, en la Figura 43 los compuestos tienen carga neutra, en la Figura 44 sobre todo positiva y en la Figura 45 positiva y/o negativa.

En las Figuras 43 y 44 A y B (Páginas 131 y 132) se encuentran los compuestos que típicamente interaccionan con P-gp, dando lugar a curvas características en forma de campana dependientes de concentración, y otros compuestos que dieron lugar a curvas con sólo activación de la actividad ATPasa de P-gp. Por el contrario, todos los compuestos de estas Figuras apenas aumentan sino más bien disminuyen la actividad ATPasa de ABCG2, indicativo de que interactúan inhibiendo directamente a ABCG2. En la Figura 44 C (Página 132) se encuentran los únicos 2 compuestos que interaccionan con ambos transportadores dando lugar a curvas en forma de campana. En la Figura 44 D (Página 132) se encuentra la familia de los antagonistas del receptor H_2, que dan lugar a curvas de sólo activación de la actividad ATPasa para los dos transportadores (excepto la ranitidina que interacciona con ABCG2 con una curva de inhibición). La Figura 45 (Página 133) incluye compuestos típicos para ABCG2 que no parecen interaccionar con P-gp; exceptuando sulfasalazina, que es el compuesto con la mayor respuesta de actividad ATPasa de ABCG2 dando lugar a una curva en forma de campana, con la mayoría de los compuestos se obtienen prácticamente sólo curvas con una ligera activación. El metotrexato no estimuló la actividad ATPasa de ninguno de los dos transportadores.

Los resultados de las Figuras 43-45 (Páginas 131 a 133) para ambos transportadores están en consonancia con otros publicados con los compuestos analizados, aunque no fueron realizados con las mismas membranas celulares. Por ejemplo, daunorubicina, metotrexato, prazosina, progesterona y tamoxifen para P-gp (Litman y cols., 1997; Ramachyra y cols., 1998) y daunorubicina, digoxina, Ko143, mitoxantrona, ranitidina, sulfasalazina, testosterona, verapamilo para ABCG2 (Ozvegy y cols., 2001; Glavinas y cols., 2007). Hay dos casos particulares en la interacción con ABCG2. Primero, el metotrexato fue transportado en membranas Sf9 y ABCG2-M-ATPasa (Ozvegy-Laczka y cols., 2005; Glavinas y cols., 2007) únicamente a concentraciones muy bajas, en el rango de pmol, y en concordancia nosotros no pudimos ver el transporte a concentraciones mayores, en el rango de µM. El otro caso es que todos los compuestos analizados en vesículas de membrana de células *L. lactis* dan curvas de activación e inhibición para la ATPasa de ABCG2 (Janvilisri y cols., 2003), por ejemplo para las hormonas, para las cuales nosotros obtenemos sólo inhibición. Las diferencias pueden ser debidas a la diferente composición lipídica entre ambos tipos celulares (In 't Veld y cols., 1991), junto con la mayor concentración de membrana utilizada por Janvilisri y cols. (2003) en los experimentos, aproximadamente 10 veces más que nosotros. Se ha comprobado que una mayor concentración de membrana en los ensayos de ATPasa favorece la obtención de actividad ATPasa (Beck y cols., 2013).

En la Tabla 9 (Página 129) se representan también los parámetros cinéticos (K_1, K_2, V_1 y V_2) obtenidos a partir de la evaluación de actividad ATPasa de ABCG2 y P-gp aplicando la Ecuación 2. Los parámetros cinéticos de la parte de inhibición (K_2, V_2) de las curvas que sólo presentaron activación de la actividad ATPasa (debido a agregación vesicular o precipitación del compuesto) no se pudieron calcular de forma apropiada, de la misma manera tampoco los parámetros de activación (K_1, V_1) de curvas que sólo presentaron inhibición.

En resumen, veinte de los compuestos analizados interaccionan con ambos transportadores; aproximadamente la mitad de ellos presentan sólo curvas de inhibición para ABCG2, y activación o curvas en forma de campana para P-gp. La otra mitad de los compuestos producen sólo activación de la actividad ATPasa de ambos transportadores o sólo de ABCG2. Sólo dos compuestos dan curvas en forma de campana para ambos transportadores (Figura 44 C, Página 132). En general, P-gp tiene mayor estimulación de la actividad ATPasa que ABCG2 para los compuestos analizados en este estudio.

Hemos comprobado que ambos transportadores, ABCG2 y P-gp, pueden dar lugar a curvas en forma de campana (primero activación a bajas concentraciones y segundo inhibición a altas concentraciones), cuya mejor interpretación es mediante el modelo de unión en "dos pasos" y la evaluación cinética mediante la ecuación modificada de Michaelis-Menten (Ecuación 2) (Litman y cols., 1997a). Comparando con la literatura publicada para ABCG2, las curvas bifásicas (en forma de campana) de actividad ATPasa se han observado en pocos casos, por ejemplo usando células *L. lactis* (Janvilisri y cols., 2003; Cooray y cols., 2004) células *high-five* de insecto (Dai y cols., 2008) o usando sulfasalazina (Glavinas y cols, 2007); en la mayoría de las publicaciones se encuentran curvas de activación o inhibición (Figura 63, Página 174) (ej: Ozvegy y cols., 2001; Ozvegy-Laczka y cols., 2004; Glavinas y cols., 2007). Eso explica porqué la evaluación de la actividad ATPasa de ABCG2 suele hacerse con la cinética simple de Michaelis-Menten (ej: Ozvegy y cols., 2001; Wu y cols., 2007; Robey y cols., 2009); de hecho, la cinética de la ecuación modificada de Michaelis-Menten, si sólo existe activación, se corresponde con la ecuación simple (Seelig y Lywojtowicz, 2000). Las curvas "simples" de actividad ATPasa, sólo activación o inhibición, encontradas de manera más habitual para ABCG2 se pueden explicar en términos de carga y concentración; los compuestos que dan curvas de inhibición son neutros y catiónicos y producen su inhibición a concentraciones en el rango de nM o µM (Ozvegy y cols., 2001; Ozvegy y cols., 2002; Ozvegy-Laczka y cols., 2004; Glavinas y cols, 2007), la parte de activación es más difícil de conseguir experimentalmente por encontrarse a concentraciones sumamente bajas. Los sustratos típicos de ABCG2 son sobre todo aniónicos e zwiteriónicos (con carga positiva y negativa), y suelen dar curvas sólo de activación de actividad ATPasa (Ozvegy y cols., 2001; Glavinas y cols, 2007) porque a la parte de inhibición es difícil de llegar debido a que a tan altas concentraciones se dan problemas de agregación. De hecho, como se verá más adelante, para estos compuestos también es complicado obtener medidas de SAM, la CMC no se puede alcanzar debido a problemas de agregación.

Basándose en este set de compuestos analizados es posible clasificarlos de acuerdo a su carga eléctrica frente a la tendencia de los resultados de actividad ATPasa con ABCG2 y P-gp (Tabla 10, Página 135). Los compuestos neutros o catiónicos inducen la activación de P-gp e inhiben la ABCG2. Los compuestos que tienen una ligera carga positiva también pueden activar ABCG2. Por otra parte, los compuestos zwiteriónicos y aniónicos interaccionan sólo con ABCG2. Existen dos excepciones de compuestos aniónicos: glibenclamida que interacciona con P-gp, y metotrexato, que no interacciona con ninguno de los dos transportadores (aunque, como hemos comentado, interaccionará activando ABCG2

a concentraciones menores de las que se pueden utilizar en nuestros experimentos). Nuestros resultados están en concordancia con lo que ya se sabía para P-gp, los compuestos neutros y catiónicos interaccionan con él, pero no los que tienen carga negativa (Schinkel y cols., 1996; Seelig, 1998; Sharom, 2008). Referido a ABCG2, se ha dicho que transporta moléculas cargadas negativa y positivamente y también neutras (Xia y cols., 2005; Krishnamurthy y Schuetz, 2006; Ni y cols., 2010); nuestros resultados dan diferentes comportamientos de actividad ATPasa para estos compuestos (Tabla 10, Página 135), los neutros y catiónicos tienen una alta afinidad por ABCG2, mientras que los negativos y zwiteriónicos se unen de manera menos fuerte y son transportados más rápidamente.

Los sustratos típicos de ABCG2 no dan curvas de actividad ATPasa para P-gp (Figura 45, Página 133, no hay resultados para P-gp), indicando que apenas existe interacción con P-gp. Los sustratos típicos de ABCG2 no son anfifílicos y están altamente cargados con al menos una carga negativa, por tanto difunden despacio a través de la membrana; ambos factores no favorecen en absoluto la interacción con P-gp, primero porque la difusión es el factor limitante para la interacción con P-gp (Seelig y Lywojtowicz, 2000; Aänismaa y Seelig, 2007) y segundo porque los compuestos aniónicos apenas interaccionan con P-gp (Seelig, 1998). Por tanto, debido a las características físico-químicas de los sustratos típicos de ABCG2, si son transportados por P-gp, serán transportados despacio.

La hidrofobicidad ha sido una característica común en los modelos SAR y QSAR publicados para ABCG2 y P-gp (Seelig, 1998; Seelig y Lywojtowicz, 2000; Gandhi y Morris, 2009). En un análisis exhaustivo de nuestros datos se comprueba ve que para los compuestos muy hidrofílicos se obtienen curvas casi completas en forma de campana de actividad ATPasa de ABCG2 y no se puede alcanzar inhibición en el caso de P-gp, mientras que para los compuestos muy hidrofóbicos apenas hay activación en ABCG2 y se dan curvas completas para P-gp (Figuras 43 y 44, Páginas 131 y 132). De acuerdo con nuestras conclusiones, los compuestos hidrofílicos han sido descritos en la literatura como muy buenos sustratos pero no inhibidores de ABCG2, mientras que los hidrofóbicos actúan como inhibidores (Matsson y cols., 2007); clásicamente se ha considerado que P-gp interacciona con compuestos hidrofóbicos (Gottesman y Pastan, 1993; Schinkel y cols., 1996; Sharom, 2008). En relación a las interacciones de P-gp con los compuestos, se sabe que los máximos de actividad requieren altas concentraciones en el rango milimolar para compuestos muy hidrofílicos, micromolares para hidrofóbicos y nanomolares para los muy hidrofóbicos (Aänismaa y Seelig, 2007); lo cual parece ser también válido para ABCG2 (Figuras 43-45, Páginas 131 a 133).

En la Figura 42 (Página 130) se realizó una clasificación de los compuestos de acuerdo a la distribución de los centros hidrofóbicos e hidrofílicos en su molécula. Los compuestos anfifílicos normalmente presentan un centro hidrofóbico y otro hidrofílico y penetran en la membrana por el hidrofóbico (lipofílico) (tipo I). Los compuestos con dos terminaciones hidrofóbicas y un centro hidrofílico (tipo II) pueden tener estructura plana y rígida (penetran en la membrana con dificultad) o ser

capaces de doblarse y entrar en la membrana de manera análoga a los anfifílicos. Si los compuestos con estructura plana y rígida presentan carga positiva o neutra interaccionan con ambos transportadores. De manera análoga, los compuestos con dos terminaciones hidrofílicas y un centro hidrofóbico (tipo III) pueden doblarse bien o no, esto último suele ser lo habitual. Estos compuestos presentan carga aniónica o mixta (zwiteriónicos) (sustratos típicos de ABCG2 que no interaccionan con P-gp, con estructura rígida) o neutra (activan P-gp e inhiben ABCG2).

Los análisis SAR de Gandhi y Morris (2009) mostraron que un aspecto común requerido para la unión e inhibición de ABCG2 es la estructura plana; nosotros también hemos observado que la estructura plana es necesaria para la unión al transportador, sin embargo está relacionada con la activación, no con la inhibición de la actividad ATPasa de ABCG2.

Con esta combinación podemos explicar aparentes excepciones, por ejemplo, los antagonistas del receptor de H_2, interaccionan con ambos transportadores por su leve carga positiva, sin embargo, como la ranitidina es más hidrofóbica (Tabla 12, Página 138), interacciona inhibiendo directamente a ABCG2 (Figura 44, Página 132). La glibenclamida tiene carga negativa pero una estructura con dos terminaciones hidrofóbicas que le permiten penetrar bien en la membrana e interaccionar con el transportador P-gp.

Una conclusión que podemos sacar de este análisis SAR es que los compuestos que activan la actividad ATPasa de P-gp actuarán como inhibidores de ABCG2 (estos compuestos tienen carga neutra o positiva y son hidrofóbicos), excepto si tienen una carga positiva leve. Inversamente, un compuesto que activa la actividad ATPasa de ABCG2 no interaccionará con P-gp (estos compuestos tienen carga negativa y son hidrofílicos). Ambos transportadores parecen tener funciones complementarias en el tipo de compuestos transportados teniendo en cuenta su carga y su hidrofobicidad. Aunque tendrán que existir excepciones (serán necesarios más investigaciones para elucidarlo), esta pauta puede ser útil para predecir interacciones con estos dos transportadores.

Actividad ATPasa de ABCG2 con otras moléculas. Para investigar más a fondo el comportamiento de ABCG2, se testaron varios detergentes, azúcares, ácidos y lípidos cuya interacción con P-gp es bien conocida (Li-Blatter y cols., 2009; Li-Blatter y Seelig, 2010; Li-Blatter y cols., 2012). Las curvas de actividad ATPasa están representadas en la Figura 46 (Página 136) y los parámetros cinéticos derivados están expuestos en la Tabla 11 (Página 136). Los resultados obtenidos concuerdan con lo demostrado para el set de 28 compuestos; además, se comprobó que los compuestos muy hidrofóbicos inhiben directamente la actividad ATPasa de ABCG2 y los compuestos muy hidrofílicos presentan sólo la parte de activación de la curva, independientemente de su carga eléctrica. Sin embargo, para los compuestos que no presentan patrones para difundir en la membrana lipídica (no tienen patrones de tipo l ni tipo ll de HAP (Seelig, 1998)), no hay interacción con ABCG2, no hay señal de actividad ATPasa.

Estimación de la difusión pasiva. Medidas de actividad de superficie (SAM). La actividad de superficie en función de la concentración se midió para la lista de los 28 compuestos; los resultados están representados en la Figura 47 (Página 139) y los parámetros obtenidos de su evaluación están en la Tabla 12 (Página 138). Nótese que para algunos compuestos no se detectó actividad de superficie (*nd* en la Tabla 12, Página 138) y en algunos casos debido a la falta de anfifilicidad no hay apenas actividad o parte lineal; para muchos compuestos no se pudo alcanzar la CMC porque el compuesto precipitó antes o porque era demasiado hidrofílico.

Los compuestos analizados por SAM pueden ser divididos por tanto en dos grupos, el primer grupo está formado por aquellos compuestos anfifílicos con importante actividad de superficie, mostrando las típicas líneas ascendentes constantes lineales hasta la CMC desde donde se mantiene una actividad constante; estos compuestos son los sustratos característicos de P-gp. El segundo grupo son compuestos no anfifílicos con una actividad de superficie baja, dando lugar a extrañas curvas de actividad con forma sigmoidea (indicativo de absorción al teflón o de la orientación molecular de la carga (Fischer y cols., 1998)), con escalones (el compuesto forma varias monocapas dando lugar cada una a su propia actividad de superficie) y/o a cuyo CMC no se puede llegar o cuya actividad disminuye al llegar a la CMC (estos últimos dos casos se pueden explicar por problemas de agregación). Los compuestos no anfifílicos no pueden estimular apropiadamente la actividad de superficie, en consecuencia tampoco se pueden determinar de manera exacta los parámetros cinéticos derivados de SAM (Fischer y cols., 1998). En este segundo grupo se incluyen sustratos típicos de ABCG2, que muy probablemente crucen la membrana lentamente.

La calorimetría de titulación isotérmica (ITC) se utilizó como una segunda técnica para comparar los resultados obtenidos en algunos de los compuestos del segundo grupo con SAM. Los coeficientes K_{lw} obtenidos fueron mayores en ITC que en SAM (Tabla 13, Página 141); además en ITC, excepto en un caso, todos se encontraban en el rango de 10^3 M^{-1}. Consiguientemente, todos estos resultados de SAM e ITC dan una idea de la dificultad que tienen los compuestos típicos que interaccionan con ABCG2 y otros compuestos no anfifílicos para penetrar en la membrana.

Correlación de parámetros. Correlación entre V_1 y K_{tw}. Para investigar la relación entre la hidrólisis de ATP en los NBD y la unión del sustrato en los TMD, las V_1 fueron representadas en función de las energías libres de K_{tw} ($\Delta G°_{tw}$) (Figura 48, Página 142) para todos los compuestos cuyas actividades ATPasa y de superficie se pudieron determinar. Se sabe que para P-gp, cuanto más negativa es la energía libre de unión ($\Delta G°_{tw}$), mayor es la afinidad del compuesto por el transportador y menor es la actividad ATPasa, por tanto la tasa de transporte (Li-Blatter y cols., 2009). Para los compuestos típicos de P-gp (hidrofóbicos, anfifílicos y del tipo I y II; Tabla 9, Página 129) se observó esta correlación lineal entre la actividad ATPasa y la afinidad del sustrato, similar a la descrita por Aänismaa y Seelig (2007); los compuestos fuera de esta correlación son esencialmente compuestos típicos de ABCG2 (tipo III,

marcados en gris) no anfifílicos (Figura 48 A, Página 142). Por otra parte, en el caso de ABCG2, ocurre justo lo contrario (Figura 48 B, Página 142), la tasa de actividad ATPasa se incrementa linealmente al disminuir la energía libre (al incrementar la afinidad). Cada compuesto tiene mayor energía libre negativa para ABCG2 que para P-gp. Por tanto, la afinidad de sustrato es mayor para ABCG2 que para P-gp.

Correlación entre K_1 y $K_{aw.}$ Cuando se representó log ($1/K_1$) (proporcional a $\Delta G°_{tw}$, Ecuaciones 9 y 13) frente a log K_{aw} (refleja la anfifilicidad del compuesto), se obtuvo aproximadamente una correlación lineal para ambos transportadores (Figura 49, Página 144), dando lugar a K_{tl} (Ecuación 11). Destacar que los compuestos que no están en la línea de correlación sino situados más abajo, probablemente sea debido a que el pH utilizado en SAM no es favorable para estos compuestos cargados eléctricamente, pudiendo haber disociaciones que pueden afectar a los resultados.

Estudios con *Cytosensor*. Cuando se realizaron estudios con células MEF3.8 parentales y transducidas con ABCG2 humana en el microfisiómetro *Cytosensor*, ninguno de los intentos realizados a diferentes condiciones (Tabla 14, Página 145) dio lugar a una señal de acidificación atribuible al transportador. Estos resultados están probablemente relacionados no con una falta de actividad de ABCG2 con los compuestos testados (por ejemplo recuérdese que obtenemos curvas completas en ensayos de actividad ATPasa de sulfasalazina a las concentraciones utilizadas con el *Cytosensor* y que los resultados obtenidos con ambos métodos son comparables (Landwojtowicz et al., 2002; Gatlik-Landwojtowicz et al., 2004; Gatlik-Landwojtowicz et al., 2006; Aänismaa and Seelig, 2007)), sino más bien con el hecho de que debido a problemas de precipitación de los compuestos típicos de ABCG2 a concentraciones elevadas por su alta hidrofobicidad, a las concentraciones no citotóxicas con que se puede trabajar nos encontramos tan sólo al comienzo de la curva de activación ECAR, actividad ATPasa basal, donde el transportador está tomando de manera eficaz cada molécula de compuesto que cruza la membrana pero ECAR no es visible por ser muy bajas las concentraciones utilizadas del compuesto. Se sabe que las curvas de actividad ATPasa están desplazadas hacia la derecha en la escala de concentraciones en ensayos con células comparado con vesículas (Nervi y cols., 2010); por tanto, para poder observar actividad del transportador son necesarias mayores concentraciones de compuesto trabajando con el *Cytosensor*. Hasta la fecha no existe en la literatura ningún experimento con microfisiómetro *Cytosensor* estudiando el transportador ABCG2; por tanto, que sepamos, este ha sido el primer intento de medición realizado.

Con los datos obtenidos se ha realizado una **comparación entre ABCG2 y P-gp en términos cinéticos: relación de la actividad ATPasa y el transporte** que exponemos a continuación.

Se puede deducir de nuestros resultados de actividad ATPasa (Figuras 43-45, Páginas 131 a 133) que la mayoría de los compuestos inducen la actividad de P-gp de manera significativamente mayor que para ABCG2, por tanto, ABCG2 presenta generalmente una menor activación por el compuesto

comparado con P-gp. Este fenómeno se puede observar también en la mayoría resultados publicados para la actividad ATPasa de ABCG2 (Figura 63, Página 174) y ha sido relacionado con un bajo ratio de *turnover* que no permite detectar todo el fosfato inorgánico del ensayo (Glavinas y cols., 2007), con el alto nivel de actividad ATPasa basal en células Sf9 (Ozvegy y cols., 2001), o con la presencia de sustratos endógenos (Hegedus y cols., 2009).

A pesar del ratio bajo de actividad ATPasa para ABCG2, este transportador funciona de manera muy eficiente para los compuestos para los que está adaptado. Un ejemplo de ello fueron los resultados obtenidos con el *Cytosensor*, comentados anteriormente.

También **comparamos ABCG2 y P-gp en términos termodinámicos, esto es, especificidad de afinidad por el sustrato,** y exponemos nuestras conclusiones a continuación.

En relación al sitio de unión de los compuestos con ABCG2, los estudios de Rosenberg y cols. (2010) mostraron que la entrada a los NBD en la estructura abierta de ABCG2 es lo suficientemente grande como para permitir el acceso de compuestos desde el citoplasma. Por otra parte, SAM es escasamente medible para los compuestos típicos de este transportador, por lo que aparentemente K_{lw} parece no tener relevancia. Además, la escasa importancia de la anfifilicidad y la hidrofobicidad (prerrequisitos para la unión a la membrana (Seelig y Lywojtowicz, 2000; Sharom, 2008) para ABCG2, da una idea previa de que la membrana no tiene un papel significativo en el proceso de unión. Para comprobar este hecho se testaron una serie de detergentes, azúcares, ácidos y lípidos (Figura 46 y Tabla 11, Página 136) que presentan patrones que les permiten poder penetrar o no en la membrana lipídica. Encontramos que para los compuestos que no presentan patrones para difundir a la membrana lipídica, no hay interacción con ABCG2, no hay señal de actividad ATPasa. Parece por tanto, que la difusión a la membrana es un requisito para la interacción de los compuestos con ABCG2, tal y como se demostró anteriormente para P-gp. El modelo de unión en "dos pasos" es, en definitiva, adecuado para ambos transportadores (Figura 16, Página 54). Este modelo fue propuesto inicialmente para P-gp por Sauna y Ambudkar (2001) y sugerido después para ABCG2 por Matsson y cols. (2007) (Figura 10, Página 41).

De manera importante, a pesar de que la entrada en la membrana sea esencial para que los compuestos interaccionen con ABCG2, los parámetros que suelen definirlo: K_{lw}, anfifilicidad e hidrofobicidad parecen no serlo. Sin embargo, las interacciones entre sustratos y ABCG2 tienen un componente hidrofóbico, que parece explicar la mayor afinidad de los sustratos por ABCG2; este aspecto está ausente en P-gp. De hecho, fue sugerido que los sitios de unión a ABCG2 son posiblemente hidrofóbicos (Coburger y cols., 2010).

Otra conclusión importante a tener en cuenta de los ensayos de actividad ATPasa con ABCG2 para este segundo grupo de compuestos analizados es que los detergentes interaccionan con ABCG2 inhibiéndolo. Por tanto, cuando en el ABCG2 purificado con detergentes ha sido detectada una actividad basal baja (McDevitt y cols., 2006; Pozza y cols., 2006; Rosenberg y cols., 2010) la razón podría ser la

inhibición de ABCG2 por los detergentes usados. Estos detergentes también interaccionan con P-gp (Li-Blatter y cols., 2009). Por tanto, si el transportador ha sido solubilizado con detergentes, éstos podrían influir e interferir con los resultados de transporte.

Como hemos comentado anteriormente, de la Figura 48 (Página 142) se deduce que la afinidad de sustrato es mayor para ABCG2 que para P-gp, observándose de nuevo patrones complementarios entre ambos transportadores también en el caso de la afinidad como los hemos visto para la carga y la hidrofobicidad. Los compuestos con mucha afinidad por el transportador P-gp tienden a ocupar ambos sitios de unión y a inhibir P-gp (Li-Blatter y cols., 2009). Aunque existe un considerable solapamiento entre los sustratos ABCG2 y P-gp (20 de los 28 compuestos testados interaccionan con ambos transportadores), el análisis revela características diferentes para ambos en relación a la carga, hidrofobicidad, anfifilicidad y afinidad; sugiriendo que ABCG2 y P-gp tienen distintas localizaciones de unión al sustrato. Serán necesarias más investigaciones para localizar de manera precisa los sitios de unión para cada transportador pues la localización, el tipo y el número aún no están claros para estos dos transportadores ABC (Sharom y cols., 2005; Xia at al., 2005; Sauna y Ambudkar, 2007; Chen y cols., 2012).

Por último, se realizó un segundo análisis basado en grupos aceptores de hidrógeno (HAP) de la estructura molecular, teniéndose en cuenta los grupos =O, -O- y nitrógenos terciarios (Tabla 19, Página 181). De él se deduce que, en general, los compuestos típicos de ABCG2 tienen entre 4-6 HAP y el rango es más amplio para P-gp; por tanto HAP son importantes para ambos transportadores. Se ha dicho que los grupos nitrógeno e hidroxilo son importantes para el reconocimiento y la interacción con ABCG2 (Yoshikawa y cols., 2004; Saito y cols., 2006; Boumendjel y cols., 2007; Matsson y cols., 2007; Pick y cols., 2008, Gandhi y Morris, 2009; Matsson y cols., 2009). Nuestros resultados muestran que los compuestos que activan la actividad ATPasa de ABCG2 presentan siempre grupos hidroxilo y que los compuestos que interaccionan con P-gp también pueden tenerlos (Tabla 19, Página 181).

Además, el reconocimiento y la afinidad del sustrato por ABCG2 y P-gp parecen ser debidos a interacciones de puentes de hidrógeno, pues las interacciones electroestáticas y dipolares son favorecidas en un ambiente lipídico de acuerdo a la ley de Coulomb (Seelig y Gatlik-Lywojtowicz, 2005) y la entrada en la membrana del compuesto es un prerrequisito para poder interaccionar con ambos transportadores. Se ha presentado una correlación entre la afinidad del sustrato y la frecuencia de patrones de puentes de hidrógeno para P-gp (Seelig, 1998; Gatlik-Lywojtowicz y cols., 2006) y una similar ha sido sugerida para ABCG2 (Matsson y cols., 2007). Nótese que los puentes de hidrógeno han sido una característica común en SAR y QSAR en literatura (Gandhi y Morris, 2009).

Como conclusión, ambos transportadores ABCG2 y P-gp, a pesar del considerable solapamiento en los compuestos transportados, presentan características significativamente diferentes pues parecen presentar funciones y patrones complementarios (Tabla 20, Página 183). Por otra parte, tienen los

mismos elementos de reconocimiento excepto en la carga y las interacciones hidrofóbicas (Tabla 20, Página 183).

En este estudio, se ha realizado por primera vez un análisis molecular directo para ABCG2 basado en datos experimentales que ha permitido explicar y predecir las interacciones de compuestos con los transportadores ABCG2 y P-gp.

5.2. Interacción de ABCG2 y P-gp con hormonas esteroideas – análisis de correlación de la actividad ATPasa y el transporte

Para estudiar el segundo objetivo de la presente memoria relacionado con la correlación entre la tasa de hidrólisis de ATP y la tasa de transporte, escogimos seis hormonas esteroideas (cortisol, dexametasona, estradiol, progesterona, testosterona, tamoxifen) que presentan dos ventajas fundamentales, la primera que han sido extensamente testadas en experimentos de transporte y acumulación (Tabla 6, Página 67) y la segunda que la mayoría son eléctricamente neutras, lo que permite obviar posibles efectos de la carga y hacer más fácil la interpretación de las interacciones entre los transportadores y las hormonas. Teniendo en cuenta la actividad ATPasa con ABCG2 y P-gp y los parámetros obtenidos de la actividad de superficie por SAM se realizó una estimación de la difusión pasiva de estas hormonas a través de la membrana lipídica. Con estos datos se pudo discutir y correlacionar nuestros resultados con los ensayos de transporte y actividad publicados con ABCG2 y P-gp.

Medidas de actividad ATPasa en vesículas de membrana para ABCG2 y P-gp. Los datos de las Figuras 43 y 44 (Páginas 131 y 132) pertenecientes a la actividad ATPasa de ABCG2 y P-gp para hormonas esteroideas se representaron en la Figura 50 (Página 147). La actividad ATPasa de P-gp con progesterona presentó una curva característica en forma de campana casi completa. En el caso de cortisol, dexametasona, tamoxifen y testosterona, sólo se obtuvo la parte de activación, debido a que sus límites de solubilidad se encuentran alrededor del máximo de activación de la actividad ATPasa de P-gp. No se obtuvo actividad ATPasa de P-gp con estradiol. Debe decirse que a pesar de que estas hormonas tienen cargas neutra y positiva, que son apropiadas para interaccionar con P-gp (Schinkel y cols., 1996; Sharom, 2008), estos compuestos no son típicamente anfifílicos, un segundo requisito necesario para interactuar con este transportador. El estradiol no interacciona con P-gp además de por la falta de anfifilicidad, también debido a la carencia de patrones de puentes de hidrógeno (Seelig, 1998).

Por otra parte, tal como era de esperar por su carga, todos estos esteroides apenas activan sino que más bien reducen la actividad ATPasa de ABCG2 desde bajas concentraciones, indicando que interaccionan inhibiendo directamente a este transportador.

Los correspondientes parámetros cinéticos derivados de la actividad ATPasa están resumidos en la Tabla 15 (Página 148) (sustraídos de la Tabla 9, Página 129). No se pudieron calcular los parámetros cinéticos de la parte correspondiente a inhibición (K_2 y V_2) de las hormonas que sólo presentaron activación de la actividad ATPasa de P-gp; para las hormonas analizadas con ABCG2 se estimó K_1 como $K_1 = K_2 / 100$.

Los resultados de actividad ATPasa ya publicados para estas seis hormonas esteroideas se encuentran resumidos en la Tabla 21 (Página 185). Básicamente, en casi todos los resultados publicados para ABCG2 y P-gp se obtuvieron curvas completas de activación e inhibición. Los resultados publicados con P-gp son consistentes con los nuestros para cortisol y progesterona (Rao y cols., 1994; Orlowski y cols., 1996; Litman y cols., 1997; Kim y Benet., 2004). Dos de los resultados que no concuerdan con los nuestros porque los autores obtienen curvas completas para cortisol (y nosotros sólo conseguimos activación), y actividad ATPasa de P-gp para estradiol (Rao y cols., 1994) (que nosotros no observamos), se realizaron con células de insecto Sf9, cuya estructura de la membrana lipídica varía mucho respecto a la de los mamíferos, como ya se ha comentado anteriormente (In 't Veld y cols., 1991). Además estos autores utilizan una concentración de proteína unas veinte veces mayor que la nuestra, lo que favorece la obtención de activación ATPasa (Beck y cols., 2013). Los dos resultados publicados para tamoxifen (Rao y cols., 1994; Litman y cols., 1997) muestran curvas de activación e inhibición de la actividad ATPasa de P-gp, sin embargo ambos utilizan concentraciones altas de hormona con las que nosotros hemos encontrado problemas en las curvas de vanadato, probablemente reflejando problemas de agregación. Respecto a ABCG2, los experimentos publicados con las membranas ABCG2-M-ATPasa con progesterona dieron lugar a los mismos resultados que los nuestros (Glavinas y cols., 2007). La otra única publicación existente de actividad ATPasa de ABCG2 muestra curvas de activación e inhibición para las cuatro hormonas analizadas y nosotros sólo vemos inhibición (Janvilisri y cols., 2003) (Tabla 21 y Figura 50, Páginas 147 y 185). Estos autores utilizan vesículas de células *L. lactis* a una concentración diez veces mayor que la nuestra, lo que favorece la activación ATPasa (Beck y cols., 2013).

Medidas de actividad de superficie (SAM). Para estimar la capacidad de las hormonas para cruzar la membrana por difusión pasiva las hormonas esteroideas caracterizadas por SAM de la Figura 47 (Página 139) se representaron en la Figura 51 (Página 149). Dexametasona, progesterona, tamoxifen y testosterona presentaron curvas completas de SAM, las curvas de testosterona y progesterona terminaron a una presión considerablemente menor de la esperada para compuestos típicos anfifílicos (Gerebtzoff y cols., 2004). Dexametasona y tamoxifen tienen escalones en sus curvas que además son sigmoideas. Cortisol presenta una actividad de superficie pequeña, debido a su carencia de anfifilicidad; el compuesto precipita antes de alcanzar el CMC; y para estradiol la actividad de superficie es inexistente. Todos estos resultados son indicativos de nuevo de la poca anfifilicidad de estas hormonas. Es evidente que existe una correlación entre los resultados de SAM y la actividad ATPasa pues en ambos casos las curvas terminan donde comienzan los problemas de precipitación del compuesto o en el CMC

(Figuras 50 y 51, Páginas 147 y 149). Los parámetros calculados: CMC, A_D y K_{aw} (Ecuación 5), están expuestos en la Tabla 16 (Página 150) (algunos de ellos son de la Tabla 12, Página 138).

A pesar de la estructura similar de estas hormonas, pequeñas diferencias las hacen comportarse de manera diferente. Cortisol y dexametasona son los compuestos con los menores valores de K_{aw} y XLogP y con el mayor número de heteroátomos (Tablas 16 y 20, Página 150 y 183); todo ello implica que estos compuestos cruzarán la membrana con mayor dificultad. Por otra parte, tamoxifen es el compuesto con los mayores valores K_{aw} y XLogP y con pocos heteroátomos, siendo el compuesto que atraviesa la membrana más rápidamente. Estradiol, progesterona y testosterona están en la mitad.

Las predicciones de difusión pasiva para cortisol, dexametasona, progesterona y testosterona fueron calculadas utilizando los datos de SAM (Ecuación 8). La difusión pasiva en función de la concentración está representada en la Figura 52 (Página 151). Es necesario recordar que el transporte neto (de experimentos de transporte transepitelial) es la suma del transporte activo (actividad ATPasa del transportador) más la difusión pasiva del compuesto (calculada en SAM) (Seelig, 2007). El transporte activo representado en la Figura 52 (Página 151) es una media de los resultados comunes obtenidos para ABCG2 y P-gp. Para progesterona y testosterona (las más hidrofóbicas) la difusión pasiva es mayor que el transporte activo prácticamente a cualquier concentración, por tanto, aunque el transportador está obviamente funcionando, el transporte neto puede no observarse a concentraciones mayores de ~ 0,1 µM. Por el contrario, cortisol y dexametasona (las menos hidrofóbicas) si se aplican a concentraciones por debajo del rango de mM en experimentos de transporte transepitelial, su transporte neto puede ser visible debido a que el transporte activo es mayor que la difusión pasiva. Sin embargo, si se añaden a mayores concentraciones en las que la difusión pasiva comienza a ser mayor que el transporte activo, el transporte neto puede dejar de ser perceptible. Estas deducciones son aplicables a ambos transportadores.

Por último realizamos una **comparación de los resultados obtenidos de actividad ATPasa de ABCG2 y P-gp con experimentos de transporte y acumulación *in vitro*** previamente publicados (Tabla 6 y Figuras 50 y 64, Páginas 67, 147 y 188). Un estudio detallado de los resultados publicados comparados con los de actividad ATPasa refleja constantes correlaciones teniendo en cuenta el significado de transporte neto frente al activo.

Los sustratos se pueden dividir en intrínsecos, que activan la actividad ATPasa pero al ser pequeños y/o estar poco cargados, difunden rápidamente por la membrana dando lugar a ratios B-A /A-B ≈ 1 en experimentos de transporte transepitelial; no son visibles en estos experimentos, no dan transporte neto. El otro tipo de sustratos son los aparentes, que son sustratos intrínsecos lo suficientemente grandes o cargados como para difundir despacio por la membrana y que el transportador sea capaz de exportarlos eficientemente fuera de la célula (Fischer et al., 1998; Seelig and Gatlik-Landwojtowicz, 2005), y dar lugar a ratios B-A /A-B >2 en experimentos de transporte, se ve

transporte neto (Schwab y cols., 2003). Podemos decir que cortisol y dexametasona son sustratos aparentes y progesterona y testosterona son intrínsecos para los dos transportadores ABC (Figuras 52 y 64, Páginas 151 y 188). De hecho en las publicaciones de transporte transepitelial con cortisol y dexametasona, se observó transporte neto (Ueda y cols., 1992; van Kalken y cols., 1993; Schinkel y cols., 1995; Yates y cols., 2003), al utilizar concentraciones menores del rango de mM y ser entonces el transporte activo mayor que la difusión pasiva (Figura 52, Página 151). Por el contrario, la progesterona (no se encontraron ensayos realizados con testosterona) presenta actividad ATPasa para P-gp y no se encontró interacción en los experimentos de transporte a ninguna de las concentraciones utilizadas (Ueda y cols., 1992; Ushigome y cols., 2000) (Figura 64 y Tabla 6, Páginas 67 y 188), por ser el transporte activo menor que la difusión pasiva (Figura 52, Página 151). Hemos dicho que el tamoxifen es la hormona más hidrofóbica, por tanto un sustrato intrínseco descrito como no sustrato en ensayos de acumulación con P-gp (Callagan y Higgis, 1995). De forma similar a nuestros resultados de actividad ATPasa, el estradiol fue identificado como no sustrato para P-gp (Kim y Benet, 2004). El transporte neto de sustratos aparentes y de inhibidores puede ser visible a concentraciones muy bajas del compuesto, donde el transportador todavía trabaja a nivel basal (Figura 64, Página 188), por ejemplo estradiol con ABCG2 (Janvilisri y cols., 2003; Pavek y cols., 2005).

Cuando las hormonas esteroideas actúan como inhibidores al ser utilizadas a altas concentraciones, son transportadas por el transportador en un ciclo inútil pues aún siguen difundiendo rápidamente por la membrana, siendo el transporte pasivo mayor que el activo; además se impide el transporte de otros compuestos. Recuérdese que los compuestos pueden actuar como sustratos o inhibidores dependiendo de la concentración (Seelig y Lywojtowicz, 2000); el estradiol pudo verse como sustrato de ABCG2 a bajas concentraciones (Janvilisri y cols., 2003; Pavek y cols., 2005) y como inhibidor a altas (Figura 64 y Tabla 6, Páginas 67 y 188) (Imai y cols., 2002; 2003; Pavek y cols., 2005; Matsson y cols., 2007; Robey y cols., 2003). La inhibición puede ser predicha directamente a partir de la actividad ATPasa, correspondiéndose con la parte decreciente de las curvas; se puede comprobar por ejemplo con las interacciones de estradiol, tamoxifen o progesterona con ABCG2 (Imai y cols., 2003; Sugimoto y cols., 2003; Matsson y cols., 2007). En algunos casos los resultados pueden variar entre diferentes autores y/o experimentos, por ejemplo Pavek y cols. (2005) observó en un caso inhibición y en otro no utilizando dexametasona en experimentos de transporte y acumulación a la misma concentración, probablemente porque la concentración utilizada se encontraba en el límite de la inhibición (Figura 64, Página 188). Es importante saber que hay inhibición cuando ambos sitios de unión del transportador son ocupados, dependerá por tanto de la suma de concentración de todos los compuestos incluidos en el experimento. Por tanto, si un compuesto es utilizado a una concentración cercana a su V_1 de actividad ATPasa la inhibición puede ocurrir incluso si la concentración del segundo compuesto aún no es inhibitoria en su curva de actividad ATPasa. Esto es lo que puede estar ocurriendo en el caso de Elahian y cols. (2010) pues encuentran inhibición de ABCG2 por dexametasona a una concentración en la que el transportador

se encuentra funcionando a actividad basal por incluir mitroxantrona a una concentración cercana a su V_1. Otro ejemplo es el caso de van Kalken y cols. (1993) y Yang y cols. (1989); estos autores observan inhibición de testosterona y progesterona a concentraciones donde en sus curvas de ATPasa están en activación de P-gp porque añaden daunorubicina a una concentración cercana a su V_1 (Figura 64 y Tabla 6, Páginas 67 y 188). También es importante tener en cuenta el material con el que se está trabajando; en los experimentos realizados con vesículas se necesita menor concentración de cortisol para inhibir a ABCG2 pues los NBD son accesibles desde la fase acuosa (Imai y cols., 2003) que en ensayos con células (Matsson y cols., 2007; Pavek y cols., 2005), donde el compuesto tiene que atravesar la membrana lipídica para acceder a los NBD (Figuras 18 y 64, y Tabla 6, Páginas 56, 67 y 188) (Nervi y cols., 2010).

En resumen, si el transporte activo es mayor que la difusión pasiva (cortisol y dexametasona), la actividad ATPasa puede ser interpretada directamente en términos de sustrato en la parte ascendente de la curva y de inhibidor en la descendente. Si por el contrario, la difusión pasiva es mayor que el transporte activo, los compuestos no son sustratos pero pueden funcionar como inhibidores (progesterona y testosterona) (Figura 65, Página 192). Por tanto, hemos demostrado que las tasas de hidrólisis de ATP y de transporte para ABCG2 y P-gp se correlacionan teniendo en cuenta la difusión pasiva. Es posible predecir sustratos e inhibidores de estos transportadores realizando dos sencillos experimentos (medidas de actividad ATPasa y SAM).

5.3. Interacción de ABCG2 y P-gp con fluoroquinolonas – análisis de la correlación de la actividad ATPasa con otros experimentos *in vitro* e *in vivo* utilizando estos antibióticos

Aunque se sabe que la biodisponibilidad de varias fluoroquinolonas es reducida debido a ABCG2 (Merino y cols., 2006; Pulido y cols., 2006; Real y cols., 2011), esta afirmación no se ha confirmado para todos los miembros de esta familia de antibióticos. La interacción de estos antibióticos con P-gp, ha sido extensamente evaluada (ej: de Lange y cols., 2000; Lowes y Simmons, 2002). Sin embargo, aún no se han explicado de manera precisa y completa las interacciones entre esta familia de antibióticos y ABCG2 y P-gp. Para conseguir el tercer objetivo de esta tesis, evaluamos la actividad ATPasa de ABCG2 y P-gp con cinco fluoroquinolonas (ciprofloxacina, enrofloxacina, moxifloxacina, norfloxacina y pefloxacina) y completamos el estudio de sus interacciones *in vitro* e *in vivo* con el transportador ABCG2 (todos estos compuestos han sido extensamente estudiados con P-gp) realizando experimentos *in vitro* de transporte transepitelial y de acumulación e *in vivo* con ratones *wild-type* y *knockout*. Por último, se realizó una correlación entre los experimentos de transporte, acumulación e *in vivo* con los ensayos de actividad ATPasa utilizando también los datos publicados existentes de la interacción de estas cinco fluoroquinolonas con ABCG2 y P-gp.

Medidas de actividad ATPasa en vesículas de membrana para ABCG2 y P-gp. Para poder explicar la interacción de las fluoroquinolonas estudiadas con ABCG2 y P-gp a nivel molecular, se realizaron medidas de actividad ATPasa con cinco fluoroquinolonas (Figura 53, Página 153); parte los resultados están extraídos de la Figura 45 (Página 133). Para ciprofloxacina, enrofloxacina y norfloxacina sólo se pudo medir la parte de activación de la curva de actividad ATPasa de ABCG2 por problemas de solubilidad a concentraciones altas debido a su carácter hidrofílico (nótese que tienen el LogP más negativo, Tabla 12, Página 138). Este fenómeno es más marcado para la ciprofloxacina y norfloxacina, ya que la enrofloxacina parece haber alcanzado el máximo (V_1). La moxifloxacina directamente reduce la actividad ATPasa de ABCG2. La pefloxacina muestra una curva casi completa en forma de campana con ABCG2. Basándose en estos datos se puede predecir que la ciprofloxacina y norfloxacina interaccionarán como sustratos de ABCG2 en el rango de µM y mM en experimentos con células, sin embargo será difícil conseguir inhibición debido a problemas de solubilidad y agregación a concentraciones mayores. La moxifloxacina y pefloxacina se podrán observar como sustratos hasta aproximadamente 600 µM y después actuarán como inhibidores. En relación a la interacción de estas fluoroquinolonas con P-gp, sólo la moxifloxacina dio lugar a curvas de actividad ATPasa (Figura 53 B, Página 153). Los correspondientes parámetros cinéticos derivados de estas medidas están en la Tabla 17 (Página 154). El orden de los valores K_1 para ABCG2 (moxifloxacina < enrofloxacina < pefloxacina < ciprofloxacina < norfloxacina) refleja la hidrofobicidad de estos antibióticos: moxifloxacina > enrofloxacina > pefloxacina > ciprofloxacina > norfloxacina; orden también visto en los valores de LogP (Tabla 12, Página 138; LogP = -0.50 para moxifloxacina), la excepción es la moxifloxacina, que se comentará más adelante. Los valores V_1 revelan la curva obtenida para cada fluoroquinolona con ABCG2: moxifloxacina < norfloxacina < pefloxacina.

Estudios de transporte transepitelial con ABCG2. Para poder realizar el estudio comparado entre los resultados obtrenidos con los distintos experimentos, no existían ensayos de transporte transepitelial ni ensayos de acumulación de mitoxantrona con ABCG2 para moxifloxacina ni pefloxacina. Por tanto, se llevaron a cabo experimentos de transporte transepitelial utilizando monocapas de células confluyentes MDCK-II parentales y transducidas con ABCG2 humana y Abcg2 de ratón. La moxifloxacina no presentó transporte neto significativo en las células parentales y se observó un ligero transporte neto para la transducidas con ABCG2 y Abcg2 comparado con las parentales (Figura 54, Página 155), aunque los ratios de transporte calculados no mostraron diferencias significativas. Según las guías del Consorcio Internacional de Transportadores (Giacomini y cols., 2010), la moxifloxacina no es sustrato *in vitro* de ABCG2 por obtenerse unos ratios de transporte con las células transducidas con el transportador < 2. Cuando se realizaron los experimentos con el inhibidor Ko143, se redujo el bajo transporte mediado por ABCG2 aunque se siguió manteniendo un pequeño transporte en las células parentales y transducidas con ABCG2, indicativo de que otro posible transportador ABC como P-gp podría estar involucrado en el proceso. De hecho este antibiótico interacciona con P-gp (Brillault y cols., 2009) y las células MDCK-II

contienen P-gp endógeno (Goh y cols., 2002). Precisamente debido a los transportadores endógenos, se recomiendan corroboraciones con inhibidores específicos en experimentos de transporte (Giacomini y cols., 2010).

Para la pefloxacina el transporte neto en las células parentales fue nulo; las células transducidas con Abcg2 de ratón presentaron un transporte neto mediado por Abcg2 considerable pero fue algo menos pronunciado para las células con ABCG2 de humana (Figura 55, Página 157). Los ratios de transporte fueron significativamente mayores para ambas líneas celulares transducidas comparadas con las parentales, siendo mayores los de Abcg2. Utilizando Ko143, el transporte mediado por ABCG2/Abcg2 se redujo a valores similares a la línea parental. Por tanto, se puede concluir que la pefloxacina es transportada de manera eficiente por la ABCG2 humana y Abcg2 de ratón.

Acumulación de mitoxantrona. La acumulación de mitoxantrona como sustrato de ABCG2 para testar moxifloxacina y pefloxacina como inhibidores se midió utilizando células MDCK-II parentales y transducidas con ABCG2 o Abcg2 en un citómetro de flujo. No se encontró ningún efecto en la acumulación de mitoxantrona cuando moxifloxacin y pefloxacina fueron añadidas a las células transducidas, sugiriendo que estas fluoroquinolonas no actúan como inhibidores de ABCG2 a las concentraciones testadas (Figura 56, Página 158). Estos resultados están en concordancia con los obtenidos para otras fluoroquinolonas como norfloxacina, ciprofloxacina o enrofloxacina (Merino y cols., 2006; Pulido y cols., 2006).

Farmacocinéticas *in vivo* con ratones. Para completar la caracterización de la interacción de las fluoroquinolonas utilizadas en este estudio con ABCG2, basándonos en nuestros experimentos *in vitro* con pefloxacina y en otros resultados de nuestro grupo indicando que la norfloxacina es un sustrato *in vitro* (Merino y cols., 2006), estas dos fluoroquinolonas fueron testadas como sustratos *in vivo*. Destacar que la única diferencia estructural entre la pefloxacina y la norfloxacina es un grupo metilo que parece incrementar la biodisponibilidad a ~100% para pefloxacina (Hooper y Wolfson, 1985) comparado con ~40% para norfloxacina (Neu, 1992), sugiriendo la potencial relevancia de la interacción de un transportador ABC en el proceso en el caso de la norfloxacina.

Ciprofloxacina y enrofloxacina han sido descritas previamente como sustratos *in vivo* de ABCG2 (Merino y cols., 2006; Pulido y cols., 2006).

Las concentraciones en plasma después de la administración de norfloxacina fueron significativamente mayores en los ratones *knock-out* comparados con *wild-type* en todo el rango de tiempos analizados (Figura 57 A, Página 160), también las AUC calculadas; indicando el importante papel que presenta Abcg2 en la farmacocinética oral de este antibiótico. Asimismo, las concentraciones hepáticas fueron significativamente mayores en los ratones *knock-out* comparados con los *wild-type* y las biliares en los ratones *wild-type* comparados con los *knock-out* a los dos tiempos estudiados (30 y 60 min) (Figura 57 B y D, Página 160), incluso cuando se normalizó por las concentraciones de plasma

(Figura 57 C y E, Página 160), indicando el papel relevante de Abcg2 en la eliminación biliar de norfloxacina. Los niveles de norfloxacina divergieron significativamente entre *knock-out* y *wild-type* también en otros tejidos: el riñón, intestino, contenido intestinal y bazo; aunque al corregir por el plasma, las diferencias significativas permanecieron sólo para el intestino y el contenido intestinal (Figura 58 y Tabla 18, Páginas 161 y 162). La gran acumulación de norfloxacina en el contenido intestinal de los ratones *wild-type* probablemente esté relacionada con el transporte mediado por Abcg2 en el intestino y con su excreción hepatobiliar. La secreción intestinal activa de este antibiótico ya fue sugerida por Griffiths y cols. (1994), aunque el correspondiente transportador involucrado no fue identificado. Importante es destacar que la norfloxacina no se detectó en el cerebro de ningún ratón (Tabla 18, Página 161), tampoco en la leche de las hembras (Figura 59, Página 163). Comparado con datos publicados, la norfloxacina se ha detectado en la leche de ovejas (Soback y cols., 1994) y vacas (Gips y Soback, 1999), pero no de humanos después de una administración oral (Wise, 1984).

Cuando la norfloxacina fue administrada durante una semana consecutiva, los resultados reflejaron de nuevo mayores niveles de fluoroquinolona en ratones *knock-out* comparados con los *wild-type* (Figura 60, Página 164); indicando de nuevo la relevancia de Abcg2 en la farmacocinética de este antibiótico, incluso en un tratamiento crónico. En este último experimento, los ratones se mantuvieron en jaulas metabólicas y se analizaron los niveles de norfloxacina en heces y orina a las 24 h de comenzar el experimento, también la orina a los 60 min después de esta primera administración. Los niveles de antibiótico en orina fueron extremadamente superiores en los ratones *knock-out* comparados con los *wild-type* a ambos tiempos, aunque debido a la alta variación entre individuos no se obtuvieron diferencias significativas entre ambos grupos a las 24 h. Por el contrario, no se observaron diferencias en los niveles de norfloxacina en las heces de ambos genotipos.

Cuando se estudió la posible interacción de pefloxacina con Abcg2 *in vivo* no se observaron diferencias entre ambos grupos de ratones en la farmacocinética plasmática, ni tampoco en el hígado o la bilis (Figura 61, Página 165). Los niveles de pefloxacina en la leche de hembras lactantes mostraron diferencias significativas entre *knock-out* y *wild-type*; sin embargo, estas diferencias desaparecieron cuando los niveles de antibiótico en leche fueron relacionados con los niveles en plasma (Figura 62, Página 166). Parece que Abcg2 no afecta a la disposición sistémica de la pefloxacina bajo nuestras condiciones experimentales. Es posible que otros factores pudiesen están enmascarando el efecto *in vivo* de Abcg2 con la pefloxacina, como por ejemplo otros transportadores, de hecho Kodaira y cols. (2011) han demostrado interacción de la P-gp con este antibiótico.

El metabolismo de la pefloxacina se produce principalmente en el hígado, dando lugar a varios metabolitos, incluida la norfloxacina. Se ha demostrado que la norfloxacina puede ser detectada en bilis y orina en varias especies administradas con pefloxacina, pero no en la orina de ratón (Montay y cols., 1985). En nuestros experimentos, la norfloxacina se pudo detectar en algunas muestras de tejidos de

ratón administrados con pefloxacina, observándose niveles significativamente superiores en *wild-type* comparados con los *knock-out* en la bilis y el contenido intestinal. No se detectó este metabolito en plasma, cerebro, riñón ni bazo, y en leche los niveles fueron extremadamente bajos como para poder realizar una comparación. Estos hallazgos confirman que Abcg2 tiene efectos sustanciales en la eliminación hepatobiliar de norfloxacina que implican una importante relevancia a nivel terapéutico y biológico.

Nótese que los tejidos con mayores diferencias entre ambos grupos de ratones (intestino e hígado) son los tejidos con los mayores niveles de Abcg2 (Tanaka y cols., 2005), que además tienen uniones estrechas que hacen difundir al compuesto más despacio por estas membranas compactas, lo que facilita el transporte activo mediado por ABCG2.

La correlación de la actividad ATPasa de ABCG2 y P-gp con otros experimentos *in vitro* de nuestro estudio y de otros artículos publicados previamente (Tabla 7, Página 77) para las cinco fluoroquinolonas se representó en la Figura 66 (Página 194). Una observación detallada de todos los resultados refleja constantes correlaciones entre la actividad ATPasa y otros experimentos. Excepto moxifloxacina, todas las fluoroquinolonas fueron clasificadas como sustratos pero no inhibidores de ABCG2, reflejo de la activación de la actividad ATPasa en la Figura 53 (Página 153); además en general no interaccionan con P-gp en ningún experimento.

Observando los ensayos *in vitro* con ABCG2 con estas fluoroquinolonas, en la Tabla 22 (Página 193) se ve como los valores XLogP < 1, son pequeños o incluso negativos, lo que significa que estas fluoroquinolonas son muy hidrofílicas y por tanto de difusión pasiva lenta (Seelig, 2007), con la excepción de la moxifloxacina. En consecuencia, la actividad ATPasa se correlaciona directamente con el transporte neto de los experimentos de transporte bidireccional en la parte ascendente de la curva. De hecho el transporte neto es ya visible a 10 µM, concentración a la cual la actividad ATPasa se encuentra a niveles basales para todas las fluoroquinolonas (Figura 66, Página 194). Para el compuesto más hidrofóbico, la moxifloxacina (mayor XLogP, Tabla 22, Página 193), la difusión pasiva no debe ser ignorada, por consiguiente, su escaso transporte neto a 10 µM es debido a que la difusión pasiva es mayor que el transporte activo (Figura 54, 66, Páginas 155 y 194).

Los resultados de las medidas de acumulación de MXR para testar las fluoroquinolonas como inhibidores también concuerdan con los de actividad ATPasa. Considerando la moxifloxacina, la inhibición de la actividad ATPasa en vesículas comienza a la concentración de 500 μM, concentración a la que aún no se observa inhibición en experimentos de acumulación celular (Figura 56, Página 158). Se ha demostrado que en células las curvas de actividad ATPasa necesitan mayores concentraciones de compuestos que difunden despacio para alcanzar inhibición que en vesículas (Nervi y cols., 2010). Sin embargo, al ser ya 500 μM la mitad de la dosis letal para ratones (von Keutz y Schluter, 1999), no se probaron mayores concentraciones en experimentos de acumulación ni tampoco *in vivo*. Por otra parte,

en el caso de ciprofloxacin, enrofloxacina, norfloxacina y pefloxacina, no se observó inhibición de ABCG2 (Tabla 22 y Figura 66, Páginas 193 y 194) porque es difícil llegar a ella debido a problemas de solubilidad de los compuestos por su carácter zwiteriónico.

Los resultados de los estudios *in vivo* con ABCG2 pueden también explicarse teniendo en cuenta su hidrofobicidad. La ciprofloxacina, norfloxacina y enrofloxacina son las fluoroquinolonas más hidrofílicas (XLogP en Tabla 12, Página 138) y al cruzar la membrana con mayor dificultad el Abcg2 puede competir con la difusión pasiva y verse interacciones *in vivo* con el transportador. Al encontrarse la pefloxacina en la mitad de la secuencia de hidrofobicidad se explica porque unas veces puede verse transporte (*in vitro*) y otras no (*in vivo*). Finalmente, la moxifloxacina es la más hidrofóbica y por ello no se observa transporte neto *in vitro* ni *in vivo* (Tablas 12 y 22, Páginas 138 y 193).

Cuando se comparan los experimentos *in vitro* e *in vivo*, es importante considerar las diferencias en el pH pues afecta al estado de protonación de estos compuestos zwiteriónicos. Los experimentos *in vitro* se realizan a pH fisiológico pH≈7, donde funcionan como zwiteriónicos y la difusión pasiva es lenta, pudiendo ser tomados fácilmente por ABCG2 y verse como sustratos aparentes. Por el contrario, en los experimentos *in vivo* con administración oral, las fluoroquinolonas se absorben desde el estómago (pH≈2) o intestino (pH≈6), donde son débilmente catiónicas y cruzan las membranas con mayor facilidad. Esto explica porqué las fluoroquinolonas son rápidamente absorbidas desde el intestino y distribuidas por tejidos y fluidos.

Nuestros hallazgos *a priori* podrían sugerir la necesidad de estudiar la interacción de cada molécula de forma individual con los transportadores ABC pues, como hemos visto, no todos los componentes de esta familia necesariamente interaccionan de la misma manera. Además las diferencias encontradas entre los experimentos *in vitro* e *in vivo* subrayan la importancia de realizar estudios *in vivo,* de hecho el Consorcio Internacional de Transportadores (Giacomini y cols., 2010) establece que se deben utilizar estos modelos en particular con compuestos con poca solubilidad y permeabilidad, como la norfloxacina. Sin embargo, como hemos demostrado, teniendo en cuenta las propiedades fisicoquímicas de los compuestos, es posible estimar la interacción de cada compuesto con el transportador ABCG2.

Considerando las interacciones de las fluoroquinolonas con P-gp, es preciso primero tener en cuenta que en principio no se espera que haya interacción por poseer carga negativa que difícilmente es tomada por P-gp, aunque si logran atravesar la membrana de manera efectiva estos compuestos presentan patrones para poder interaccionar con el transportador (Seelig, 1998). La Figura 66 (Página 194) muestra constantes consistencias. De hecho, en concordancia con la ausencia de actividad ATPasa de P-gp, se ha encontrado que la ciprofloxacina no interacciona con P-gp *in vitro* como sustrato utilizando distintos tipos celulares (Cavet y cols., 1997; de Lange y cols., 2000; Lowes y Simmon, 2002; Yamaguchi y cols., 2004; Park y cols., 2011) ni como inhibidor (de Lange y cols., 2000; Haritova y cols.,

2007), tampoco *in vivo* (Dautrey y cols., 1999; de Lange y cols., 2000; Rodriguez-Ibañez y cols., 2006; Haslam y cols., 2011). Ruiz-García y cols. (2002) y Rodríguez-Ibañez y cols. (2003) describieron a la ciprofloxacina como sustrato de P-gp utilizando células Caco-2; hay que tener en cuenta que en estas células se expresan otros muchos transportadores, incluyendo ABCG2, que podrían interferir en los resultados (Xia y cols., 2005; Seithel y cols., 2006).

La enrofloxacina no inhibe P-gp en ensayos de acumulación (Haritova y cols., 2007) y la norfloxacina no es sustrato *in vitro* o *in vivo* (de Lange y cols., 2000) ni inhibidor de P-gp (de Lange y cols., 2000; Lowes y Simmons, 2002; Sikri y cols., 2004), de acuerdo con la ausencia de actividad ATPasa. El papel de P-gp en el transporte de la pefloxacina como sustrato *in vitro* e *in vivo* y como inhibidor también fue descartado en un principio (de Lange y cols., 2000; Tsai, 2001; Lowes y Simmons, 2002), sin embargo, más tarde se identificó la pefloxacina como sustrato en experimentos de transporte (Kodaira y cols., 2011). Esto podría ser explicado en términos de hidrofobicidad pues como la pefloxacina está en la mitad de la secuencia (Tabla 22, Página 193), podría pasar que en algunos casos la difusión pasiva fuese lo suficientemente rápida como para ser captada por P-gp a pesar de la carga negativa.

Por último la moxifloxacina es la fluoroquinolona más hidrofóbica, cruzando la membrana con facilidad. Este hecho la permite interaccionar con P-gp y obtener activación en las curvas de actividad ATPasa (Figura 53, Página 153). En los experimentos publicados Brillault y cols. (2009) pudieron identificar el compuesto como sustrato a una concentración en la que hay activación de la actividad ATPasa de P-gp; por el contrario Michot y cols. (2005) no observaron esta interacción porque testaron el antibiótico a una concentración a la que aún no hay activación de la actividad ATPasa y el transporte activo no puede superar al pasivo.

Como conclusión, debido a su carácter zwiteriónico, en general las fluoroquinolonas interaccionan como sustratos *in vitro* pero no como inhibidores de ABCG2 y no interaccionan con P-gp, a no ser que sean lo suficientemente hidrofóbicos. Además hemos demostrado que no existe interacción *in vivo* de la pefloxacina con Abcg2 pero la biodisponibilidad de la norfloxacina se ve muy afectada por este transportador. Hemos podido explicar nuestros hallazgos en cuanto a la interacción de fluoroquinolonas con ABCG2 y P-gp considerando las propiedades fisicoquímicas de los compuestos (como carga e hidrofobicidad) y su influencia en los flujos pasivo y activo. Un resumen de las conclusiones de este apartado se encuentra en la Figura 67 (Página 200).

6. Conclusiones

Primera.- Aunque existe un solapamiento considerable entre los sustratos de ABCG2 y P-gp, nuestro análisis revela importantes diferencias. Ambos transportadores parecen tener preferencia por determinados compuestos según el tipo específico de carga eléctrica, su hidrofobicidad y anfifilicidad. De esta manera, los sustratos de ABCG2 no son anfifílicos, más bien hidrofílicos y con carga negativa o son zwiteriónicos (aunque ABCG2 interacciona con compuestos con cualquier carga); mientras que compuestos que interaccionan con P-gp son anfifílicos, hidrofóbicos y eléctricamente neutros o catiónicos. ABCG2 y P-gp tienen grupos aceptores de hidrógeno como elementos de reconocimiento.

Segunda.- ABCG2 presenta menor actividad basal y generalmente también menor actividad ATPasa inducida por sustrato. Los sustratos típicos de ABCG2, si son transportados por P-gp, son transportados despacio. A pesar de la relativa baja tasa de actividad ATPasa y de transporte, ABCG2 transporta compuestos que no son anfifílicos de manera eficaz porque estos compuestos tienen generalmente una tasa lenta de difusión a través de la bicapa lipídica.

Tercera.- Para ambos transportadores, ABCG2 y P-gp, se obtuvieron curvas de actividad ATPasa en forma de campana y los dos transportadores se unen a sus sustratos en la bicapa lipídica, por tanto, un modelo de unión en "dos pasos" es válido para ambos.

Cuarta.- ABCG2 presenta mayor afinidad por el sustrato en comparación con P-gp. La afinidad de ABCG2, así como de P-gp por sus sustratos, parece ser esencialmente debida a interacciones de puentes de hidrógeno. La mayor afinidad de ABCG2 por sus sustratos en la membrana lipídica parece tener una contribución hidrofóbica que no se da en el caso de P-gp. Mientras la tasa de transporte en P-gp disminuye al incrementarse la afinidad del compuesto por el transportador, en ABCG2 esta tasa aumenta al incrementarse dicha afinidad. Los sustratos de ABCG2 y P-gp parecen tener distintos sitios de unión al transportador.

Quinta.- La tasa de hidrólisis de ATP y la tasa de transporte se correlacionan inequívocamente. Esto se puede demostrar teniendo en cuenta la difusión pasiva a través de la membrana lipídica. Si la actividad del transportador puede superar a la difusión pasiva, las curvas de actividad ATPasa pueden ser interpretadas directamente en términos de transporte. Es decir, los compuestos actúan como sustrato en el rango de concentraciones de la parte ascendente de la curva de actividad ATPasa y como inhibidores en el rango de concentraciones de la parte descendente de la curva. Si la difusión pasiva es mayor que la actividad exportadora del transportador, los compuestos no aparecen como sustratos en experimentos de transporte pero aún pueden actuar como inhibidores.

Sexta.- Los sustratos de ABCG2 y P-gp pueden ser predichos de manera fiable a cualquier concentración combinando los resultados de la actividad ATPasa con los de la actividad de superficie. Los inhibidores de ABCG2 y P-gp pueden ser inferidos directamente de los ensayos de actividad ATPasa.

Esta combinación de ambos experimentos revela bajo qué condiciones un compuesto actúa como sustrato y/o como inhibidor para los transportadores ABCG2 y P-gp. Además, permite conseguir un mayor entendimiento de la función del transportador.

Séptima.- Es posible estimar la interacción de cada compuesto con los transportadores ABCG2 y P-gp teniendo en cuenta sus propiedades físico-químicas (como carga e hidrofobicidad). Debido al carácter zwiteriónico de su carga, en general las fluoroquinolonas interaccionan como sustratos *in vitro* pero no como inhibidores de la proteína ABCG2 humana; por otra parte, apenas interaccionan con el transportador P-gp.

Octava.- No hay una interacción *in vivo* de moxifloxacina y pefloxacina con el transportador Abcg2 de ratón; sin embargo, la biodisponibilidad de norfloxacina se ve muy afectada por el transportador.

Novena.- El par ABCG2 y P-gp exhibe una asociación perfecta. Ambos transportadores funcionan óptimamente para el tipo de compuestos para los que se han adaptado. Los dos transportadores exportan compuestos que son a la vez solubles en agua y en la membrana. Debido al solapamiento en la especificidad es complicado que se escape algún compuesto al interior de la célula sin ser transportado por alguna de estas dos proteínas.

References

Aänismaa P, Gatlik-Landwojtowicz E, Seelig A. P-glycoprotein senses its substrates and the lateral membrane packing density: consequences for the catalytic cycle. Biochemistry. 2008;47(38):10197-207

Aänismaa P, Seelig A. P-Glycoprotein kinetics measured in plasma membrane vesicles and living cells. Biochemistry. 2007;46(11):3394-404

Abd El-Aty AM, Goudah A. Some pharmacokinetic parameters of pefloxacin in lactating goats. Vet Res Commun. 2002;26(7):553-61

Abuznait AH, Kaddoumi A. Role of ABC transporters in the pathogenesis of Alzheimer's disease. ACS Chem Neurosci. 2012;3(11):820-31

Adeoya-Osiguwa SA, Markoulaki S, Pocock V, Milligan SR, Fraser LR. 17beta- Estradiol and environmental estrogens significantly affect mammalian sperm function, Hum Reprod. 2003;18:100–107

Agarwal S, Elmquist WF. Insight into the cooperation of P-glycoprotein (ABCB1) and breast cancer resistance protein (ABCG2) at the blood-brain barrier: a case study examining sorafenib efflux clearance. Mol Pharm. 2012;9(3):678-84

Ahmed F, Arseni N, Glimm H, Hiddemann W, Buske C, Feuring-Buske M. Constitutive expression of the ATP-binding cassette transporter ABCG2 enhances the growth potential of early human hematopoietic progenitors. Stem Cells. 2008;26:810-18

Ahmed-Belkacem A, Pozza A, Muñoz-Martínez F, Bates SE, Castanys S, Gamarro F, Di Pietro A, Pérez-Victoria JM. Flavonoid structure-activity studies identify 6-prenylchrysin and tectochrysin as potent and specific inhibitors of breast cancer resistance protein ABCG2. Cancer Res. 2005;65:4852-4860

Aleksunes LM, Cui Y, Klaassen CD. Prominent expression of xenobiotic efflux transporters in mouse extraembryonic fetal membranes compared with placenta. Drug Metab Dispos. 2008;36:1960–1970

Allen JD, Brinkhuis RF, Wijnholds J, Schinkel AH. The mouse Bcrp1/ Mxr/Abcp gene: amplification and overexpression in cell lines selected for resistance to topotecan, mitoxantrone, or doxorubicin. Cancer Res. 1999;59:4237–41

Allen JD, van Loevezijn A, Lakhai JM, van der Valk M, van Tellingen O, Reid G, Schellens JH, Koomen GJ, Schinkel AH. Potent and specific inhibition of the breast cancer resistance protein multidrug transporter in vitro and in mouse intestine by a novel analogue of fumitremorgin C. Mol Cancer Ther. 2002;1:417- 425

Allen JD, Brinkhuis RF, van Deemter L, Wijnholds J, Schinkel AH. Extensive contribution of the multidrug transporters P-glycoprotein and Mrp1 to basal drug resistance. Cancer Res. 2000;60(20):5761-6

Allen JD, Brinkhuis RF, van Deemter L, Wijnholds J, Schinkel AH. Extensive contribution of the multidrug transporters P-glycoprotein and Mrp1 to basal drug resistance. Cancer Res. 2000;60(20):5761-6

Aller SG, Yu J, Ward A, Weng Y, Chittaboina S, Zhuo R, Harrell PM, Trinh YT, Zhang Q, Urbatsch IL, Chang G. Structure of P-glycoprotein reveals a molecular basis for poly-specific drug binding. Science. 2009;323(5922):1718–1722

Allikmets R, Schriml LM, Hutchinson A, Romano-Spica V,MDean M. A human placenta- specific ATP-binding cassette gene (ABCP) on chromosome 4q22 that is involved in multidrug resistance. Cancer Res 1998; 58: 5337-5339

Alqawi O, Bates S, Georges E. Arginine482 to threonine mutation in the breast cancer resistance protein ABCG2 inhibits rhodamine 123 transport while increasing binding. Biochem J. 2004;382(Pt 2):711–716

Al-Shawi MK, Polar MK, Omote H, Figler RA. Transition state analysis of the coupling of drug transport to ATP hydrolysis by P-glycoprotein. J Biol Chem. 2003;278(52):52629-40

Al-Shawi MK, Urbatsch IL, Senior AE. Covalent inhibitors of P-glycoprotein ATPase activity. J Biol Chem. 1994;269(12):8986-92

Al-Shawi MK, Senior AE. Characterization of the adenosine triphosphatase activity of Chinese hamster P-glycoprotein. J Biol Chem. 1993;268(6):4197-206

Álvarez AI, Vallejo F, Barrera B, Merino G, Prieto JG, Tomás-Barberán F, Espín JC. Bioavailability of the glucuronide and sulfate conjugates of genistein and daidzein in breast cancer resistance protein 1 knockout mice. Drug Metab Dispos. 2011;39(11):2008-12

Ambudkar SV, Cardarelli CO, Pashinsky I, Stein WD. Relation between the turnover number for vinblastine transport and for vinblastine-stimulated ATP hydrolysis by human P-glycoprotein. J Biol Chem. 1997;272(34):21160-6

Ambudkar SV, Dey S, Hrycyna CA, Ramachandra M, Pastan I, Gottesman MM. Biochemical, cellular, and pharmacological aspects of the multidrug transporter. Annu Rev Pharmacol Toxicol. 1999;39,361-398

Ambudkar SV, Kim IW, Sauna ZE. The power of the pump: mechanisms of action of P-glycoprotein (ABCB1). Eur J Pharm Sci. 2006;27, 392-400

Ambudkar SV. Drug-stimulatable ATPase activity in crude membranes of human MDR1-transfected mammalian cells. Methods Enzymol. 1998;292:504-14

Ando T, Kusuhara H, Merino G, Alvarez AI, Schinkel AH,MSugiyama Y. Involvement of breast cancer resistance protein (ABCG2) in the biliary excretion mechanism of fluoroquinolones. Drug Metab Dispos 2007; 35: 1873- 1879

Asashima T, Hori S, Ohtsuki S, Tachikawa M, Watanabe M, Mukai C, Kitagaki S, Miyakoshi N, Terasaki T. ATP-binding cassette transporter G2 mediates the efflux of phototoxins on the luminal membrane of retinal capillary endothelial cells. Pharm Res. 2006;23:1235–1242

Aust S, Obrist P, Jaeger W, Klimpfinger M, Tucek G, Wrba F, Penner E and Thalhammer T. Subcellular localization of the ABCG2 transporter in normal and malignant human gallbladder epithelium. Lab Invest. 2004; 84: 1024-1036

Avdeef A, Berger CM. pH-metric solubility. 3. Dissolution titration template method for solubility determination. Eur J Pharm Sci. 2001;14(4):281-91

Bailey-Dell KJ, Hassel B, Doyle LA, Ross DD. Promoter characterization and genomic organization of the human breast cancer resistance protein (ATP-binding cassette transporter G2) gene. Biochimica et Biophysica Acta. 2001;1520:234–241

Bakos E, Evers R, Sinkó E, Váradi A, Borst P, Sarkadi B. Interactions of the human multidrug resistance proteins MRP1 and MRP2 with organicanions. Mol Pharmacol. 2000;57(4):760-8

Ball P. Quinolone generations: natural history or natural selection? J Antimicrob Chemother. 2000;46(Suppl 3):17-24

Barbosa J, Barrón D, Cano J, Jiménez-Lozano E, Sanz-Nebot V, Toro I. Evaluation of electrophoretic method versus chromatographic, potentiometric and absorptiometric methodologies for determing pK(a) values of quinolones in hydroorganic mixtures. J Pharm Biomed Anal. 2001;24(5-6):1087-98

Barnes KM, Dickstein B, Cutler GB Jr, Fojo T, Bates SE. Steroid treatment, accumulation, and antagonism of P-glycoprotein in multidrug-resistant cells. Biochemistry. 1996;35(15):4820-7

Bassi C, Pederzoli P, Vesentini S, Falconi M, Bonora A, Abbas H, Benini A, Bertazzoni EM. Behavior of antibiotics during human necrotizing pancreatitis. Antimicrob Agents Chemother. 1994;38(4):830-6

Bates SE, Robey R, Miyake K, Rao K, Ross DD, Litman T. The role of half-transporters in multidrug resistance. J Bioenerg Biomembr. 2001;33:503-511

Beck A, Aänismaa P, Li-Blatter X, Dawson R, Locher K, Seelig A. Sav1866 from Staphylococcus aureus and P-Glycoprotein: Similarities and Differences in ATPase Activity Assessed with Detergents as Allocrites. Biochemistry. 2013

Bekaii-Saab TS, Perloff MD, Weemhoff JL, Greenblatt DJ, von Moltke LL. Interactions of tamoxifen, N-desmethyltamoxifen and 4-hydroxytamoxifen with P-glycoprotein and CYP3A.Biopharm Drug Dispos. 2004;25(7):283-9

Bhatia A, Schafer HJ, Hrycyna CA. Oligomerization of the human ABC transporter ABCG2: evaluation of the native protein and chimeric dimers. Biochemistry. 2005;44(32):10893–10904

Biedler JL, Riehm H.Cellular resistance to actinomycin D in Chinese hamster cells in vitro: cross-resistance, radioautographic, and cytogenetic studies. Cancer Res. 1970;30(4):1174-84

Bihorel S, Camenisch G, Lemaire M, Scherrmann JM. Influence of breast cancer resistance protein (Abcg2) and p-glycoprotein (Abcb1a) on the transport of imatinib mesylate (Gleevec) across the mouse blood-brain barrier. J Neurochem. 2007;102:1749–1757

Blondeau JM. Fluoroquinolones: mechanism of action, classification, and development of resistance. Surv Ophthalmol. 2004;49 Suppl 2:S73-8

Bodo A, Bakos E, Szeri F, Varadi A, Sarkadi B. Differential modulation of the human liver conjugate transporters MRP2 and MRP3 by bile acids and organic anions. J Biol Chem. 2003;278:23529–23537

Boesen JJ, Niericker MJ, Dieteren N, Simons JW. How variable is a spontaneous mutation rate in cultured mammalian cells? Mutat Res. 1994;307:121-129

Borst P, Elferink RO. Mammalian ABC transporters in health and disease. Annu Rev Biochem. 2002;71, 537–592

Borst P, Ouellette M. New mechanisms of drug resistance in parasitic protozoa. Annu Rev Microbiol. 1995;49,427-60

Borst P, Schinkel AH. P-glycoprotein ABCB1: a major player in drug handling by mammals. J Clin Invest. 2013;123(10):4131-3

Borst P, Schinkel AH. What have we learnt thus far from mice with disrupted P-glycoprotein genes? Eur J Cancer. 1996;32A, 985–990

Borst P, Evers R, Kool M, Wijnholds J. A family of drug transporters: the multidrug resistance-associated proteins. J Natl Cancer Inst. 2000;92(16):1295-302

Boumendjel A, Macalou S, Ahmed-Belkacem A, Blanc M, Di Pietro A. Acridone derivatives: design, synthesis, and inhibition of breast cancer resistance protein ABCG2. Bioorg Med Chem. 2007;15(8):2892-7

Box K, Ruiz R, Comer JE, Takacs-Novak, K , Bosch E, Rafols C, Roses M. Physicochemical Properties of a New Multicomponent Cosolvent System for the pKa Determination of Poorly Soluble Pharmaceutical Compounds. Helvetica Chimica Acta. 2007;90:1538-53

Breedveld P, Pluim D, Cipriani G, Wielinga P, van Tellingen O, Schinkel AH, Schellens JH. The effect of Bcrp1 (Abcg2) on the in vivo pharmacokinetics and brain penetration of imatinib mesylate (Gleevec): implications for the use of breast cancer resistance protein and P-glycoprotein inhibitors to enable the brain penetration of imatinib in patients. Cancer Res. 2005;65:2577–2582

Breedveld P, Pluim D, Cipriani G, Dahlhaus F, van Eijndhoven MA, de Wolf CJ, Kuil A, Beijnen JH, Scheffer GL, Jansen G, Borst P, Schellens JH. The effect of low pH on breast cancer resistance protein (ABCG2)-mediated transport of methotrexate, 7-hydroxymethotrexate, methotrexate diglutamate, folic acid, mitoxantrone, topotecan, and resveratrol in in vitro drug transport models. Mol Pharmacol. 2007;71(1):240-9

Brillault J, De Castro WV, Harnois T, Kitzis A, Olivier JC, Couet W. P-glycoprotein-mediated transport of moxifloxacin in a Calu-3 lung epithelial cell model. Antimicrob Agents Chemother. 2009;53(4):1457-62

Brouwer MC, McIntyre P, de Gans J, Prasad K, van de Beek D. Corticosteroids for acute bacterial meningitis. Cochrane Database Syst Rev. 2010;(9):CD004405

Bruggemann EP, Currier S J, Gottesman MM, Pastan I. Characterization of the azidopine and vinblastine binding site of P-glycoprotein. J Biol Chem. 1992;267:21020-6

Bunting KD. ABC transporters as phenotypic markers and functional regulators of stem cells. Stem Cells. 2002;20:11-20

Burkhart CA, Watt F, Murray J, Pajic M, Prokvolit A, Xue C, Flemming C, Smith J, Purmal A, Isachenko N, Komarov PG, Gurova KV, Sartorelli AC, Marshall GM,Norris MD, Gudkov AV, Haber M. Small-molecule multidrug resistance-associated protein 1 inhibitor reversan increases the therapeutic index of chemotherapy in mouse models of neuroblastoma. Cancer Res. 2009;69:6573-80

Buxbaum E. Co-operating ATP sites in the multiple drug resistance transporter Mdr1. European Journal of Biochemistry. 1999;265:54–63

Calcabrini A, Meschini S, Stringaro A, Cianfriglia M, Arancia G, Molinari A. Detection of P-glycoprotein in the nuclear envelope of multidrug resistant cells. Histochem J. 2000;32, 599-606

Callaghan R, Higgins CF. Interaction of tamoxifen with the multidrug resistance P-glycoprotein. Br J Cancer. 1995;71(2):294-9

Cao J, Stieger B, Meier PJ, Vore M. Expression of rat hepatic multidrug resistance-associated proteins and organic anion transporters in pregnancy. Am J Physiol Gastrointest Liver Physiol. 2002;283: G757–G766

Carani C, Qin K, Simoni M, Faustini-Fustini M, Serpente S, Boyd J, Korach KS, Simpson ER. Effect of testosterone and estradiol in a man with aromatase deficiency. The New England Journal of Medicine. 1997;337 (2): 91–5

Carreau S, Lambard S, Delalande C, Denis-Galeraud I, Bourguiba S. Aromatase expression and role of estrogens in male gonad : a review. Reproductive Biology and Endocrinology. 2003;1: 35

Cavet ME, West M, Simmons NL. Fluoroquinolone (ciprofloxacin) secretion by human intestinal epithelial (Caco-2) cells. Br J Pharmacol. 1997;121(8):1567-78

Chearwae W, Anuchapreeda S, Nandigama K, Ambudkar SV, Limtrakul P. Biochemical mechanism of modulation of human P-glycoprotein (ABCB1) by curcumin I, II, and III purified from turmeric powder. Biochem Pharmacol. 2004;68:2043-52

Chen G, Durán GE, Steger KA, Lacayo NJ, Jaffrézou JP, Dumontet C, Sikic BI. Multidrug-resistant human sarcoma cells with a mutant P-glycoprotein, altered phenotype, and resistance to cyclosporins. J Biol Chem. 1997;272, 5974–5982

Chen J, Lu G, Lin J, Davidson AL, Quiocho FA. A tweezers-like motion of the ATP-binding cassette dimer in an ABC transport cycle. Mol Cell. 2003;12, 651-661

Chen L, Li Y, Yu H, Zhang L, Hou T. Computational models for predicting substrates or inhibitors of P-glycoprotein. Drug Discov Today. 2012;17(7-8):343-51

Chen Y, Pant AC, Simon SM. P-glycoprotein does not reduce substrate concentration from the extracellular leaflet of the plasma membrane in living cells. Cancer Res. 2001;61, 7763-7769

Chen ZS, Lee K, Walther S, Raftogianis RB, Kuwano M, Zeng H, Kruh GD. Analysis of methotrexate and folate transport by multidrug resistance protein 4 (ABCC4): MRP4 is a component of the methotrexate efflux system. Cancer Res. 2002;62(11):3144-50

Chen CJ, Chin JE, Ueda K, Clark DP, Pastan I, Gottesman MM, Roninson IB. Internal duplication and homology with bacterial transport proteins in the mdr1 (P-glycoprotein) gene from multidrug-resistant human cells. Cell. 1986;47(3):381-9

Chen ZS, Robey RW, Belinsky MG, Shchaveleva I, Ren XQ, Sugimoto Y, Ross DD, Bates SE, Kruh GD. Transport of methotrexate, methotrexate polyglutamates, and 17beta-estradiol 17-(beta-D-glucuronide) by ABCG2: effects of acquired mutations at R482 on methotrexate transport. Cancer Res. 2003;63(14):4048-54

Cisternino S, Mercier C, Bourasset F, Roux F, Scherrmann JM. Expression, upregulation, and transport activity of the multidrug-resistance protein Abcg2 at the mouse blood-brain barrier, Cancer Res. 2004;64:3296–3301

Clark R, Kerr ID, Callaghan R. Multiple drug binding sites on the R482G isoform of the ABCG2 transporter. Br J Pharmacol. 2006;149(5):506–515

Coburger C, Wollmann J, Krug M, Baumert C, Seifert M, Molnár J, Lage H, Hilgeroth A. Novel structure-activity relationships and selectivity profiling of cage dimeric 1,4-dihydropyridines as multidrug resistance (MDR) modulators. Bioorg Med Chem. 2010;18(14):4983-90

Coderre L, Srivastava AK, Chiasson JL. Role of glucocorticoid in the regulation of glycogen metabolism in skeletal muscle. Am J Physiol. 1991;260(6 Pt 1):E927–32

Cole SP, Bhardwaj G, Gerlach JH, Mackie JE, Grant CE, Almquist KC, Stewart AJ, Kurz EU, Duncan AM, Deeley RG. Overexpression of a transporter gene in a multidrug-resistant human lung cancer cell line. Science. 1992;258(5088):1650-4

Cooray HC, Blackmore CG, Maskell L, Barrand MA. Localisation of breast cancer resistance protein in microvessel endothelium of human brain. Neuroreport. 2002;13:2059–2063

Cooray HC, Janvilisri T, van Veen HW, Hladky SB, Barrand MA. Interaction of the breast cancer resistance protein with plant polyphenols. Biochem Biophys Res Commun. 2004;317(1):269-75

Cordon-Cardo C, O'Brien JP, Boccia J, Casals D, Bertino JR, Melamed MR. Expression of the multidrug resistance gene product (P-glycoprotein) in human normal and tumor tissues. J Histochem Cytochem. 1990;38, 1277– 1287

Cramer J, Kopp S, Bates SE, Chiba P, Ecker GF. Multispecificity of drug transporters: probing inhibitor selectivity for the human drug efflux transporters ABCB1 and ABCG2. ChemMedChem. 2007;2:1783–8

Crisp TM, Clegg ED, Cooper RL, Wood WP, Anderson DG, Baetcke KP, Hoffmann JL, Morrow MS, Rodier DJ, Schaeffer JE, Touart LW, Zeeman MG, Patel YM. Environmental endocrine disruption: An effects assessment and analysis. Environ Health Perspect. 1998;106 (Suppl 1): 11–56

Croop JM, Tiller GE, Fletcher JA, Lux ML, Raab E, Goldenson D, Son D, Arciniegas S, Wu RL. Isolation and characterization of a mammalian homolog of the Drosophila white gene. Gene. 1997;185:77–85

Dai CL, Tiwari AK, Wu CP, Su XD, Wang SR, Liu DG, Ashby CR Jr, Huang Y, Robey RW, Liang YJ, Chen LM, Shi CJ, Ambudkar SV, Chen ZS, Fu LW. Lapatinib (Tykerb, GW572016) reverses multidrug resistance in cancer cells by inhibiting the activity of ATP-binding cassette subfamily B member 1 and G member 2. Cancer Res. 2008;68(19):7905-14

Darby RA, Callaghan R, McMahon RM. P-glycoprotein inhibition: the past, the present and the future. Curr Drug Metab. 2011;12:722-31

Dassa E, Bouige P. The ABC of ABCS: a phylogenetic and functional classification of ABC systems in living organisms. Res Microbiol. 2001;152(3-4):211-29

Dautrey S, Felice K, Petiet A, Lacour B, Carbon C, Farinotti R. Active intestinal elimination of ciprofloxacin in rats: modulation by different substrates. Br J Pharmacol. 1999;127(7):1728-34

Davidson AL, Dassa E, Orelle C, Chen J. Structure, function, and evolution of bacterial ATP-binding cassette systems. Microbiol. Mol Biol Rev. 2008;72, 317-364

Davis SR, Moreau M, Kroll R, Bouchard C, Panay N, Gass M, Braunstein GD, Hirschberg AL, Rodenberg C, Pack S, Koch H, Moufarege A, Studd J. APHRODITE Study Team. Testosterone for low libido in postmenopausal women not taking estrogen. N Engl J Med. 2008;359(19):2005-17

Dawson RJ, Locher KP. Structure of a bacterial multidrug ABC transporter. Nature. 2006;443(7108):180–185

de Lange EC, Marchand S, van den Berg D, van der Sandt IC, de Boer AG, Delon A, Bouquet S, Couet W. In vitro and in vivo investigations on fluoroquinolones; effects of the P-glycoprotein efflux transporter on braindistribution of sparfloxacin. Eur J Pharm Sci. 2000;12(2):85-93

Dean M, Fojo T, Bates S. Tumour stem cells and drug resistance. Nat Rev Cancer. 2005;5:275-84

Dean M, Rzhetsky A, Allikmets R. The human ATP-binding cassette (ABC) transporter superfamily. Genome Res. 2001;11:1156-1166

Dehghan A, Kottgen A, Yang Q, Hwang SJ, Kao WL. Rivadeneira F, Boerwinkle E, Levy D, Hofman A, Astor BC et al. Association of three genetic loci with uric acid concentration and risk of gout: a genome- wide association study. Lancet. 2008;372:1953–1961

Demel MA, Krämer O, Ettmayer P, Haaksma EE, Ecker GF. Predicting ligand interactions with ABC transporters in ADME. Chem Biodivers. 2009;6:1960–1969

Demel MA, Schwaha R, Krämer O, Ettmayer P, Haaksma EE, Ecker GF. In silico prediction of substrate properties for ABC-multidrug transporters. Expert Opin Drug Metab Toxicol. 2008;4(9):1167-80

Demmer A, Andreae S, Thole H, Tummler B. Iodomycin and iodipine, a structural analogue of azidopine, bind to a common domain in hamster P-glycoprotein. Eur J Biochem. 1999;264, 800-5

Devault A, Gros P. Two members of the mouse mdr gene family confer multidrug resistance with overlapping but distinct drug specificities. Mol Cell Biol. 1990;10:1652–1663

Dey S, Ramachandra M, Pastan I, Gottesman MM, Ambudkar SV. Evidence for two nonidentical drug-interaction sites in the human Pglycoprotein. Proc Natl Acad Sci USA. 1997;94, 10594-10599

Diestra JE, Scheffer GL, Catalaı, Maliepaard M, Schellens JH, Scheper RJ, Germa - Lluch JR, Izquierdo MA. Frequent expression of the multi-drug resistance-associated protein CRP/MXR/ABCP/ABCG2 in human tumours detected by the BXP-21 monoclonal antibody in paraffin-embedded material. J Pathol. 2002;198:213–219

Dietrich CG, Geier A, Oude Elferink RP. ABC of oral bioavailability: transporters as gatekeepers in the gut. Gut. 2003;52:1788- 1795

Djurhuus CB, Gravholt CH, Nielsen S, Mengel A, Christiansen JS, Schmitz OE, Moller N. Effects of cortisol on lipolysis and regional interstitial glycerol levels in humans. Am J Physiol Endocrinol Metab. 2002;283(1): E172–7

Doige CA, Yu X, Sharom FJ. ATPase activity of partially purified P-glycoprotein from multidrug-resistant Chinese hamster ovary cells. Biochim Biophys Acta. 1992;1109(2):149-60

Dong X, Mumper RJ. Nanomedicinal strategies to treat multidrug-resistant tumors: current progress. Nanomedicine (Lond). 2010;5:597-615

Doyle LA, Yang W, Abruzzo LV, Krogmann T, Gao Y, Rishi AK, Ross DD. A multidrug resistance transporter from human MCF-7 breast cancer cells. Proc Natl Acad Sci U S A. 1998;95:15665-15670

Drozdzik M, Bialecka M, Mysliwiec K, Honczarenko K, Stankiewicz J, Sych Z. Polymorphism in the P-glycoprotein drug transporter MDR1 gene: A possible link between environmental and genetic factors in Parkinson's disease. Pharmacogenetics. 2003;13:259–263

Duan Z, Choy E, Hornicek FJ. NSC23925, identified in a high-throughput cell-based screen, reverses multidrug resistance. PLoS One. 2009;4(10):7415

Dumanović D, Juranić I, Dzeletović D, Vasić VM, Jovanović J. Protolytic constants of nizatidine, ranitidine and N,N'-dimethyl-2-nitro-1,1-ethenediamine; spectrophotometric and theoretical investigation. J Pharm Biomed Anal. 1997;15(11):1667-78

Ecker GF, Stockner T, Chiba P. Computational models for prediction of interactions with ABC-transporters. Drug Discov Today. 2008;13(7-8):311-7.

Ee PL, He X, Ross DD, Beck WT. Modulation of breast cancer resistance protein (BCRP/ABCG2) gene expression using RNA interference. Mol Cancer Ther. 2004; 3: 1577- 1583

Ee PL, Kamalakaran S, Tonetti D, He X, Ross DD, Beck WT. Identification of a novel estrogen response element in the breast cancer resistance protein (ABCG2) gene. Cancer Res. 2004;64(4):1247-51

Eisenblatter T, Huwel S, Galla HJ. Characterisation of the brain multidrug resistance protein (BMDP/BCRP/ABCG2) expressed at the blood-brain barrier. Brain Res. 2003;971:221–31

Ejendal KF, Diop NK, Schweiger LC, Hrycyna CA. The nature of amino acid 482 of human ABCG2 affects substrate transport and ATP hydrolysis but not substrate binding. Protein Sci. 2006;15(7):1597–1607

Ejendal KF, Hrycyna CA. Differential sensitivities of the human ATP-binding cassette transporters ABCG2 and P-glycoprotein to cyclosporin A. Mol Pharmacol. 2005;67(3):902-11

Elahian F, Kalalinia F, Behravan J. Evaluation of indomethacin and dexamethasone effects on BCRP-mediated drug resistance in MCF-7 parentaland resistant cell lines. Drug Chem Toxicol. 2010;33(2):113-9

Endres CJ, Hsiao P, Chung FS, Unadkat JD. The role of transporters in drug interactions. Eur J Pharm Sci. 2006;27(5):501-17

Enokizono J, Kusuhara H, Ose A, Schinkel AH, Sugiyama Y. Quantitative investigation of the role of breast cancer resistance protein (Bcrp/Abcg2) in limiting brain and testis penetration of xenobiotic compounds. Drug Metab Dispos. 2008;36:995–1002

Enokizono J, Kusuhara H, Sugiyama Y. Effect of breast cancer resistance protein (Bcrp/Abcg2) on the disposition of phytoestrogens. Mol Pharmacol. 2007;72:967– 975

Escribano E, Calpena AC, Garrigues TM, Freixas J, Domenech J, Moreno J. Structure-absorption relationships of a series of 6-fluoroquinolones. Antimicrob Agents Chemother. 1997;41(9):1996-2000

Eugster EA, Shankar R, Feezle LK, Pescovitz OH. Tamoxifen treatment of progressive precocious puberty in a patient with McCune-Albright syndrome. J Pediatr Endocrinol Metab. 1999;12(5):681-6

Eytan GD, Regev R, Oren G, Assaraf YG. The role of passive transbilayer drug movement in multidrug resistance and its modulation. J Biol Chem. 1996;271, 12897–12902

Falasca M, Linton KJ. Investigational ABC transporter inhibitors. Expert Opin Investig Drugs. 2012;21(5):657-66

Farrell RJ, Menconi MJ, Keates AC, Kelly CP. P-glycoprotein-170 inhibition significantly reduces cortisol and ciclosporin efflux from human intestinal epithelialcells and T lymphocytes. Aliment Pharmacol Ther. 2002;16(5):1021-31

Ferenci T, Boos W, Schwartz M, Szmelcman S. Energy-coupling of the transport system of Escherichia coli dependent on maltose-binding protein. Eur J Biochem. 1977;75:187-193

Fetsch PA, Abati A, Litman T, Morisaki K, Honjo Y, Mittal K, Bates SE. Localization of the ABCG2 mitoxantrone resistanceassociated protein in normal tissues. Cancer Lett. 2006;235: 84-92

Fischer H, Gottschlich R, Seelig A. Blood-brain barrier permeation: molecular parameters governing passive diffusion. Journal of Membrane Biology. 1998;165(3):201-11

Fletcher JI, Haber M, Henderson MJ, Norris MD. ABC transporters in cancer: more than just drug efflux pumps. Nat Rev Cancer. 2010;10:147-56

Fonseca EB, Celik E, Parra M, Singh M, Nicolaides KH. Fetal Medicine Foundation Second Trimester Screening Group. Progesterone and the risk of preterm birth among women with a short cervix. N Engl J Med. 2007;357(5):462-9

Fouad M, Gallagher JC. Moxifloxacin as an alternative or additive therapy for treatment of pulmonary tuberculosis. Ann Pharmacother. 2011;45, 1439-1444

Frézard F, Garnier-Suillerot A. Permeability of lipid bilayer to anthracycline derivatives. Role of the bilayer composition and of the temperature. Biochim Biophys Acta. 1998;1389(1):13-22

Fu D, Bebawy M, Kable E, Roufogalis BD. Subcellular localization of P-glycoprotein- EGFP fusion protein: implication in multidrug resistance in cancer. Int J Cancer. 2004;109:174–81

Fu D, Roufogalis BD. Actin disruption inhibits endosomal traffic of Pglycoprotein- EGFP and resistance to daunorubicin. Am J Physiol Cell Physiol. 2007;292:C1543–52

Fu D, Arias IM. Intracellular trafficking of P-glycoprotein. Int J Biochem Cell Biol. 2012;44(3):461-4

Gadsby DC, Vergani P, Csanady L. The ABC protein turned chloride channel whose failure causes cystic fibrosis. Nature. 2006;440:477-483

Gandhi YA, Morris ME. Structure-activity relationships and quantitative structure-activity relationships for breast cancer resistance protein (ABCG2). Aaps J. 2009;11(3):541–552

Garcia MA, Solans C, Aramayona JJ, Rueda S, Bregante MA. Development of a method for the determination of danofloxacin in plasma by HPLC with fluorescence detection. Biomed Chromatogr. 2000,142:89-92

Gardner ER, Ahlers CM, Shukla S, Sissung TM, Ockers SB, Price DK, Hamada A, Robey RW, Steinberg SM, Ambudkar SV, Dahut WL, Figg WD. Association of the ABCG2 C421A polymorphism with prostate cancer risk and survival. BJU Int. 2008;102(11):1694-9

Garrigos M, Mir LM, Orlowski S. Competitive and non-competitive inhibition of the multidrug-resistanceassociated P-glycoprotein ATPase-further experimental evidence for a multisite model. Eur J Biochem. 1997;244:664–673

Gatlik-Landwojtowicz E, Aänismaa P, Seelig A. The rate of P-glycoprotein activation depends on the metabolic state of the cell. Biochemistry. 2004;43(46):14840-51

Gatlik-Landwojtowicz E, Aänismaa P, Seelig A. Quantification and characterization of P-glycoprotein-substrate interactions. Biochemistry. 2006;45(9):3020-32

Gatti L, Cossa G, Beretta GL, Zaffaroni N, Perego P. Novel insights into targeting ATP-binding cassette transporters for antitumor therapy. Curr Med Chem 2011;18:4237-49

Gedeon C, Anger G, Piquette-Miller M, Koren G. Breast cancer resistance protein: mediating the trans-placental transfer of glyburide across the human placenta. Placenta. 2008;29:39–43

Gennaro AR. Remington: The science and practice of pharmacy. Vol. II. 19th ed. Easton, PA: Mack Publishing. 1995; p1257.

George AM, Jones PM. Perspectives on the structure-function of ABC transporters: the Switch and Constant Contact models. Prog Biophys Mol Biol. 2012;109(3):95-107

Gerebtzoff G, Li-Blatter X, Fischer H, Frentzel A, Seelig A. Halogenation of drugs enhances membrane binding and permeation. Chembiochem. 2004;5(5):676-84

Gerk PM, Kuhn RJ, Desai NS, McNamara PJ. Active transport of nitrofurantoin into human milk. Pharmacotherapy. 2001;21:669–675

Germann UA, Chambers TC, Ambudkar SV, Licht T, Cardarelli CO, Pastan I, Gottesman MM. Characterization of phosphorylationdefective mutants of human P-glycoprotein expressed in mammalian cells. J Biol Chem. 1996;271:1708-16

Giacomini KM, Huang SM, Tweedie DJ, Benet LZ, Brouwer KL, Chu X, Dahlin A, Evers R, Fischer V, Hillgren KM, Hoffmaster KA, Ishikawa T, Keppler D, Kim RB, Lee CA, Niemi M, Polli JW, Sugiyama Y, Swaan PW, Ware JA, Wright SH, Yee SW, Zamek-Gliszczynski MJ, Zhang L. Membrane transporters in drug development. Nat Rev Drug Discov. 2010;9(3):215-36

Giamarellou H, Kolokythas E, Petrikkos G, Gazis J, Aravantinos D, Sfikakis P. Pharmacokinetics of three newer quinolones in pregnant and lactating women. Am J Med. 1989;87(5A):49S-51S

Gil S, Saura R, Forestier F, Farinotti R. P-glycoprotein expression of the human placenta during pregnancy. Placenta. 2005;26: 268–270

Gilfillan EC, Pelak BA, Bland JA, Malatesta PF, Gadebusch HH. Pharmacokinetic studies of norfloxacin in laboratory animals. Chemotherapy. 1984;30(5):288-96

Gillet JP, Gottesman MM. Advances in the molecular detection of ABC transporters involved in multidrug resistance in cancer. Curr Pharm Biotechnol. 2011;12:686-92

Gilson E, Higgins CF, Hofnung M, Ferro-Luzzi Ames G, Nikaido H. Extensive homology between membrane-associated components of histidine and maltose transport systems of Salmonella typhimurium and Escherichia coli. J Biol Chem. 1982;257:9915-9918

Gips M, Soback S. Norfloxacin pharmacokinetics in lactating cows with sub-clinical and clinical mastitis. J Vet Pharmacol Ther. 1999;22(3):202-8

Giri N, Agarwal S, Shaik N, Pan G, Chen Y, Elmquist WF. Substrate-dependent breast cancer resistance protein (Bcrp1/Abcg2)-mediated interactions: consideration ofmultiple binding sites in in vitro assay design. Drug Metab Dispos. 2009;37(3):560-70

Glavinas H, Kis E, Pal A, Kovacs R, Jani M, Vagi E, Molnar E, Bansaghi S, Kele Z, Janaky T, Bathori G, von Richter O, Koomen GJ, Krajcsi P. ABCG2 (breast cancer resistance protein/mitoxantrone resistance-associated protein) ATPase assay: a useful tool to detect drug-transporter interactions. Drug Metab Dispos. 2007;35(9):1533–1542

Glavinas H, Krajcsi P, Cserepes J, Sarkadi B. The role of ABC transporters in drug resistance, metabolism and toxicity. Curr Drug Deliv. 2004;1:27-42

Goh LB, Spears KJ, Yao D, Ayrton A, Morgan P, Roland Wolf C, Friedberg T. Endogenous drug transporters in in vitro and in vivo models for the prediction of drug disposition in man. Biochem Pharmacol. 2002;64(11):1569-78

Goossens H, Ferech M, Vander Stichele R, Elseviers M, ESAC Project Group. Outpatient antibiotic use in Europe and association with resistance: a cross-national database study. Lancet. 2005;365(9459):579-87

Gordeliy VI, Kiselev MA, Lesieur P, Pole AV, Teixeira J. Lipid membrane structure and interactions in dimethyl sulfoxide/water mixtures. Biophys J. 1998;75(5):2343-51.

Gottesman MM, Fojo T, Bates SE. Multidrug resistance in cancer: role of ATP-dependent transporters. Nat Rev Cancer. 2002;2: 48–58

Gottesman MM, Ling V. The molecular basis of multidrug resistance in cancer: the early years of P-glycoprotein research. FEBS Lett. 2006;580:998e1009

Gottesman MM, Pastan I, Ambudkar SV. P-glycoprotein and multidrug resistance. Curr Opin Genet Dev. 1996; 6:610–617

Gottesman MM, Pastan I. Biochemistry of multidrug resistance mediated by the multidrug transporter. Annu Rev Biochem. 1993;62:385-427

Goudah A, Shah SS, Shin HC, Chang BJ, Shim JH, Abd El-Aty AM. Concentration-time courses of pefloxacin in plasma and milk of lactating she-camels (Camelus dromedarius). Berl Munch Tierarztl Wochenschr. 2008;121(11-12):432-9

Greenberger LM. Major photoaffinity drug labeling sites for iodoaryl azidoprazosin in P-glycoprotein are within, or immediately C-terminal to, transmembrane domains 6 and 12. J Biol Chem. 1993;268:11417-25

Griffiths NM, Hirst BH, Simmons NL. Active intestinal secretion of the fluoroquinolone antibacterials ciprofloxacin, norfloxacin and pefloxacin; acommon secretory pathway? J Pharmacol Exp Ther. 1994;269(2):496-502

Gupta A, Zhang Y, Unadkat JD, Mao Q. HIV protease inhibitors are inhibitors but not substrates of the human breast cancer resistance protein (BCRP/ABCG2). J Pharmacol Exp Ther. 2004;310(1):334-41

Gutmann H, Hruz P, Zimmermann C, Beglinger C, Drewe J. Distribution of breast cancer resistance protein (BCRP/ABCG2) mRNA expression along the human GI tract. Biochem Pharmacol. 2005;70:695–699

Ha SN, Hochman J, Sheridan RP. Mini review on molecular modeling of P-glycoprotein (P-gp). Curr Top Med Chem. 2007;7(15):1525-9

Haber M, Smith J, Bordow SB, Flemming C, Cohn SL, London WB, Marshall GM, Norris MD. Association of high-levelMRP1 expression with poor clinical outcome in a large prospective study of primary neuroblastoma. J Clin Oncol. 2006;24:1546-53

Hall MD, Handley MD, Gottesman MM. Is resistance useless? Multidrug resistance and collateral sensitivity. Trends Pharmacol Sci. 2009;30:546-56

Harangi M, Kaminski WE, Fleck M, Orsó E, Zeher M, Kiss E, Szekanecz Z, Zilahi E, Marienhagen J, Aslanidis C, Paragh G, Bolstad AI, Jonsson R, Schmitz G. Homozygosity for the 168His variant of the minor histocompatibility antigen HA-1 is associated with reduced risk of primary Sjogren's syndrome. Eur J Immunol. 2005;35:305-17

Haritova AM, Schrickx JA, Fink-Gremmels J. Functional studies on the activity of efflux transporters in an ex vivo model with chicken splenocytes andevaluation of selected fluoroquinolones in this model. Biochem Pharmacol. 2007;73(6):752-9

Hasegawa J, Fujita T, Hayashi Y, Iwamoto K, Watanabe J. pKa determination of verapamil by liquid-liquid partition. J Pharm. Sci. 1984;73: 442-445

Haslam IS, Wright JA, O'Reilly DA, Sherlock DJ, Coleman T, Simmons NL. Intestinal ciprofloxacin efflux: the role of breast cancer resistance protein (ABCG2). Drug Metab Dispos. 2011;39(12):2321-8

Hazai E, Bikadi Z. Homology modeling of breast cancer resistance protein (ABCG2). J Struct Biol. 2008;162(1):63–7

Hegedus C, Szakacs G, Homolya L, Orban TI, Telbisz A, Jani M, Sarkadi B. Ins and outs of the ABCG2 multidrug transporter: an update on in vitro functional assays. Adv Drug Deliv Rev. 2009;61(1):47–56

Higgins CF, Linton KJ. The ATP switch model for ABC transporters. Nat. Struct Mol Biol. 2004; 11:918-926

Hirai K, Aoyama H, Irikura T, Iyobe S, Mitsuhashi S. Differences insusceptibility to quinolones of outer membrane mutants of Salmonella typhimurium and Escherichia coli. Antimicrob Agents Chemother. 1986;29:535–8

Hirai K, Suzue S, Irikura T, Iyobe S, Mitsuhashi S. Mutations producing resistance to norfloxacin in Pseudomonas aeruginosa. Antimicrob Agents Chemother. 1987;31:582–6

Hirano M, Maeda K, Matsushima S, Nozaki Y, Kusuhara H, Sugiyama Y. Involvement of BCRP (ABCG2) in the biliary excretion of pitavastatin. Mol Pharmacol 2005;68:800-807

Hirohashi T, Suzuki H, Chu XY, Tamai I, Tsuji A, Sugiyama Y. Function and expression of multidrug resistance-associated protein family in human colon adenocarcinoma cells (Caco-2). J Pharmacol Exp Ther. 2000;292:265–270

Hochman JH, Chiba M, Nishime J, Yamazaki M, Lin JH. Influence of P-glycoprotein on the transport and metabolism of indinavir in Caco-2 cells expressing cytochrome P-450 3A4. J Pharmacol Exp Ther. 2000;292:310-8

Holland IB, Blight MA. ABC-ATPases, adaptable energy generators fuelling transmembrane movement of a variety of molecules in organisms from bacteria to humans. J Mol Biol. 1999; 293:381-399

Homolya L, Orbán TI, Csanády L, Sarkadi B. Mitoxantrone is expelled by the ABCG2 multidrug transporter directly from the plasma membrane. Biochim Biophys Acta. 2011;1808(1):154-63

Honjo Y, Hrycyna CA, Yan QW, Medina-Perez WY, Robey RW, van de Laar A, Litman T, Dean M, Bates SE. Acquired mutations in the MXR/BCRP/ABCP gene alter substrate specificity in MXR/BCRP/ABCP-overexpressing cells. Cancer Res. 2001;61:6635–6639

Honorat M, Mesnier A, Di Pietro A, Lin V, Cohen P, Dumontet C, Payen L. Dexamethasone down-regulates ABCG2 expression levels in breast cancer cells. Biochem Biophys Res Commun. 2008;375(3):308-14

Hooper DC. New uses for new and old quinolones and the challenge of resistance. Clin Infect Dis 2000;30(2):243-54

Hooper DC: Mechanisms of fluoroquinolone resistance. Drug Resist Updates. 1999;2:38–55

Hooper DC, Wolfson JS. The fluoroquinolones: pharmacology, clinical uses, and toxicities in humans. Antimicrob Agents Chemother. 1985;28(5):716-21

Hrycyna CA, Airan LE, Germann UA, Ambudkar SV, Pastan I, Gottesman MM. Structural flexibility of the linker region of human Pglycoprotein permits ATP hydrolysis and drug transport. Biochemistry. 1998;37:13660- 73

Huang H, Wang H, Sinz M, Zoeckler M, Staudinger J, Redinbo MR, Teotico DG, Locker J, Kalpana GV, Mani S. Inhibition of drug metabolism by blocking the activation of nuclear receptors by ketoconazole. Oncogene 2007;26:258-68

Huang L, Be X, Tchaparian EH, Colletti AE, Roberts J, Langley M, Ling Y, Wong BK, Jin L. Deletion of Abcg2 has differential effects on excretion and pharmacokinetics of probe substrates in rats. J Pharmacol Exp Ther. 2012;343(2):316-24

Huang Y, Sadee W: Membrane transporters and channels in chemoresistance and sensitivity of tumor cells. Cancer Lett. 2006;239:168–182

Huisman MT, Smit JW and Schinkel AH. Significance of Pglycoprotein for the pharmacology and clinical use of HIV protease inhibitors. Aids. 2000;14:237-42

Huisman MT, Smit JW, Wiltshire HR, Beijnen JH, Schinkel AH. Assessing safety and efficacy of directed P-glycoprotein inhibition to improve the pharmacokinetic properties of saquinavir coadministered with ritonavir. J Pharmacol Exp Ther. 2003;304:596-602

Ieiri I. Functional significance of genetic polymorphisms in P-glycoprotein (MDR1, ABCB1) and breast cancer resistance protein (BCRP, ABCG2). Drug Metab Pharmacokinet. 2012;27(1):85-105

Imai Y, Ishikawa E, Asada S, Sugimoto Y. Estrogen-mediated post transcriptional down- egulation of breast cancer resistance protein/ABCG2. Cancer Research. 2005;65:596– 604

Imai Y, Asada S, Tsukahara S, Ishikawa E, Tsuruo T, Sugimoto Y. Breast cancer resistance protein exports sulfated estrogens but not free estrogens. Mol Pharmacol. 2003;64(3):610-8

Imai Y, Tsukahara S, Ishikawa E, Tsuruo T, Sugimoto Y. Estrone and 17beta-estradiol reverse breast cancer resistance protein-mediated multidrug resistance. Jpn J Cancer Res. 2002;93(3):231-5

In 't Veld G, Driessen AJ, Op den Kamp JA, Konings WN. Hydrophobic membrane thickness and lipid-protein interactions of the leucine transport system of Lactococcus lactis. Biochim Biophys Acta. 1991;1065(2):203-12

Inagaki N, Gonoi T, Clement JPt Namba N, Inazawa J, Gonzalez G, Aguilar-Bryan L, Seino S, Bryan J. Reconstitution of IKATP: an inward rectifier subunit plus the sulfonylurea receptor. Science. 1995;270:1166–1170

Ishikawa T, Sakurai A, Kanamori Y, Nagakura M, Hirano H, Takarada Y, Yamada K, Fukushima K, Kitajima M. High-speed screening of human ATP-binding cassette transporter function and genetic polymorphisms: new strategies in pharmacogenomics. Methods Enzymol. 2005;400:485-510

Ishikawa T, Kasamatsu S, Hagiwara Y, Mitomo H, Kato R, Sumino Y. Expression and functional characterization of human ABC transporter ABCG2 variants in insect cells. Drug Metab Pharmacokinet. 2003;18(3):194-202

Islam MS, Narurkar MM. Solubility, stability and ionization behaviour of famotidine. J Pharm Pharmacol. 1993;45(8):682-6

Ito K, Hirai K, Inoue M, et al. In vitro antibacterial activity of AM-715, a new nalidixic acid analog. Antimicrob Agents Chemother. 1980;17:103–8

Jansen RS, Küçükosmanoglu A, de Haas M, Sapthu S, Otero JA, Hegman IE, Bergen AA, Gorgels TG, Borst P, van de Wetering K. ABCC6 prevents ectopic mineralization seen in pseudoxanthoma elasticum by inducing cellular nucleotiderelease. Proc Natl Acad Sci U S A. 2013;110(50):20206-11

Janvilisri T, Venter H, Shahi S, Reuter G, Balakrishnan L, van Veen HW. Sterol transport by the human breast cancer resistance protein (ABCG2) expressed in Lactococcus lactis. J Biol Chem. 2003;278(23):20645-51

Johnstone RW, Ruefli AA, Smyth MJ. Multiple physiological functions for multidrug transporter P-glycoprotein? Trends Biochem Sci. 2000;25:1-6

Jones PM, George AM. Opening of the ADP-bound active site in the ABC transporter ATPase dimer: evidence for a constant contact, alternating sites model for the catalytic cycle. Proteins. 2009;75:387-396

Jonker JW, Buitelaar M, Wagenaar E, Van Der Valk MA, Scheffer GL, Scheper RJ, Plosch T, Kuipers F, Elferink RP, Rosing H, Beijnen JH, Schinkel AH. The breast cancer resistance protein protects against a major chlorophyll-derived dietary phototoxin and protoporphyria. Proc Natl Acad Sci USA. 2002;99:15649–15654

Jonker JW, Freeman J, Bolscher E, Musters S, Alvi AJ, Titley I, Schinkel AH, Dale TC. Contribution of the ABC transporters Bcrp1 and Mdr1a/1b to the side population phenotype in mammary gland and bone marrow of mice. Stem Cells. 2005b; 23:1059–1065

Jonker JW, Merino G, Musters S, van Herwaarden AE, Bolscher E, Wagenaar E, Mesman E, Dale TC, Schinkel AH. The breast cancer resistance protein BCRP (ABCG2) concentrates drugs and carcinogenic xenotoxins into milk. Nat Med. 2005a;11:127–129

Jonker JW, Smit JW, Brinkhuis RF, Maliepaard M, Beijnen JH, Schellens JH, Schinkel AH. Role of breast cancer resistance protein in the bioavailability and fetal penetration of topotecan. J Natl Cancer Inst. 2000;92:1651–1656

Jonker JW, Merino G, Musters S, van Herwaarden AE, Bolscher E, Wagenaar E, Mesman E, Dale TC, Schinkel AH. The breast cancer resistance protein BCRP (ABCG2) concentrates drugs and carcinogenic xenotoxins into milk. Nat Med. 2004;11:127-129

Jordan VC. Tamoxifen (ICI46,474) as a targeted therapy to treat and prevent breast cancer. Br J Pharmacol. 2006;147 Suppl 1:S269-76

Juliano RL, Ling V. A surface glycoprotein modulating drug permeability in Chinese hamster ovary cell mutants. Biochim Biophys Acta. 1976; 455:152-162

Kage K, Tsukahara S, Sugiyama T, Asada S, Ishikawa E, Tsuruo T, Sugimoto Y. Dominant-negative inhibition of breast cancer resistance protein as drug efflux pump through the inhibition of S-S dependent homodimerization. Int J Cancer. 2002;97(5):626–630

Kannan P, Brimacombe KR, Kreisl WC, Liow JS, Zoghbi SS, Telu S, Zhang Y, Pike VW, Halldin C, Gottesman MM, Innis RB, Hall MD. Lysosomal trapping of a radiolabeled substrate of P-glycoprotein as a mechanism for signal amplification in PET. Proc Natl Acad Sci U S A. 2011;108(6):2593-8

Karssen AM, Meijer OC, van der Sandt IC, Lucassen PJ, de Lange EC, de Boer AG, de Kloet ER. Multidrug resistance P-glycoprotein hampers the access of cortisol but not of corticosterone to mouse andhuman brain. Endocrinology. 2001;142(6):2686-94

Katoh M, Nakajima M, Yamazaki H, Yokoi T. Inhibitory effects of CYP3A4 substrates and their metabolites on P-glycoprotein-mediated transport. Eur J Pharm Sci. 2001;12(4):505-13

Kawabata S, Oka M, Shiozawa K, Tsukamoto K, Nakatomi K, Soda H, Fukuda M, Ikegami Y, Sugahara K, Yamada Y, Kamihira S, Doyle LA, Ross DD, Kohno S. Breast cancer resistance protein directly confers SN-38 resistance of lung cancer cells. Biochem Biophys Res Commun. 2001;280:1216-1223

Kelly RJ, Draper D, Chen CC, Robey RW, Figg WD, Piekarz RL, Chen X, Gardner ER, Balis FM, Venkatesan AM, Steinberg SM, Fojo T, Bates SE. A pharmacodynamic study of docetaxel in combination with the P-glycoprotein antagonist tariquidar (XR9576) in patients with lung, ovarian, and cervical cancer. Clin Cancer Res. 2011;17:569-80

Kim WY, Benet LZ. P-glycoprotein (P-gp/MDR1)-mediated efflux of sex-steroid hormones and modulation of P-gp expression in vitro. Pharm Res. 2004;21(7):1284-93

Kimchi-Sarfaty C, Marple AH, Shinar S, Kimchi AM, Scavo D, Roma MI, Kim IW, Jones A, Arora M, Gribar J, Gurwitz D, Gottesman MM. Ethnicity-related polymorphisms and haplotypes in the human ABCB1 gene. Pharmacogenomics. 2007;8:29–39

Kimura Y, Morita S-Y, Matsuo M, Ueda K. Mechanism of multidrug recognition by MDR1/ABCB1. Cancer Science. 2007;98:1303–1310

Kioka N, Tsubota J, Kakehi Y, Komano T, Gottesman MM, Pastan I, Ueda K. P-glycoprotein gene (MDR1) cDNA from human adrenal: normal P-glycoprotein carries Gly185 with an altered pattern of multidrug resistance. Biochem Biophys Res Commun. 1989;162:224–231

Klaassen CD, Aleksunes LM. Xenobiotic, bile acid, and cholesterol transporters: function and regulation. Pharmacol Rev. 2010;62(1):1-96

Knutsen T, Rao VK, Ried T, Mickley L, Schneider E, Miyake K, Ghadimi BM, Padilla-Nash H, Pack S, Greenberger L, Cowan K, Dean M, Fojo T, Bates S. Amplification of 4q21-q22 and the MXR gene in independently derived mitoxantrone-resistant cell lines. Genes Chromosomes & Cancer. 2000;27:110–116

Kobayashi D, Irokawa M, Maeda T, Tsuji A, Tamai I. Carnitine/organic cation transporter OCTN2-mediated transport of carnitine in primary-cultured epididymal epithelial cells. Reproduction. 2005;130:931–937

Kodaira H, Kusuhara H, Ushiki J, Fuse E, Sugiyama Y. Kinetic analysis of the cooperation of Pglycoprotein (P-gp/Abcb1) and breast cancer resistance protein (Bcrp/Abcg2) in limiting the brain and testis penetration of erlotinib, flavopiridol, and mitoxantrone. J Pharmacol Exp Ther. 2010;333(3):788–796

Kodaira H, Kusuhara H, Fujita T, Ushiki J, Fuse E, Sugiyama Y. Quantitative evaluation of the impact of active efflux by p-glycoprotein and breast cancer resistance protein at theblood-brain barrier on the predictability of the unbound concentrations of drugs in the brain using cerebrospinalfluid concentration as a surrogate. J Pharmacol Exp Ther. 2011;339(3):935-44

Kowalski P, Farley KM, Lage H, Schneider E. Effective knock down of very high ABCG2 expression by a hammerhead ribozyme. Anticancer research. 2004;24:2231-2235

Kowalski P, Stein U, Scheffer GL, Lage H. Modulation of the atypical multidrug-resistant phenotype by a hammerhead ribozyme directed against the ABC transporter BCRP/ MXR/ABCG2. Cancer Gene Ther. 2002;9:579-586

Kowalski P, Wichert A, Holm PS, Dietel M, Lage H. Selection and characterization of a high-activity ribozyme directed against the antineoplastic drug resistance-associated ABC transporter BCRP/MXR/ABCG2. Cancer Gene Ther. 2001;8:185-192

Krishna R, Mayer LD. Multidrug resistance (MDR) in cancer. Mechanisms, reversal using modulators of MDR and the role of MDR modulators in influencing the pharmacokinetics of anticancer drugs. Eur J Pharm Sci. 2000;11,265- 83

Krishnamurthy P, Ross DD, Nakanishi T, Bailey-Dell K, Zhou S, Mercer KE, Sarkadi B, Sorrentino BP, Schuetz JD. The stem cell marker BCRP/ABCG2 enhances hypoxic cell survival through interactions with heme. Journal of Biological Chemistry. 2004;279:24218–24225

Krishnamurthy P, Schuetz JD. Role of BCRP/ABCG2 in biology and medicine. Annu Rev Pharmacol Toxicol. 2006;46:381–410

Krishnamurthy P, Xie T, Schuetz JD. The role of transporters in cellular heme and porphyrin homeostasis, Pharmacol Ther. 2007;114:345–358

Kruijtzer CM, Beijnen JH, Rosing H, ten Bokkel Huinink WW, Schot M, Jewell RC, Paul EM, Schellens JH. Increased oral bioavailability of topotecan in combination with the breast cancer resistance protein and P-glycoprotein inhibitor GF120918. J Clin Oncol. 2002;20:2943-2950

Kusuhara H, Sugiyama Y. ATP-binding cassette, subfamily G (ABCG family). Pflugers Arch. 2007;453(5):735-44

Lancet JE, Baer MR, Duran GE, List AF, Fielding R, Marcelletti JF, Multani PS, Sikic BI. A phase I trial of continuous infusion of the multidrug resistance inhibitor zosuquidar with daunorubicin and cytarabine in acute myeloid leukemia. Leuk Res. 2009;33:1055-61

Landwojtowicz E, Nervi P, Seelig A. Real-time monitoring of P-glycoprotein activation in living cells. Biochemistry. 2002;41(25):8050-7

Lee CG, Gottesman MM, Cardarelli CO, Ramachandra M, Jeang KT, Ambudkar SV, Pastan I, Dey S. HIV-1 protease inhibitors are substrates for the MDR1 multidrug transporter. Biochemistry. 1998;37,3594-601

Lee JS, Paull K, Alvarez M, Hose C, Monks A, Grever M, Fojo AT, Bates SE. Rhodamine efflux patterns predict P-glycoprotein substrates in the National Cancer Institute drug screen. Mol Pharmacol. 1994;46(4):627-38

Lee YJ, Kusuhara H, Jonker JW, Schinkel AH, Sugiyama Y. Investigation of efflux transport of dehydroepiandrosterone sulfate and mitoxantrone at the mouse blood-brain barrier: a minor role of breast cancer resistance protein. J Pharmacol Exp Ther. 2005;312:44–52

Lee W, Kim RB. Transporters and renal drug elimination. Ann. Rev. Pharmacol. Toxicol. 2004;44:137-166

Leo JC, Guo C, Woon CT, Aw SE, Lin VC. Glucocorticoid and mineralocorticoid cross-talk with progesterone receptor to induce focal adhesion and growthinhibition in breast cancer cells. Endocrinology. 2004;145(3):1314-21

Leschziner GD, Andrew T, Pirmohamed M, Johnson MR. ABCB1 genotype and P-GP expression, function and therapeutic drug response: a critical review and recommendations for future research. Pharmacogenomics J. 2007;7:154–179

Leslie EM, Deeley RG, Cole SPC. Multidrug resistance proteins: role of P-glycoprotein, MRP1, MRP2, and BCRP (ABCG2) in tissue defense. Toxicol Appl Pharmacol. 2005;204:216–237

Li YF, Polgar O, Okada M, Esser L, Bates SE, Xia D. Towards understanding the mechanism of action of the multidrug resistance-linked half-ABC transporter ABCG2: a molecular modeling study. J Mol Graph Model. 2007;25(6):837–851

Li L, Sham YY, Bikadi Z, Elmquist WF. pH-Dependent transport of pemetrexed by breast cancer resistance protein. Drug Metab Dispos. 2011;39(9):1478-85

Liang E, Proudfoot J, Yazdanian M. Mechanisms of transport and structure-permeability relationship of sulfasalazine and its analogs in Caco-2 cellmonolayers. Pharm Res. 2000;17(10):1168-74

Li-Blatter X, Beck A, Seelig A. P-glycoprotein-ATPase modulation: the molecular mechanisms. Biophys J. 2012 ;102(6):1383-93

Li-Blatter X, Nervi P, Seelig A. Detergents as intrinsic P-glycoprotein substrates and inhibitors. Biochim Biophys Acta. 2009;1788(10):2335-44

Li-Blatter X, Seelig A. Exploring the P-glycoprotein binding cavity with polyoxyethylene alkyl ethers. Biophys J. 2010;99(11):3589-98

Lindner S, Halwachs S, L Wassermann, Honscha W. Expression and subcellular localization of efflux transporter ABCG2/BCRP in important tissue barriers of lactating dairy cows, sheep and goats. J Vet Pharmacol Ther 2013; 36(6): 562-70

Linder JA, Huang ES, Steinman MA, Gonzales R, Stafford RS. Fluoroquinolone prescribing in the United States: 1995 to 2002. Am J Med. 2005;118(3):259-68

Linton KJ, Higgins CF. Structure and function of ABC transporters: the ATP switch provides flexible control. Pflugers Arch. 2007;453:555-567

Linton KJ. Structure and function of ABC transporters. Physiology (Bethesda). 2007;22:122-30

Lipsky BA, Baker CA. Fluoroquinolone toxicity profiles: a review focusing on newer agents. Clin Infect Dis. 1999;28(2):352-64

Litman T, Brangi M, Hudson E, Fetsch P, Abati A, Ross DD, Miyake K, Resau JH, Bates SE. The multidrug-resistant phenotype associated with overexpression of the new ABC half-transporter, MXR (ABCG2). J Cell Sci. 2000;113:2011-2021

Litman T, Druley TE, Stein WD, Bates SE. From MDR to MXR: new understanding of multidrug resistance systems, their properties and clinical significance. Cell Mol Life Sci. 2001;58, 931–959

Litman T, Jensen U, Hansen A, Covitz KM, Zhan Z, Fetsch P, Abati A, Hansen PR, Horn T, Skovsgaard T, Bates SE. Use of peptide antibodies to probe for the mitoxantrone resistanceassociated protein MXR/BCRP/ABCP/ABCG2. Biochim Biophys Acta. 2002;1565(1):6–16

Litman T, Zeuthen T, Skovsgaard T, Stein WD. Competitive, non-competitive and cooperative interactions between substrates of P-glycoprotein as measured by its ATPase activity. Biochim Biophys Acta. 1997a;1361:169–176

Litman T, Zeuthen T, Skovsgaard T, Stein WD. Structure activity relationships of p-glycoprotein interacting drugs: kinetic characterization of their effects on atpase activity. Biochimica et Biophysica Acta. 1997b;1361(2):159-68

Liu XL, Tee HW, Go ML. Functionalized chalcones as selective inhibitors of P-glycoprotein and breast cancer resistance protein. Bioorg Med Chem. 2008;16(1):171-80

Locher KP. Structure and mechanism of ATP-binding cassette transporters. Philos Trans R Soc Lond B Biol Sci. 2009;364(1514):239-45

Loe DW, Almquist KC, Deeley RG, Cole SP. Multidrug resistance protein (MRP)- mediated transport of leukotriene C4 and chemotherapeutic agents in membrane vesicles. Demonstration of glutathione-dependent vincristine transport. J Biol Chem. 1996;271:9675–9682

Loo TW, Bartlett MC, Clarke DM. Simultaneous binding of two different drugs in the binding pocket of the human multidrug resistance P-glycoprotein. J Biol Chem. 2003;278:39706–39710

Loo TW, Clarke DM. Functional consequences of glycine mutations in the predicted cytoplasmic loops of P-glycoprotein. J Biol Chem. 1994;269:7243-8

Loo TW, Clarke DM. Vanadate trapping of nucleotide at the ATPbinding sites of human multidrug resistance P-glycoprotein exposes different residues to the drug-binding site. Proc Natl Acad Sci USA. 2002;99:3511-3516

Loscher W, Potschka H. Role of multidrug transporters in pharmacoresistance to antiepileptic drugs. J Pharmacol Exp Ther. 2002;301:7-14

Lowes S, Simmons NL. Multiple pathways for fluoroquinolone secretion by human intestinal epithelial (Caco-2) cells. Br J Pharmacol. 2002;135(5):1263-75

Lugo MR, Sharom FJ. Interaction of LDS-751 and rhodamine 123 with P-glycoprotein: evidence for simultaneous binding of both drugs. Biochemistry. 2005;44:14020-9

Luker GD, Nilsson KR, Covey DF, Piwnica-Worms D. Multidrug resistance (MDR1) P-glycoprotein enhances esterification of plasma membrane cholesterol. J Biol Chem. 1999;274:6979-91

Maliepaard M, Scheffer GL, Faneyte IF, van Gastelen MA, Pijnenborg AC, Schinkel AH, van De Vijver MJ, Scheper RJ, Schellens JH. Subcellular localization and distribution of the breast cancer resistance protein transporter in normal human tissues. Cancer Res. 2001;61:3458-3464

Mandell L, Tillotson G. Safety of fluoroquinolones: an update. Can J Infect Dis. 2002;13(1):54-61

Mao Q, Conseil G, Gupta A, Cole SP, Unadkat JD. Functional expression of the human breast cancer resistance protein in Pichia pastoris. Biochem Biophys Res Commun. 2004;320(3):730–737

Mao Q, Leslie EM, Deeley RG, Cole SP. ATPase activity of purified and reconstituted multidrug resistance protein MRP1 from drug-selected H69AR cells. Biochim Biophys Acta. 1999;1461(1):69– 82

Mao Q. BCRP/ABCG2 in the placenta: expression, function and regulation. Pharm Res. 2008;25:1244–1255

Marchetti S, Mazzanti R, Beijnen JH, Schellens JH. Concise review: Clinical relevance of drug drug and herb drug interactions mediated by the ABCtransporter ABCB1 (MDR1, P-glycoprotein). Oncologist. 2007;12(8):927-41

Martin C, Berridge G, Higgins CF, Mistry P, Charlton P, Callaghan R. Communication between multiple drug binding sites on P-glycoprotein. Molecular Pharmacology. 2000a;58:624–632

Martin C, Berridge G, Mistry P, Higgins C, Charlton P, Callaghan R. Drug binding sites on P-glycoprotein are altered by ATP binding prior to nucleotide hydrolysis. Biochemistry. 2000b;39:11901–11906

Martinez M, McDermott P, Walker R. Pharmacology of the fluoroquinolones: a perspective for the use in domestic animals. Vet J. 2006;172(1):10-28

Marzolini C, Paus E, Buclin T, Kim RB. Polymorphisms in human MDR1 (P-glycoprotein): recent advances and clinical relevance. Clin Pharmacol Ther. 2004;75(1):13-33

Mathias AA, Hitti J, and Unadkat JD. P-glycoprotein and breast cancer resistance protein expression in human placentae of various gestational ages. Am J Physiol Regul Integr Comp Physiol. 2005;289: R963–R969

Matsson P, Englund G, Ahlin G, Bergstrom CA, Norinder U, Artursson P. A global drug inhibition pattern for the human ATP-binding cassette transporter breast cancer resistance protein (ABCG2). J Pharmacol Exp Ther. 2007;323(1):19–30

Matsson P, Pedersen JM, Norinder U, Bergström CA, Artursson P. Identification of novel specific and general inhibitors of the three major human ATP-binding cassette transporters P-gp, BCRP and MRP2 among registered drugs. Pharm Res. 2009;26(8):1816-31.

Matsunaga T, Kose E, Yasuda S, Ise H, Ikeda U, Ohmori S. Determination of p-glycoprotein ATPase activity using luciferase. Biol Pharm Bull. 2006;29(3):560-4

Matsuo H, Takada T, Ichida K, Nakamura T, Nakayama A, Ikebuchi Y, Ito K, Kusanagi Y, Chiba T, Tadokoro S Takada Y, Oikawa Y, Inoue H, Suzuki K, Okada R,Nishiyama J, Domoto H, Watanabe S, Fujita M, Morimoto Y, Naito M, Nishio K, Hishida A, Wakai K, Asai Y, Niwa K, Kamakura K, Nonoyama S, Sakurai Y,Hosoya T, Kanai Y, Suzuki H, Hamajima N, Shinomiya N. Common defects of ABCG2, a high-capacity urate exporter, cause gout: a function-based genetic analysis in a Japanese population. Sci Transl Med. 2009;1:5-11

McConnell HM, Owicki JC, Parce JW, Miller DL, Baxter GT, Wada HG, Pitchford S. The cytosensor microphysiometer: biological applications of silicon technology. Science. 1992;257(5078):1906-12

McDevitt CA, Collins R, Kerr ID, Callaghan R. Purification and structural analyses of ABCG2. Adv Drug Deliv Rev. 2009;61(1):57–65

McDevitt CA, Collins RF, Conway M, Modok S, Storm J, Kerr ID, Ford RC, Callaghan R. Purification and 3D structural analysis of oligomeric human multidrug transporter ABCG2. Structure. 2006;14(11):1623–1632

McDevitt CA, Crowley E, Hobbs G, Starr KJ, Kerr ID, Callaghan R. Is ATP binding responsible for initiating drug translocation by the multidrug transporter ABCG2? Febs J. 2008;275(17):4354–4362

Mechetner EB, Roninson I. B. Efficient inhibition of P-glycoproteinmediated multidrug resistance with a monoclonal antibody. Proc Natl Acad Sci USA. 1992;89:5824-8

Memin E, Panteix G, Revol A. Is the uptake of pefloxacin in human blood monocytes a simple diffusion process? J Antimicrob Chemother. 1996; 38, 787-798

Merino G, Alvarez AI, Pulido MM, Molina AJ, Schinkel AH, Prieto JG. Breast cancer resistance protein (BCRP/ABCG2) transports fluoroquinolone antibiotics and affects their oral availability, pharmacokinetics, and milk secretion. Drug Metab Dispos. 2006;34:690- 695

Merino G, Jonker JW, Wagenaar E, van Herwaarden AE, Schinkel AH. The breast cancer resistance protein (BCRP/ABCG2) affects pharmacokinetics, hepatobiliary excretion, and milk secretion of the antibiotic nitrofurantoin. Mol Pharmacol. 2005b;67:1758–1764

Merino G, Real R, Baro MF, Gonzalez-Lobato L, Prieto JG, Alvarez AI, Marques MM. Natural allelic variants of bovine ATP-binding cassette transporter ABCG2: increased activity of the Ser581 variant and development of tools for the discovery of new ABCG2 inhibitors. Drug Metab Dispos. 2009;37(1):5-9

Merino G, van Herwaarden AE, Wagenaar E, Jonker JW, Schinkel AH. Sex-dependent expression and activity of the ATP-binding cassette transporter breast cancer resistance protein (BCRP/ABCG2) in liver. Mol Pharmacol. 2005a;67:1765–71

Michiels F, van der Kammen RA, Janssen L, Nolan G, Collard JG. Expression of Rho GTPases using retroviral vectors. Methods Enzymol. 2000; 325:295– 302

Michot JM, Van Bambeke F, Mingeot-Leclercq MP, Tulkens PM. Active efflux of ciprofloxacin from J774 macrophages through an MRP-like transporter. Antimicrob Agents Chemother. 2004;48(7):2673-82

Michot JM, Seral C, Van Bambeke F, Mingeot-Leclercq MP, Tulkens PM. Influence of efflux transporters on the accumulation and efflux of four quinolones (ciprofloxacin, levofloxacin,garenoxacin, and moxifloxacin) in J774 macrophages. Antimicrob Agents Chemother. 2005;49(6):2429-37

Miravitlles M, Anzueto A. Moxifloxacin: a respiratory fluoroquinolone. Expert Opin Pharmacother. 2008;9(10):1755-72

Mitomo H, Kato R, Ito A, Kasamatsu S, Ikegami Y, Kii I, Kudo A, Kobatake E, Sumino Y, Ishikawa T. A functional study on polymorphism of the ATP-binding cassette transporter ABCG2: critical role of arginine-482 in methotrexate transport. Biochem. 2003;J373:767–774

Miyake K, Mickley L, Litman T, Zhan Z, Robey R, Cristensen B, Brangi M, Greenberger L, Dean M, Fojo T, Bates SE. Molecular cloning of cDNAs which are highly overexpressed in mitoxantrone-resistant cells: demonstration of homology to ABC transport genes. Cancer Res. 1999;59:8-13

Mizuno N, Suzuki M, Kusuhara H, Suzuki H, Takeuchi K, Niwa T, Jonker JW, Sugiyama Y. Impaired renal excretion of 6-hydroxy-5,7-dimethyl-2-methylamino-4-(3-pyridylmethyl) benzothiazole (E3040) sulfate in breast cancer resistance protein (BCRP1/ABCG2) knockout mice. Drug Metab Dispos. 2004;32:898-901

Mo W, Zhang JT. Human ABCG2: structure, function, and its role in multidrug resistance. Int J Biochem Mol Biol. 2012;3(1):1-27

Molinari A, Calcabrini A, Meschini S, Stringaro A, Del Bufalo D, Cianfriglia M, Arancia G. Detection of P-glycoprotein in the Golgi apparatus of drug-untreated human melanoma cells. Int J Cancer. 1998;75:885-93

Montay G, Tassel JP. Improved high-performance liquid chromatographic determination of pefloxacin and its metabolite norfloxacin in human plasma and tissue. J Chromatogr. 1985; 339, 214-218

Mulgaonkar A, Venitz J, Sweet DH. Fluoroquinolone disposition: identification of the contribution of renal secretory and reabsorptive drugtransporters. Expert Opin Drug Metab Toxicol. 2012;8(5):553-69

Munteanu E, Verdier M, Grandjean-Forestier F, Stenger C, Jayat-Vignoles C, Huet S, Robert J, Ratinaud MH. Mitochondrial localization and activity of P-glycoprotein in doxorubicin-resistant K562 cells. Biochem Pharmacol. 2006;71:1162-74

Nabekura T. Overcoming multidrug resistance in human cancer cells by natural compounds. Toxins (Basel). 2010;2:1207-24

Nakanishi T, Doyle LA, Hassel B, Wei Y, Bauer KS, Wu S, Pumplin DW, Fang HB, Ross DD. Functional characterization of human breast cancer resistance protein (BCRP, ABCG2) expressed in the oocytes of Xenopus laevis. Mol Pharmacol. 2003;64(6):1452–1462

Nakanishi T, Ross DD. Breast cancer resistance protein (BCRP/ABCG2): its role in multidrug resistance and regulation of its gene expression. Chin J Cancer. 2012;31(2):73-99

Natarajan K, Xie Y, Baer MR, Ross DD. Role of breast cancer resistance protein (BCRP/ABCG2) in cancer drug resistance. Biochem Pharmacol. 2012;83(8):1084-103

Nelson JM, Chiller TM, Powers JH, Angulo FJ. Fluoroquinolone-resistant Campylobacter species and the withdrawal of fluoroquinolones from use in poultry: apublic health success story. Clin Infect Dis. 2007;44(7):977-80

Nervi P, Li-Blatter X, Aänismaa P, Seelig A. P-glycoprotein substrate transport assessed by comparing cellular and vesicular ATPase activity. Biochim Biophys Acta. 2010;1798(3):515-25

Neu HC. Quinolone antimicrobial agents. Annu Rev Med. 1992;43:465-86

Ni Z, Bikadi Z, Rosenberg MF, Mao Q. Structure and function of the human breast cancer resistance protein (BCRP/ABCG2). Curr Drug Metab. 2010b;11(7):603-17

Ni Z, Mark ME, Cai X, Mao Q. Fluorescence Resonance Energy Transfer (FRET) Analysis Demonstrates Dimer/Oligomer Formation of the Human Breast Cancer Resistance Protein (BCRP/ ABCG2) in Intact Cells. Int J Biochem Mol Biol 2010a;1(1):1–11

Ni Z, Bikadi Z, Cai X, Rosenberg MF, Mao Q. Transmembrane helices 1 and 6 of the human breast cancer resistance protein (BCRP/ABCG2): identification ofpolar residues important for drug transport. Am J Physiol Cell Physiol. 2010c;299(5):C1100-9

Nicolle E, Boumendjel A, Macalou S, Genoux E, Ahmed-Belkacem A, Carrupt PA, Di Pietro A. QSAR analysis and molecular modeling of ABCG2-specific inhibitors. Adv Drug Deliv Rev. 2009;61(1):34–46

Noguchi K, Kawahara H, Kaji A, Katayama K, Mitsuhashi J, Sugimoto Y. Substrate-dependent bidirectional modulation of P-glycoprotein-mediated drug resistance by erlotinib. Cancer Sci. 2009;100:1701–7

Oldham ML, Davidson AL, Chen J. Structural insights into ABC transporter mechanism. Curr Opin Struct Biol. 2008;18(6):726-33

Oliphant CM, Green GM. Quinolones: a comprehensive review. Am Fam Physician 2002;65(3):455-65

Omote H, Al-Shawi MK. A novel electron paramagnetic resonance approach to determine the mechanism of drug transport by P-glycoprotein. J Biol Chem. 2002;277(47):45688-94

Oo CY, Kuhn RJ, Desai N, and McNamara PJ. Active transport of cimetidine into human milk. Clin Pharmacol Ther. 1995;58:548–555

Orbán TI, Seres L, Ozvegy-Laczka C, Elkind NB, Sarkadi B, Homolya L. Combined localization and real-time functional studies using a GFP-tagged ABCG2 multidrug transporter. Biochem Biophys Res Commun. 2008;367(3):667-73

Orlowski S, Mir LM, Belehradek J Jr, Garrigos M. Effects of steroids and verapamil on P-glycoprotein ATPase activity: progesterone, desoxycorticosterone,corticosterone and verapamil are mutually non-exclusive modulators. Biochem J. 1996;317 (Pt 2):515-22

Ozols RF, Cunnion RE, Klecker RW Jr, Hamilton TC, Ostchega Y, Parrillo JE, Young RC. Verapamil and adriamycin in the treatment of drug-resistant ovarian cancer patients. J Clin Oncol. 1987;5:641-7

Ozvegy C, Litman T, Szakacs G, Nagy Z, Bates S, Varadi A, Sarkadi B. Functional characterization of the human multidrug transporter, ABCG2, expressed in insect cells. Biochem Biophys Res Commun. 2001;285(1):111–117

Ozvegy C, Varadi A, Sarkadi B. Characterization of drug transport, ATP hydrolysis, and nucleotide trapping by the human ABCG2 multidrug transporter. Modulation of substrate specificity by a point mutation. J Biol Chem. 2002;277(50):47980–47990

Ozvegy-Laczka C, Cserepes J, Elkind NB, Sarkadi B. Tyrosine kinase inhibitor resistance in cancer: role of ABC multidrug transporters. Drug Resist Update. 2005;8:15-26

Ozvegy-Laczka C, Várady G, Köblös G, Ujhelly O, Cervenak J, Schuetz JD, Sorrentino BP, Koomen GJ, Váradi A, Német K, Sarkadi B. Function-dependent conformational changes of the ABCG2 multidrug transporter modify its interaction with amonoclonal antibody on the cell surface. J Biol Chem. 2005b;280(6):4219-27

Ozvegy-Laczka C, Hegedus T, Várady G, Ujhelly O, Schuetz JD, Váradi A, Kéri G, Orfi L, Német K, Sarkadi B. High-affinity interaction of tyrosine kinase inhibitors with the ABCG2 multidrug transporter. Mol Pharmacol. 2004;65(6):1485-95

Pajeva IK, Globisch C, Wiese M. Structure-function relationships of multidrug resistance Pglycoprotein. J Med Chem. 2004;47:2523–2533

Pal A, Mehn D, Molnar E, Gedey S, Meszaros P, Nagy T, Glavinas H, Janaky T, von Richter O, Bathori G, Szente L, Krajcsi P. Cholesterol potentiates ABCG2 activity in a heterologous expression system: improved in vitro model to study function of human ABCG2. J Pharmacol Exp Ther. 2007;321(3):1085–1094

Parce JW, Owicki JC, Kercso KM, Sigal GB, Wada HG, Muir VC, Bousse LJ, Ross KL, Sikic BI, McConnell HM. Detection of cell-affecting agents with a silicon biosensor. Science. 1989;246(4927):243-7

Park MS, Okochi H, Benet LZ. Is Ciprofloxacin a Substrate of P-glycoprotein? Arch Drug Inf. 2011;4(1):1-9

Paulusma CC, Bosma PJ, Zaman GJ, Bakker CT, Otter M, Scheffer GL, Scheper RJ, Borst P, Oude Elferink RP. Congenital jaundice in rats with a mutation in a multidrug resistance-associated protein gene. Science. 1996;271:1126-8

Pavek P, Merino G, Wagenaar E, Bolscher E, Novotna M, Jonker JW, Schinkel AH. Human breast cancer resistance protein: interactions with steroid drugs, hormones, the dietary carcinogen 2-amino-1-methyl-6-phenylimidazo(4,5-b)pyridine, and transport of cimetidine. J Pharmacol Exp Ther. 2005;312(1):144-52

Pearce HL, Safa AR, Bach NJ, Winter MA, Cirtain MC, Beck WT. Essential features of the P-glycoprotein pharmacophore as defined by a series of reserpine analogs that modulate multidrug resistance. Proc Natl Acad Sci USA. 1989;86:5128–5132

Peng H, Dong Z, Qi J, Yang Y, Liu Y, Li Z, Xu J and Zhang JT. A Novel Two Mode-Acting Inhibitor of ABCG2-Mediated Multidrug Transport and Resistance in Cancer Chemotherapy. PLoS ONE. 2009;4:5676

Peng H, Qi J, Dong Z, Zhang JT. Dynamic vs Static ABCG2 Inhibitors to Sensitize Drug Resistant Cancer Cells. PLoS One. 2010;5:15276

Peterson LR. Management of fluoroquinolone use to avoid microbial resistance in clinical practice. Postgrad Med. 2001;109(2 Suppl):51-9

Pichler A, Zelcer N, Prior JL, Kuil AJ, Piwnica-Worms D. In vivo RNA interference-mediated ablation of MDR1 P-glycoprotein. Clin Cancer Res. 2005;11:4487-94

Pick A, Müller H, Wiese M. Structure-activity relationships of new inhibitors of breast cancer resistance protein (ABCG2). Bioorg Med Chem. 2008;16(17):8224-36

Poguntke M, Hazai E, Fromm MF, Zolk O. Drug transport by breast cancer resistance protein. Expert Opin Drug Metab Toxicol. 2010;6(11):1363-84

Polgar O, Ierano C, Tamaki A, Stanley B, Ward Y, Xia D, Tarasova N, Robey RW, Bates SE. Mutational analysis of threonine 402 adjacent to the GXXXG dimerization motif in transmembrane segment 1 of ABCG2. Biochemistry. 2010;49(10):2235–2245

Polli JW, Olson KL, Chism JP, John-Williams LS, Yeager RL, Woodard SM, Otto V, Castellino S, Demby VE. An unexpected synergist role of P-glycoprotein and breast cancer resistance protein on the central nervous system penetration of the tyrosine kinase inhibitor lapatinib (N-{3-chloro-4-[(3- fluorobenzyl)oxy]phenyl}-6-[5-({[2-(methylsulfonyl)ethy l]amino}methyl)-2-furyl]-4-quinazolinamine, GW572016). Drug Metab Dispos. 2009;37(2):439–442

Polli JW, Wring SA, Humphreys JE, Huang L, Morgan JB, Webster LO, Serabjit-Singh CS. Rational use of in vitro P-glycoprotein assays in drug discovery. Int J Clin Pharmacol Ther. 2001; 299, 620–628

Potocnik U, Ferkolj I, Glavac D, Dean M. Polymorphisms in multidrug resistance 1 (MDR1) gene are associated with refractory Crohn disease and ulcerative colitis. Genes Immun. 2004;5:530–539

Potocnik U, Glavac MR, Golouh R, Glavac D: The role of P-glycoprotein (MDR1) polymorphisms and mutations in colorectal cancer. Pflugers Arch. 2001;442:R182–R183

Pozza A, Perez-Victoria JM, Sardo A, Ahmed-Belkacem A, Di Pietro A. Purification of breast cancer resistance protein ABCG2 and role of arginine-482. Cell Mol Life Sci. 2006;63(16):1912–1922.

Pulido MM, Molina AJ, Merino G, Mendoza G, Prieto JG, Alvarez AI. Interaction of enrofloxacin with breast cancer resistance protein (BCRP/ABCG2): influence of flavonoids and role in milk secretion in sheep. J Vet Pharmacol Ther. 2006;29:279–287

Putman M, Koole LA, van Veen HW, Konings WN. The secondary multidrug transporter LmrP contains multiple drug interaction sites. Biochemistry. 1999;38(42):13900-5

Raaijmakers MH, de Grouw EP, Heuver LH, van der Reijden BA, Jansen JH, Scheper RJ, Scheffer GL, de Witte TJ, Raymakers RA. Breast cancer resistance protein in drug resistance of primitive CD34+38- cells in acute myeloid leukemia. Clin Cancer Res. 2005;11:2436-2444

Rabbaa L, Dautrey S, Colas-Linhart N, Carbon C, Farinotti R. Intestinal elimination of ofloxacin enantiomers in the rat: evidence of a carrier-mediated process. Antimicrob Agents Chemother. 1996;40(9):2126-30

Ramachandra M, Ambudkar SV, Chen D, Hrycyna CA, Dey S, Gottesman MM, Pastan I. Human P-glycoprotein exhibits reduced affinity for substrates during a catalytic transition state. Biochemistry. 1998;37:5010-5019

Rao US, Fine RL, Scarborough GA. Antiestrogens and steroid hormones: substrates of the human P-glycoprotein. Biochem Pharmacol. 1994;48(2):287-92

Raub TJ. P-glycoprotein recognition of substrates and circumvention through rational drug design. Molecular Pharmacology. 2006;3:3–25

Real R, Egido E, Pérez M, González-Lobato L, Barrera B, Prieto JG, Alvarez AI, Merino G. Involvement of breast cancer resistance protein (BCRP/ABCG2) in the secretion of danofloxacin into milk: interaction with ivermectin. J Vet Pharmacol Ther. 2011;34(4):313-21

Riordan JR, Ling V. Purification of P-glycoprotein from plasma membrane vesicles of Chinese hamster ovary cell mutants with reduced colchicines permeability. J Biol Chem. 1979;254(24):12701-5

Riordan JR, Rommens JM, Kerem B, Alon N, Rozmahel R, Grzelczak Z, Zielenski J, Lok S, Plavsic N, Chou JL, et al. Identification of the cystic fibrosis gene: cloning and characterization of complementary DNA. Science. 1989; 245;1066-1073

Robert J, Jarry C: Multidrug resistance reversal agents. J Med Chem. 2003;46:4805–4817

Robey RW, Honjo Y, van de Laar A, Miyake K, Regis JT, Litman T, Bates SE. A functional assay for detection of the mitoxantrone resistance protein, MXR (ABCG2). Biochim Biophys Acta. 2001;1512(2):171-82

Robey RW, To KK, Polgar O, Dohse M, Fetsch P, Dean M, Bates SE. ABCG2: a perspective. Adv Drug Deliv Rev. 2009;61(1):3-13

Robey RW, Honjo Y, Morisaki K, Nadjem TA, Runge S, Risbood M, Poruchynsky MS, Bates SE. Mutations at amino-acid 482 in the ABCG2 gene affect substrate and antagonist specificity. Br J Cancer. 2003;89(10):1971-8

Rodríguez-Ibáñez M, Nalda-Molina R, Montalar-Montero M, Bermejo MV, Merino V, Garrigues TM. Transintestinal secretion of ciprofloxacin, grepafloxacin and sparfloxacin: in vitro and in situ inhibition studies. Eur J Pharm Biopharm. 2003;55(2):241-6

Rodríguez-Ibáñez M, Nalda-Molina R, Montalar-Montero M, Bermejo MV, Merino V, Garrigues TM. Transintestinal secretion of ciprofloxacin, grepafloxacin and sparfloxacin: in vitro and in situ inhibition studies. Eur J Pharm Biopharm. 2003;55(2):241-6

Rodríguez-Ibáñez M, Sánchez-Castaño G, Montalar-Montero M, Garrigues TM, Bermejo M, Merino V. Mathematical modelling of in situ and in vitro efflux of ciprofloxacin and grepafloxacin. Int J Pharm. 2006;307(1):33-41

Rodríguez-Ibáñez M, Sánchez-Castaño G, Montalar-Montero M, Garrigues TM, Bermejo M, Merino V. Mathematical modelling of in situ and in vitro efflux of ciprofloxacin and grepafloxacin. Int J Pharm. 2006;307(1):33-41

Rodríguez-Ibáñez M, Nalda-Molina R, Montalar-Montero M, Bermejo MV, Merino V, Garrigues TM. Transintestinal secretion of ciprofloxacin, grepafloxacin and sparfloxacin: in vitro and in situ inhibition studies. Eur J Pharm Biopharm. 2003;55(2):241-6

Rodríguez-Ibáñez M, Sánchez-Castaño G, Montalar-Montero M, Garrigues TM, Bermejo M, Merino V. Mathematical modelling of in situ and in vitro efflux of ciprofloxacin and grepafloxacin. Int J Pharm. 2006;307(1):33-41

Romsicki Y, Sharom F. The ATPase and ATP-binding functions of P-glycoprotein modulation by interaction with defined phospholipids. European Journal of Biochemistry. 1998;256:170–178

Romsicki Y, Sharom FJ. The membrane lipid environment modulates drug interactions with the P- glycoprotein multidrug transporter. Biochemistry. 1999;38:6887-6896

Rosenberg MF, Bikadi Z, Chan J, Liu X, Ni Z, Cai X, Ford RC, Mao Q. The human breast cancer resistance protein (BCRP/ABCG2) shows conformational changes with mitoxantrone. Structure. 2010;18:482-493

Ross DD, Karp JE, Chen TT, Doyle LA. Expression of breast cancer resistance protein in blast cells from patients with acute leukemia. Blood. 2000;96:365-368

Ross DD, Nakanishi T. Impact of breast cancer resistance protein on cancer treatment outcomes. In: Zhou J, editor. Methods in Molecular Biology. New York: Humana Press, Springer. 2010:251–90

Ruff P, Vorobiof DA, Jordaan JP, Demetriou GS, Moodley SD, Nosworthy AL, Werner ID, Raats J, Burgess LJ. A randomized, placebo-controlled, double-blind phase II study of docetaxel compared to docetaxel plus zosuquidar (LY335979) in women with metastatic or locally recurrent breast cancer who have received one prior chemotherapy regimen. Cancer Chemother Pharmacol. 2009;64:763-8

Ruiz-García A, Lin H, Plá-Delfina JM, Hu M. Kinetic characterization of secretory transport of a new ciprofloxacin derivative (CNV97100) across Caco-2 cellmonolayers. J Pharm Sci. 2002;91(12):2511-9

Rust S, Rosier M, Funke H, Real J, Amoura Z, Piette JC, Deleuze JF, Brewer HB, Duverger N, Denèfle P, Assmann G. Tangier disease is caused by mutations in the gene encoding ATP-binding cassette transporter 1. Nat Genet. 1999;22:352-5

Sai Y, Nies AT, Arias IM. Bile acid secretion and direct targeting of mdr1-green fluorescent protein from Golgi to the canalicular membrane in polarized WIF-B cells. J Cell Sci. 1999;112:4535–45

Saison C, Helias V, Ballif BA, Peyrard T, Puy H, Miyazaki T, Perrot S, Vayssier-Taussat M, Waldner M, Le Pennec PY, Cartron JP, Arnaud L. Null alleles of ABCG2 encoding the breast cancer resistance protein define the new blood group system Junior. Nat Genet. 2012;44(2):174-7

Saito H, Hirano H, Nakagawa H, Fukami T, Oosumi K, Murakami K, Kimura H, Kouchi T, Konomi M, Tao E, Tsujikawa N, Tarui S, Nagakura M, Osumi M, Ishikawa T. A new strategy of high-speed screening and quantitative structure-activity relationship analysis to evaluate human ATP-binding cassette transporter ABCG2-drug interactions. J Pharmacol Exp Ther. 2006;317(3):1114–1124

Sarkadi B, Price EM, Boucher RC, Germann UA, Scarborough GA. Expression of the human multidrug resistance cDNA in insect cells generates a high activity drug-stimulatedmembrane ATPase. J Biol Chem. 1992;267(7):4854-8

Sarkadi B, Homolya L, Szakács G, Váradi A. Human multidrug resistance ABCB and ABCG transporters: participation in a chemoimmunity defense system. Physiol Rev. 2006;86(4):1179-236

Sauna Z, Ambudkar SV. About a switch: how P-glycoprotein (ABCB1) harnesses the energy of ATP binding and hydrolysis to do mechanical work. Mol Cancer Ther. 2007;6:13–23

Sauna ZE, Ambudkar SV. Evidence for a requirement for ATP hydrolysis at two distinct steps during a single turnover of the catalytic cycle of human P-glycoprotein. Pro Natl Acad Sci USA. 2000;97:2515-2520

Sauna ZE, Ambudkar SV. Characterization of the catalytic cycle of ATP hydrolysis by human P-glycoprotein. The two ATP hydrolysis events in a single catalytic cycle are kinetically similar but affect different functional outcomes. J Biol Chem. 2001;276(15):11653-61

Schinkel AH, Jonker JW: Mammalian drug efflux transporters of the ATP binding cassette (ABC) family: an overview. Adv Drug Deliv Rev. 2003;55:3–29

Schinkel AH, Mol CA, Wagenaar E, van Deemter L, Smit J J, Borst P. Multidrug resistance and the role of P-glycoprotein knockout mice. Eur J Cancer. 1995;31A:1295-8

Schinkel AH, Wagenaar E, Mol CA, van Deemter L. Pglycoprotein in the blood-brain barrier of mice influences the brain penetration and pharmacological activity of many drugs. J Clin Invest. 1996;97:2517-24

Schinkel AH, Mayer U, Wagenaar E, Mol CA, van Deemter L, Smit JJ, van der Valk MA, Voordouw AC, Spits H, van Tellingen O, Zijlmans JM, Fibbe WE, Borst P. Normal viability and altered pharmacokinetics in mice lacking mdr1-type (drug-transporting) P-glycoproteins. Proc. Natl Acad Sci USA. 1997;94:4028–4033

Schinkel AH, Wagenaar E, van Deemter L, Mol CA, Borst P. Absence of the mdr1a P-Glycoprotein in mice affects tissue distribution and pharmacokinetics of dexamethasone, digoxin, and cyclosporin A. J Clin Invest. 1995;96(4):1698-705

Schinkel AH. The physiological function of drug-transporting P-glycoproteins. Semin Cancer Biol. 1997;8(3):161-70

Schlatter P, Gutmann H, Drewe J. Primary porcine proximal tubular cells as a model for transepithelial drug transport in human kidney. Eur J Pharm Sci. 2006;28(1-2):141-54

Schnepf R, Zolk O. Effect of the ATP-binding cassette transporter ABCG2 on pharmacokinetics: experimental findings and clinical implications. Expert Opin Drug Metab Toxicol. 2013;9(3):287-306

Scholar E. Fluoroquinolones: past, present and future of a novel group of antibacterial agents. Am J Pharm Educ. 2002;66(2):164-71

Schroder J. Enrofloxacin: a new antimicrobial agent. J S Afr Vet Assoc. 1989;60(2):122-4

Schwab D, Fischer H, Tabatabaei A, Poli S, Huwyler J. Comparison of in vitro p-glycoprotein screening assays: recommendations for their use in drug discovery. Journal of Medicinal Chemistry. 2003a;46(9):1716-25

Schwab M, Eichelbaum M, Fromm MF. Genetic polymorphisms of the human MDR1 drug transporter. Annu Rev Pharmacol Toxicol. 2003b;43:285–307

Schwab M, Schaeffeler E, Marx C, Fromm MF, Kaskas B, Metzler J, Stange E, Herfarth H, Schoelmerich J, Gregor M, Walker S, Cascorbi I, Roots I, Brinkmann U,Zanger UM, Eichelbaum M. Association between the C3435T MDR1 gene polymorphism and susceptibility for ulcerative colitis. Gastroenterology. 2003c;124:26-33

Seeger MA, van Veen HW. Molecular basis of multidrug transport by ABC transporters. Biochim Biophys Acta. 2009;1794:725–737

Seelig A, Gatlik-Landwojtowicz E. Inhibitors of multidrug efflux transporters: their membrane and protein interactions. Mini Rev Med Chem. 2005;5(2):135-51

Seelig A, Gerebtzoff G. Enhancement of drug absorption by noncharged detergents through membrane and p-glycoprotein binding. Expert Opin Drug Metab Toxico.2006;2(5):733-52

Seelig A, Gottschlich R, Devant RM. A method to determine the ability of drugs to diffuse through the blood-brain barrier. Proc Natl Acad Sci USA. 1994;91(1):68-72

Seelig A, Landwojtowicz E. Structure-activity relationship of Pglycoprotein substrates and modifiers. Eur J Pharm Sci. 2000;12:31-40

Seelig A. A general pattern for substrate recognition by P-glycoprotein. Eur J Biochem. 1998;251(1-2):252-61

Seelig A. The role of size and charge for blood-brain barrier permeation of drugs and fatty acids. J Mol Neurosci. 2007;33(1):32-41

Seigneuret M; Garnier-Suillerot A. A structural model for the open conformation of the mdr1 P-glycoprotein based on the MsbA crystal structure. J Biol Chem. 2003;278:30115–30124

Seiler P. Interconversion of lipophilicities from hydrocarbonwater systems into octanol-water system. Eur J Med Chem. 1974;9: 473-479

Seithel A, Karlsson J, Hilgendorf C, Björquist A, Ungell AL. Variability in mRNA expression of ABC- and SLC-transporters in human intestinal cells: comparison between human segments and Caco-2 cells. Eur J Pharm Sci. 2006;28(4):291-9

Senior AE, Al-Shawi MK, Urbatsch IL. The catalytic cycle of P-glycoprotein. FEBS Lett. 1995;377:285-289

Senior AE, Bhagat S. P-glycoprotein shows strong catalytic cooperativity between the two nucleotide sites. Biochemistry. 1998;37:831-836

Shapiro AB, Fox K, Lam P, Ling V. Stimulation of Pglycoprotein- mediated drug transport by prazosin and progesterone. Evidence for a third drug-binding site. Eur J Biochem. 1999;259:841-850

Shapiro AB, Ling V. Extraction of Hoechst 33342 from the cytoplasmic leaflet of the plasma membrane by P-glycoprotein. Eur J Biochem. 1997;250:122-129

Sharom FJ, Lugo MR, Eckford PD. New insights into the drug binding, transport and lipid flippase activities of the P-glycoprotein multidrug transporter. J Bioenerg Biomembr. 2005;37:481–487

Sharom FJ, Yu X, Lu P, Liu R, Chu JW, Szabó K, Müller M, Hose CD, Monks A, Váradi A, Seprôdi J, Sarkadi B. Interaction of the P-glycoprotein multidrug transporter (MDR1) with high affinity peptide chemosensitizers inisolated membranes, reconstituted systems, and intact cells. Biochem Pharmacol. 1999;58(4):571-86

Sharom FJ. The p-glycoprotein effux pump: how does it transport drugs? Journal of Membrane Biology. 1997;160(3):161-75

Sharom FJ. ABC multidrug transporters: structure, function and role in chemoresistance. Pharmacogenomics. 2008;9(1):105-27

Sheppard DN, Robinson KA. Mechanism of glibenclamide inhibition of cystic fibrosis transmembrane conductance regulator Cl- channelsexpressed in a murine cell line. J Physiol. 1997;503(Pt 2):333-46

Sheps JA, Ralph S, Zhao Z, Baillie DL, Ling V. The ABC transporter gene family of Caenorhabditis elegans has implications for the evolutionary dynamics of multidrug resistance in eukaryotes. Genome Biol. 2004;5(3):R15

Shilling RA, Venter H, Velamakanni S, Bapna A, Woebking B, Shahi S, Van Veen HW. New light on multidrug binding by an ATP-binding-cassette transporter. Trends in Pharmacology Sciences. 2006;27:195–203

Shulenin S, Nogee LM, Annilo T, Wert SE, Whitsett JA, Dean M. ABCA3 gene mutations in newborns with fatal surfactant deficiency. N Engl J Med. 2004;350:1296-303

Siegsmund M, Brinkmann U, Schäffeler E, Weirich G, Schwab M, Eichelbaum M, Fritz P, Burk O, Decker J, Alken P, Rothenpieler U, Kerb R, Hoffmeyer S,Brauch H. Association of the P-glycoprotein transporter MDR1 C3435T polymorphism with the susceptibility to renal epithelial tumors. J Am Soc Nephrol. 2002;13:1847–1854

Sikic BI. Modulation of multidrug resistance: a paradigm for translational clinical research. Oncology. 1999;13:183–7

Sikic BI. Multidrug resistance and stem cells in acute myeloid leukemia. Clin Cancer Res. 2006;12:3231-2

Sikri V, Pal D, Jain R, Kalyani D, Mitra AK. Cotransport of macrolide and fluoroquinolones, a beneficial interaction reversing P-glycoprotein efflux. Am J Ther. 2004;11(6):433-42

Simerly RB. Wired for reproduction: organization and development of sexually dimorphic circuits in the mammalian forebrain. Annu Rev Neurosci. 2002;25:507-36.

Simmons PS, Miles JM, Gerich JE, Haymond MW. Increased proteolysis. An effect of increases in plasma cortisol within the physiologic range. J Clin Invest. 1984;73(2): 412–20

Soback S, Gips M, Bialer M, Bor A. Effect of lactation on single-dose pharmacokinetics of norfloxacin nicotinate in ewes. Antimicrob Agents Chemother. 1994;38(10):2336-9

Solomkin JS, Mazuski JE, Bradley JS, Rodvold KA, Goldstein EJ, Baron EJ, O'Neill PJ, Chow AW, Dellinger EP, Eachempati SR, Gorbach S, Hilfiker M, May AK, Nathens AB, Sawyer RG, Bartlett JG. Diagnosis and management of complicated intra-abdominal infection in adults and children:guidelines by the Surgical Infection Society and the Infectious Diseases Society of America. Surg Infect (Larchmt). 2010;11(1):79-109

Sorgel F, Jaehde U, Naber KG, Stephan U. Pharmacokinetic disposition of quinolones in human body fluids and tissues. Clin Pharmacokinet. 1989;16(Suppl 1):5-24

Sprandel KA, Rodvold KA. Safety and tolerability of fluoroquinolones. Clin Cornerstone. 2003;5(Suppl 3):S29-36

Stahlmann R, Lode H. Fluoroquinolones in the elderly: safety considerations. Drugs Aging 2003;20(4):289-302

Stahlmann R. Clinical toxicological aspects of fluoroquinolones. Toxicol Lett. 2002;127(1-3):269-7

Stass H, Kubitza D, Halabi A, Delesen H. Pharmacokinetics of moxifl oxacin, a novel 8-methoxy-quinolone, in patients with renal dysfunction. Br J Clin Pharmacol. 2002;53:232-7

Stass H, Kubitza D, Schühly U. Pharmacokinetics, safety and tolerability of moxifl oxacin, a novel 8-methoxyfl uoroquinolone, after repeated oral administration. Clin Pharmacokinet. 2001;40 (Suppl 1):1-9

Steck TL, Weinstein RS, Straus JH, Wallach DF. Inside-out red cell membrane vesicles: preparation and purification. Science. 1970;168(3928):255-7

Stein GE. Pharmacokinetics and pharmacodynamics of newer fluoroquinolones. Clin Infect Dis. 1996;23(Suppl 1):S19-24

Steinbach D, Sell W, Voigt A, Hermann J, Zintl F, Sauerbrey A. BCRP gene expression is associated with a poor response to remission induction therapy in childhood acute myeloid leukemia. Leukemia. 2002;16(8):1443–1447

Steiner AZ, Terplan M, Paulson RJ. Comparison of tamoxifen and clomiphene citrate for ovulation induction: a meta-analysis. Hum Reprod. 2005;20(6):1511-5

Stenham DR, Campbell JD, Sansom MS, Higgins CF, Kerr ID, Linton KJ. An atomic detail model for the human ATP binding cassette transporter P-glycoprotein derived from disulfide cross-linking and homology modeling. FASEB J. 2003;17:2287–2289

Storch CH, Ehehalt R, Haefeli WE, Weiss J. Localization of the human breast cancer resistance protein (BCRP/ABCG2) in lipid rafts/caveolae and modulation of its activity by cholesterol in vitro. J Pharmacol Exp Ther. 2007;323:257–264

Strautnieks SS, Bull LN, Knisely AS, Kocoshis SA, Dahl N, Arnell H, Sokal E, Dahan K, Childs S, Ling V, Tanner MS, Kagalwalla AF, Németh A, Pawlowska J, Baker A, Mieli-Vergani G, Freimer NB, Gardiner RM, Thompson RJ. A gene encoding a liver-specific ABC transporter is mutated in progressive familial intrahepatic cholestasis. Nat Genet. 1998;20:233-8

Sugimoto Y, Tsukahara S, Imai Y, Sugimoto Y, Ueda K, Tsuruo T. Reversal of breast cancer resistance protein-mediated drug resistance by estrogen antagonists and agonists. Mol Cancer Ther. 2003;2(1):105-12

Sun H, Pang KS. Permeability, transport, and metabolism of solutes in Caco-2 cell monolayers: a theoretical study. Drug Metab Dispos. 2008;36(1):102-23

Susa M, Iyer AK, Ryu K, Choy E, Hornicek FJ, Mankin H, Milane L, Amiji MM, Duan Z. Inhibition of ABCB1 (MDR1) expression by an siRNA nanoparticulate delivery system to overcome drug resistance in osteosarcoma. PLoS One. 2010;5:10764

Szakács G, Váradi A, Ozvegy-Laczka C, Sarkadi B. The role of ABC transporters in drug absorption, distribution, metabolism, excretion andtoxicity (ADME-Tox). Drug Discov Today. 2008;13(9-10):379-93

Szakács Z, Noszál B. Determination of dissociation constants of folic acid, methotrexate, and other photolabile pteridines by pressure-assisted capillary electrophoresis. Electrophoresis. 2006;27(17):3399-409

Takada Y, Yamada K, Taguchi Y, Kino K, Matsuo M, Tucker SJ, Komano T, Amachi T, Ueda K. Non-equivalent cooperation between the two nucleotide-binding folds of P-glycoprotein. Biochim Biophys Acta. 1998;1373:131-6

Tamura A, Onishi Y, An R, Koshiba S, Wakabayashi K, Hoshijima K, Priebe W, Yoshida T, Kometani S, Matsubara T, Mikuriya K, Ishikawa T. In vitro evaluation of photosensitivity risk related to genetic polymorphisms of human ABC transporter ABCG2 and inhibition by drugs. Drug Metab Pharmacokinet. 2007;22:428–440

Tamura A, Watanabe M, Saito H, Nakagawa H, Kamachi T, Okura I, Ishikawa T. Functional validation of the genetic polymorphisms of human ATPbinding cassette (ABC) transporter ABCG2: identification of alleles that are defective in porphyrin transport. Mol Pharmacol. 2006;70:287–296

Tanaka Y, Slitt AL, Leazer TM, Maher JM, Klaassen CD. Tissue distribution and hormonal regulation of the breast cancer resistance protein (Bcrp/Abcg2) in rats and mice. Biochem. Biophys Res Commun. 2005;326:181–87

Tang SC, Lagas JS, Lankheet NA, Poller B, Hillebrand MJ, Rosing H, Beijnen JH, Schinkel AH. Brain accumulation of sunitinib is restricted by P-glycoprotein (ABCB1) and breast cancer resistance protein (ABCG2) and can be enhanced by oral elacridar and sunitinib coadministration. Int J Cancer. 2012;130(1):223-33

Tang SC, de Vries N, Sparidans RW, Wagenaar E, Beijnen JH, Schinkel AH. Impact of P-glycoprotein (ABCB1) and breast cancer resistance protein (ABCG2) gene dosage on plasma pharmacokinetics and brain accumulation of dasatinib, sorafenib, and sunitinib. J Pharmacol Exp Ther. 2013;346(3):486-94

Tarr PT, Tarling EJ, Bojanic DD, Edwards PA, Baldan A. Emerging new paradigms for ABCG transporters. Biochim Biophys Acta. 2009;1791:584–593

Tatsuta T, Naito M, Oh-hara T, Sugawara I, Tsuruo T. Functional involvement of P-glycoprotein in blood-brain barrier. J Biol Chem. 1992;267:20383-91

Taub ME, Podila L, Ely D, Almeida I. Functional assessment of multiple P-glycoprotein (P-gp) probe substrates: influence of cell line and modulatorconcentration on P-gp activity. Drug Metab Dispos. 2005;33(11):1679-87

Telbisz A, Müller M, Ozvegy-Laczka C, Homolya L, Szente L, Váradi A, Sarkadi B. Membrane cholesterol selectively modulates the activity of the human ABCG2 multidrug transporter. Biochim Biophys Acta. 2007;1768(11):2698-713

Thibault MB, Koumare B, Soussy CJ, Duval J. [Structure-activity relationships in the quinolone group: antibacterial activity of two new compounds (author's transl)]. Ann. Microbiol. (Paris). 1981; 132, 267-281

Thiebaut F, Tsuruo T, Hamada H, Gottesman MM, Pastan I, Willingham MC. Cellular localization of the multidrug-resistance gene product P-glycoprotein in normal human tissues. Proc Natl Acad Sci USA. 1987;84:7735–7738

Thomas H, Coley HM. Overcoming multidrug resistance in cancer: an update on the clinical strategy of inhibiting p-glycoprotein. Cancer Control. 2003;10:159-65

Tsai TH. Pharmacokinetics of pefloxacin and its interaction with cyclosporin A, a P-glycoprotein modulator, in rat blood, brain and bile, using simultaneous microdialysis. Br J Pharmacol. 2001; 132, 1310-1316

Tsuruo T, Iida H, Tsukagoshi S, Sakurai Y. Overcoming of vincristine resistance in P388 leukemia in vivo and in vitro through enhanced cytotoxicity of vincristine and vinblastine by verapamil. Cancer Res. 1981;41:1967-72

Ueda K, Okamura N, Hirai M, Tanigawara Y, Saeki T, Kioka N, Komano T, Hori R. Human P-glycoprotein transports cortisol, aldosterone, and dexamethasone, but not progesterone. J Biol Chem. 1992;267(34):24248-52

Ueda K. ABC proteins protect the human body and maintain optimal health. Biosci Biotechnol Biochem. 2011;75(3):401-9

Ueda T, Brenner S, Malech HL, Langemeijer SM, Perl S, et al. Cloning and functional analysis of the rhesus macaque ABCG2 gene. Forced expression confers an SP phenotype among hematopoietic stem cell progeny in vivo. J Bio Chem. 2005;280:991–98

Ueda K, Cornwell MM, Gottesman MM, Pastan I, Roninson IB, Ling V, Riordan JR. The mdr1 gene, responsible for multidrug-resistance, codes for P-glycoprotein. Biochem Biophys Res Commun. 1986;141(3):956-62

Urbatsch IL, Sankaran B, Weber J, Senior AE. (1995) P-glycoprotein is stably inhibited by vanadate-induced trapping of nucleotide at a single catalytic site. J Biol Chem.1995; 270:19383-90

Ushigome F, Takanaga H, Matsuo H, Yanai S, Tsukimori K, Nakano H, Uchiumi T, Nakamura T, Kuwano M, Ohtani H, Sawada Y. Human placental transport of vinblastine, vincristine, digoxin and progesterone: contribution of P-glycoprotein. Eur J Pharmacol. 2000;408(1):1-10

Vallet CM, Marquez B, Nhiri N, Anantharajah A, Mingeot-Leclercq MP, Tulkens PM, Lallemand JY, Jacquet E, Van Bambeke F. Modulation of the expression of ABC transporters in murine (J774) macrophages exposed to large concentrations of the fluoroquinolone antibiotic moxifloxacin. Toxicology. 2011;290(2-3):178-86

Valverde MA, Diaz M, Sepulveda FV, Gill DR, Hyde SC, Higgins CF. Volume-regulated chloride channels associated with the human multidrug-resistance P-glycoprotein. Nature. 1992;355:830-3

Van Asperen J, Van Tellingen O, Beijnen JH. The pharmacological role of p-glycoprotein in the intestinal epithelium. Pharmacological Research. 1998;37(6):429-35

Van Bambeke F, Balzi E and Tulkens PM. Antibiotic efflux pumps. Biochem Pharmacol. 2000;60:457-70

van Breemen RB, Li Y. Caco-2 cell permeability assays to measure drug absorption. Expert Opin Drug Metab Toxicol. 2005;1(2):175-85

van der Bliek AM, Kooiman PM, Schneider C, Borst P. Sequence of mdr3 cDNA encoding a human P-glycoprotein. Gene. 1988;71:401–411

van der Does C, Tampe R. How do ABC transporters drive transport? Biol Chem. 2004;385:927-933

van Helvoort A, Smith AJ, Sprong H, Fritzsche I, Schinkel AH, Borst P, van Meer G. MDR1 P-glycoprotein is a lipid translocase of broad specificity, while MDR3 P-glycoprotein specifically translocates phosphatidylcholine. Cell. 1996;87:507-17

van Herwaarden AE, Wagenaar E, Karnekamp B, Merino G, Jonker JW, Schinkel AH. Breast cancer resistance protein (Bcrp1/Abcg2) reduces systemic exposure of the dietary carcinogens aflatoxin B1, IQ and Trp-P-1 but also mediates their secretion into breast milk. Carcinogenesis. 2006;27:123–130

van Herwaarden AE, Wagenaar E, Merino G, Jonker JW, Rosing H, Beijnen JH, Schinkel AH. Multidrug transporter ABCG2/breast cancer resistance protein secretes riboflavin (vitamin B2) into milk. Mol Cell Biol. 2007;27:1247-1253

van Kalken CK, Broxterman HJ, Pinedo HM, Feller N, Dekker H, Lankelma J, Giaccone G. Cortisol is transported by the multidrug resistance gene product P-glycoprotein. Br J Cancer. 1993;67(2):284-9

van Loevezijn A, Allen JD, Schinkel AH and Koomen GJ. Inhibition of BCRP-mediated drug efflux by fumitremorgin-type indolyl diketopiperazines. Bioorg Med Chem Lett 2001;11:29-32

van Veen HW, Higgins CF, Konings WN. Molecular basis of multidrug transport by ATP-binding cassette transporters: a proposed two-cylinder engine model. J Mol Microbiol Biotechnol. 2001;3:185-92

van Veen HW, Konings WN. The ABC family of multidrug transporters in microorganisms. Biochim. Biophys. Acta. 1998;1365;31-36

van Waterschoot RA, Lagas JS, Wagenaar E, et al. Individual and combined roles of CYP3A, P-glycoprotein (MDR1/ABCB1) and MRP2 (ABCC2) in the pharmacokinetics of docetaxel. Int J Cancer. 2010;127:2959-64

Vlaming ML, Lagas JS, Schinkel AH. Physiological and pharmacological roles of ABCG2 (BCRP): recent findings in Abcg2 knockout mice. Adv Drug Deliv Rev. 2009;61(1):14-25

Vlaming ML, van Esch A, van de Steeg E, Pala Z, Wagenaar E, van Tellingen O, Schinkel AH. Impact of abcc2 [multidrug resistance-associated protein (MRP) 2], abcc3 (MRP3), and abcg2 (breast cancer resistance protein) on the oral pharmacokinetics of methotrexate and its main metabolite 7-hydroxymethotrexate. Drug Metab Dispos. 2011;39(8):1338-44

Völgyi G, Ruiz R, Box K, Comer J, Bosch E, Takács-Novák K. Potentiometric and spectrophotometric pKa determination of water-insoluble compounds: validation study in anew cosolvent system. Anal Chim Acta. 2007;583(2):418-28

Volk EL, Farley KM, Wu Y, Li F, Robey RW, Schneider E. Overexpression of wild-type breast cancer resistance protein mediates methotrexate resistance. Cancer Res. 2002;62:5035–5040

von Keutz E, Schlüter G. Preclinical safety evaluation of moxifloxacin, a novel fluoroquinolone. J Antimicrob Chemother. 1999;43 Suppl B:91-100

Wahrle SE, Jiang H, Parsadanian M, Kim J, Li A, Knoten A, Jain S, Hirsch-Reinshagen V, Wellington CL, Bales KR, Paul SM, Holtzman DM. Overexpression of ABCA1 reduces amyloid deposition in the PDAPP mouse model of Alzheimer disease. J Clin Invest. 2008;118:671-82

Wang EJ, Casciano CN, Clement RP, Johnson WW. In vitro flow cytometry method to quantitatively assess inhibitors of P-glycoprotein. Drug Metab Dispos. 2000; 28:522–528

Wang H, Lee EW, Cai X, Ni Z, Zhou L, Mao Q. Membrane topology of the human breast cancer resistance protein (BCRP/ABCG2) determined by epitope insertion and immunofluorescence. Biochemistry. 2008a;47(52):13778–13787

Wang H, Zhou L, Gupta A, Vethanayagam RR, Zhang Y, Unadkat JD, et al. Regulation of BCRP/ABCG2 expression by progesterone and 17{beta}-estradiol in human placental BeWo cells. American Journal of Physiology: Endocrinology and Metabolism. 2006;290(5):98–807

Wang H, Lee EW, Zhou L, Leung PC, Ross DD, Unadkat JD, Mao Q. Progesterone receptor (PR) isoforms PRA and PRB differentially regulate expression of the breast cancerresistance protein in human placental choriocarcinoma BeWo cells. Mol Pharmacol. 2008c;73(3):845-54

Wang L, Leggas M, Goswami M, Empey PE, and McNamara PJ. N-(4-[2- (1,2,3,4-tetrahydro-6,7-dimethoxy-2-isoquinolinyl)ethyl]-phenyl)-9 ,10-dihydro-5- methoxy-9-oxo-4-acridine carboxamide (GF120918) as a chemical ATP-binding cassette transporter family G member 2 (Abcg2) knockout model to study nitrofurantoin transfer into milk. Drug Metab Dispos. 2008b;36:2591–2596

Ward A, Reyes CL, Yu J, Roth CB, Chang G. Flexibility in the ABC transporter MsbA: Alternating access with a twist. Proc Natl Acad Sci USA. 2007;104(48):19005–19010

Weber PC, Salemme FR. Applications of calorimetric methods to drug discovery and the study of protein interactions. Curr Opin Struct Biol. 2003 Feb;13(1):115-21

Weiner M, Burman W, Luo CC, Peloquin CA, Engle M, Goldberg S, Agarwal V, Vernon A. Effects of rifampin and multidrug resistance gene polymorphism on concentrations of moxifloxacin. Antimicrob Agents Chemother. 2007;51(8):2861-6

Wilma van Esse G, Westphal AH, Surendran RP, Albrecht C, van Veen B, Borst JW, de Vries SC. Quantification of the brassinosteroid insensitive1 receptor in planta. Plant Physiol. 2011;156(4):1691-700

Wise R. Norfloxacin--a review of pharmacology and tissue penetration. J Antimicrob Chemother. 1984;13 Suppl B:59-64

Woehlecke H, Osada H, Herrmann A, Lage H. Reversal of breast cancer resistance protein- mediated drug resistance by tryprostatin A. Int J Cancer 2003;107:721-728

Wolfger H, Mamnun YM, Kuchler K. Fungal ABC proteins: pleiotropic drug resistance, stress response and cellular detoxification. Res Microbiol. 2001;152, 375-89

Woodward OM, Kottgen A, Coresh J, Boerwinkle E, Guggino WB, Kottgen M. Identification of a urate transporter, ABCG2, with a common functional polymorphism causing gout. Proc Natl Acad Sci USA. 2009;106:10338-10342

Woodward OM, Köttgen A, Köttgen M. ABCG transporters and disease. FEBS J. 2011;278(18):3215-25

Wu CP, Shukla S, Calcagno AM, Hall MD, Gottesman MM, Ambudkar SV. Evidence for dual mode of action of a thiosemicarbazone, NSC73306: a potent substrate of the multidrug resistance linked ABCG2 transporter. Mol Cancer Ther. 2007;6(12 Pt 1):3287-96

Xia CQ, Yang JJ, Gan LS. Breast cancer resistance protein in pharmacokinetics and drug-drug interactions. Expert Opin Drug Metab Toxicol. 2005;1(4):595-611

Xiong H, Callaghan D, Jones A, Bai J, Rasquinha I, Smith C, Pei K, Walker D, Lue LF, Stanimirovic D, Zhang W. ABCG2 is upregulated in Alzheimer's brain with cerebral amyloid angiopathy and may act as a gatekeeper at theblood-brain barrier for Abeta(1-40) peptides. J Neurosci. 2009;29(17):5463-75

Xu J, Liu Y, Yang Y, Bates S, Zhang JT. Characterization of oligomeric human half ABC transporter BCRP/ABCG2/MXR/ABCP in plasma membranes. J Biol Chem. 2004;279(19):19781–19789

Yague E, Higgins CF, Raguz S. Complete reversal of multidrug resistance by stable expression of small interfering RNAs targeting MDR1. Gene Ther. 2004;11:1170-4

Yahya AM, McElnay JC, D'Arcy PF. Drug sorption to glass and plastics. Drug Metab. Drug Interact. 1988;6:1-45

Yamaguchi H, Yano I, Saito H, Inui K. Effect of cisplatin-induced acute renal failure on bioavailability and intestinal secretion of quinolone antibacterialdrugs in rats. Pharm Res. 2004;21(2):330-8

Yang CP, DePinho SG, Greenberger LM, Arceci RJ, Horwitz SB. Progesterone interacts with P-glycoprotein in multidrug-resistant cells and in the endometrium of gravid uterus. J Biol Chem. 1989;264(2):782-8

Yates CR, Chang C, Kearbey JD, Yasuda K, Schuetz EG, Miller DD, Dalton JT, Swaan PW. Structural determinants of P-glycoprotein-mediated transport of glucocorticoids. Pharm Res. 2003;20(11):1794-803

Yildiz A, Guleryuz S, Ankerst DP, Ongür D, Renshaw PF. Protein kinase C inhibition in the treatment of mania: a double-blind, placebo-controlled trial of tamoxifen. Arch Gen Psychiatry. 2008;65(3):255-63

Yoshikawa M, Ikegami Y, Hayasaka S, Ishii K, Ito A, Sano K, Suzuki T, Togawa T, Yoshida H, Soda H, Oka M, Kohno S, Sawada S, Ishikawa T, Tanabe S. Novel camptothecin analogues that circumvent ABCG2-associated drug resistance in human tumor cells. Int J Cancer. 2004;110(6):921–927

Zamora JM, Pearce HL, Beck WT. Physical-chemical properties shared by compounds that modulate multidrug resistance in human leukemic cell. Mol Pharmacol. 1988;33:454– 462

Zelinski T, Coghlan G, Liu XQ, Reid ME. ABCG2 null alleles define the Jr(a-) blood group phenotype. Nat Genet. 2012;44(2):131-2

Zhang Y, Wang H, Unadkat JD, Mao Q. Breast cancer resistance protein 1 limits fetal distribution of nitrofurantoin in the pregnant mouse. Drug Metab Dispos. 2007;35:2154–2158

Zhou L, Naraharisetti SB, Wang H, Unadkat JD, Hebert MF, Mao Q. The breast cancer resistance protein (Bcrp1/Abcg2) limits fetal distribution of glyburide in the pregnant mouse: an Obstetric-Fetal Pharmacology Research Unit Network and University of Washington Specialized Center of Research Study. Mol Pharmacol. 2008;73:949–959

Zhou S, Morris JJ, Barnes YX, Lan L, Schuetz JD, Sorrentino BP: Bcrp1 gene expression is required for normal numbers of side population stem cells in mice, and confers relative protection to mitoxantrone in hematopoietic cells in vivo. Proc Natl Acad Sci USA. 2002;99:12339–12344

Zhou S, Schuetz JD, Bunting KD, Colapietro AM, Sampath J, Morris JJ, Lagutina I, Grosveld GC, Osawa M, Nakauchi H, Sorrentino BP. The ABC transporter Bcrp1/ABCG2 is expressed in a wide variety of stem cells and is a molecular determinant of the side-population phenotype. Nat Med. 2001;7:1028-1034

Zhou SF. Structure, function and regulation of P-glycoprotein and its clinical relevance in drugdisposition. Xenobiotica. 2008;38(7-8):802-32

Zlotos G, Buucker A, Kinzig Schippers M, Sorgel F, Holzgrabe U. Plasma protein binding of gyrase inhibitors. J Pharm Sci. 1998;87(2):215-20